

General Disclaimer

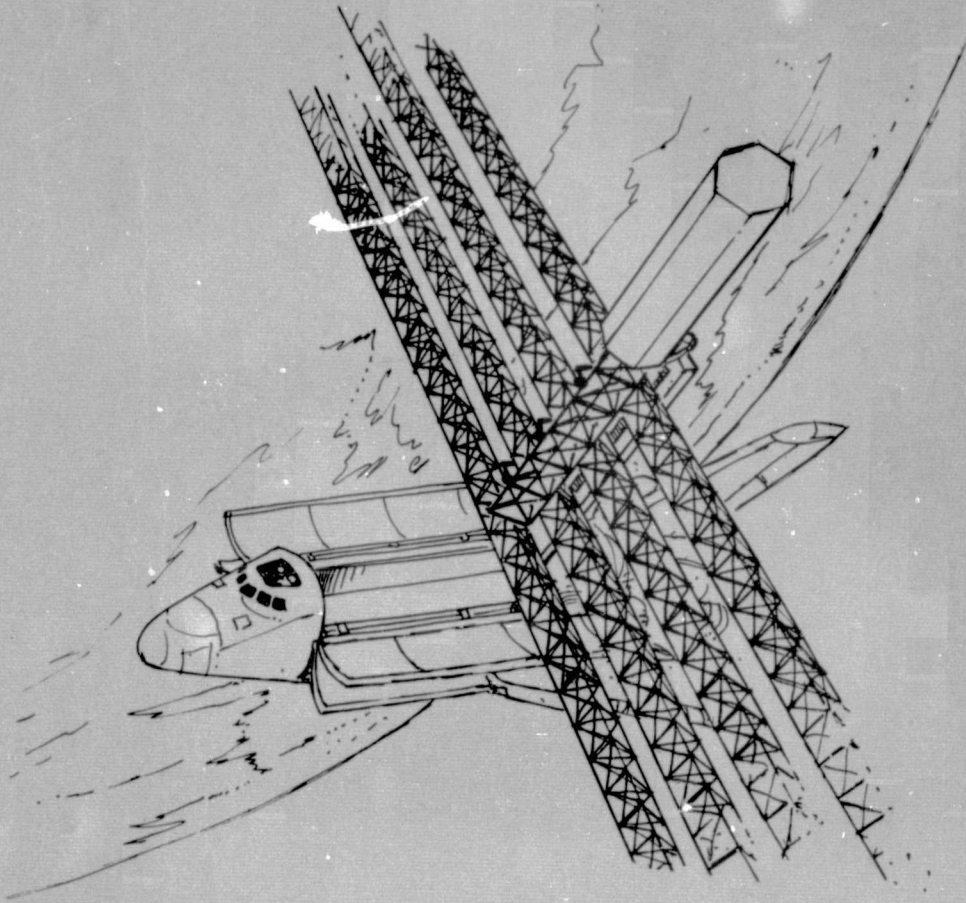
One or more of the Following Statements may affect this Document

- This document has been reproduced from the best copy furnished by the organizational source. It is being released in the interest of making available as much information as possible.
- This document may contain data, which exceeds the sheet parameters. It was furnished in this condition by the organizational source and is the best copy available.
- This document may contain tone-on-tone or color graphs, charts and/or pictures, which have been reproduced in black and white.
- This document is paginated as submitted by the original source.
- Portions of this document are not fully legible due to the historical nature of some of the material. However, it is the best reproduction available from the original submission.

CASD-ASP77-017

NASA CR-

151730



SPACE CONSTRUCTION AUTOMATED FABRICATION EXPERIMENT DEFINITION STUDY (SCAFEDS)

FINAL REPORT
VOLUME II + STUDY RESULTS

CONTRACT NO. NAS9-15310

DRL NO. T-1346

DRD NO. MA-664T

LINE ITEM NO. 3



GENERAL DYNAMICS

Convair Division

Kearny Mesa Plant, P.O. Box 80847
San Diego, California 92138
Advanced Space Programs

(NASA-CR-151730) SPACE CONSTRUCTION
AUTOMATED FABRICATION EXPERIMENT DEFINITION
STUDY (SCAFEDS). VOLUME 2: STUDY RESULTS
Final Report (General Dynamics/Convair)
382 p HC A17/MF A01

N78-25112

Unclas

CSCI 22A G3/12 21624

CASD-ASP77-017

**SPACE CONSTRUCTION AUTOMATED FABRICATION
EXPERIMENT DEFINITION STUDY (SCAFEDS)**

FINAL REPORT

VOLUME II ♦ STUDY RESULTS

CONTRACT NO. NAS9-15310

DRL NO. T-1346

DRD NO. MA-664T

LINE ITEM NO. 3

26 May 1978

Submitted to
National Aeronautics and Space Administration
LYNDON B. JOHNSON SPACE CENTER
Houston, Texas 77058

Prepared by
GENERAL DYNAMICS CONVAIR DIVISION
P.O. Box 80847
San Diego, California 92138

FOREWORD

This final report was prepared by General Dynamics Convair Division for NASA/JSC in accordance with Contract NAS9-15310, DRL No. T-1346, DRD No. MA-664T, Line Item No. 3. It consists of three volumes: (I) A brief Executive Summary; (II) a comprehensive set of Study Results; and (III) a compilation of Requirements suitable for use as a preliminary system specification for subsequent Phase B studies.

The principal study results were developed from April 1977 through January 1978, followed by a beam fabrication task and final documentation. Reviews were presented at JSC on 19 July 1977, 1 September 1977, 9 November 1977, and 3 February 1978 and at NASA Headquarters on 10 February 1978.

Due to the broad scope of this study, many individuals were involved in providing technical assistance. General Dynamics Convair personnel who significantly contributed to the study include:

Study Manager	-	Lee Browning
Mechanical Design	-	John Bodle, Des Kozmary, Bob Trussell, Maurice Butler, A. D. McFarlan
Avionics & Controls	-	Jack Fisher, Dave Sears, Ron Newby
Requirements & Operations	-	Charlie Hyde, Jim Peterson, John Maloney, Tad Winięcki
EVA/IVA	-	Kent Geyer, Mike Byrd
Structural Design	-	Lee Browning, Des Vaughan
Structural Analysis	-	Denny Laue, Jack Dyer
Structural Dynamics	-	Des Pengelley, Mike Shafir, Jack Weber
Stability & Control	-	Bill Stubblefield
Thermodynamics	-	Bruce Kaser
Mass Properties	-	Dave Johnston, John Kessler, Marv French, Julie Richardson
Materials & Processes	-	Jules Hertz, Chuck May, Herb Urbach, Joe Villa, Carlos Portugal
Manufacturing R&D	-	Jerry Peddie
Economic Analysis	-	Bob Bradley
Test Integration	-	Phil Gardner

The study was conducted in Convair's Advanced Space Programs department, directed by J. B. (Jack) Hurt. The NASA-JSC COR is Lyle Jenkins of the Spacecraft Design Division, under Allen J. Louviere, Chief.

For further information contact:

**Lyle M. Jenkins, Code EW4
NASA/JSC
Houston, TX 77058
(713) 483-4483**

**D. Lee Browning, MZ 21-9504
General Dynamics Convair Division
P. O. Box 80847
San Diego, CA 92138
(714) 277-8900, X 2815**

TABLE OF CONTENTS

Section	Page
1.0 INTRODUCTION	1-1
1.1 Scope	1-1
1.2 Study Overview	1-1
1.3 Summary	1-3
2.0 SYSTEM DESIGN	2-1
2.1 Structure/Materials	2-1
2.1.1 Baseline Platform	2-1
2.1.2 Materials	2-15
2.1.3 Alternative Platform Concepts	2-31
2.2 Platform Fabrication System	2-35
2.2.1 Beam Builder	2-35
2.2.2 Assembly Jig	2-82
2.2.3 Avionics and Controls	2-111
2.3 Alternative Beam Concept	2-143
2.3.1 Structural Efficiency Analysis	2-144
2.3.2 Beam Design	2-166
2.3.3 Beam Fabricator	2-168
3.0 FLIGHT EXPERIMENT INTEGRATION	3-1
3.1 Mission Requirements and Guidelines	3-1
3.1.1 Orbital Altitude and Inclination	3-2
3.1.2 Fabrication Orientation	3-3
3.2 Fabrication and Construction Experiment Requirements	3-9
3.2.1 NASA Design Guidelines/Requirements	3-9
3.2.2 Derived Performance Requirements	3-10
3.2.3 Derived Ground Operations Guidelines/Requirements	3-13
3.2.4 Derived Beam Builder and Assembly Jig Functional Requirements	3-13
3.3 Structural Test Description	3-15
3.3.1 First Beam Dynamics Experiment	3-15
3.3.2 Complete Platform Dynamics Experiment	3-18
3.3.3 Thermal Effects Test	3-21
3.3.4 Separation/Recapture Demonstration	3-23

TABLE OF CONTENTS (Contd)

Section	Page
3.4 Post Separation Experiments	3-26
3.4.1 Geodynamic Experiment	3-26
3.4.2 Atmospheric Composition Experiment	3-27
3.5 Future Applications	3-27
3.6 Mission Operations	3-29
3.6.1 Mission Profile	3-29
3.6.2 Experiments Timeline	3-35
3.6.3 Supporting Subsystem	3-36
3.6.4 EVA	3-41
3.6.5 Ground Operations	3-46
3.6.6 Mission Options	3-49
3.7 Orbiter Compatibility/Interfaces	3-54
3.7.1 Mass Properties	3-54
3.7.2 Structural Supports	3-55
3.7.3 Remote Manipulator System (RMS)	3-57
3.7.4 Subsystem Interfaces	3-57
3.7.5 Aft Cabin Viewing/Illumination	3-61
3.7.6 Scafe Aft Station Control/Display Provisions.	3-66
3.7.7 Orbiter RCS Propellant Requirements	3-71
4.0 ANALYSES	4-1
4.1 Mass Properties	4-1
4.1.1 Preliminary Analyses	4-1
4.1.2 Final Analyses.	4-1
4.2 Stability and Control	4-6
4.2.1 Orbiter/Platform Response	4-6
4.2.2 Platform Stability During Free Flight Mode	4-15
4.3 Structural Dynamics	4-20
4.3.1 Single Beam Attached to Orbiter	4-21
4.3.2 Completed Platform Attached to Orbiter	4-24
4.3.3 Free Platform.	4-26
4.4 Stress Analysis	4-28
4.4.1 Element Section and Material Properties	4-28
4.4.2 Loads	4-33
4.4.3 Preload in Diagonals.	4-38
4.4.4 Open Section Caps	4-44
4.4.5 Differential Drive Effects	4-49
4.4.6 Thermal Distortion Analysis	4-53
4.4.7 Final Analysis	4-55

TABLE OF CONTENTS (Contd)

Section	Page
4.5 Thermodynamics	4-58
4.5.1 Beam Builder Power and Cooling Requirements	4-58
4.5.2 Space Heating	4-64
5.0 PROGRAMMATICS	5-1
5.1 Program Definition for Development Plan and Cost Estimation	5-1
5.1.1 Objectives and Guidelines	5-1
5.1.2 Mission Operations Summary	5-2
5.1.3 Ground Operations Summary	5-4
5.1.4 Technology Advancement	5-6
5.2 Preliminary Development Plan	5-11
5.2.1 Schedule	5-11
5.2.2 Development & Qualification Test Program	5-13
5.3 Cost Analysis	5-13
5.3.1 Work Breakdown Structure	5-13
5.3.2 Cost Analysis	5-23
5.3.3 SCAFE Program Cost Estimate	5-35
6.0 MANUFACTURING	6-1
6.1 Design	6-1
6.2 Fabrication	6-1
7.0 CONCLUSIONS AND RECOMMENDATIONS	7-1
7.1 Conclusions	7-1
7.1.1 System Design	7-1
7.1.2 Flight Mission	7-3
7.1.3 Analyses	7-4
7.1.4 Programmatic	7-4
7.1.5 Fabrication	7-5
7.2 Recommendations	7-5
7.2.1 Platform Applications	7-5
7.2.2 SCAFE Development	7-6
7.2.3 Beam Builder Development Article	7-8
7.2.4 Manufacture and Test	7-8
7.2.5 Alternative Beam Concept	7-8

LIST OF FIGURES

Figure		Page
1-1	Study approach - Part I	1-2
1-2	Study approach - Part II	1-3
1-3	Baseline system concept	1-4
2-1	Selected platform	2-3
2-2	Typical beam	2-3
2-3	Cap section	2-3
2-4	Cross-member section	2-3
2-5	Joints	2-4
2-6	Original platform structure concept	2-5
2-7	Cargo bay and assembly jig geometry constraints	2-6
2-8	Local clearance concerns at beam intersection	2-7
2-9	Platform overall transverse geometry	2-8
2-10	Assembly geometry with tolerance considerations	2-8
2-11	Local element geometry considerations	2-9
2-12	Beam construction concepts	2-13
2-13	Flow chart of materials evaluation effort	2-16
2-14	TiO ₂ Absorptance vs. time	2-31
2-15	Maximum temperature vs α/ϵ	2-31
2-16	Mission temperature histories	2-31
2-17	Single planar platforms	2-32
2-18	Dual planar platforms	2-32
2-19	Large T-Beam	2-33
2-20	Large triangular beams	3-34
2-21	Study method and issues	3-36
2-22	Cyclic feed fabricator functional schematic	2-37
2-23	Constant feed fabricator functional schematic	2-39
2-24	Baseline beam builder excitation timeline	2-39
2-25	Beam dynamic characteristics	2-40
2-26	Cap and cross member material storage options	2-42
2-27	Cord storage options	2-42
2-28	Material heating options	2-43
2-29	Relative efficiencies of heating process options	2-43
2-30	Material cooling options	2-44
2-31	Cap drive options	2-45
2-32	Cross-member positioner options	2-47
2-33	Cutoff options	2-48
2-34	Independent cooling system	2-48

LIST OF FIGURES (Contd)

Figure		Page
2-35	Beam builder concept 1 layout	2-51
2-36	Beam builder concept 2 layout	2-53
2-37	Baseline beam assembly sequence	2-55
2-38	Beam builder concept 2A layout	2-57
2-39	Beam builder concept 3 layout	2-59
2-40	Beam builder concept 4 layout	2-63
2-41	Beam builder concept 4 assembly sequence	2-65
2-42	SCAFEDS beam builder selected concept	2-66
2-43	Beam builder general arrangement	2-71
2-44	Cap forming machine general arrangement	2-73
2-45	Cord pleyer and welding mechanism general arrangement	2-75
2-46	Cross-member clip and positioner mechanism	2-77
2-47	Beam builder structure	2-79
2-48	Cord pleyer timing sequence	2-80
2-49	Assembly jig functional diagram	2-84
2-50	SCAFE stowage options	2-85
2-51	SCAFE jig and beam builder deployment sequence	2-85
2-52	Jig deployment drive options	2-86
2-53	Beam builder roll-and-turn mechanism options	2-87
2-54	Beam builder carriage mechanism options	2-88
2-55	Beam builder support options	2-89
2-56	Beam builder umbilicals and service lines	2-89
2-57	Umbilical and service line rigging options	2-90
2-58	Beam retention and guide mechanism options	2-91
2-59	Platform drive mechanism option	2-92
2-60	Cross beam retention and positioning options	2-93
2-61	Cross-beam-to-longitudinal-beam joining options	2-94
2-62	Corss-beam-to-longitudinal-beam ultrasonic welding mechanism	2-95
2-63	Cross-beam-to-longitudinal-beam joining technique options	2-96
2-64	Platform separation options	2-97
2-65	Assembly jig concept 1	2-98
2-66	Assembly jig concept 1A	2-99
2-67	Assembly jig concept 2	2-100
2-68	Assembly jig concept 3	2-101
2-69	Preliminary design layout of the SCAFE assembly jig	2-103
2-70	Preliminary design layout of the SCAFE assembly jig	2-105
2-71	Flight support provisions	2-107
2-72	Assembly jig structure	2-111

LIST OF FIGURES (Contd)

Figure		Page
2-73	Baseline assembly fig control diagram	2-113
2-74	Assembly jig setup control diagram	2-113
2-75	Beam builder positioning control diagram	2-115
2-76	Longitudinal beam handling control diagram	2-117
2-77	Cross beam assembly control diagram	2-118
2-78	Baseline beam builder control system	2-119
2-79	Beam control unit alternate concept	2-121
2-80	Cap member subsystem control diagram	2-121
2-81	Heater/sensor control elements	2-122
2-82	Beam control/alignment requirements	2-123
2-83	Manufacturing accuracy effects	2-125
2-84	Structural consideration limit correction capability	2-126
2-85	Alternate manufacturing error control methods	2-127
2-86	Cap travel alignment sensors method	2-128
2-87	External alignment sensor	2-128
2-88	Cross-member positioning control diagram	2-130
2-89	Beam tension cord drive control diagram	2-131
2-90	Beam ultrasonic weld control diagram	2-133
2-91	Executive software systems	2-134
2-92	ACU application software modules	2-135
2-93	BCU executive software	2-135
2-94	Control avionics packaging configuration	2-140
2-95	Beam builder avionics interconnect diagram	2-143
2-96	Mesh tube concepts	2-144
2-97	Task flow	2-145
2-98	Minimum coil diameter vs. element size for candidate fiber materials	2-152
2-99	Modulus vs. laminate thickness	2-159
2-100	Critical axial load vs. unit weight	2-164
2-101	Cylindrical geodetic beam	2-166
2-102	In-plane beam/beam joint concept	2-167
2-103	Geodetic beam joint concepts	2-169
2-104	Beam fabricator concept	2-170
2-105	Helix element storage cylinder detail	2-170
2-106	Feed/weld/cutoff assembly	2-171

LIST OF FIGURES (Contd)

Figure		Page
3-1	SCAFE program top level activities	3-2
3-2	Cargo weight vs. altitude	3-3
3-3	Orbit lifetime	3-3
3-4	Graphical determination of SCAFE orbit geometry	3-4
3-5	Candidate orientation families	3-4
3-6	Reference fabrication orientation	3-5
3-7	Stable axis orientation	3-5
3-8	Phase planes for rate-mode VRCS operation	3-6
3-9	Sunward viewing due to attitude oscillation	3-6
3-10	Orbiter-TDRS antenna coverage	3-8
3-11	Baseline system concept	3-10
3-12	Initial platform baseline	3-11
3-13	First beam dynamics experiment system diagram	3-16
3-14	Platform dynamics experiment system diagram	3-19
3-15	Laser beacon, detector array concept	3-20
3-16	Location of sun shade and temperature sensors	3-22
3-17	Thermal deflection experiment system diagram	3-22
3-18	Beam cap temperature measurements	3-22
3-19	End effector/grapple fitting capture and rigidize sequence	3-24
3-20	RMS/grapple fitting relationship	3-25
3-21	Scientific experiments system diagrams	3-26
3-22	Position accuracy relative requirements for future applications of platform	3-28
3-23	SCAFE flight profile	3-31
3-24	SCAFE stowage concept	3-32
3-25	Beam/platform/Orbiter positions	3-33
3-26	Platform equipment general arrangement (Experiment plus Subsystems)	3-34
3-27	Subsystem installation	3-35
3-28	SCAFE program mission profile	3-36
3-29	Experiment timeline	3-37
3-30	Overall mission experiment timeline	3-38
3-31	Solar array installation	3-38
3-32	Power profile-limiting case	3-39
3-33	Platform dynamics/thermal deflection experiments power requirements	3-40
3-34	Crew activities	3-42
3-35	Astronaut wearing MMU	3-43
3-36	EVA work station	3-43

LIST OF FIGURES (Contd)

Figure		Page
3-37	Equipment module installation	3-45
3-38	Instrument installation concepts	3-45
3-39	Wiring shuttle concept	3-46
3-40	Platform repair using MMU	3-46
3-41	Timeline Day 6 EVA activity	3-47
3-42	Preliminary Level IV integration flow diagram	3-50
3-43	Preliminary Level III/II payload integration flow diagram	3-53
3-44	Weight/ X_{cg} compatibility	3-55
3-45	Weight/ Z_{cg} compatibility	3-55
3-46	Baseline Orbiter interface block diagram	3-58
3-47	Orbiter software system block diagram	3-60
3-48	SCAFE major function support software	3-60
3-49	Aft cabin viewing with fixed eye positions (JSC 07700)	3-62
3-50	Aft cabin viewing with normal eye/head movement	3-63
3-51	SCAFE illumination	3-63
3-52	Locations and FOVs of Orbiter CCTV cameras	3-64
3-53	FOV and two TV cameras at aft end of cargo bay	3-65
3-54	Orbiter/RMS CCTV viewing	3-65
3-55	IVA payload support displays and controls	3-67
4-1	Structural/mechanical evaluation task flow of combined shuttle, fabrication system, and platform structure	4-2
4-2	Structural/mechanical evaluation task flow of free-flying platform	4-3
4-3	Thermal evaluation task flow	4-3
4-4	Mass properties for analyses	4-6
4-5	Mass properties variation with mission event	4-7
4-6	Orbiter VRCS operation	4-9
4-7	VRCS thruster operational details	4-11
4-8	Environmental torques	4-15
4-9	Orbiter VRCS operation, Phase 2-1	4-16
4-10	Orbiter VRCS operation, Phase 3	4-16
4-11	Platform stable release orientation	4-18
4-12	Mode shapes: single beam and Orbiter	4-22
4-13	Dynamic response: Single beam, roll pulse	4-22
4-14	Clearance loss due to dynamic response	4-23
4-15	Beam root yaw bending moment	4-23
4-16	Beam tip response sensitivity to pulse duration	4-23
4-17	Beam tip response sensitivity to pulse timing	4-23
4-18	Math model: Platform with Orbiter	4-24

LIST OF FIGURES (Contd)

Figure		Page
4-19	Mode shapes: Platform and Orbiter	4-25
4-20	Platform tip response, yaw pulse	4-26
4-21	Mode Shape: Free platform	4-28
4-22	SCAFE beam cap geometry and section properties	4-28
4-23	SCAFE cross-member geometry and section properties	4-29
4-24	Finite element model for determining torsional constant	4-32
4-25	Torque applied to model	4-32
4-26	Orbiter/beam configuration	4-33
4-27	Preliminary beam limit reaction loads on jig	4-36
4-28	Preliminary internal limit loads in bay (N)	4-37
4-29	Final internal ultimate loads in bay (N)	4-37
4-30	Final beam limit reactions loads on jig	4-37
4-31	Maximum platform joint loads	4-38
4-32	Details of longitudinal/cross beam joint	4-39
4-33	Minimum required preload in diagonals	4-39
4-34	Typical beam geometry	4-40
4-35	Beam bending loads	4-41
4-36	Beam torsion due to diagonal cord preload unbalance	4-43
4-37	Beam bending due to diagonal cord preload unbalance	4-43
4-38	Beam distortion due to diagonal cord preload unbalance	4-44
4-39	Cap geometry used for comparison	4-45
4-40	Column allowable for open section caps	4-45
4-41	Flow chart of STAGS cap stability analysis	4-46
4-42	Post buckling load-displacement curve	4-49
4-43	Finite element geometry for differential cap drive study	4-49
4-44	Internal load distribution for differential drive	4-50
4-45	Spot weld geometry for cap/cross-member joint	4-52
4-46	Worst case beam thermal loading	4-54
4-47	Beam tip clearance	4-54
4-48	Beam cap strip material thermal model	4-60
4-49	Temperature vs. distance - longitudinal direction	4-60
4-50	Transverse temperature vs. distance, two laminates	4-61
4-51	Transverse temperature vs. time, radiation/intra-conductive cooling	4-62
4-52	Transverse temperature vs. time, platen cooling	4-63
4-53	Temperature decay vs. time, insulated storage reel	4-64
4-54	Start-up heating	4-65
4-55	Preliminary space heating analysis	4-66
4-56	Axial temperature distribution, beam cap No. 1	4-66
4-57	Updated space heating analysis	4-67

LIST OF FIGURES (Concl'd)

Figure		Page
5-1	Platform characteristics	5-8
5-2	Preliminary SSAFE program development schedule	5-12
5-3	Work breakdown structure	5-24
6-1	Prototype beam segment	6-3
6-2	Part and joint numbers	6-5
6-3	Flat-weld setup: first cap	6-5
6-4	Flat-weld setup: cross-section completion	6-5
6-5	Typical flat-weld preparation	6-5
6-6	Cord installation/pierce-weld setup.	6-5
6-7	Completed beam segment	6-6

LIST OF TABLES

Table		Page
2-1	Governing gap Δ	2-11
2-2	Beam concept evaluation	2-14
2-3	Fiber candidates	2-16
2-4	Typical values for graphite fiber properties used for study	2-17
2-5	Thermoplastic resin candidates	2-18
2-6	Typical properties of polysulfone	2-19
2-7	Estimated lamina properties	2-20
2-8	Candidate laminates	2-23
2-9	Laminate properties/unidirection tape (57% fiber volume)	2-24
2-10	Laminate properties/hybrid (57% fiber volume)	2-25
2-11	Laminate properties/woven (%0%±45/%90) (57% fiber volume)	2-26
2-12	Laminate properties/tape (pseudoisotropic) (±60, 0) _s (57% fiber volume)	2-26
2-13	Laminate properties/summary of candidate laminates (57% fiber volume)	2-28
2-14	Cord candidates/evaluation	2-30
2-15	Beam builder power and energy requirements compared	2-62
2-16	Concept evaluation	2-62
2-17	Summary Assessment	2-65
2-18	Beam builder preliminary design and performance data	2-67
2-19	Assembly jig concept evaluation	2-102
2-20	Beam builder positioning sequence	2-116
2-21	BCU software summary	2-120
2-22	Software function sizing assumptions	2-136
2-23	ACU software sizing estimates	2-137
2-24	BCU software sizing estimates	2-138
2-25	Early beam builder power requirements	2-139
2-26	Baseline beam builder power & energy requirements	2-139
2-27	Beam builder equipment list and characteristics	2-141
2-28	Options for column size relationship	2-146
2-29	Geodetic column element size	2-150
2-30	Candidate graphite/polysulfone materials	2-151
2-31	Minimum coil diameter for candidate materials	2-152
2-32	Summary of baseline geodetic beam characteristics	2-156
2-33	Triangular beam weight breakdown	2-161
2-34	Geodetic vs. triangular beam comparison	2-161
2-35	Triangular beam weight summary	2-164

LIST OF TABLES (Contd)

Table		Page
3-1	Platform data rates for dynamics, deformation, and docking experiments	3-7
3-2	Equipment list	3-17
3-3	Equipment list	3-20
3-4	Equipment list	3-23
3-5	Potential future SCAFE platform activities and uses	3-30
3-6	Attitude control system	3-41
3-7	On-orbit experiment instrumentation	3-44
3-8	On-orbit structural fabrication equipment support subsystems	3-44
3-9	Extended mission crew provisions	3-48
3-10	Level IV integration requirements summary	3-51
3-11	Level III/II integration requirements	3-52
3-12	Level I integration requirements	3-52
3-13	Selected support locations	3-56
3-14	Support reaction compatibility	3-56
3-15	SCAFE control/monitor software capabilities	3-61
3-16	Summary of simultaneous task/work station analysis	3-71
3-17	RCS propellant usage	3-73
4-1	Beam builder weight summary	4-4
4-2	Assembly jig weight summary	4-4
4-3	Free platform/equipment mass properties	4-5
4-4	Orbiter/SCAFE properties with mission phase	4-5
4-5	Gravity gradient stabilization	4-8
4-6	Roll duty cycles	4-10
4-7	Pitch duty cycles	4-10
4-8	Yaw duty cycles	4-10
4-9	Thruster control accelerations	4-12
4-10	Case 2 thrust factors	4-13
4-11	Case 3 thrust factors	4-13
4-12	Final pitch duty cycles	4-17
4-13	Final yaw duty cycles	4-17
4-14	Final roll duty cycles	4-17
4-15	Bare platform response	4-18
4-16	Bare platform environmental torques	4-19
4-17	Platform response systems installed	4-19
4-18	Platform with systems environmental torques	4-19
4-19	Response to environment disturbance torques	4-20
4-20	Mode frequencies: Single beam and Orbiter	4-21

LIST OF TABLES (Contd)

Table		Page
4-21	Displacement response: Single beam, roll pulse	4-22
4-22	Mode frequencies: Platform and Orbiter	4-24
4-23	Platform tip displacements	4-26
4-24	Platform dynamic response loads	4-27
4-25	Mode frequencies: Free platform	4-27
4-26	Cap material properties, VSA-11 (120/W-705 ₃ /120)	4-29
4-27	Material properties, VSA-11 (120/W705 ₂ /120) cross member	4-30
4-28	Beam stiffness properties	4-33
4-29	Orbiter mass properties	4-33
4-30	Orbiter VRCS torques	4-34
4-31	Preliminary single beam design loads	4-36
4-32	Maximum spotweld loads in platform	4-38
4-33	Beam parameters	4-40
4-34	Candidate graphite/thermoplastic laminates	4-47
4-35	Lamina properties* for candidate graphite/thermoplastic laminates	4-47
4-36	Results of STAGS stability analysis	4-48
4-37	Minimum margins of safety	4-58
4-38	Heating/forming power requirement history	4-58
4-39	Estimated laminate thermal properties	4-62
5-1	Baseline mission characteristics	5-3
5-2	On-orbit structural fabrication equipment and scientific experiment support subsystems	5-5
5-3	On-orbit experiment instrumentation	5-7
5-4	Typical Level IV integration tasks	5-9
5-5	GSE - Experiment Peculiar	5-9
5-6	Unique facilities/special test equipment	5-10
5-7	Preliminary technology demonstration assessment	5-10
5-8	SCAFE development and qualification ground test program	5-14
5-9	SCAFE program cost summary	5-36
5-10	Total SCAFE program cost estimate	5-37
5-11	Annual funding requirements	5-38

1

INTRODUCTION

1.1 SCOPE

This is the second of three volumes comprising the SCAFED Study Final Report. It contains the detailed results of all study tasks. Other volumes provide an Executive Summary and a comprehensive Requirements Document.

This section provides a study overview and a top level summary of the study effort.

1.2 STUDY OVERVIEW

The top-level objectives of this definition study are:

- a. Define the techniques, processes, and equipment required for automatic fabrication and assembly of structural elements in space using Shuttle as a launch vehicle and construction base
- b. Identify and define additional construction/systems/operational techniques, processes, and equipment which can be developed/demonstrated in the same program to provide further risk reduction benefits to future large space systems.

The corresponding objectives for downstream program phases consist of the development and flight demonstration of the techniques, processes, and equipment identified and defined during this study.

Study activities were divided into two parts, each of approximately four months duration. The task flow for Part I is shown in Figure 1-1.

Part I involved a predominately linear flow proceeding from requirements analysis through a series of converging design trade-offs addressing beam builder options, structural platform alternatives, and associated jigs and fixtures. Baseline concepts for the platform structure and beam builder were used as reference configurations in these trade-offs. Materials, processes, and techniques were evaluated in parallel supporting tasks. These efforts, plus an evaluation of mission options, including preliminary timelines and EVA assessment, led to a Convair/NASA joint selection of a preferred total system concept at the end of Part I.

Two additional tasks were also accomplished in Part I. A preliminary development plan and cost analysis for the total SCAFE program was submitted to support long range NASA/JSC program planning, and preliminary evaluation of an alternative geodesic beam concept, with potential application to future large space systems, was conducted.

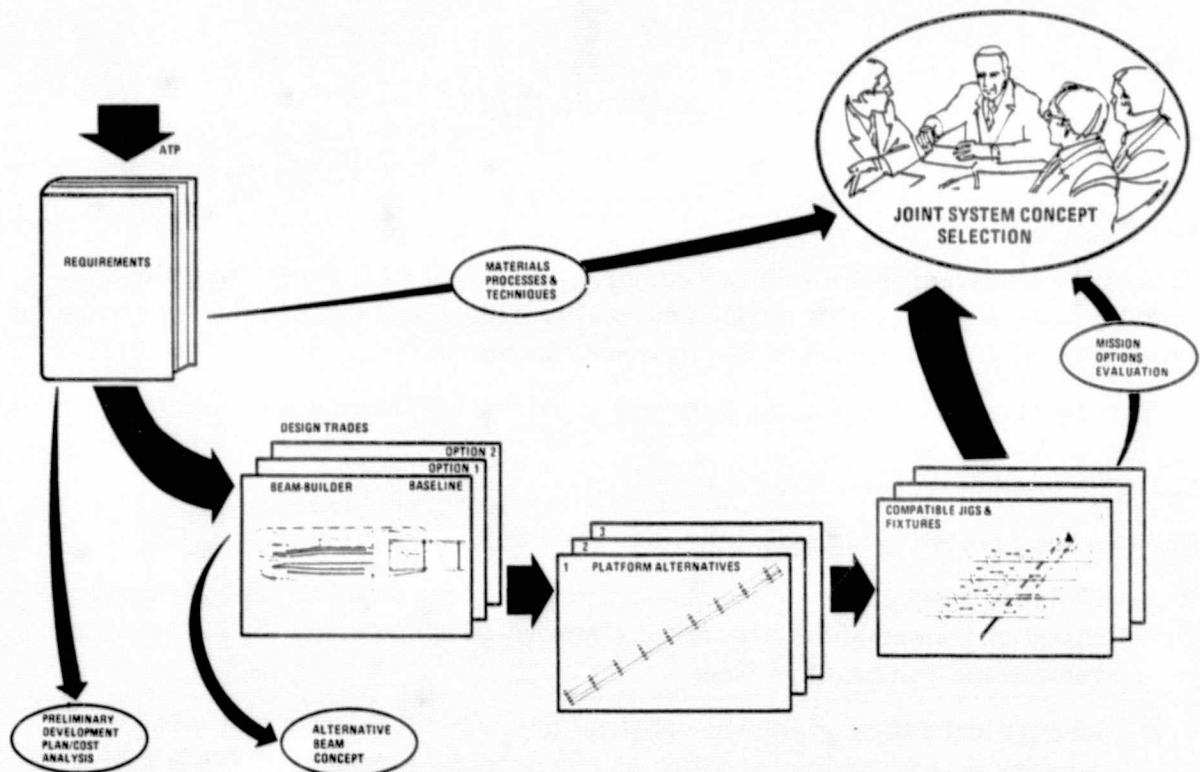


Figure 1-1. Study approach - Part I.

In Part II, as illustrated in the task flow of Figure 1-2, conceptual designs of the selected total system concept were prepared first. This effort led to definition of platform performance verification tests and associated subsystem equipment. Coordinated stress, dynamics, stability and control, thermal, and mass properties analyses supported both efforts.

A parallel task series assessed STS compatibility, analyzed mission options, and evaluated the role of EVA in the experiment. The study concluded with definition of development program plans and associated cost analyses, which updated the Part I preliminary data by incorporating study-generated data.

The requirements document was also updated at study conclusion and is published as Volume III of the Final Report. It is expected to serve as an initial version of the SCAFE Program System Specification to support subsequent program phases.

In addition to engineering effort, the study also included one manufacturing task. A full-scale prototype beam segment, reflecting the selected structural concept, was designed and built.

Study output includes both summary documentation and recommendations for follow-on activities.

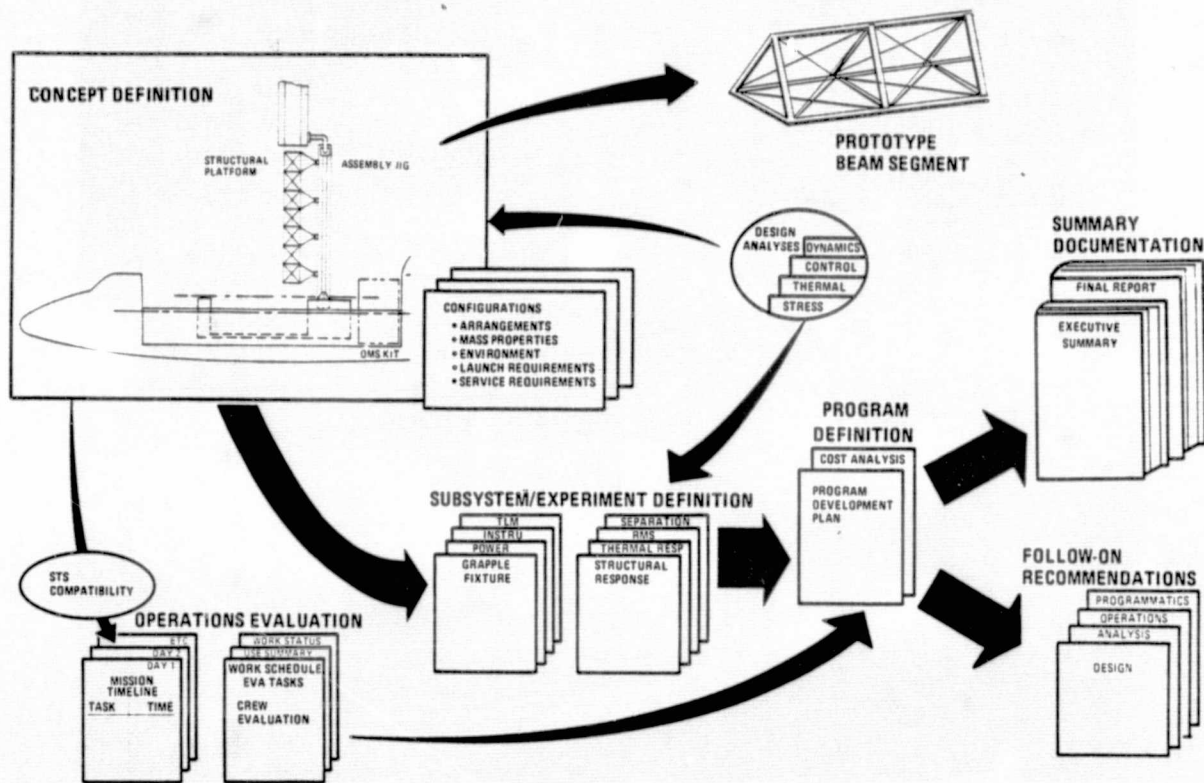


Figure 1-2. Study approach - Part II.

Comprehensive task descriptions, input/output requirements, detailed study logic diagrams, schedules, study organization, and task participation by technical disciplines are summarized in Study Plans submitted at the start of Parts I and II.

1.3 SUMMARY

The baseline SCAFE system concept is shown in Figure 1-3. In mid-1982, fabrication/assembly systems, prepackaged raw materials, and experiment systems are delivered by the Space Shuttle to a 556 km circular orbit.

Upon system deployment from the stowed position, a beam-builder, moving to successive positions along an Orbiter-attached assembly jig, automatically fabricates four triangular beams, each 200 meters long. Retention of the completed beams is provided by the assembly jig.

The beam builder then moves to the position shown and fabricates the first of nine shorter, but otherwise identical, cross-beams. After cross-beam attachment, the partially completed assembly is automatically transported across the face of the assembly jig to the next cross-beam location, where another cross-beam is fabricated and installed. This process repeats until the "ladder" platform assembly is complete. During this process, an opportunity to develop/evaluate EVA is provided by the difficult-to-automate task of sensor/equipment attachment, as shown.

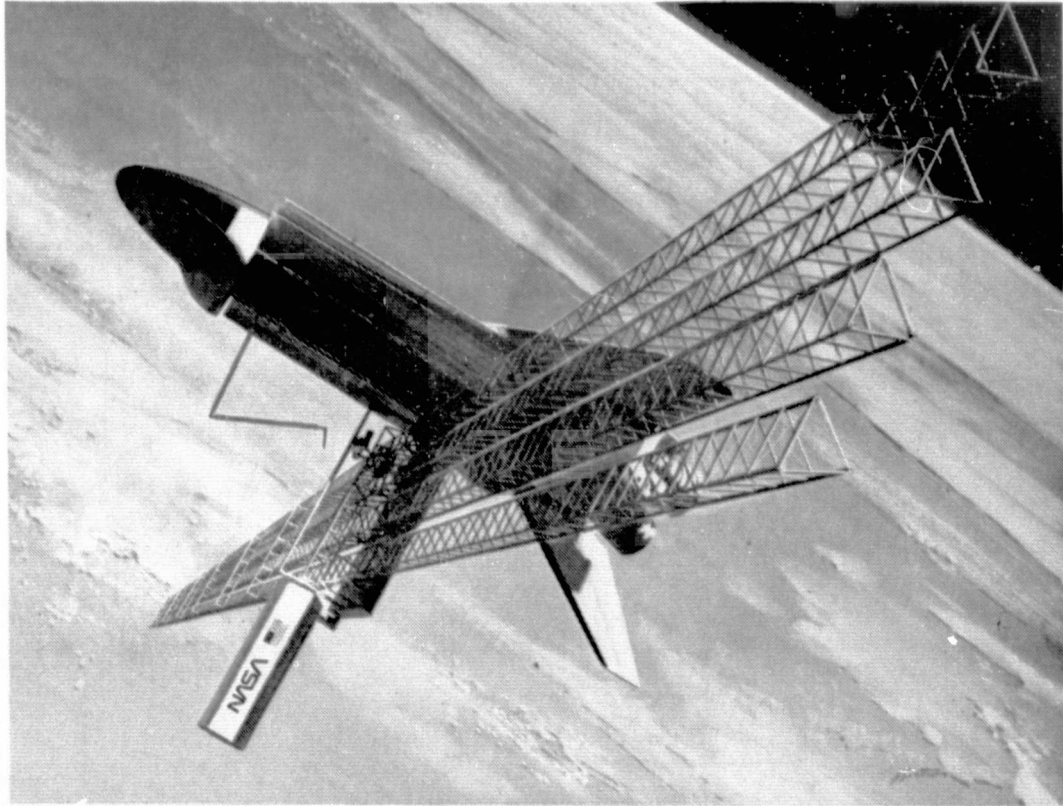


Figure 1-3. Baseline system concept.

Upon platform assembly completion, both structural and thermal response tests are conducted and RMS/platform release/recapture techniques are developed, completing the seven-day mission cycle.

Details supporting the SCAFE system concept development are discussed in the body of this volume. The presentation has been grouped by topic and discipline, rather than by individual study task, to avoid fragmenting the treatment of effort in specific disciplines.

2

SYSTEM DESIGN

Conceptual and preliminary design studies were conducted in the areas of structures/materials, mechanisms, and avionics in order to evaluate both the SCAFE platform and various alternative concepts, and to define the associated fabrication equipment. The following sections summarize this design activity.

2.1 STRUCTURE/MATERIALS

Structural design concentrated on development of a recommended experiment platform incorporating the preferred beam concept in turn selected as a result of an integrated beam/beam builder trade study.

Parallel materials evaluations led to selection of: (1) a laminate material providing desirable structural, thermal, and processing characteristics; (2) a continuous cord material for beam diagonals; and (3) an integral coating suitable for the SCAFE mission. An additional study identified and compared alternative platform concepts with the baseline arrangement. Each of these activities is discussed in the following sections.

2.1.1 BASELINE PLATFORM

2.1.1.1 Selected Concept. The selected platform concept is illustrated in Figure 2-1. The 4×9 beam "ladder" arrangement is virtually identical to the baseline arrangement adopted at Study ATP which, in turn, was similar to the NASA-JSC in-house concept provided in the SCAFEDS RFP. Specific evolutionary changes and their justification are discussed in later paragraphs.

Platform width is limited to approximately the cross-beam dimension shown to permit inter-beam assembly using a simple tilt-up Orbiter-mounted jig whose length, in turn, is constrained by available Orbiter cargo bay length. Details of the assembly jig and its installation within the Orbiter are discussed in Sections 2.2.2 and 3.7.2, respectively.

No firm requirement drives platform length or beam quantity. The practical upper limit on total beam length achievable in the platform assembly results from limitations on beam builder material storage canister diameter imposed by both the cargo bay envelope and the beam builder/assembly jig stowage concept. Ultimately, platform length and beam arrangement may be driven by selected post-separation platform uses.

Platform longitudinal and cross beams are identical in size, construction, bay spacing, and detail element characteristics. As also shown in Figure 2-1, they differ only in the number of bays: each longitudinal beam comprises 139 identical bays plus an allowance at each end for cutoff by the beam builder; each cross-beam comprises 7 bays plus identical end cutoff allowances.

Figure 2-2 illustrates the typical beam bay and end cutoff. Each beam consists of three continuous cap members, equally spaced upright cross members, and continuous diagonal cord cross-bracing, with joints accomplished by ultrasonic welding. Overall beam dimensions have been reduced somewhat during study execution as discussed below. This beam construction concept was selected as a result of a compound trade study which considered several beam concepts and the characteristics of their corresponding beam builders.

Structural properties for the beam and its elements have been developed for use in supporting analyses and are given in Section 4.4

The beam cap section is shown in Figure 2-3. The 60° apex angle is dictated by the selected equilateral beam concept, which permits the three cap sections to be identical. (Cap section congruence is not a requirement for automated fabrication, however, but is indicated for this initial experiment program to minimize development costs.) The use of the open cross-section simplifies two automated beam builder operations (cap forming and cap/cross-member joining) with a possible sacrifice in maximum compressive load capability when compared with a similar closed cross-section. However, the selected section exhibits a large margin of safety with respect to conservative loads, developed from analyses discussed in Sections 4.2 and 4.3, and applied in Section 4.4. The side flats accommodate cross-member and diagonal cord attachment and are stabilized by the adjacent lips. The relatively generous radii reflect the results of a detailed stability evaluation of the open section, also reported in Section 4.4. The cap section is formed, by the beam builder rolltrusion process, from a continuous pre-consolidated hybrid-material flat strip laminate.

The specific laminate consists of outer layers of style 120 glass cloth with three plies of predominately unidirectional pitch graphite fabric between. Selection of this laminate resulted from a comprehensive trade study reported in Section 2.1.2.

The beam cross-member section is presented in Figure 2-4. The side flares are provided to enhance packaging in the beam builder clip feed system. (See Section 2.2.1.) Base width is selected to accommodate the spotweld pattern at the cross-member/cap joint, while small corner radii are used to minimize cross section developed length. Flat sides are used for simplicity and exhibit adequate margin of safety for conservatively developed loads, as reported in Section 4.4, in spite of their one-edge-free configuration. Added capability is achievable, if desired, by incorporation of stabilizing lips. Future effort should consider this revision in view of both increased structural capability and possible improvement of the clip feed system. Cross members use a hybrid laminate similar to the cap section, but requiring only two inner graphite fabric plies to provide sufficient strength and stability.

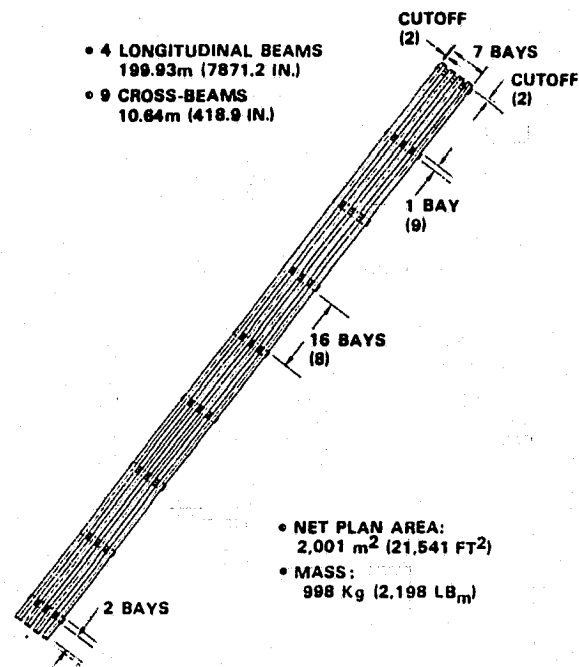


Figure 2-1. Selected platform.

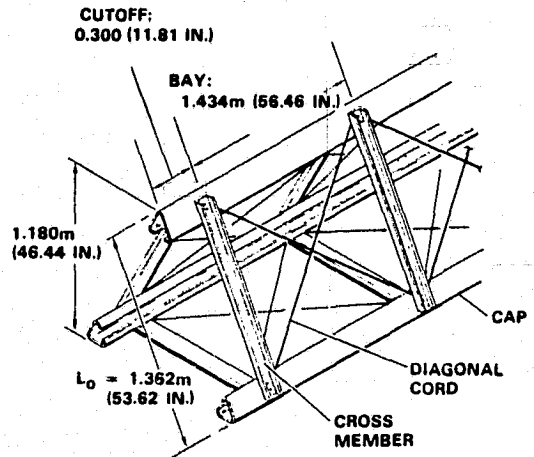


Figure 2-2. Typical beam.

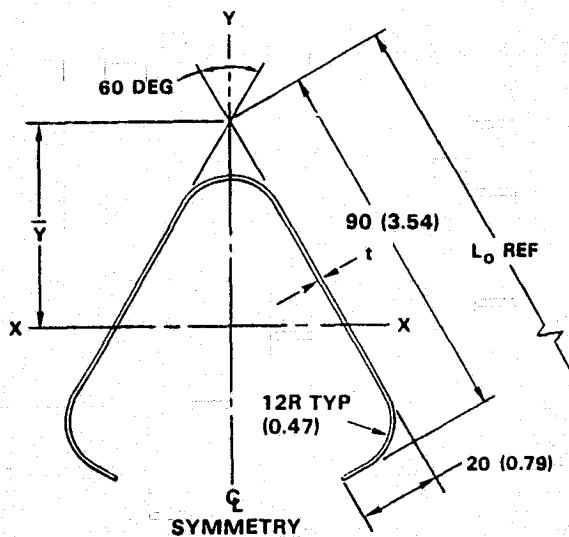


Figure 2-3. Cap section.

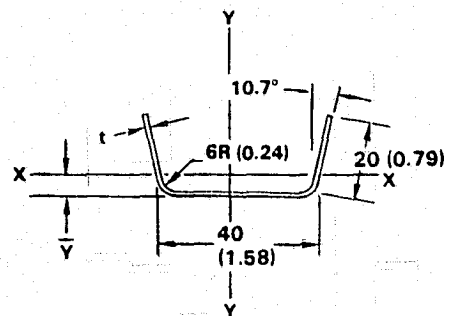


Figure 2-4. Cross-member section.

cated an improved envelope for the pattern as shown, as opposed to the prior pattern with the cord capture spot nearest the end of the cross-member.

2.1.1.2 Platform Configuration Development. The original platform structure, shown in Figure 2-6, reflects an earlier NASA-developed reference configuration, with slight dimensional changes which resulted from interacting studies of the beam, beam builder, and assembly jig, as influenced by one another and by the Orbiter interfaces and orbital environment. The NASA reference configuration employed a beam cross-section slant height of 1.50 m and an identical bay spacing. During the proposal period the development of cross-member and weld pattern geometries necessitated a somewhat smaller beam side than bay spacing to permit the orthogonal long-/cross-beam platform joints without interference between elements of interfacing beams. In addition, evaluation of cargo bay diameter influence on available assembly jig width, and allowance for retention/translation of the longitudinal beams throughout fabrication, assembly, and later platform positioning resulted in a bay spacing reduction to 1.434 m. Further, provisions for cutoff of completed beams added a small increment at the ends of all beams. The given dimensions resulted, and were adopted as the study baseline until Part II detailed design activity necessitated further beam size reductions as discussed below.

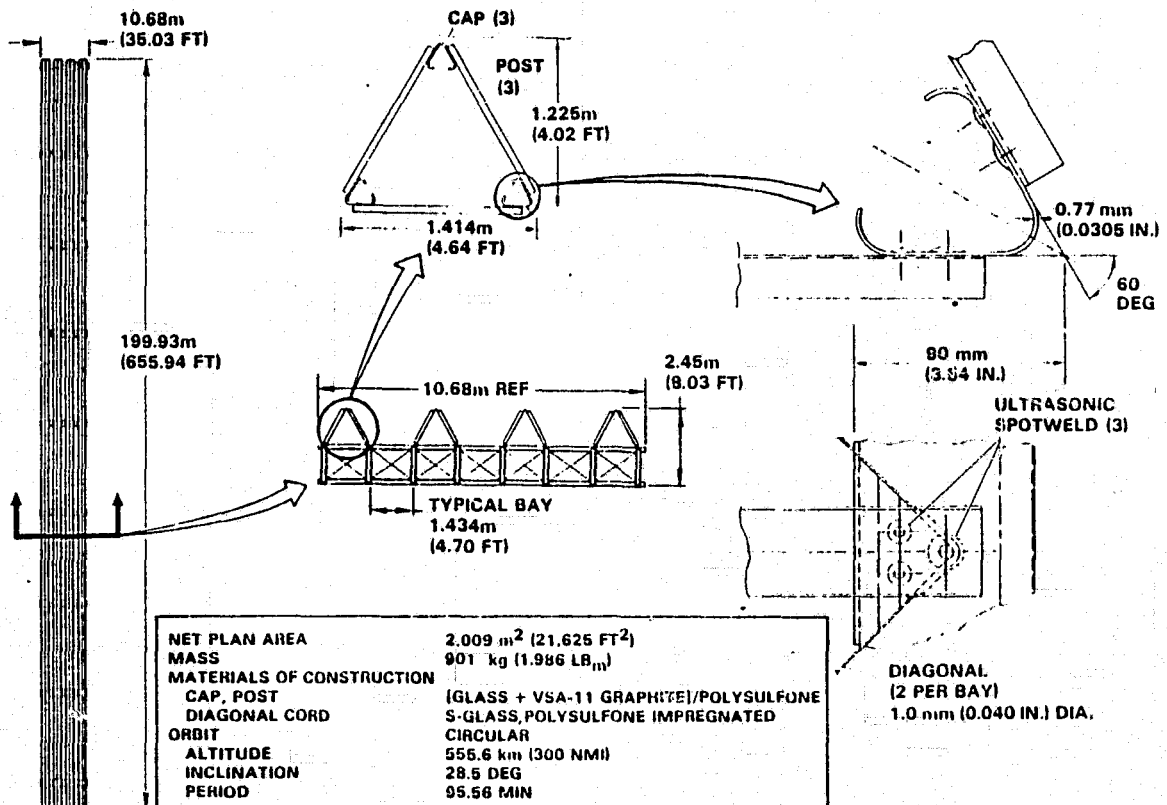


Figure 2-6. Original platform structure concept.

From the discussion above, assembly jig/Orbiter bay compatibility, assembly jig retention/translation of longitudinal beams, and element clearances at beam-to-beam joints were the primary considerations in initial selection of bay spacing and beam size. The previous values were reassessed and refined somewhat to reflect Part II design and analysis of assembly and handling provisions.

As illustrated in Figure 2-7, the preferred Orbiter stowage technique suggests a 4.343 m maximum working surface width to provide 5 cm cargo bay envelope clearance for the 0.523-m deep assembly jig.

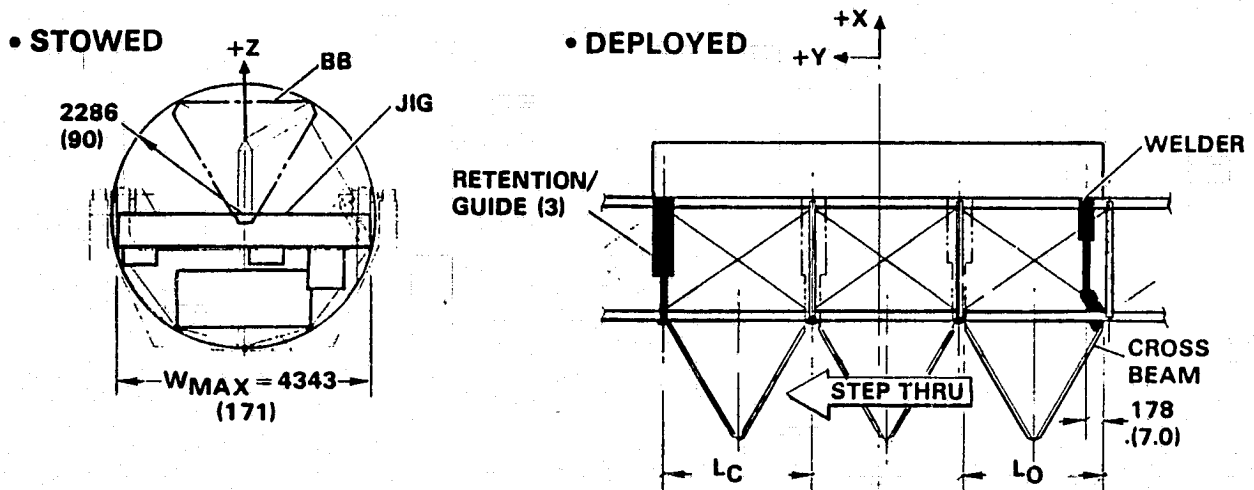


Figure 2-7. Cargo bay and assembly jig geometry constraints.

On the deployed jig, permissible beam bay spacing (L_C) and overall beam mold line width (L_O) are influenced by both size and location limits of the guide/retention system (19 cm dia base) and the cross-beam attachment welders (15.2 cm dia base). Also, in the interest of system simplification, an objective of Part II was to eliminate, if possible, the "flip-out" portion of the assembly jig concept selected at the end of Part I. (See Section 2.2.2.5 for discussion of the assembly jig concept trade study.) This was achievable if two issues were met throughout the cross-beam "step-thru" process: (1) can three guide/retention devices be provided within the basic jig width, such that moment-carrying beam-support can be achieved by any two; and (2) will the resulting support spans sustain the predicted loads?

In resolving the first issue, the problem, illustrated in Figure 2-8, is to determine the condition governing the minimum clearance between a cross-beam cap and either the assembly jig retention/guide roller or the adjacent longitudinal beam post in its worst-tolerance position. In conjunction with the assembly jig detail predesign (Section 2.2.2) a retention/guide roller design was developed. Its position on the crown of the longitudinal beam cap, and its clearance, Δ_2 , from the cross beam elements are shown in Figure 2-8. A value of 12.5 mm was selected for Δ_2 to ensure positive clearance in conjunction with the dynamic start/stop sequence associated with the step-through process.

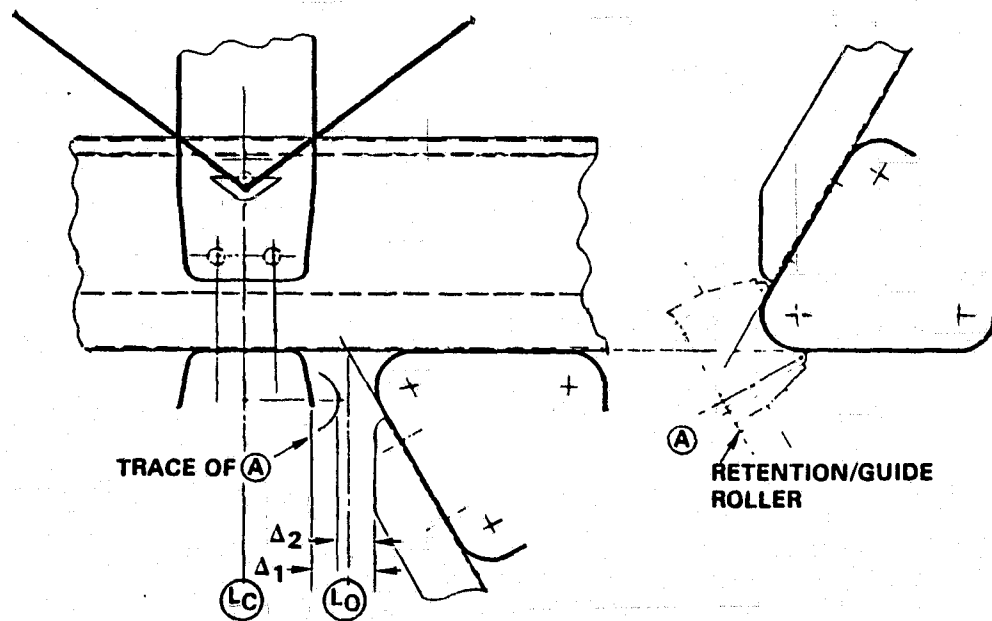


Figure 2-8. Local clearance concerns at beam intersection.

A value for Δ_1 was developed from a detailed study of tolerances on beam and beam element sizes, cross-member spacing (L_C), and beam-to-beam spacing. Figures 2-9, 2-10, and 2-11 illustrate the pertinent geometrical features. The driving consideration is the sensitivity of the permissive range of the dimension i (i.e., $i_{\max} - i_{\min}$) to the controlling local dimensions and their tolerances. For example, in Figure 2-10, permissible i_{\max} (a_{\max} in this case) to avoid interference is determined by setting δ_1 and δ_4 to zero and taking worst case tolerances on the contributing dimensions:

$$a_{\max} = 3 L_{C_{\min}} - W_{\max} - L_{T_{\max}}$$

From similar considerations over several bays, the following general relationship was developed:

$$i_{\max} - i_{\min} = 2 [(L_C - W - L_T) - (\overline{W} + \overline{L_T} + N \overline{L_C})]$$

in which \overline{W} , $\overline{L_T}$, and $\overline{L_C}$ are the tolerances on the associated dimensions and N is the number of bays within the span i . This expression indicates that the beam-to-beam locating tolerances in the transverse direction (i.e., considering spacing between longitudinal beams) are very sensitive to $\overline{L_C}$. This is important, since the beams are dimensioned from a common datum, as shown in Figure 2-9. In the longitudinal direction, $i_{\max} - i_{\min}$ becomes very large (since $N_{\max} = 137$), even for very small L_C , if the cross-beams are also dimensioned from a common datum. However, there is no requirement to datum-dimension the cross-beams, since by providing a post-locating sensor in the beam drive system, each cross-beam can be located solely with respect to the adjacent posts in the adjoining longitudinal beams, without regard to other cross-beam locations.

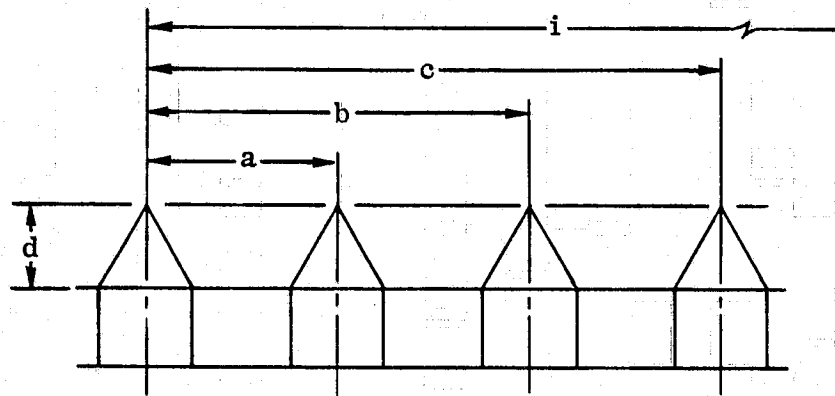


Figure 2-9. Platform overall transverse geometry.

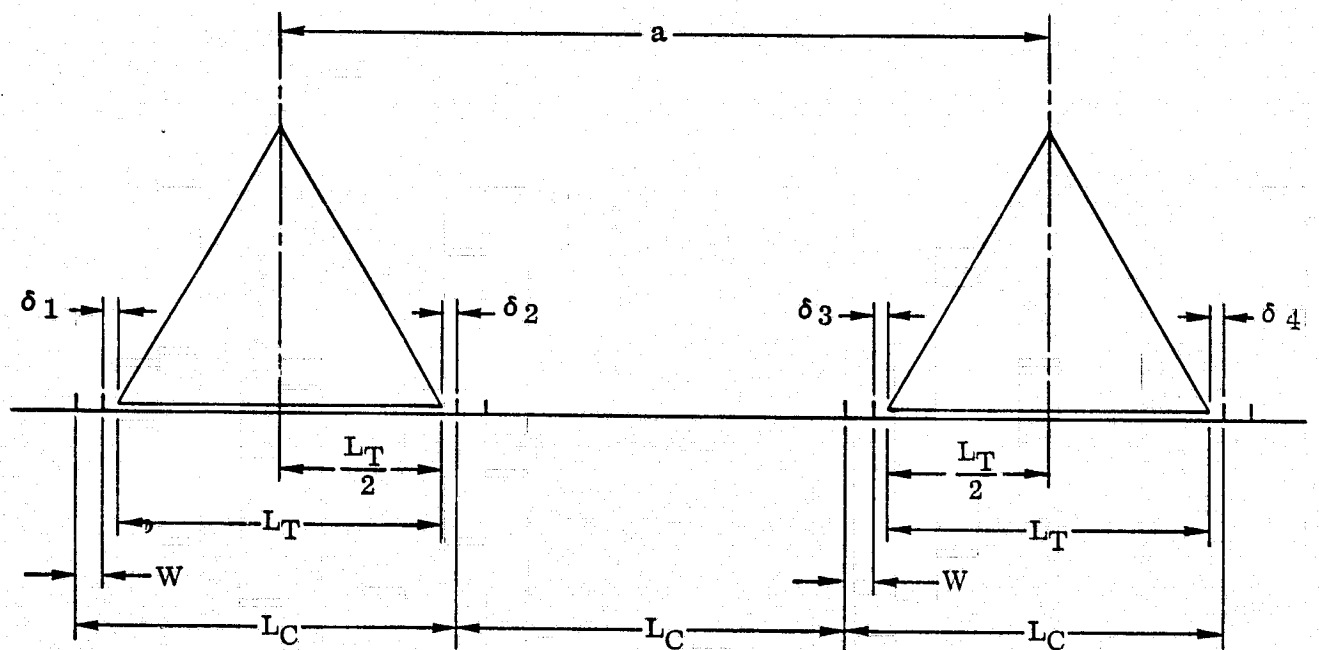


Figure 2-10. Assembly geometry with tolerance considerations.

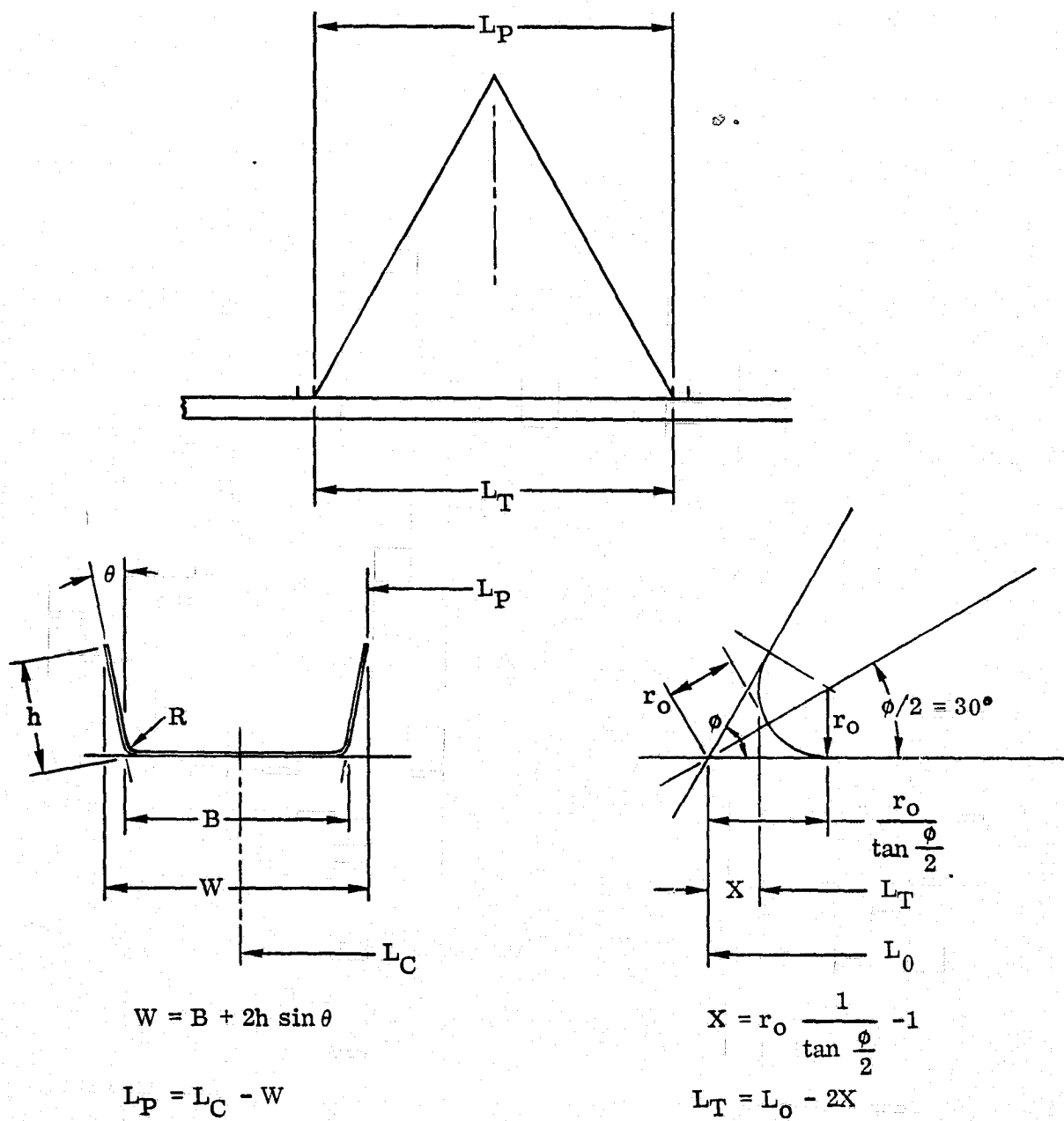


Figure 2-11. Local element geometry considerations.

Selecting appropriate tolerances is principally a matter of judgement based on prior experience, and the following values were chosen for the reasons noted:

- \bar{W} = 0.060 cm (0.025 in): typical for similar formed metallic parts.
- \bar{L}_T = 0.030 cm (0.012 in): typical for precision-located machine elements such as beam builder cooling platens and weld station elements which dictate relative cap positions.

$\overline{L}_c = 0.025 \text{ cm (0.010 in)}$: normally considered very tight for located parts, but readily achievable using the beam builder differential drive straightness-control provisions (Section 2.2.3.2).

$i_{\max} - i_{\min} = 0.025 \text{ N cm (0.010 N in)}$: similar to \overline{L}_T .

Furthermore, from Figure 2-11:

$$W = 4.74 \text{ cm}$$

$$L_T = 139.54 \text{ cm (for } L_O = 141.4 \text{ cm)}$$

Then, by rearranging the above general relationship:

$$\begin{aligned} L_c &= \frac{i_{\max} - i_{\min}}{2} + W + L_T + \overline{W} + \overline{L}_T + N\overline{L}_c \\ &= \frac{0.025 \text{ N}}{2} + 4.74 + 139.54 + 0.06 + 0.03 + 0.025 \text{ N} \\ &= \frac{3}{2} (0.025 \text{ N}) + 144.37 \end{aligned}$$

For the worst case in the transverse direction, $N = 6$ ($i = c$, Figure 2-9), and:

$$L_c = 144.60 \text{ cm}$$

Also, from Figure 2-10:

$$\begin{aligned} \Delta_1 &= \frac{1}{2} (L_c - L_T - W) \\ &= \frac{144.60 - 139.54 - 4.74}{2} = 0.16 \text{ cm} \end{aligned}$$

In the longitudinal direction, the equation for L_c can be modified for two reasons:

- a. Since datum dimensioning is not required, the term in i can be deleted.
- b. It is highly unlikely that one longitudinal beam would be fabricated with all maximum length bays and another with all minimum length bays (the condition indicated by the $N\overline{L}_c$ term). A more reasonable approach would be to RSS the bay length variation in which case the last term becomes:

$$\sqrt{N\overline{L}_c^2} = \sqrt{N} \overline{L}_c$$

and:

$$\begin{aligned} L_C &= W + L_T + \bar{W} + \bar{L}_T + N \bar{L}_C \\ &= 4.74 + 139.54 + 0.06 + 0.03 + \sqrt{137} (0.025) \\ &= 144.66 \text{ cm} \end{aligned}$$

Then:

$$\Delta_1 = \frac{144.66 - 139.54 - 4.74}{2} = 0.20 \text{ cm}$$

In either case, Δ_1 is considerably smaller than Δ_2 , which, therefore, governs cross-beam clearance requirements as summarized in Table 2-1. Although not governing relative beam dimensions in this case, the tolerance study highlights the accuracy with which large, lightweight beams can be fabricated and assembled for other applications where high precision is required.

Table 2-1. Governing gap Δ .

Condition	Value	Use
Δ_1 (Cross)	1.6 (0.063)	
Δ_1 (Longit)	2.0 (0.077)	
Δ_2	12.5 (0.49)	✓

Also, from Figure 2-7, the following relation between bay spacing, L_C , and assembly jig width, W_j , exists:

$$W_j = 3 L_{C_{\max}} + 9.5 - 17.8 + 7.6 = 3 L_{C_{\max}} - 0.7 = 434.3$$

From which:

$$L_{C_{\max}} = \frac{434.3 + 0.7}{3} = 145.0 \text{ cm}$$

From the layout on which Figure 2-8 is based plus the relationships in Figure 2-11:

$$\begin{aligned} L_T &= L_C - 9.1 \\ L_O - L_T &= 1.9 \text{ cm} \end{aligned}$$

Then

$$\begin{aligned} L_O &= L_T + 1.9 \\ &= L_C - 9.1 + 1.9 \\ &= L_C - 7.2 \end{aligned}$$

ORIGINAL PAGE IS
OF POOR QUALITY

and:

$$\begin{aligned}L_{O_{\max}} &= L_{C_{\max}} - 7.2 \\ &= 145.0 - 7.2 \\ &= 137.8\end{aligned}$$

But $L_{C_{\max}}$ only slightly exceeds the original value:

$$\Delta L_C = 145.0 - 143.4 = 1.6 \text{ cm (0.63 in)}$$

However, to change would have required revision of prior developed models/data based on the original L_C , without any apparent benefit. Consequently, the baseline 1.434 m (56.46 inch) bay spacing was retained and the beam size, L_O , reduced as required to reflect the governing roller/beam clearance gap, Δ_2 .

The resulting beam size is:

$$L_O = 143.4 - 7.2 = 136.2 \text{ cm}$$

2.1.1.3 Beam Configuration Development. The basic beam structural concept was chosen as the result of a trade study investigating both a series of beam concept options and the characteristics of the beam builders required by each. The beam builder portion of this compound trade is reported in Section 2.2.1.

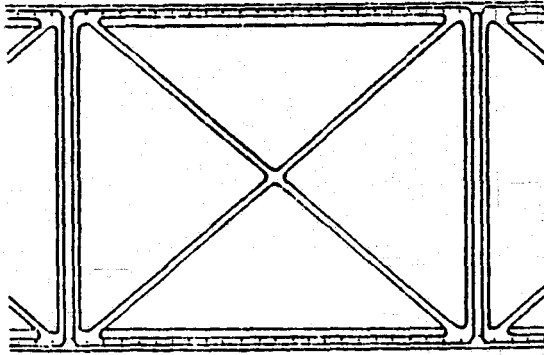
Three basic structural concepts have been found applicable to lightweight triangular truss beam construction: (1) single piece precut side panels, (2) rigid posts with tension-only diagonals, and (3) rigid posts/diagonal bracing. Due to variations within each of these concept families, a total of seven specific beam designs was identified and conceptual design layouts prepared for each.

The overall beam builder concept was influenced differently by each of the seven options. However, major machine differences were associated with families rather than individual options, except that tension-only diagonals may either zig-zag along each beam side or wrap spirally about the beam perimeter, resulting two distinctly different machine options. Consequently, the four structural concepts shown in Figure 2-12 were traded against one another and also used to develop beam builder concepts.

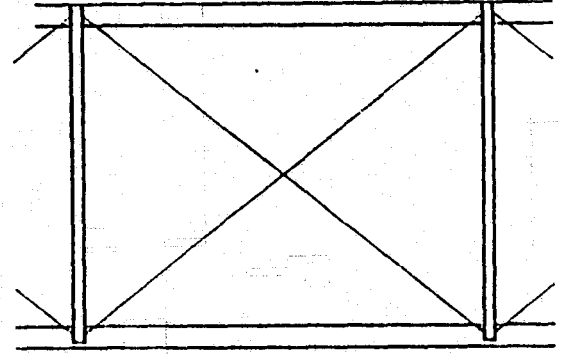
Concept 1 integrates the vertical posts (initially flat), the diagonal tension members, and nonstructural longitudinal connecting strips into one continuous, preconsolidated sheet, which is precut on the ground. Post cross-section is achieved by forming on-orbit. The diagonals sustain tension loads only, yet cannot be preloaded. Consequently, a potentially undesirable shear stiffness loss occurs in the neutral (i.e., undeflected) beam position. It is also the heaviest of the four systems, weighing 1.5 kg/m,

due largely to layup requirements in the precut webs to provide fibers in the various element directions. In addition, the horizontal strips would require a large number of closely spaced spotwelds to develop them as effective cap material. Since this would increase beam builder mechanical complexity with limited structural benefit, the strips act as parasitic non-structural material.

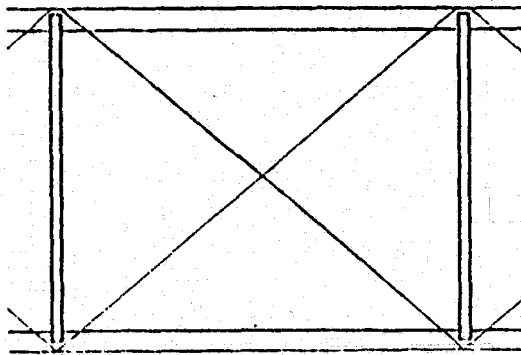
• CONCEPT 1: PRECUT SIDE PANELS



• CONCEPT 2: ZIG-ZAG CORD DIAGONALS



• CONCEPT 3: SPIRAL WOUND DIAGONALS



• CONCEPT 4: RIGID BRACING

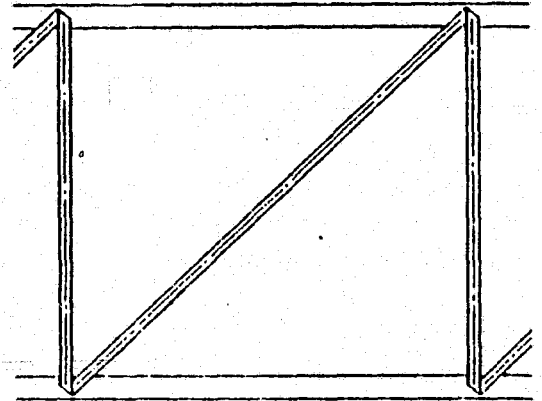


Figure 2-12. Beam construction concepts.

Concepts 2 and 3 are very attractive structurally since, due to the extremely low shear stress intensity induced in the beam, the shear-carrying capability can be met with small-diameter tension cords. The cords can be preloaded during beam fabrication to provide constant shear stiffness regardless of beam position. These systems are lightest, 1.0 kg/m, since they avoid the parasitic longitudinal strips of Concept 1 and the diagonal cross-section required for compressive stability in Concept 4.

Concept 4 is the simplest structural system, in which minimal cross-section tension diagonals are replaced by a single heavier compression-critical member in each bay. Consequently, beam weight increases to 1.4 kg/m. A potential advantage accrues from the opportunity to use the same cross-section for all side bracing.

The four beam candidates were evaluated in terms of unit weight, beam size scale-up potential, and structural performance as shown in Table 2-2. Concept 1 was promptly rejected since: (1) it is heaviest; (2) both its weight (which influences transportation

costs) and the fixed width of the precut roll-on web limit its scale-up to larger or varied beam sizes; and (3) the inability to preload the diagonals limits beam behavior predictability due to the shear stiffness non-linearity. From a structural point of view, Concepts 2 and 3 are virtually identical, although Concept 3 may permit a simpler cord/cap joint but will also require the cap transverse fibers to transmit loads in the diagonals into the posts. Concept 4 performs well (provided the diagonals don't "spiral" around the beam in successive bays, in which case a beam torsional weakness occurs), is heavy, and scale-up compatibility is somewhat constrained by the fairly rapid weight growth in the diagonals to retain stability as single span beam columns as their span increases.

Table 2-2. Beam concept evaluation.

Concept	Structure		
	Weight	Scale-Up	Performance
1	15	Poor	?
2	10	Good	✓
3	10	Good	✓
4	14	Fair	✓

The cap geometry has remained virtually constant throughout the study with one exception: bend radii were reduced from 15 mm to 12 mm to help reduce thermal energy requirements for forming and to enhance cross-section stability in response to a preliminary analysis reported in Section 4.4. It was found, in a later analysis, that a decrease in radius reduces cross-section stability, hence, the radius reduction was perhaps unnecessary for structural reasons. However, the later analysis used the 12 mm radius section as one reference configuration and determined a large margin of safety under conservative loads. Consequently, cap radius increase is presently unwarranted.

The post (cross-member) geometry has evolved from vertical sides to flared sides of first 7.5° and finally 10.7°. This resulted from the mid-study elimination of cross-member on-orbit forming in favor of a clip feed system dispensing preformed elements. The side flares permit "nesting" of posts in the clip, thereby minimizing clip length and weight. Initially, posts and caps used the same laminate (two glass fabric plies sandwiching three graphite fabric plies). However, once preliminary loads were developed, it was found that a satisfactory margin of safety could be maintained if one graphite ply was omitted from the post laminate, and the design was revised accordingly. As noted above in Section 2.1.1.1, a potential future post cross-section change might involve the addition of lips on the sides to both increase structural capability and possibly simplify the beam builder clip feed system.

The cross-member/cap joint detail was also revised during the study. The initial design used a spotweld pattern in which the cord capture spot was circular and was located nearest the end of the post, as shown in Figure 2-6. A subsequent assembly jig welder access study, reported above and illustrated in Figure 2-5, showed that placing the cord capture spot furthest from the post end improved welder clearances. In addition, a non-circular cross-section was developed for the cord capture spot (also shown in Figure 2-5) to minimize spot size (and welder weight and power) while still providing sufficient capture length to fully develop the diagonal cords.

Laminates for both the caps and cross-members were revised from the original (0/±60) pseudo-isotropic all-graphite fiber system to the hybrid glass fabric/graphite fabric system mentioned above as a result of a trade study and supporting thermal analysis, reported in Sections 2.1.2 and 4.5, respectively.

Element and overall beam stiffnesses and mass properties have evolved throughout the study and are discussed in Section 4.4 and 4.1, respectively.

2.1.2 MATERIALS

2.1.2.1 Laminate Evaluation/Selection. A materials evaluation/selection trade-off study was performed to determine the proper laminate material for the SCAFEDS program application.

- a. Procedure. The flow chart shown in Figure 2-13 is a summary of the procedure followed for the materials evaluation effort. The chart traces the history of the analysis and, therefore, forms an outline for the materials evaluation section of this report.
- b. Fiber Candidates. The representative graphite fibers were chosen from the four general classes of fibers as shown in Table 2-3. The purpose of this was to restrict the number of candidates and yet be able to generalize the results across the spectrum of graphite fibers. The fibers chosen are the ones most commonly used at Convair. Table 2-4 gives the fiber properties used in this study.
- c. Raw Material. The form of the raw material is also a major consideration in evaluating candidate materials. As the flow chart shows, three forms were considered, standard unidirectional tape layups, single ply "woven" fabrics, and tube construction. The tape layups can be either all graphite material or a hybrid of graphite and glass in a resin matrix. All-glass is not a consideration for this study because of its low stiffness and high coefficient of thermal expansion (CTE). Typical tape material is 19.05 cm wide and extremely long. With these dimensions and in light of manufacturing considerations, a laminate in the form of $(\pm 0, \theta)_s$ may not be practical, and only $(0^\circ, 90^\circ)$ type layups may be possible. For this study though, cross plies at angles were considered.

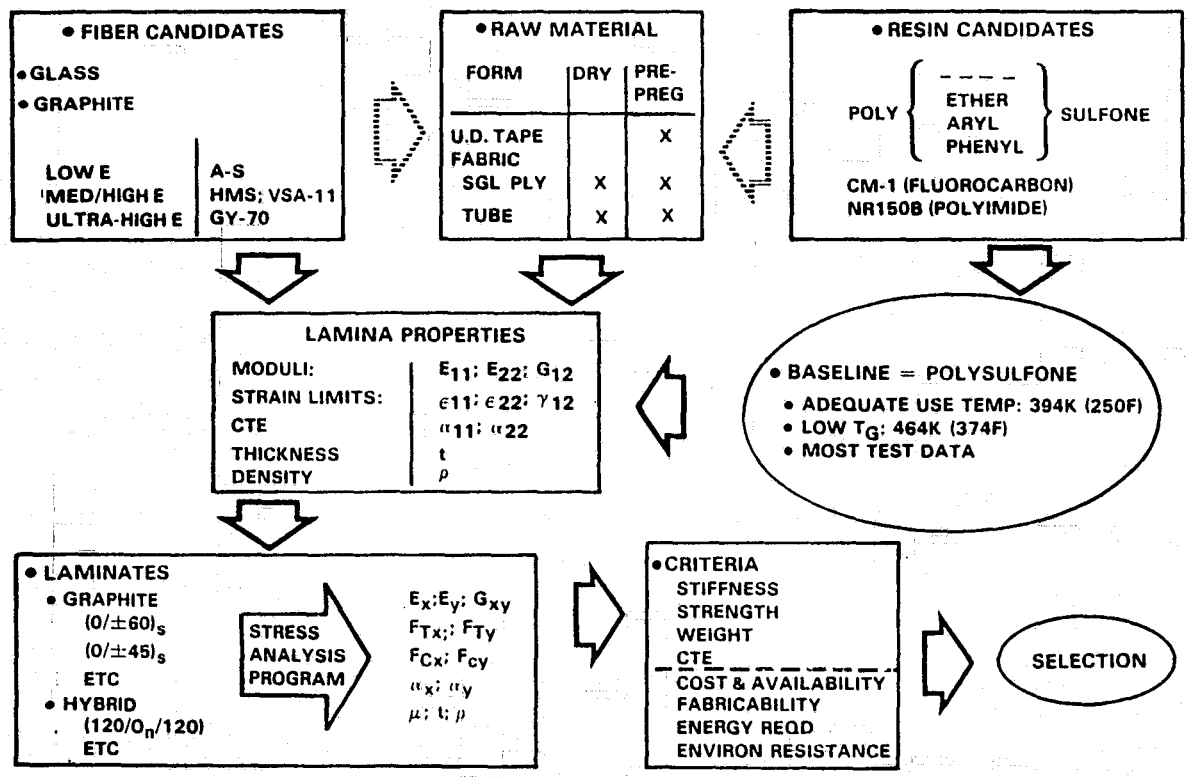


Figure 2-13. Flow chart of materials evaluation effort.

Table 2-3. Fiber candidates.

Low Modulus, Low to Ultra High Strength	Medium Modulus, High Strength	High Modulus, Medium Strength	Ultra High Modulus, Medium Strength
Hercules Type A-S*	Hercules HT-S	Hercules HM-S*	Celanese Celion GY-70*
Stackpole Panex 30/A	Courtaulds HT-S	Courtaulds HM-S	Thornel 75
Courtaulds Type A	Morganite II	Morganite I	
Morganite Type III	Modmor Type II*	Modmor Type I	
Union Carbide Thornel* 300	Fortafil 4-T	Fortafil 5-T	
Great Lakes Fortafil 3-T	Polycarbon T	Fortafil 6-T	
Thornel 400		Thornel 50	
Polycarbon A		Hitco HMG-50	
Celion 3000		Polycarbon M	
Celion 6000		Thornel VSA-11*	
		Stackpole Panex 50	

ORIGINAL PAGE IS OF POOR QUALITY

* Chosen candidate fibers

Table 2-4. Typical values for graphite fiber properties used for study.

Fiber	F_{tu} (GN/m ²)	E_t (GN/m ²)	α_x ($\mu\text{m}/\text{m}/\text{K}$)	ρ (Kg/m ³)
AS*	2689	193	-0.90	1811.4
T300	2413 (0.96) [†]	221	-0.90	1755.7
Modmor II	2758 (0.78)	276	-0.90	1755.7
HMS	2344 (0.65)	359	-1.098	1895.0
VSA-11	1207 (0.65)	345	-1.08	2006.5
GY-70	1724 (0.67)	490	-1.127	1978.6

*Values not used because unidirectional test data for AS/P-1700 are available.

[†]Tensile allowables shown for fibers were used to compute lamina tensile allowables by rule-of-mixtures. The lamina tensile allowables were then reduced by the factor shown in parentheses. The reduction factor is an efficiency factor for that fiber in a matrix derived by comparing test values versus theoretical values for various fiber/epoxy systems.

A disadvantage of the unidirectional tape layups is the possibility of a delamination occurring during the heating/forming process (assuming use of a thermoplastic resin). The single ply "woven" fabric and tube construction would eliminate the delamination problem by making a single ply to the required thickness by weaving tows of the proper diameter. At the present time, it is not clear whether anything but a (0°/90°) type weave would be possible to manufacture for a single ply made in the flat. It would be possible to mix fiber types, graphite and glass as an example, in almost any fiber volume distribution to achieve the desired stiffness and CTE requirements. A significant amount of material testing would be required to verify analytical predictions for woven fabrics.

Similar to the flat woven fabric concept is weaving the material in a tube or "sock". This method allows a cross ply orientation other than 90° and is within the present state of the art. The tube material after weaving can either be slit along the length and opened up to form a single ply or flattened and bonded together to form a two ply system.

- d. Resin Candidates. Initially both epoxy and thermoplastic resins were considered as candidates for large space structures. As the design of the beam builder evolved, the use of a thermoplastic resin became a necessity because of the use of heat forming in space and joining of parts by ultrasonic welding. The use of thermoplastics also allows all curing to be done on the ground while the use of epoxy in space would result in undesirable outgassing of volatiles during curing. Epoxy resins cannot be heated and formed like the thermoplastics.

Table 2-5 lists the thermoplastic resin candidates considered. Polysulfone (P-1700) was chosen for this study because it has the lowest glass transition temperature along with an acceptable working temperature. Polysulfone also has the most test data available in graphite composites. Table 2-6 gives the typical properties for polysulfone used for this study.

Table 2-5. Thermoplastic resin candidates.

Resin	T _G °K (°F)	Use Temp °K (°F)
Polysulfone	464 (374)	381 (225)
Polyethersulfone	506 (450)	422 (300)
CM-1 (fluorocarbon)	492 (425)	478 (400)*
NR 150B (polyimide)	622 (660)	589 (600)
Polyphenylsulfone	485 (413)	TBD

*The crystalline structure of CM-1 allows use to a higher percentage of T_G.

The question of outgassing of graphite/thermoplastic composition was answered when samples of Type A-S/P1700 were submitted to NASA-MSFC by Convair in 1975 and tested to the requirements of the ATM Specification 50-MO-2442. The samples were heated to 373°K in a vacuum and any outgassing products were collected. No outgassing products were collected from the A-S/P1700 samples and, thus, the material is considered acceptable for space applications by NASA-MSFC.

- e. Lamina Properties. As the flow chart in Figure 2-13 shows, with the selection of fiber candidates, raw material form, and resin the lamina properties were derived. The rule-of-mixture formulas, test data, and representative graphite/epoxy values were used in preparation of the lamina properties. Table 2-7 is a summary of the estimated material properties of the representative graphite/polysulfone laminae chosen for this study. The data are in a form that is used by the SQ5 program to predict laminate properties, except they are converted to SI units to satisfy NASA requirements. All of the lamina properties were normalized to a 57% fiber volume. This is a typical state-of-the-art value for polysulfone. The values listed for AS/P1700 are actual test data. (Ref. University of Dayton Research Institute, "Mechanical Property Data AS/3004 Graphite/Polysulfone Composite," Air Force Materials Laboratory, Contract F33615-75-C-5085, November, 1976.)

Table 2-6. Typical properties of polysulfone.

Property	P1700
General	
Density, kg/m ³	1240
Mechanical	
Tensile Strength at Yield, GN/m ²	0.0703
Tensile Modulus, GN/m ²	2.482
Tensile Elongation at Break, %	50 to 100
Flexural Strength, GN/m ²	0.1062
Flexural Modulus, GN/m ²	2.689
Izod Impact at 295°K, N-m/cm	0.694
Rockwell Hardness	R120
Thermal	
Heat Distortion Temperature at 1820 kN/m ² , °K	447
Coefficient of Linear Thermal Expansion, m/m/°K	5.58×10^{-5}
Thermal Conductivity, watts/m-°K, Flammability	0.26 Non-burning
Electrical	
Dielectric Strength, V/mil	425
Volume Resistivity, 295°K, ohm-cm	5×10^{16}
Dielectric Constant, 295°K, 60 Hz to 1 MHz	3.07 to 3.03
Dissipation Factor, 295°K, 60 Hz to 1 MHz	0.0008 to 0.0034

Reference, "Investigation of Reinforced Thermoplastics for Naval Aircraft Structural Applications," Boeing Aerospace Co., Report No. D180-17531-1, May 1973, Contract N00019-72-C-0526.

The material properties listed in Table 2-7 for glass/polysulfone fabrics are values taken from MIL-HDBK-17 for glass/epoxy fabrics. The glass fabric Style 104 was chosen because it is a minimum gage fabric, just enough to hold a hybrid laminate together. The glass fabric Style 120 was chosen because it has an intermediate thickness with equal properties in the warp and fill directions. The glass fabric Style 143 was chosen for its high stiffness in the warp direction for applications where high stiffnesses are required.

Table 2-7. Estimated lamina properties.

Property	UD Graphite @ 57% Fiber Volume						Glass Fabric			Woven
	AS/P-1700	HMS/P-1700	T300/P-1700	GY-70/P-1700	VSA-11/P-1700	MODII/P-1700	104 Glass	120 Glass	143 Glass	VSA-11 (W-705)
E_{11} (GN/m ²)	112.4	205.5	131.0	279.9	197.9	158.6	20.0	18.1	32.5	187.5
E_{22} (GN/m ²)	7.93	5.72	5.72	5.72	5.72	5.72	11.03	17.86	13.51	6.00
G_{12} (GN/m ²)	3.86	5.86	5.52	6.55	5.86	4.90	6.21	4.00	4.07	6.89
ν_{12}	0.34	0.20	0.30	0.294	0.20	0.33	0.15	0.15	0.15	0.25
α_{11} ($\mu\text{m}/\text{m}/^\circ\text{K}$)	-0.0108	-0.8028	-0.450	-0.9108	-0.7722	-0.5184	10.98	9.9	9.9	-0.756
α_{22} ($\mu\text{m}/\text{m}/^\circ\text{K}$)	30.60	28.80	28.80	30.24	28.80	28.80	17.28	12.06	12.06	27.00
ϵ_{11}^c ($\mu\text{m}/\text{m}$)	-5896	-4300	-7750	-2350	-2265	-7740	-12000	-17110	-12712	-2265
ϵ_{22}^c ($\mu\text{m}/\text{m}$)	-11813	-12290	-12300	-12290	-12290	-12290	-8455	-16833	-13418	-11724
ϵ_{11}^t ($\mu\text{m}/\text{m}$)	11534	4300	7750	2350	2265	7740	11000	17110	18008	2265
ϵ_{22}^t ($\mu\text{m}/\text{m}$)	4348	5300	5300	5285	5285	5285	7750	16872	5204	5434
ϵ_{12} ($\mu\text{m}/\text{m}$)	28571	13000	14500	10500	11800	10990	23000	20345	13322	15000
μ (cm)	0.0127	0.0127	0.0127	0.0127	0.0144	0.0127	0.0025	0.0102	0.0203	0.0191
ρ (KG/m ³)	1522.4	1605.4	1522.4	1660.8	1660.8	1522.4	2020.6	2020.6	2020.6	1688.5

The rule-of-mixtures expressions used are:

$$E_{11} = E_f V_f^{\circ} + E_m V_m^{\circ}$$

$$E_{22} = \frac{1}{\frac{V_f^{\circ}}{E_f} + \frac{V_m^{\circ}}{E_m}}$$

$$\alpha_{11} = \frac{E_f \alpha_f V_f^{\circ} + E_m \alpha_m V_m^{\circ}}{E_f V_f^{\circ} + E_m V_m^{\circ}}$$

$$F_{11} = F_f V_f^{\circ} + F_m V_m^{\circ}$$

$$F_{22} = F_m V_m^{\circ}$$

$$\rho = \rho_f V_f^{\circ} + \rho_m V_m^{\circ}$$

Subscript:

f = FIBER

M = MATRIX

V[°] = % by VOLUME

E = ELASTIC MODULUS

α = Coefficient of Thermal Expansion, CTE

F = STRENGTH

ρ = DENSITY

The other values were estimated from equivalent graphite/epoxy properties.

As stated earlier, the material properties listed in Table 2-7 are analytical predictions; but, for design tradeoffs, the values show the proper trend or relationship between the candidates even though the values are probably not correct. The final material selection should be well characterized by test.

- f. Laminate Analysis. The next step in the material evaluation is the laminate analysis. Two general criteria exist for large space structures, high stiffness applications and/or low CTE applications. For a first cut at appropriate laminate configurations to satisfy these criteria, three thickness ranges per criterion were picked:

$$T_1 \quad 0.0381 \text{ to } 0.0508 \text{ cm}$$

$$T_2 \quad 0.0635 \text{ to } 0.0762 \text{ cm}$$

$$T_3 \quad 0.1016 \text{ to } 0.1270 \text{ cm}$$

For the laminate study the number of graphite fiber candidates was reduced to four. T-300 was dropped because it is similar to AS and test data for AS/P1700 exists. Modmor II was also eliminated because its medium stiffness, high strength characteristics were not required. Both VSA-11 (pitch) and HMS were retained even though they have similar properties because they are, at this time, of different thickness, and availability of VSA-11 in large amounts is not known.

Table 2-8 has three basic composite configurations. The layup of unidirectional tape is the common configuration used in the industry today. The hybrid laminate consists of unidirectional graphite tape in the middle with either 104, 120, or 143 woven glass fabric on the outside "to hold the laminate together." The woven fabric represents the single ply fabric or tube construction. The values shown in the brackets are the percentages of fibers in the (0°, ±45, 90°) directions. At the time this chart was prepared it was felt cross plies at angles were not within practical manufacturing technology for such large quantities.

The woven fabrics can be made in an almost infinite combination of fiber percentages in warp and fill directions plus mixing of fiber types. Picking a few examples, as in this table, does not truly represent the possibilities. It was suggested by the composites group to reduce the stiffnesses for the woven fabrics by 10% and increase the CTEs by 10% because of the "weaviness" of the fibers in the fabric.

The laminate analysis SQ5 computer program was used to calculate laminate material properties. Tables 2-9, 2-10, and 2-11 present the results of these runs. The allowable stresses (F_x and F_y) show both tension and compression values.

In the tables the laminates are labelled as being either one designed for high stiffness, STF, or one designed for low coefficient of thermal expansion, CTE.

In addition to the laminates listed in Table 2-8, several more (the Hybrids) were analyzed and are listed at the end of Table 2-10. These entries include the hybrids where the graphite laminas are actually a woven fabric, W-705, consisting of 95% VSA-11 (pitch) in the warp direction and 5% glass in the fill direction. This form of composite prepreg is apparently preferred over the conventional unidirectional tapes by the prepreg suppliers because of its easier handling characteristics. The cost of the woven fabric is also projected to be lower than the unidirectional tape.

Also in this group of laminates at the end of Table 2-10 are two laminates where the 120 glass laminas are rotated 45° to the warp directional in an attempt to increase the shear modulus. This gave a 25% increase in the shear modulus of the laminate but also increased the CTE in the X-direction significantly.

Also, in addition to the laminate candidates listed in Table 2-8, the pseudo-isotropic layups for AS, HMS, VSA-11, and GY-70 were run with the results shown in Table 2-12.

Table 2-8. Candidate laminates.

Graphite Fiber	Criteria	Gage	Tape	Hybrid	Woven (0°/45°/90°) %
AS	STIFF	1	(+15) _s	(104/0 ₃ /104)	(80/0/20)
		2	(+20/0)	(120/0 ₄ /120)	
		3	(+30/0 ₂) _s	(120/0 ₇ /120)	
	CTE	1	(0/90/0) _T	(120/0 ₂ /120)	(70/0/30)
		2	(0 ₂ /90)	(143/0 ₂ /143)	
		3	(0 ₃ /90) _s	(143/0 ₅ /143)	
HMS	STIFF	1	(+15) _s	(104/0 ₃ /104)	(80/0/20)
		2	(+20/0)	(120/0 ₄ /120)	
		3	(+30/0 ₂) _s	(120/0 ₇ /120)	
	CTE	1	(0/90/0) _T	(120/0 ₂ /120)	(60/0/40)
		2	(0 ₂ /90)	(143/0 ₂ /143)	
		3	(0 ₃ /90) _s	(143/0 ₅ /143)	
VSA-11	STIFF	1	(0/90/0) _T	(104/0 ₃ /104)	(80/0/20)
		2	(+15) _s	(120/0 ₂ /120)	
		3	(0 ₂ /90) _s	(120/0 ₄ /120)	
	CTE	1	(0/90/0) _T	(120/0/120)	(60/0/40)
		2	(0/90) _s	(143/0 ₂ /143)	
		3	(0/90/0) _s	(143/0 ₃ /143)	
GY-70	STIFF	1	(+15) _s	(104/0 ₃ /104)	(80/0/20)
		2	(+20/0)	(120/0 ₄ /120)	
		3	(+30/0 ₂) _s	(120/0 ₇ /120)	
	CTE	1	(0/90/0) _T	(120/0 ₂ /120)	(50/0/50)
		2	(+60/0)	(143/0 ₂ /143)	
		3	(0 ₂ /90) _s	(143/0 ₅ /143)	

GAGES
 1. 0.0381 - 0.0508 CM
 2. 0.0635 - 0.0762 CM
 3. 0.1016 - 0.1270 CM

g. Laminate Selection. With the laminate data generated and tabulated, a final selection of laminates for the triangular beam can be made based upon a set of criteria as shown in Figure 2-13. High stiffness, low cost, low CTE, availability, and good fabricability were the primary selection criteria with strength, weight, and environmental resistance playing a lesser role in the selection. A trade study of the energy requirements during the forming process of the cap played an important role in the final selection of a laminate. The detailed analysis of the heat transfer within the laminate (Section 4.5.1) shows the hybrid laminates were best suited for local heating and forming because there is little transverse heat transfer in the laminate.

Since the proposal called for a pseudoisotropic layup of graphite/polysulfone with a thickness of 6 plies, or 0.0762 cm, the final selected laminate thickness was also chosen to be in the 0.0762 cm range. The information on thinner and thicker laminates will be valuable for other applications.

Table 2-9. Laminate properties/unidirection tape (57% fiber volume).

Laminate Description	E_X GN/m ²	E_Y GN/m ²	ν	G GN/m ²	α_X m/m/°K	α_Y m/m/°K	F_X^T 10 ⁶ N/m ²	F_X^C 10 ⁶ N/m ²	F_Y^T 10 ⁶ N/m ²	F_Y^C 10 ⁶ N/m ²	F_s 10 ⁶ N/m ²	t cm	kg/m ³
AS(+15) _s - STF	90.74	8.00	0.100	10.14	-1.6164	28.2960	1206.59	-444.03	37.23	-101.35	176.51	0.0508	1605.
AS(+20/0) _s - STF	88.18	8.34	0.100	10.76	-1.6524	26.6760	1006.64	-369.56	36.54	-98.60	197.88	0.0762	1605.
AS(+30/0) _{2s} - STF	78.19	10.14	0.100	13.31	-1.6542	20.8080	896.32	-328.88	44.13	-119.28	180.64	0.1016	1605.
AS(0/90/0) _T - CTE	78.05	43.02	0.060	3.86	1.5912	4.3200	339.22	-459.88	186.85	-253.73	110.32	0.0381	1605.
AS(0 ₂ /90) _s - CTE	78.05	43.02	0.060	3.86	1.5912	4.3200	339.22	-459.88	186.85	-253.04	110.32	0.0762	1605.
AS(0 ₃ /90) _s - CTE	86.74	34.47	0.080	3.86	1.2276	5.8500	337.15	-511.59	148.93	-202.02	110.32	0.1016	1605.
HMS(+15) _s - STF	159.06	6.62	1.700	17.44	-2.2446	22.9860	834.27	-556.41	37.92	-87.56	219.94	0.0508	1605.
HMS(+20/0) _s - STF	154.58	7.45	1.630	18.62	-2.1942	20.0880	664.66	-501.94	39.30	-91.70	203.40	0.0762	1605.
HMS(+30/0) _{2s} - STF	137.41	11.24	1.390	23.24	-1.9800	12.2940	590.88	-522.63	59.30	-137.90	230.98	0.1016	1605.
HMS(0,90,0) _T - CTE	139.00	72.40	0.016	5.86	-0.2484	0.9072	597.78	-597.78	310.96	-310.96	64.12	0.0381	1605.
HMS(0 ₂ /90) _s - CTE	139.00	72.40	0.016	5.86	-0.2484	0.9072	597.78	-597.78	310.96	-310.96	64.12	0.0762	1605.
HMS(0 ₃ /90) _s - CTE	155.68	55.71	0.021	5.86	-0.3852	1.6236	669.49	-669.49	239.94	-239.94	64.12	0.1016	1605.
VSA-11(0/90/0) _T - STF	133.97	69.84	0.016	5.86	-0.1988	0.9972	303.37	-303.37	157.89	-157.89	68.95	0.0610	1661.
VSA-11(+15) _s - STF	153.96	6.62	1.640	16.96	-2.2014	22.9950	423.34	-423.34	37.92	-87.56	153.75	0.0813	1661.
VSA-11(0 ₂ /90) _s - STF	133.97	69.84	0.016	5.86	-0.1980	0.9972	303.37	-303.37	157.89	-157.89	68.95	0.1219	1661.
VSA-11(0/90) _s - CTE	101.91	101.91	0.011	5.86	0.2142	0.2142	230.98	-230.98	230.98	-230.98	68.95	0.0813	1661.
VSA-11(0/90/0) _s - CTE	121.14	82.67	0.014	5.86	-0.0581	0.6120	274.41	-274.41	187.54	-187.54	68.95	0.1016	1661.
GY-70(+15) _s - STF	207.19	6.83	2.190	22.61	-2.4138	23.3910	619.15	-619.15	38.61	-90.32	212.36	0.0508	1661.
GY-70(+20/0) _s - STF	201.81	7.93	2.040	24.20	-2.3076	19.7298	474.36	-474.36	42.06	-97.22	177.20	0.0762	1661.
GY-70(+30/0) _{2s} - STF	180.64	13.03	1.610	30.61	-1.9818	10.9782	424.72	-424.72	68.95	-159.96	166.16	0.1016	1661.
GY-70(0/90/0) _T - CTE	188.85	97.29	0.017	6.55	-0.4230	0.4842	444.03	-444.03	228.91	-228.91	68.95	0.0381	1661.
GY-70(+60,0) _s - CTE	100.73	100.73	0.300	38.61	-0.1134	-0.1134	236.49	-236.49	350.95	-350.95	186.85	0.0762	1661.
GY-70(0 ₂ /90/0) _{2s} - CTE	143.07	143.07	0.012	6.55	-11.2662	-11.2662	336.47	-336.47	336.47	-336.47	68.95	0.1016	1661.

2-24

ORIGINAL PAGE IS
OF POOR QUALITY

Table 2-10. Laminate properties/hybrid (57% fiber volume).

Laminate Description	F_X GN/m ²	E_Y GN/m ²	ν	G GN/m ²	α_X m/m/°K	α_Y m/m/°K	F_X^T 10 ⁶ N/m ²	F_X^C 10 ⁶ N/m ²	F_Y^T 10 ⁶ N/m ²	F_Y^C 10 ⁶ N/m ²	F_s 10 ⁶ N/m ²	t cm	kg/m ³
AS(104/0 ₃ /104) _T - STF	101.56	8.27	0.310	4.14	0.2682	28.6740	1116.96	-598.47	35.85	-68.95	95.15	0.0432	1661.
AS(120/0 ₄ /120) _T - STF	85.56	10.82	0.250	3.93	0.6930	22.2840	985.96	-504.70	46.88	-128.24	111.70	0.0711	1716.
AS(120/0 ₇ /120) _T - STF	94.94	9.86	0.270	3.86	0.4176	24.6240	1094.89	-559.86	42.75	-115.83	111.01	0.1092	1688.
AS(120/0 ₂ /120) _T - CTE	70.60	12.48	0.220	3.93	1.2528	19.3032	813.59	-416.45	54.47	-146.86	112.39	0.0457	1799.
AS(143/0 ₃ /143) _T - CTE	71.29	10.82	0.220	4.00	2.4390	19.0620	820.48	-419.89	27.10	-128.24	113.07	0.0787	1827.
AS(143/0 ₅ /143) _T - CTE	81.29	10.14	0.240	3.93	1.6380	21.2940	937.69	-479.19	44.13	-119.28	112.39	0.1041	1772.
HMS(104/0 ₃ /104) _T - STF	183.68	6.34	0.190	5.93	-0.6498	26.7588	792.90	-792.90	33.78	-53.78	64.12	0.0432	1661.
HMS(120/0 ₄ /120) _T - STF	151.96	9.31	0.170	5.31	-0.4266	20.2536	652.94	-652.94	48.95	-114.45	57.92	0.0711	1716.
HMS(120/0 ₇ /120) _T - STF	170.65	8.07	0.180	5.52	-0.5832	21.6000	730.85	-730.85	42.75	-98.60	59.98	0.1092	1688.
HMS(120/0 ₂ /120) _T - CTE	122.24	11.24	0.160	5.03	-0.0828	17.8110	525.38	-525.38	59.98	-138.59	55.16	0.0457	1799.
HMS(143/0 ₂ /143) _T - CTE	99.08	10.55	0.160	4.76	1.3752	16.4628	426.10	-426.10	55.85	-129.62	51.71	0.0660	1799.
HMS(143/0 ₅ /143) _T - CTE	137.96	8.83	0.170	5.17	0.1944	19.4922	592.95	-592.95	46.88	-108.25	56.54	0.1041	1772.
VSA-11(104/0 ₂ /104) _T - STF	178.09	6.34	0.190	5.93	-0.6228	26.8596	403.35	-403.35	33.10	-53.78	69.64	0.0457	1799.
VSA-11(120/0 ₃ /120) _T - STF	152.93	8.83	0.170	5.38	-0.4446	20.9448	346.81	-346.81	46.88	-108.94	63.43	0.0813	1799.
VSA-11(120/0 ₄ /120) _T - STF	161.89	8.20	0.180	5.52	-0.5238	22.0428	366.80	-366.80	43.44	-101.35	64.81	0.1016	1772.
VSA-11(120/0/120) _T - CTE	108.04	11.93	0.160	4.96	0.1386	17.1288	244.77	-244.77	63.43	-146.86	57.92	0.0406	1855.
VSA-11(143/0 ₂ /143) _T - CTE	108.04	11.93	0.160	4.96	0.1386	17.1288	260.62	-260.62	51.02	-118.59	58.61	0.0813	1855.
VSA-11(143/0 ₃ /143) _T - CTE	131.76	8.89	0.170	5.17	0.2952	19.3320	298.54	-298.54	46.88	-108.94	60.67	0.1016	1799.
GY-70(104/0 ₃ /104) _T - STF	249.38	6.34	0.260	6.48	-0.7920	27.9036	586.06	-586.06	33.78	-53.78	68.26	0.0432	1716.
GY-70(120/0 ₄ /120) _T - STF	205.19	9.31	0.210	5.79	-0.6120	20.8980	481.95	-481.95	48.95	-114.45	61.36	0.0711	1772.
GY-70(120/0 ₇ /120) _T - STF	231.25	8.07	0.230	6.07	-0.7326	23.2200	543.31	-543.31	42.75	-98.60	64.12	0.1092	1744.
GY-70(120/0 ₂ /120) _T - CTE	163.61	11.31	0.190	5.45	-0.3456	18.2394	384.73	-384.73	59.30	-138.59	56.54	0.0457	1827.
GY-70(143/0 ₂ /143) _T - CTE	127.76	10.55	0.180	5.03	0.8172	16.8156	299.92	-299.92	55.85	-129.62	52.40	0.0660	1882.
GY-70(143/0 ₅ /143) _T - CTE	183.40	8.83	0.210	5.58	-0.1350	20.0844	430.93	-430.93	46.20	-108.25	58.61	0.1041	1799.
HMS(120 _{45°} /0 ₄ /120 _{45°}) _T	150.24	8.20	0.330	6.41	-0.5868	22.4190	646.04	-646.04	43.44	-100.66	70.33	0.0711	1716.
VSA-11(120/0 ₂ /120) _T	137.96	9.86	0.170	5.24	-0.2916	19.4166	312.33	-312.33	52.40	-121.35	60.67	0.0610	1799.
VSA-11(120 _{45°} /0 ₂ /120 _{45°}) _T	135.90	8.62	0.340	6.55	0.4878	21.6918	308.20	-308.20	45.51	-105.49	77.22	0.0610	1799.
VSA-11(120/W-705 ₂ /120) _T	128.66	10.27	0.190	5.86	-0.2088	18.6462	291.65	-291.65	55.85	-119.97	88.25	0.0584	1799.
VSA-11(120/W-705 ₃ /120) _T	143.14	9.17	0.200	6.14	-0.3798	19.9998	323.37	-323.37	50.33	-107.53	91.70	0.0775	1772.

2-25

Table 2-11. Laminate properties/woven (%0/%±45/%90) (57% fiber volume).

Laminate Description	E_X GN/m ²	E_Y GN/m ²	ν	G GN/m ²	α_X m/m/°K	α_Y m/m/°K	F_X^T 10 ⁶ N/m ²	F_X^C 10 ⁶ N/m ²	F_Y^T 10 ⁶ N/m ²	F_Y^C 10 ⁶ N/m ²	F_S 10 ⁶ N/m ²	t cm	kg/m ³
AS(80/0/20) - STF	82.74	26.20	0.090	3.45	1.1340	7.9200	954.93	-954.93	301.30	99.29	-301.30	0.0508	0.1016
AS(70/0/30) - CTE	73.08	35.85	0.070	3.45	1.5840	5.3280	846.68	-846.68	410.24	99.29	-410.24	0.0508	0.1016
HMS(80/0/20) - STF	148.93	41.37	0.030	5.31	-0.5040	2.5380	641.22	-641.22	177.20	60.67	-177.20	0.0508	0.1016
HMS(60/0/40) - CTE	113.07	77.22	0.010	5.31	-0.1260	0.5940	492.98	-492.98	331.64	60.67	-331.64	0.0508	0.1016
VSA-11(80/0/20) - STF	143.41	39.99	0.030	5.31	-0.4500	2.6820	325.43	-325.43	90.32	62.05	-90.32	0.0508	0.1016
VSA-11(60/0/40) - CTE	108.94	74.46	0.010	5.31	-0.0720	0.6660	246.83	-246.08	168.92	62.05	-168.92	0.0508	0.1016
GY-70(80/0/20) - STF	202.71	54.47	0.030	5.93	-0.6480	1.7640	476.43	-476.43	128.24	62.05	-128.24	0.0508	0.1016
GY-70(50/0/50) - STF	128.93	130.31	0.010	5.93	-0.1260	-0.1260	302.68	-302.68	302.68	62.05	-302.68	0.0508	0.1016

NOTE: Stiffness reduced by 10% (Also allowable Stress)
CTE increased by 10%

2-26

Table 2-12. Laminate properties/tape (pseudoisotropic) (±60,0)_S (57% fiber volume).

Laminate Description	E_X GN/m ²	E_Y GN/m ²	ν	G GN/m ²	α_X m/m/°K	α_Y m/m/°K	F_X^T 10 ⁶ N/m ²	F_X^C 10 ⁶ N/m ²	F_Y^T 10 ⁶ N/m ²	F_Y^C 10 ⁶ N/m ²	F_S 10 ⁶ N/m ²	t cm	kg/m ³
AS(±60/0) _S	43.23	43.23	0.320	16.48	2.5758	2.5758	280.61	-255.10	188.22	-380.59	223.39	0.0762	1605.
HMS(±60/0) _S	75.29	75.29	0.300	29.09	0.1494	0.1494	324.05	-324.05	399.20	-479.18	288.89	0.0762	1605.
VSA-11(±60,0) _S	72.80	72.80	0.290	28.13	0.2142	0.2142	164.78	-164.78	243.38	-243.38	146.85	0.1219	1661.
GY-70(±60,0) _S	100.73	100.73	0.300	38.61	-0.1134	-0.1134	236.49	-236.49	350.94	-350.94	209.60	0.0762	1661.

Table 2-13 is a summary of the candidate laminates resulting from scanning the tables laminate properties. The pseudoisotropic candidates were retained because of their choice in the proposal. The GY-70 ($\pm 60/0$)_S was used as a baseline for analysis in the proposal. The HMS layup is shown here because it probably is cheaper, although it does not exhibit as good properties as GY-70. The pitch pseudoisotropic layup is also shown but it is too thick for this application (0.12192 cm).

In general, the selected HMS, VSA-11 (pitch) laminates have similar properties, with the pitch fiber possibly having lower cost. However, since the pitch fiber is relatively new and not as well characterized, the HMS laminates were retained for further evaluation.

The hybrid laminates, glass and graphite, exhibit high longitudinal stiffness and relatively low CTEs but also exhibit low shear and transverse moduli and strength which may make the joints of caps and side posts critical. The low shear modulus also raises the questions of low cap torsional stability. Further analysis showed that the above mentioned concerns were not a problem because of the low loads in the structure (see Section 4.4).

When such large amounts of material are involved as in this application, cost becomes a critical item. In general, the fibers in the PAN family with the highest stiffnesses, such as GY-70, are the most expensive. Recently, the pitch fibers VSA-11 and now VSB-32T have been developed that combine the high stiffness and low cost.

The VSB-32T is a higher strength pitch fiber than the VSA-11 but with the same stiffness. The VSA-11 fiber was used for this tradeoff because VSB-32T had not yet become widely available and tested. The hybrids are attractive from the cost standpoint because the glass is much cheaper than graphite for providing transverse strength and stiffness.

Thus, the hybrid combination of graphite and glass, specifically, VSA-11 and 120 glass was chosen as the preferred material for the SCAFE program. This combination provided the high axial stiffness, low CTE, adequate strength, low energy consumption during forming, and lower cost. Currently the caps are designed to be made of VSA-11 (120/W-705₃/120), $t = 0.07747$ cm and the cross-member posts are VSA-11 (120/W-705₃/120), $t = 0.05842$ cm.

2.1.2.2 Cord Material. Selection of a cord material for the beam diagonals was based on considering the desired characteristics summarized below.

- Low Preload Required
 - Sufficient Strength
- Low $E \alpha$

—————→ { 445N Applied
22N Preload
22N Preload Tolerance
22N Thermal

—————→ 511 N × 2.0 Min = 1022N

Table 2-13. Laminate properties/summary of candidate laminates (57% fiber volume).

Laminate Description	E_X GN/m ²	E_Y GN/m ²	ν	G GN/m ²	α_X m/m/°K	α_Y m/m/°K	F_X^T 10 ⁶ N/m ²	F_X^C 10 ⁶ N/m ²	F_Y^T 10 ⁶ N/m ²	F_Y^C 10 ⁶ N/m ²	F_s 10 ⁶ N/m ²	t cm	kg/m ³
HMS(0 ₂ /90) _B	139.00	72.40	0.016	5.86	-0.248	0.907	597.78	-597.88	310.96	-310.96	64.12	0.0762	1605.
HMS(±60/0) _B	75.29	75.29	0.300	29.10	0.149	0.149	324.06	-324.06	399.21	-479.19	288.89	0.0762	1605.
VSA11(±60/0) _B	72.81	72.81	0.290	28.13	0.214	0.214	164.79	-164.79	243.39	-243.39	146.86	0.1219	1661.
GY-70(±60/0) _B	100.73	100.73	0.300	38.61	-0.113	-0.113	236.49	-236.49	350.95	-350.95	209.60	0.0762	1661.
VSA11(0/90/0) _T	133.97	69.84	0.016	5.86	-0.198	0.997	303.37	-303.37	157.89	-157.89	68.95	0.0610	1661.
HMS(120/0 ₄ /120) _T	151.96	9.31	0.170	5.31	-0.427	20.254	652.94	-652.94	48.95	-114.45	57.92	0.0711	1716.
VSA11(120/0 ₂ /120) _T	137.96	9.86	0.170	5.24	-0.292	19.417	312.33	-312.33	52.40	-121.35	60.67	0.0610	1799.
VSA11(120/0 ₃ /120) _T	152.93	8.83	0.170	5.38	-0.445	20.945	346.81	-346.81	46.88	-108.94	63.43	0.0813	1799.
VSA11(120/W705 ₂ /120)	128.66	10.27	0.190	5.86	-0.209	18.646	291.65	-291.65	55.85	-119.97	88.25	0.0584	1799.
VSA11(120/W705 ₃ /120)	143.14	9.17	0.200	6.14	-0.380	20.000	323.37	-323.37	50.33	-107.56	91.70	0.0775	1772.

2-28

ORIGINAL PAGE IS
OF POOR QUALITY

- Preload Retention → Resin impregnate, cure
- Compatible with Welding → Thermoplastic resin, withstand temperature
- Compact Storage → High ϵ_{TU}
- Compatible with Environment → Radiation Resistant

The preference for low preload helps minimize the total required cord strength, thereby minimizing cord cross-sectional area and enhancing the cord capture joint simplicity/reliability through the associated cord diameter reduction. Sufficient cord strength is desirable, not only for the obvious reason of assuring positive safety margin under design loads but also to minimize the sustained stress due to preload to prevent creep and consequent loss of preload. (Note that a low ratio of preload to maximum design load is desirable for this reason, further justifying the preference for low preload.) Development of maximum applied load and preload requirements is discussed in Section 4.4.

To assure cord dimensional stability and eliminate inter-fiber slip and relaxation, resin impregnation and ground cure are required. The particular choice of resin is nominally open to thermosets as well as thermoplastics. However, the nature of the direct cord capture joint concept suggests thermoplastic resin to permit cord flattening during welding (to minimize the local cap/post surface gap) and to contribute additional resin to the joint. Compatibility with the welding process also influences cord selection, since the fiber material must be compatible with the peak temperatures occurring in the joint area during welding. The required cord storage volume is a function of the minimum radius to which the cured cord can be coiled for long periods of time without creep or fracture. A similar problem occurs in laminate storage, as thicknesses increase. Derivation of the governing relationship, driven by the ultimate tensile strain, ϵ_{TU} , is provided in Section 2.3. For SCAFE, and particularly in other potential longer term applications, the diagonal cord material must avoid degradation by the radiation environment in the mission orbit.

Candidate cord fibers are identified and evaluated in Table 2-14. Among available candidates, Kevlar 29 provides the best mechanical/physical properties but is subject to degradation by UV radiation and possibly by heat generated during joining. Since preload requirements are quite low (the given value in Table 2-14 is based on Kevlar 29), either of the glass candidates provides good ultimate strain with little increase in preload due to higher $E\alpha$. Of the two, impregnated/cured S-glass roving provides approximately the desired breaking strength. The S-glass candidate was therefore selected.

2.1.2.3 Coatings. A baseline surface coating system consisting of titanium dioxide (TiO_2) powder dispersed in polysulfone resin (50/50 by weight, 0.05 mm thick) has been selected for use on beam caps and cross-members. Specific features of the coating are:

- Provides Temperature Control
- Has Dimensional Stability
- Limits Resin Max Temperature
- Compatible with Processing
 - Readily Applied by Spray-on or as Laminated Film
 - Flexible
 - Joinable
- Radiation Exposure Degrades Optical Properties

Table 2-14. Cord candidates/evaluation.

Material	Filament Properties		Compatibility	
	$E\alpha$ (KN/m ² - °K)	ϵ_{TU} (μ m/m)	Temp	UV Rad.
AS Graphite	-199	12188	✓	✓
Kevlar 49	-259	21053	?	?
Kevlar 29	112	44444	?	?
E-Glass	209	38095	✓	✓
S-Glass	246	44355	✓	✓
Quartz	40	23810	✓	✓

Application of a thermal control coating on the otherwise dark surface of a graphite/thermoplastic laminate reduces both maximum temperature and the temperature range experienced in a typical orbital cycle. If used, the selected coating must be compatible with both the processing and service environments. As shown in Figures 2-14, 2-15, and 2-16, the titanium dioxide coating satisfies these requirements in SCAFE and subsequent applications with service life in the 5 to 10 year range.

A reduction in coating efficiency arises from an increase in absorptance, α , with continued exposure to UV, electron, and proton radiation. Limited test data are available for long-term optical property degradation, but the trend can be seen in Figure 2-14. A new time scale has been overplotted on the existing test data curve, with $t = 0$ occurring at the α_s intercept corresponding to the Convair-measured value for the TiO₂/polysulfone coating. The difference in α_s at $t = 0$ appears to result from the polysulfone resin in which the TiO₂ is dispersed for this application. Values of α at 6 months (SCAFE mission duration) and 4 years are shown and their corresponding maximum temperatures found to be well within the maximum use temperature for the polysulfone resin system, as shown in Figure 2-15.

Temperature histories for several α/ϵ ratios are shown in Figure 2-16 to illustrate the initially available temperature reduction (vs. bare surfaces), the effect of coating application technique, and the effects of coating degradation with time.

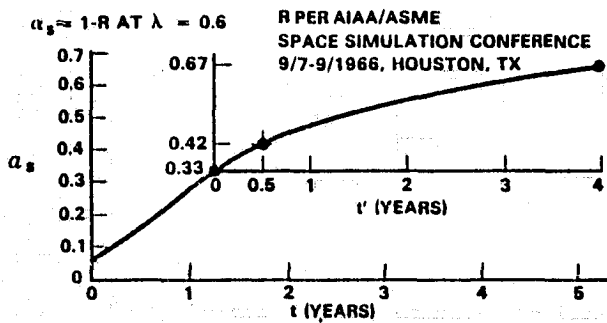


Figure 2-14. TiO_2 Absorptance vs. time.

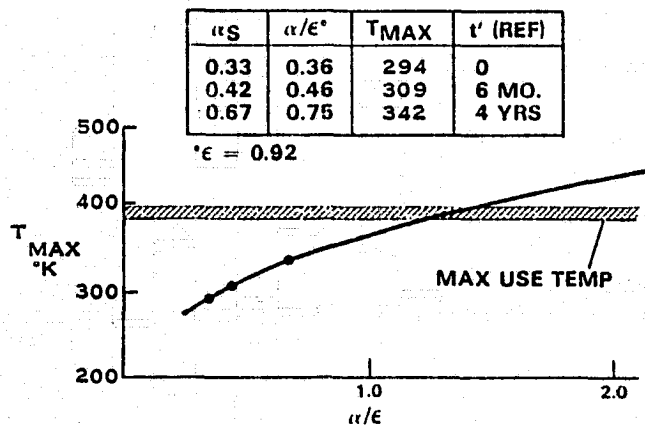


Figure 2-15. Maximum temperature vs α/ϵ .

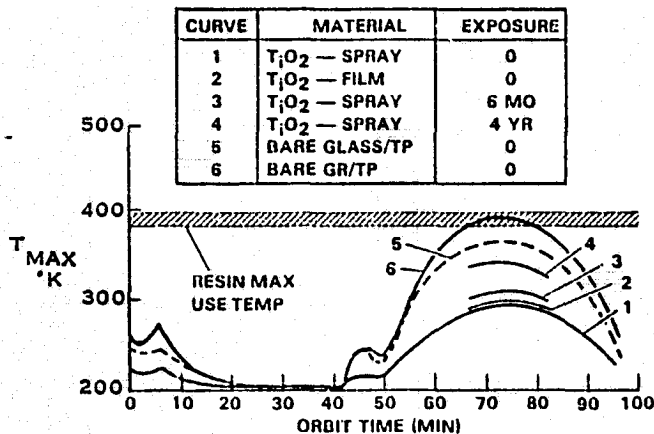


Figure 2-16. Mission temperature histories.

and, therefore, imply added complexity to provide jig fold-out.

In addition to the single planar platform variations (Figure 2-17), a number of dual platform/central hub concepts, suitable for either single- or two-mission construction, are also compatible with the baseline SCAFE concept.

2.1.3 ALTERNATIVE PLATFORM CONCEPTS.

In addition to the baseline 4×9 platform, several variations on the size and grid spacing were identified for potential application to the SCAFE mission, as shown in Figure 2-17.

Although material quantities and total system weight are well within maximum capabilities, reduction in beam element quantity may yet be required to satisfy either of two possible constraints. The mission timeline indicates a very full day on Day 3 to accomplish cross-beam fabrication/joining plus equipment/sensor installation using EVA. If necessary, the schedule can be eased by adopting the appropriate reduced cross-beam arrangement. The resulting platform lengths would vary only slightly from the baseline.

Although not indicated by current analyses in which Orbiter VRCS duty cycle impulses are applied to an Orbiter/platform model (Sections 4.2 and 4.3), future analysis may indicate beam tip displacement responses sufficient to cause potential impact between adjacent longitudinal beams with baseline spacing. If required, reduction in longitudinal beam quantity can be accomplished easily with no change in cross beam bay spacing.

Larger platforms can also be fabricated/assembled if warranted by end usage requirements, such as the NASA/JSC Microwave Transmission Test Article (MTTA) concept, but involve increased assembly jig length

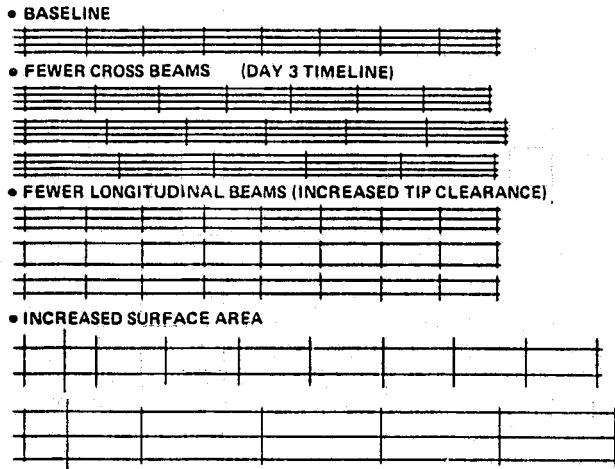


Figure 2-17. Single planar platforms.

As illustrated in Figure 2-18, there are three principal distinctions among these concepts: (1) alignment between longitudinal beams in the two platforms; (2) beam/hub segment interface relationships; and (3) hub concepts. Hub elements may be either preassembled (including required subsystems) and delivered to orbit with the platform construction equipment, or portion(s) of the assembly jig can be separated to act as the hub. However, the assembly jig hub concept is limited to two-mission construction since, due to cargo bay envelope constraints, it appears unlikely that dual jigs could be used on a single mission (nor does

it make sense to do so, since the second jig is effectively a preassembled hub segment with extensive mechanization it doesn't need to simply retain a completed platform section).

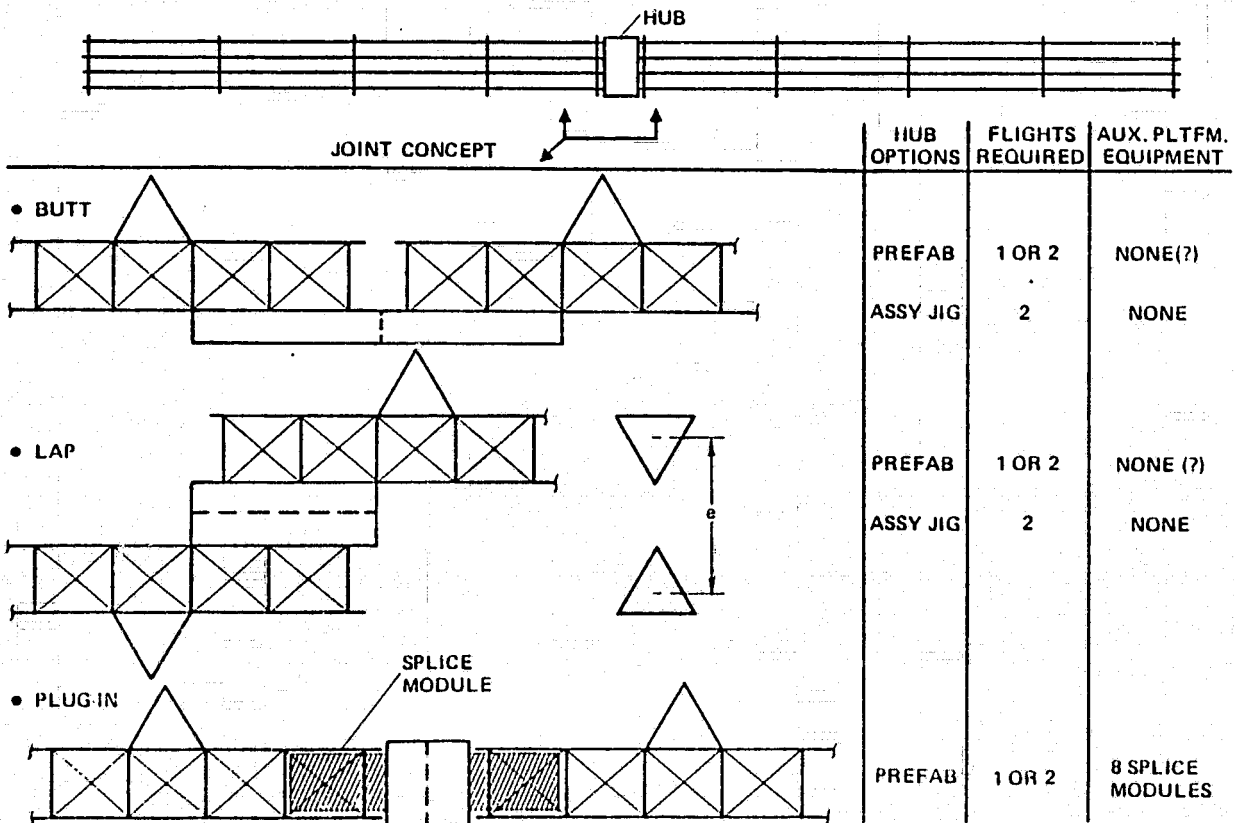


Figure 2-18. Dual planar platforms.

The plug-in concept provides minimum load path eccentricity (if important) but requires several splice modules to permit assembly. This offers no advantage over the other options if the joint is to be permanent but is a decided advantage in an application involving periodic separation/docking.

Using the baseline beams and platform as building blocks, two alternative three-dimensional large beams can be developed. The first of these is a Tee, shown in Figure 2-19.

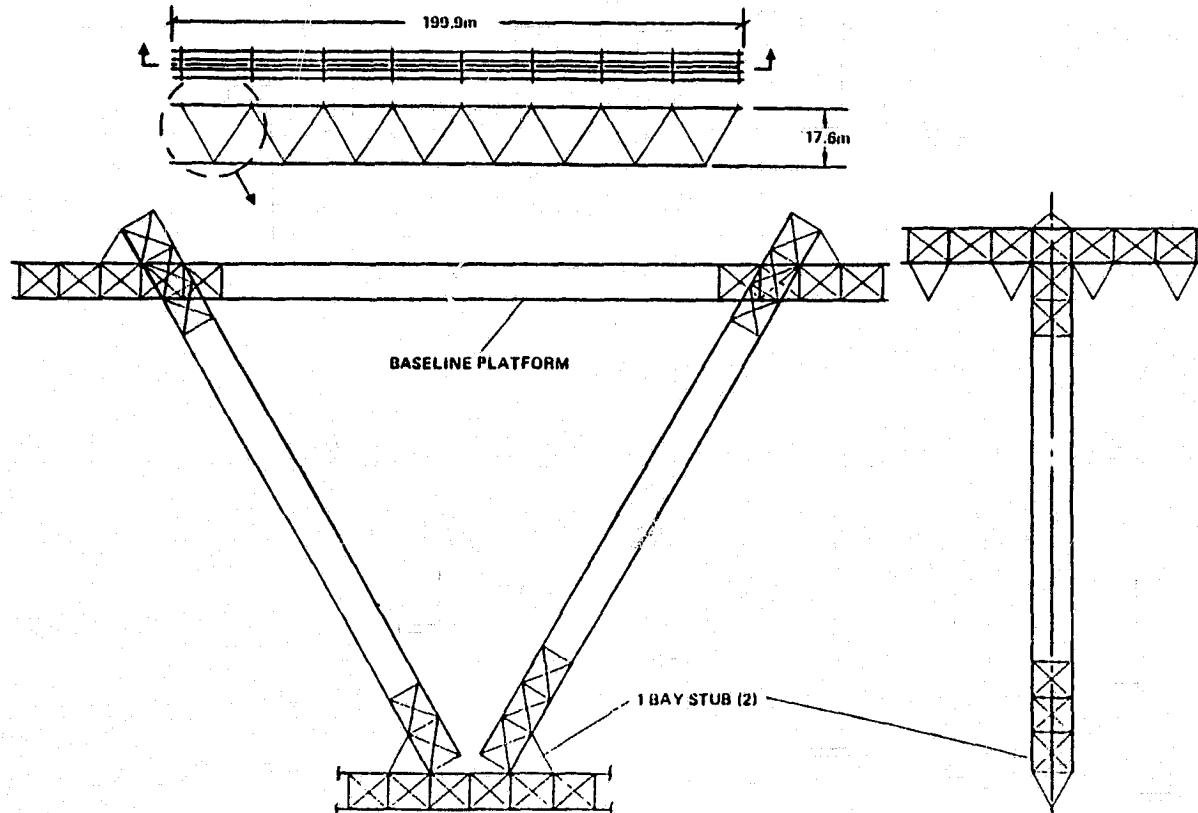


Figure 2-19. Large T-Beam.

For the nine-cross-member baseline, the resulting depth between longitudinal beam centroids is 17.6 m. Diagonal beams are coplanar and located on the platform centerline. Consequently, either of the two-longitudinal-beam platform concepts of Figure 2-17 may also be used, but the three-beam option is precluded.

Geometry at beam-to-beam joints is identical to that in the planar systems (flat on flat). This joint concept requires single bay beam stubs at the diagonal/keel intersections, as shown.

The second large beam concept directly developable from the baseline beam/platform geometry is the triangular arrangement of Figure 2-20. Again, all joints use the baseline flat-on-flat concept.

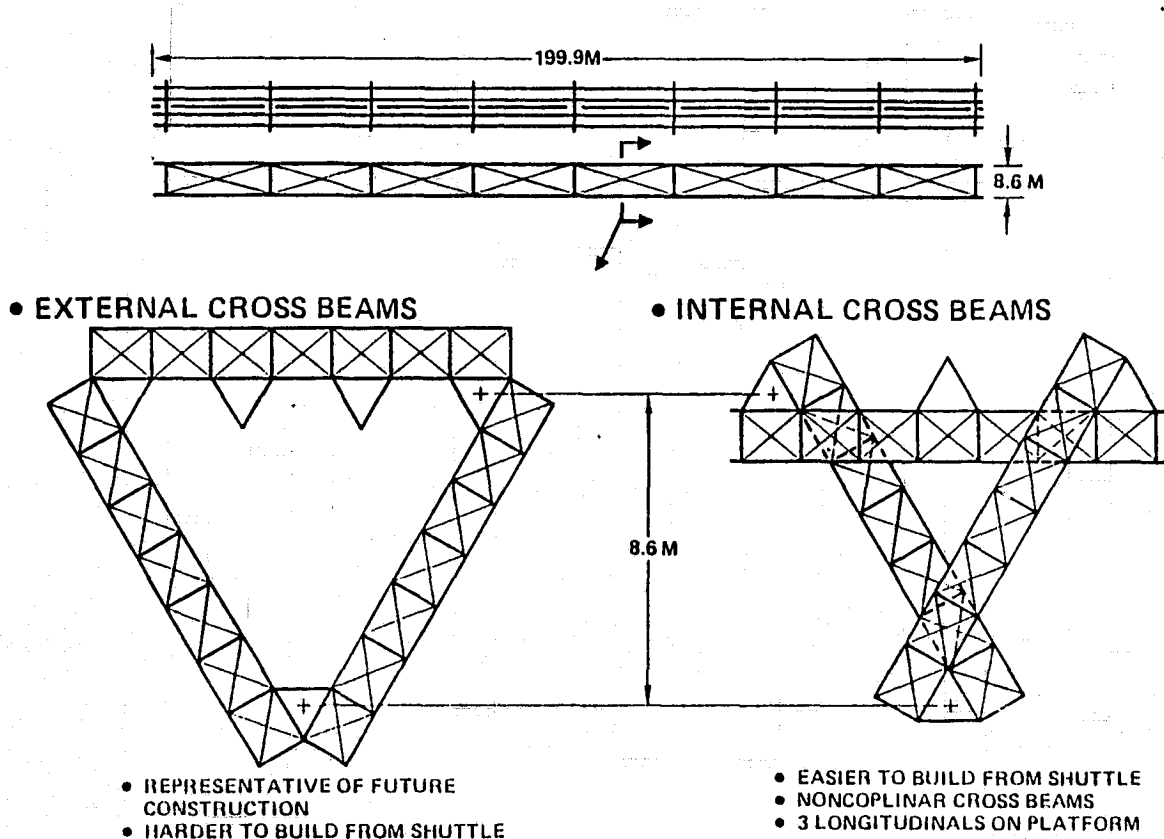


Figure 2-20. Large triangular beams.

Either of two feasible arrangements provides a centroidal depth of 8.6 meters between the platform and keel. The external cross-beam concept has been widely shown as an element of future large systems such as SPS. However, an assembly sequence flow using the baseline Shuttle-attached assembly jig concept indicates that the internal cross-beam option is easier to build.

Various longitudinal beam quantities can be incorporated into either arrangement, although the four-beam baseline is not recommended for the internal cross-beam option due to resulting handling clearance constraints during cross-beam positioning.

If required, zig-zag preloaded tension diagonals can be installed during assembly in much the same manner as in baseline beam fabrication.

At present, there is no reason to adopt any of the alternative beam concepts. However, future studies of platform usage and applications may generate new requirements which may be more readily satisfied by one of these alternatives than by the current baseline platform.

2.2 PLATFORM FABRICATION SYSTEM

The SCAFE platform fabrication system includes all mechanical, structural, and avionics subsystems necessary to automatically fabricate continuous beams to required lengths and assemble the beams into the baseline platform configuration. The fabrication system also includes equipment and software for:

- a. Mechanical and avionics interfaces with the Shuttle Orbiter.
- b. Deployment from the Orbiter payload bay.
- c. EVA support equipment.
- d. Post-experiment stowing in the Orbiter payload bay.
- e. Payload safety and monitoring devices.

The three major subsystems of the SCAFE fabrication system are the beam builder, the assembly jig, and the avionics subsystems. The selected concepts provide a totally automated platform fabrication technique which allows maximum use of EVA time for equipment installation and experimentation. This section presents the selected design concepts, preliminary performance data, and the design concept selection trade studies for the platform fabrication system.

2.2.1 BEAM BUILDER. This section gives the trade study methodology and issues for the beam builder and its basic processes. Concept layouts of the candidate beam builder configurations are presented along with concept sketches of the process options. The selected beam builder concept is presented in preliminary design layout drawings.

The SCAFE beam builder is an automatic machine process which fabricates beam assemblies from non-metallic materials stored within the machine. The materials are preconsolidated thermoplastic graphite/fiberglass composites which are manufactured in a convenient form for small volume storage. The thermoplastic composite materials not only provide excellent properties for space structures, but lend themselves to automatic fabrication techniques because they are heat formable and can be joined by efficient spot welding techniques.

The selected beam builder concept satisfies the following design criteria:

- a. Power utilization well within Orbiter capability.
- b. Automatic quality control.
- c. Least amount of material.
- d. Fewest number of beam weld joints.
- e. No growth limitations.
- f. Low weight.

**ORIGINAL PAGE IS
OF POOR QUALITY**

2.2.1.1 Study Method and Issues. The trade study approach to selecting the beam builder concept is diagrammed in Figure 2-21. Thermosetting resins were excluded from consideration by Convair IRAD programs which established graphite/thermo-plastic as the best material system.

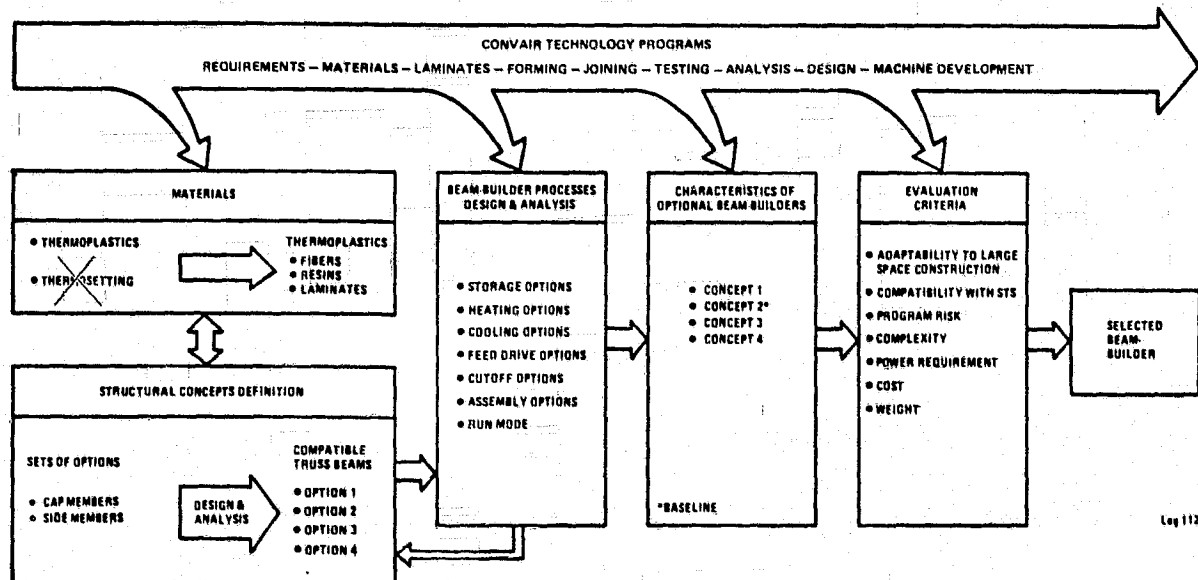


Figure 2-21. Study method and issues.

Three beam options were selected in addition to the baseline beam as candidates for trade. These concepts were used to define applicable beam builder processes. Various process options were then evaluated and selected processes used to develop three beam builder concepts and update our baseline beam builder. Where applicable, beam options were revised for compatibility with process options and beam builder concepts.

Beam builder concepts included machine layouts plus controls system and software definition to allow total system evaluation. The four beam builder concepts were evaluated with respect to the evaluation criteria indicated. Beam builder selection was based on the results of these evaluations.

2.2.1.2 Beam Builder Baseline Concept. The basic processes of the original baseline beam builder are illustrated schematically in Figure 2-22. The baseline beam described in Section 2.1.2 is constructed of three formed caps, joined to channel-shaped cross-members, and stabilized with six zig-zag plyed tension cord diagonals. Fabrication of this beam requires these processes:

- a. Storage. Flat strip material for the caps and cross-members, and the cord for the diagonals are stored by a process which provides safe, positive containment and dispenses the material with ease.

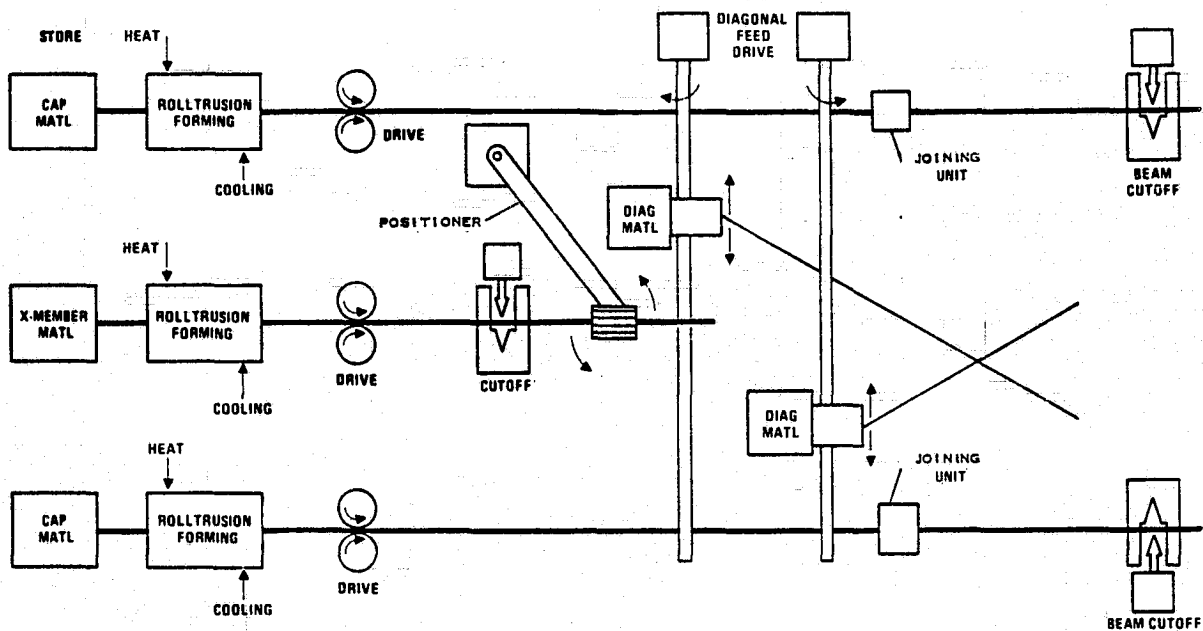


Figure 2-22. Cyclic feed fabricator functional schematic.

- b. **Heating.** The flat strip material for the caps and cross-members is fed through a heating section in preparation for forming. The heating section applies heat only to bend zones in order to conserve energy. The bend zones are heated to the plastic state prior to entering the forming section.
- c. **Forming.** The heated caps and cross-members are formed to the desired cross sectional shape by the Convair-developed rolltrusion process's.
- d. **Cooling.** On exit from the forming process, the beam members are cooled to a satisfactory use temperature before exposure to load.
- e. **Drive.** The beam is moved through the fabrication process and deployed into space by a drive mechanism on each cap member. The drive mechanism also provides the force necessary to extract the cap and cross-member material from storage and pull it through the forming process.
- f. **Diagonal Cord Applicator.** As the beam advances through the fabrication process, the diagonal cord members are plyed across each face of the beam. The cords are properly tensioned and positioned for joining.
- g. **Cross-Member Positioner.** Before the finished cross-members are cut to length, a positioner grasps the member. After cutoff, the positioners rotate and translate the cross-members into position for joining to the caps.
- h. **Joining.** When the cross-members are positioned and the cords are positioned and tensioned, the joining process permanently joins the beam elements together.
- i. **Cutoff.** Cutoff devices are required to cut cross-members to length and to cut off finished lengths of beam.

Two approaches to beam fabrication were considered: (1) cyclic feed, whereby the beam advances one bay length, then pauses to allow the assembly operations to be performed in place; and (2) constant feed, where the beam advances at a constant rate and assembly operations are performed in motion relative to the beam builder.

The cyclic-feed beam builder illustrated in Figure 2-22 operates for a 40-second run period during which the caps and beam are advanced at 2.2 meters per minute. After 1.434 meter beam extension, a pause of 40 seconds is made for cross-member and diagonal cord attachment. During the pause period, the formed cross-members are grasped by the positioner, cut off, and positioned on the caps. The diagonal cords are aligned between the cap and cross member by the cord feed mechanisms and the cord and cap are ultrasonic weld joined to the cap. The beam builder then repeats the operating cycle.

The constant-feed beam builder illustrated in Figure 2-23 installs cross members and positions cords while the caps are moving at 1.1 meter per minute. A reciprocating carriage is provided for cross-member attachment. The carriage-mounted assembly units move at the same feed rate as the caps and cross-members, and are thus able to grasp, cutoff, position, and attach the cross-members as the beam advances at a constant speed. After a 40-second working cycle, the carriage is returned to the start position in 40 seconds and then advanced for another work cycle.

The cyclic feed fabrication process was selected for SCAFE based on the following considerations:

- a. Mission Compatibility. It was determined that both processes were compatible with SCAFE. Both have the same fabrication rate. Both have the same dynamic impulse history.

A timeline of baseline beam builder events which control start/stop motion of the beam and masses within the machine allowed an impulse history to be developed (Figure 2-24). This impulse history was used to determine the potential for exciting natural modes in the beam as its length progressively increases. The step functions indicate start of power application and are not meant to imply sudden stop and start of the beam.

The two curves in Figure 2-25 show free-free yaw bending frequency and cantilever torsional frequency as a function of length of a single beam. Impulse timelines shown in Figure 2-24 indicate that periods of repetitive impulses may occur at 80, 40, and 20 seconds. While some pulses occur three or four times in a sequence at intervals of approximately one second, the lowest continuously repetitive period is about 20 seconds. The repetitive impulses represent frequencies of 0.013, 0.025, and 0.050 Hz, respectively, which are all well below natural frequencies of a beam of 200 m or less in length. Consequently, it is not anticipated that any first order resonances will be excited.

If it is determined that higher order resonances may be excited, it is feasible to deliberately program the control system to vary the impulse history as a function of beam length to avoid potential resonances.

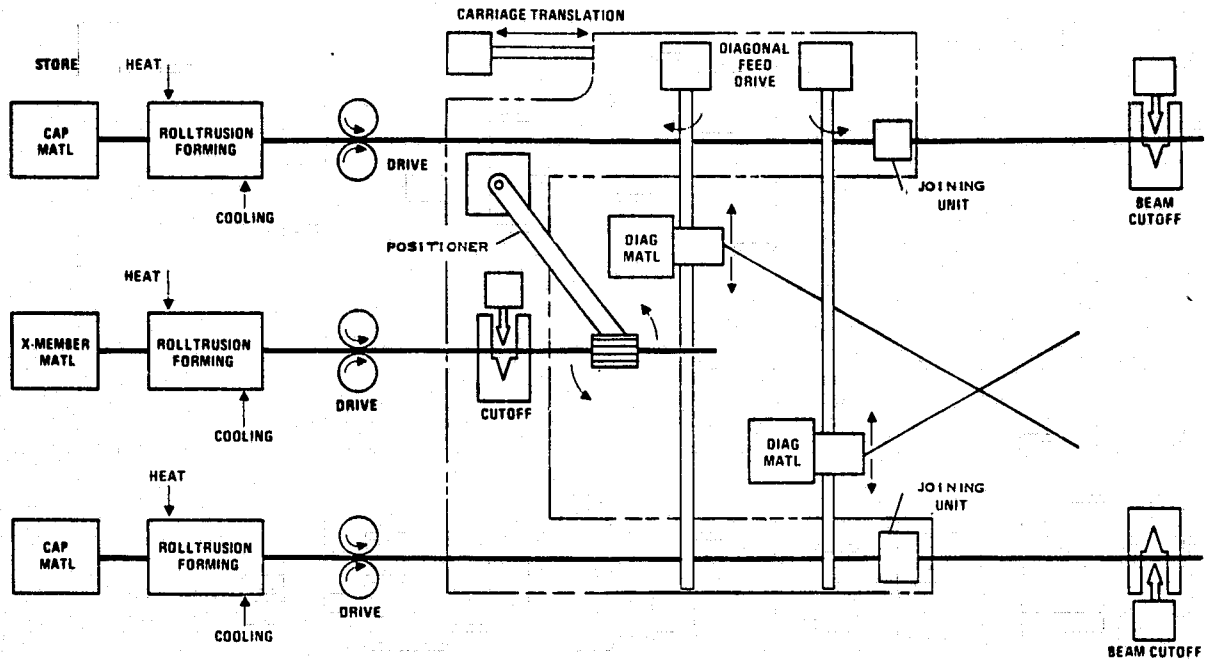


Figure 2-23. Constant feed fabricator functional schematic.

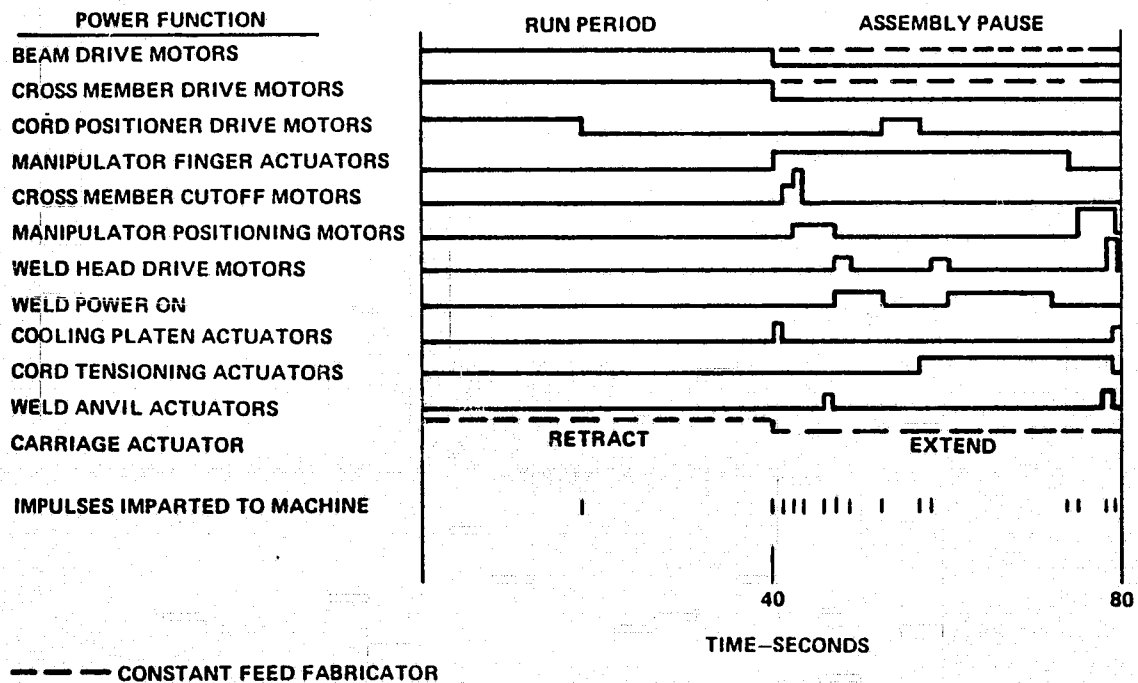


Figure 2-24. Baseline beam builder excitation timeline.

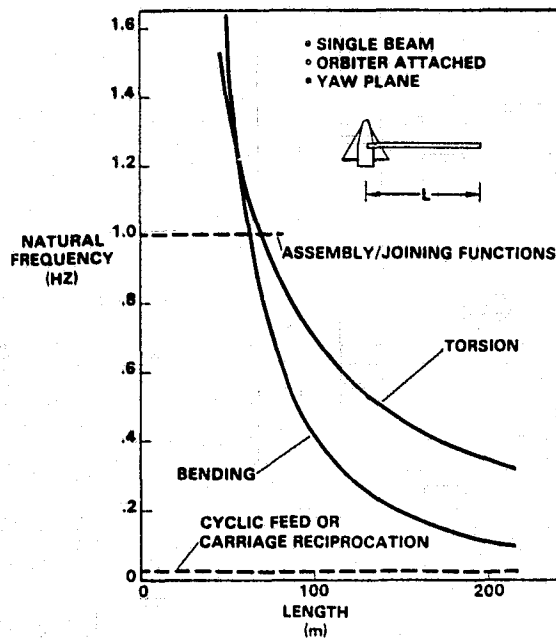


Figure 2-25. Beam dynamic characteristics.

length of beam. The use of cooling platens also allows the machine speed to be increased, if necessary.

Cooling the material in a constant-run fabricator requires a more complex system if the machine is to operate at the same fabrication rate as the cyclic-feed fabricator. Possible solutions include radiation to a cryogenically cooled box, reciprocating platens, or multiple contacting rollers which are fluid cooled.

- d. Process Quality Control. An important advantage of cyclic feed is the ability to automatically assess the quality control parameters under static conditions during assembly operations. If an out-of-tolerance conditions is detected, the cycle is automatically interrupted while the beam is not in motion, and the process has not advanced beyond the faulty operation. A continuous run process will advance beyond the faulty operation because of the time delay in stopping the beam and traveling carriage. This can cause greater difficulty in recovering to a ready-to-run status.
- e. Growth Capability. The adaptability of cyclic-feed fabricators to larger beam cross sections and lengths may be limited by beam dynamic responses and axial inertial loads created by the run/pause cycle. Such limitations must be determined individually with respect to any given beam configuration. Further study of potential scale-up beam candidate configurations is required to identify growth constraints.

- b. Machine Size and Complexity. The travelling carriage on the continuous-feed fabricator causes the overall machine length, weight, and complexity to be greater. All of these factors contribute to higher cost.

The SSAFE beam builder is cantilevered off the assembly jig during platform fabrication. A shorter machine is more desirable to reduce bending loads on the beam builder supports so as to simplify the support arrangement.

- c. Material Cooling. Analysis of the cooling behavior of the selected material presented in Section 4.5.1 indicates conducting cooling platens are required for the current fabrication rate of 80 seconds per bay

2.2.1.3 PROCESSES AND TECHNIQUES. Concept options for each of the beam builder machine processes and techniques were developed and compared. This section presents the results of those trades.

2.2.1.3.1 Storage. Material storage options are compared in Figures 2-26 and 2-27. The following storage options were selected:

- a. Roll in a Can. The concept of winding and storing the strips of cap material in rolls rather than on reels was considered worth developing further in this study for several reasons:
 1. Storage reels present a disposal problem to future large scale space construction projects.
 2. A reel tends to unwind by clock spring action of the roll and inertia. It must be controlled by a friction clutch and contained in an enclosure to guard against clutch failure. The clutch friction also causes higher load on the cap drive.
 3. The heating section can be readily integrated with the storage canister. This provides two advantages. First, the overall length of the beam builder is reduced by 1 meter. Second, any back-face radiation from the heated zones of the material passing by the heaters can be absorbed by the subsequent layer of material on the roll to gain some power utilization advantage.
- b. Clip Storage of Cross-members. Although the original beam builder baseline and alternate beam builder concepts all used on-orbit forming of cross-members, the energy savings provided by ground forming and sizing was determined to be significant. The clip storage process was ultimately selected for cross-member storage not only for power reduction, but to allow an alternate process concept to be developed as part of this study.
- c. Cord Spool. Consideration of the cord storage options shown in Figure 2-27 led to the selection of the spool. The wound ball concepts leave no core to dispose of, but are considered unreliable because they tend to unravel without the containment provided by a spool. A spindle feed ensures no backlash but introduces a twist to the cord as it is dispensed. There is also concern that the spindle may dispense several loops at a time, which may become tangled or knotted. Twisting of the cord may have detrimental effects on the strength of the cord when it is subjected to repeated tension cycles.

2.2.1.3.2 Heating. Material strip heating options are compared in Figures 2-28 and 2-29. Electric resistance element heating was selected because its high efficiency ensures that heating power requirements are maintained well within the Orbiter payload power limitation at the desired forming rate. Ultrasonic heating techniques for graphite/thermoplastic materials have been under investigation through Convair IRAD and may become a suitable alternative pending further investigation.

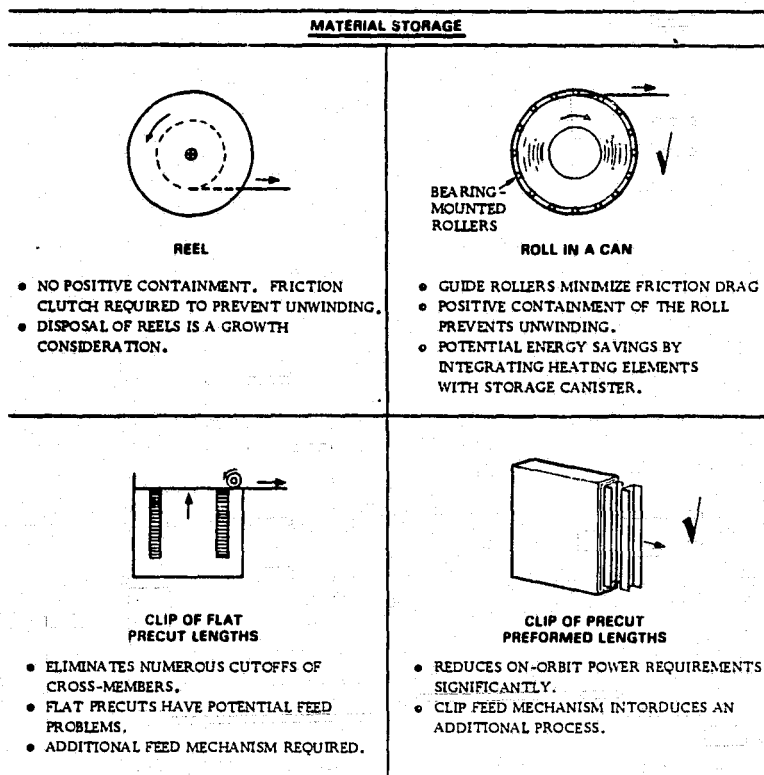


Figure 2-26. Cap and cross member material storage options.

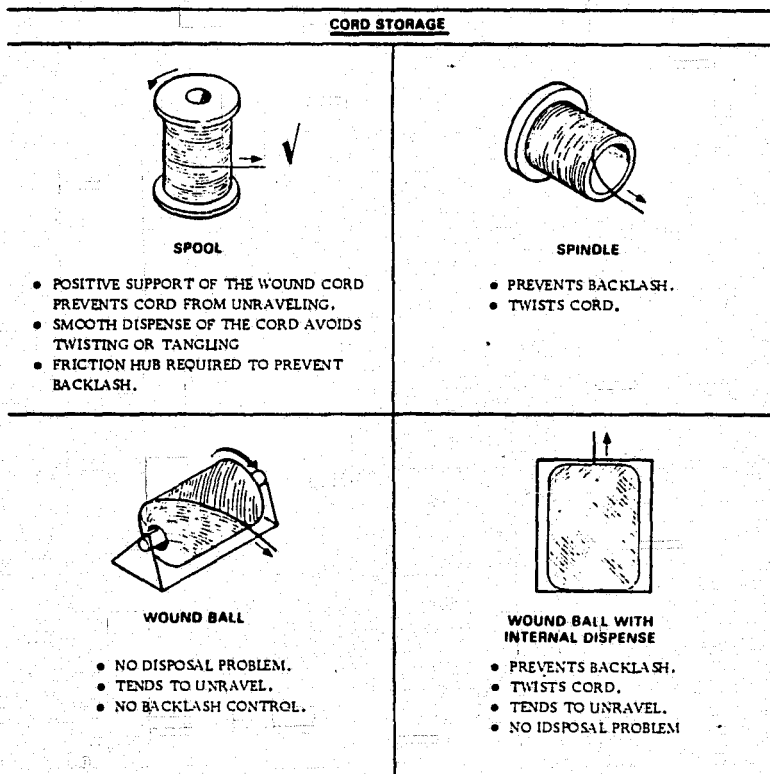


Figure 2-27. Cord storage options.

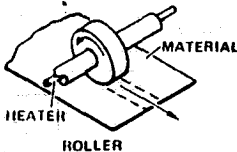
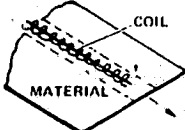
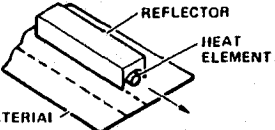
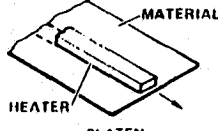
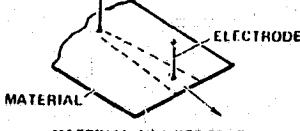
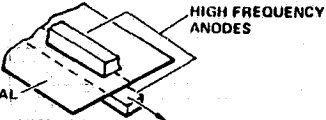
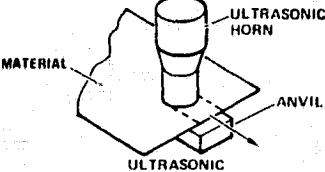
CONDUCTION	INDUCTION	RADIATION
 <p>ROLLER</p> <ul style="list-style-type: none"> • CONTACT RESISTANCE VARIABLE • SMALL CONTACT AREA REQUIRES LARGE NUMBER OF ROLLERS. 	 <p>ELECTROMAGNETIC</p> <ul style="list-style-type: none"> • LOW EFFICIENCY, GRAPHITE FIBERS SUPPRESS EDDY CURRENTS 	 <p>ELECTRICAL RESISTANCE ELEMENT</p> <ul style="list-style-type: none"> • HIGH EFFICIENCY. • HEATS MOVING AND STATIONARY SURFACES. • NO CONTACT WITH MATERIAL. • GOOD PREDICTABILITY OF HEAT TRANSFER.
 <p>PLATEN</p> <ul style="list-style-type: none"> • CONTACT RESISTANCE VARIABLE. • CAN ONLY BE APPLIED TO STATIONARY SURFACE. MOVING PLATENS REQUIRED. • CONTACT PRESSURE VARIABLE. 	 <p>MATERIAL AS A RESISTOR</p> <ul style="list-style-type: none"> • PENETRATION OF PROBES DAMAGES MATERIAL. 	 <p>MICROWAVE/RF</p> <ul style="list-style-type: none"> • LOW EFFICIENCY. • REQUIRES SHIELDING.
	 <p>ULTRASONIC</p> <ul style="list-style-type: none"> • MINIMIZES LENGTH OF HEATING SECTION • IRAD DEVELOPMENT ITEM. 	<p>✓ ALTERNATE</p>

Figure 2-28. Material heating options.

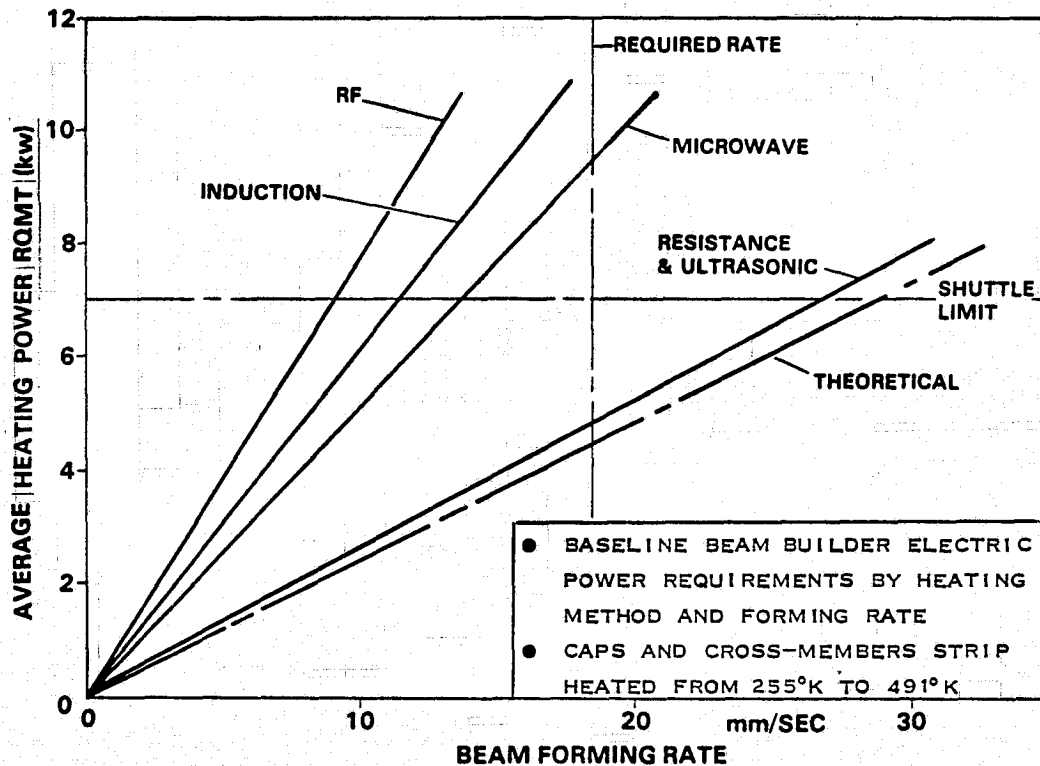


Figure 2-29. Relative efficiencies of heating process options.

In Figure 2-29, the theoretical power curve represents the energy rate necessary to bring pseudoisotropic graphite/thermoplastic material from 255°K to a required temperature of 491°K in the heating section and maintain this temperature in the forming section for a cyclic feed machine operation. The four heating process curves represent the electric power input to each of the candidate processes necessary to provide the theoretical material heat input. Subsequent to the initial heating process selection, several energy saving process and material selections were made which have reduced the heating power requirements by 74%, as will be discussed in subsequent sections.

2.2.1.3.3 Forming. The baseline forming process assumed for SCAFEDS is the GDC-developed rolltrusion process. No trade studies were performed on alternate forming processes.

2.2.1.3.4 Cooling. Cooling mechanism options are shown in Figure 2-30. Fluid-cooled aluminum platens were selected because they provide the fastest method of cooling the material to the desired structural use temperature of 380°K. They also maintain the straightness and uniformity of the formed member during the cooling period.

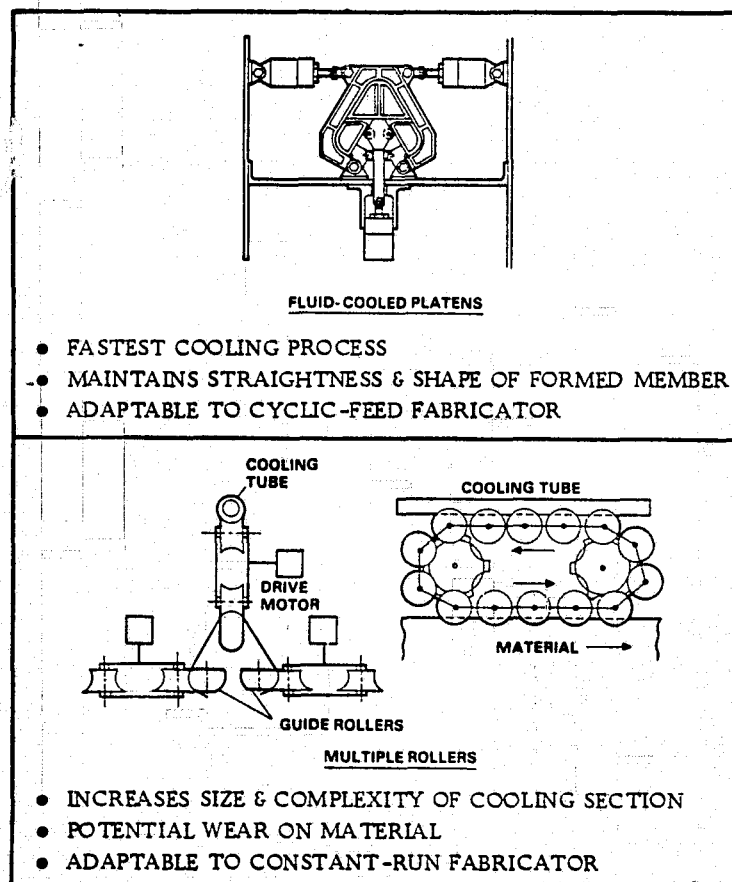


Figure 2-30. Material cooling options.

Because platens can only be applied to stationary surfaces, they are best suited for a cyclic-feed fabrication process. For constant-run fabrication, a multiple roller arrangement was considered. This approach uses a chain of sprocket-driven rollers which contact the heat-affected zones of the material on the inboard stroke and expel heat to a cooling tube on the outboard stroke. This method is undesirable because of added complexity, weight, power requirement, and potential wear on the material.

2.2.1.3.5 Drive. Cap drive options are illustrated in Figure 2-31. Estimated drive forces necessary to pull the material from the storage roll through the heating and forming process and advance the beam is 311 N maximum. A single set of contoured drive rollers with drive input to all four rollers has a calculated cap drive force capability of 534 N maximum.

The contoured friction roller drive was selected for SCAFE primarily because it provides more efficient drive force distribution (all rollers are powered), and it maintains the alignment of the caps regardless of the contact forces. It is also simple to add additional sets of drive rollers in the drive train without adding additional drive motors should the single set prove to be marginal.

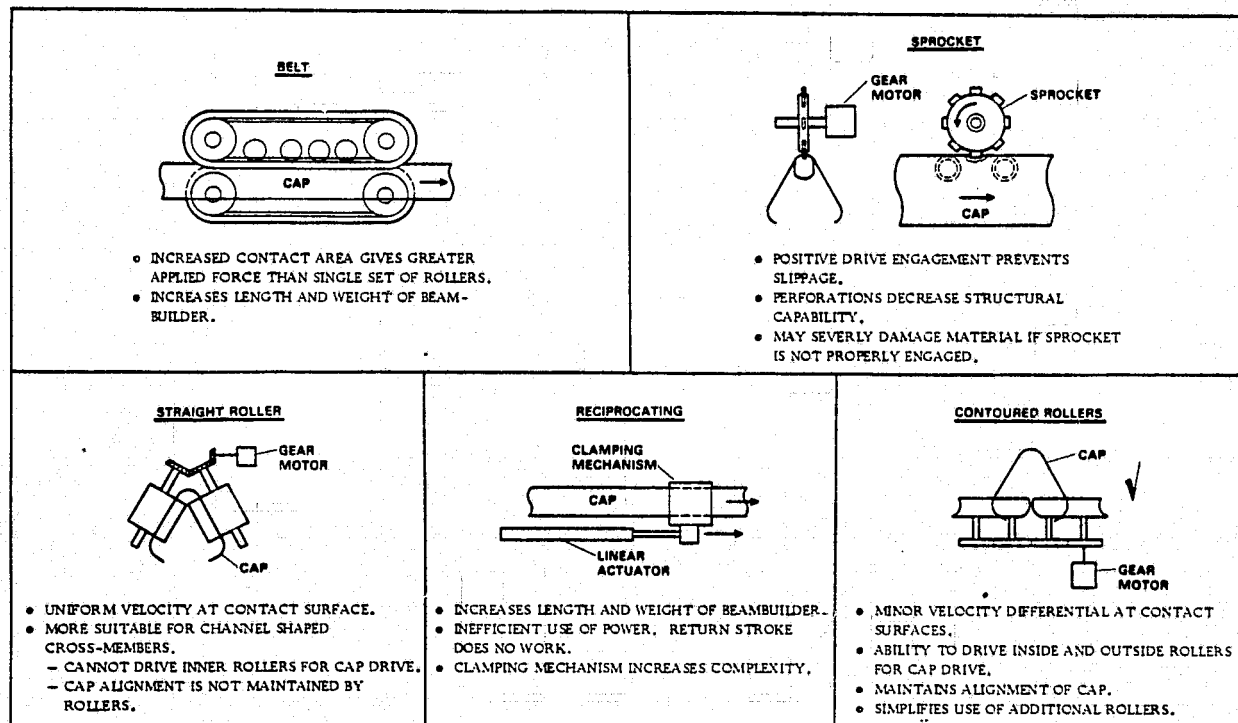


Figure 2-31. Cap drive options.

Future scale-up of the beam builder will require multiple roller sets or belt drives to deliver higher drive forces.

For cross-member forming processes, the drive rollers would be straight; however, the cross-member shape will allow both inside and outside rollers to be driven.

2.2.1.3.6 Cross-member Positioner. The original beam builder baseline included on-orbit forming and sizing of cross-members. For this reason several cross-member positioner options were considered to handle cross-members as they came out of the forming machine, as illustrated in Figure 2-32. For this case, the positioning of a cross-member requires three operations. The member is extended to clear the cutter, rotated normal to the cap members, and positioned on the caps for joining. This can be accomplished by a wide variety of mechanisms, as shown. A common device is assumed for each manipulator to grip the cross-member. The eccentric arm and screw jack was selected for the baseline beam builder to minimize drive requirements and provide fixed mechanical alignment and positioning of cross-members.

For clip-fed preformed, precut cross-members, two options were considered as shown in Figure 2-32. The track-driven swing arm was selected for the final beam builder concept because it is more compact, simplest to design, and simplest to adjust for close-tolerance positioning accuracy.

2.2.1.3.7 Joining. The baseline beam assembly joining process for SCAFEDS is ultrasonic spot welding. The advantages of this method of joining graphite/glass/thermoplastic include:

- a. No loose or expendable joining materials, such as fasteners, brackets, clips, or adhesives to handle.
- b. Efficient use of power.
- c. Short weld time required.
- d. Ability to verify weld quality by monitoring weld energy.
- e. Ability to pierce and join caps and cross-members without producing debris.
- f. Produces permanent joints.

2.2.1.3.8 Cutoff. The beam cutoff process options are compared in Figure 2-33. The shears mechanism was selected because of its clean, positive cutoff characteristics. The ultrasonic cutting characteristics are very clean, but the use of multiple cutting horns with attendant power supplies makes it very cumbersome for this application. Processes which produce substantial debris or outgassing of thermoplastic resin were eliminated as such contaminants are potentially detrimental to equipment and spacecraft.

2.2.1.3.9 Integral Cooling vs. Orbiter Cooling. A fluid-coolant loop is required in the beam builder to control the temperature of the cooling platens and the heater reflectors. A study was conducted to determine the advantages of an independent cooling system for the beam builder as an alternative to using the Orbiter coolant supply system.

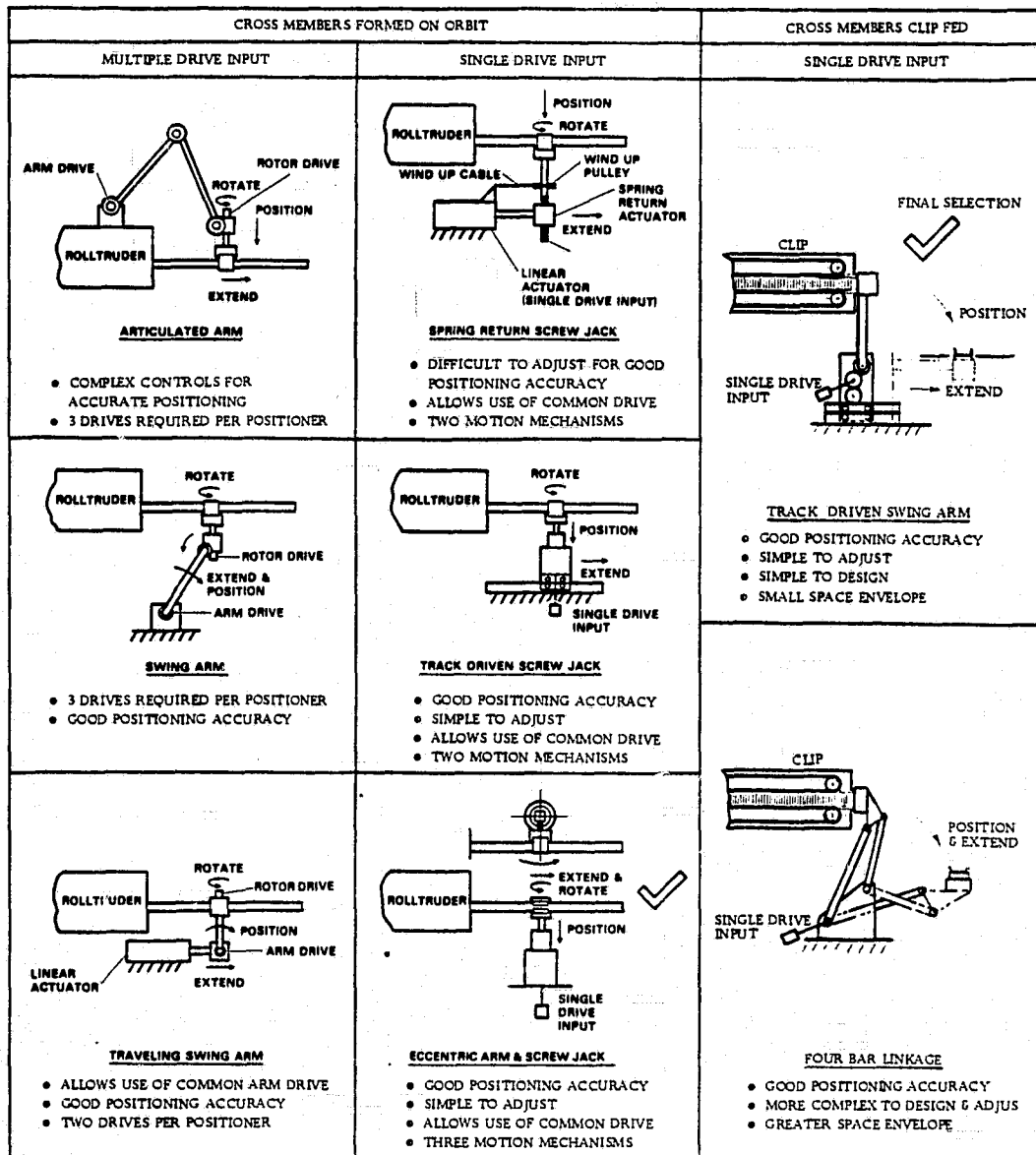


Figure 2-32. Cross-member positioner options.

A simple schematic of the independent cooling system concept is shown in Figure 2-34. The coolant (F-21 or equivalent) is circulated through the cooling platens and heater reflectors in the heating and forming sections of the three cap forming machines. The coolant removes an estimated 448 watts total from the platens and reflectors. The high temperature coolant then flows through the radiator panel where the excess heat is radiated to space. The radiating area shown is sized to reject the 448 watts cooling load under maximum solar heat influx conditions. The silver backed teflon tape provides high emittance and low absorptance to minimize the thermal impact of solar heating.

The pump operates with a power demand of 58 watts. Overall system weight is estimated to be 15.3 kg.

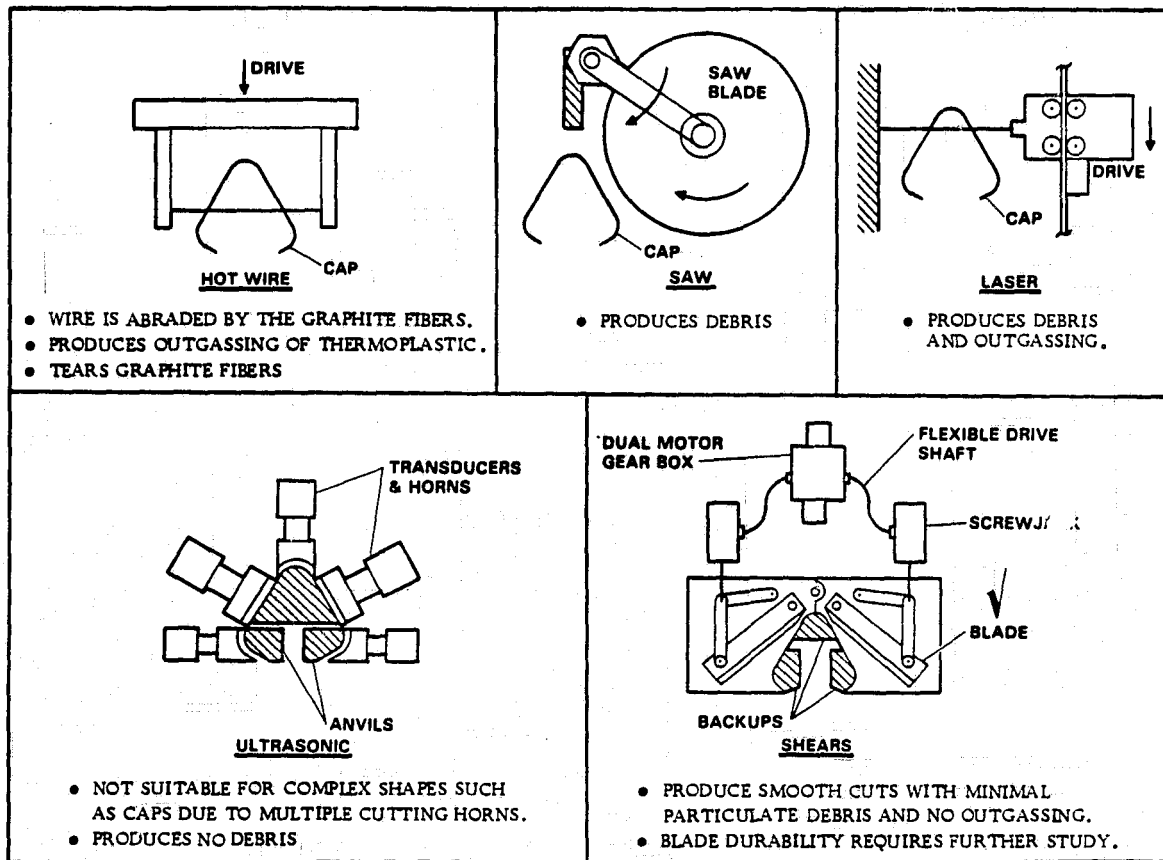


Figure 2-33. Cutoff options.

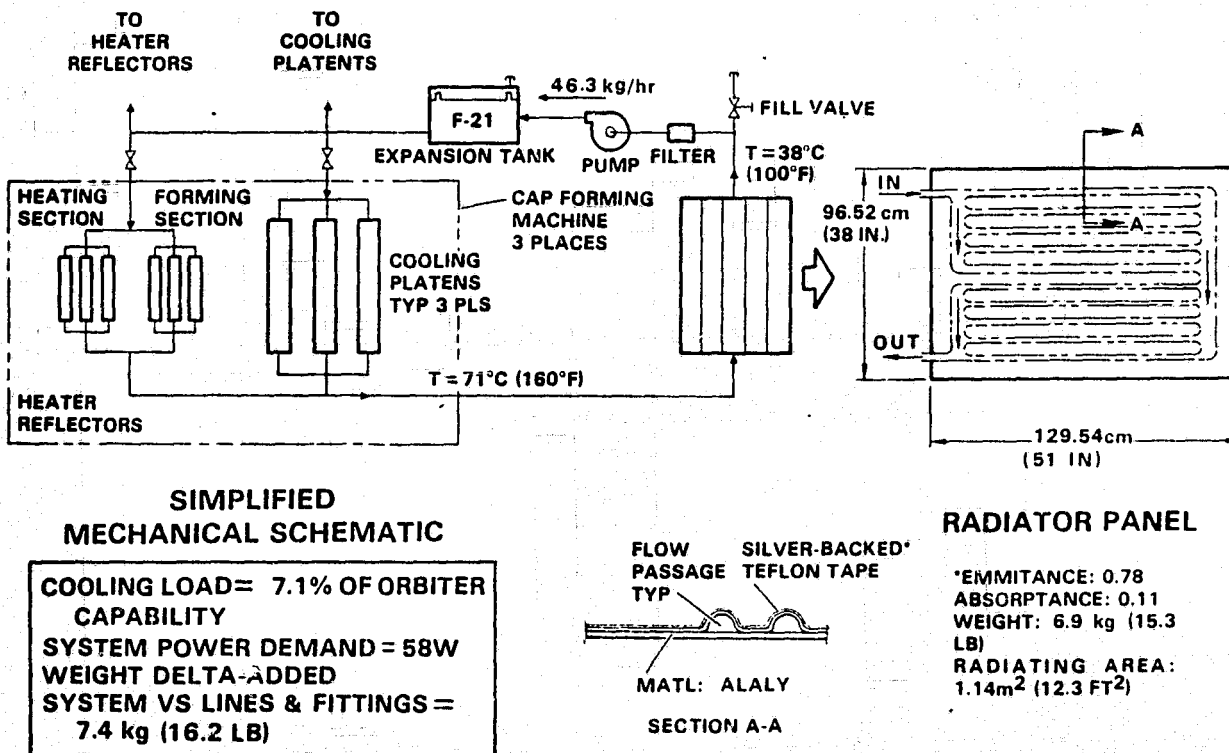


Figure 2-34. Independent cooling system.

The cooling load of the beam builder represents 7.1% of the Orbiter capability. The interface between the beam builder and the Orbiter would require long runs (21 m) of fluid lines including a 15 m length of flex hose in the supply and return lines to allow for relative motion between the beam builder and assembly jig. The estimated weight of lines and fittings for the interfacing fluid lines is 8 kg.

The independent cooling system is recommended because of these advantages:

- a. Requires a small amount of electrical power to operate (58 W).
- b. Does not add significantly to the weight of the payload (7.3 kg).
- c. Eliminates the potential leakage and handling problems associated with long lengths of flexible fluid lines.
- d. Precludes additional cooling load on the Orbiter cooling system.

2.2.1.4 Beam Builder Concept Selection. Concept layouts for each of the candidate beam builders are shown in Figures 2-35 through 2-40. Each concept was developed to fabricate one of the four candidate beam configurations described in Section 2.1.2. Wherever applicable, the same processes were used in each concept in order to prevent process options from becoming discriminators in the concept selection evaluations. For example, all of the concepts use reel storage and common cap forming machine assemblies. The principal discriminators are in the fabrication and assembly techniques used for side members.

2.2.1.4.1 Beam Builder Concept 1. Concept 1, shown in Figure 2-35, fabricates a beam from three baseline caps joined to prefabricated continuous-strip side panels. The three side panel strips are rolled on storage reels. From there they pass through a heating, forming, and cooling process. This forms a stiffening bead along each lateral cross-member. During the pause period, one panel cross-member in each panel is strip heated in a heater section as the preceding panel cross-member is simultaneously formed and cooled in a set of fluid-cooled dies.

Perforations along each side panel edge allow synchronized drive belts to pull the panels from the reels through the forming process and feed them into the assembly process. Notches in the edge of the panels at the ends of the beads permit the panels to pass through the belt drive without crushing the beads.

The panels are loosely guided into place along the sides of the beam by guide rollers. A final set of synchronous guide rollers flatten the panels against the caps for joining.

The panels are spot welded to the caps by twelve ultrasonic weld heads as shown in the weld detail. The weld heads are engaged during the pause period, then sequentially energized to limit peak power requirements. At the conclusion of the weld operations, the weld heads are retracted and the beam is advanced one bay length by the cap drive mechanisms.

The beam cutoff shears are located so as to sever the beam by cutting through the caps. This leaves a nearly one bay length tail-piece at the end of each beam due to inability of the machine to produce variable (i.e., shorter) bay lengths.

The major advantage of Concept 1 is that it precludes multiple side member handling and attaching mechanisms and processes. The major disadvantages are:

- a. Higher weight and volume due to the following factors may limit growth capability:
 1. A high percentage of the volume of the material roll is created by voids in the "doily-like" precut material.
 2. Much of the material, e.g., longitudinal sections, performs no structural function but is required for handling the panels.
 3. The wide panels drive the size of the storage reels up.
- b. Panel production is costly. If panels are blanked out, it results in a large quantity of high-dollar non-recyclable waste material. If they are done by special layup, manufacturing manhours could be staggering. Development of automatic manufacturing processes could be equally expensive for limited quantities.
- c. Requires development of two different forming processes.
- d. Pretensioning of the diagonals is not controlled, therefore, torsional stiffness and beam twist are not controlled. The effects of diagonal pretensioning are discussed in Section 2.1.2.

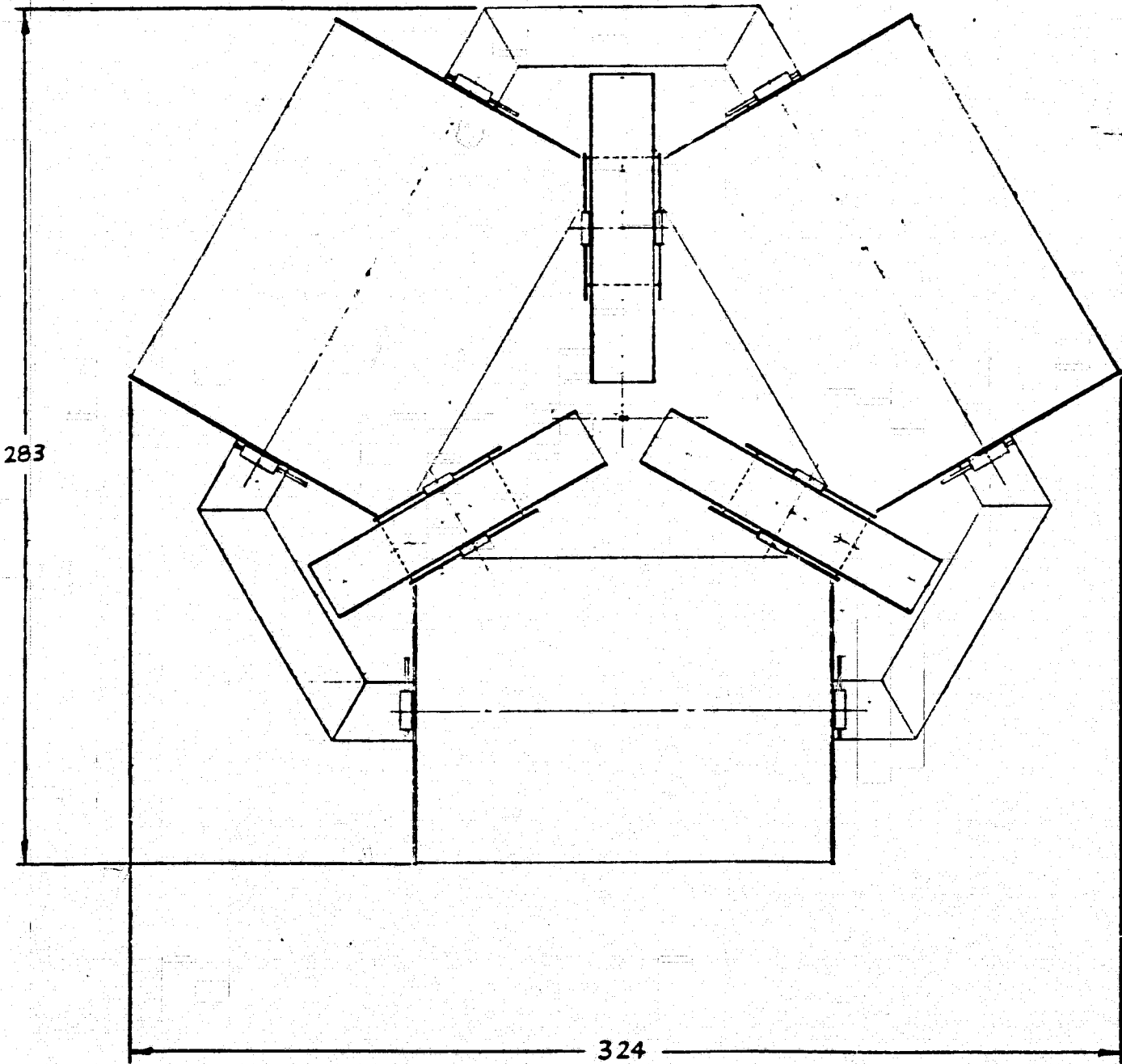
2.2.1.4.2 Beam Builder Concept 2. The baseline beam builder concept is shown in Figure 2-36. This machine fabricates a beam from three rolltrusion-formed cap members, joined to rolltrusion-formed cross-members, and pretensioned diagonal cord members plyed across the sides of the beam in a zig-zag path.

During the run period, fore and aft cord plyers shuttle across the faces of the beam in opposite directions, as illustrated in Figure 2-37. Cap drive force pulls the six cords from their storage spools through the cord tensioning and cord pleyer mechanisms. Cord tensioners apply an equal preload to each cord after the cord plyers are at the end of their strokes.

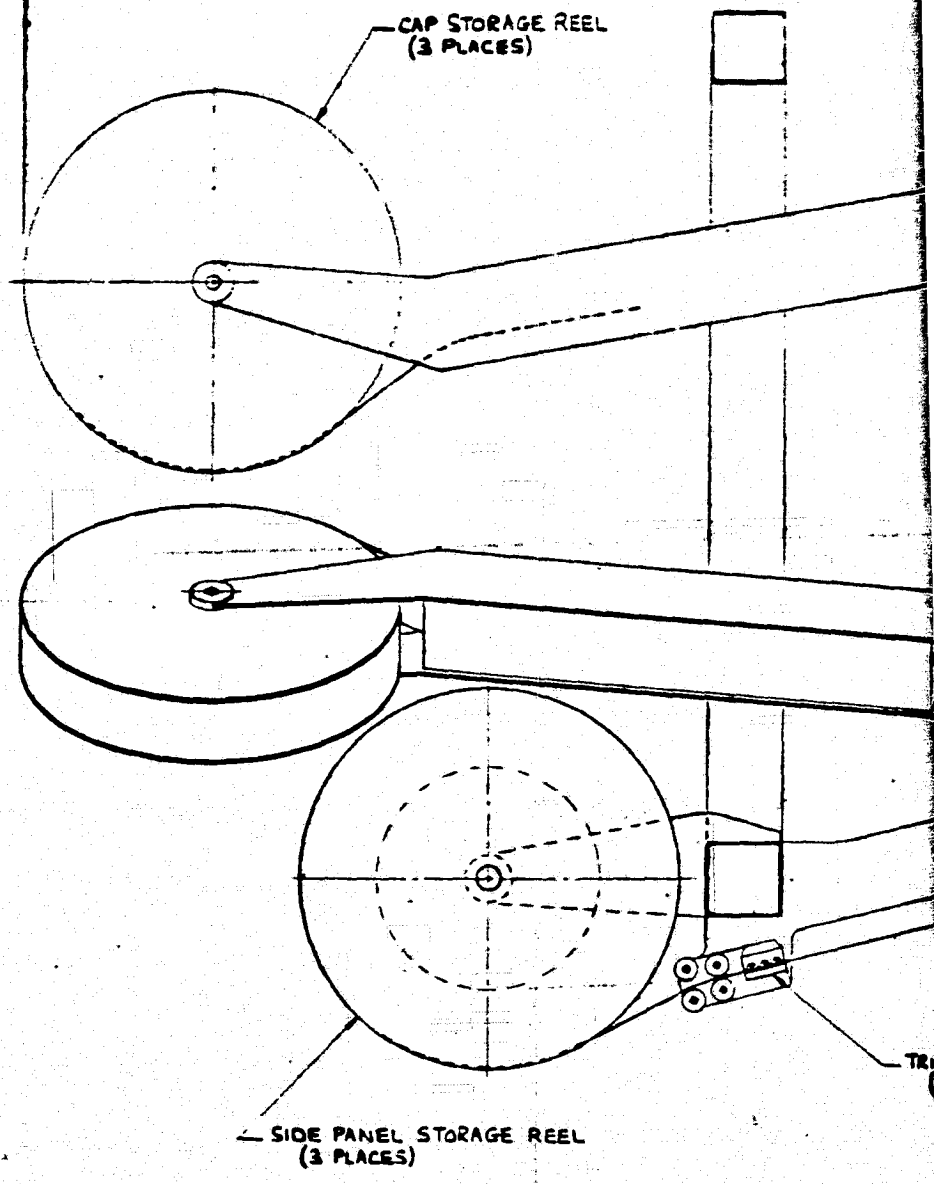
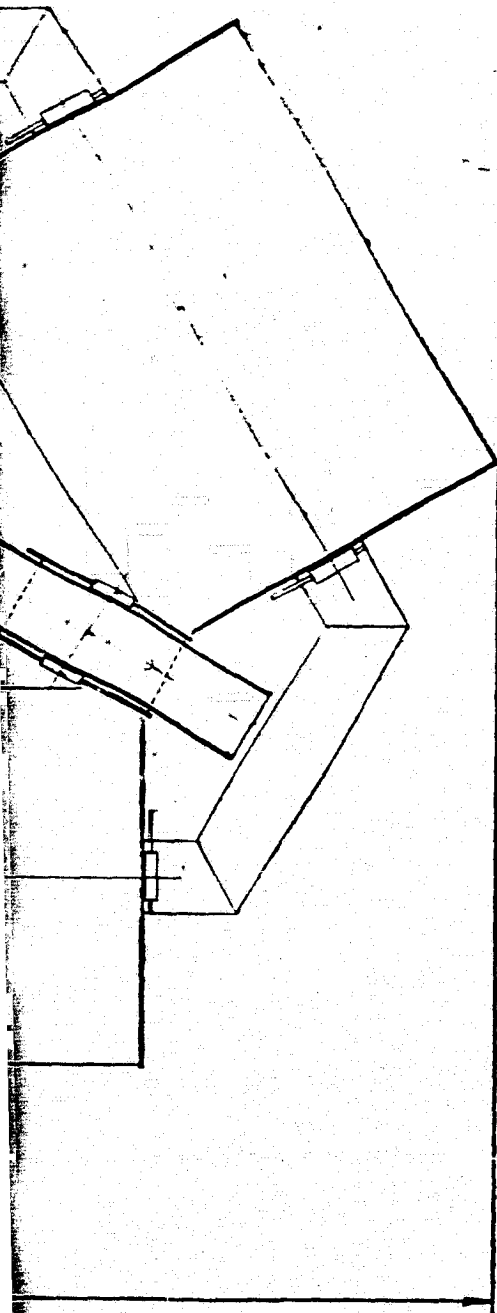
When the beam has paused for the assembly operations, the cross-members are cut off and positioned on the beam by three eccentric arm and screw jack positioner/handler mechanisms. Six ultrasonic weld heads are activated and a pin in each weld horn hot pierces through the caps and cross-members. The cord plyers are then driven inward and the cords are pulled over the piercing pins to the normally installed angle with the cap. The weld heads are then driven against the weld anvils and sequentially energized to make the permanent welded joints, which also captures each cord between a cap and a cross-member. The weld heads are retracted and the cycle repeated.

BUILDING FRAME

1



~~REVISION~~ 2



696

~~WELDING PLANT~~

3

CAP FORMING ASSY
(3 PLACES)

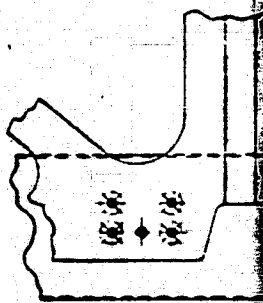
DUAL WELD HEAD
(6 PLACES)

SYNCHRONOUS ROLLER
(3 PLACES)

SYNCHRONOUS
DRIVE BELT

FORMING &
COOLING DIES

TRIPLE HEATING STRIP
(3 PLACES)

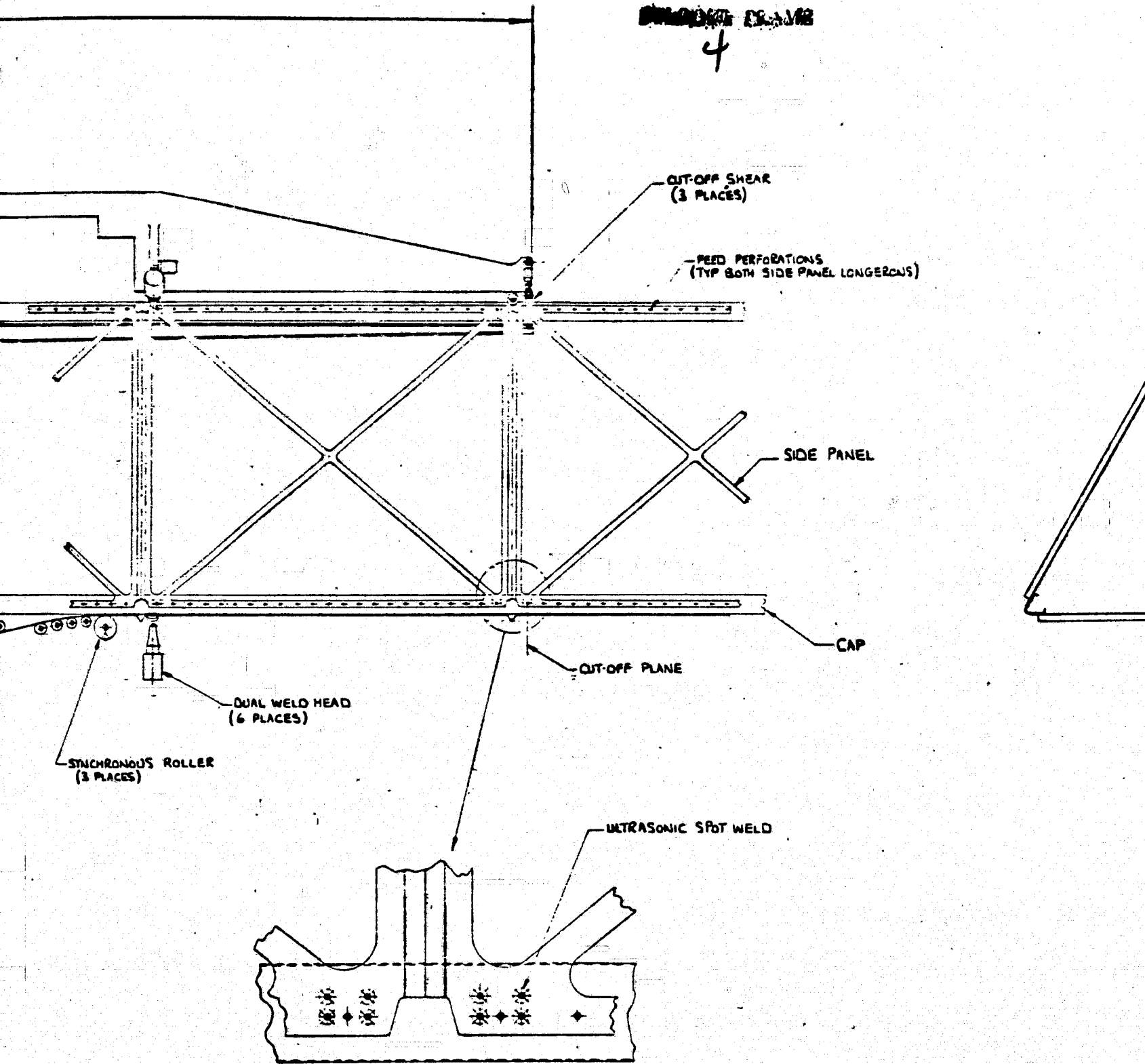


WELD ON
SQUARE

7

BRIDGE DECK

4



WELD DETAIL
 SQUARE TO FACE SCALE: 1/2

ATIONS
(DE PANEL LONGERONS)

SIDE PANEL

CAP

FORMED CROSS MEMBER BEAD

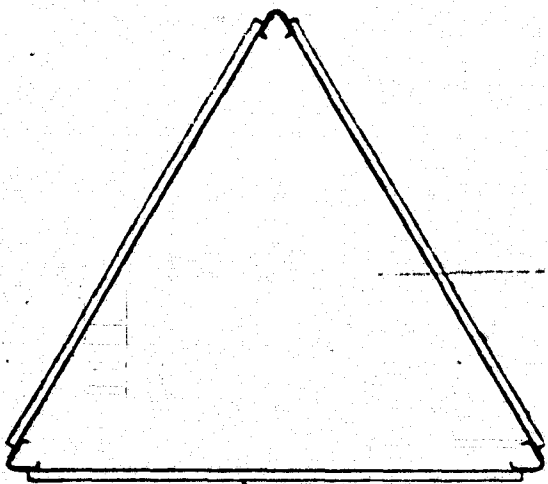


Figure 2-35. Beam builder concept 1 layout.

~~SECRET~~

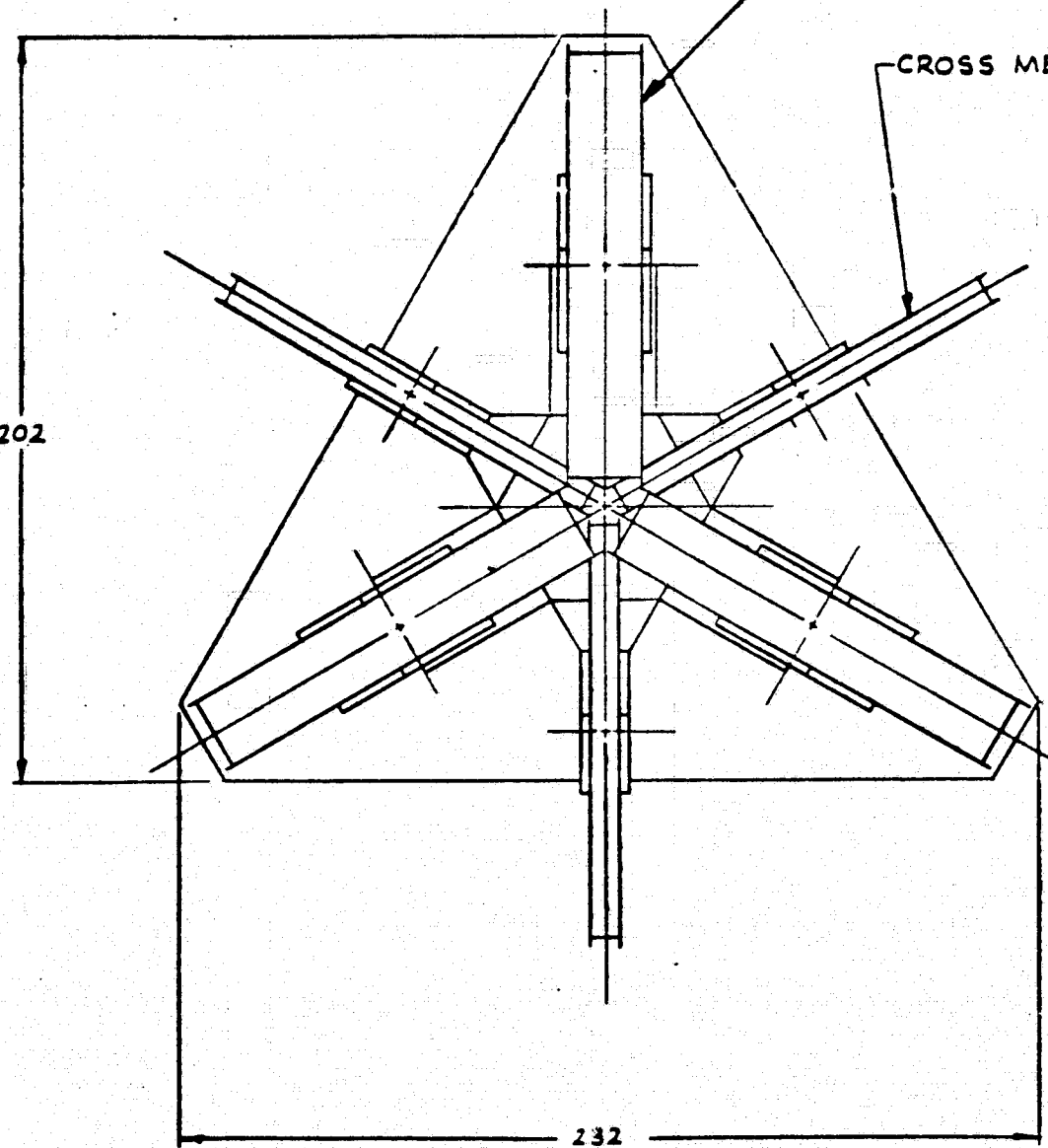
1

CAP MATERIAL STORAGE REE

CROSS MEMBER MATERIAL ST

202

232



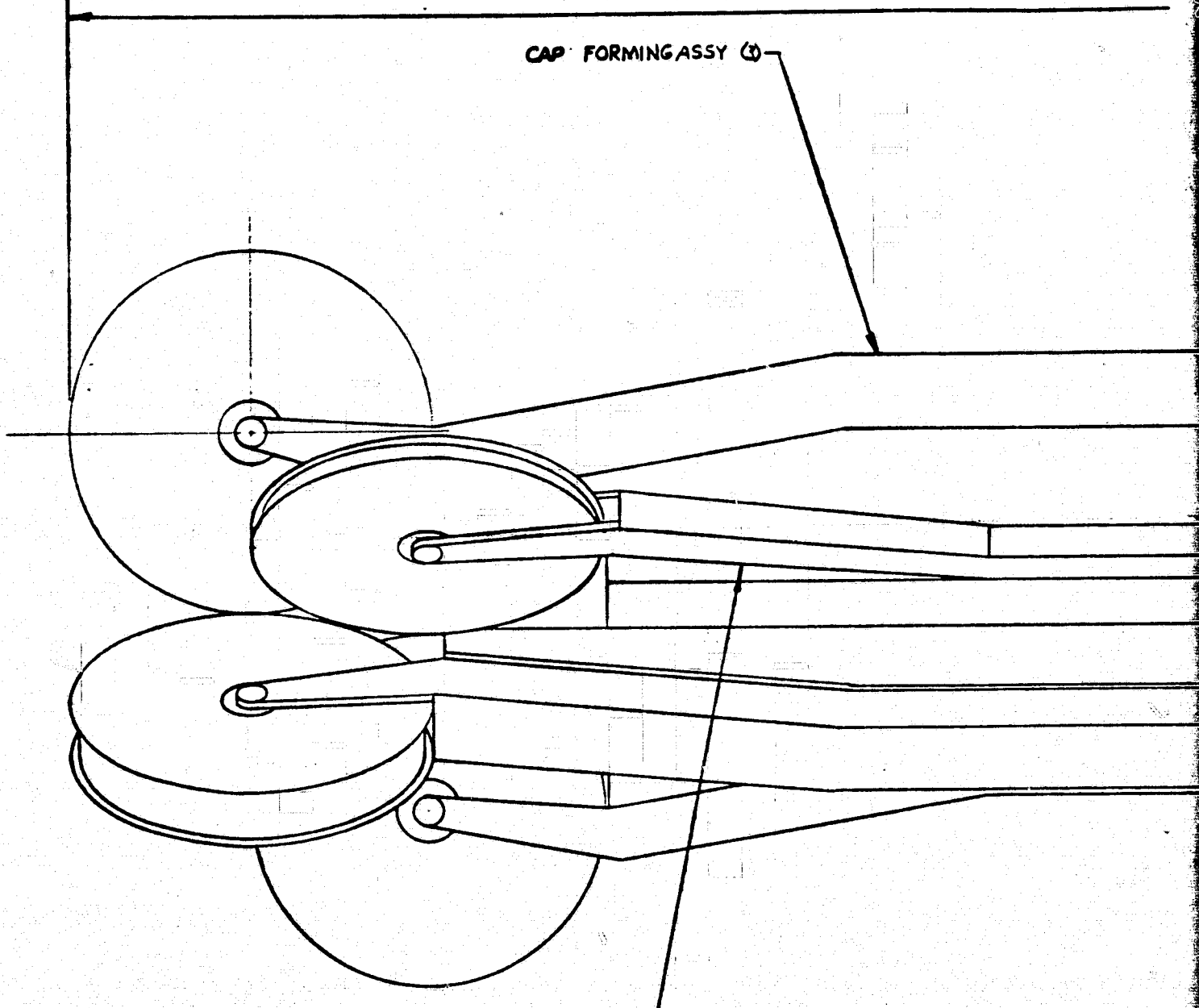
~~RELATION DRAWING~~

2

(3)

STORAGE REEL (3)

CAP FORMING ASSY (3)



CROSS MEMBER FORMING ASSY (3)

~~FRAME~~

3

732

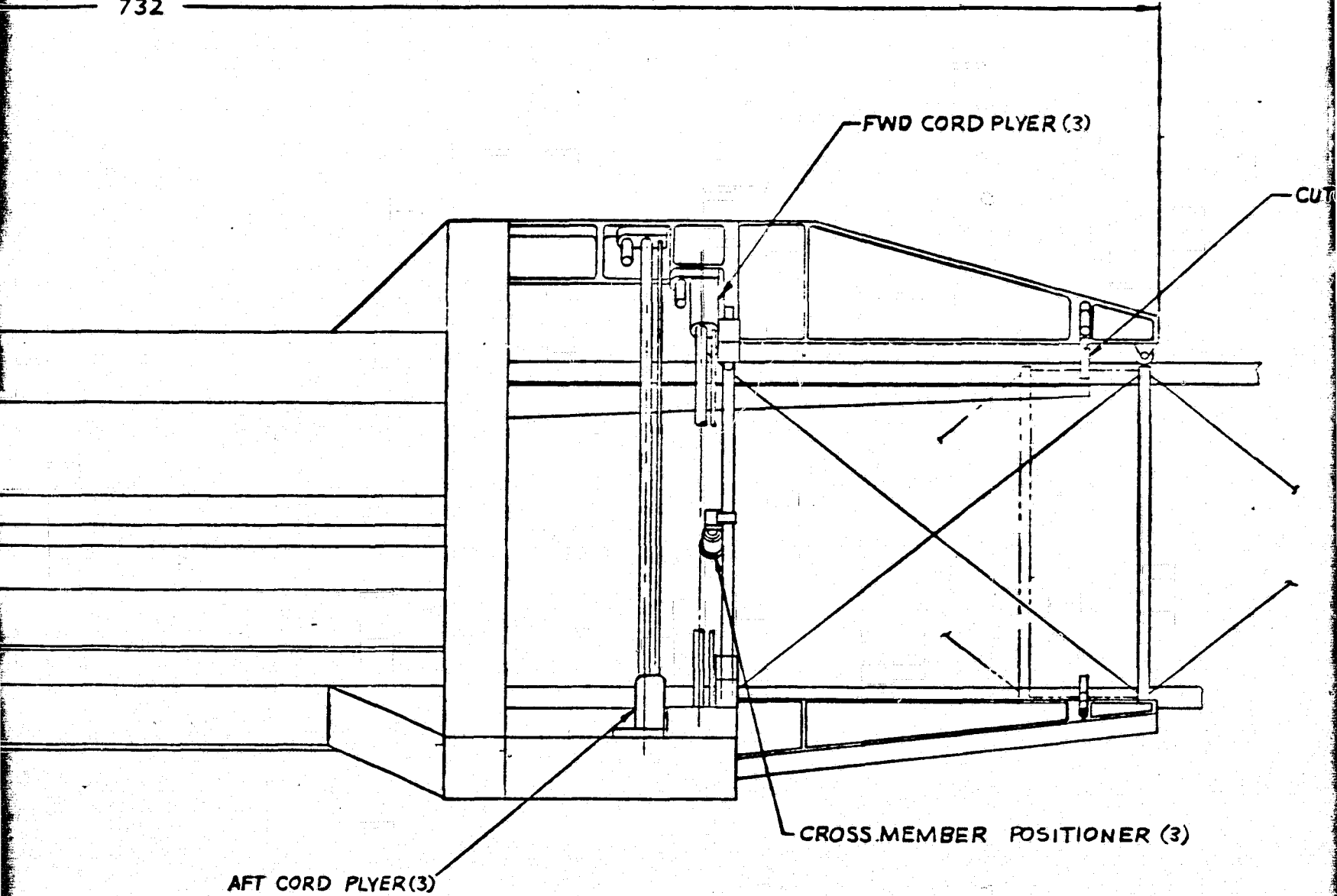


Figure 2-

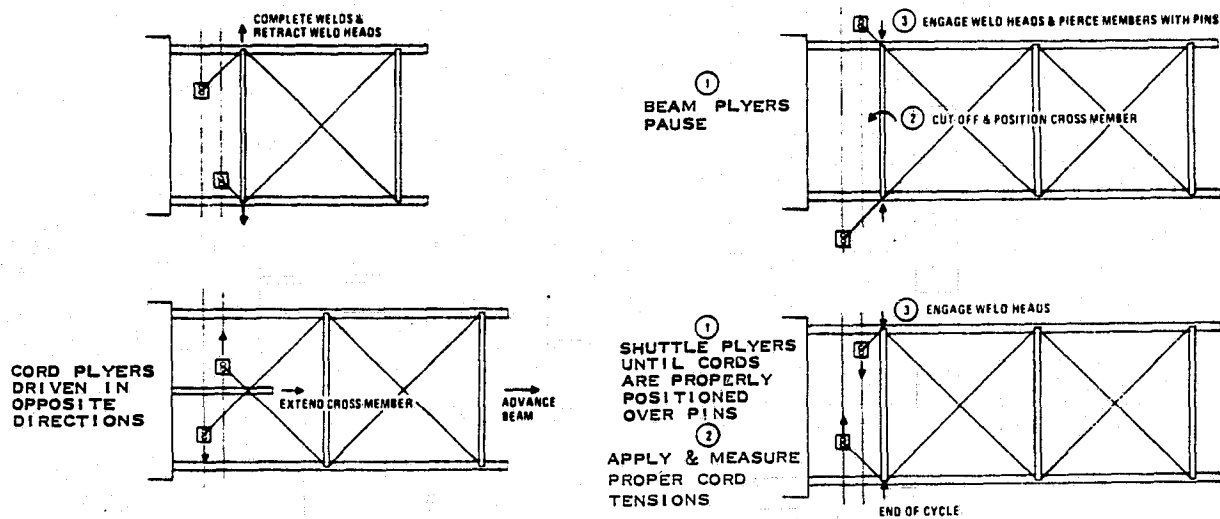


Figure 2-37. Baseline beam assembly sequence.

The baseline cap and cross-member forming machines include these processes:

- a. Storage - Flat continuous strips wound in rolls, cord wound on spools.
- b. Heating - Electrical resistance wire, reflective strip heaters.
- c. Forming - Rolltrusion.
- d. Cooling - Fluid-cooled platens.
- e. Drive - Friction roller drive.
- f. Cutoff - Shears.

The baseline beam builder can be programmed to fabricate a short (60 cm) bay for cutoff purposes. During this cycle, the cords are positioned along the caps during the welding sequence on the last cross-member set in the finished beam. The cords are positioned to the normal angle with the caps for the welding sequence on the first set of cross-members on the following beam. When the beam is advanced to the shear cutters, the caps are sheared in the center of the short bay which also severs the cords. Each end of each finished beam thus has 28 cm long cap stubs and loose cord ends.

The major advantages of this baseline concept are:

- a. Uses one type of forming process.
- b. Provides positive control of diagonal pretensioning.
- c. Requires least amount of material.
- d. Requires fewest number of welds.
- e. Has no major growth limitation.

Since energy use is a major driver for the SCAFE mission, an alternative concept was developed which would significantly reduce the energy required to operate the baseline machine. This alternative is shown in Figure 2-38 as Concept 2A.

Concept 2A uses the same processes and techniques as Concept 2 for cap forming, cord application, welding, and beam cutoff. Concept 2A uses prefabricated cross-members which are stacked closely and stored in a clip mechanism. The clip has a belt feed mechanism which advances the stack one member separation distance at a time. The cross-members are positioned by a swing arm positioner/handler mechanism.

2.2.1.4.3 Beam Builder Concept 3. The third beam builder candidate is shown in Figure 2-39. This concept uses the same basic processes as the baseline machine (Concept 2), except for the cord application process and welding technique.

The six diagonal cords are applied to the beam in a spiral pattern. The cord dispensers, tensioners, and storage spools are mounted on large diameter counter-rotating rings with three applicators per ring. The rings are the outer races of large diameter bearings.

As the beam advances during the run period, the two rings rotate 120° each in opposite directions until the cords are layed flat along the sides of the caps. Tension is applied to each cord by the cord tensioners. As the beam pauses, the cross-members are positioned and the weld heads are engaged. Six weld heads are used to spot weld the cross-members to the caps. Another six weld heads spot weld the cords to the caps.

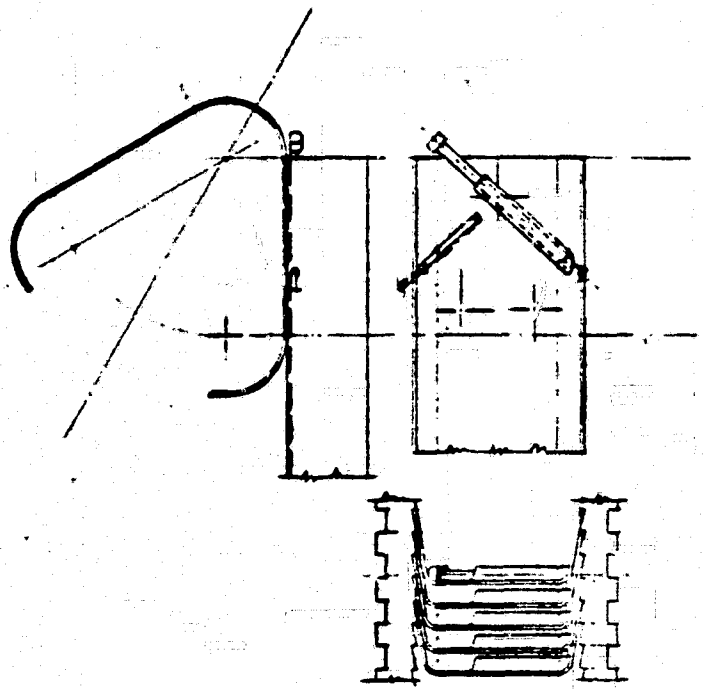
The major advantage of Concept 3 is that it greatly simplifies the cord application process. The disadvantages are:

- a. Six additional weld heads are required.
- b. The cord welds may affect the strength of the cord.
- c. Placing controls on the cord applicators is complicated by inability to use hardlines.
- d. The weight and reliability of large diameter bearings may be a growth limitation.

2.2.1.4.4 Beam Builder Concept 4. The fourth beam builder concept, shown in Figure 2-40, constructs the beam from rigid members. Beam builder Concept 4 has three cap forming machines and three side-member forming machines. These forming machines are like the baseline machines, except the side-member machines have larger storage reels and each machine alternately produces cross-members and diagonal members.

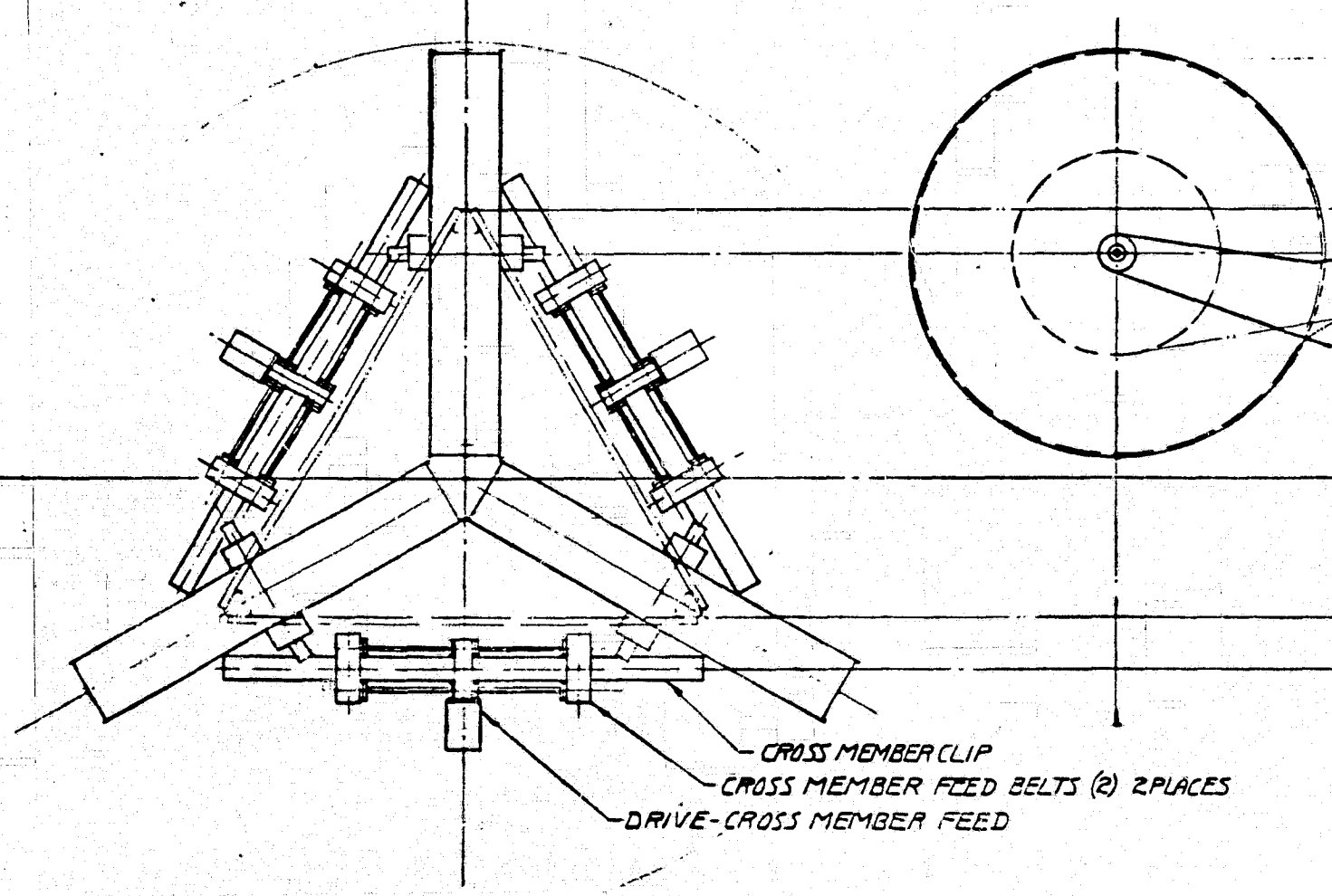
Concept 4 uses 12 ultrasonic weld heads and two weld stations. The forward weld station joins the forward end of the diagonal members to the caps. The aft weld station joins the aft end of the diagonals and the cross-members to the caps.

~~SECRET~~



DETAILS OF NESTED CROSS MEMBERS
AND CROSS MEMBER ATTACHMENT TO CAP SECTION

mm 0 50 100



- CROSS MEMBER CLIP
- CROSS MEMBER FEED BELTS (2) 2 PLACES
- DRIVE-CROSS MEMBER FEED

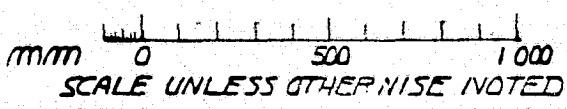
~~FRAME~~
2

CAP SECTION ROLLTRUDER

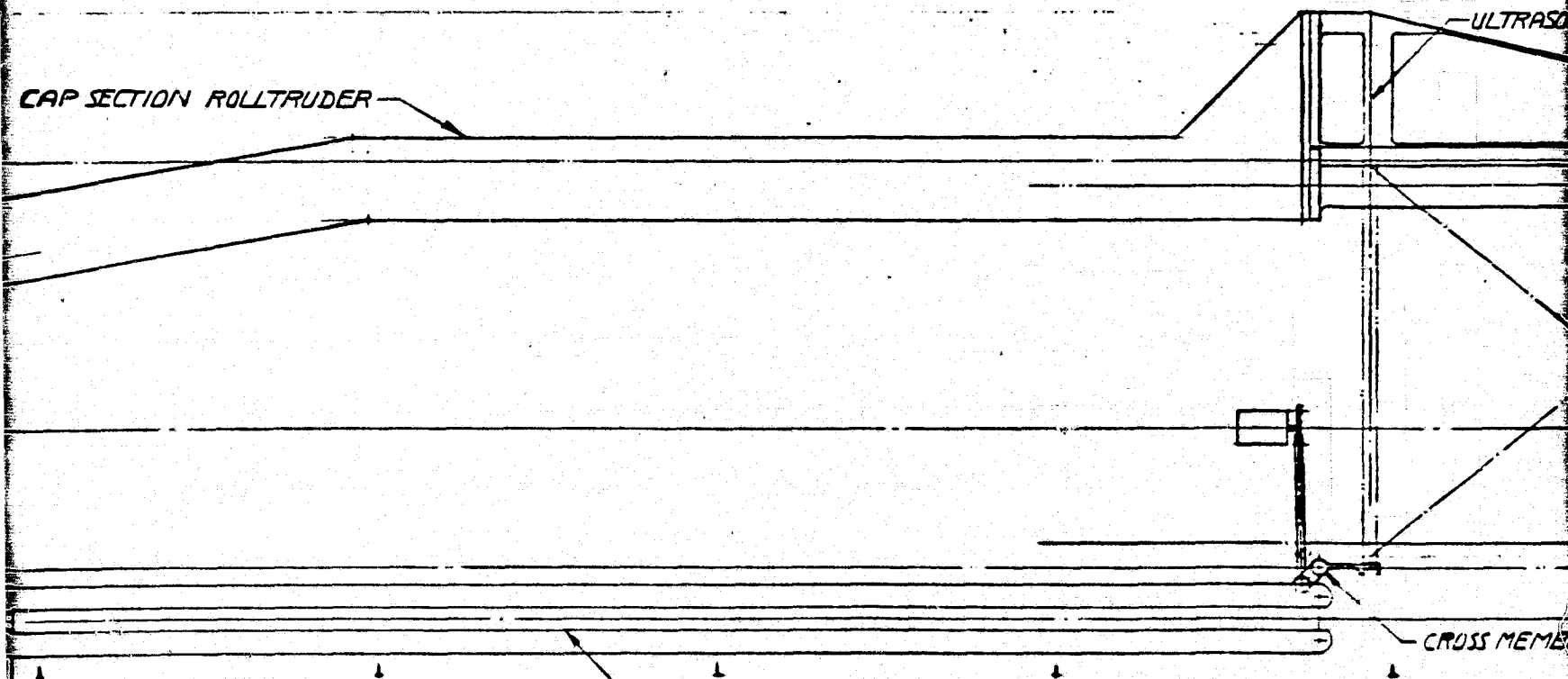
ULTRAS

CROSS MEME

CROSS MEMBER CLIP



OUT OF PLANE EQUIPMENT OMITTED FOR CLARITY



ORIGINAL PAGE IS
OF POOR QUALITY

~~FIGURE 2-38~~

3

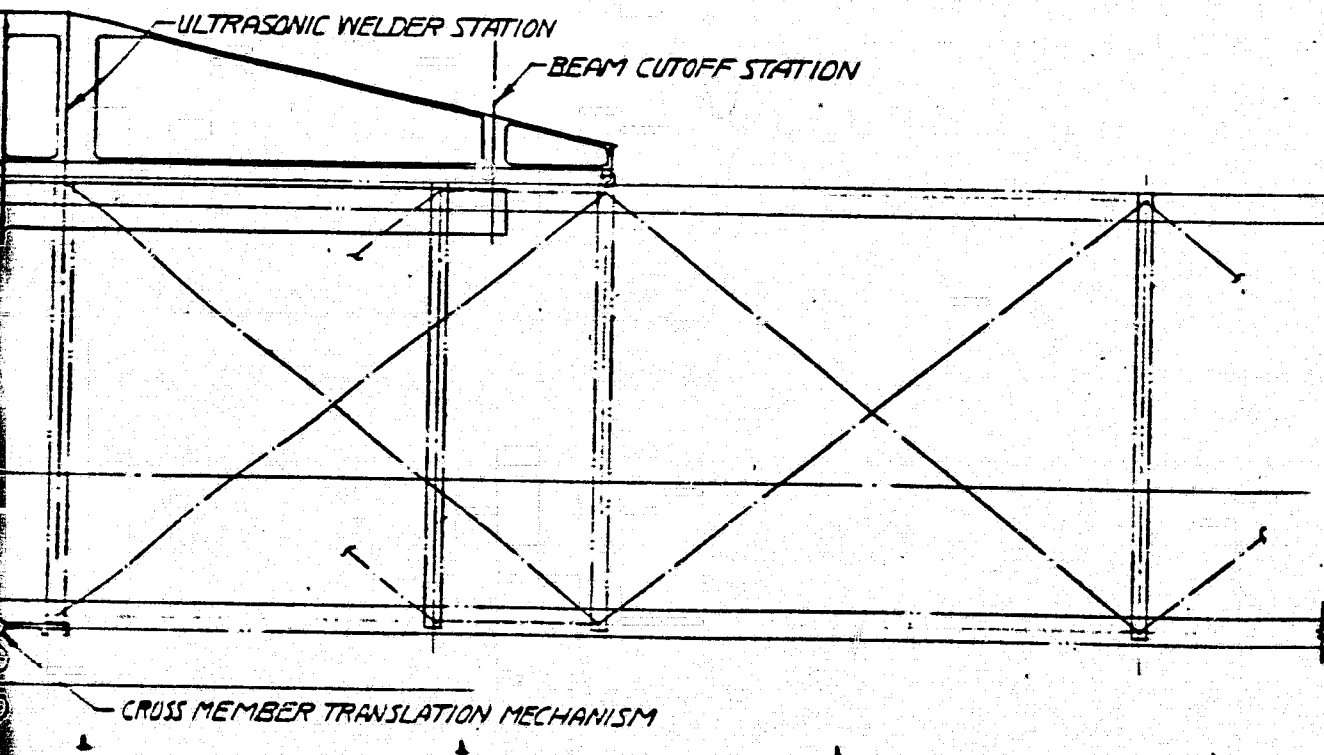
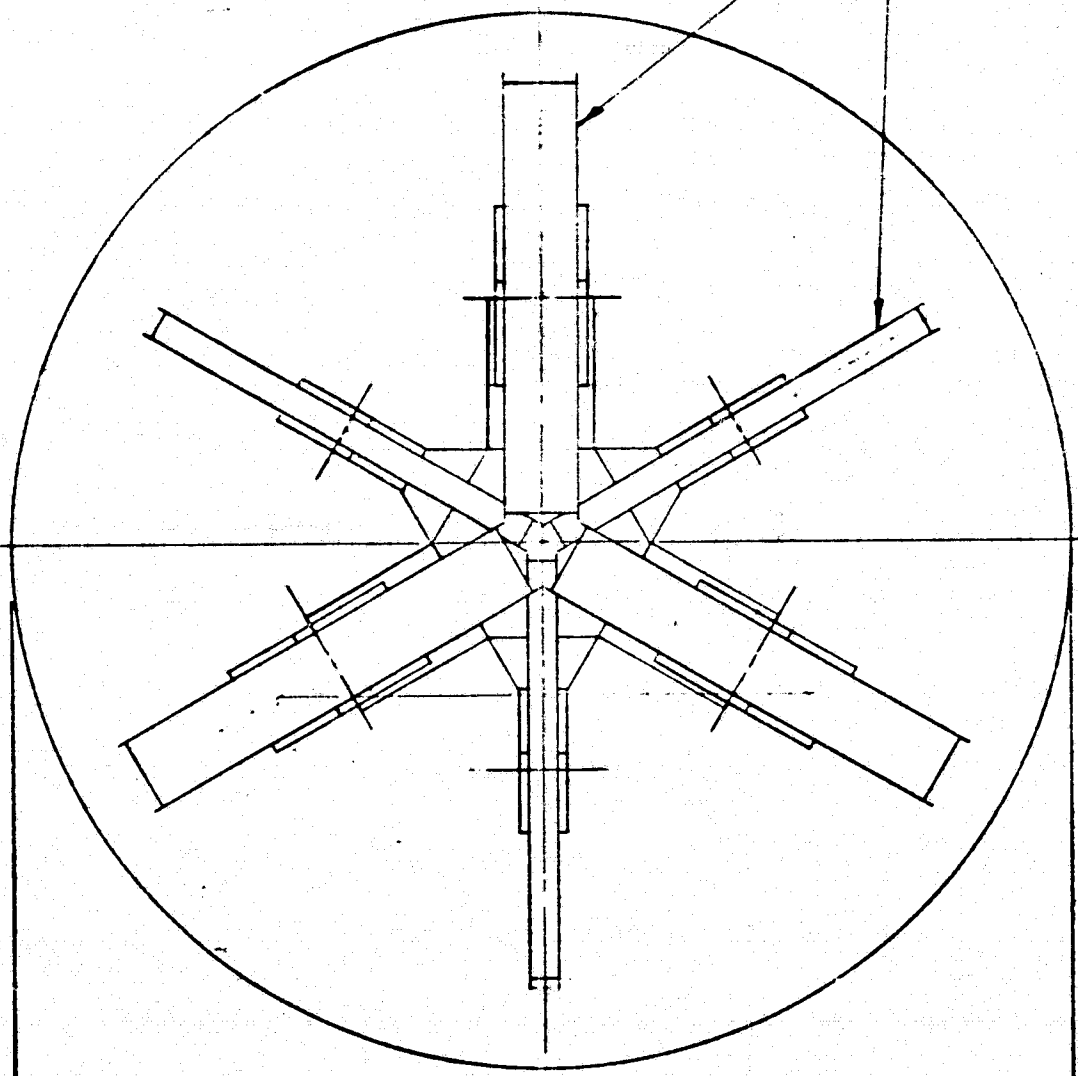


Figure 2-38. Be

~~SECRET~~ CB-14

1

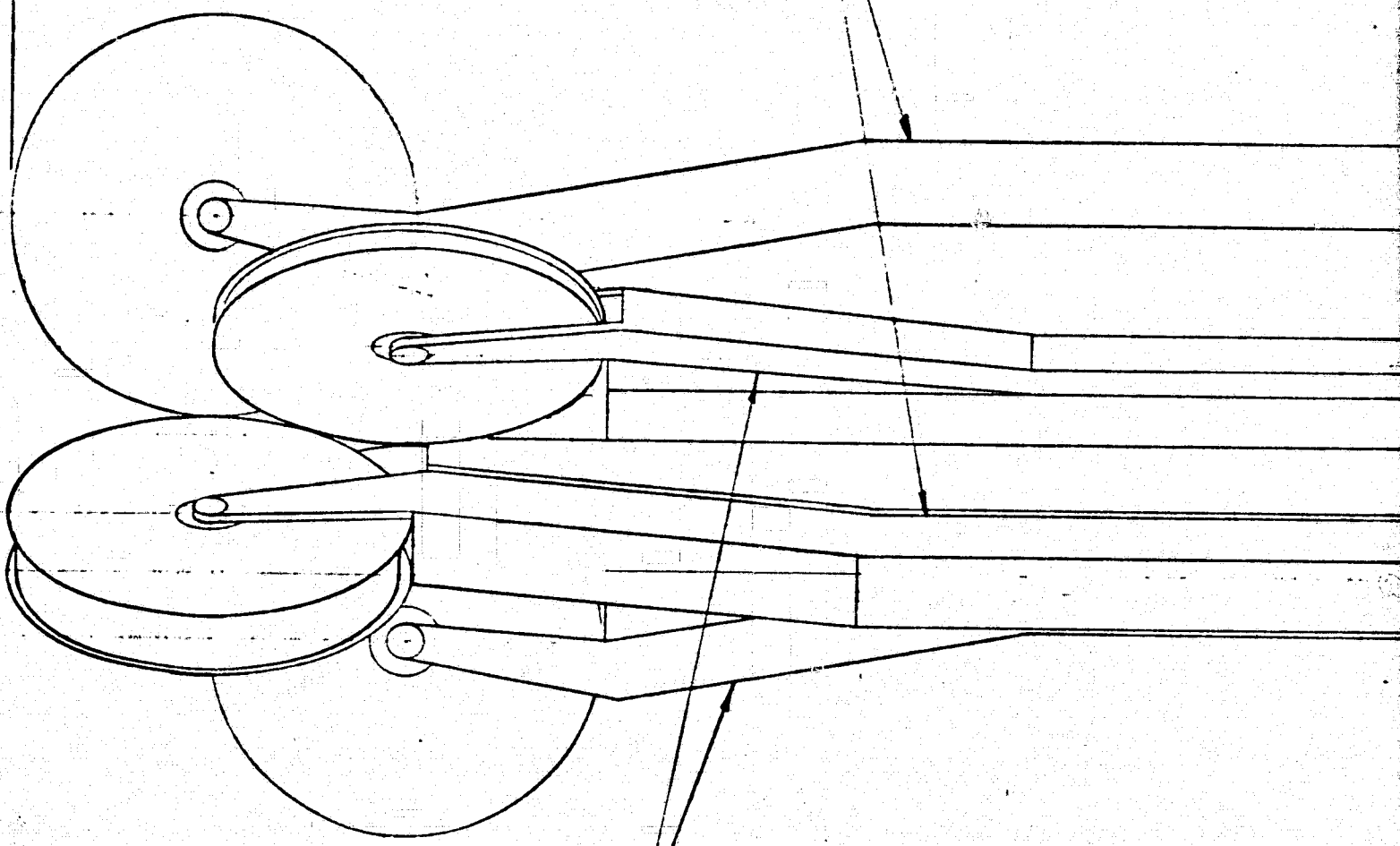
MATERIAL STORAGE REEL (6)



282
DIA

2

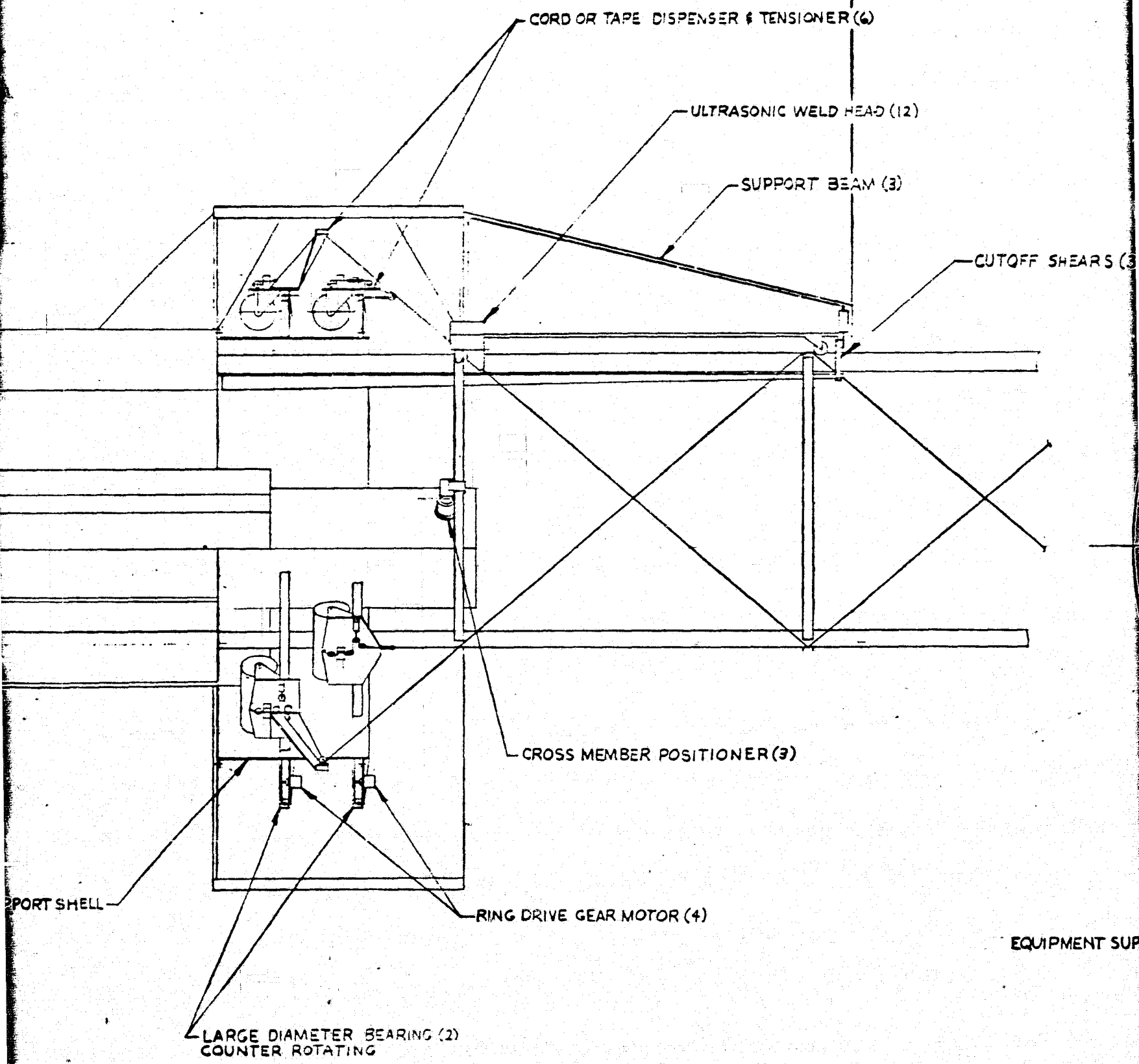
CAP FORMING ASSY (3)



CROSS MEMBER FORMING ASSY (3)

INNER SUPPORT

3



EQUIPMENT SUP

~~SECRET~~

4

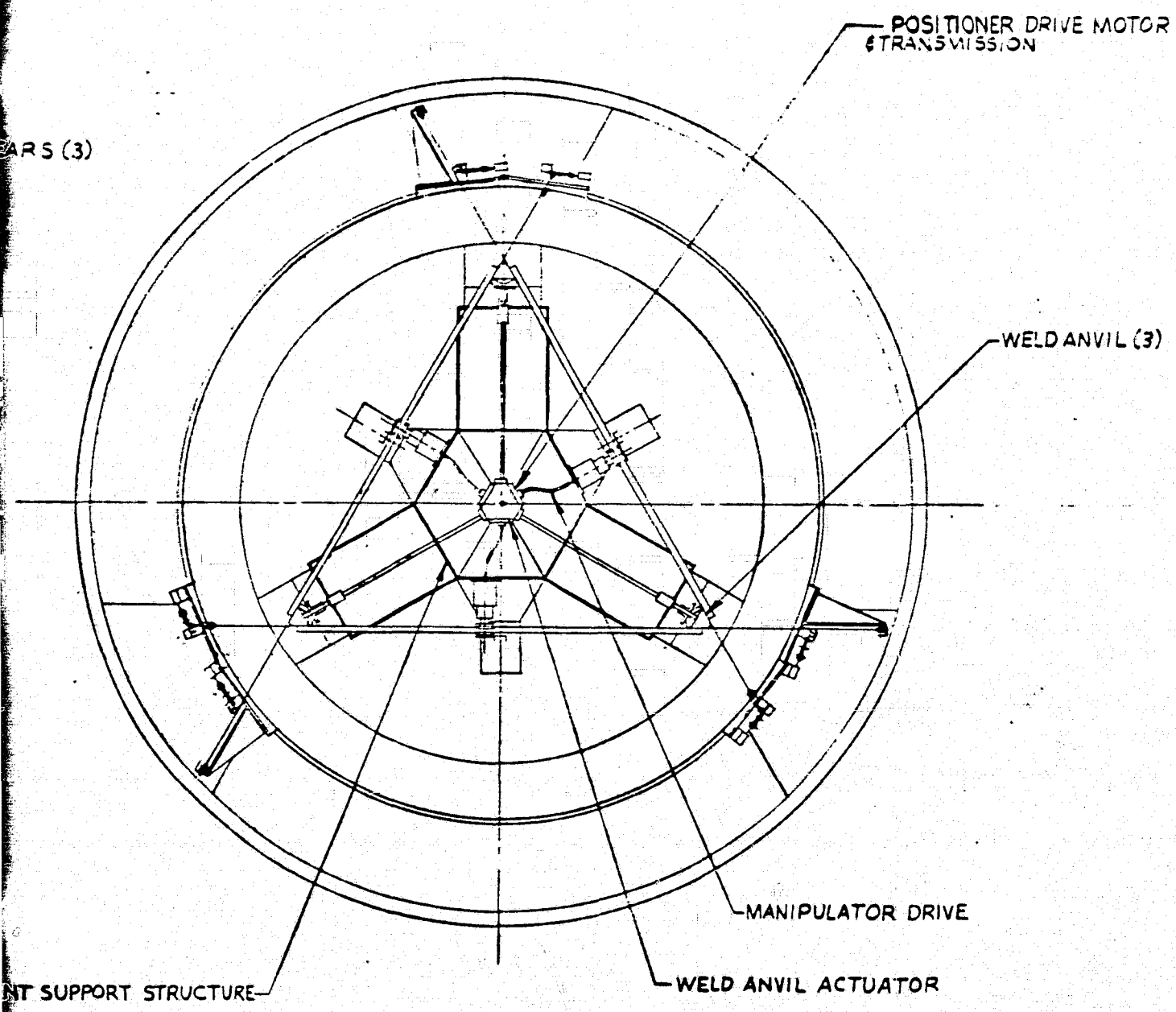


Figure 2-39. Beam

The side-member forming machines each have two cutoff stations to allow the lengths of the side-members and cross-members to be alternately set with the member centered on the handler/positioner mechanism. The handler/positioner grasps each member, rolls it 90° to put the base side toward the beam, then translates and rotates the member into position.

The assembly sequence for an 80-second cycle per bay length of beam is shown in Figure 2-41. The side-member forming machines must run 164% faster than the baseline cross-member forming machines in order to achieve a comparable beam production rate. This indicates a potential growth constraint with respect to beam fabrication rates. The major advantage of Concept 4 is that it eliminates the mechanisms and controls for applying diagonal cord members. The major disadvantages are: (1) the overall machine length is 2 m greater than the baseline concept due to the extra weld station and the large side-member material storage reel, and (2) heating and welding of the diagonal members causes this concept to have the highest energy requirements.

2.2.1.4.5 Concept Evaluation. Power and energy requirements for five beam builder concepts were determined and are compared in Table 2-15. These results indicate that Concept 2A requires the least on-orbit power and, with 8kW, Concept 4 requires the most power. It is further indicated that the bulk of the beam builder energy requirements result from the cap and cross-member heating sections (70% and 22%, respectively) and that welding and control operations are of minimal consideration. The greatest potential area for reducing power demand is to improve the material heating technique. Two methods were subsequently adopted: (1) maintaining a material bulk temperature above 294°K on the ground and maintaining it on orbit with insulation, and (2) use of a material with a lower transverse conductivity such as the hybrid glass/graphite laminate.

To aid selection of candidate options for further definitions, the baseline machine (Concept 2) and three other machine options were evaluated in terms of the criteria shown in Table 2-16. In addition, the beam structures produced by these machines were evaluated in terms of beam weight, beam size, scale-up potential, and structural performance.

The evaluation was performed using a numerical rating system. The resulting values shown in the table are based on assigning each option points using the selection criteria from the lower table and then normalizing each evaluation category to a base of ten to avoid decimals in the comparisons. Consequently, low values are good and percentage comparisons with the norm for the column are obtained by inspection. Cost and reliability considerations, while numerically not determined for each option, are assumed proportional to the averaged values of the design complexity, operating complexity, and production risk categories.

Table 2-15. Beam builder power and energy requirements compared.

- LEAST ON-ORBIT POWER WITH OPTION 2A
- APPROXIMATELY 70% OF POWER FOR CAP HEATING
- CONTROL/WELDING POWER MINIMAL CONSIDERATION
- STORAGE REEL PREHEATING OFFERS POTENTIAL POWER SAVING (47% AT 200°F)

PROCESS/BAY	BASELINE (OPTION 2)			
	ENERGY	AVE PWR.	PEAK POWER	% ENERGY
CAP HEATING/FORMING*	336.3KJ/BAY	4204.W	3876.1W 655.2 4531.3W	70.3%
CROSS MEMBER HEATING/FORMING*	106.9 KJ/BAY	1336.W	973.33 724.9 1698.W	22.3%
WELDING	21.6 WJ/BAY	270.W	900.W	4.5%
SUBSYSTEM ASSEMBLY & CONTROL	13.6 KJ/BAY	170.W	368.W	2.9%
TOTALS/BAY	478.4 KJ/BAY	5980.W	7497.3	100%

OPTION	1	2 BASELINE	2A	3	4
POWER AVE (W)	5196	5980	4570	6115	9063
POWER PW (W)	6377	7497	5662	7497	9347
ENERGY KJ/BAY	415.7	476.7	365.5	489.2	645.

*HEATING VALUES BASED ON PSEUDO ISOTROPIC TYPE MATERIAL

Table 2-16. Concept evaluation.*

Concept	Machine							Structure		
	Energy Use	System Complexity		Operational Complexity	Program Risk	Weight	Scale-Up	Weight	Scale-Up	Performance
		Mechanical	Control/Software							
1	18	22	10	12	12	43	Poor	15	Poor	?
2	27	12	15	12	15	10	Good	10	Good	✓
2A	10	10	10	10	10	11	Fair	10	Good	✓
3	29	18	15	15	17	14	Fair	10	Good	✓
4	52	24	18	15	19	15	Fair	14	Fair	✓

CRITERIA

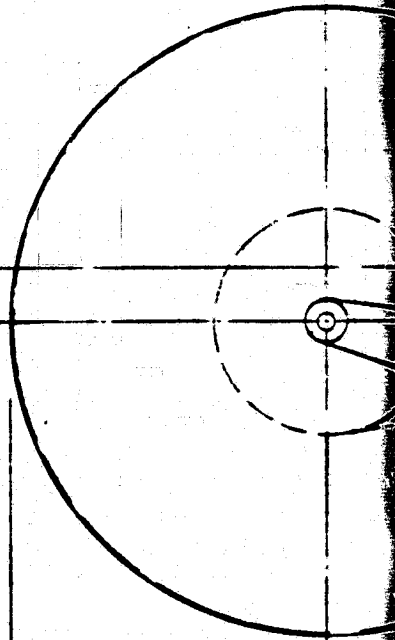
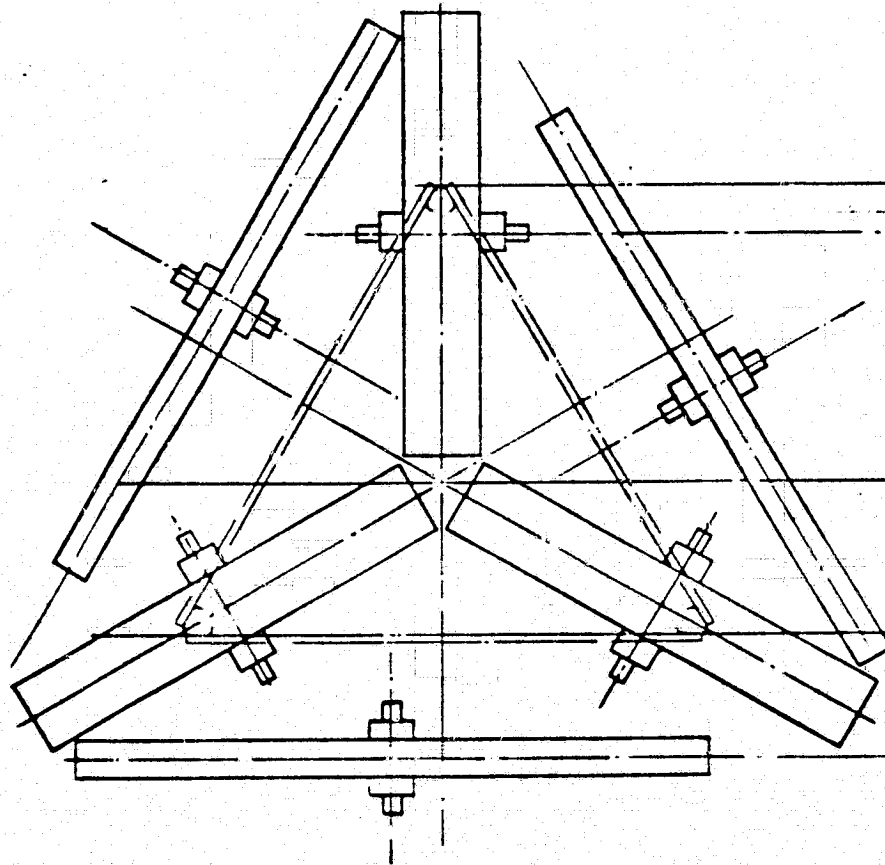
- Energy
- Mechanical
- Control/Software Complexity
- Operational Complexity
- Program Risk
- Weight - Machine
- Structure
- Scale-Up - Machine
- Structure
- Structure Performance

ASSESSMENT FACTORS

- 1 point per 10 K Joules over 300 K Joules
- 1 to 3 points per major assembly based on complexity
- 1 point per 20 motors, actuators, and sensors
- 1 point per assembly operating cycle per bay
- 4 points per new assembly design (no experience)
- 3 points per new assembly design (similar to previous design)
- 2 points per modification of new design
- 1 point per copy of new design
- 1 point per 100 lb over 5000 lbs
- 1 point per 1.0 kg/m unit weight
- Judgement based on amount of new design required to fabricate larger beams
- Judgement: Structure weight, potential transportation cost increases
- Judgement: Side member behavior predictability

* Assessment factors totaled and normalized to 10 for lowest sum.

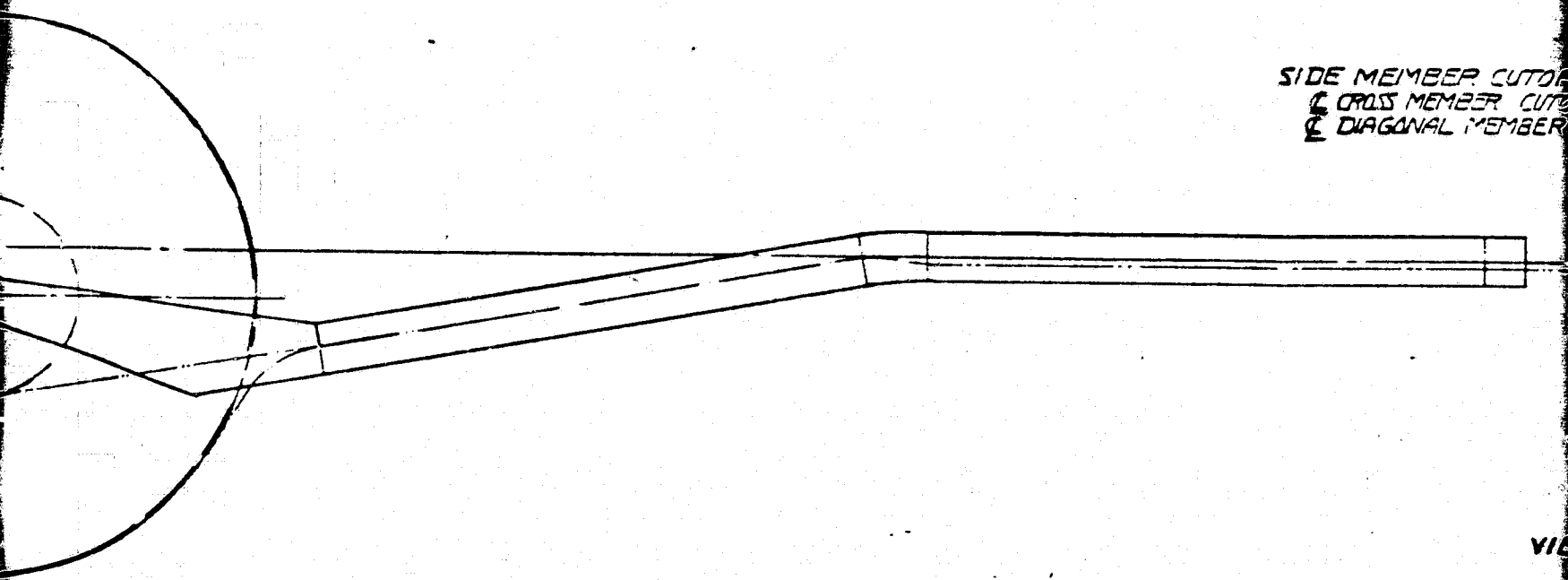
PROJECT FRAME



A

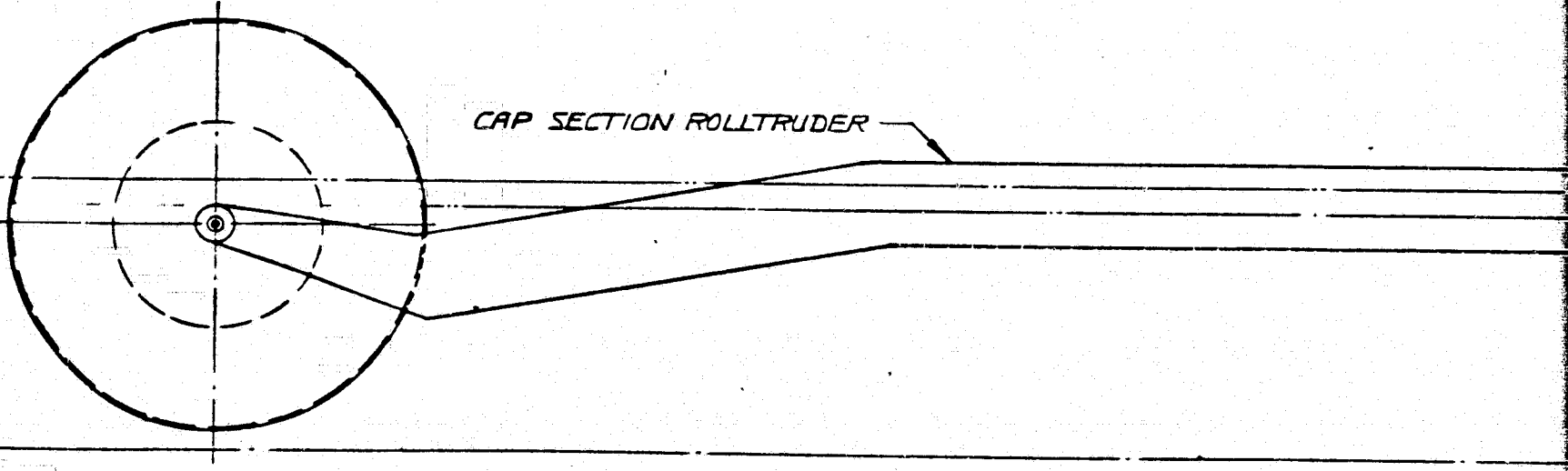
~~SECRET~~
2

SIDE MEMBER CUTOUT
C CROSS MEMBER CUTOUT
E DIAGONAL MEMBER

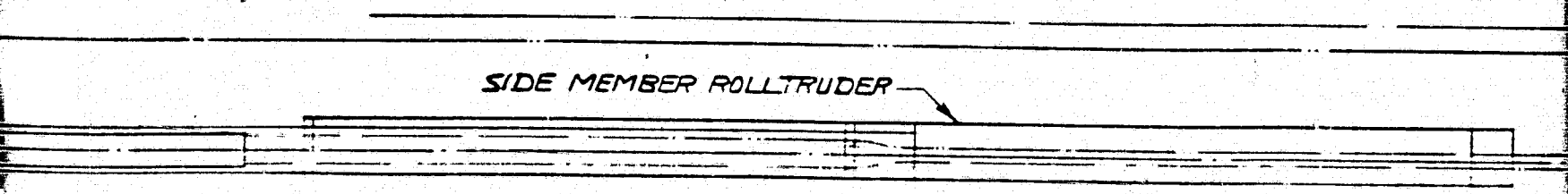


VIE

9 475.0



CAP SECTION ROLLTRUDER



SIDE MEMBER ROLLTRUDER

SIDE MEMBER MANIPULATOR STATIONS
 Ⓢ CROSS MEMBER DELIVERY STATION
 Ⓢ PICKUP STATION
 Ⓢ DIAGONAL MEMBER DELIVERY STATION

MEMBER CUTOFF STATIONS
 Ⓢ MEMBER CUTOFF STATION
 Ⓢ DIAGONAL MEMBER CUTOFF STATION

VIEW A-A

475.0

Ⓢ WELD STATION { BOTH ENDS OF CROSS MEMBER
 TRAILING END OF DIAGONAL MEMBER
 Ⓢ WELD STATION (LEADING END OF DIAGONAL)
 Ⓢ BEAM CUTOFF

3

Figure 2-40. Beams

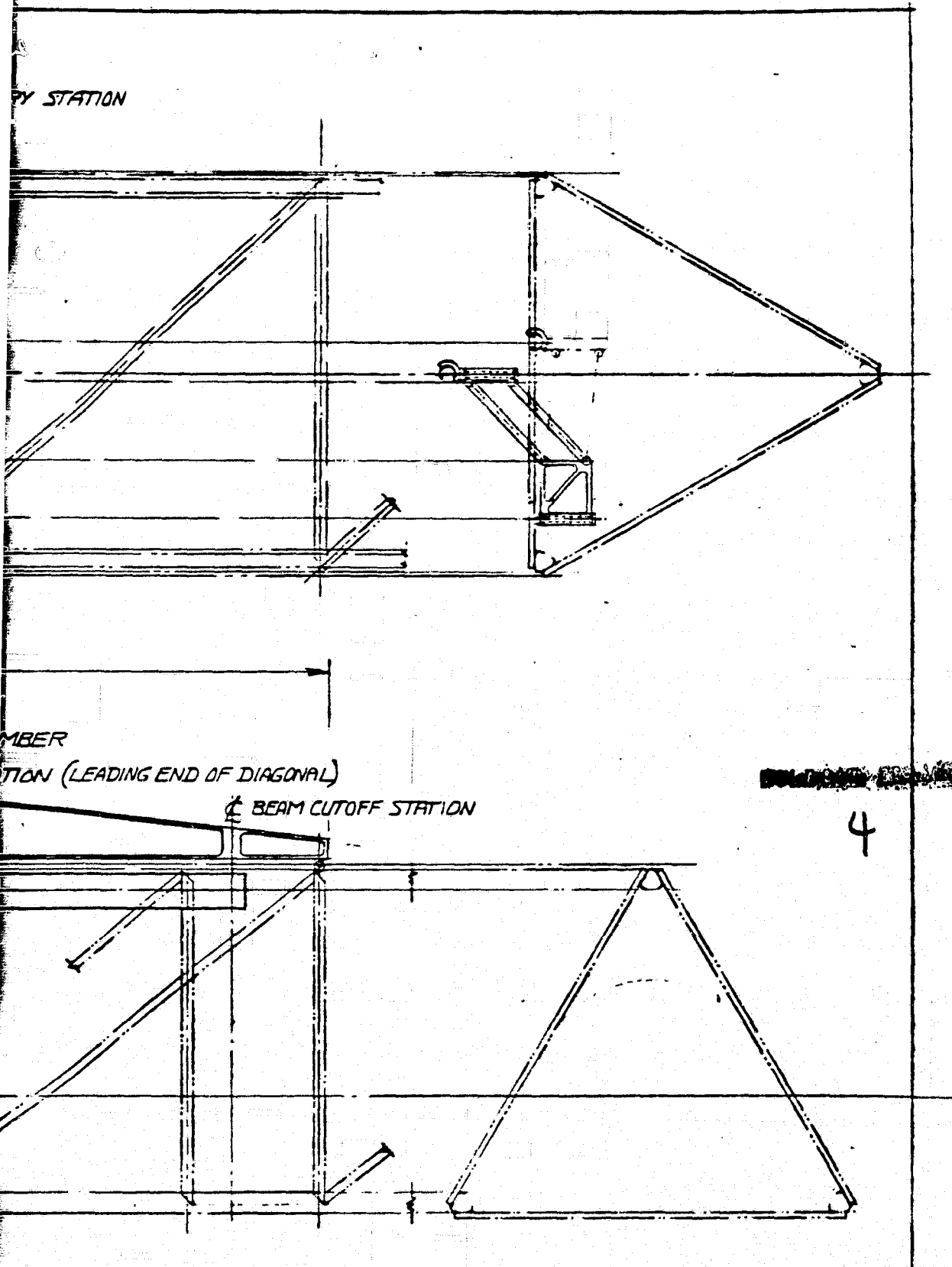


Figure 2-40. Beam builder concept 4 layout.

2-63/-64

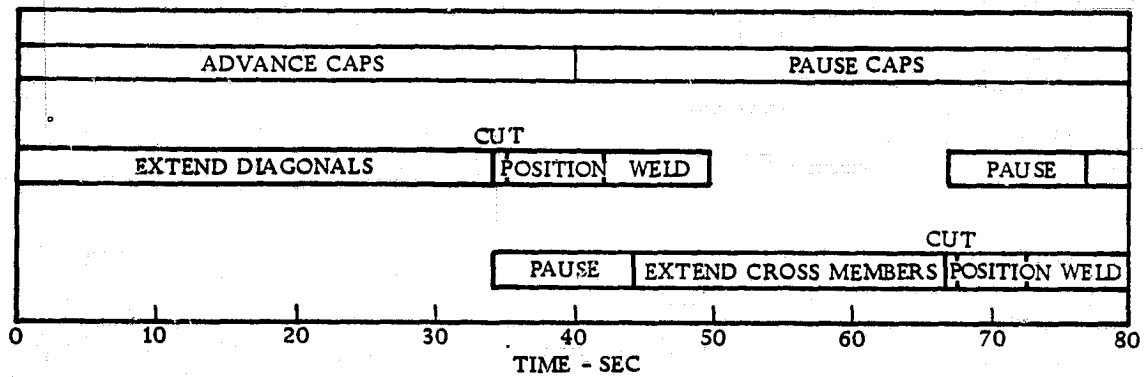


Figure 2-41. Beam builder concept 4 assembly sequence.

2.2.1.4.6 Concept Selection. The results of the concept assessment are summarized in Table 2-17. The selection became a choice between Concept 2 and Concept 2A. It was a decision between the machine with the best scale-up capability which has more energy requirements versus the machine with the lowest energy requirements but not as suitable for scale-up.

Table 2-17. Summary Assessment.

Concept	Principal Discriminators	
	Pro	Con
1	<ul style="list-style-type: none"> ● Low Energy ● Simple Control/Software 	<ul style="list-style-type: none"> ● Heavy Machine, Structure ● Poor Machine, Structure Scale-up ● Diagonal Preload ??
2	<ul style="list-style-type: none"> ● Low Risk ● Light Machine, Structure ● Low Mechanical Complexity ● Good Machine, Structure Scale-up 	<ul style="list-style-type: none"> ● Intermediate Energy
2A	<ul style="list-style-type: none"> ● Low Energy ● Low Overall Complexity ● Low Program Risk ● Light Machine and Structure ● Good Structure Scale-up 	<ul style="list-style-type: none"> ● Fair Machine Scale-up
3	<ul style="list-style-type: none"> ● Low Risk ● Light Structure ● Good Structure Scale-up 	<ul style="list-style-type: none"> ● Fair Machine Scale-up (Bearings) ● Moderate Design Complexity ● Intermediate Energy
4	<ul style="list-style-type: none"> ● Simple Structure 	<ul style="list-style-type: none"> ● High Energy ● High Machine Complexity ● High Structure Weight ● High Risk ● Fair Scale-up

Development of Concept 2A in SCAFEDS provides an alternative process for the fabrication and installation of cross-members. Concept 2 uses the same basic roll-trusion process for fabrication of cross-members. This factor plus the assurance of low energy use led to the final selection of Concept 2A as the SCAFE beam builder.

2.2.1.5 Selected Beam Builder Preliminary Design. The Part I trade studies of beam builder candidates, and process and technique options resulted in the selection of the configuration shown in Figure 2-42 as the baseline for Part II preliminary design development. This configuration operates as a cyclic feed fabricator, i.e., the machine is programmed to extend the beam one bay length in 40 seconds, then pause 40 seconds to permit assembly and joining of the beam members. Other preliminary performance data are summarized in Table 2-18.

Preliminary design layouts of the selected beam builder concept are shown in Figures 2-43 through 2-47. This section presents the description and function of the mechanical subsystems.

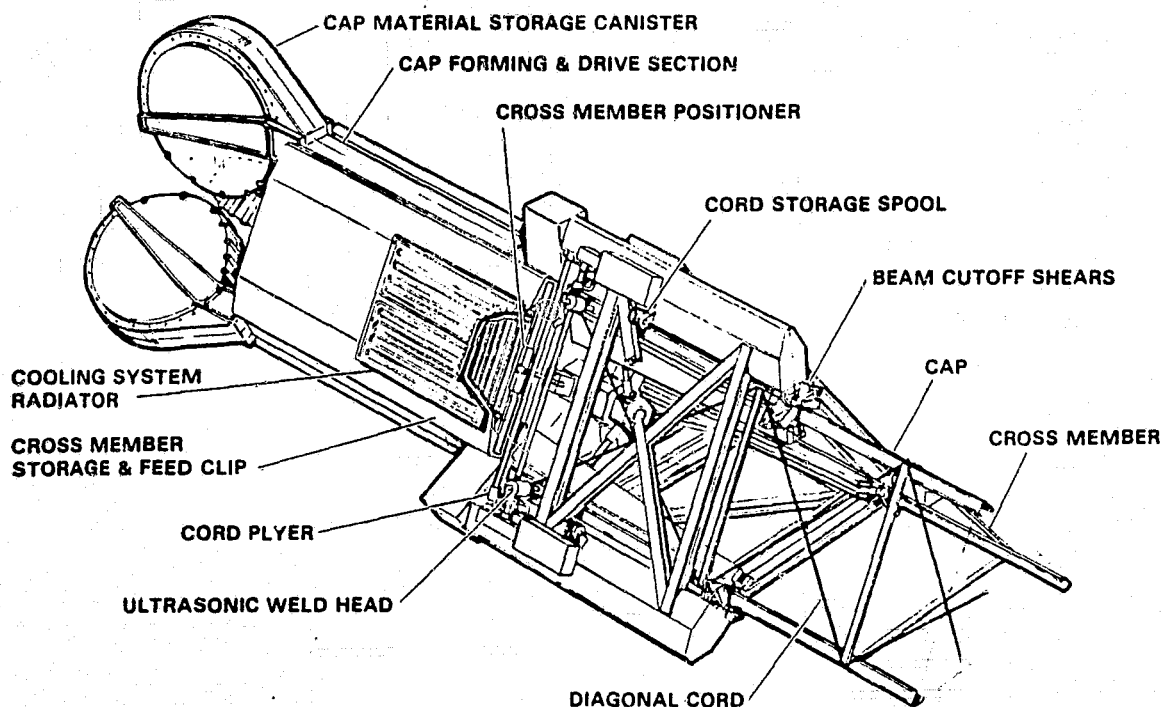


Figure 2-42. SCAFEDS beam builder selected concept.

2.2.1.5.1 Cap Forming Machine Subsystem. The cap forming machine subsystem general arrangement is shown in Figure 2-44.

The cap forming machine assembly contains all elements necessary to continuously process flat strip glass/graphite/thermoplastic material into the baseline cap configuration. Approximately 918 m of material is coiled in the roll retained in the storage canister. The roll turns freely on bearing-mounted rollers and unwinds uniformly as

Table 2-18. Beam builder preliminary design and performance data.

PROCESS OR SUBSYSTEM	PARAMETER	LIMITS OR TOLERANCE
Material Storage	Roll O.D.	121.4 cm Max
	Roll I.D.	60 cm Min
	Roll Length	918.2 m
	Roll Width	19.05 cm
	Roll Weight	262.2 kg
Heating	Temperature Limits:	
	1st Stage	482°K
	2nd Stage	707°K
	Forming Section	707°K
	Start-Up Time	430 seconds
Forming	Forming Section Length	
	Max. Forming Rate	Not Determined
Cooling	Actuation Time	0.2 seconds
	Actuator Stroke	0.32 cm
	Max. Cooling Time	12 seconds
Drive	Cap Stroke Tolerance	± TBD
	Cap Speed	3.585 cm/sec
	Max. Acceleration	1.3 cm/sec ²
	Max. Force Capability	533N
	Max. Force Required	311N
	Run Time	40 seconds
	Pause Time	40 seconds
Cord Storage	Cord on Spool:	
	Length	1219 m
	O.D.	13.12 cm
	I.D.	7.62 cm
	Width	13.12 cm
	Weight per Spool	2.13 kg
	Spool Drag Torque	56.5 ± 5.6 N-cm
Cord Tensioner	Tensioning Force	44.5 ± 8.9 N
	Spring Stroke	21.2 cm
	Spring Load Rating	89 N
	Max. Cord Speed	11.3 cm/sec
	Pulley Diameter	7.1 cm
Cord Plyer	Travel Speed	10.7 cm/sec
	Pulley Diameter	7.1 cm

C-2

Table 2-18. Beam builder preliminary design and performance data. (Concl'd)

PROCESS OR SUBSYSTEM	PARAMETER	LIMITS OR TOLERANCE
Clip Storage and Feed	Capacity	650 pieces
	Weight of Cross-Members	79.8 kg
	Feed Rate	0.4 cm/sec
Cross-Member Positioner	Time to Position Cross-Member	3 sec
	Separation Time	1 sec
	Return Time	4 sec
Welding Mechanism	Stroke	4 cm
	Time to Engage and Pierce	3 sec
	Time to Engage for Weld	0.2 sec
	Weld Time	2 sec
	Cooling Time	1 sec
Cutoff Mechanism	Retraction Time	3 sec
	Time to Engage and Shear	1 sec
	Time to Retract	1 sec

material is used. The canister is in two halves, with one half hinged to permit the material roll to be inserted. When the canister is closed and latched, an access panel in the hinged half is opened to allow the material to be manually routed over the heating section guide rollers into the forming section manual feed rollers.

The heating section is partially built into the storage canister with resistance strip heaters and parabolic reflectors mounted on the access panel. The heating section extends from the access panel up to the point where the material starts to form.

The material passes from the heating section through the forming section. The rolltrusion forming section is also equipped with strip heaters which heat the partially formed material in preparation for start-up of the machine.

The material then passes from the forming section into the cooling section where it is contact cooled by aluminum platens. Cooling fluid is supplied to the inside cooling platens and expelled as waste heat by an independent cooling system in the beam builder. Waste heat is also extracted from the heater reflectors by the cooling fluid loop. The cooling platens cool one bay length of cap section during the 40-second pause period.

The drive section has four friction-drive rollers which provide the necessary pull force on the cap to draw the material from the storage roll through the heat/form/cool sections. The three cap drive sections also provide the push force to advance the beam out of the beam builder.

2.2.1.5.2 Cross-Member Subsystem. The cross-member subsystem general arrangement is shown in Figure 2-46.

The cross-member clip is constructed of machined aluminum sections. Two mating center support panels are joined by two end piece assemblies to form the basic clip structure.

The stack of cross-members is supported and fed to the beam assembly process by four timing belts. The clips are indexed on the belts by serrations on the mating surfaces of the belts. The belt drive and belt pulleys are mounted on the center support panels. The clip holds 650 cross-members.

The clip is loaded and assembled by laying the stack of cross-members on one of the center support/belt drive subassemblies. The second center support/belt drive subassembly is then layed on the stack and all belts inspected for proper mesh with the cross-members. The end pieces, which consist of two mated halves, are bolted to the center supports.

The feed drive is a redundant motor drive which provides simultaneous output to all four feed belts. The retainer mechanisms at the output end of the clip are described below.

Mounting pads on the inboard center support allow the clip assembly to be bolted to the beam builder structure.

The cross-member positioner/handler mechanism transports one cross-member at a time from the storage clip to the installation position on the beam. During the run period, when the beam is advancing one bay length, the positioner/handler is fully retracted with the handler below the plane of the beam side. This allows the last cross-member installed to clear the handler and also allows the cord plyers to pass over the handler/positioner.

At some time after the cord plyers have completed their stroke, each position arm is rotated and translated into position for receiving the next cross-member from the clip. The cross-member retainers on each end of the next cross-member are retracted and the clip drive stepper motors are activated. When the stack has moved about 0.4 cm, a sensor in the cross-member handler is triggered. This causes the clip drive motors to stop and cross-member retainers to engage and retain the next to last cross-member. The fingers on the handler also close and grasp the next cross-member to be installed.

The cross-member positioner arm is rotated and translated to remove the cross-member from the clip and lay it in proper position for welding to the cap members. After welding is complete, but before the beam is advanced, the handler fingers are opened and the positioner arm rotated to drop the handler below the plane of the beam side.

2.2.1.5.3 Diagonal Cord Applicator Subsystem. The subsystem arrangement for applying the diagonal cord members is shown in Figure 2-45. The cord storage and tensioner mechanisms are shown in Figure 2-43.

The cord pleyer mechanism consists of six reciprocating cord pleyer subassemblies. Each pleyer is driven along a guide beam by a motor-driven ball reverser lead screw. Each guide beam is equipped with position sensors to monitor the six positions of each cord pleyer. Cord is supplied to each pleyer from a storage spool over a series of pulleys. The inboard pulleys on the cord pleyers are mounted on swivels to allow the cord to be properly aligned as the cord pleyer changes position.

Forward and aft cord pleyers permit the two cords on each side of the beam to be applied without interference between the moving pleyers. The aft cord pleyers have a longer stroke than the forward cord pleyers because they are set back 13.5 cm from the forward cord pleyers. This requires more lateral motion to achieve the required angle between the cord and the caps.

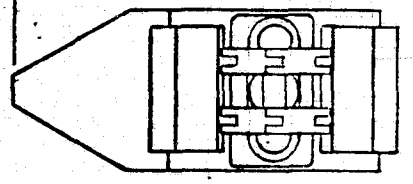
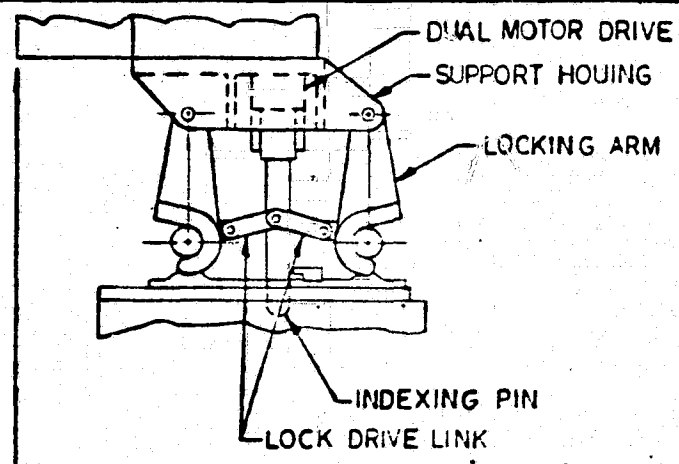
The forward cord pleyer must always complete its stroke to the outboard position ahead of the aft cord pleyer to avoid a collision with the cord of the aft pleyer at the apex of the beam. Similarly, the aft cord pleyer must always move from the outboard position first.

The forward and aft cord pleyers each have redundant motor drives. Two of the three lead screws are motor driven while the third is driven at either end by a flexible drive shaft. Should one of the two drives fail, the other would drive all three lead screws. The cord pleyers are all driven at an average velocity of 10.7 cm/sec.

The cord tensioner mechanism operates in two modes. The first mode is the supply mode where cord passes freely from the storage spool to the cord pleyers. The second mode is the tensioning mode whereby the free-turning capstan is stopped and held by an electric-operated clutch brake. This causes the traveling pulley to extend under the force applied by the constant-force spring. A tension force equal to one-half the spring force is thus applied to the cord. Total spring force is measured by a force transducer attached to a guide pulley.

A cord tension force of 44.5 ± 8.9 N is applied to each cord during assembly. This preloads the cords sufficiently to preclude any slackening or over tensioning due to thermal and deflection effects. The ± 8.9 N variation limits the theoretical twist and deflection in the beam to less than 1.2° of twist and 0.5 cm of tip deflection for a 200 m beam.

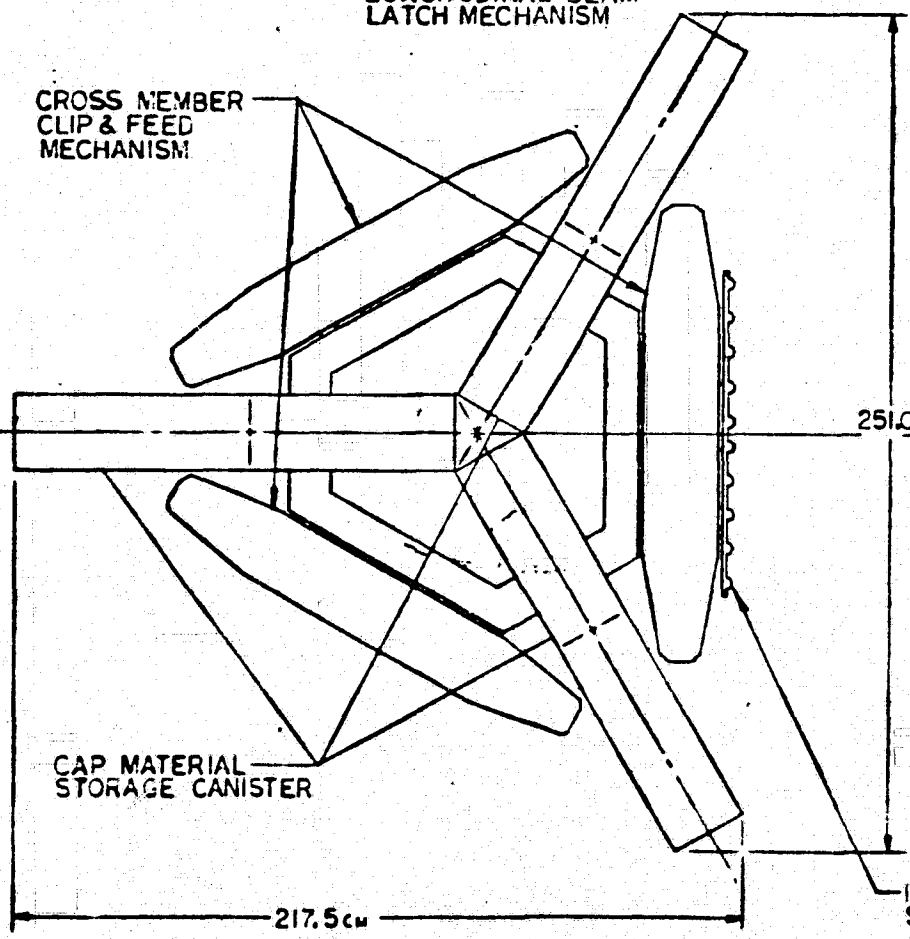
The stroke of the traveling pulley assures that a constant force is maintained on the cord throughout the assembly sequent. As the cord pleyers move from the outboard position to the ready-to-weld position, the traveling pulley automatically compensates for the change in cord length. The cord pleyer timing sequence is illustrated in Figure 2-48.



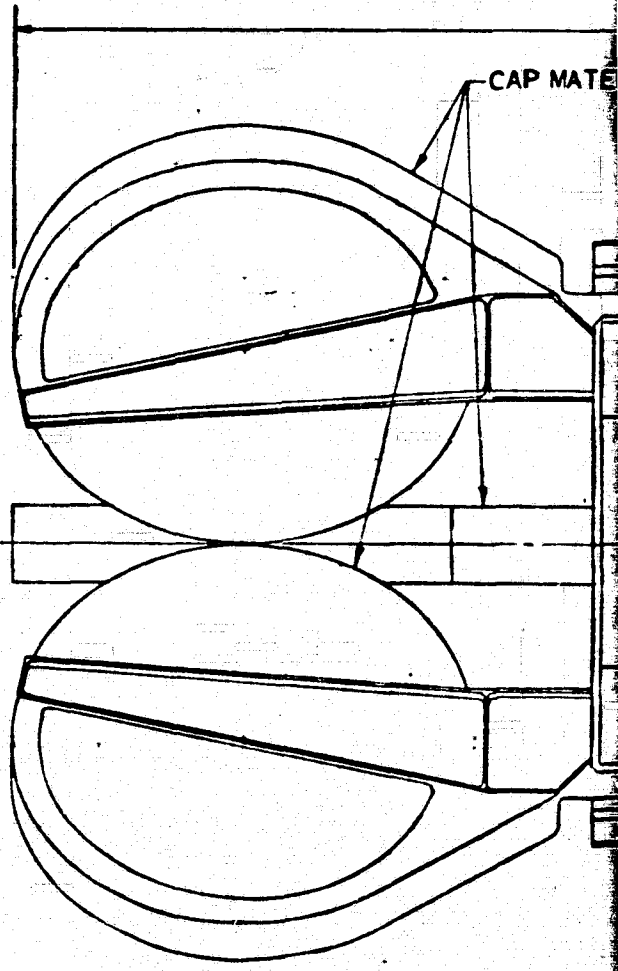
DETAIL T
SCALE 1/3
LONGITUDINAL BEAM
LATCH MECHANISM

~~SECRET~~

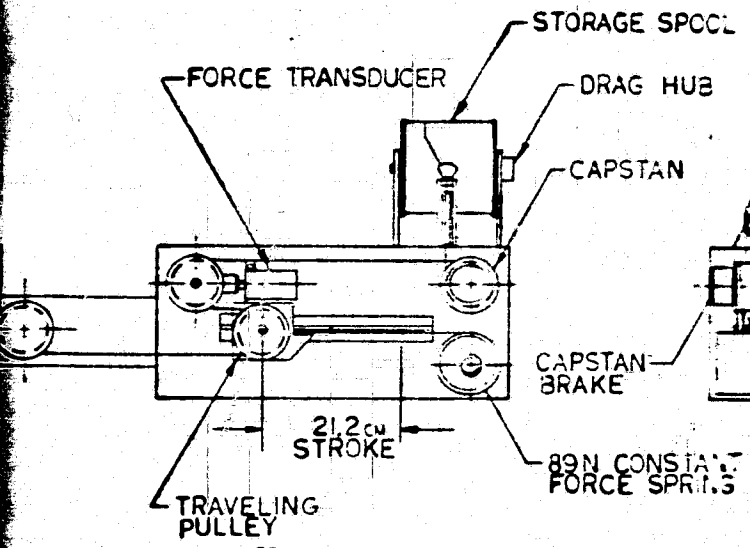
CROSS MEMBER
CLIP & FEED
MECHANISM



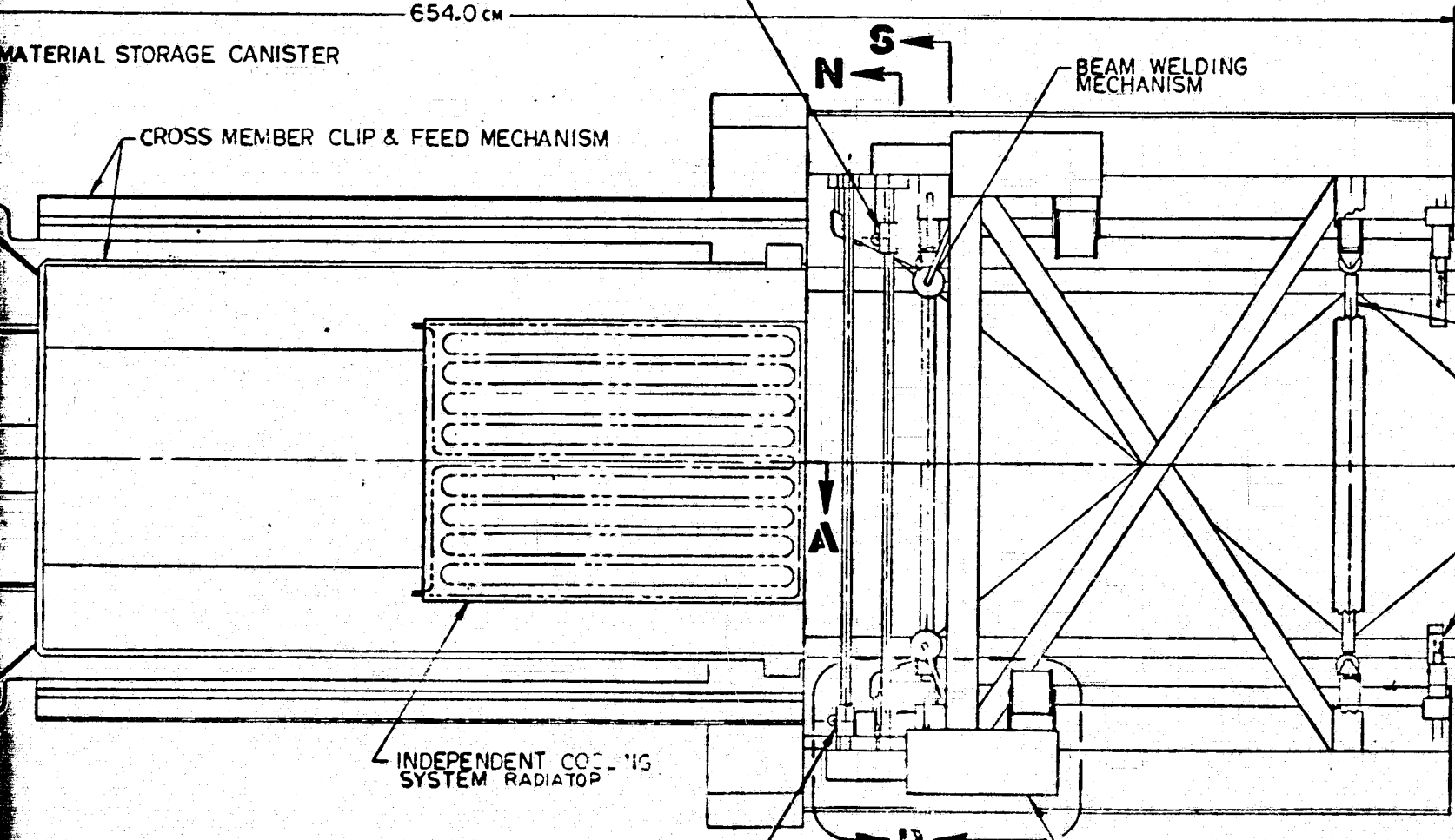
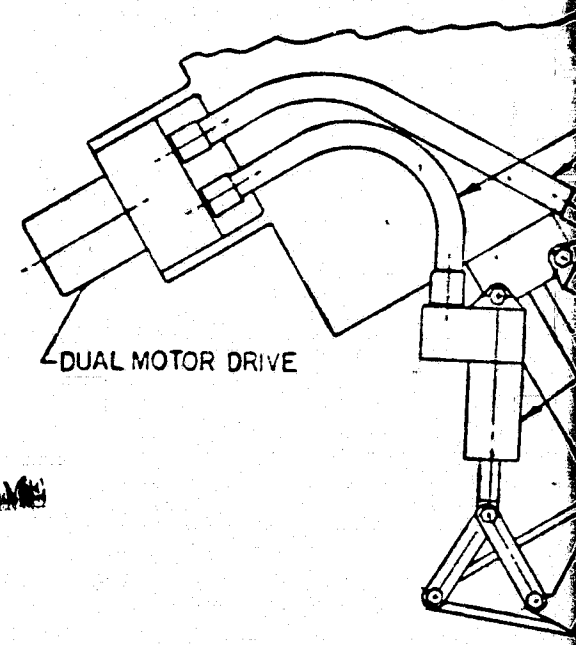
CAP MATERIAL
STORAGE CANISTER



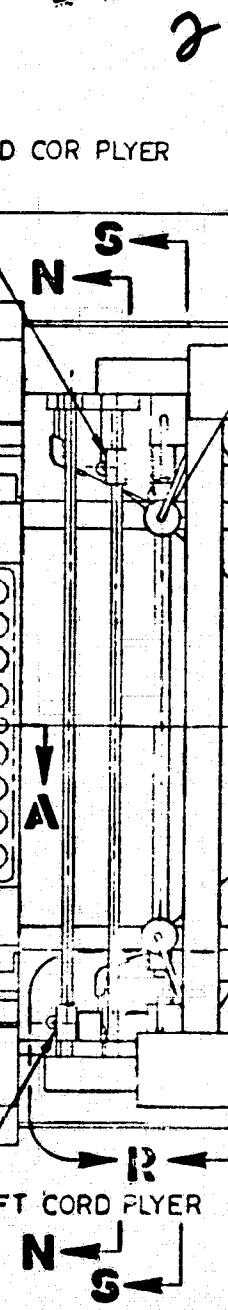
INDEPENDENT COOLING
SYSTEM RADIATOR



DETAIL R
 SCALE 1/5
 CORD TENSIONER



GENERAL ARRANGEMENT
 SCALE 1/10



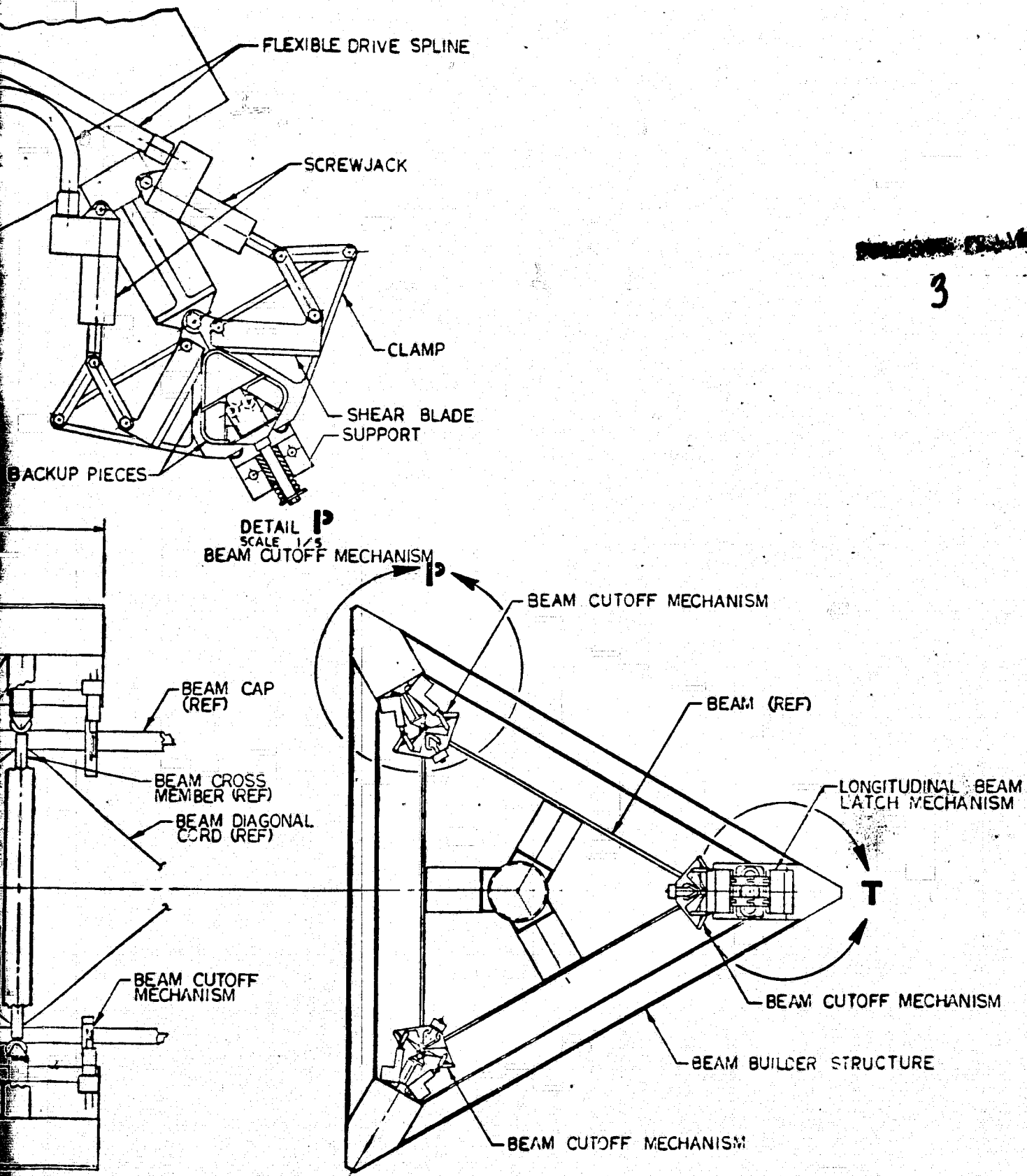


Figure 2-43. Beam builder general arrangement.

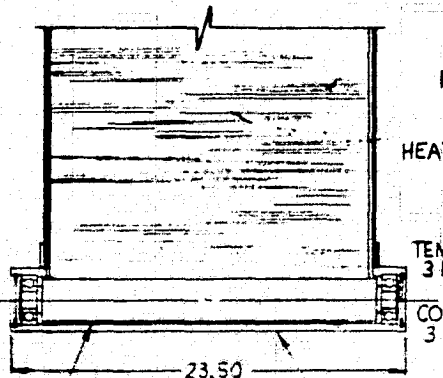
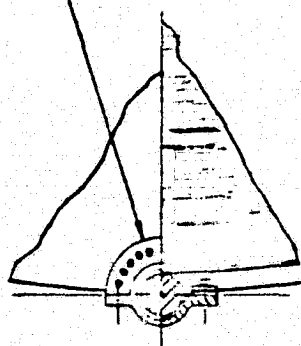
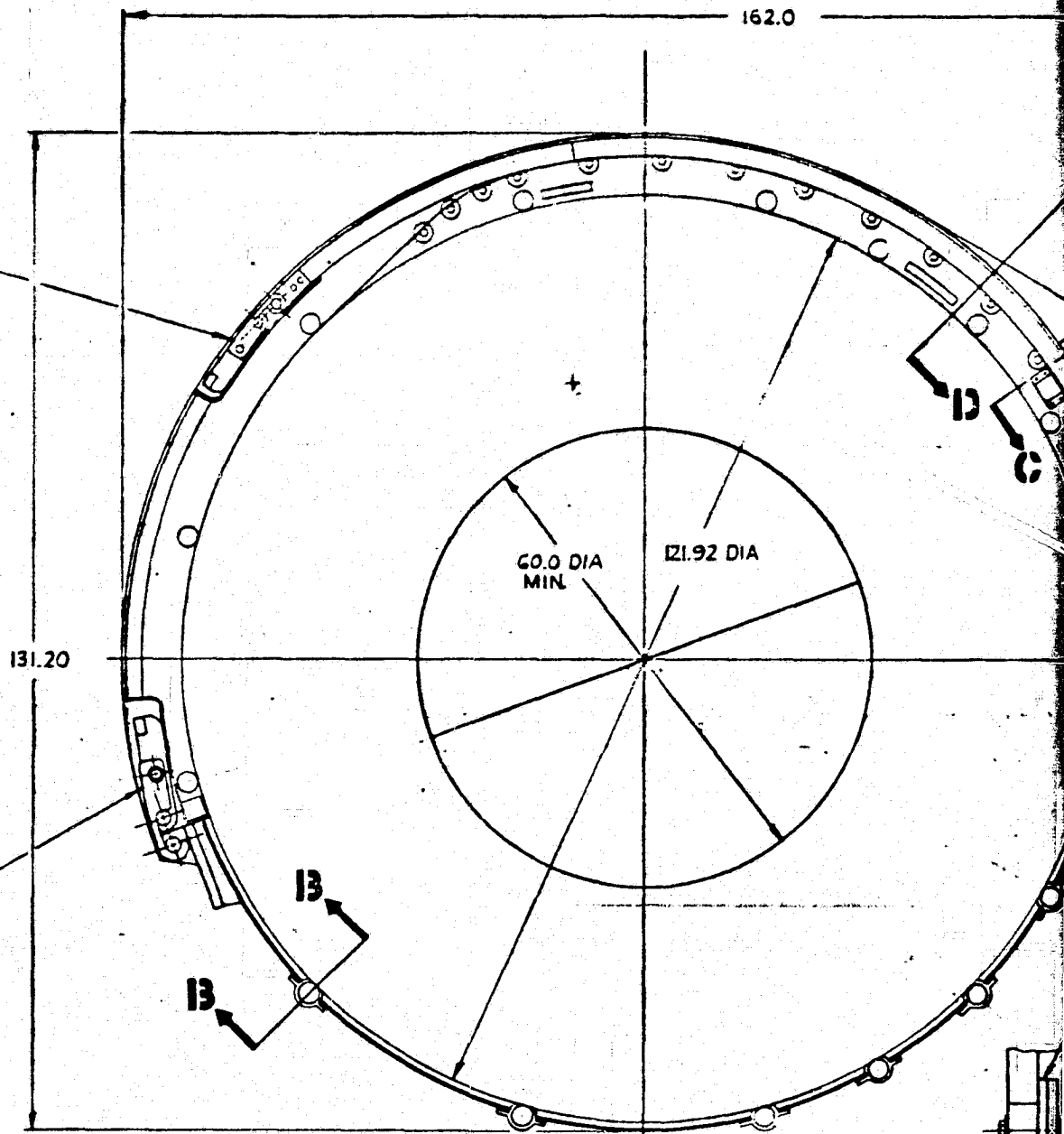
2-71/72

~~WELDING FRAME~~

ACCESS PANEL LATCH

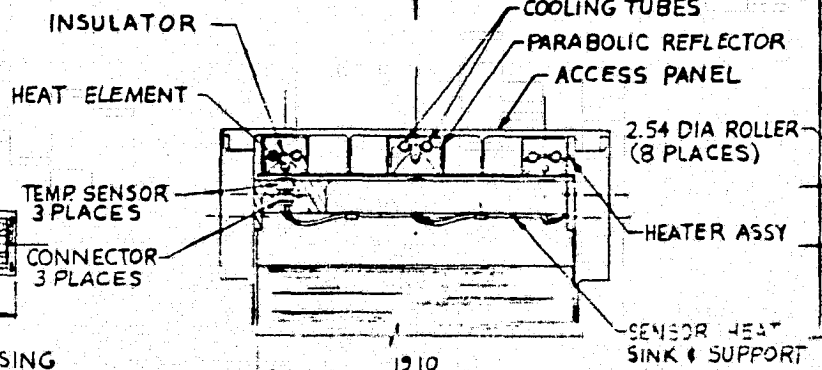
CANISTER LATCH

ROLLER MOUNT

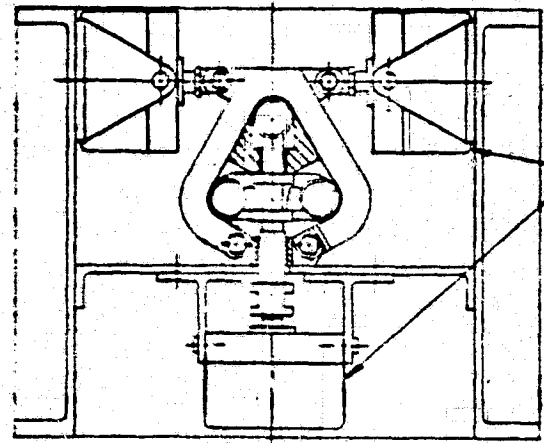
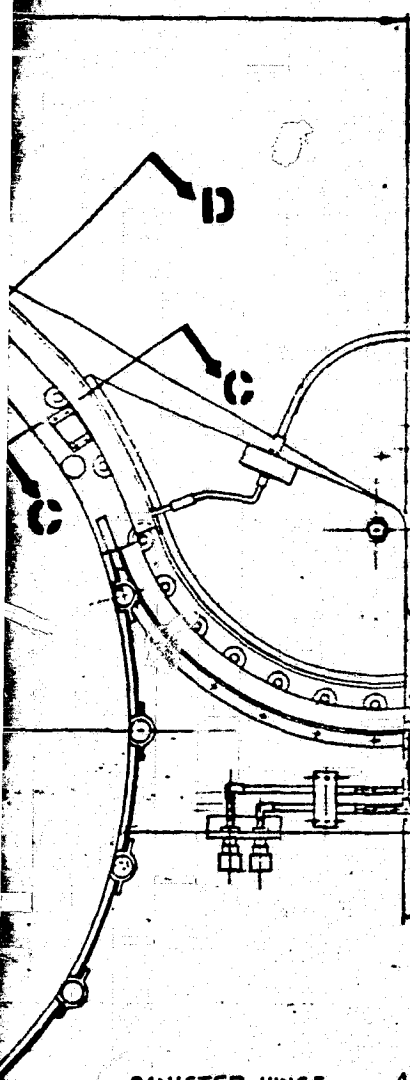


2.54 DIA ROLLER - HOUSING

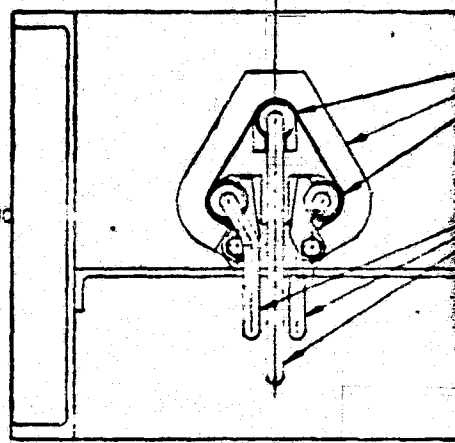
SECTION 13-13
SCALE 1/2
OUTSIDE ROLLER ASSY INSTL
9 PLACES



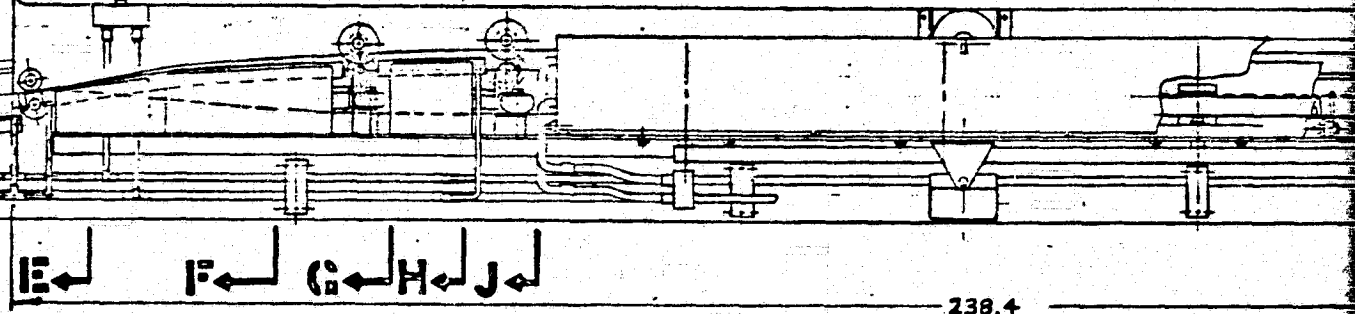
SECTION C-C
SCALE 1/2
HEATING SECTION CONTROL STATION NO 1



SECTION **K-K**
SCALE 1/2
COOLING PLATEN ACTUATORS

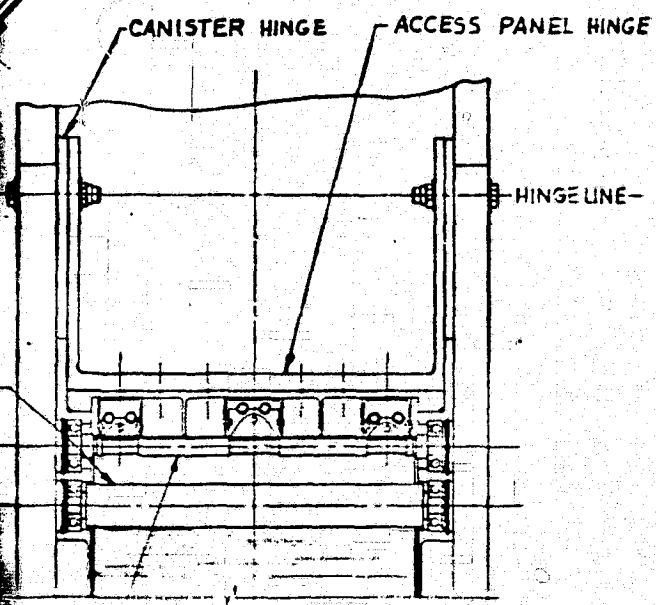


SECTION **L-L**
SCALE 1/2
COOLING SECTION LINES E-E & H-H

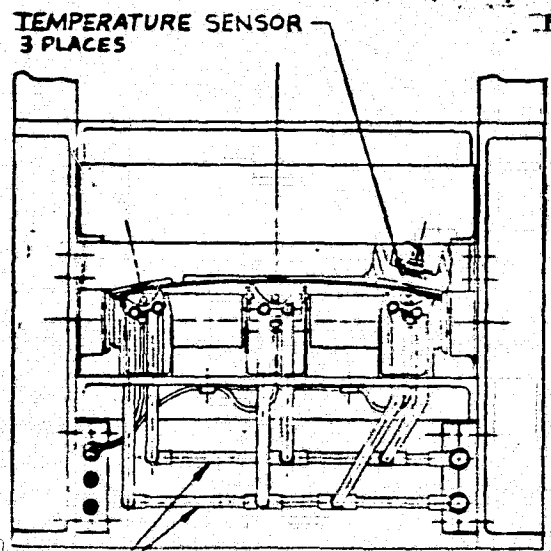


DETAIL **A**
SCALE 1/4
CAP FORMING MACHINE ASSY
GENERAL ARRANGEMENT

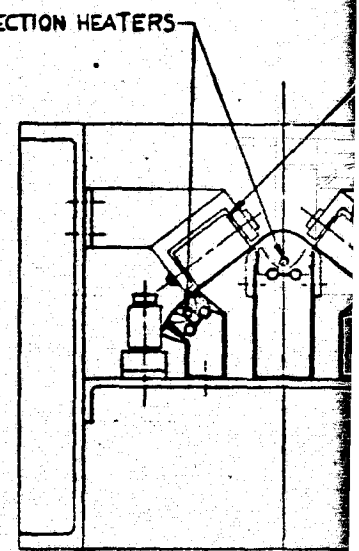
238.4



1.0 DIA GUIDE ROLLER (20 PLACES)
SECTION **D-D**
SCALE 1/2
HINGE & GUIDE DETAIL



TEMPERATURE SENSOR
3 PLACES
SECTION **E-E**
SCALE 1/2
HEATING SECTION CONTROL STATION NO2



FORMING SECTION HEATERS
SECTION **F-F**
SCALE 1/2
TYPICAL FORMING SECTION

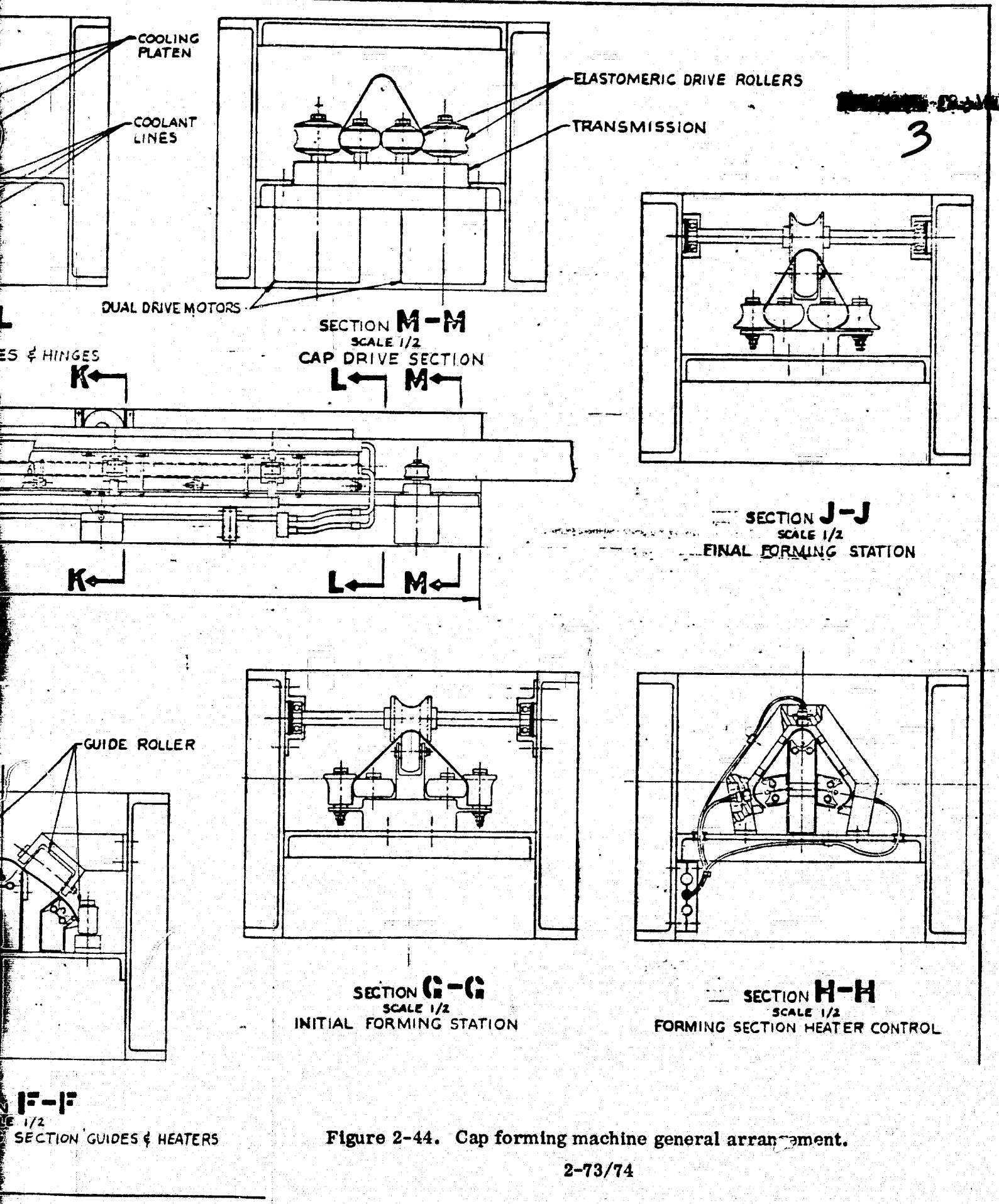
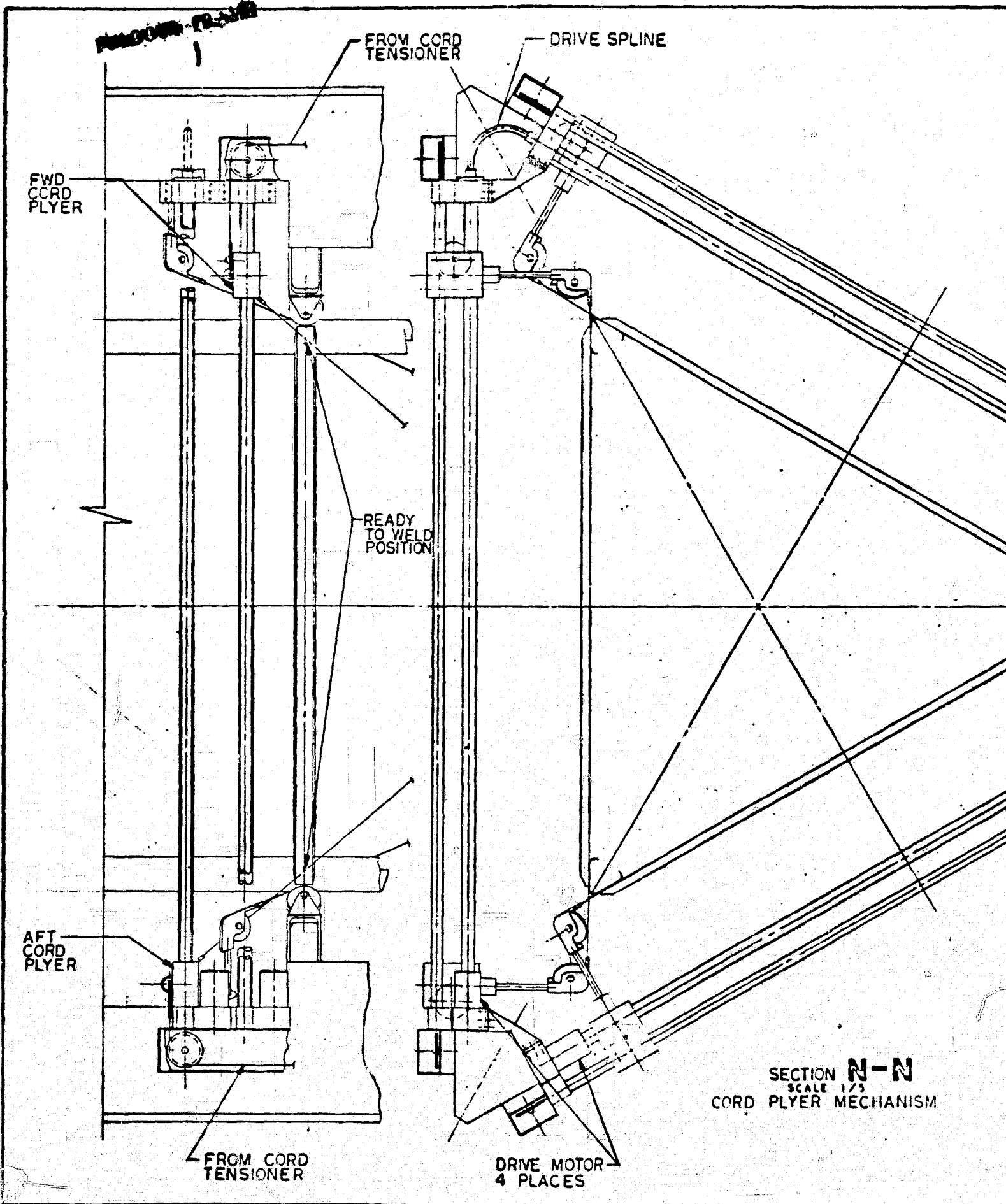


Figure 2-44. Cap forming machine general arrangement.

2-73/74



~~SECTION N-N~~

FROM CORD TENSIONER

DRIVE SPLINE

FWD CORD PLYER

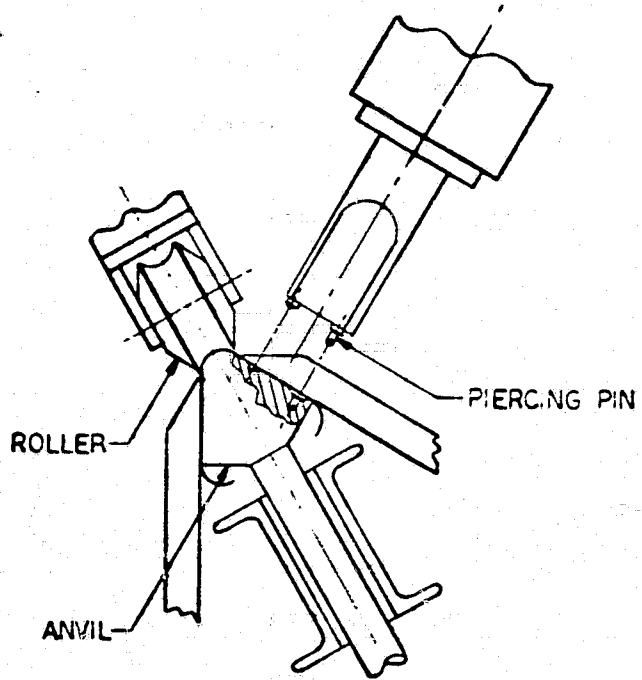
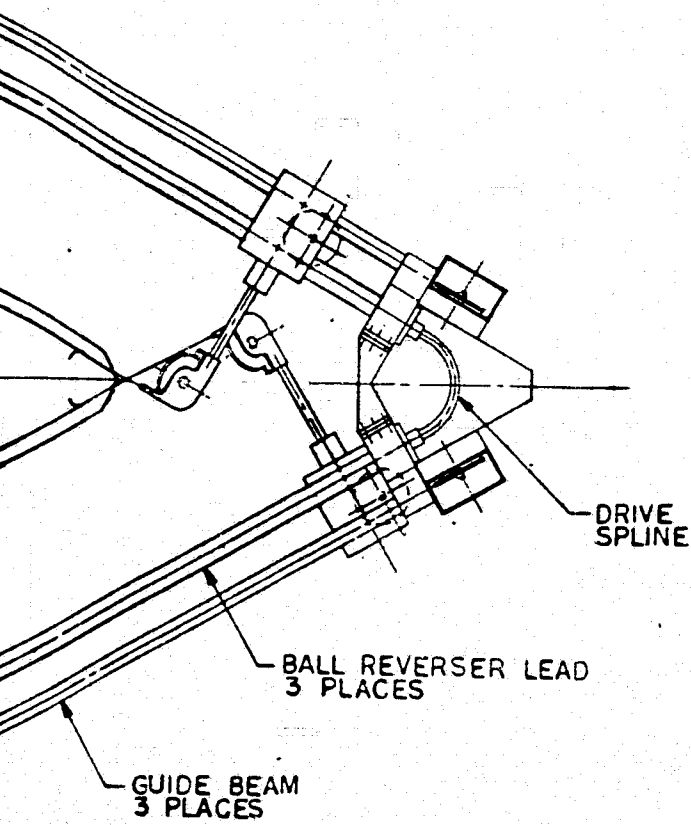
READY TO WELD POSITION

AFT CORD PLYER

FROM CORD TENSIONER

DRIVE MOTOR 4 PLACES

SECTION **N-N**
SCALE 1/2
CORD PLYER MECHANISM

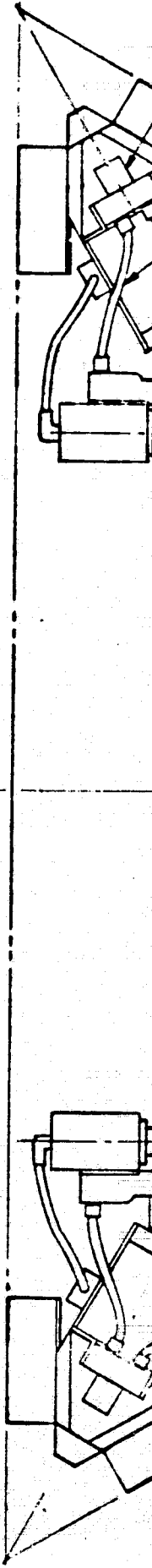


DETAIL **Z**
SCALE 1/2

~~XXXXXXXXXX~~

2

ORIGINAL PAGE IS
OF POOR QUALITY



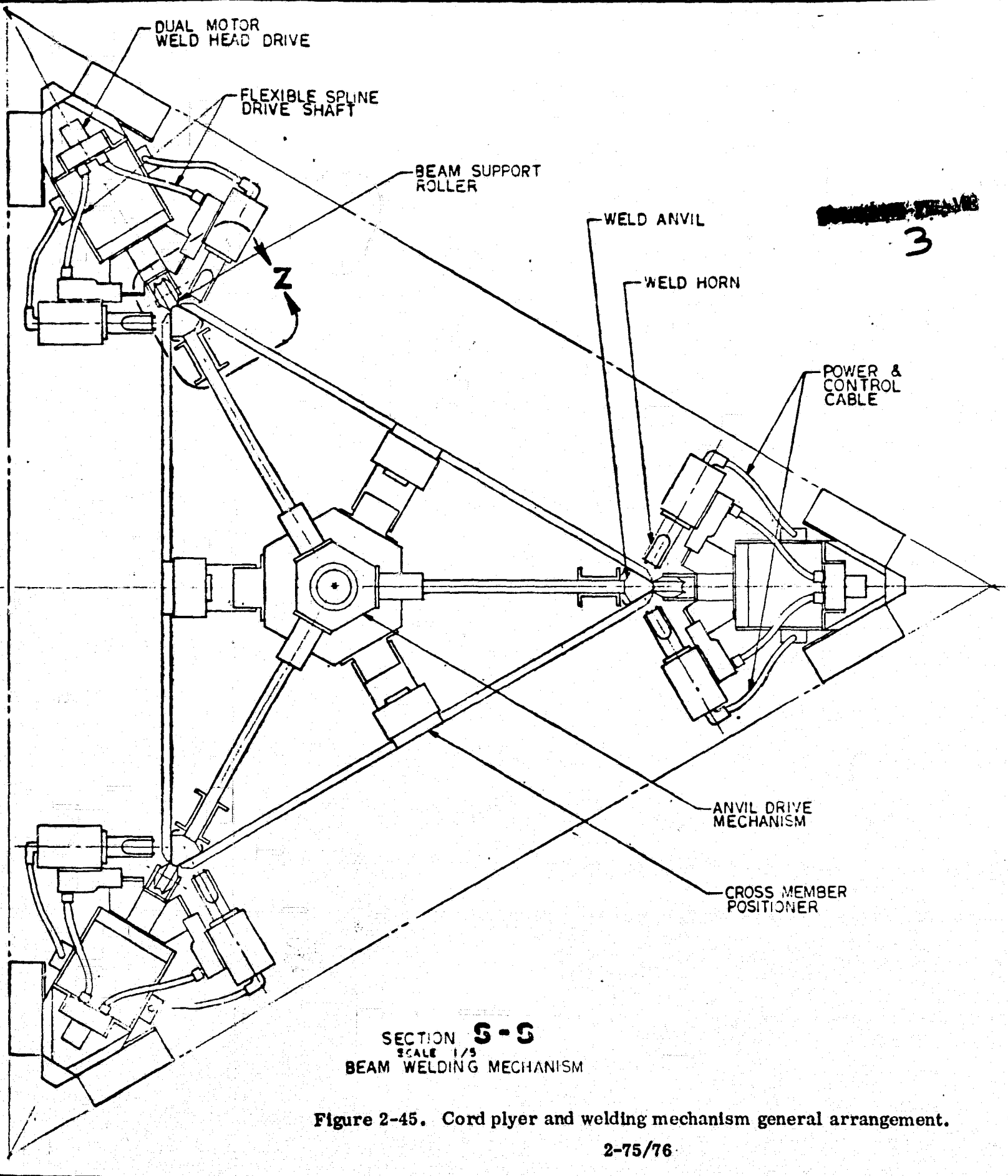
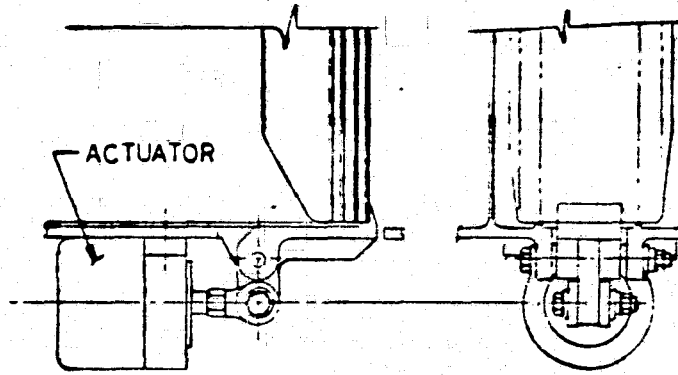
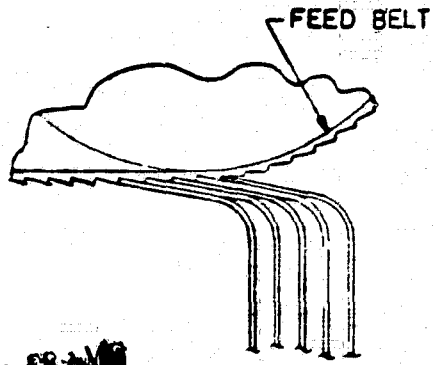
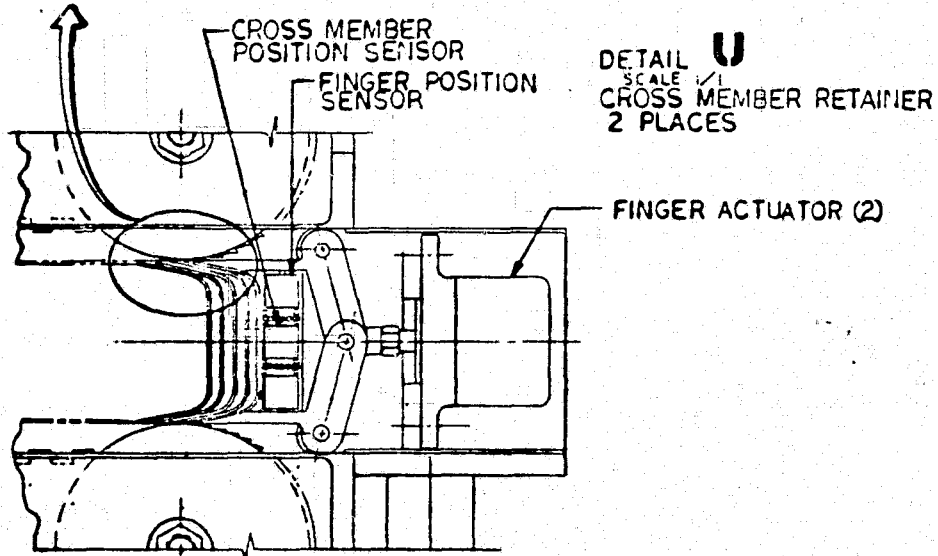


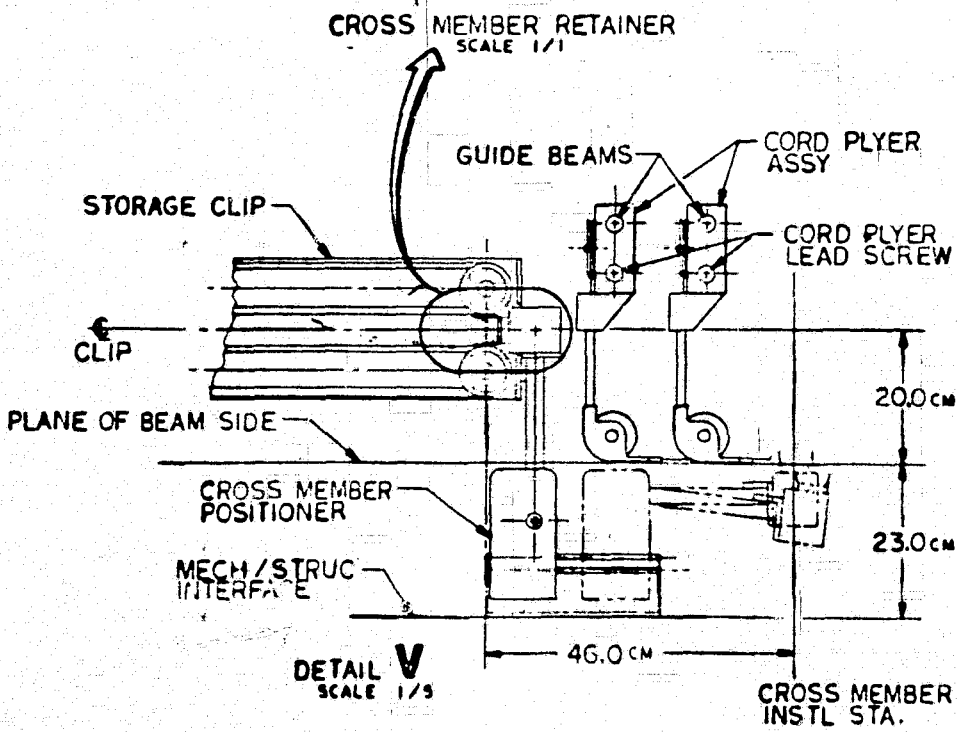
Figure 2-45. Cord pleyer and welding mechanism general arrangement.



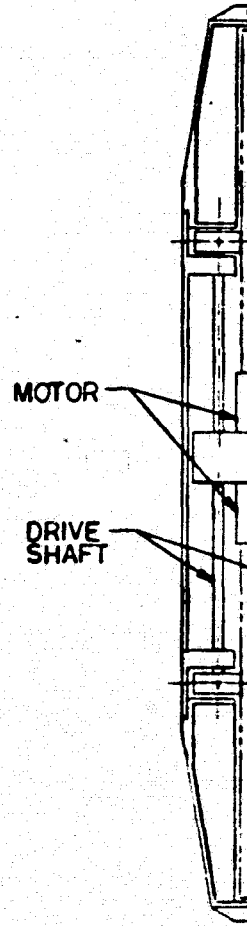
~~SECRET~~ **SECRET**



DETAIL U
SCALE 1/1
CROSS MEMBER RETAINER
2 PLACES

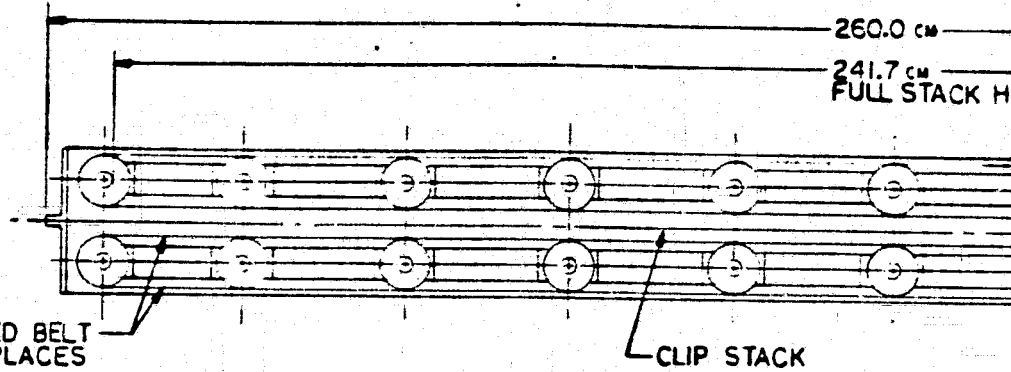
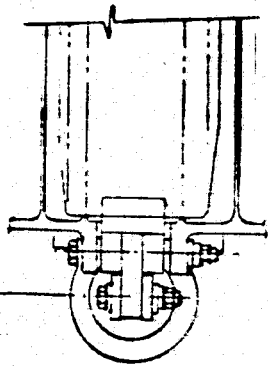


DETAIL V
SCALE 1/5

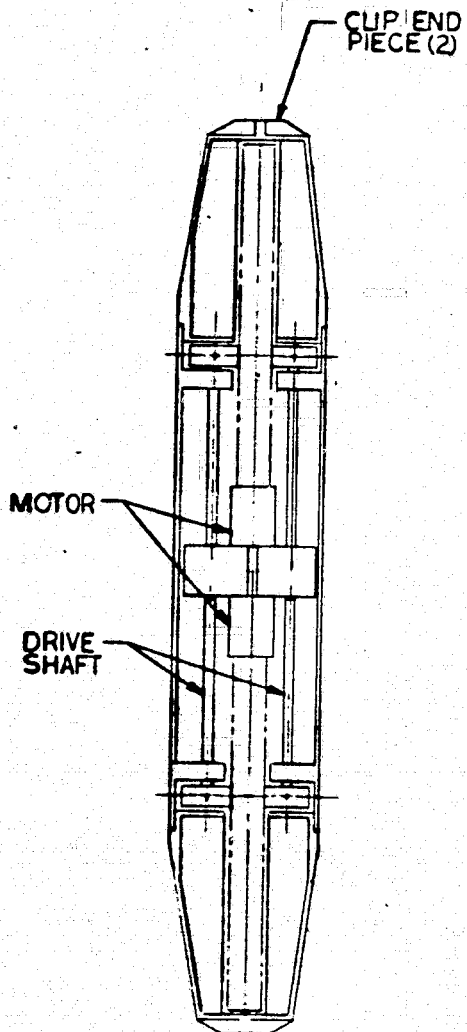


SECTION
SCALE 1/1

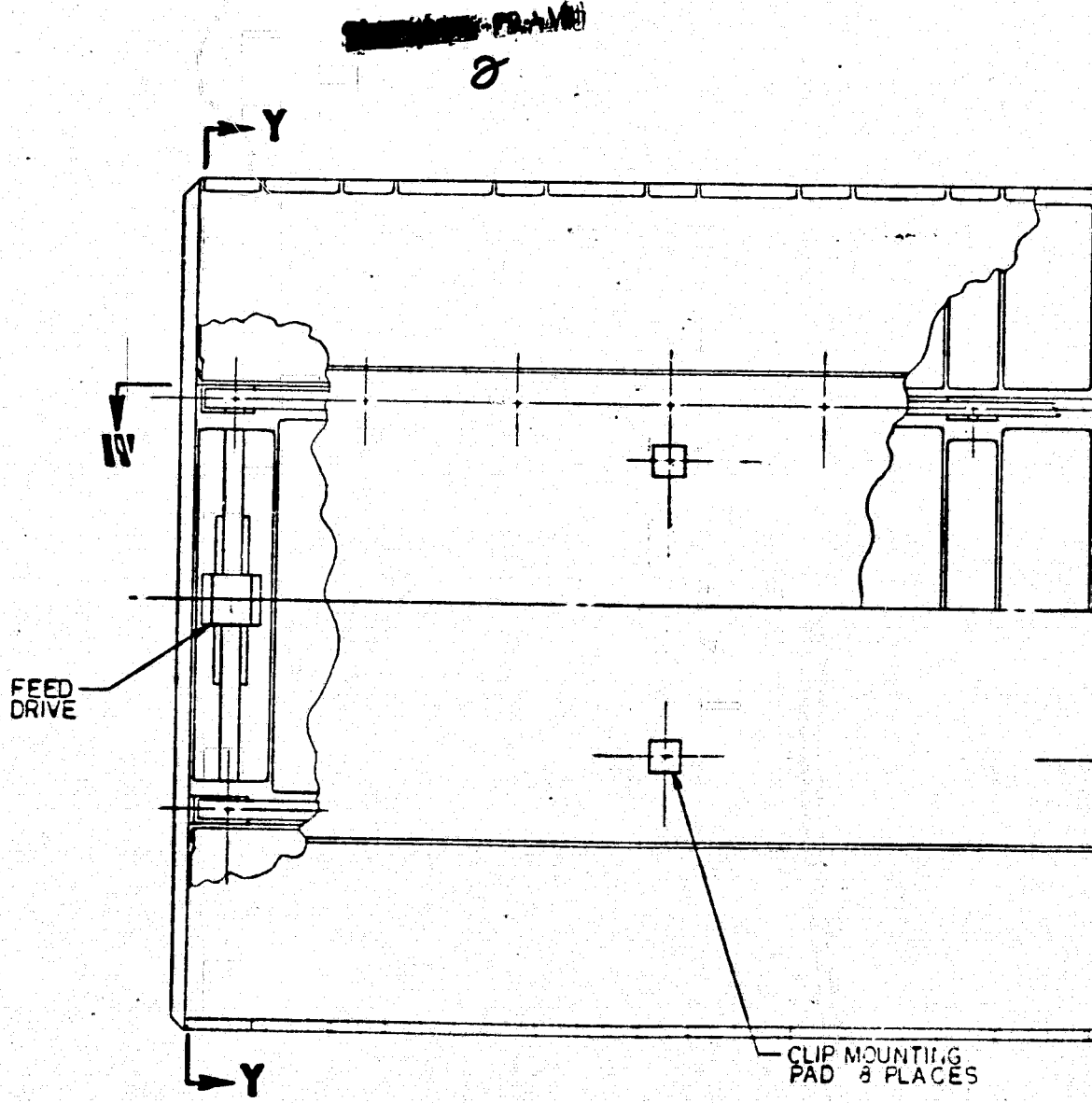
ORIGINAL PAGE IS
OF POOR QUALITY



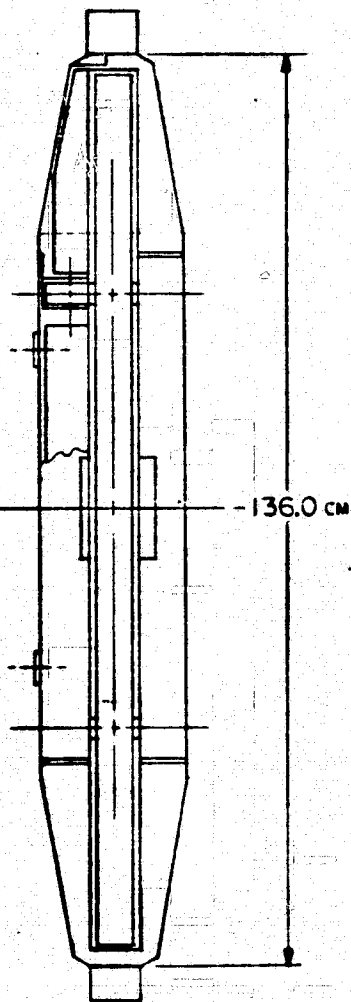
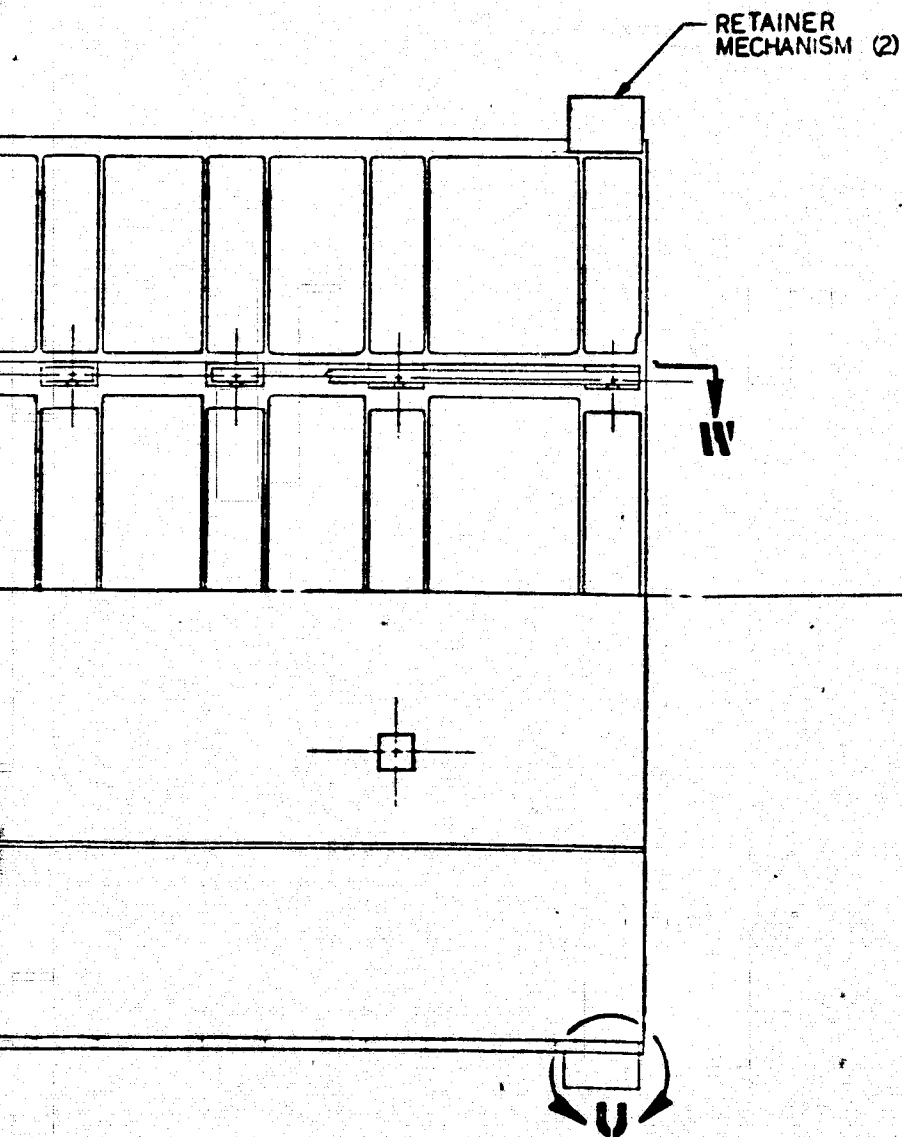
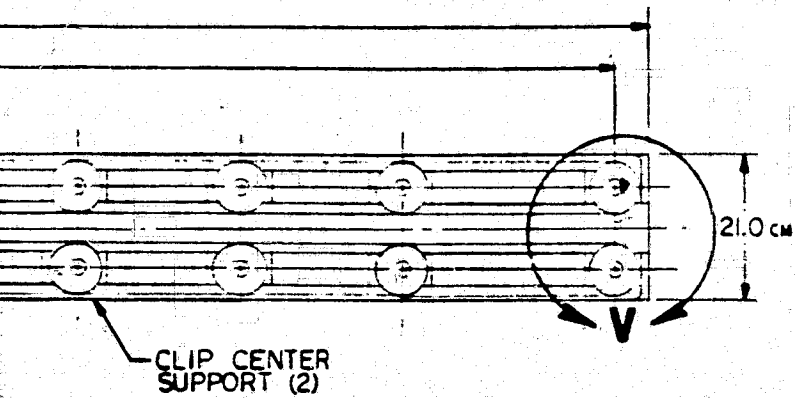
SECTION **W-W**
SCALE 1/5



SECTION **Y-Y**
SCALE 1/5



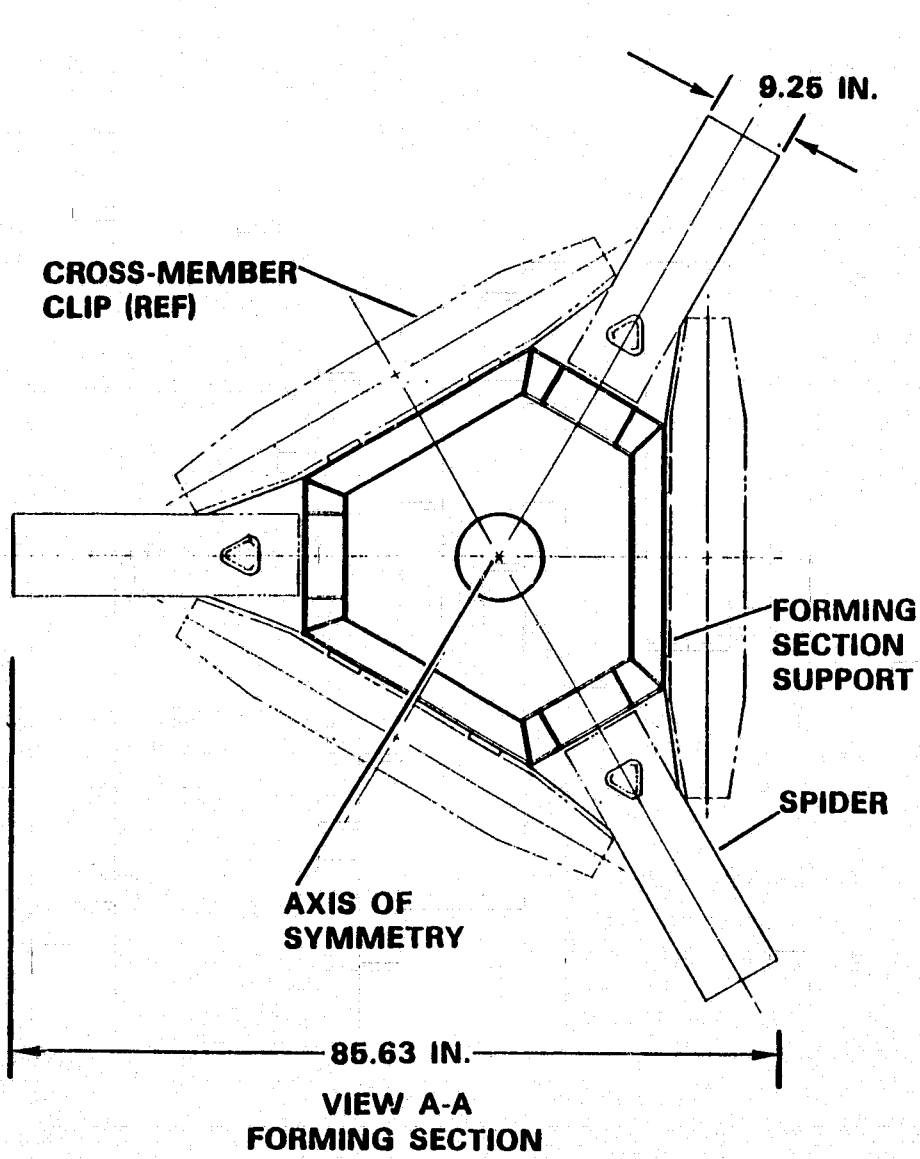
CROSS MEMBER CLIP & FEED M
SCALE 1/5



~~SECRET~~
3

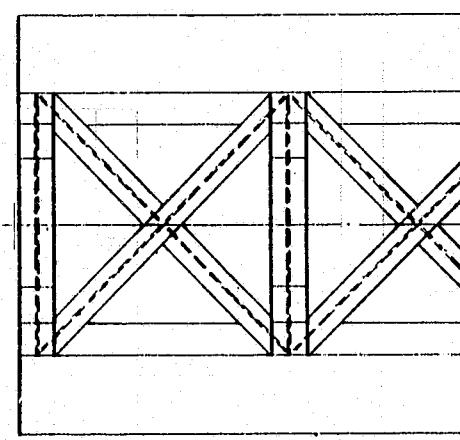
Figure 2-46. Cross-member clip and positioner mechanism

2-77/78

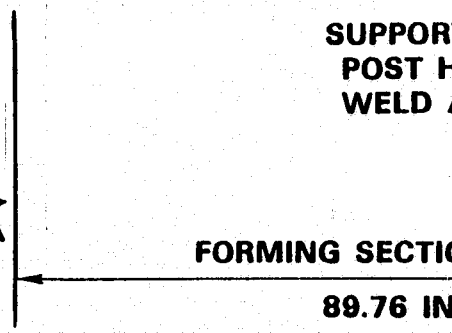


A

- MATERIAL/CONSTRUCTION: AL ALLOY PLATE & S
- WEIGHT 1,456 LB



A



~~FORMING SECTION~~

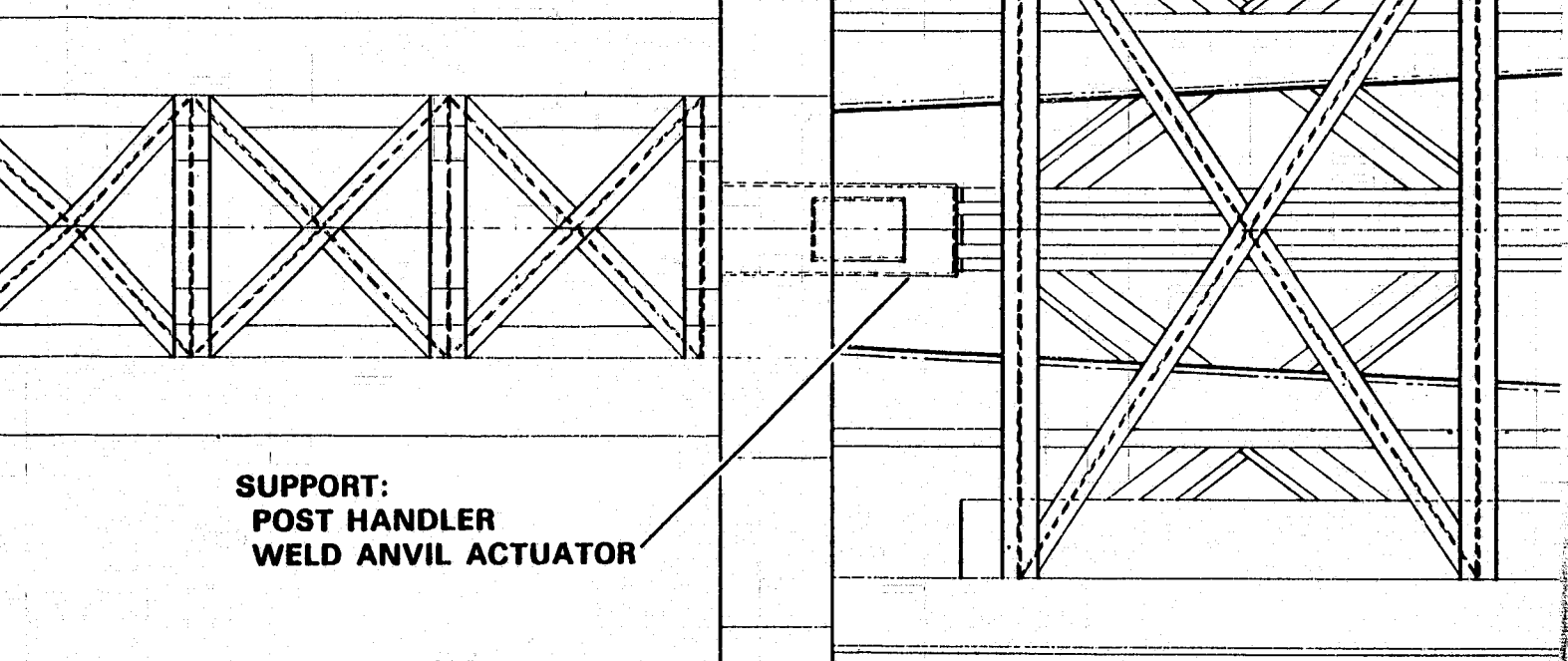
ROLL/TURN
MECHANISM
INTERFACE

EXTERNAL
SUPPORT
BEAM (3)

INTERNAL
SUPPORT
BEAM (3)

• MATERIAL/CONSTRUCTION:
AI ALLOY PLATE & SHAPES, WELDED

• WEIGHT 1,456 LB



SUPPORT:
POST HANDLER
WELD ANVIL ACTUATOR

FORMING SECTION SUPPORT

89.76 IN.

SPIDER

12.60 IN.

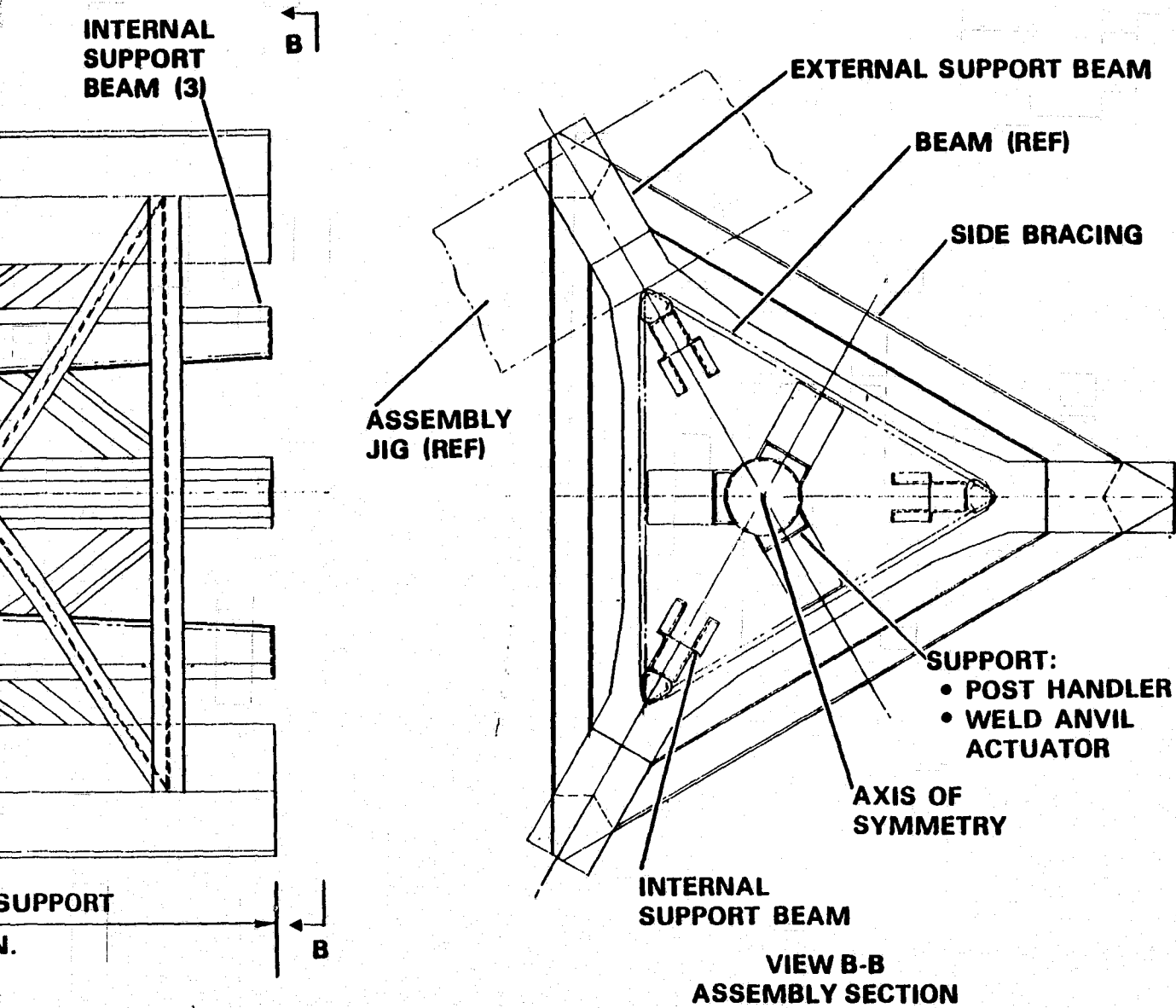
ASSY SECTION SUPPORT

86.30 IN.

~~XXXXXXXXXX~~

2

ORIGINAL PAGE IS
OF POOR QUALITY



~~SECRET~~
3

Figure 2-47. Beam builder structure.

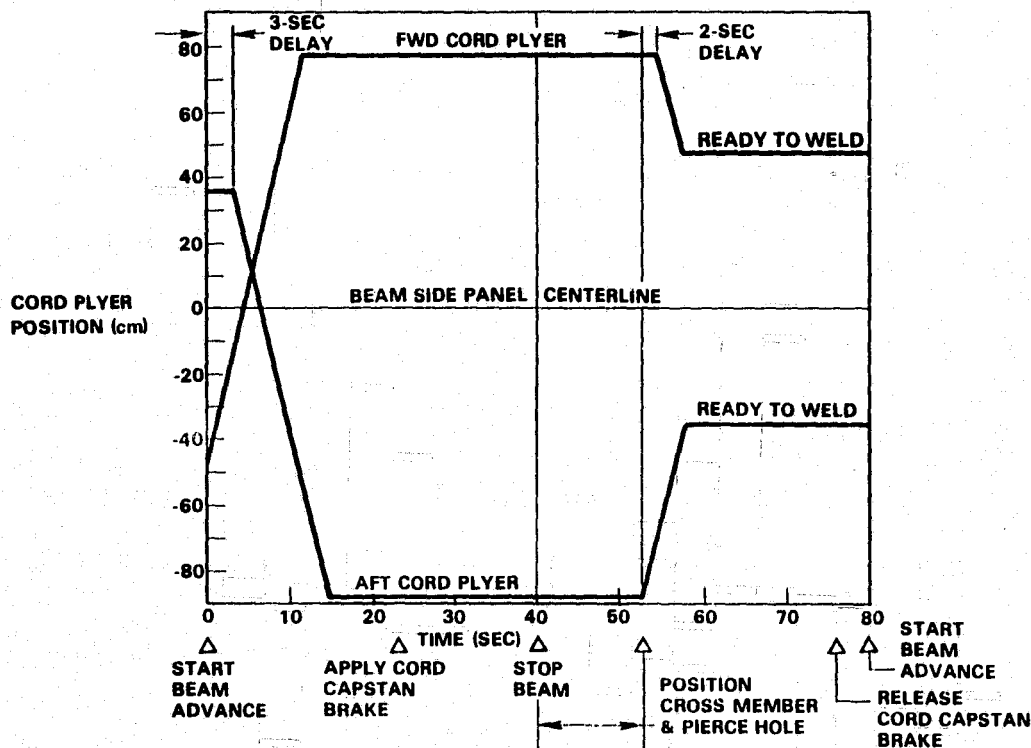


Figure 2-48. Cord pleyer timing sequence.

As the beam starts to advance in the beam builder, the cord tensioners are in the free feed mode and the forward cord pleyer drive is activated. A 3-second delay is provided before start of the aft cord pleyer drive so that the forward cord pleyers reach their outboard position first.

The cord pleyers stop at their outboard positions and, after 23 seconds, the cord tensioner capstan brakes are applied. The beam drive thus applies the necessary force to extend the cord tensioner constant force springs to the proper stroke.

After the beam is stopped and the cross-members to be attached are in position, the ultrasonic welding heads are advanced and activated momentarily to allow a pin on each weld head to pierce the cross-member and cap just below each cord. When the piercing is completed, the aft cord pleyer drive is activated. A 2-second delay permits the aft cord pleyer cords to move clear of the forward cord pleyers before the forward pleyers start to move. The forward and aft cord pleyers move to the ready-to-weld position while the cord tension is maintained by the cord tensioning mechanism.

At the ready-to-weld position, the cords have been strung over the piercing pins and are at their final assembled angle to the beam caps. At the conclusion of the welding operation, the cord tensioner capstan brakes are released and the next cycle is ready to begin.

2.2.1.5.4 Beam Welding Subsystem. The beam welding mechanism, shown in Figure 2-44, has six ultrasonic weld head assemblies, which are driven in pairs by a redundant motor drive for each pair. The three weld head positions are: (1) fully retracted to allow the cross-members to be positioned by the cross-member positioners; (2) pierce position, where the piercing pin on each weld horn has penetrated the cross-member and cap; and (3) the weld position, where the weld horn is engaged and properly loaded to enable the welds to be accomplished.

Each weld horn is equipped to perform two dimple spot welds and one special cord capturing weld simultaneously. The weld horns act against internal anvils, which are extended against the inside surface of the caps by a common dual motor-driven cam mechanism. The weld station is supported and sized by the combined action of the weld anvils and the beam support rollers located on the centerline of the weld station. A spring cartridge on each anvil actuator-rod limits the engagement force. The weld anvils are retracted to allow the weld dimples to pass and to minimize friction drag on the caps.

2.2.1.5.5 Beam Support Subsystem. The beam is supported at two stations by precision located metal rollers as shown in Figure 2-43. The roller support stations fall on the centerline of the beam cross-members when the beam builder is in the assembly pause mode. The rollers maintain beam straightness during assembly and react bending moments during beam extension.

2.2.1.5.6 Coolant Subsystem. The independent cooling system was described in Section 2.2.1.3.9. The radiator for this system is mounted to one of the clip housings as shown in Figure 2-43. The remaining components are installed inside the beam builder structure beneath the clips.

2.2.1.5.7 Beam Cutoff Subsystem. The beam cutoff mechanism, shown in Figure 2-43, shears each cap and cord member to separate a complete beam from the beam builder. The clamping device is normally retracted to allow the cross-members to travel past the outer clamps.

In preparation for beam cutoff, a short cutoff bay (60 cm) is manufactured by the beam builder. The cords are laid along the caps within this short bay rather than crossing over in diagonal directions as they do in normal bay construction. The short bay is advanced to the point where the cutoff shears are in the center of the short bay as the next complete bay is in assembly. When the next bay is assembled, the beam builder sequence is interrupted to permit beam cutoff and beam builder or platform repositioning.

Dual motor drives operate each cutter. As the actuators are extended, the clamps engage the internal backup mechanism and force the backups into position. The shear blades are spring loaded to allow the clamps to fully engage before the shear blades penetrate the cap. The shear blades are then driven through the caps as the actuators continue to extend. This also shears the cords as they lay along the sides of the cap.

2.2.1.5.8 Beam Builder Structural Subsystem. The beam builder structure is composed of welded aluminum elements, arranged as shown in Figure 2-47. A preliminary analysis indicates a weight of 660 kg for the complete assembly.

The structure consists of three major segments: a forming section support, a central "spider", and an assembly section support. The forming section support is a trussed hexagonal system whose external surfaces provide support for the three machine storage/forming sections and the three cross member storage clips. To maintain precise alignment of machine elements, local pads, machined after weld completion are provided at machine/structure interfaces.

The central spider is a three-legged box structure providing a transition load path from the internal forming section support to the external portions of the assembly section supports. It also provides an interface with the beam builder roll/turn positioning mechanism as well as supporting three cantilevered internal support beams and a support pedestal for the cross-member handler and weld anvil actuators.

The three external beams in the assembly section support provide mounting for the cord pleyer/tensioner mechanisms, the ultrasonic weld station, the cutoff mechanism, and guide rollers at the weld and exit stations. One of these three beams also supports the beam builder/assembly jig latch system. As a consequence of this eccentric support, the three beams are connected by a cross-bracing system to provide system torsional rigidity, particularly needed in view of the reduced beam section, near the spider attachment plane, to accommodate cord pleyer installation.

2.2.1.5.9 Beam Builder Support Subsystem. The support subsystem includes the mechanisms and controls which support the beam builder during platform fabrication.

A handling arm assembly attaches to the spider section of the beam builder structure. The handling arm is connected to a mechanism on the assembly jig which positions the beam builder as described in the next section.

A longitudinal beam latch mechanism, shown on Figure 2-43, aligns and couples the beam builder with the assembly jig. It provides the added support necessary to prevent relative motion between the beam builder and assembly jig during longitudinal beam fabrication. A cross-beam latch mechanism (not shown) is also required to align and support the beam builder during cross-beam fabrication.

2.2.2 ASSEMBLY JIG. The SSAFE assembly jig is an automatic machine process for positioning and receiving beams from the beam builder and assembling them into a baseline platform configuration. The selected assembly jig configuration satisfies the following design criteria:

- a. Low power dissipation.
- b. Automatic quality control.
- c. Permits platform separation and remating options.
- d. Permits platform to be driven back and forth across the jig.

- e. Conforms to Shuttle Orbiter interface requirements.
- f. Uses automatic techniques for highly repetitive operations.
- g. Provides for use of EVA for specialized operations.
- h. Assures safety of crew and Orbiter.

This section gives the trade study methodology and issues for the assembly jig and its basic processes. Concept layouts and sketches of the candidate assembly jig configurations are presented and the selected assembly jig concept is presented in preliminary design layout drawings.

2.2.2.1 Study Method and Issues. The trade study approach to selecting the assembly jig concept was to first identify the processes and techniques required to assemble the baseline platform. Process option concepts were developed for each process and evaluated in terms of compatibility with the Orbiter and SCAFE, safety, complexity, and performance. The processes were used to develop three assembly jig concepts. The assembly jig concepts were then evaluated in terms of complexity, program risk, weight, and operational compatibility.

2.2.2.2 Assembly Jig Functional Concept. The functional processes of the assembly jig are diagrammed in Figure 2-49. The function of the assembly jig is to automatically assemble the baseline platform. To accomplish this, it must perform the following operations in this sequence:

- a. Position and support the beam builder for fabrication of each of four longitudinal beams. This requires a carriage and a roll-and-turn mechanism, as well as a latching mechanism to secure the beam builder to the jig.
- b. Grasp and retain each longitudinal beam in position after it is completed and cut off from the beam builder. This requires a retractable retention and guide mechanism.
- c. Position and support the beam builder for fabrication of cross beams. This is accomplished with the carriage and roll-and-turn mechanism.
- d. Advance all four longitudinal beams into position for joining to each cross beam. This is accomplished with a drive mechanism provided for each beam.
- e. Grasp and place each cross beam into position after it is completed and cut off from the beam builder. This requires a cross beam positioner mechanism.
- f. Join the cross beam to the four longitudinal beams using automatic joining mechanisms.
- g. Permit EVA personnel to traverse the platform and perform equipment installation tasks. An EVA bridge and personnel carriage is required for this purpose.
- h. Allow the platform to be quickly released for deployment to space. This is another function of the beam retention and guide mechanisms.

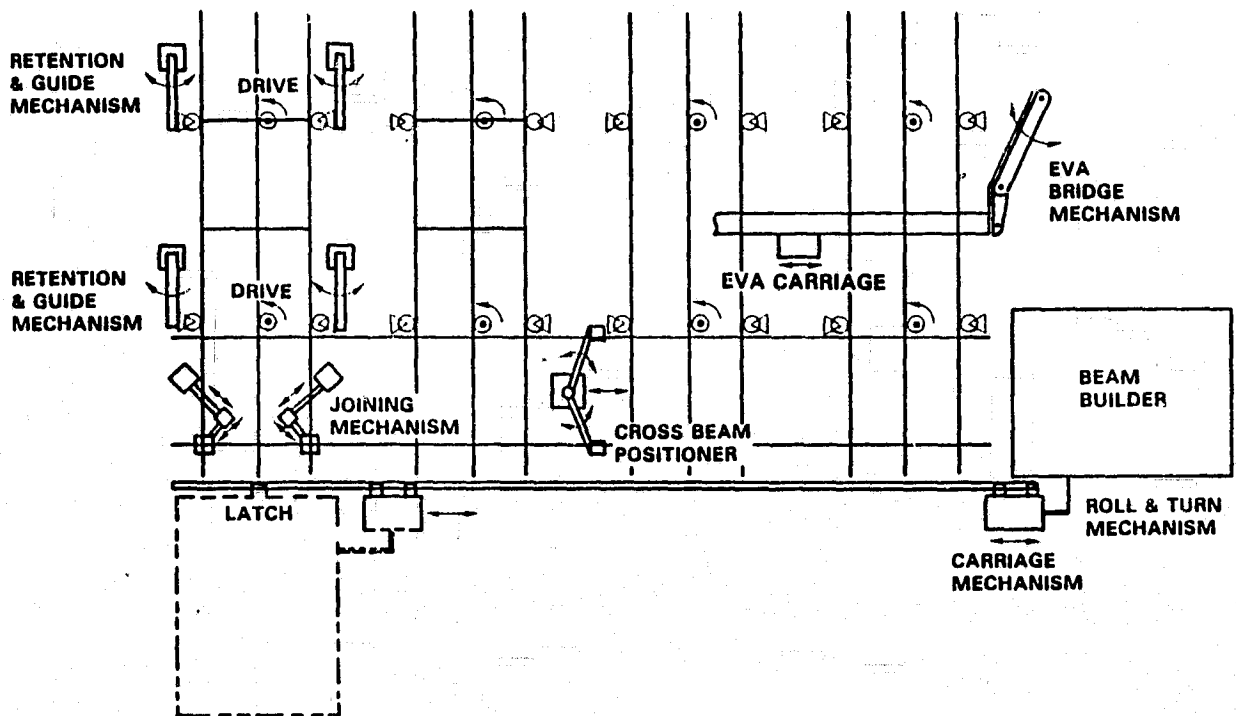


Figure 2-49. Assembly jig functional diagram.

2.2.2.3 Stowage and Deployment Concept. Two optional SCAFE stowage concepts are shown in Figure 2-50. Both options use a short cradle at the aft end of the assembly jig to provide X, Y, and Z load reactions. A pair of trunion pins mounted near the forward end of the jig provides the forward Z load reaction.

Option 1 is the selected approach since it provides these advantages:

- a. Best access to the beam builder.
- b. Beam builder does not interfere with mechanisms on the face of the jig.
- c. It permits the forward Z load fitting to be located nearer the c.g. of the payload.
- d. It allows equipment stowage in the cargo bay area in the best location for use.

Option 2 cargo stowed on the back of the jig is simpler to support, but it must be repositioned with the RMS after deployment of the assembly jig.

Figure 2-51 illustrates the concept for deployment of the assembly jig and beam builder. The assembly jig is deployed by unlatching the forward Z support pins and rotating the jig about an axle concentric with the aft X-Z trunion support pin. When the longitudinal axis of the jig is parallel to the Z axis, the jig is locked in position and the beam builder is unlatched for deployment.

Beam builder deployment and positioning is described as a series of operations by the roll-and-turn mechanism. The beam builder is rolled 180° to the orientation for longitudinal beam fabrication in two steps as shown in Steps 3 and 4. It is then turned 90° as shown in Step 5 to position the axis of the longitudinal beams normal to the longitudinal axis of the jig.

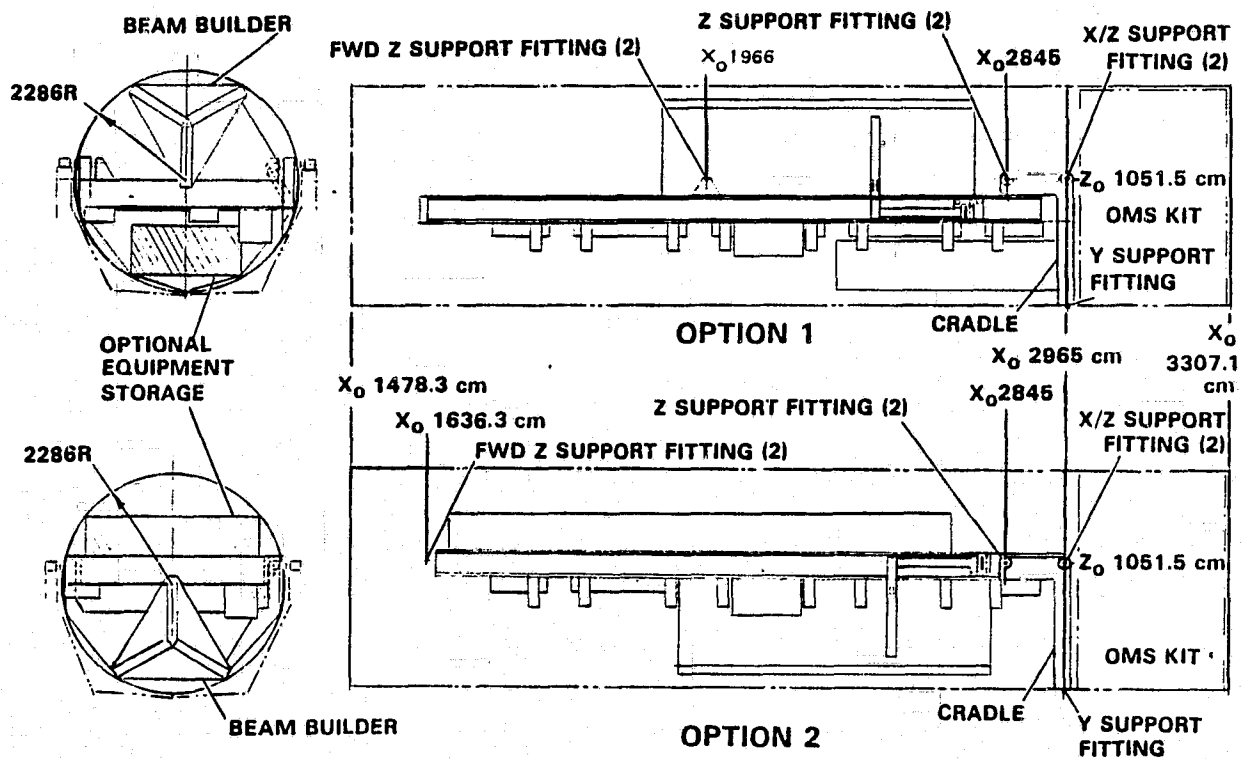


Figure 2-50. SCAFE stowage options.

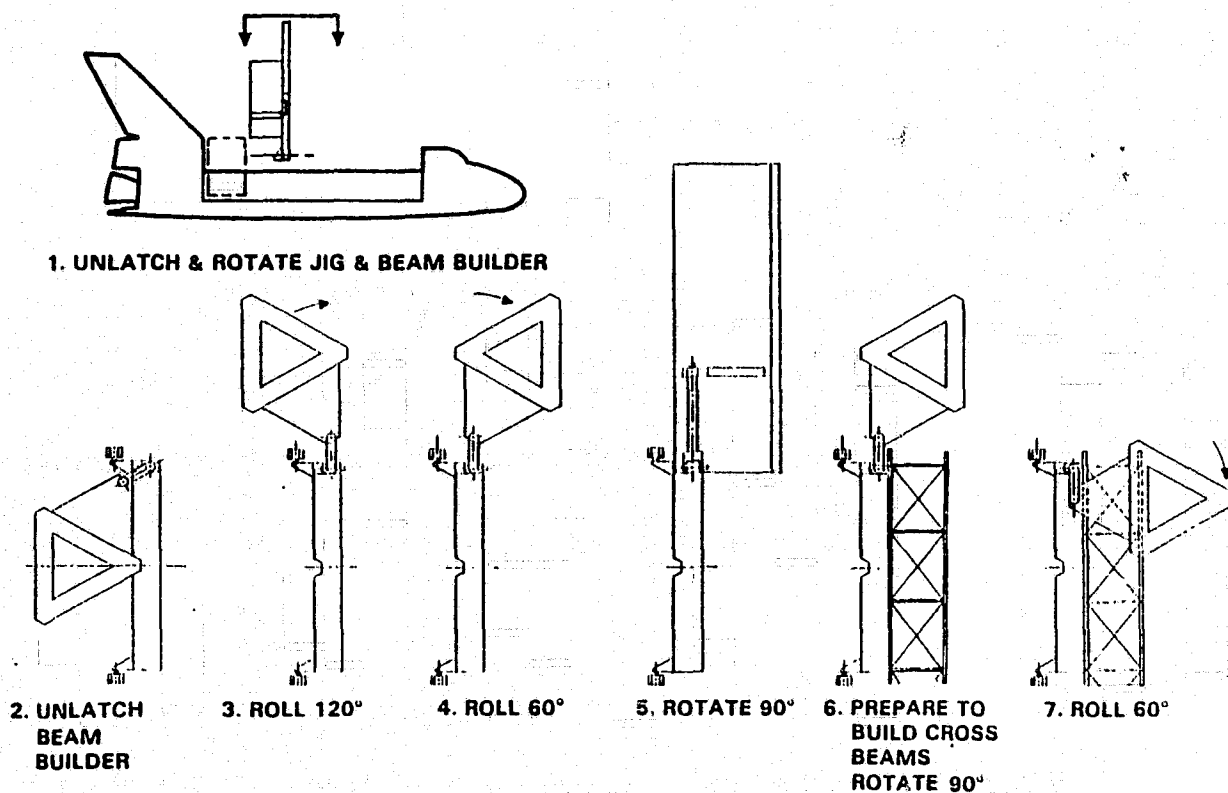


Figure 2-51. SCAFE jig and beam builder deployment sequence.

To reorient the beam builder for cross beam fabrication, it is first turned back 90°. The roll link then rotates 180° as the beam builder counter rotates 120° resulting in a net rotation of the beam builder of 60° and a lateral translation to the desired position.

2.2.2.4 Processes and Techniques. Concept options for each of the assembly jig machine processes and techniques were developed and compared. This section presents the results of those trades.

2.2.2.4.1 Jig Deployment Drive. The three jig deployment drive options are compared in Figure 2-52. A single-point connection to the jig is favored because it requires only a single pin puller to separate for payload jettison. The dual gear motor drive interferes with installation of separation latches at the jig pivot axle. The noted disadvantages of a telescoping pneumatic actuator eliminate it as a candidate. The linear screw drive actuator was, therefore, selected as the option which met all the necessary criteria for a deployment drive.

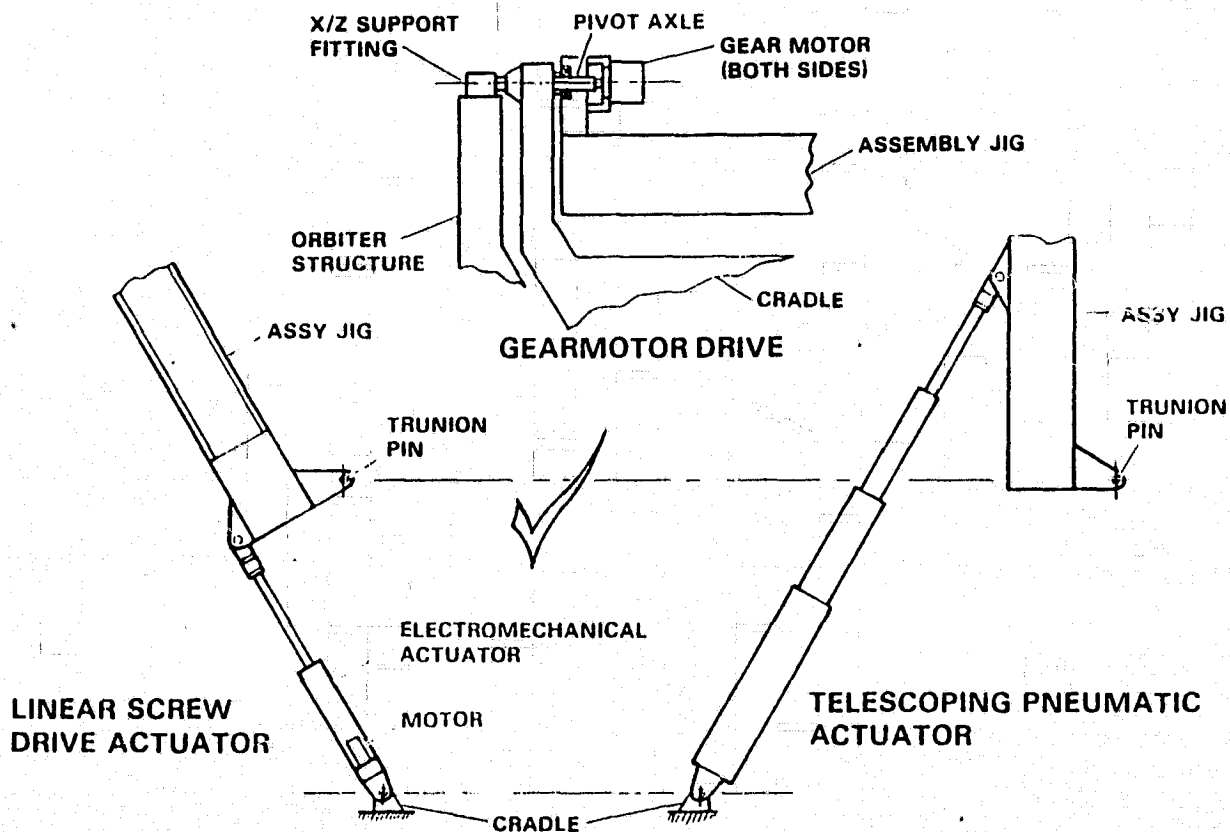


Figure 2-52. Jig deployment drive options.

2.2.2.4.2 Roll-and-Turn Mechanism. The deployment and positioning sequence dictates the nature of the beam builder roll-and-turn mechanism. The two options shown in Figure 2-53 will accomplish the desired sequence, with one being only a variation of the other. The turn arm option was selected over the roll/turn link primarily because the maximum bending moments at the carriage pivot axis are reacted through bearings on a shaft rather than through the gear train of the drive motor. It also allows the beam builder handling arm to be designed symmetrical.

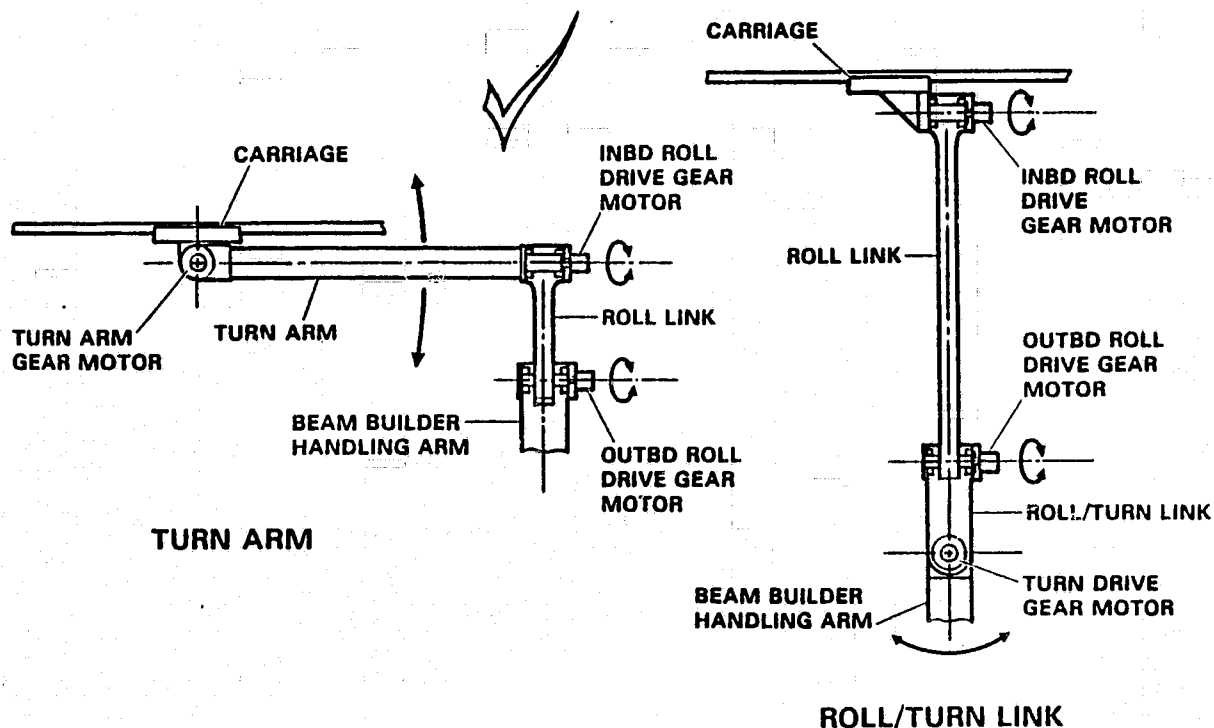


Figure 2-53. Beam builder roll-and-turn mechanism options.

2.2.2.4.3 Beam Builder Carriage Mechanism. There are numerous combinations of guide way bearings and drive mechanisms to consider as options for the beam builder carriage mechanism as illustrated in Figure 2-54. Although a friction drive has a number of advantages which make it simpler to manufacture and operate, it does not have the positive engagement necessary to ensure accurate positioning of the beam builder on the jig. A rack and pinion drive is the selected drive option since it is the positive engagement drive option most adaptable to space environment.

Linear ball bearings were selected over ball or roller bearings in order to minimize the contact stresses between the bearings and the guideways so as to avoid potential fretting problems due to thin dry film lubrication of the guide way surfaces. Round guide ways are less costly to produce and lighter weight than a machined groove track assembly.

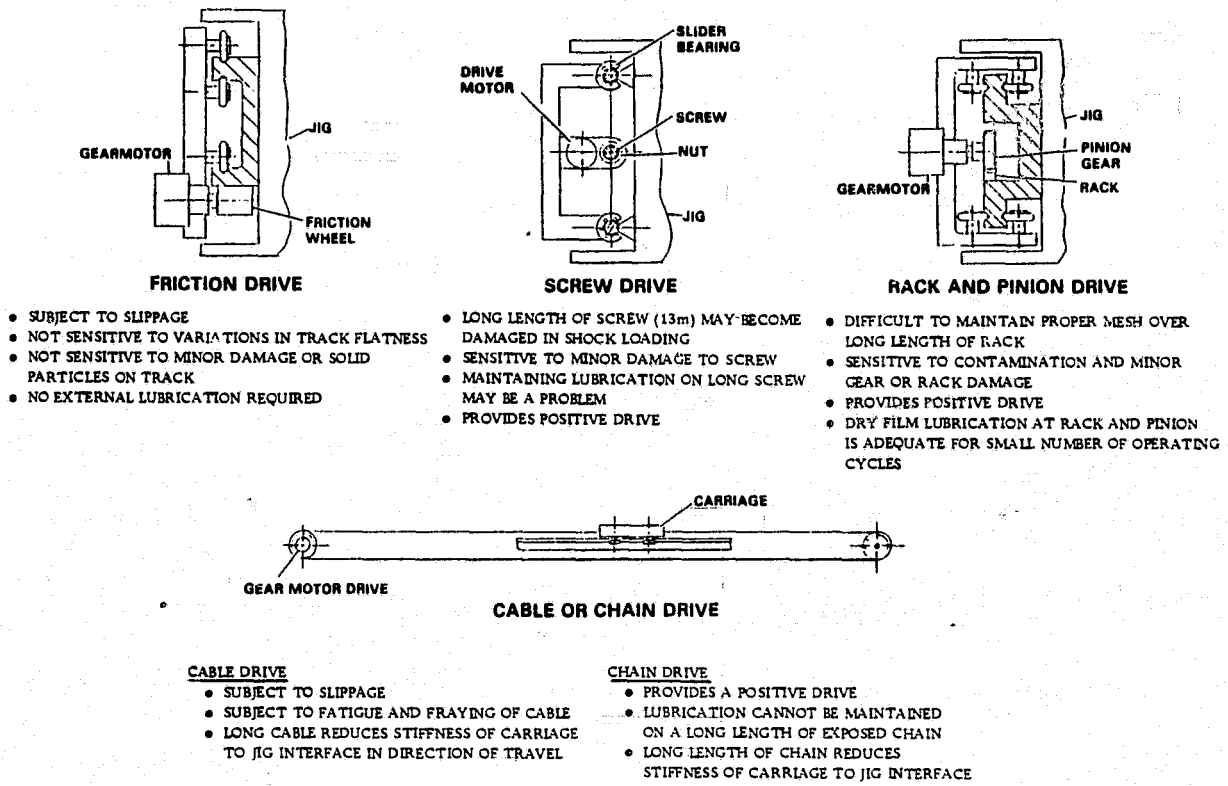


Figure 2-54. Beam builder carriage mechanism options.

2.2.2.4.4 Beam Builder Support. The support of the beam builder is determined by the loads environment during beam fabrication. Inadequate stiffness in the support scheme may cause greater tip deflection of the beam under accelerations imposed by the VRCS. Three support options are shown in Figure 2-55.

Supporting the beam builder by the positioner only provides the least amount of stiffness. For the beam deflection analysis it was assumed that a rigid latching coupler which connected the front end of the beam builder to the assembly jig was installed. This coupler has bending moment capability in all three axes.

A parametric study of the coupler stiffness is necessary to determine the stiffness required. The coupler stiffness must then be evaluated in order to prove its adequacy.

2.2.2.4.5 Beam Builder Umbilicals. The beam builder interfaces include electrical power, a control link, a data link, and, possibly, coolant liquid supply and return lines. Flexible interconnects are required to transfer these services between the jig and the beam builder. Optional methods are shown in Figure 2-56.

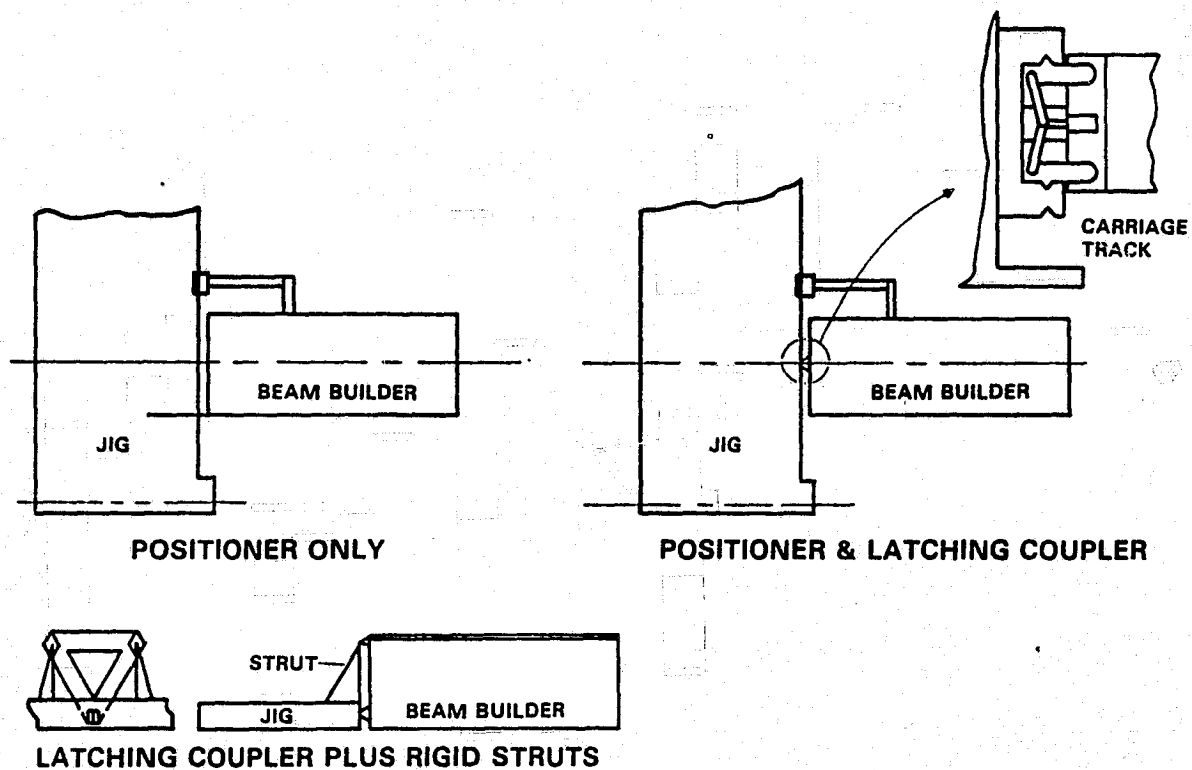
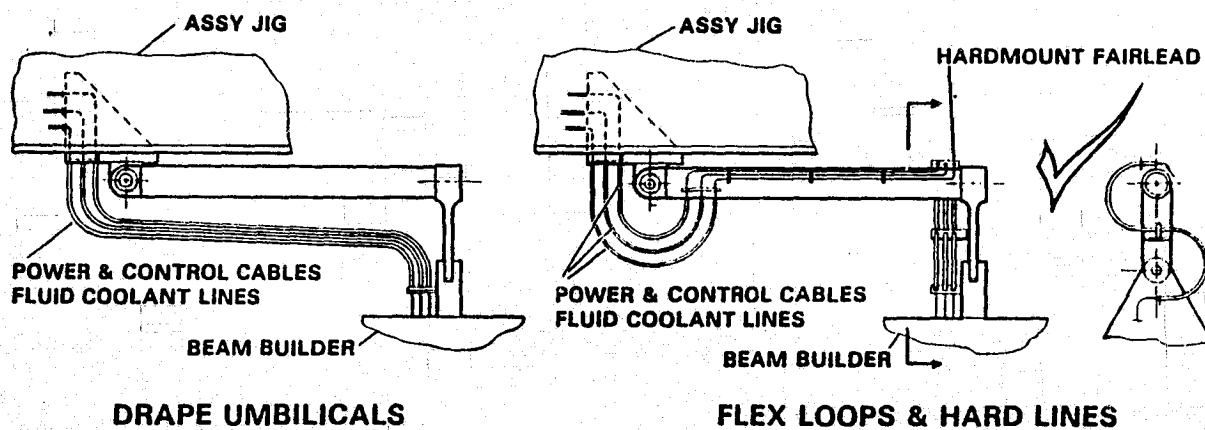


Figure 2-55. Beam builder support options.



OTHER OPTIONS
 SWIVEL JOINTS
 RF LINKS TO BEAM BUILDER
 SELF-CONTAINED COOLING SYSTEM

Figure 2-56. Beam builder umbilicals and service lines.

ORIGINAL PAGE IS
 OF POOR QUALITY

Drape umbilicals are not suitable for this application because the rolling and turning operations on the beam builder would cause severe twisting of the cables and flex hoses. A suitable alternative is to provide flexible loops about each axis of rotation with interconnecting hardlines and hard-mounted harnesses.

Use of swivel joints for fluid lines is not considered as reliable in preventing leakage as flex hose with permanent tube joint connections.

Possible ways to reduce the number of umbilicals were considered. RF data and control links to the beam builder would be costly and less reliable than hard wire links. Incorporation of a self-contained cooling system in the beam builder, as described in Section 2.2.1.3.9, eliminates umbilicals for coolant and eliminates additional load on the shuttle cooling system.

As the beam builder travels along the jig, the trailing umbilicals and service lines must be guided to prevent kinking or hangups which could damage them.

For the rigging scheme shown in Figure 2-57, the pulley guide moves at half the displacement of the beam builder carriage and must be controlled to maintain a positive return force on the umbilicals when the carriage is returned to its original position for stowage of the beam builder.

A simple spring return on the pulley guide was selected since it requires no power or control. A motorized follower would have to be controlled to not more than half the speed of the carriage to prevent overloading the umbilicals.

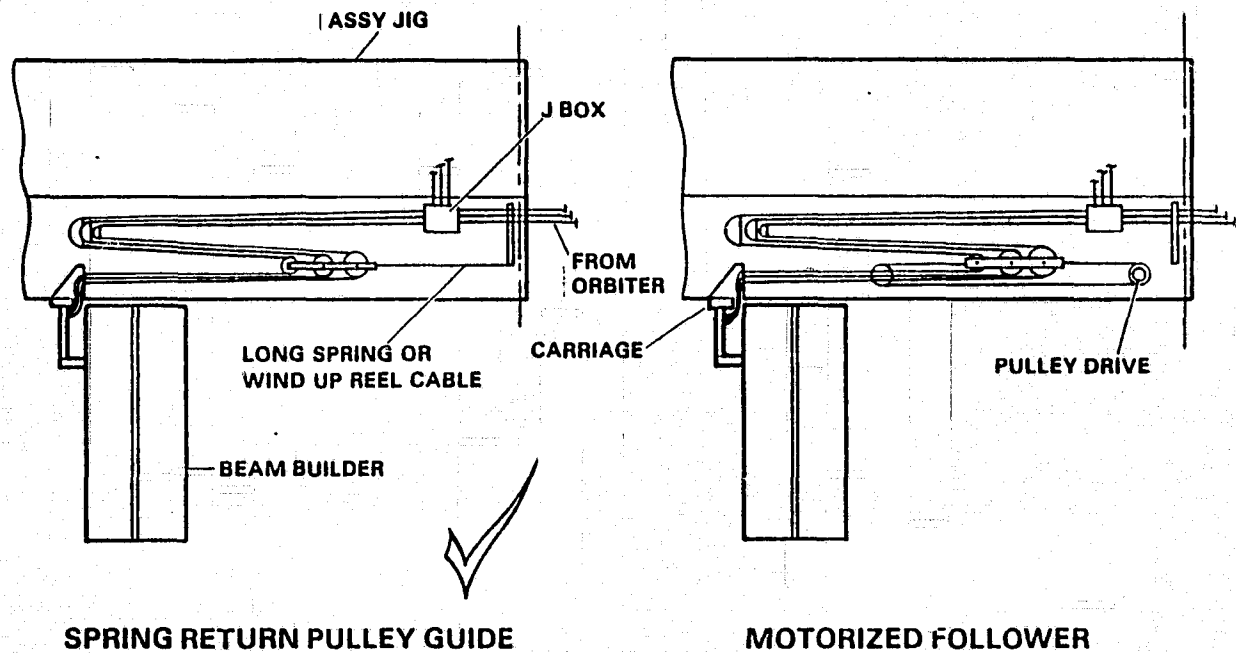
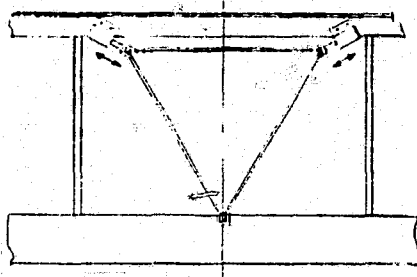


Figure 2-57. Umbilical and service line rigging options.

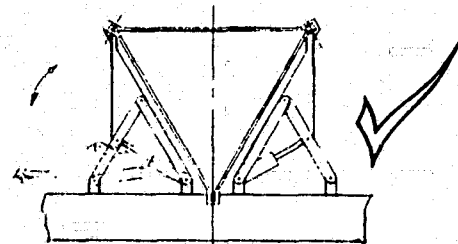
2.2.2.4.6 Retention and Guide Mechanism (RGM). As the longitudinal beams are manufactured by the beam builder, they are supported by the beam builder and have no contact with the assembly jig mechanisms. This is to prevent unnecessary bending moments on the beam during manufacture as a result of misalignment interferences with the assembly jig. Once the beam is finished it must be grasped by the assembly jig RGM before severing it from the beam builder. The RGM then functions to hold the beam in place until platform separation. It must also allow the beam to be translated across the jig by the platform drive system.

Four RGM options are compared in Figure 2-58. The linkage mechanism RGM provides the greatest number of advantages. For platform separation and remating operations, this option assures adequate clearance for the platform. It is the only option which allows the platform to be automatically translated back and forth across the jig.



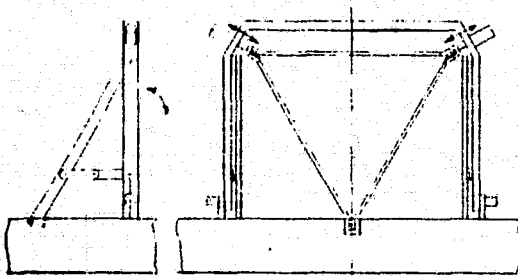
SOLID FRAME

- NOT COMPATIBLE WITH STOWAGE
- INTERFERES WITH PLATFORM SEPARATION
- SIMPLEST SUPPORT SYSTEM



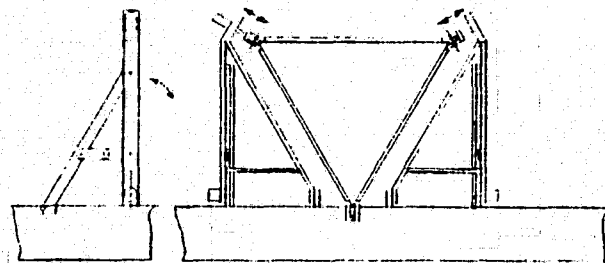
LINKAGE MECHANISM

- AUTOMATICALLY DEPLOYABLE
- AUTOMATICALLY STOWABLE FOR PLATFORM SEPARATION
- GREATER DESIGN COMPLEXITY
- BEST USE OF SPACE. LEAVES LONG AISLE WAYS FOR STOWAGE OF OTHER EQUIPMENT



RIGID WRAP AROUND FRAME

- MANUALLY DEPLOYMENT
- INTERFERES WITH PLATFORM SEPARATION



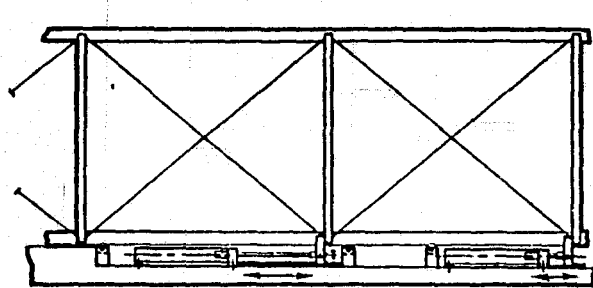
RIGID SIDE FRAMES

- MANUALLY DEPLOYABLE
- AUTOMATIC RETRACTION FOR PLATFORM SEPARATION REQUIRES TWO MORE ACTUATORS
- STOWAGE DIRECTION INTERFERES WITH STOWAGE OF OTHER EQUIPMENT E.G., EVA BRIDGE OR PLATFORM EXTENSION

Figure 2-58. Beam retention and guide mechanism options.

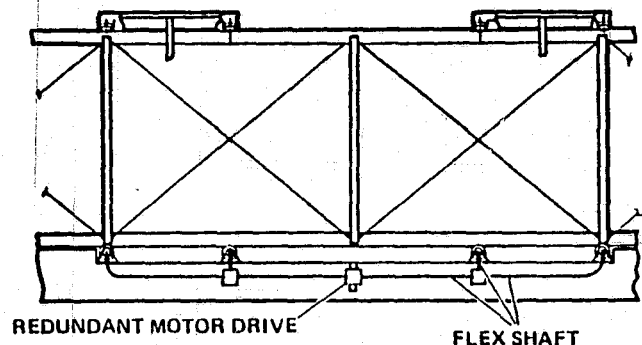
2.2.2.4.7 Platform Drive Mechanism (PDM). The four longitudinal beams are translated into position for joining of the first cross beam. When the beams have been joined, all subsequent drive inputs to the longitudinal beams must be synchronized in displacement and displacement rate. The synchronization of beam drives is a controls consideration discussed in Section 2.2.3. The individual beam drive mechanism options are compared in Figure 2-59.

The roller drive option was selected because it is not potentially damaging to the beam, as is the reciprocating drive, and it provides the widest span of force input distribution with the least amount of hardware, i.e., drive rollers can be set at each station where an RGM roller is located. The drive rollers can be coated with a friction material compatible with the thermal environment, whereas heating the flexible belt for low temperature operation (143°K) or use of metal belts is an added complexity. Drive rollers are adequate to deliver the relatively low (~ 22N) drive force required.



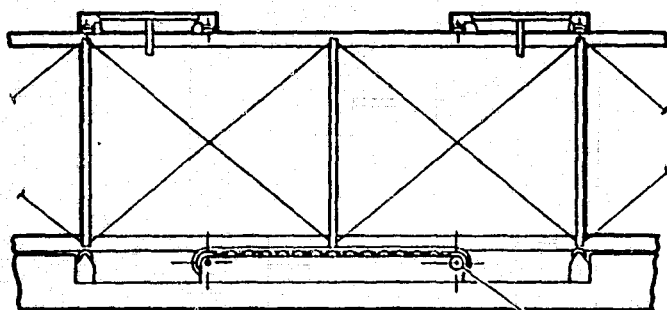
**RECIPROCATING DRIVE
(HAND OVER HAND)**

- POSITIVE DRIVE ENGAGEMENT
- PLACES SHEAR LOAD ON CROSS MEMBER JOINTS
- GREATER COMPLEXITY OF CONTROL



ROLLER DRIVE

- SIMPLE CONTROL
- SUBJECT TO SLIPPAGE
- MULTIPLE ROLLERS ENSURE ADEQUATE CONTACT FORCE ON AT LEAST ONE ROLLER AT ALL TIMES
- DRIVE TRAIN IS MORE COMPLEX



BELT DRIVE

- SIMPLE DRIVE TRAIN AND CONTROL
- BELT MECHANISM MORE COMPLEX THAN ROLLERS
- HIGHER DRIVE FORCE CAPABILITY THAN ROLLERS
- BUT ALSO SUBJECT TO SLIPPAGE
- ELASTOMERS IN BELT SUBJECT TO EMBRITTLEMENT AT LOW TEMPERATURE

Figure 2-59. Platform drive mechanism option.

2.2.2.4.8 Cross Beam Retention and Positioning Mechanism. The options for handling cross beams are illustrated in Figure 2-60. The selected device for cross beam positioning is a translating mechanism, which has an actuator to grip the beam. A second actuator moves the mechanism along a track to align the cross beam with the longitudinal beams, and a third actuator lowers the cross beam into position for joining. A variation of the translating mechanism incorporates a deployment arm and actuator. This device is required for assembly jig option 2 described in Section 2.2.2.5.3.

A swing boom positioner was considered as a means of allowing the beam builder to produce cross beams in a direction parallel to the longitudinal beams. This device would tend to interfere with EVA operations. The assembly jig would require deployable extension to allow the beam builder to move outboard far enough to produce the cross beams.

Use of the RMS was rejected because its positioning accuracy of ± 7.62 cm is not compatible with cross beam positioning requirements (± 0.15 cm). The use of EVA personnel to manually position the cross beams was also rejected because it would be very time consuming and preclude other EVA activities.

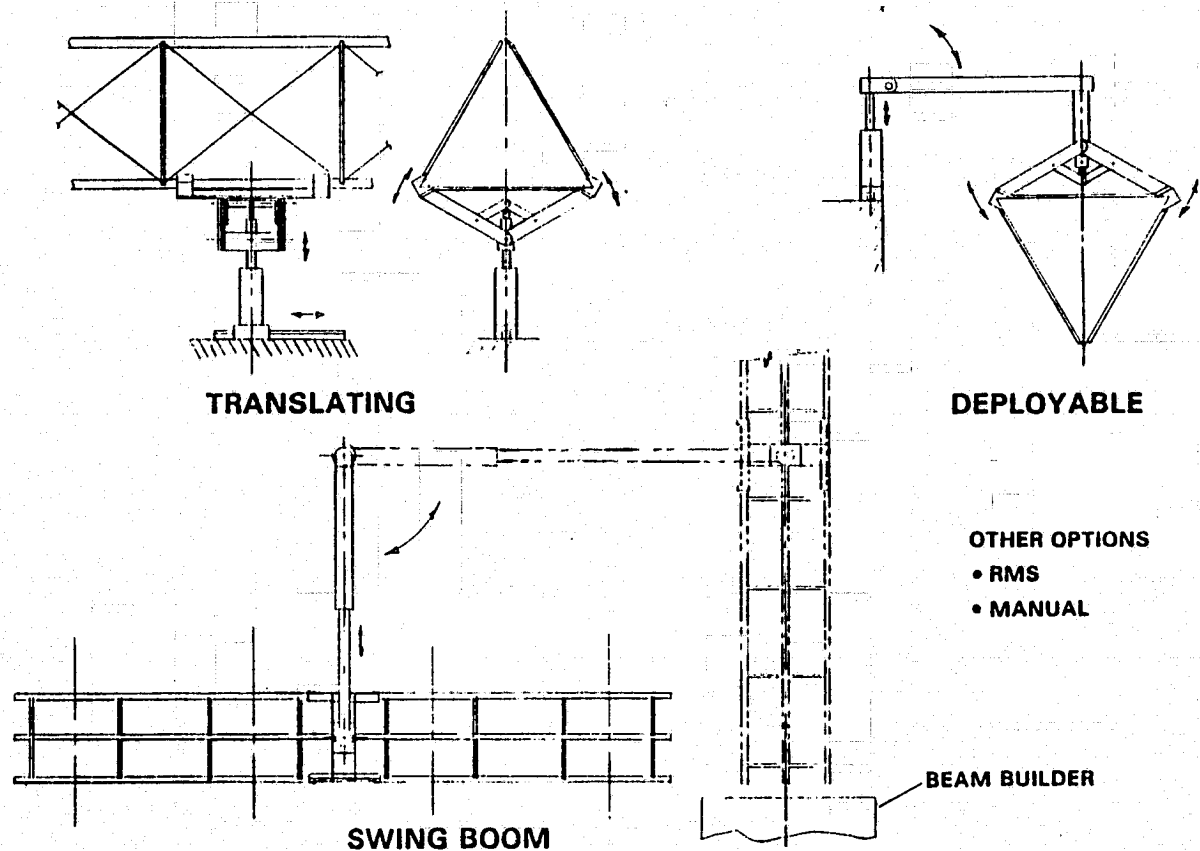


Figure 2-60. Cross beam retention and positioning options.

ORIGINAL PAGE IS
OF POOR QUALITY

2.2.2.4.9 Beam-to-Beam Joining Options. There are several techniques to consider as candidates for joining cross beams to longitudinal beams as indicated in Figure 2-61. Convair has experimentally pursued ultrasonic welding on IRAD funds. It offers the advantages previously mentioned in Section 2.2.1.3.7. A cap-to-cap ultrasonic weld joint at each cap intersection was, therefore, selected for cross-beam-to-longitudinal-beam joining.

JOINING TECHNIQUE	JOINT OPTIONS	
	CAP TO CAP	CAP TO POST
ULTRASONIC WELD	o ✓	
HOT MELT LAP	o	
HOT MELT FILLET	o	o
ADHESIVE TAPE LAP	o	
ADHESIVE LIQUID LAP	o	
VELCRO	o	
FASTENERS	o	
CLIPS	o	o

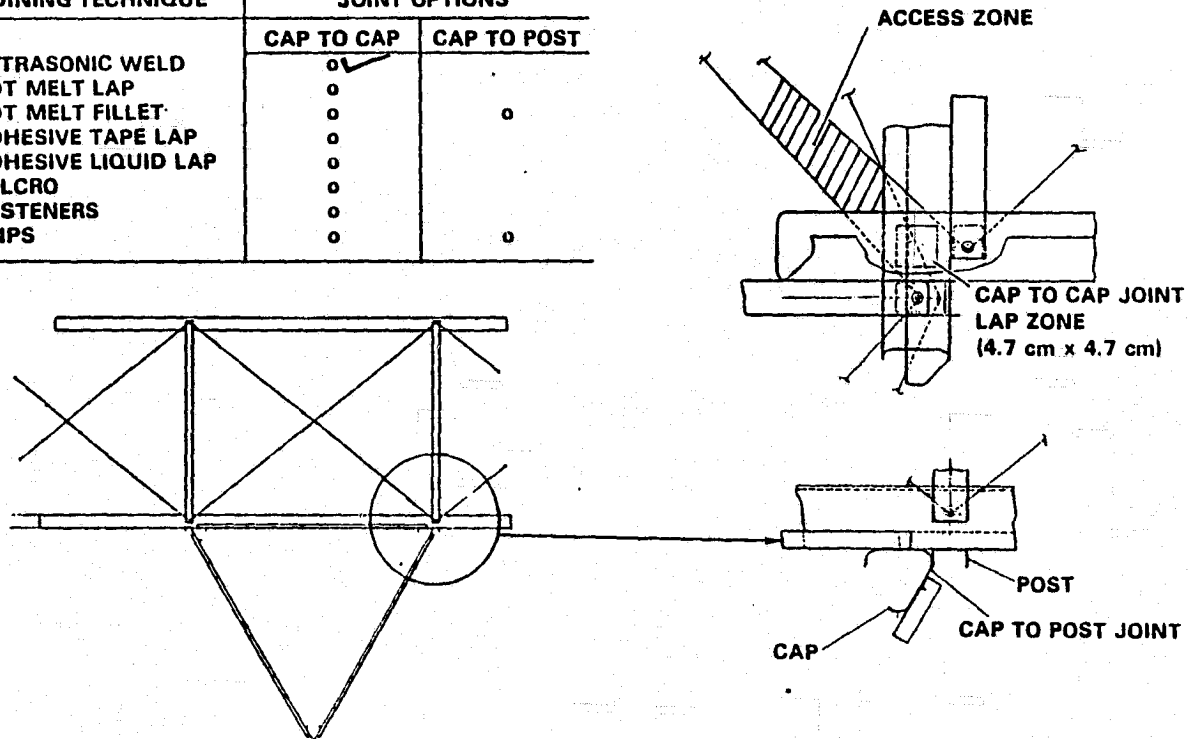


Figure 2-61. Cross-beam-to-longitudinal-beam joining options.

It is feasible to make cap-to-cap joints by inserting the weld horn and anvil into the caps. A view in the plane of the cap-to-cap lap joint (Figure 2-61) shows a narrow access zone occurs between the tensioning cord members. The welding head anvil will be inserted between the cords in this zone as shown in Figure 2-62.

With the cross beam positioned on the longitudinal beams by the assembly jig, the weld heads are aligned with the access zones. Each weld head is raised to a preset height and the weld head engagement drive is activated. The weld horn is inserted at an angle into the lower cap while a drive linkage rotates the weld anvil into the upper cap until the horn and anvil apply contact pressure to the weld zone. On application of the proper contact pressure the weld horn is activated to initiate the weld, then deactivated for a brief cooling period. The weld head engagement drive is reversed and the extend/retract drive lowers the weld head clear of the beams. A rotary indexing drive allows the weld head to be rotated 90° for insertion for the next row of welds where single row welding is employed as described in the next section.

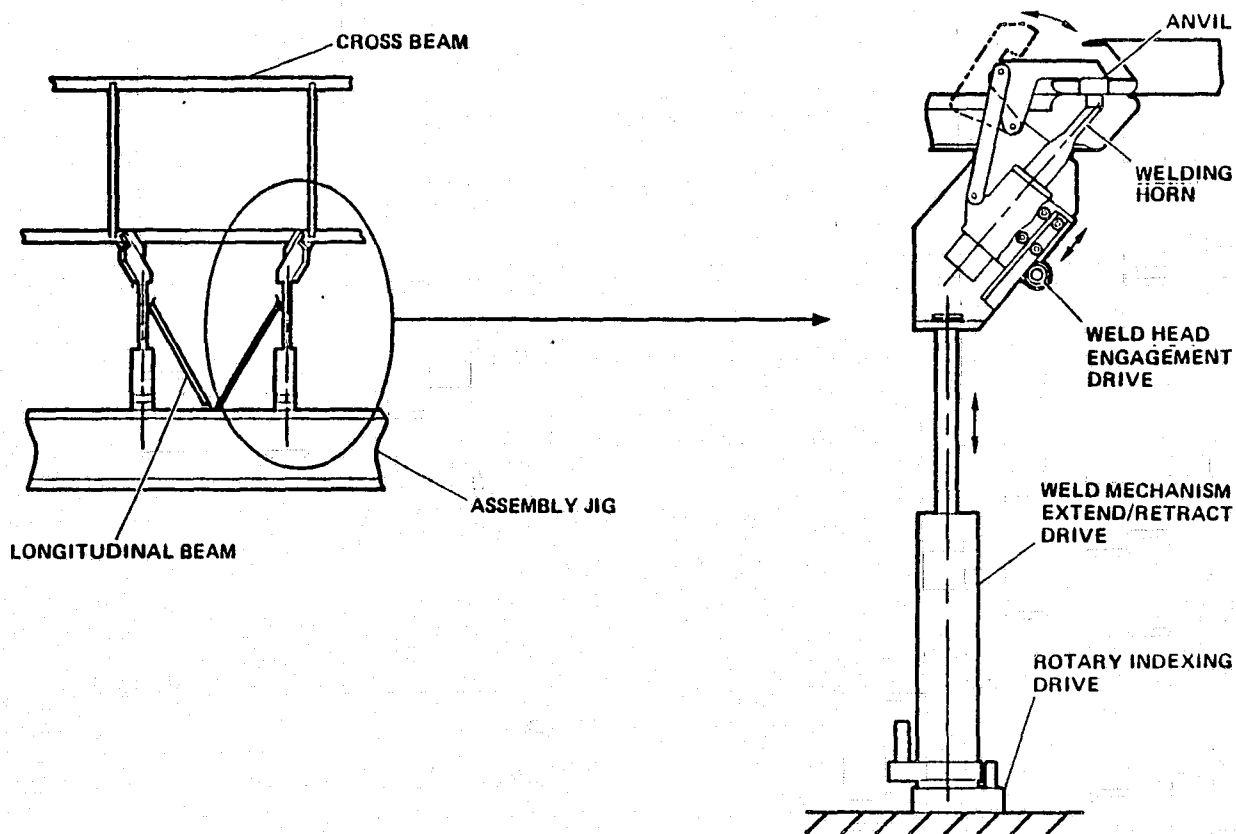


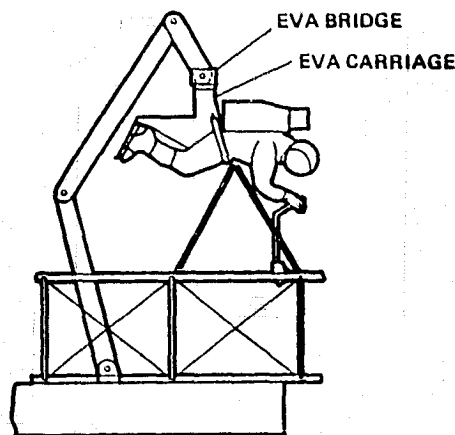
Figure 2-62. Cross-beam-to-longitudinal-beam ultrasonic welding mechanism.

2.2.2.4.10 Beam-to-Beam Joining Techniques. Manual and automatic beam joining techniques are compared in Figure 2-63. Use of EVA personnel for performing cross-beam-to-longitudinal-beam joining is considered too time consuming and would interfere with other EVA activities where manual action is more advantageous, e.g., installing instrumentation or connecting instrument wires.

The single row traveling welder makes two weld joints at a time, then rotates and translates to the next beam. When the first row of beam-to-beam welds is completed, the platform advances to the next row and the process is repeated. The time to perform this operation is estimated to be 15 minutes minimum. This adds over 2 hours to the total platform assembly time, which is not acceptable if the platform is to be constructed in a 3-day period.

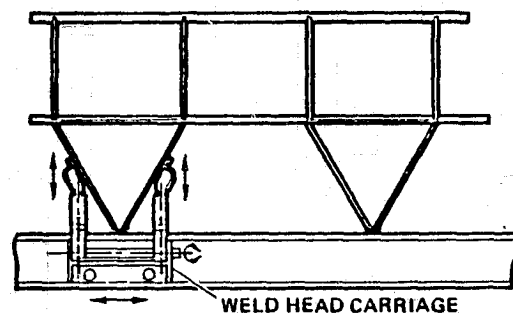
The double row of fixed welders can make all 16 weld joints in about 40 seconds. All 16 weld heads are raised, engaged, sequentially activated, disengaged, and lowered during this period.

The single row fixed welders are raised, engaged, sequentially activated, disengaged, and lowered. The platform then advances 1 m as the weld heads are rotated 45°. The next row of welds is then completed in the same sequence then the weld heads are indexed back 45° as the platform advances to the next cross beam installation station. The time estimated for making the 16 weld joints is 100 seconds.



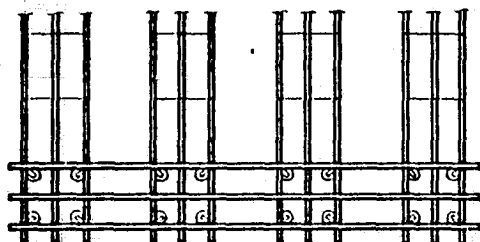
HAND-HELD WELD HEAD

- SLOWEST JOINING METHOD
- INTERFERES WITH ESSENTIAL EVA ACTIVITIES



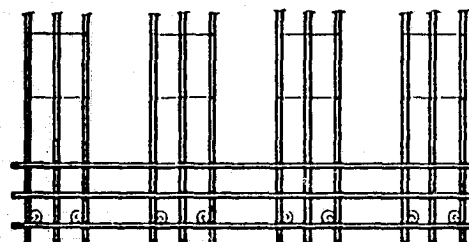
SINGLE ROW TRAVELING WELDER

- GREATEST CONTROL COMPLEXITY
- SLOWEST AUTOMATIC JOINING METHOD
- ADDS A SPECIAL CARRIAGE MECHANISM
- MINIMUM NUMBER OF WELD HEADS FOR LEAST POWER UTILIZATION



DOUBLE ROW FIXED

- FASTEST JOINING METHOD
- MAXIMUM NUMBER OF WELD HEADS (16) INCREASES POWER REQUIREMENTS
- SIMPLEST WELDING MECHANISM
- LEAST NUMBER OF CONTROL FUNCTIONS



SINGLE ROW FIXED

- PERMITS WELDING OPERATIONS WITHIN REASONABLE TIME LIMITS WITH FEWER WELD HEADS (8)
- HALF THE POWER USAGE OF DOUBLE ROW WELDERS
- ADDS INDEX DRIVE MECHANISM TO WELDING MECHANISM
- ADDS TO COMPLEXITY OF PLATFORM DRIVE CONTROL

Figure 2-63. Cross-beam-to-longitudinal-beam joining technique options.

The single row fixed welder technique was selected because it accomplishes the required weld operations in an acceptable amount of time with the least number of weld heads.

2.2.2.4.11 Platform Separation. To aid in determining assembly jig options, the potential options for platform separation shown in Figure 2-64 were taken into consideration. It is considered feasible to perform any of these platform separation options with the candidate assembly jig options presented in the next section.

RMS-aided separation would use the RMS to engage the platform at an appropriate point and move it clear of the assembly jig.

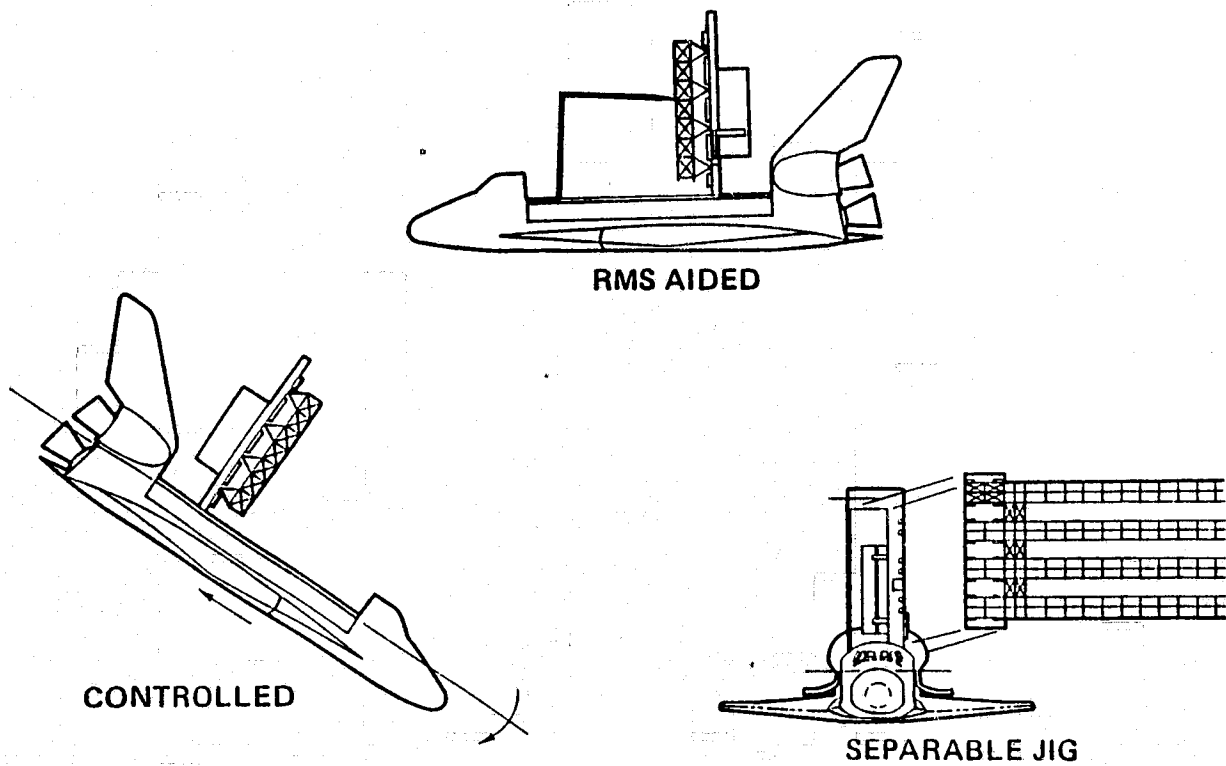


Figure 2-64. Platform separation options.

A controlled separation might consist of either driving the platform out of the assembly jig while adjusting the attitude of the Orbiter or simply releasing the platform from the jig while adjusting the attitude of the Orbiter to clear the platform.

The NASA/JSC concept for retaining the jig with the platform to act as a docking module and integrated subsystems attachment is accomplished by detaching the portion of the jig which has the retention mechanisms attached leaving a partial structure to support the beam builder for the return flight. The partial structure would also contain all the welders, positioners, and umbilicals.

2.2.2.5 Assembly Jig Concept Selection. Concept layouts for each of the candidate assembly jigs are shown in Figures 2-65 through 2-68. Selected process concepts are employed wherever applicable. The principle discriminator is the issue of platform retraction capability. The major considerations of platform retraction capability are:

- a. With Platform Retract Capability
 1. Allows equipment to be installed on platform after platform fabrication and assembly is complete.
 2. Allows return to a section of platform for repair or equipment replacement.
 3. Requires more complex drive/support system to allow step through drive past cross beams.

b. Without Platform Retract Capability

1. Must install equipment on platform during platform assembly.
2. Must interrupt platform fabrication and assembly to make necessary repairs and equipment replacement if failures are detected within a reasonable distance from the Orbiter.
3. Requires fewest drive/support mechanisms.

2.2.2.5.1 Assembly Jig Concept 1. The baseline assembly jig concept shown in Figure 2-65 orients the longitudinal beams with the apex toward the jig. This permits all assembly mechanisms to have a fixed position on the jig. The assembly jig width, however, only allows two rows of beam retention and guide mechanisms of the style shown to be installed. This precludes the ability to retract the platform across the face of the jig since three rows of retention and guide mechanisms are required to allow the cross beams to pass.

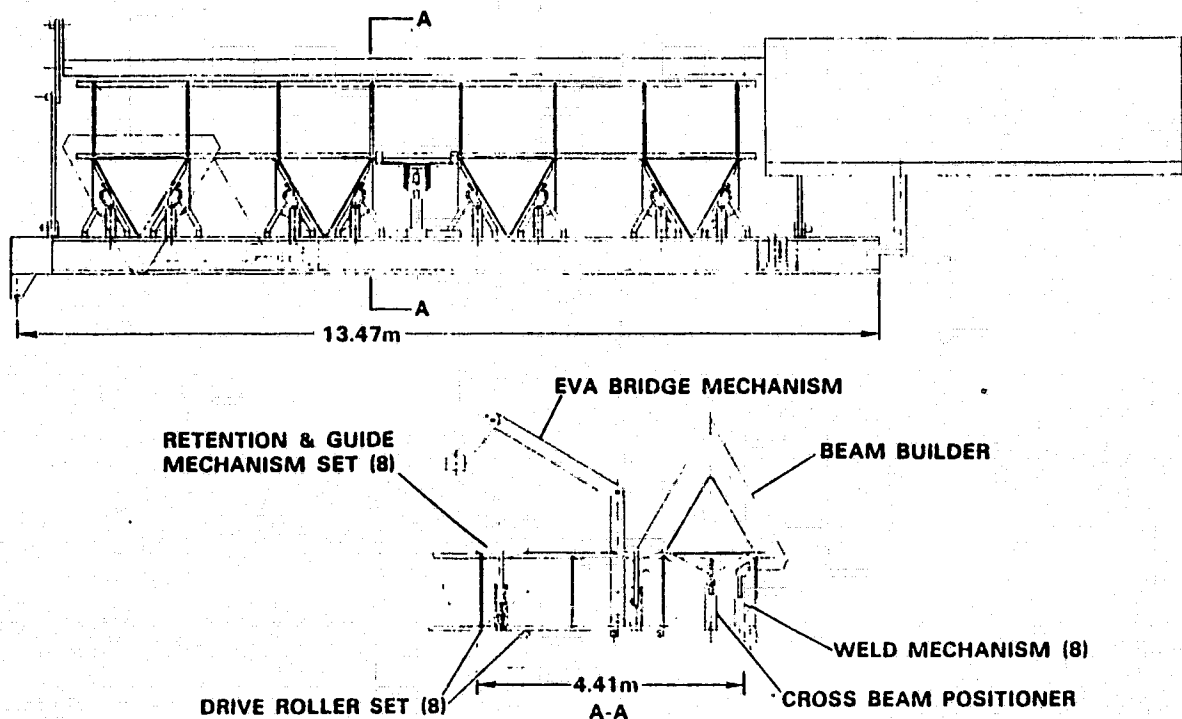


Figure 2-65. Assembly jig concept 1.

At the time the baseline jig concept was developed, it was assumed that each RGM would require two rollers to distribute the moment reaction loads and prevent overstressing the caps at mid-bay. Beam loads analysis subsequently showed that single roller RGMs are permissible. Assembly jig concept 1A was developed as a result of the original RGM concept.

2.2.2.5.2 Assembly Jig Concept 1A. Assembly jig concept 1A, shown in Figure 2-66 is the same as concept 1, except platform retraction capability is added. A third row of RGMs allows the cross beam to step through the retention and guide mechanisms in the following sequence:

- a. As a cross beam approaches the first row of RGMs, the entire row retracts to clear the cross beam leaving the platform supported by the second and third rows of RGMs.
- b. The cross beam advances to the next row of RGMs and the platform pauses.
- c. The first row of RGMs is engaged and the second row retracts leaving the platform supported by the first and third rows. The platform is advanced.
- d. As the cross beam approaches the third row of RGMs, the platform pauses. The second row is engaged and the third row retracted leaving the platform supported by the first and second rows. The platform is advanced.
- e. The third row of RGMs engages after the cross beam passes and the platform continues to advance until the next cross beam is encountered, at which time the step-through process is repeated.

In order to add a third row of double roller RGMs, a fold-out extension jig is added to the baseline configuration.

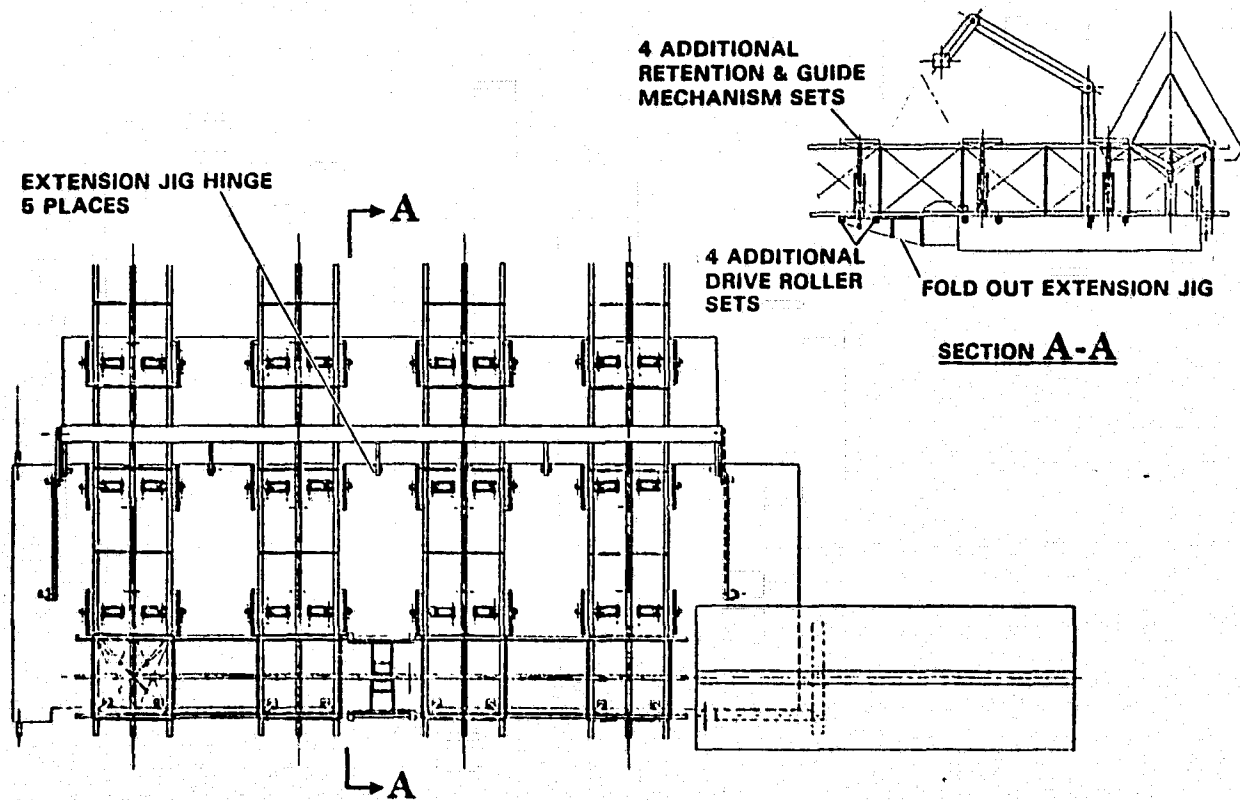


Figure 2-66. Assembly jig concept 1A.

2.2.2.5.3 Assembly Jig Concept 2. Assembly jig concept 2, shown in Figure 2-67, orients the longitudinal beams with the apex away from the jig. To reach the cross beam, the cross beam positioner and the weld mechanisms must be equipped with deployment mechanisms. Advantages of this approach are:

- a. The beam builder handling arm is eliminated.
- b. Size of the assembly jig structure is reduced.
- c. Reduces number of retention and guide retraction linkage mechanisms from 16 to 18.

Disadvantages include:

- a. Precludes any capability to retract the platform.
- b. Deployable mechanisms increase mechanical and controls complexity.
- c. Higher risk of interference with assembly jig mechanisms during platform separation.

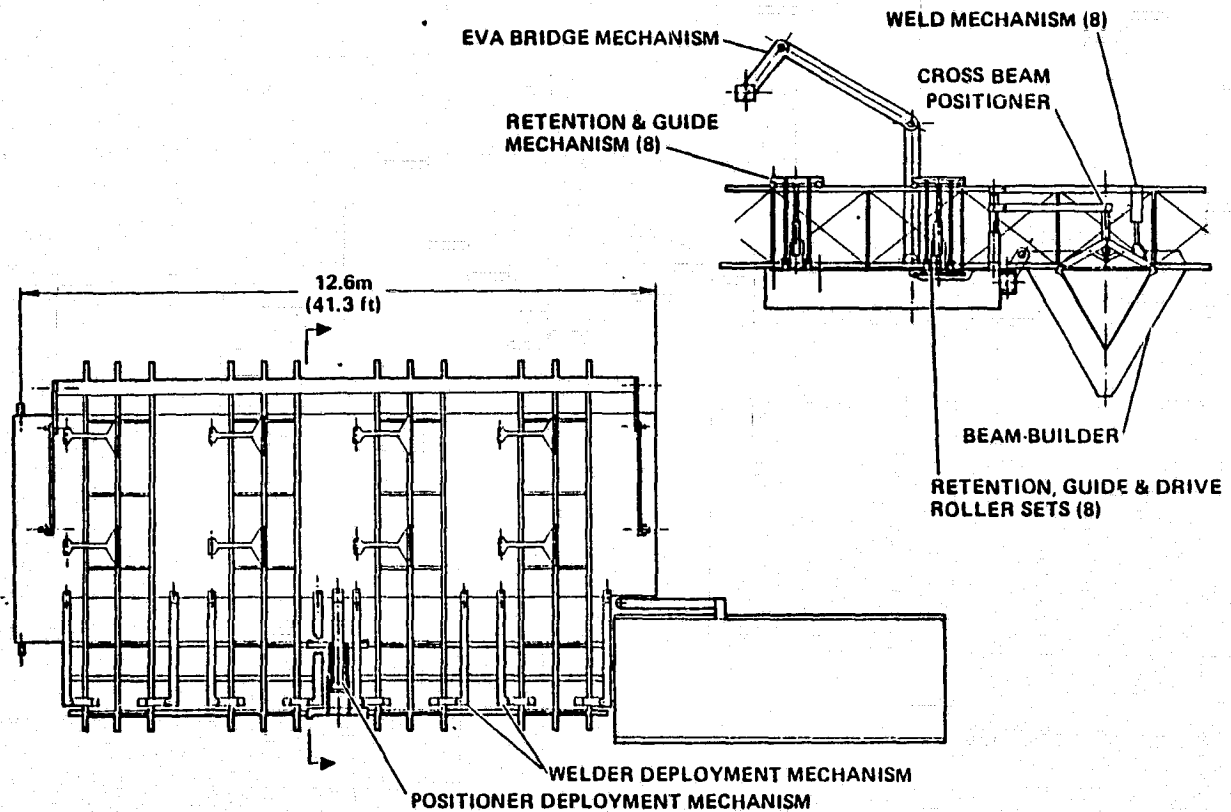


Figure 2-67. Assembly jig concept 2.

2.2.2.5.4 Assembly Jig Concept 3. Assembly jig concept 3, shown in Figure 2-68, has the same features as concept 1, with the exception that the beam builder would have only two positions for beam fabrication rather than five positions. A beam transporter would grasp each longitudinal beam as it is completed and, following beam cut-off, transport the beam to its respective position on the jig. The potential advantage of eliminating the beam builder carriage mechanism is offset by the following disadvantages.

- a. Added mechanical and control complexity of the beam transporter mechanism.
- b. Increased width of assembly jig would require an extension to be added.
- c. Ability to retract all assembly mechanisms below the face of the jig to allow the longitudinal beams to pass would increase the size and structural complexity of the jig.

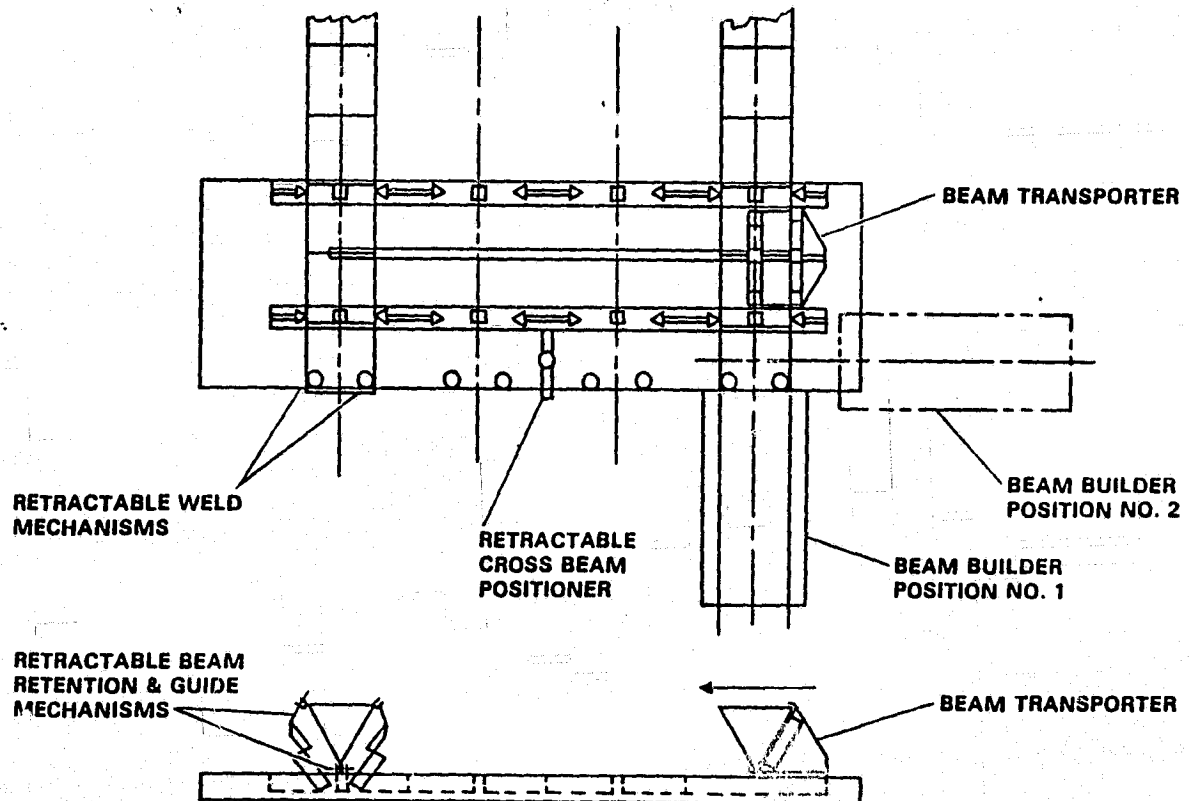


Figure 2-68. Assembly jig concept 3.

2.2.2.5.5 Concept Evaluation and Selection. The four assembly jig concepts were derived using the baseline platform as the article to be produced. As a result, all four concepts perform the same basic functions with some degree of variation in the machine functions and control operations. These variations have obvious impact on the selected evaluation criteria. This allowed a relative rating system rather than a numerical rating system to be used for concept evaluation. The evaluation criteria and results are given in Table 2-19.

Table 2-19. Assembly jig concept evaluation.

CONCEPT	SYSTEM COMPLEXITY		PROGRAM RISK	WEIGHT	OPERATIONAL COMPATIBILITY
	MECHANICAL	CONTROL/SOFTWARE			
1	LOW	LOW	LOW	LOW	FAIR
1A	LOW	LOW	LOW	MEDIUM	GOOD
2	MEDIUM	MEDIUM	MEDIUM	LOW	FAIR
3	HIGHEST	HIGHEST	HIGHEST	HIGHEST	POOR

• CONTROL & WELDING POWER IS A MINIMAL CONSIDERATION

<u>CRITERIA</u>	<u>DESCRIPTION</u>
MECHANICAL COMPLEXITY	RELATIVE NUMBER OF ACTIVE MECHANISMS REQUIRED
CONTROL/SOFTWARE COMPLEXITY	RELATIVE NUMBER OF MACHINE OPERATIONS TO MONITOR AND CONTROL
PROGRAM RISK	RELATIVE NUMBER OF DIFFERENT KINDS OF MECHANISMS TO DESIGN AND DEVELOP
WEIGHT	APPARENT RELATIVE WEIGHT OF THE ASSEMBLY JIG
OPERATIONAL COMPATIBILITY	APPARENT COMPATIBILITY WITH STS POTENTIAL MISSION REQUIREMENTS

Concept 1A was selected because of its low overall complexity and risk ranking, and good operational compatibility rating. Its primary advantage is the ability to retract the platform for post-fabrication operations. Its medium weight rating stems from the jig extension; however, further study showed there was no need for this extension.

2.2.2.6 Selected Assembly Jig Preliminary Design. Preliminary design layouts of the selected SSAFE assembly jig are presented in Figures 2-69 and 2-70. The selected assembly jig concept orients the longitudinal beams with the apex toward the jig. This permits all assembly mechanisms to have a fixed position on the jig. Three rows of retention and guide mechanisms (RGM) provide the capability to retract the platform. The cross beams step through the RGMs as described in Section 2.2.2.5. The mechanical subsystems are described in the following sections.

TELESCOPING LINEAR SCREW ACTUATOR

ROTARY INDEXING DRIVE

STRUCTURAL SUPPORT

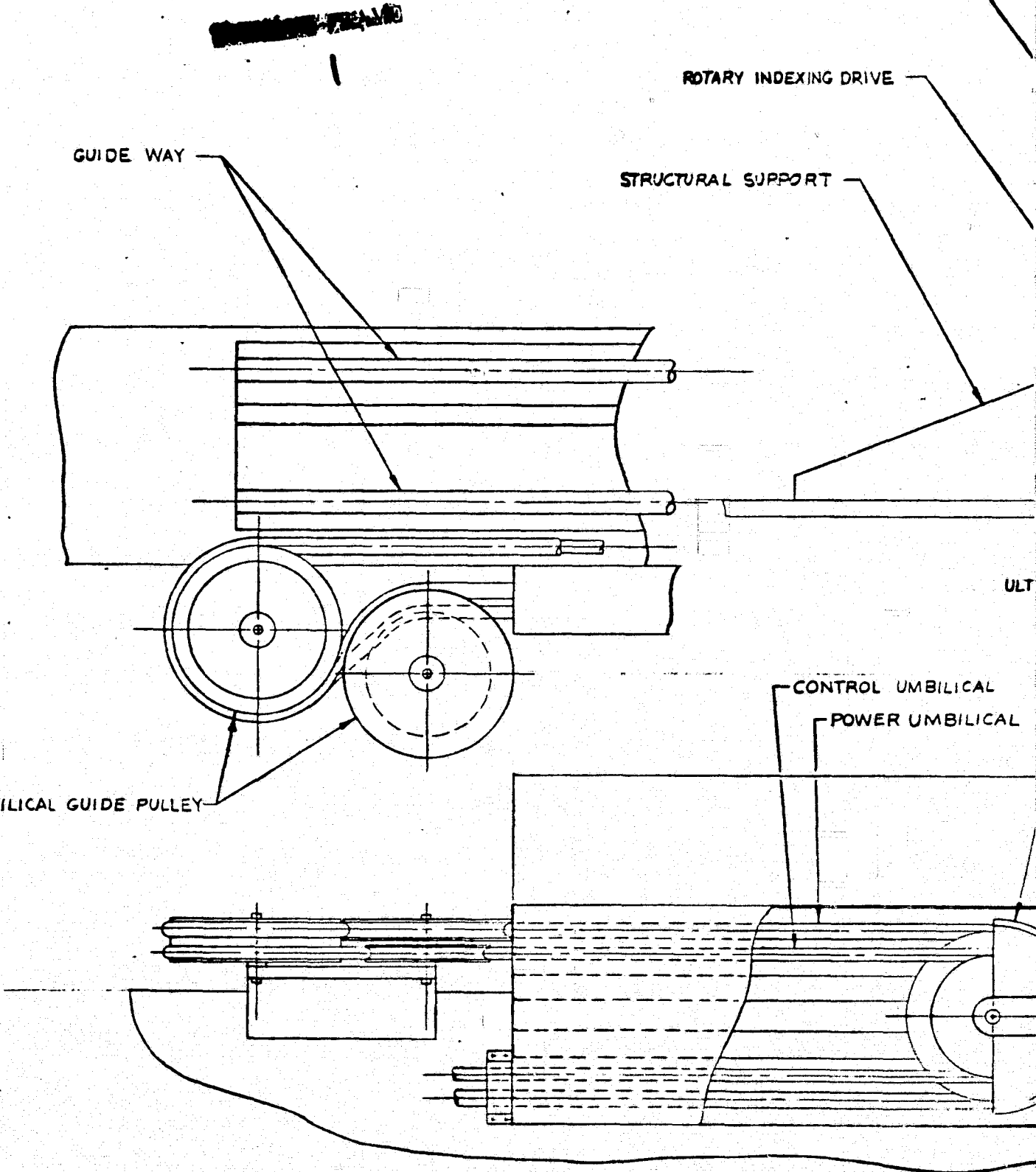
GUIDE WAY

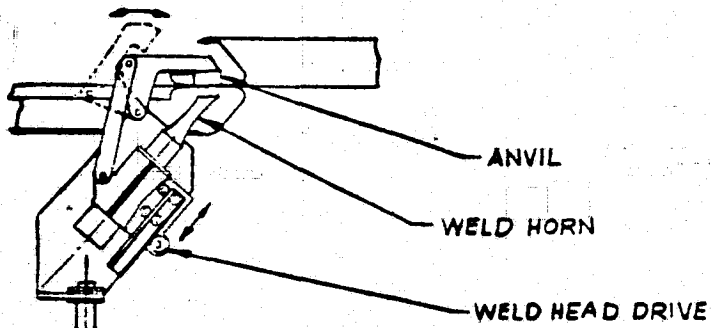
ULT

CONTROL UMBILICAL

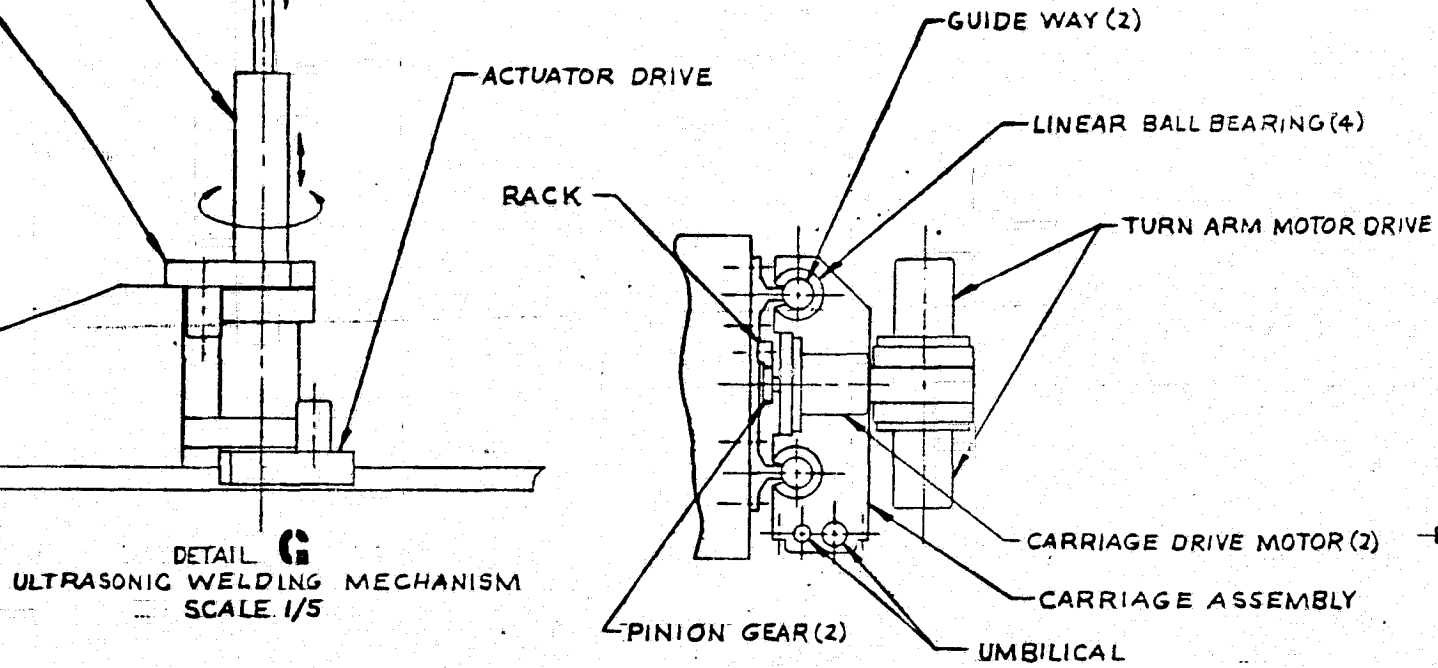
POWER UMBILICAL

UMBILICAL GUIDE PULLEY

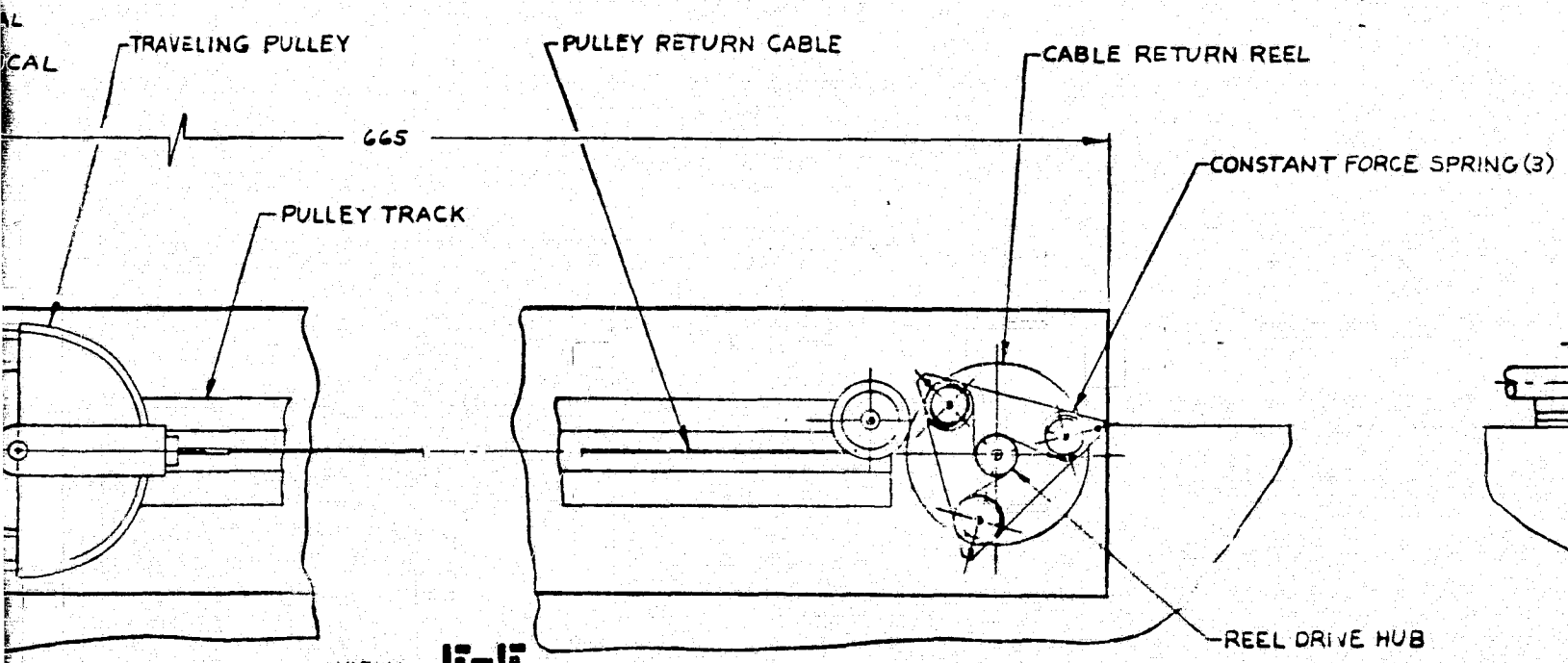




~~FIGURE 2~~
2



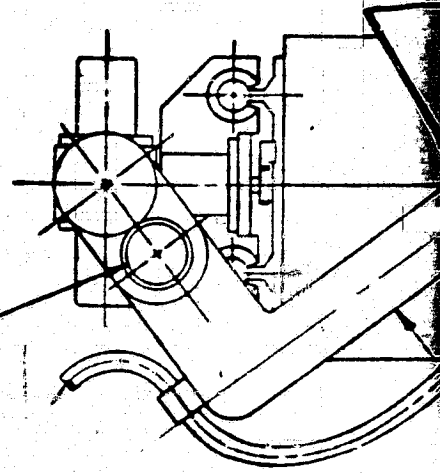
DETAIL C
ULTRASONIC WELDING MECHANISM
SCALE 1/5



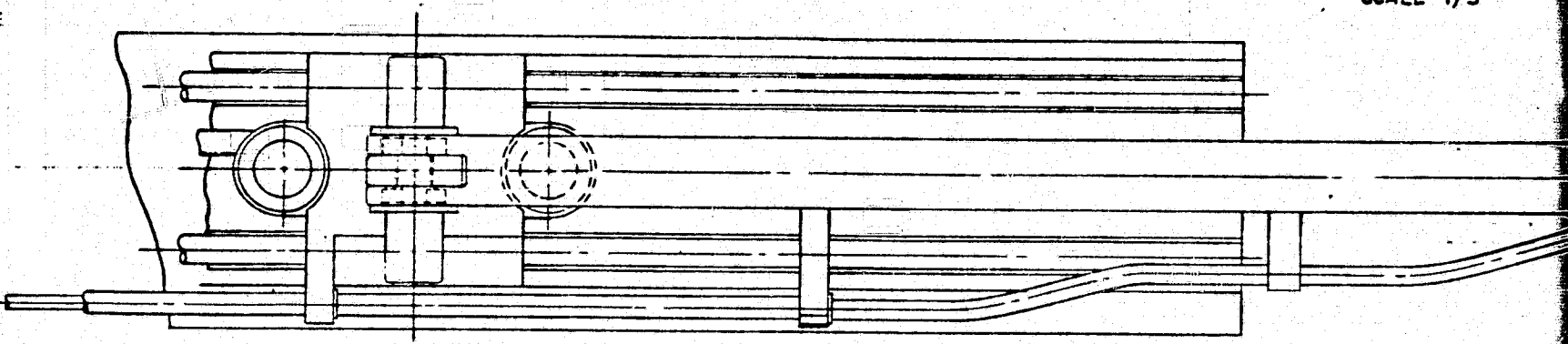
VIEW F-F
UMBILICAL SLACK CONTROL MECHANISM
SCALE 1/5

~~FIGURE 2-69~~
3

INBOARD ROLL
DRIVE MOTOR (REF)

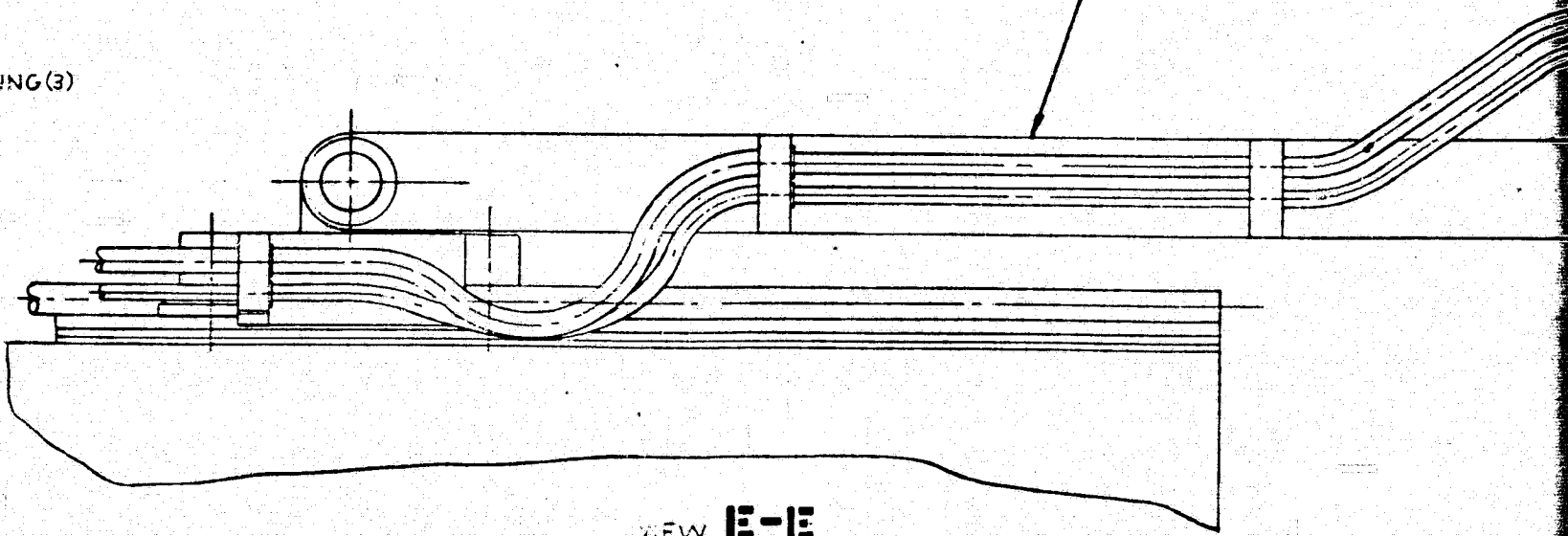


VIEW H-H
ROLL LINK MECHANISM
SCALE 1/5



E SPRING(3)

TURN ARM



VIEW E-E
BEAM BUILDER ROLL/TURN MECHANISM
SCALE 1/5

Figure 2-69. Preliminary

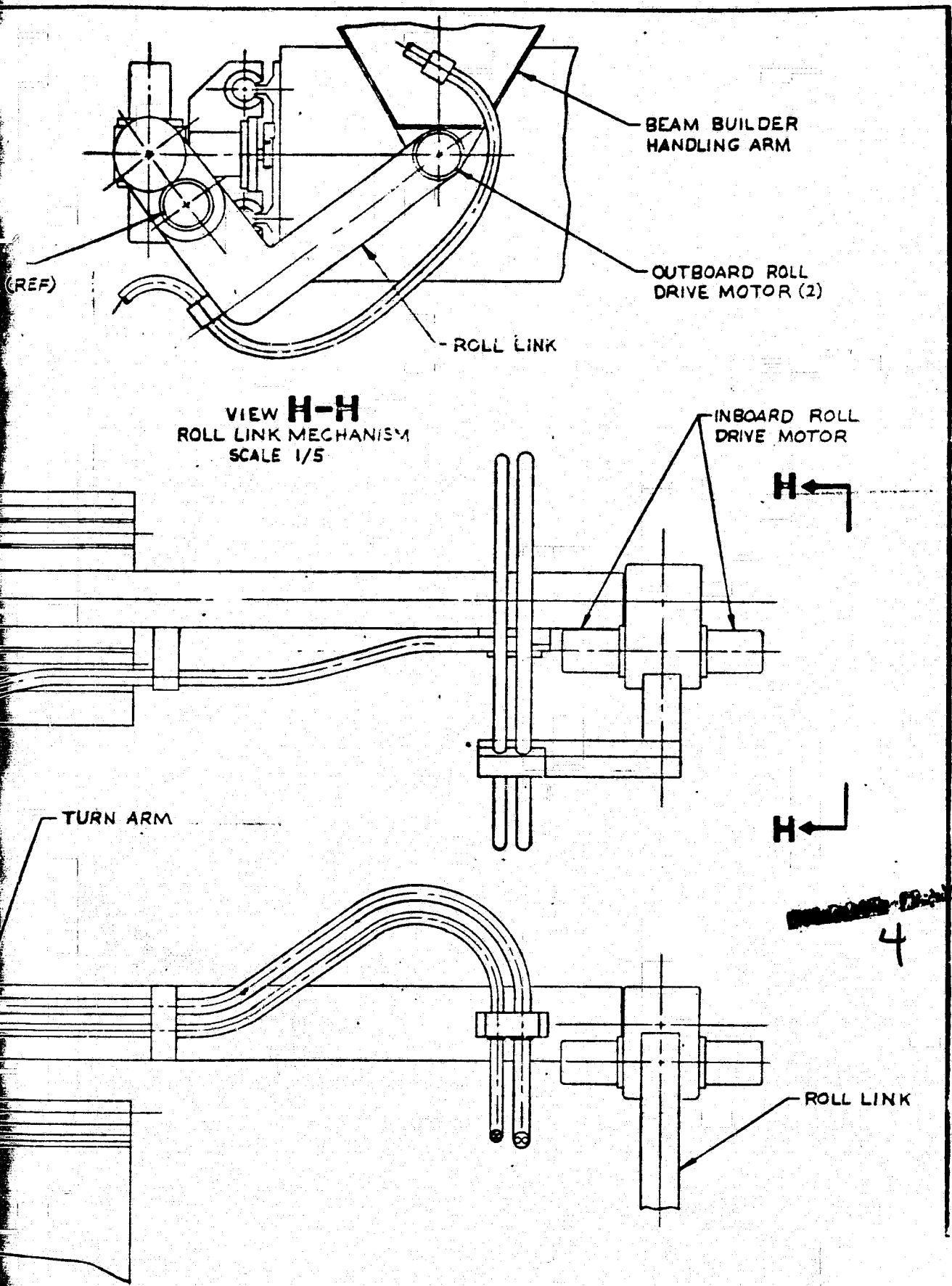
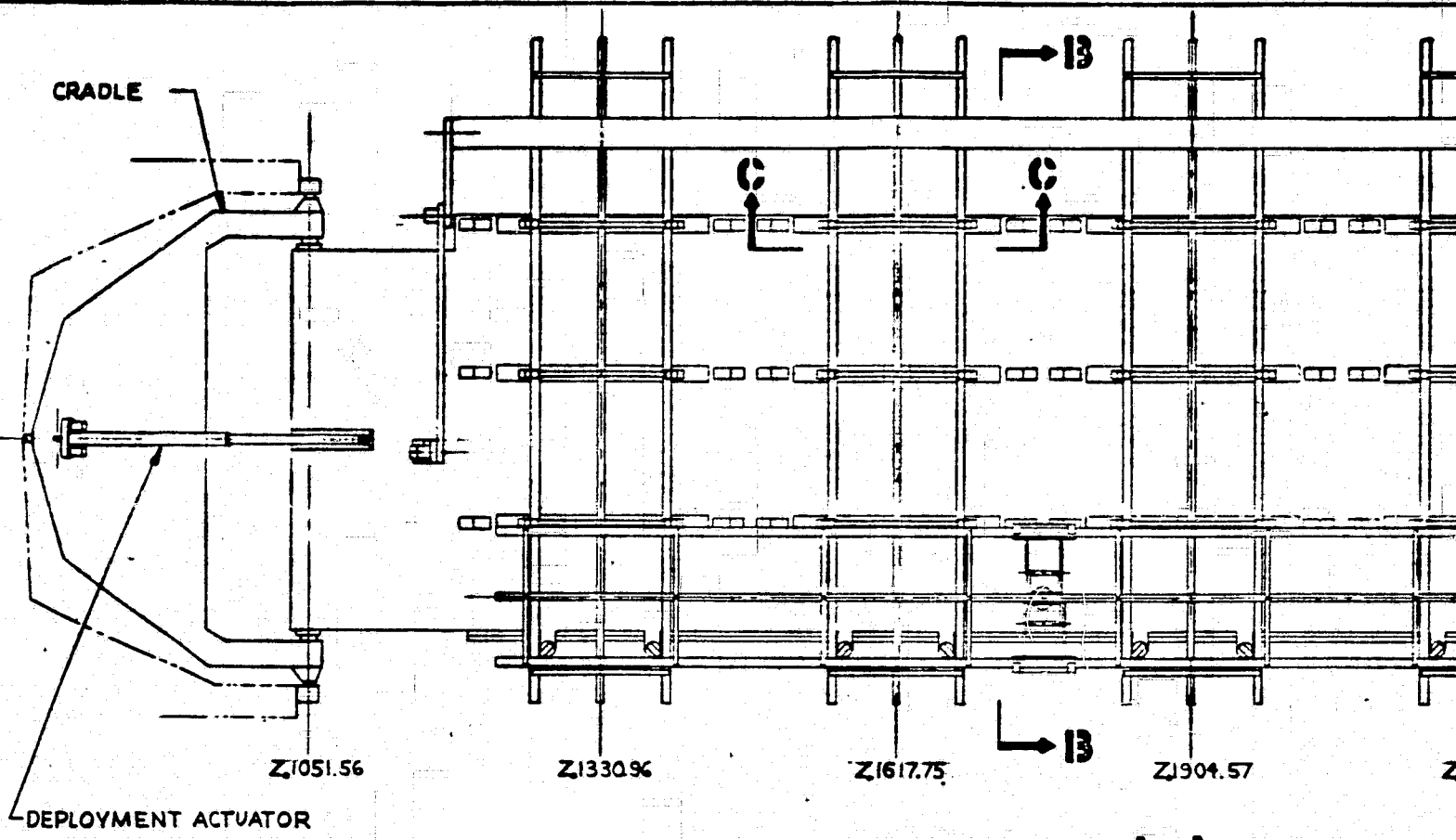
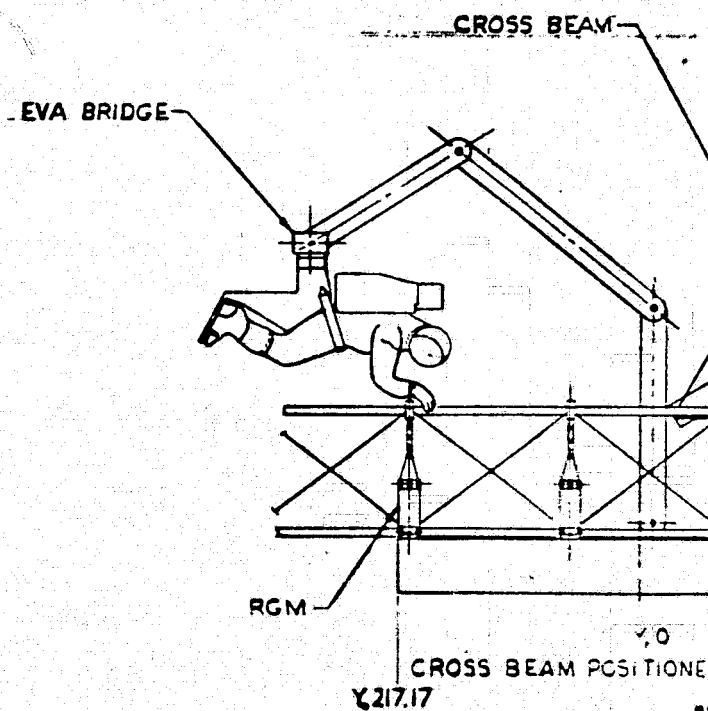


Figure 2-69. Preliminary design layout of the SSAFE assembly. ORIGINAL PAGE IS OF POOR QUALITY

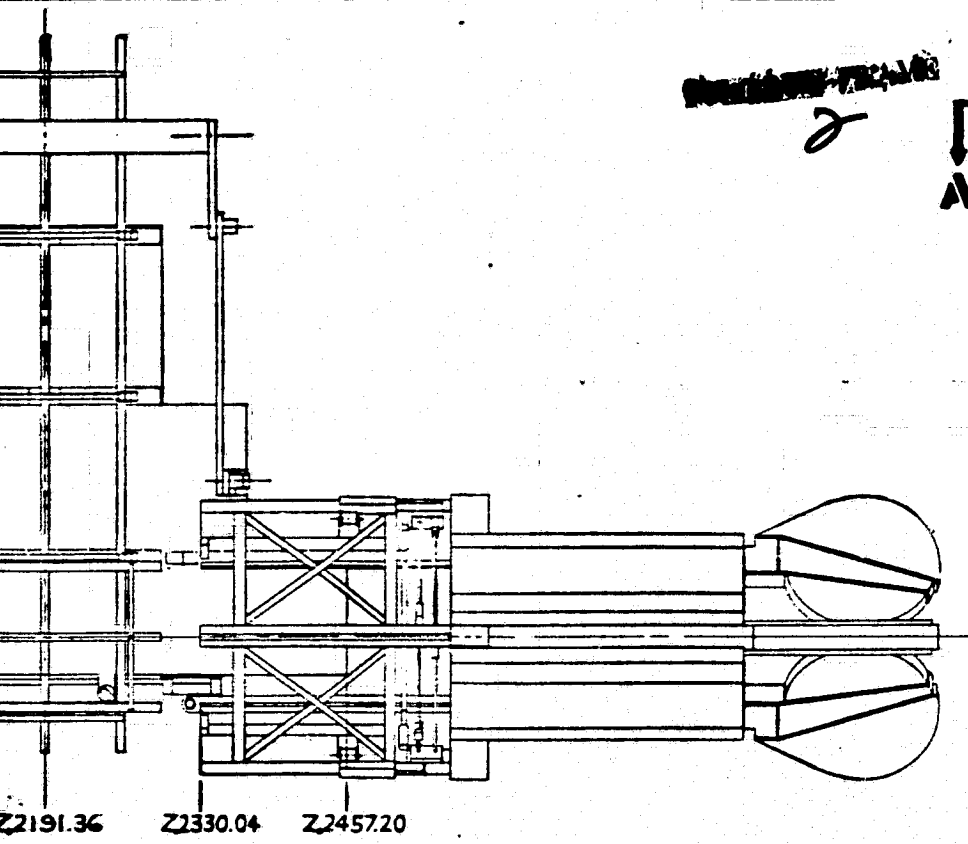


~~FRAME~~

ORIGINAL PAGE IS
OF POOR QUALITY



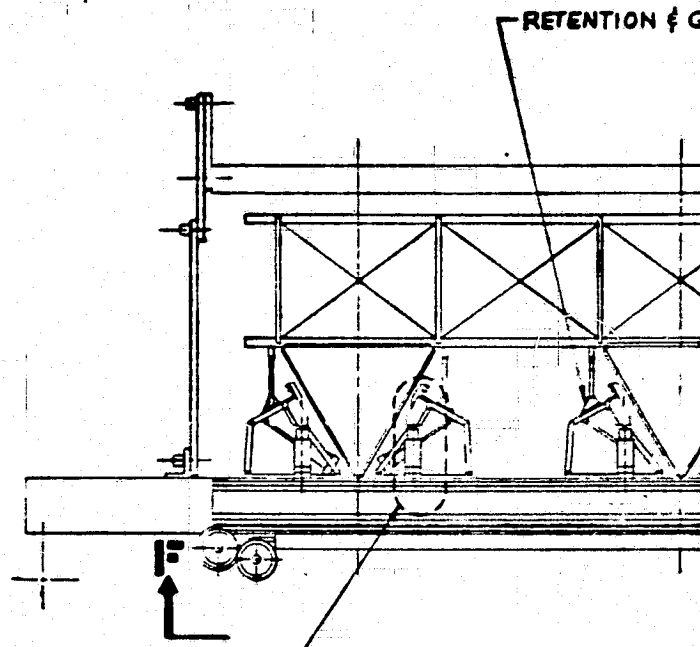
SECTION 13
PLATFORM CON
PROCESS
SCALE 1/



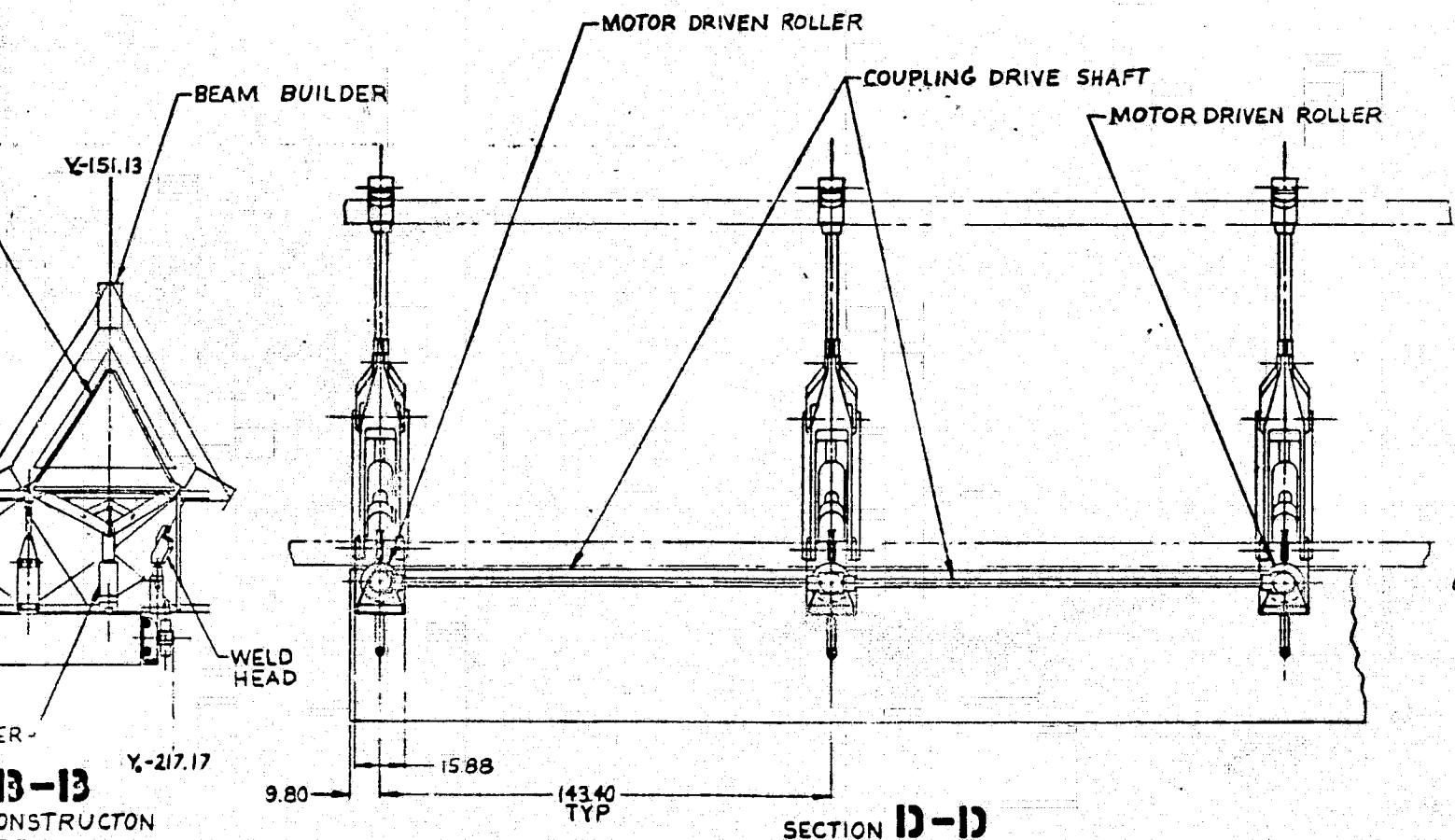
~~RETENTION FRAME~~

2

A



DETAIL C SH2 WELDING MECHANISM



3-13
CONSTRUCTION
SE S
1/30

FLEXIBLE COUPLER

MECHANISM (RGM)

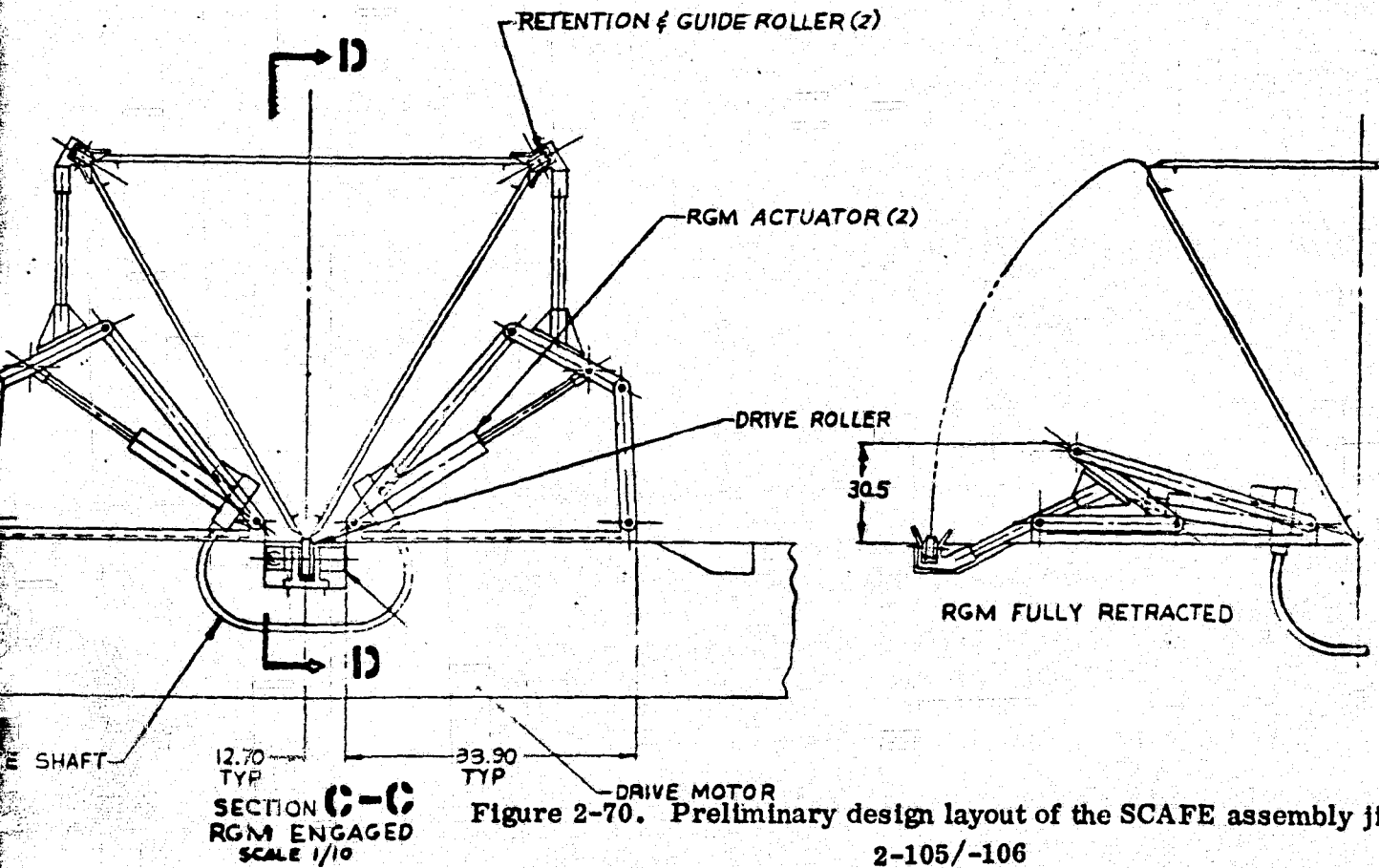
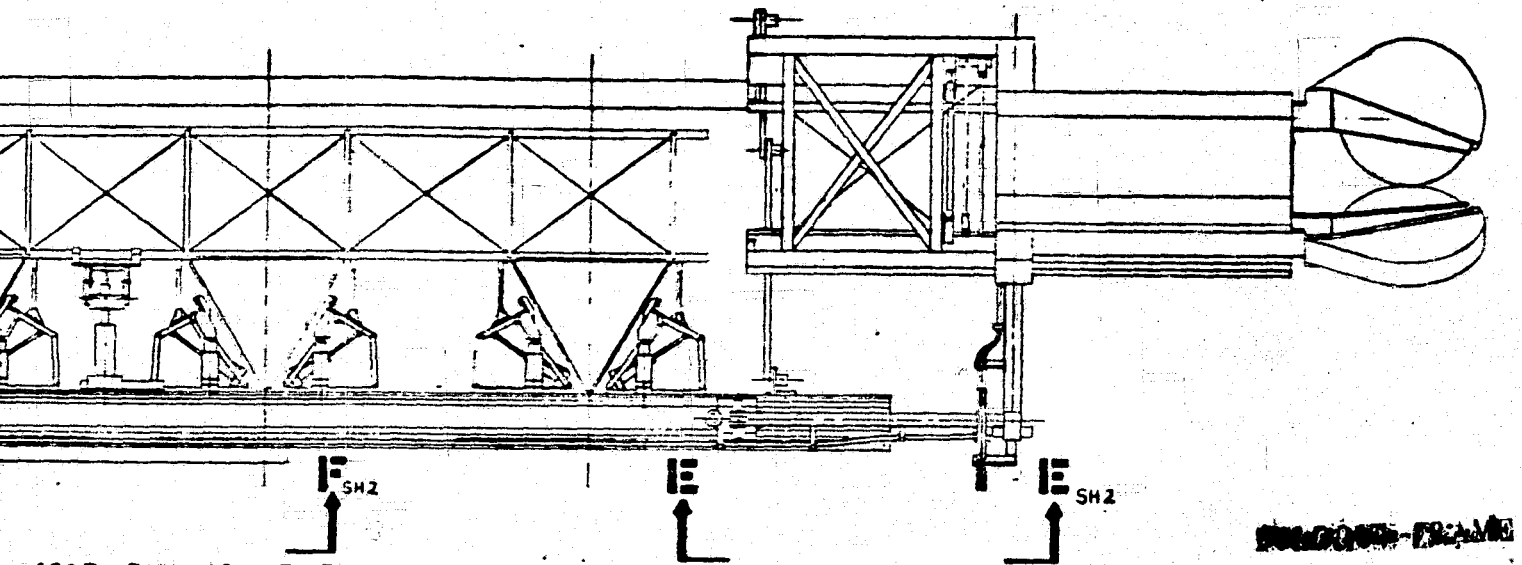


Figure 2-70. Preliminary design layout of the SSAFE assembly jig.

2-105/-106

2.2.2.6.1 Flight Support Subsystem. The flight support subsystem includes all the mechanisms necessary to secure the SCAFE assembly jig and cradle assembly to each other and to the Orbiter payload bay, as shown in Figure 2-71. Included are provisions for jettison capability and deployment of the assembly jig from the Orbiter payload bay. This subsystem requires the following mechanisms:

- a. Deployment mechanism (D) includes a dual motor-driven screw actuator with integral latching capability and necessary position sensors.
- b. Beam builder holddown latch mechanisms (B), which secure the beam builder to the assembly jig during ascent and descent and are automatically disengaged for beam builder deployment.
- c. Forward support fittings (F) and deployment latch mechanism. The Orbiter-mounted deployment latch mechanism is assumed to be a government furnished device, including all controls.
- d. Cradle support fittings (C) which allow the jig to rotate in the cradle, and jettison latch mechanisms (J) to permit automatic separation of the assembly jig from the cradle.

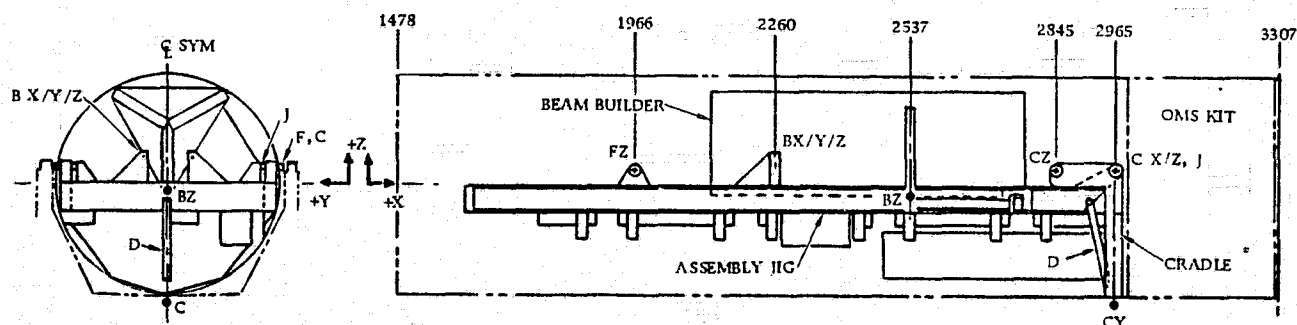


Figure 2-71. Flight support provisions.

2.2.2.6.2 Beam Builder Positioning Subsystem. The beam builder positioning subsystem includes all mechanisms necessary to deploy and position the beam builder with respect to the assembly jig. The mechanism concepts for this subsystem shown in Figure 2-70 are described as follows:

- a. The carriage mechanism travels along two round guide ways on four linear ball bearings. Dual drive redundancy is provided by two independent gear motors which operate pinion gears in a common spur gear rack. Each drive may be automatically disengaged through magnetic clutch mechanisms. The carriage body includes the support link for the turn arm and a fairlead clamp, which secures the umbilicals to the carriage in such a way as to allow a pull force to be exerted on the umbilicals. The ground guide ways are fastened to a machined support which, in turn, is fastened to the assembly jig structure.

- b. The turn arm mechanism rotates about a shaft which is keyed to the carriage support link. Dual drive redundancy is provided by two independent gear motors of the same design as the carriage drive motors. The motor shafts are splined or keyed inside the clevis shaft. Roller bearings are provided in both sides of the clevis. All bearings are compatible with maximum VRCS imposed loads; however, loads are minimized if VRCS is not activated during beam builder positioning operations.

The other end of the turn arm is a straight shaft about which the roll link rotates on roller bearings mounted inside the inboard end of the roll link. Umbilical supports and clamps are mounted on the turn arm to provide cable loops about each axis of rotation in such a way as to prevent twisting of umbilicals as the beam builder is rotated and translated.

- c. The roll link mechanism has an inboard and outboard rotating drive. The inboard roll drive has two redundant gear motors similar to the carriage drive motors.

Each motor operates a spur gear which acts against a gear mounted on the turn arm shaft. The outboard roll drive has two similar motors which are keyed or splined to a clevis shaft mounted on the beam builder handling arm. Both sides of the outboard clevis are provided with roller bearings. An umbilical support and clamp are mounted on the roll link to provide cable loops about each axis of rotation.

- d. The umbilical handling mechanism uses a track guided traveling double pulley, which is connected to a spring return reel. As the beam builder carriage moves up the jig, it pulls on the power and control umbilicals which are routed over two guide pulleys. The pull force displaces the traveling pulley half the distance of the carriage travel. As the carriage returns, the spring return reel retracts the traveling pulley which takes up the umbilical slack.

2.2.2.6.3 Longitudinal Beam Handling Subsystem. The longitudinal beam handling subsystem includes all the mechanisms required to retain and position the longitudinal beams on the assembly jig. These mechanisms are described as follows:

- a. The retention and guide mechanism (RGM) clamps each longitudinal beam to the jig and guides the beam as it is translated by the platform drive mechanism (PDM). The twelve RGMs consist of a pair of rollers each mounted on a semi-rigid shaft attached to a four bar linkage mechanism. Each four bar linkage is driven by a linear screw drive actuator. Each actuator has a single motor drive which can be automatically disengaged by a magnetic clutch mechanism. Each pair of actuators is drive coupled through a flexible drive shaft. This arrangement provides dual motor drive redundancy for each RGM.

The RGMs are fully retracted for flight and platform separation. During step-through operation, the RGMs are partially retracted in sequence to clear the cross beams as they pass over.

- b. The PDM acts as a friction holding device to prevent beam translation on the jig when clamped on the RGMs. Three friction drive wheels apply drive force to each longitudinal beam such that the beams can be individually positioned or driven in unison. Platform mating guides (not shown) are required to guide the platform into the PDMs during platform capture and remating operations.

Dual motor drive redundancy is provided by coupling three rollers to a common drive shaft with motor drive input to each end roller. Either motor can be automatically disengaged by a clutch mechanism, should the other motor fail. The technique for hand-off of a beam from the beam builder to the RGM is as follows:

1. The beam builder is closely aligned with the center of the RGMs by an index pin which is driven by the longitudinal beam latch mechanism on the beam builder into an indexing hole in the side of the jig as shown in Figure 2-43. The latch mechanism engages the carriage ways, which assures angular alignment with the RGM.
2. The vertical alignment of the beam with the PDM is biased during machine setup and alignment to ensure a small (1 to 2 mm) clearance will exist during beam fabrication between the drive rollers and the beam.
3. When the beam is complete and ready for handoff, the two RGMs farthest from the beam builder are engaged. The span between the beam builder and the RGMs allows sufficient deflection to take place such that the gap between the drive rollers and the beam can be closed without damaging the beam.
4. The beam is severed from the beam builder by the cutoff mechanisms before engaging the third RGM. The beam builder is unlatched and translated to the next position leaving the beam retained by the RGMs.

2.2.2.6.4 Cross Beam Handling Subsystem. The cross beam handling subsystem is comprised of the cross beam positioner mechanism. This device is driven laterally along a short track to a preset position directly under the center of the finished cross beam as it is supported in the beam builder. The handler arm mechanism is raised to a preset position by a linear screw drive actuator. The beam handler arms are engaged to grasp the cross beam on two caps by a second screw drive actuator. After the beam is severed from the beam builder, the positioner is driven laterally to a preset position which aligns the cross beam with the longitudinal beam cross-members. The linear screw drive actuator then lowers the beam into contact with the longitudinal beams. When the first row of cap-to-cap weld joints is complete, the second screw drive actuator retracts the handler arms below the cross beam and the platform is advanced to the next weld station. All positioner/handler drives are dual motor redundant.

2.2.2.6.5 Platform Assembly Subsystem. The platform assembly subsystem has eight platform welding mechanisms. The function of the single row fixed welding mechanisms was described in Section 2.2.2.4.10. Each drive function is dual motor redundant.

2.2.2.6.6 EVA Support Subsystem. The EVA support subsystem includes all mechanisms and controls required to aid EVA personnel in accomplishing platform equipment installation tasks. The principle aid is the EVA bridge mechanism. This device allows one man to position and support his body over any position on the platform within the reach of the bridge mechanism.

The two control arm assemblies have synchronized motor drives for each link. These control arms move the bridge up and down as well as longitudinally back and forth. A carriage mechanism traverses the bridge to allow lateral positioning of the man restrained by the traveling chair. The chair provides foot restraints as well as body restraints to allow a neutral body position to be maintained.

The chair is equipped with a local control panel to permit the man to manually control his position with respect to the platform. Safety position limit sensors prevent inadvertent collision of the man with the platform. The chair position can also be manually controlled from a second control station located in the payload bay on the end of the assembly jig.

The traveling chair is detached and stowed for flight to allow the EVA bridge to lie flat on the face of the jig.

2.2.2.6.7 Structure. The assembly jig structure is composed of welded and mechanically assembled elements, arranged as shown in Figure 2-72. The main structure is a closed box with an internal matrix of longitudinal and transverse beams.

Beam locations are dictated by the RGM drive support provisions. Rather than sacrifice overall structural depth, a recessed pan is used at each RGM drive location. The pans are incorporated into full-depth welded fittings which also include splice provisions for the longitudinal beams. Transverse beams are continuous across the full jig width.

Shallow pans are also provided between longitudinal beams along the two inboard RGM axes to accommodate the upper RGM rollers in the maximum open position. Along the outboard RGM axis ($Y_0 + 207.4$ cm) the structure outboard of the closing spar is simply omitted to provide the same mechanism foldout clearance.

The shear covering on both jig surfaces consists of integrally stiffened aluminum plate with simple blade stiffeners in the longitudinal direction only. Skin splicing is accomplished by beam flanges. At two locations, at $Y_0 0.0$, skin panel pans are provided to accommodate beam builder stowage.

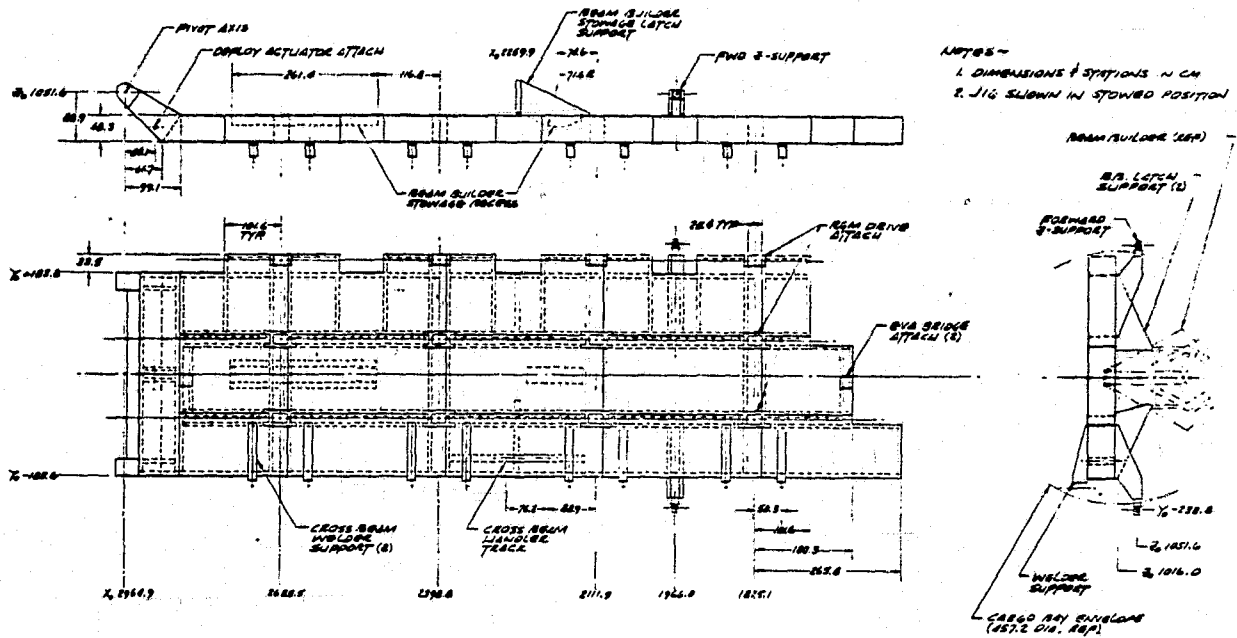


Figure 2-72. Assembly jig structure.

Auxiliary bolt-on fittings are provided at eight locations to support the cross beam welders, and two places to provide forward interface attachment in the Orbiter cargo bay. Tension ties are also provided between the transverse beams and the Y_0 -183.6 cm spar to transmit beam builder latch loads.

Local mounting provisions and associated substructure are provided for EVA bridge supports (2 places), cross beam handler track installation, deployment actuator attachment, and pivot bearing installation (2 places).

2.2.3 AVIONICS AND CONTROLS. The control and monitor functions associated with the SCAFE are performed by three semi-independent systems. Executive control of SCAFE operation is conducted by the Orbiter crew using primarily Orbiter control and monitor equipment located in the aft cabin and a sub-set of available payload support equipment. (Reference Section 3.7.4.) Using this equipment and associated Orbiter/SCAFE interface, the crew is able to control and monitor all SCAFE operations. These include: (1) assembly jig and beam builder on latching, (2) assembly jig and beam builder deployment, (3) beam builder positioning about the assembly jig, (4) assembly jig operations, (5) beam builder initialization, and (6) beam builder automated assembly operations.

The remaining two systems consist of automated control and monitor subsystems associated with both the assembly jig and the beam builder machine. The following two sections discuss the functions and operation of the assembly jig and beam builder controls.

ORIGINAL PAGE IS
OF POOR QUALITY

2.2.3.1 Assembly Jig. The assembly jig control and monitor functions are performed via the assembly control unit (ACU). The ACU performs overall control and monitoring of assembly jig operations and contains a microprocessor with interval timer, approximately 4K of memory, and input/output interfaces to the Orbiter and four assembly jig control subsystems.

The ACU functions are controlled by a software system containing an executive system and four categories of application software for the specific assembly jig control. These software functions were identified and sized to verify that ACU control and monitor functions were within the baseline capability. Results indicate that approximately 3783 bytes of memory and a speed capability of 32 KOPS (thousands of operations per second) are required. The derivation of these requirements is discussed in greater detail in Section 2.2.3.3. In addition, the ACU interfaces with the equivalent unit in the beam builder. The executive control from the Orbiter is performed via an extension of the Orbiter data bus system with an Orbiter MDM unit co-located with the ACU within the assembly jig.

The four assembly jig subsystems which operate under the control of the ACU are:

- a. Assembly jig setup
- b. Beam builder positioner
- c. Longitudinal beam handling
- d. Cross beam assembly subsystem.

These five functions are shown in Figure 2-73.

The assembly jig setup subsystem contains those motor/actuator controls and sensors necessary to deploy the assembly jig from the cargo bay and position the EVA bridge.

Assembly jig setup is initiated after the Orbiter cargo bay doors are opened by commanding the assembly jig forward latch actuators (Orbiter-supplied) to open and commanding the assembly jig power control ARM/SAFE switch to ARM. This action frees the assembly jig to rotate about its aft hinges and applies power to all assembly jig motors and actuators.

Redundant motors associated with the assembly jig deployment actuator are then activated via operator commands via the ACU, causing the assembly jig to be rotated out of the cargo bay into the beam fabrication position. Two up sensors and two down sensors are used for monitoring this operation. After the assembly jig has been erected, the EVA bridge mechanism will be deployed into position from its stowed position along the assembly jig surface. Three sets of redundant motor drives are used for this purpose on each side of the mechanism: the deployment drive, arm drive, and wrist drive functions. A fourth set of redundant motors is used to drive the EVA transport carriage. Dual controls associated with the carriage allow it to be operated either from the aft cabin or by the crew control panel associated with the carriage. Two sensors are used to indicate the carriage stowed position and another 12 sensors are used to indicate three operating positions associated with each EVA bridge drive or carriage function. See Figure 2-74 for details.

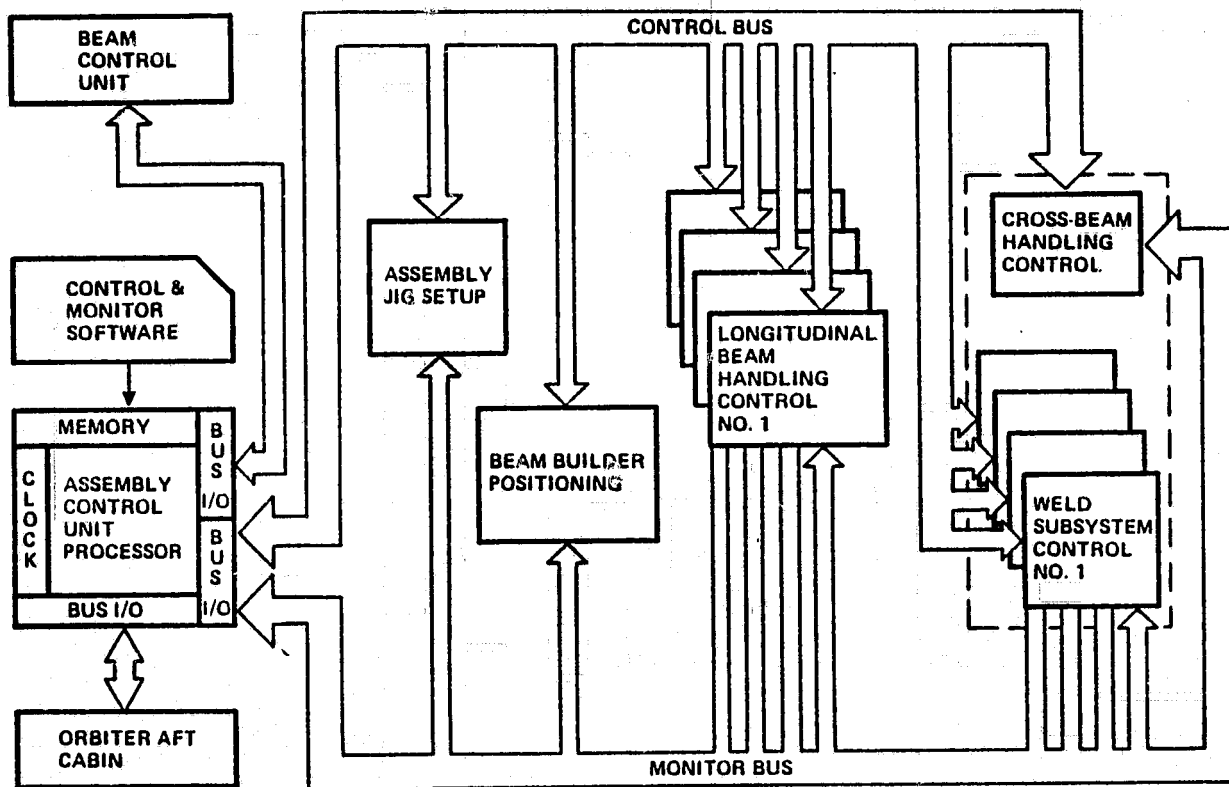


Figure 2-73. Baseline assembly jig control diagram.

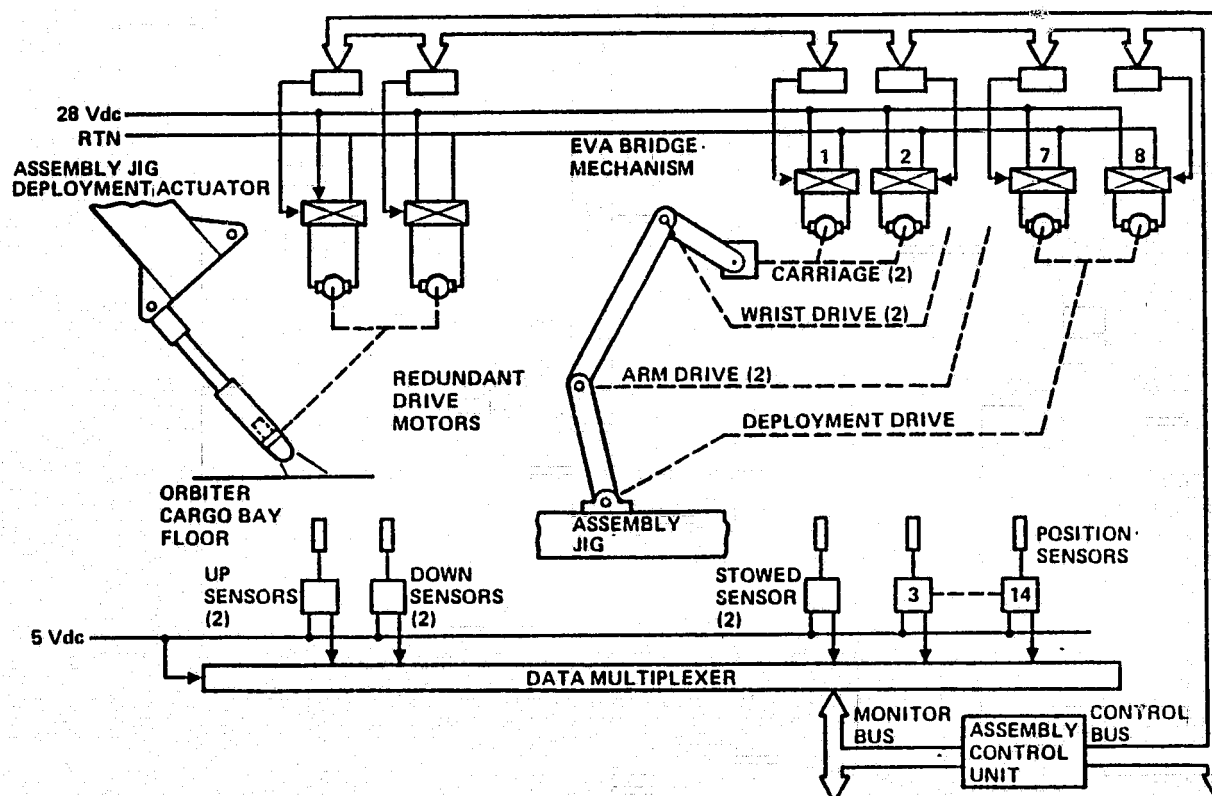


Figure 2-74. Assembly jig setup control diagram.

The beam builder positioner subsystem contains the motor/actuator controls and sensors required to translate and position the beam builder about the assembly jig and into the selected longitudinal and cross beam fabrication positions. This is accomplished by five sets of redundant motor-drive mechanisms which:

- a. Rotate the beam builder from its stowed position on the assembly jig and into the longitudinal beam attitude.
- b. Translate the beam builder along the assembly jig and into one of four longitudinal beam fabrication locations, or into a fifth position for cross-member fabrication.
- c. Latch the beam builder into the position at each beam builder location.

These mechanisms, shown in Figure 2-75, consist of:

- a. Inboard rotation drive
- b. Outboard rotation drive
- c. Turn arm drive
- d. Beam builder carriage drive
- e. Beam builder latch actuator.

The inboard rotation drive allows rotation of the beam builder about the yaw axis to positions 120 deg and 300 deg from the cradle stowage position (0 deg). Three sets of redundant position sensors are used to control the beam builder to these three desired locations.

The outboard rotation drive permits further yaw rotation about an axis offset from the inboard yaw axis. Rotation of ± 60 deg from the stowage position allows the beam builder beam axis to be set for both longitudinal and cross beam generation. Three sets of redundant sensors will be required for position sensing of these three locations.

The turn arm drive permits rotation of the beam builder from zero deg to 90 deg, and 180 deg about the roll axis. These correspond to the longitudinal beam builder position (beam axis aligned with Orbiter pitch axis) and the cross beam generation position, respectively. Redundant sensors associated with each position will aid positioning control for these three positions.

Once in the longitudinal beam building attitude, the beam builder carriage drive control system allows positioning of the beam builder at one of six locations along the edge of the assembly jig. These correspond to: (0) the stowed position, (1) thru (4) longitudinal beam positions 1 thru 4, respectively, and (5) the cross beam location. It should be noted, however, that the cross beam position falls between longitudinal positions 3 and 4. As in the other subsystems, discrete position sensors will aid accurate positioning of the beam builder at its designated parking positions.

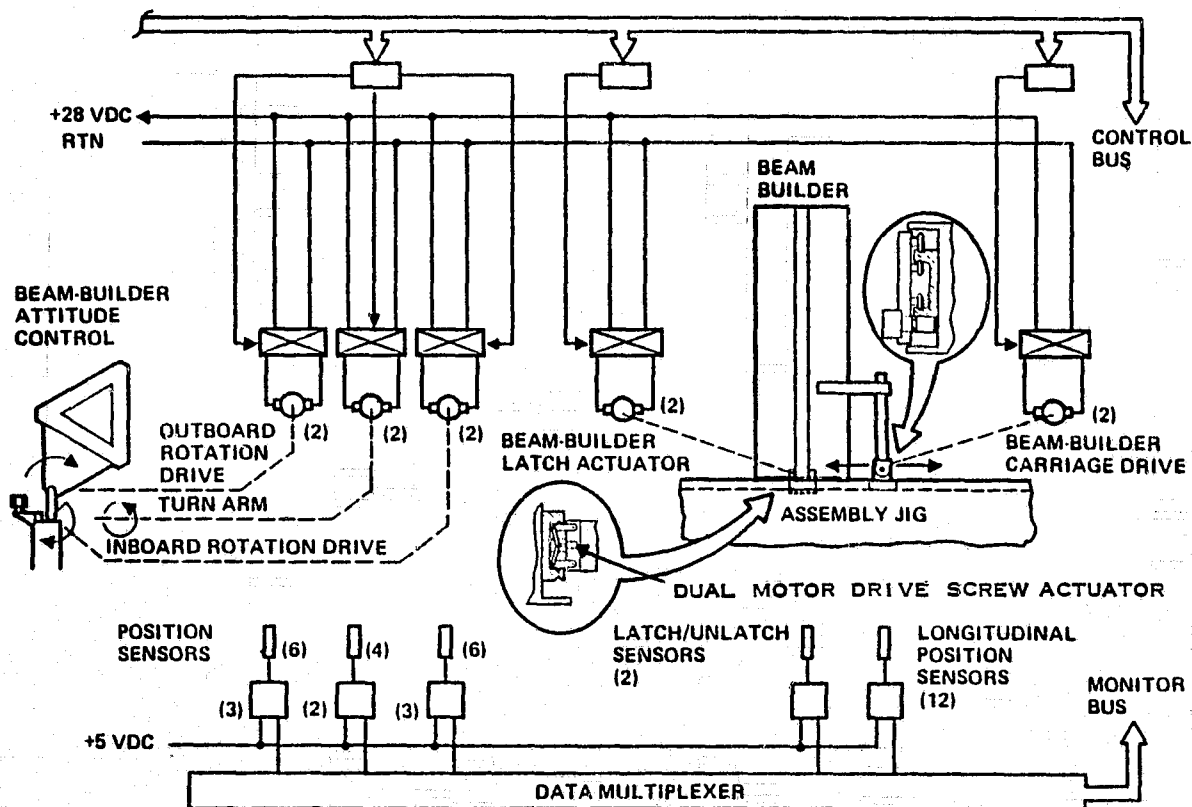


Figure 2-75. Beam builder positioning control diagram.

The final motor/actuator of this subsystem is the beam builder latch actuator used to stabilize the beam builder/assembly jig structural interface during beam fabrication. Once the beam builder is positioned at one of the five beam building locations, the latch actuator motors are activated, attaching the beam builder to the assembly jig when in the stowage position prior to deployment. This same latch actuator is also used to attach the beam builder into its assembly jig stowage position during launch and descent operations.

The sequence of command for these operations is shown in Table 2-20, and depicted in Figure 2-51.

Eight beam retention and guide mechanisms (RGM) (two per longitudinal beam) are used to guide and stabilize the beam segment as it is being generated by the beam builder. These RGMs are deployed from their stowed position and into the guide position by a motor associated with each half of each mechanism (thus a total of 16 motors is required). Redundancy is accomplished by linking each motor of a set with a spline. When the longitudinal beam is fabricated to the proper length, the RGM for that beam is commanded to the clamp position securing the beam to the assembly jig. The beam is then cutoff by the beam builder and the RGM commanded back to the guide position and translated away from the beam builder a distance of 10 cm (to allow beam builder clearance), where it is recommended to the clamp position. These operations are accomplished with the aid of redundant sets of discrete position sensors for the stowed, guide, and clamp positions, respectively.

Table 2-20. Beam builder positioning sequence.

Step	Function	Activity
1	Unlatch B/B from A/J	a. CMD B/B Ascent/Descent Latch Actuators to Release
2	B/B to First Longitudinal Position	a. CMD Inboard Drive Motors to roll B/B +127° b. CMD Outboard Drive Motors to roll B/B +53° c. CMD Turn Arm Motors to turn +90° d. CMD B/B Carriage Drive to Longitudinal Position No. 1 e. CMD B/B Carriage Latch Actuator to Latch Position
3 to 5	B/B to Nth Longitudinal position 2, 3, and 4	a. CMD B/B Carriage Latch Actuator to Open b. CMD B/B Carriage Drive to Longitudinal Position No. N c. CMD B/B Carriage Latch Actuator to Latch Position
6	B/B to Cross Beam Position	a. CMD B/B Carriage Latch Actuator to Open b. CMD B/B Carriage Drive to Position No. 5 c. CMD Turn Arm Motors to 0° Position d. CMD Inboard Drive to roll B/B +180° and Outboard Drive to roll B/B -120° e. CMD B/B Support Latch Actuator to Latch Position
7	B/B to Stowed Position	a. CMD B/B Support Latch Actuator to Unlatch b. CMD Inboard Drive to roll B/B -180° c. CMD Outboard Drive to roll B/B +67° d. CMD B/B Carriage Drive to Position No. 0 e. CMD Inboard Drive to roll B/B -127° f. CMD B/B Ascent/Descent Actuators to Latch Position

B/B = Beam Builder

A/J = Assembly Jig

CMD = Command

The longitudinal beam handling system contains those motor/actuators and sensors used to grasp and position longitudinal beam segments along the assembly jig. It consists of two types of mechanisms which are used to: (1) secure the longitudinal beams to the assembly jig, and (2) translate the beams longitudinally across the assembly jig.

Longitudinal beam translation is accomplished by four beam drive mechanisms (one for each beam). Each drive mechanism is independent. Thus, each may be operated singularly or simultaneously with the others to effect both single beam or platform translation. The drive mechanism is operated by two drive motors connected to the outer two of three drive rollers. The third drive roller (middle) is powered by a spline connection to each end roller drive thus also incorporating redundancy. Beam and platform longitudinal positioning along the assembly jig is accomplished with the aid of two travel-resolver-wheel-type sensors associated with each beam drive mechanism. The outputs of these sensors are transmitted to the ACU to allow accurate positioning of the beam or platform for cross beam assembly and equipment installation purposes. These sensors and associated mechanisms are shown in Figure 2-76.

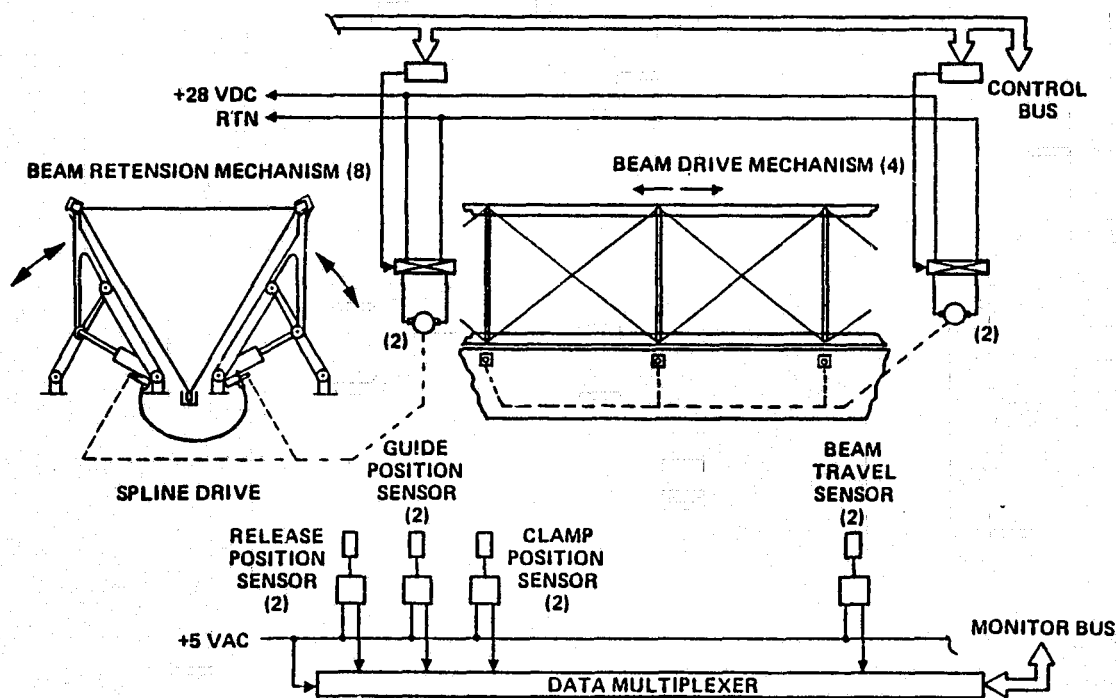


Figure 2-76. Longitudinal beam handling control diagram.

The cross beam assembly subsystem consists of the motors and actuators required to grasp, position, and weld the cross beams to the longitudinal beams. This is accomplished with: (1) cross beam handling mechanisms, and (2) the cross beam/longitudinal beam weld subsystem. See Figure 2-77. The cross beam handling mechanism is located between the second and third longitudinal beams on the assembly jig and grasps the newly generated cross beam segment, holds it during cutoff, and places it in the weld position. Grasping operation is performed via a scissors-type clamp driven by redundant holder drive motors. Position sensors (closed and open) and spring-loaded jaws are used by the ACU for control, without over-stressing beam sections. After the cross beam segment is cut off, it is translated along its axis to clear the beam builder machine by the carriage drive. When the carriage drive sensors indicate to the ACU the cross beam is in the proper lateral position, it activates

the two positioner drive motors to lower the cross beam into its weld position. Redundant sensors are used for these functions in a similar manner to other mechanisms discussed above. After welding is completed, the handler is released and retracted to the beam clearance position while the platform is translated into the next cross beam fabrication position. It is then translated to the grab position (laterally) to restart the sequence. Once the cross member is in position, the weld head is commanded to the correct attitude via the weld rotation drive and raised to the operating position via the weld positioning drive motors. The weld head drive is then activated causing the weld heads to enter the cap member' channel and clamp the cap sections to be welded together. Clamp pressure is controlled using sensors associated with the weld control unit. When the correct weld pressure is achieved, the weld control unit activates the weld process and transmits weld process control data back to the ACU. These data, which include pressure, current, voltage, and weld time are analyzed in the ACU to determine if a satisfactory weld was performed. Following the weld operation, the weld heads are retracted, lowered, and rotated 90 deg to accommodate the final two welds between intersecting cross and longitudinal beams.

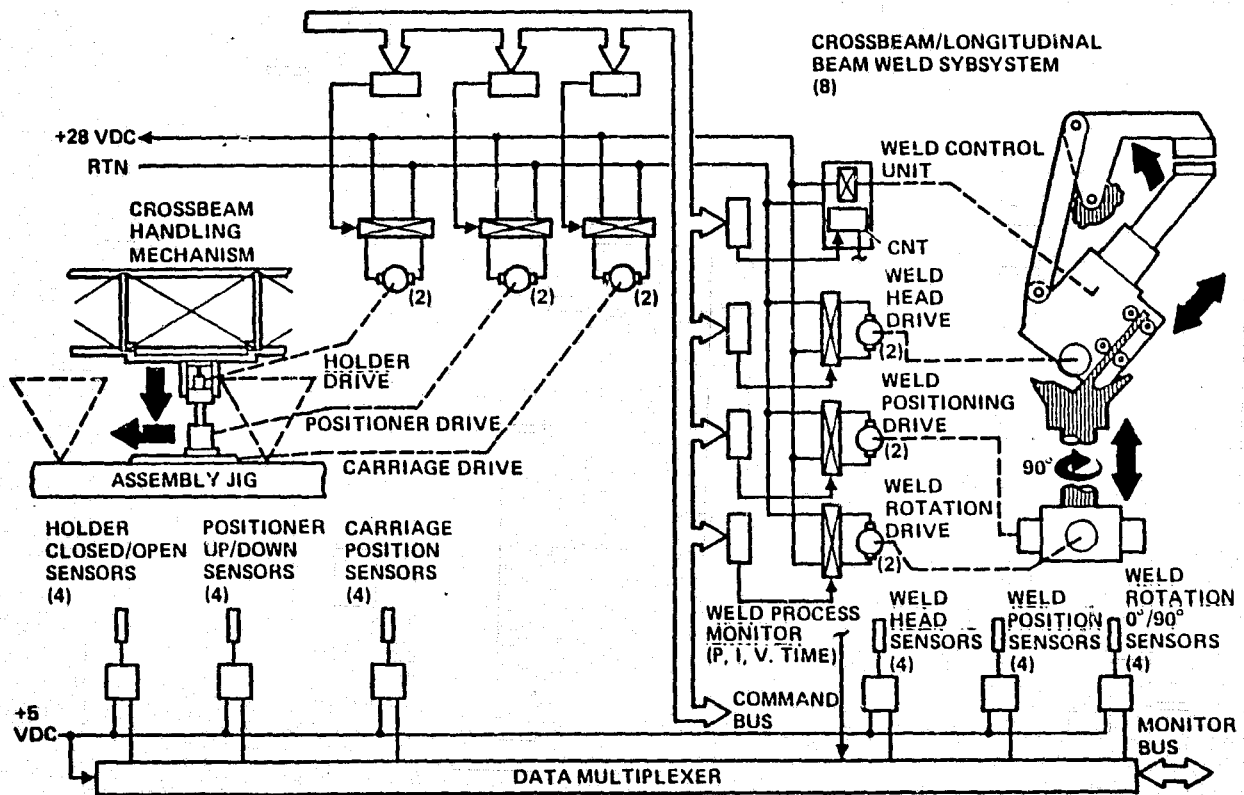


Figure 2-77. Cross beam assembly control diagram.

2.2.3.2 Beam Builder. The beam builder control and monitor system is housed within the beam builder machine and provides the real-time process control operations to fabricate beam elements to the correct length and straightness. It receives executive control from the Orbiter crew via the Orbiter MDM/data bus interface located on the assembly jig, and provides status data back to the crew. Another data link is used to coordinate assembly jig and beam builder activities. An example of the latter occurs during beam cutoff when the assembly jig ACU must signal the beam builder that the beam is secured to the assembly jig before executing the cutoff operation.

This subsystem is made up of four major subsystem functions. These are the: (1) beam control unit, (2) cap fabrication subsystem, (3) cross-member positioning subsystem, and (4) beam fabrication subsystem. These subsystems are shown in Figure 2-78 and discussed in the following paragraphs.

The beam control unit (BCU) is analogous to the ACU in concept and performs overall process control of the beam fabrication operation. In concept, the BCU and ACU may be implemented using the same hardware and executive software with different application programs for performing the unique control monitor tasks.

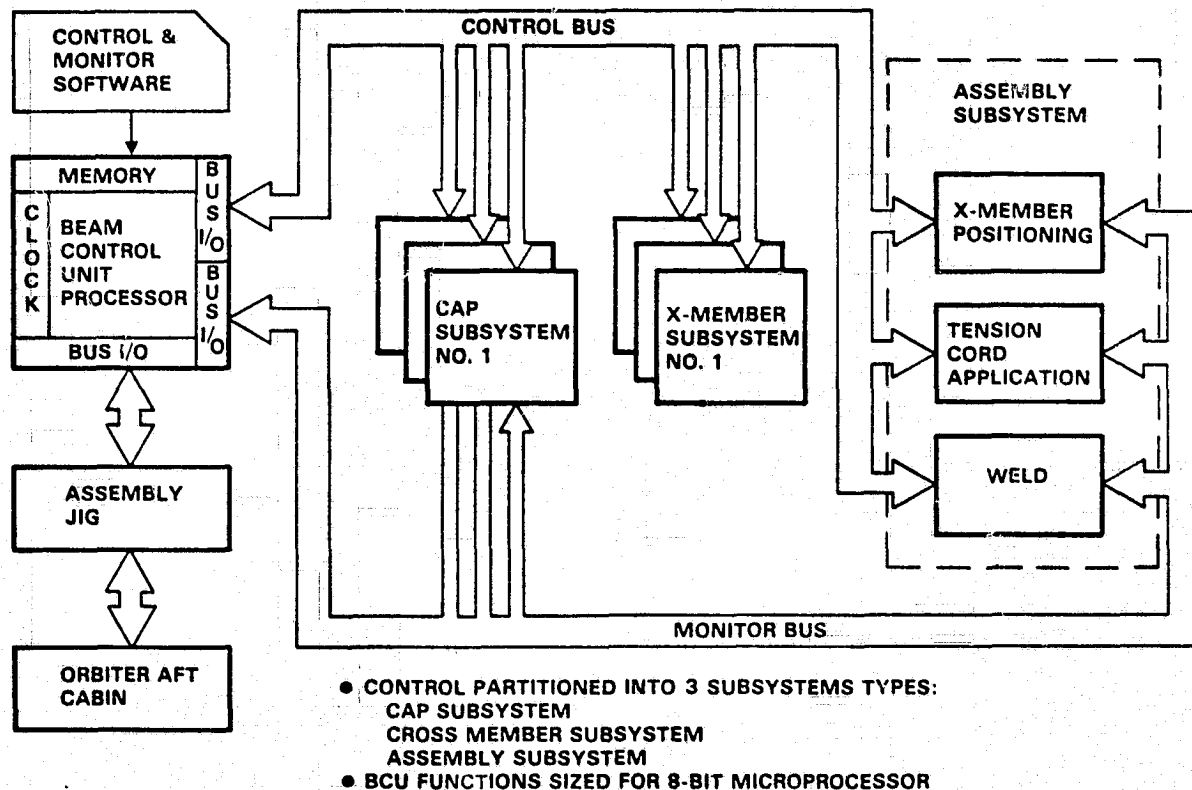


Figure 2-78. Baseline beam builder control system.

2.2.3.2.1 Beam Control Unit. The baseline BCU uses a microcomputer for control with interval timer, approximately 4K of memory, and input/output data bus interfaces to the other fabrication subsystems, plus the communications interface with the Orbiter and the ACU.

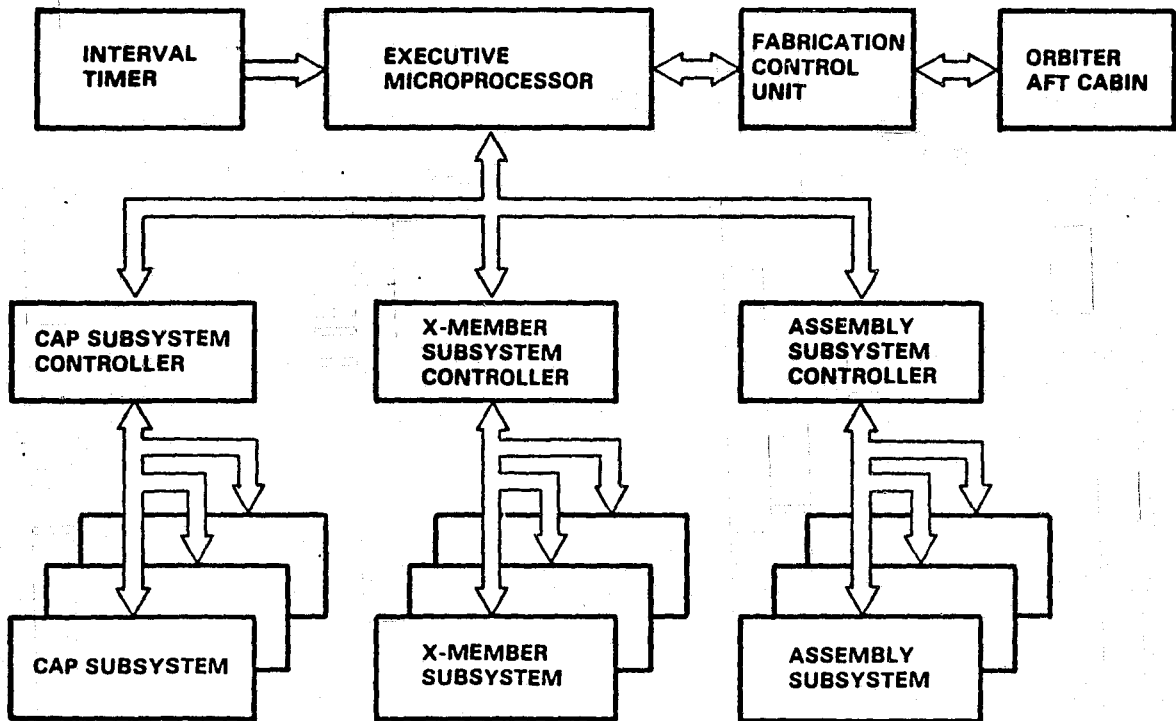
The BCU software requirements for control and monitor functions were identified and estimated in terms of program size and processor operating speed requirements. This was done to verify the baseline concept (using a microprocessor). The results indicate that 2651 software instructions (approximately 3200 bytes of memory) and a speed capacity of 52 KOPS will be required. Thus, beam builder processor requirements fall within the capability spectrum of current commercial microprocessors and microcomputers. For instance, the Intel MCS-48 speed capability is approximately 267 KOPS. This provides a factor of five for growth and unknowns. These results are summarized in Table 2-21 and are discussed in greater detail in Section 2.2.3.3, ACU/BCU Software.

Table 2-21. BCU software summary.

Beam Control Unit Software	Program Size (Instructions)	Program Speed (KOPS)
Executive Software		
Process Control	800	22.1
Peripheral Control	490	3.4
Software Task Modules		
Cap Subsystem Control	759	7.1
Cross-Member Control	282	1.1
Assembly Control	320	18.4
Totals	2651	52.1
Memory: (1.2 × Instructions)	(3181 Bytes)	

An alternate BCU concept which was investigated is shown in Figure 2-79. In this configuration an executive microprocessor is used to perform timing, task scheduling, control communication, and top level beam builder fabrication control. Three additional microprocessors would then control and monitor the detailed fabrication tasks associated with cap forming, cross-member forming, and beam assembly functions, respectively. This configuration has the advantage that real-time time-share operations between the three fabrication tasks are reduced and additional processor speed is available at low cost. Although not required for the current beam builder concept, it provides a convenient fall-back positions should beam builder fabrication complexity grow significantly or if beam fabrication rates were speeded up by a factor of four.

2.2.3.2.2 Cap Control. The cap subsystems contain those motor/actuator controls and sensors necessary to control fabrication of the three cap member sections. These are shown in Figure 2-80, and consist of: (1) the heater section, (2) platen controls, (3) cap drive subsystem, and (4) beam cutoff subsystem.



● ALTERNATE CONCEPT TO BE EVALUATED IF PROCESS SYNCHRONIZATION/DUTY-CYCLE REQUIREMENTS EXCEED SINGLE MICROCONTROLLER CAPABILITY

Figure 2-79. Beam control unit alternate concept.

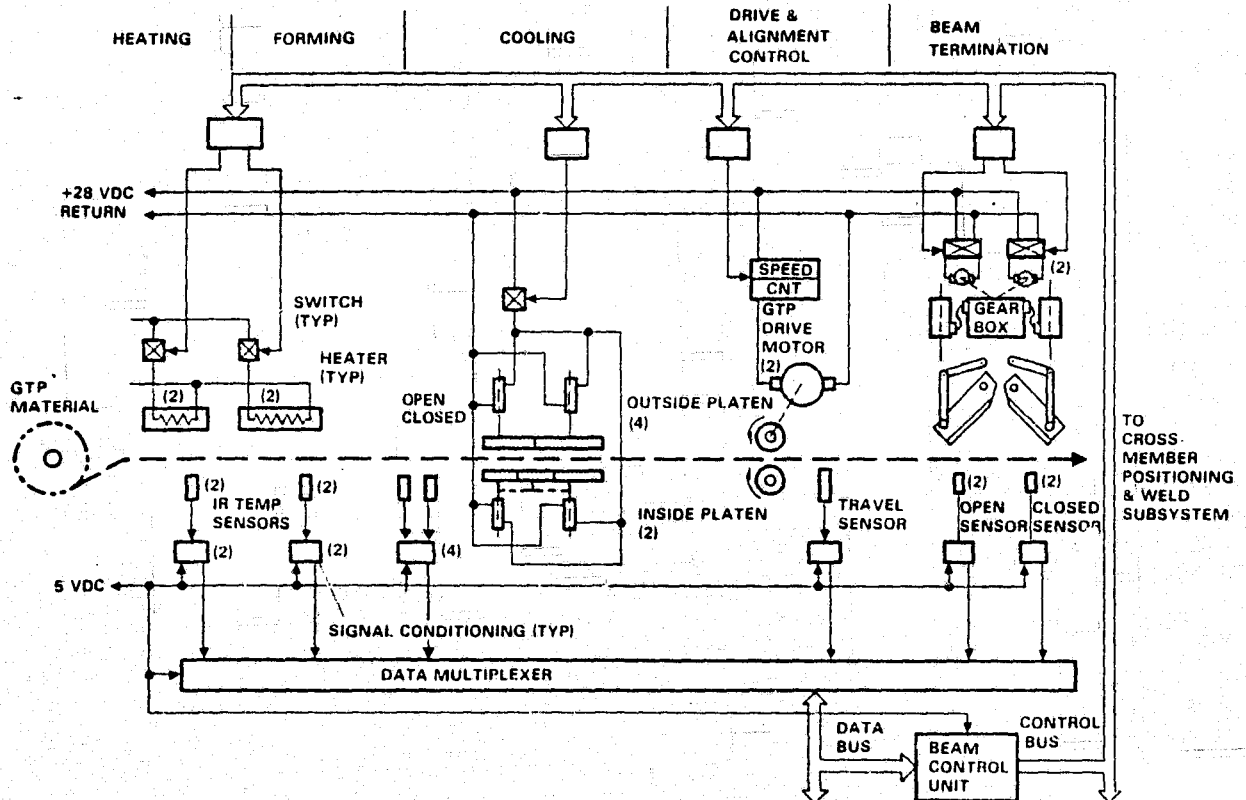


Figure 2-80. Cap member subsystem control diagram.

2.2.3.2.3 Heater Control. In the first step of the beam fabrication process, flat graphite thermoplastic material from the storage reel is heated and formed into beam-section length cap members. Upon entering this subsystem, the material is heated to 425°F in the heating section and maintained at that temperature in the forming sections. Heating is accomplished by a heater/temperature sensor set in both the heater and forming sections of each cap system. Each set consists of two helically wound nickel chrome heater elements under individual BCU control. Control monitoring is provided to the BCU by a thermopile (non-contact IR type) sensor and conditioning circuitry located opposite each heater element. (See Figure 2-81.) Alternate concepts which were identified and investigated are discussed in Section 2.2.1.3.2. These include the baseline electrical resistance element and others, such as ultrasonics techniques, which show promise but require greater development. The electrical resistance technique selected was developed under a companion NASA/MSFC effort (NAS8-32471) and adopted with few modifications to the SSAFE requirements. Operationally, the BCU measures the 12 temperature measurements ten times per second. Individual heaters are turned off when temperatures exceed 430°F and are turned on when temperature drops below 420°F.

From the heaters the material passes into the cooling platen section where three inside and two outside platens will be commanded closed under BCU control for 38 seconds during the assembly portion of the cycle. For redundancy purpose, two actuators per outside platen section will be used for this purpose. The three inside platens are driven together and are operated by dual actuators. A discrete sensor, indicating platen open/closed condition, is provided for each redundant actuator pair. Sensor outputs are transmitted to the BCU for status and control monitoring.

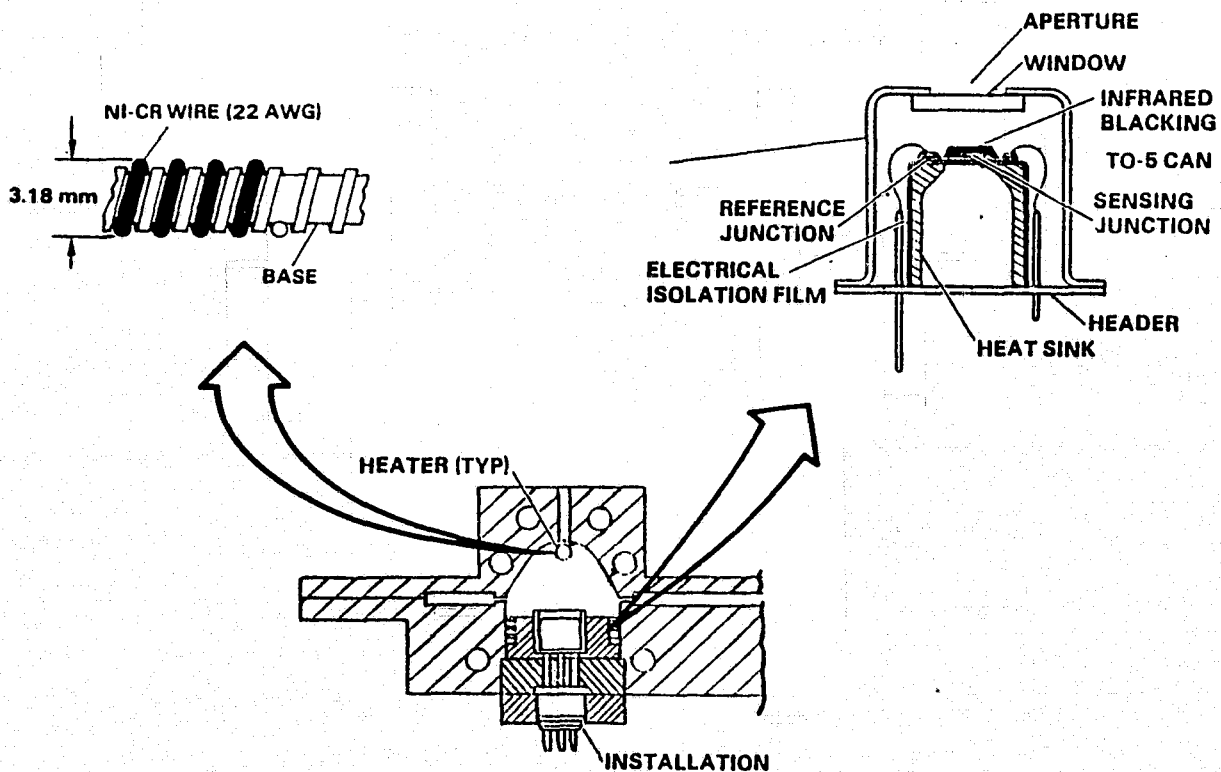


Figure 2-81. Heater/sensor control elements.

2.2.3.2.4 Cap Drive and Beam Alignment. The single most critical control function associated with the beam builder machine is the cap drive and alignment control subsystem. The function of this system is twofold: (1) it provides drive control and timing to advance the three cap sections sequentially through the beam-fabrication processes, and (2) it provides the fine control and sensors necessary to accurately adjust the length of each beam segment for straightness control. As shown in Figure 2-80, for each cap system, this subsystem consists of redundant variable-speed cap drive motor units, dual motor speed controllers, and a redundant cap length travel sensor unit.

In operation, the travel sensor system will provide cap length data with a resolution of 0.25 mm for each cap to the BCU processor where they will be compared. Cap length calculations will then be performed for the next beam bay length to maintain or correct for beam misalignment. These calculations will result in cap drive motor speed commands for the run period of the next bay length.

Each cap will be driven at constant speed during the first 37 seconds of the 40-second run cycle. Final positioning will be accomplished during the final 3 seconds of the cap drive cycle where the cap drive speed is progressively reduced to zero as the desired position (length) is reached. BCU software for this function was based on performing 100 length monitor/speed control cycles per cap during this period.

2.2.3.2.5 Beam Alignment Error Control. The cap drive and beam alignment control subsystem implementation discussed above was based on an analysis involving several interrelated factors: (1) alignment requirements, (2) structural capabilities, and (3) techniques/sensor trades. These are briefly discussed below.

2.2.3.2.6 Alignment Requirements. Beam alignment and distortion requirements are a function of the intended purpose of the beam. Observed beam distortion, however, is equal to the sum of the distortions resulting from both environmental causes and from manufacturing induced errors. Distortions due to environmental factors during beam manufacture were determined, along with desired beam alignment characteristics for three selected large space structure applications. Refer to Figure 2-82.

$$\text{ENVIRONMENT} + \text{MANUFACTURING ERRORS} = \text{TOTAL DISTORTION}$$



ENVIRONMENT	INDUCED DISTORTION	ALIGNMENT REQUIREMENT	SPACE STRUCTURE*	SOLAR COLLECTOR*	LARGE ANTENNA**		
					DISK	ARRAY	LENS
THERMAL	30 mm	WARP	1.2 m (0.07 mm/m)	±8 DEG (2 mm/m)	$\frac{\lambda}{20}$	$\frac{\lambda}{10}$	$\frac{\lambda}{4}$
DRAG	0.03 mm				0.5 cm	1 cm	2.5 cm
DYNAMICS	130 mm	TORSION	5° (0.025°/m)	±8 DEG (0.04°/m)	0.41° (0.0004°/m)	0.82° (0.0008°/m)	2.05° (0.0010°/m)

*FOR 200 m BEAM

** 3 GHz $\lambda = 10$ cm
 1 GHz $\lambda = 30$ cm
 0.3 GHz $\lambda = 100$ cm

Figure 2-82. Beam control/alignment requirements.

For the baseline 200-meter beam, lateral beam displacements at the end of the beam for thermal-, drag-, and Orbiter-induced dynamics effects were estimated to be 30 mm, 0.03 mm, and 130 mm, respectively. Manufacturing alignment requirement upper limits of 0.07 mm/m (0.004 m/bay) in warp and 0.025°/m (0.036°/bay) in torsion were calculated for structural assemblies based on allowable cap forces required for correction. Limits of 2 mm/meter (2.9 mm/bay) and 0.04 deg/meter (0.06 deg/bay) are required to keep solar panel structures oriented to within 8° of normal, representing a 1% efficiency loss. Antenna applications, however, require much tighter overall alignment tolerances, as indicated by the RMS deviations shown. These results indicate that, even with perfectly straight beams, environmental factors such as thermally-induced warp will cause distortions beyond some of the applications tolerance limits. For example, a high frequency phased array antenna may require a 1-cm maximum distortion, which is exceeded by a 3-cm thermal distortion effect. Thus, additional techniques beyond building straight beams will be required for some applications. In other applications, such as structural systems and solar collectors, the required straightness is much less than the environment-induced distortions and less stringent manufacturing requirements may be determined. Correction of manufacturing error tolerances in real-time during fabrication will be complicated by other environmentally induced errors (such as dynamics effects), which are expected to be continuously variable as the beam is fabricated. These errors may tend to mask the small changes in manufacturing errors being monitored for correction purposes.

2.2.3.2.7 Manufacturing Error Sources. Beam manufacturing inaccuracy is manifested in two ways: warp and twist. Twist is caused by preload differences among the diagonal cords. In Section 4.4.3 it is shown that a constant preload bias, equal to 100% of the nominal preload 22.2N, produced a twist angle of only 0.1 radians (6°). Consequently, it is concluded that twist is not a major problem, and the relatively low beam torsional stiffness permits post-fabrication realignment, if needed, with low induced load. Warp, however, is a more serious concern, the principal issue being cap length inequality between the three caps. As shown in Figure 2-83, a constant error bias of 2.5 mm per beam bay (0.0018 m/m in a typical 1.434 m bay) results in an unacceptable tip deflection of 30.5 m. Cap length inequality can result from various causes, the most significant of which is variation in drive roller diameter. In the simplest machine concept, the length of cap driven by the rollers in one cycle could be deduced from the number of drive roller revolutions. In such a system, the indicated error would be highly probable (and constant). However, any system that either directly measures the length of cap driven, or measures and relieves the cap load difference (which must accompany length inequality), can eliminate the majority of this effect.

Cap temperature inequality, even of the magnitude shown, is highly unlikely since, at this point in the process, all three caps have been cooled by relatively massive platens, in turn cooled by the Orbiter coolant loop, and have not yet exited the machine with potentially varying radiant heating view factors. The effect is, therefore, considered negligible.

TYPE	WARP			TWIST										
EFFECT		<table border="1"> <thead> <tr> <th>$\frac{\Delta L}{BAY}$ (cm)</th> <th>δ (cm)</th> </tr> </thead> <tbody> <tr> <td>.25</td> <td>3075.0</td> </tr> <tr> <td>.025</td> <td>307.5</td> </tr> <tr> <td>.0025</td> <td>30.8</td> </tr> <tr> <td>.00025</td> <td>3.1</td> </tr> </tbody> </table>	$\frac{\Delta L}{BAY}$ (cm)	δ (cm)	.25	3075.0	.025	307.5	.0025	30.8	.00025	3.1		
$\frac{\Delta L}{BAY}$ (cm)	δ (cm)													
.25	3075.0													
.025	307.5													
.0025	30.8													
.00025	3.1													
SOURCE	<table border="1"> <thead> <tr> <th>TYPE</th> <th>MAGNITUDE</th> <th>$\Delta L/BAY$ (cm)</th> </tr> </thead> <tbody> <tr> <td>Δ ROLLER DIA</td> <td>.0025 cm</td> <td>.094</td> </tr> <tr> <td>Δ CAP TEMP</td> <td>2.8°K</td> <td>.00043</td> </tr> <tr> <td>Δ CAP INERTIA LOAD</td> <td>1172 N</td> <td>.0061</td> </tr> </tbody> </table>	TYPE	MAGNITUDE	$\Delta L/BAY$ (cm)	Δ ROLLER DIA	.0025 cm	.094	Δ CAP TEMP	2.8°K	.00043	Δ CAP INERTIA LOAD	1172 N	.0061	Δ CORD PRELOAD: 22.2 N/BAY → 0.1 RAD
TYPE	MAGNITUDE	$\Delta L/BAY$ (cm)												
Δ ROLLER DIA	.0025 cm	.094												
Δ CAP TEMP	2.8°K	.00043												
Δ CAP INERTIA LOAD	1172 N	.0061												
CONTROL TECHNIQUE	DURING BEAM FAB: DIFFERENTIAL CAP DRIVE AFTER FAB COMPLETE: EXTERNAL FORCE			N.A. ✓										

STRUCTURAL CAPABILITY MAY LIMIT EXTENT OF CORRECTION

Figure 2-83. Manufacturing accuracy effects.

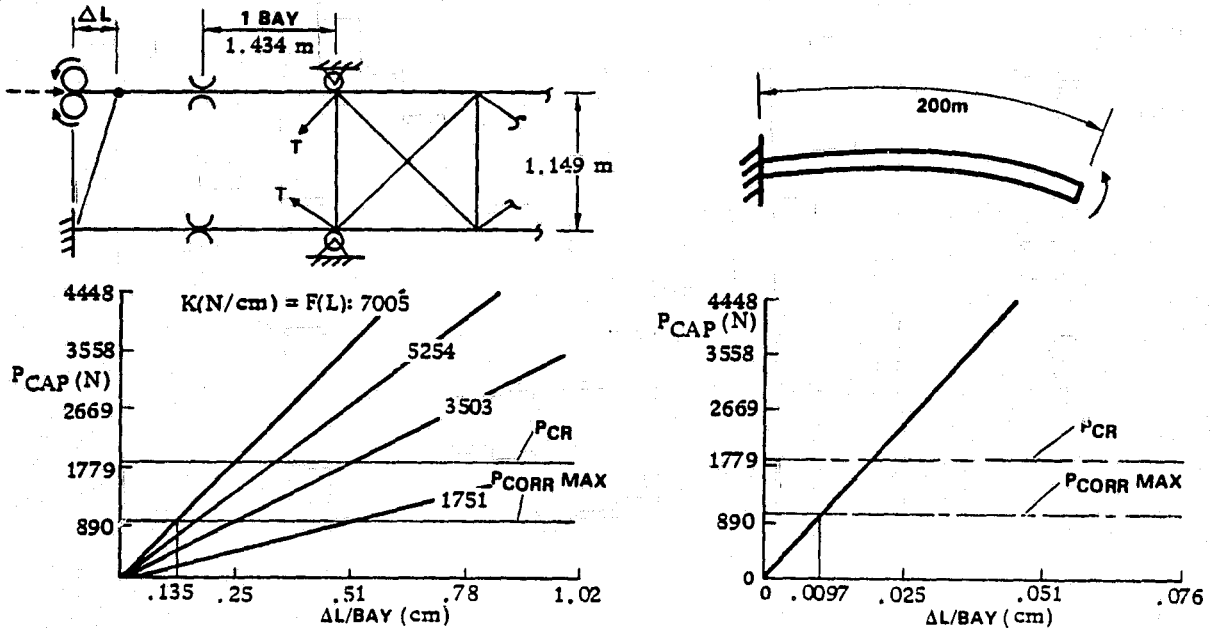
Two techniques investigated for correcting beam warping due to manufacturing inaccuracy are: (1) in-process bay "square-up" by differential cap drive, and (2) post-fabrication straightening by external load application. See Figure 2-84. Implementation of either technique necessarily subjects at least one beam cap to compressive loading, the permissible magnitude of which may be limited by axial load capability.

In the differential cap drive technique, the beam-bay cap lengths required to square up the bay are computed and the three caps driven to the proper accuracy by differential drive. Once square, the bay is completed by joining of cross-members and diagonal cords to the caps. Differential cap load effects are absorbed by a combination of bay sway and beam tip deflection due to induced "quasi" bending. The effective stiffness is a function of beam length, the sway contribution dominating initially, and the bending contribution later controlling over the majority of beam length. A preliminary analysis indicates a maximum effective stiffness of approximately 7000 N/cm. The permissible load induced by the correction process (965 N) is based on the previously given critical axial load (1846 N) reduced by the maximum operating load (587 N) with a 50% safety factor applied. As indicated, the differential drive option can accommodate an error of 1.35 mm/bay, which exceeds the maximum expected value, without cap buckling.

ISSUE: DOES STRUCTURAL CAPABILITY LIMIT INACCURACY CORRECTION?

• DIFFERENTIAL CAP DRIVE

• EXTERNAL LOAD



**DIFFERENTIAL CAP DRIVE IS PREFERRED CONTROL TECHNIQUE
 ACCOMMODATES MAXIMUM ERROR WITHOUT BUCKLING CAP
 REQUIRES ORDER OF MAGNITUDE LESS MEASUREMENT PRECISION**

Figure 2-84. Structural consideration limit correction capability.

In external load option, the cantilever beam stiffness must be overcome, resulting in considerably higher induced cap loads. The resulting tolerable error limit per bay is .10 mm, an order of magnitude more demanding than that accommodated by differential cap drive. Accordingly, differential cap drive is the recommended option for beam accuracy control.

2.2.3.2.8 Error Sensing. Two methods of sensing beam misalignment were investigated. These are: (1) use of error feedback internal to the beam builder to sense errors, and (2) use of error feedback data derived external to the beam builder to determine manufacturing corrections. Refer to Figure 2-85. Based on application requirements investigated, a cap length control capability of 0.1 mm/m has been established as a baseline requirement. In the internal error feedback control concept, a cap travel sensor is used to determine beam cap lengths. The BCU would be programmed to try to achieve zero total cap length difference between the three beam caps over the length of the beam. Errors induced through beam builder mechanical tolerance buildup would be removed for each bay length by controlling each cap length to the baseline tolerance. In this method, an external alignment sensor would not be required for manufacturing purposes, and the effects of environmentally-induced errors may be eliminated by using a beam clamp device at the entrance to the beam builder during the cap length adjustment phase.

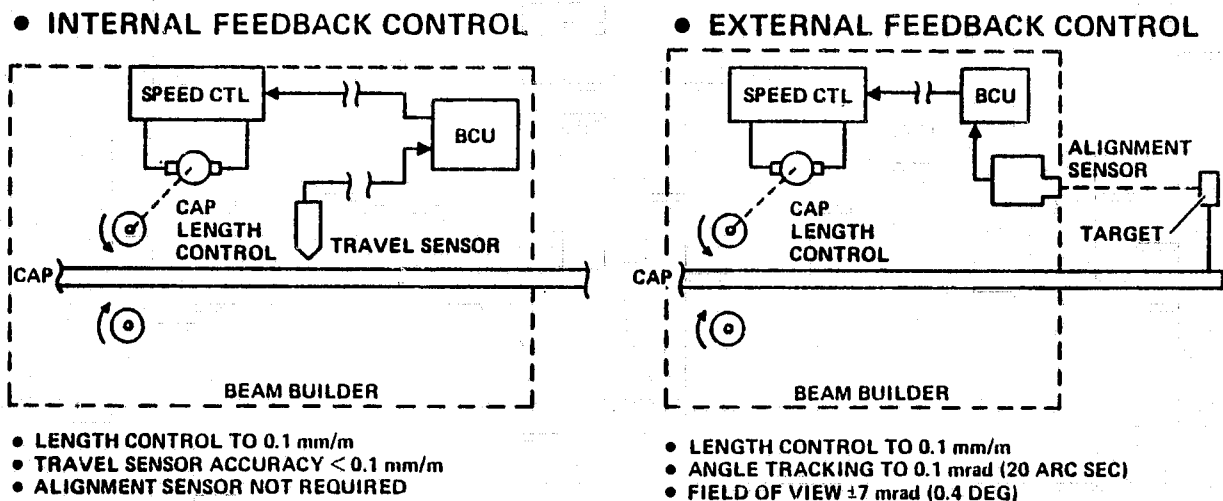


Figure 2-85. Alternate manufacturing error control methods.

Three methods of monitoring cap length to accuracies of better than 0.1 mm/m were investigated. These include both optical and magnetic coding techniques as shown in Figure 2-86. In option 1, cap length would be determined by counting reflective strips applied to the cap surface. Counting would be performed using a light emitting diode (LED) source to illuminate the 0.02 mm wide strip through an optical fiber link and monitoring the reflected light via a second optical fiber link and detector logic. Using this technique, resolution of 0.04 mm (0.0016 inch) should be readily achievable. General Dynamics Fort Worth division is involved in related activity for an F-16 air data sensor.

The resolver wheel approach of option 2 is a modification of option 1 which allows increased accuracies. In this technique, resolution capabilities at the wheel edge are multiplied by the ratio of the bearing surface diameter to edge diameter. Resolution to 0.02 mm for a 20 cm wheel with a ratio of two are predicted, with higher accuracies achievable by increasing the ratio and/or using finer marker spaces on the wheel.

Option 3 represents the baseline and is based on use of a magnetically encoded strip applied to the beam cap material. Calculations based on standard computer magnetic tape character densities (315 characters/cm) indicate that length resolution to 0.032 mm (0.00126 inch) is achievable. This technique also allows three strips of magnetic material to be applied to the composite cap material and coded simultaneously prior to cutting (into three cap tapes). Thus, additional accuracy would be achieved through elimination of errors in coding relative to the three tapes which would average out.

External feedback would be implemented using a beam builder-mounted tracker to monitor the locations of targets associated with the fabricated beam. Three methods of incorporating external alignment sensors were studied and are shown in Figure 2-87.

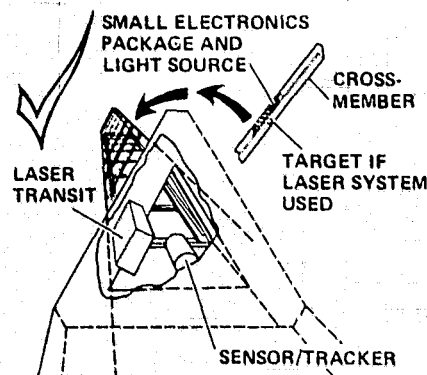
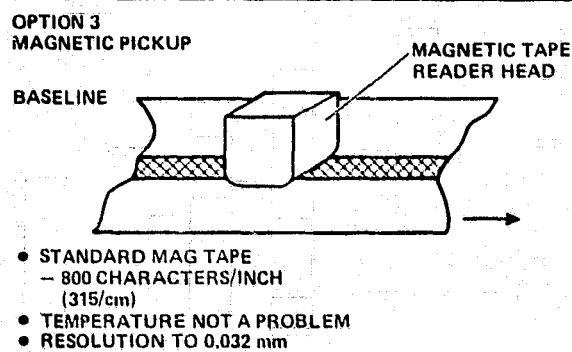
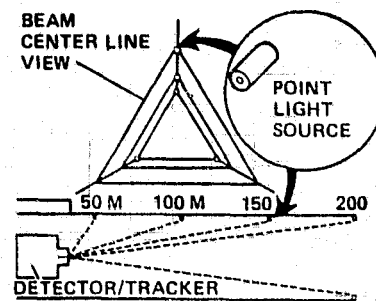
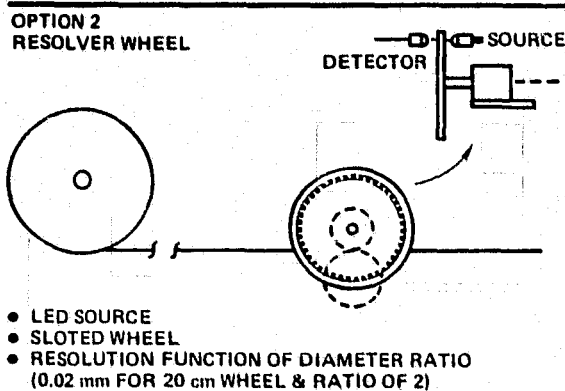
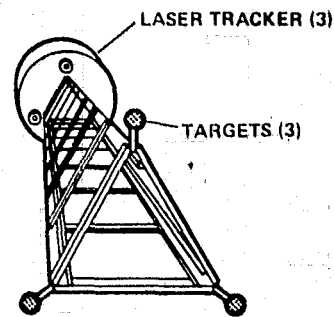
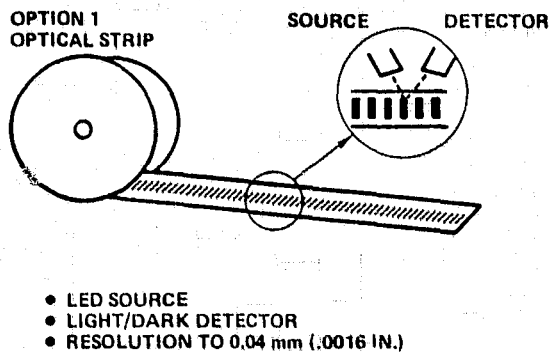


Figure 2-86. Cap travel alignment sensors method.

Figure 2-87. External alignment sensor.

In each option either an active or passive target located on the longitudinal beam is tracked as the beam is fabricated. To achieve 0.1 mm/m cap accuracies, sensor tracking to 0.1 mrad (20 arc sec) would be required. In addition, a tracking field of view capability of approximately $\pm\pi$ radians ($\pm 180^\circ$) for targets near the beam builder narrowing to ± 7 mrad (0.4 deg) for a target at 200 meters would be required. These values include tracking of both environmentally-induced errors as well as manufacturing-induced errors. This method has the advantage that, if alignment sensors are required for detached platform/beam monitoring (and if the beam builder accompanies the platform), one system could serve both needs.

Option 1 uses three laser transits, each located on the beam builder structure out-board from each emerging beam cap. Passive targets would be manually attached to the caps at the first beam bay and tracked in the X-Y plane. Computer analysis of the output signals would be required to separate environmental noise errors from manufacturing errors. Separated errors would then be converted into cap length correction requirements for the succeeding bay length.

Option 2 represents a TRW concept and is based on use of a dual detector located at the beam builder centerline to track active targets located inside the beam caps. The active target would be located in each cap in the first bay length and at 50 m intervals in the upper cap. In this scheme, a variable focal length detector would track the three bay No. 1 targets to determine warp and torsion error. The second fixed focal length detector would be used to track the upper beam cap line of targets and determine beam bending modes. The prime disadvantage of this system is that at 0.1 mm/m induced error causes the first bay length to become displaced 1.2 m (at 200 meters), thus, causing the detector to lose line of sight with the target. As with option 1, computerized processing of output data would be required to separate manufacturing error from environmentally-induced noise.

Option 3 represents a hybrid technique applicable to both option 1 and option 2 trackers. In this technique, the target is located at the center of a beam cross-member facing the sensor. A passive device (small corner reflector) may be used for the laser tracker; for an active target, the emitter optics and associated electronics may be packaged within the channel volume. This technique has the advantage that cross-members and targets may be loaded into the clip-feed mechanisms prior to flight. This allows them to be automatically attached to the beam at predetermined intervals, thus eliminating EVA operations. Intra-target set intervals of 50 meters or less will prevent loss of target line of sight and are expected to reduce target signal-to-noise ratio (due to operation in a more linear portion of the beam free-free dynamic mode).

2.2.3.2.9 Beam Cutoff. The final step of the cap control subsystem functions occurs when the desired length of beam has been fabricated. Using the cap length/travel sensors associated with the cap drive and alignment system for beam length data, the BCU keeps a running record of total beam length produced. When the proper beam length has been produced, the BCU will transmit that status to the Orbiter crew and go into a pause mode. Upon confirming correct beam length, the crew will initiate beam cutoff via Orbiter CRT/keyboard command back to the beam builder. The BCU will then cause a short beam segment to be fabricated without cross-cords. This causes the last bay of the current beam to be finished and the first bay of the next beam to be started. It also positions the midpoint of the interconnecting short section under the beam cutoff mechanism, and transmits a cutoff ready signal to the assembly jig. Upon receiving this signal, the ACU will command the retention and guide subsystem for that beam to the clamp position and transmit a "clamp ready" status back to the beam builder BCU. The BCU will then activate the three beam cutoff mechanisms. The beam cutoff mechanisms (Figure 2-80), driven by two redundant reversible motors

each, shear off the three beam caps. Shear open/closed sensors are used to monitor this function and return the cutoff shears to the open position. Once this operation is complete, the BCU transmits this status to the ACU, which causes the new beam to be translated 10 cm in the +Y direction to provide beam builder clearance when moved to its next beam fabrication position. This status is reported to the Orbiter crew via the data bus and both assembly jig and beam builder assume a pause mode while awaiting the next executive crew control command.

2.2.3.2.10 Cross-Member Positioning Control. The cross-member positioning system is operated during the assembly pause portion of the beam fabrication cycle to remove cross-members from their storage clips and position them for welding to the cap members. See Figure 2-88. In the baseline configuration, 650 cross-members are packaged in each of three motorized clips.

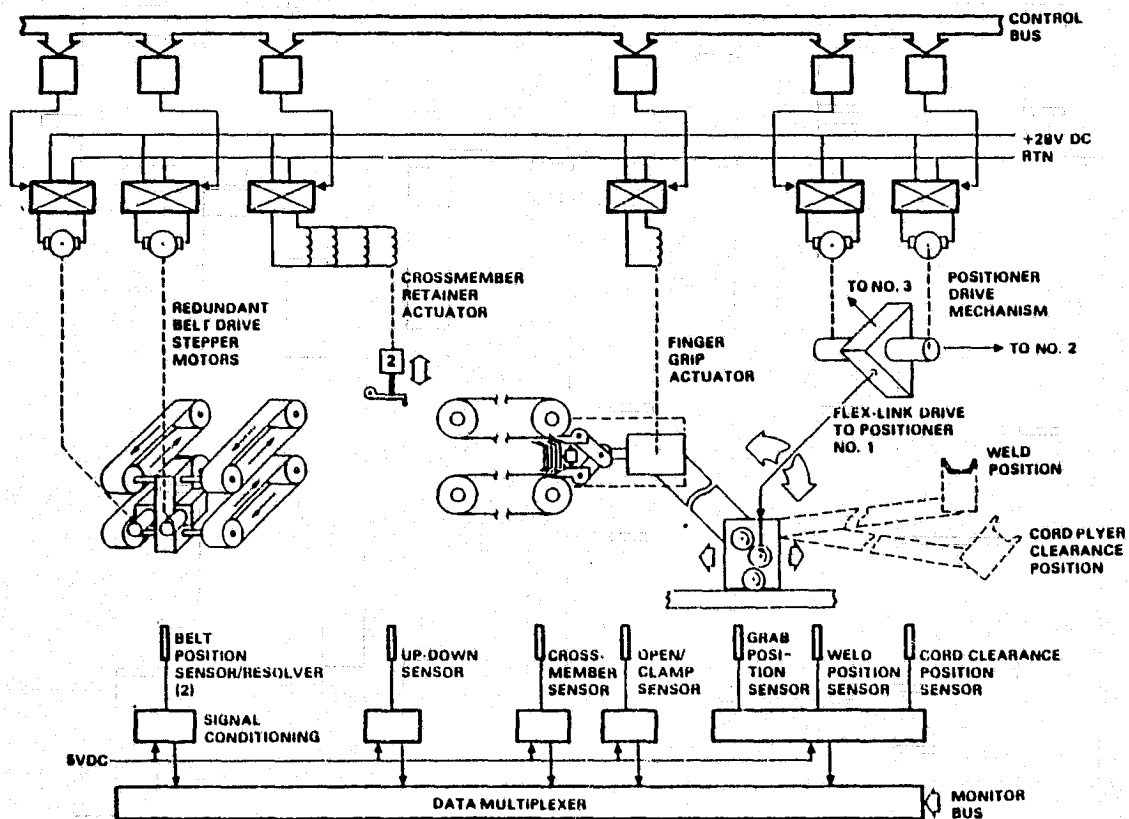


Figure 2-88. Cross-member positioning control diagram.

In operation the cross-member positioner is first driven into position at the clip. Sensing this position, the BCU then commands the clip feed belts to advance one step delivering one cross-member into the positioner finger mechanism. Cross-members are made available to the positioner mechanism via two sets of belts in the clip. These belts are driven forward one position once for each bay length. Redundant stepper motors under control of the BCU are used for this function. Two clip retainer actuators prevent premature cross-member ejection from the clip. When this is sensed

by the BCU via the cross-member sensor, the finger mechanism actuator and clip retainer actuators are activated, thus, gripping and releasing the cross-member. The BCU then activates the positioner drive mechanism causing the positioner arm and attached cross-member to be rotated and translated into the weld position. Dual reversible drive motors are used for this function. After the weld operation is complete, the finger mechanism is commanded to release the cross-member and the positioner arm is commanded to its third position to provide clearance for the subsequent cord pleyer operation. Following cord pleyer operation, the positioner drive is then run in reverse to reposition the arm and finger actuator at the original belt clip position. Discrete sensors are used by the BCU to sense the mechanism positions discussed.

2.2.3.2.11 Beam Tension Cord Drive and Tension Control. During the cap drive portion of the fabrication process, the beam cord pleyer drives are also activated. As shown in Figure 2-89, each of the two cord pleyer mechanisms is driven by two redundant motors with the lead crews coupled via interconnecting spline drivers. Controlled by BCU stop/start commands, the motors position the six cord pleyer mechanisms for the weld operation joining the cap member, cross-member, and tension cord segment. Discrete position sensors are used by the BCU to control this process and include sensors to indicate: (1) the cord is in position for the punch-through portion of the weld step, (2) the cord pleyer is in the ready-to-weld position, and (3) the cord pleyer is in the short bay section position.

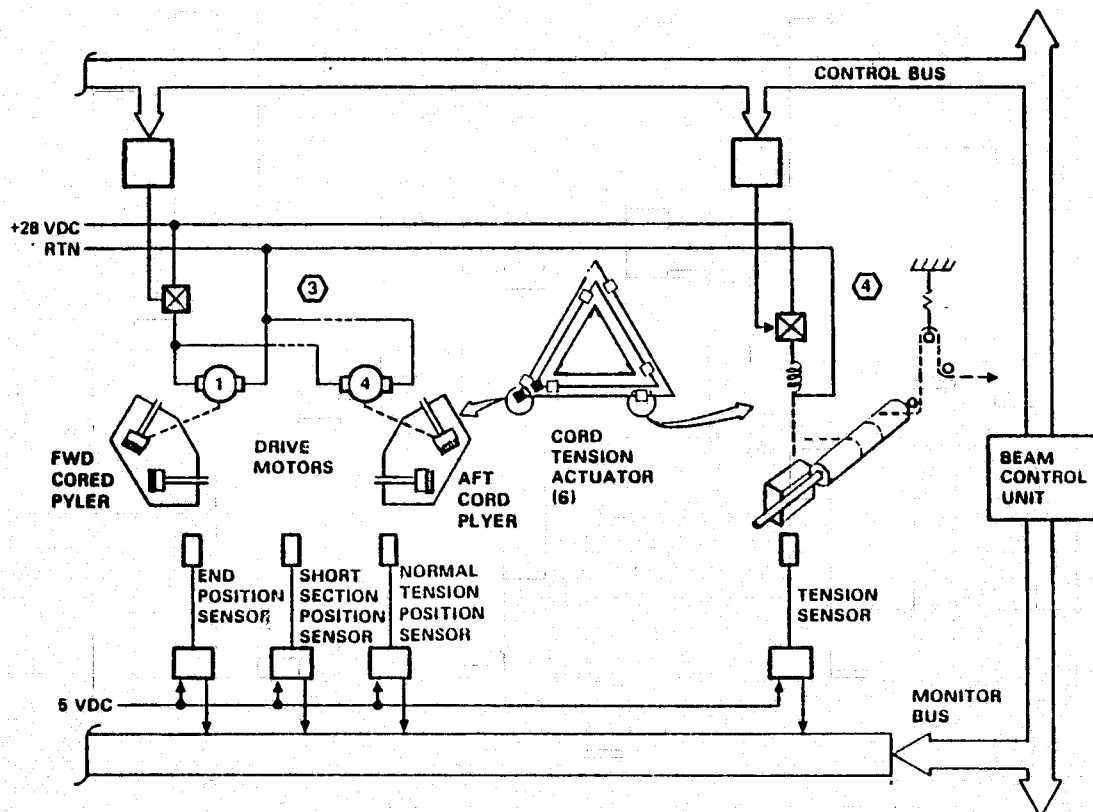


Figure 2-89. Beam tension cord drive control diagram.

Cord tensioning is controlled by the BCU via an electromechanical clutch-brake associated with each cord tensioning mechanism. In this configuration, the tension cord makes two loops around a capstan before passing through the constant-force spring and plyer mechanisms. Cord tensioning is accomplished by stopping the normally free-spinning capstan before the cord plyer reaches the weld position location. Thus, further cord payout is halted, the slack is taken out, and the cord is tensioned by the combined action of the cord plyer being driven to the weld position and the constant-force spring mechanism. After the weld operation is complete, the clutch/brake is released and the next cycle is begun. The BCU control timing for this sequence is shown in Figure 2-48. Tension sensors, shown in Figure 2-89, are for monitoring purposes only.

2.2.3.2.12 Beam Ultrasonic Weld Control. The beam ultrasonic weld control function is activated after the cross-members and tension cord are in place during the assembly phase. This operation is performed in several steps which are controlled by the BCU. In the first step, the weld head sets for each cap and weld anvil are commanded to the weld position where weld pressure is applied. In step two, the six individual weld heads are energized sequentially for 2 seconds via the weld control unit. This action allows penetration of the center portion of the weld tip probe providing a wrap-around pin for the tension cord. After the cord is positioned and tensioned (cord plyer in ready-to-weld position), the weld control units are reenergized sequentially to complete the weld process. The weld heads and weld anvil are then commanded to return to the start positions. In addition to the head position and pressure sensors data necessary to perform this operation, the weld control unit will transmit weld time, current, and voltage data to the BCU, where a weld quality assessment will be made via the BCU software. This weld quality assessment will then be transmitted to the aft cabin and displayed to the crew via the CRT. See Figure 2-90.

2.2.3.3 ACU/BCU Software. All of the beam fabrication and platform functions performed by the assembly jig and beam builder are under the direct control of the software associated with the ACU and BCU. This software: (1) controls the execution of all commands to motor/actuator subsystems, (2) synchronizes operations and timing between and within the assembly jig and beam builder unit, and (3) monitors the activity, health, and performance of the system and resulting beam.

During this study we have: (1) defined a baseline software concept design, (2) identified the major software tasks, and (3) estimated the size and computer speed requirements for these tasks. To keep cost and complexity low, maximum use of common software modules is desired. This has been implemented in our concept design by use of almost identical processor hardware and executive software for both ACU and BCU functions.

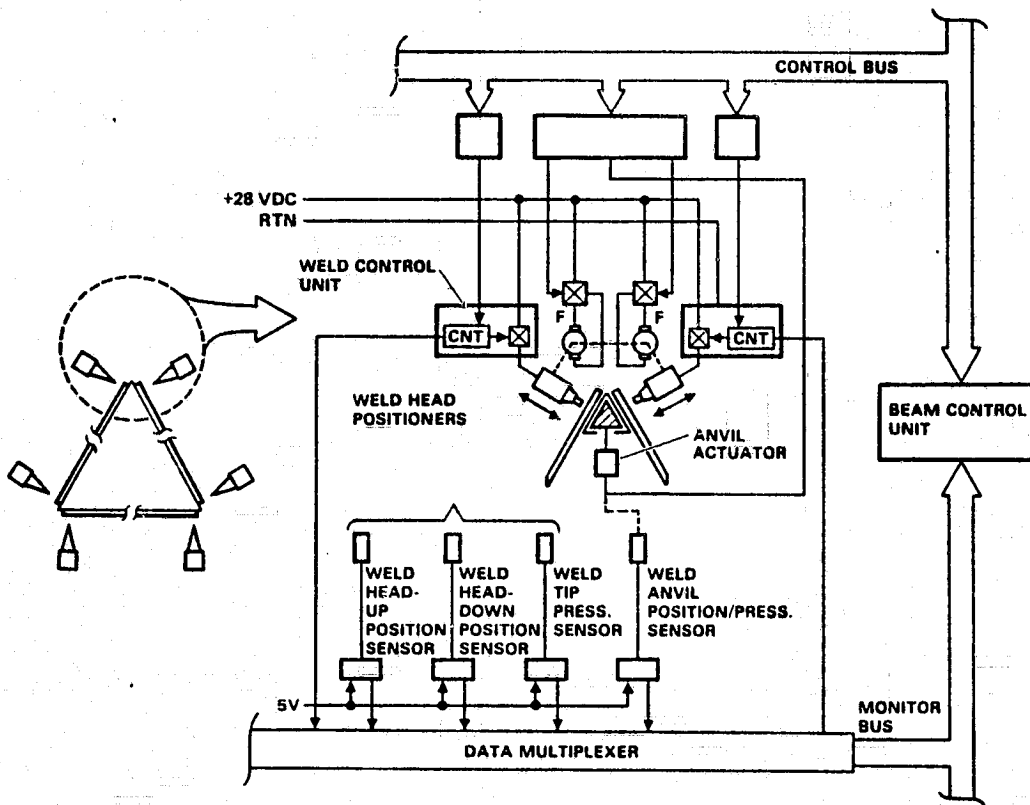


Figure 2-90. Beam ultrasonic weld control diagram.

2.2.3.3.1 Executive Software. The executive software for both ACU and BCU contains software modules for performing six functions as shown in Figure 2-91. These are: (1) process control, (2) interrupt times, (3) machine command bus I/O, (4) machine monitor bus I/O, (5) Orbiter communications I/O, and (6) its associated command decoder function.

The process control function contains five task modules which control the second-to-second real-time operations as well as collect and process status data. It uses timing data resulting from the interrupt time function. The task scheduler controls normal time share operations which govern which application task, or portion thereof, is to be run at any instant in time. The task controller function causes the specific application task functions to be performed at the proper time and in the sequence desired. The interrupt handling module responds to input indicating very fast real-time response is necessary, identifies the task, and interrupts scheduled operations to accomplish it. The housekeeping and status modules collect, update, and store the data base, monitoring data, and providing status or flag problems to the crew.

The command bus interface accepts commands from the process control function/assembly process, formats them for transmission, and operates the data bus interface to the motor/actuator subsystems. Its complement for receiving status or data from these functions is the monitor bus interface. Communication with the Orbiter is handled by the Input/Output (I/O) command decoder and communications interface, which performs the necessary formatting and handshaking tasks to communicate via the Orbiter data bus terminal unit.

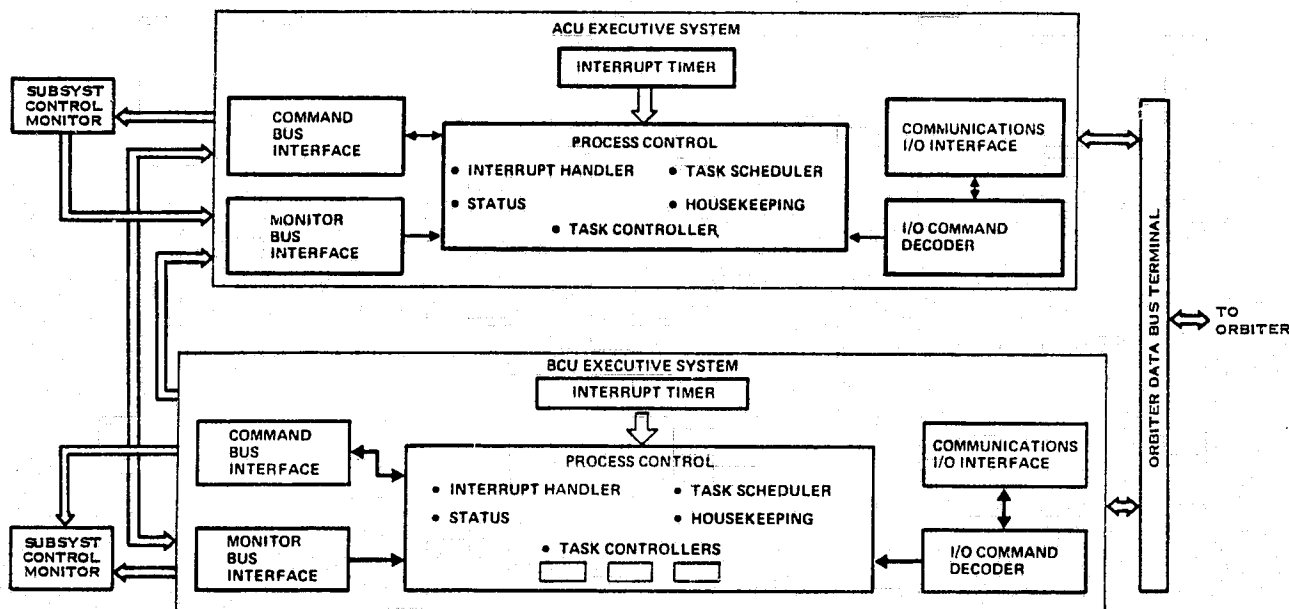


Figure 2-91. Executive software systems.

The major differences between the ACU and BCU executive software involves the task controller functions. The controller for the BCU monitors three sets of functions for each cap system as opposed to the serial task functions of the ACU.

2.2.3.3.2 Applications Software. Applications software modules comprise those programs which do the actual control and monitor task associated with subsystem tasks, such as (1) heater control, or (2) cross-member positioning control. These programs have been identified for ACU and BCU functions as shown in Figures 2-92 and 2-93.

Program sizing was performed by either flow diagramming the major steps of each program or estimating them based on a similar function. Sizing estimates were based on the number of instructions required to perform each basic type of function as shown in Table 2-22.

Program processing speed requirements are a function of the time allowed to perform a function and the total instruction loop size, and are expressed in thousands of operations per second (KOPS). The program sizing and speed requirements results are shown in Tables 2-23 and 2-24 for ACU and BCU functions, respectively.

2.2.3.4 Beam Builder Power and Energy. Beam builder power and energy requirements were estimated early in the study and have been updated regularly since. Early estimates shown in Table 2-25, indicated relatively high peak and average power consumption of 7497W and 5980W. Although these did not exceed Orbiter payload user capabilities, several beam builder process improvements were made to reduce total power and energy requirements. A 66% reduction was accomplished by: (1) switching to the hybrid-glass laminate GTP material, (2) elimination of cross-member heating/

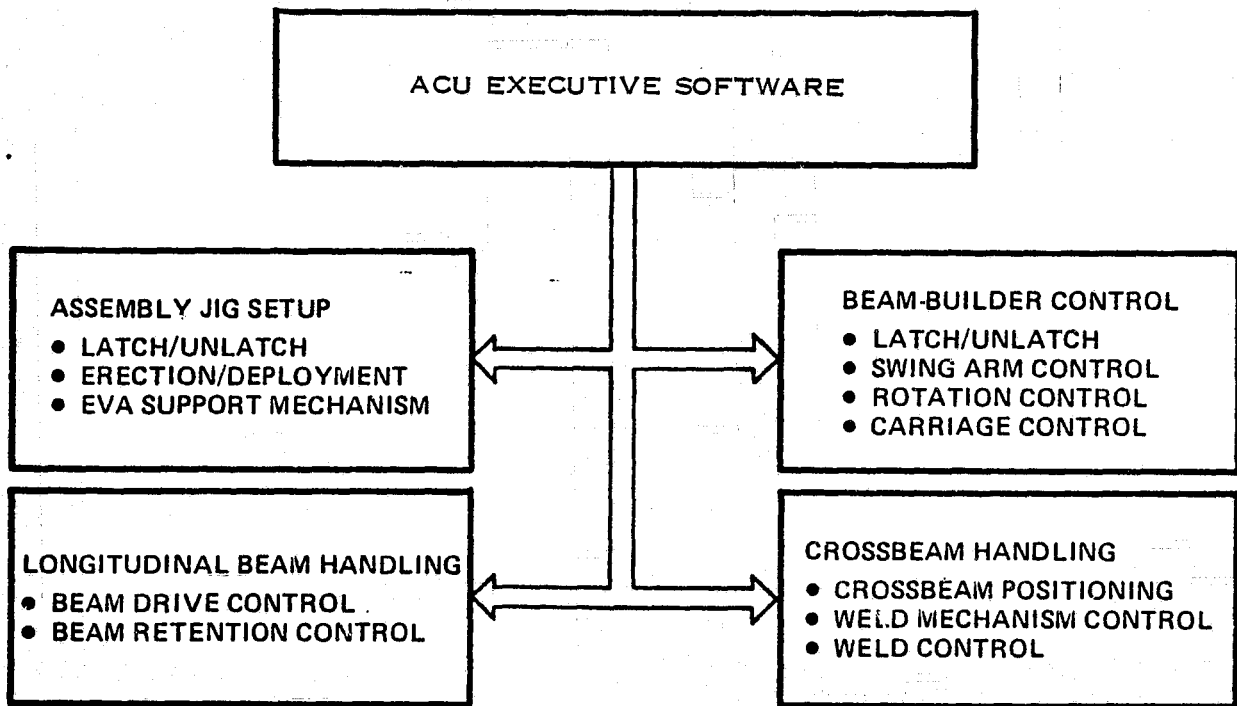


Figure 2-92. ACU application software modules.

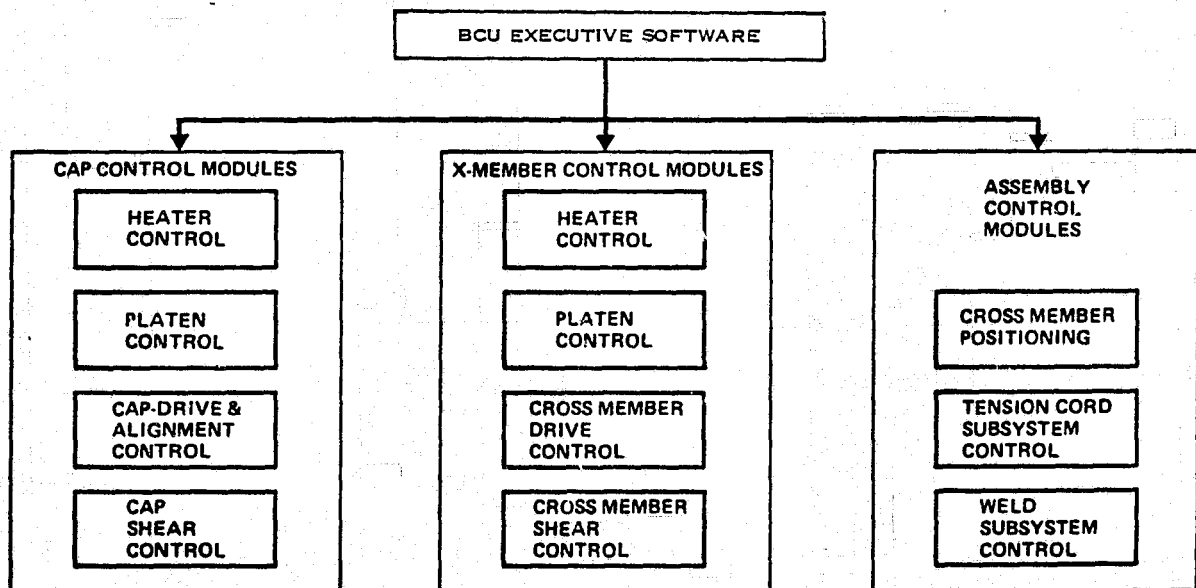


Figure 2-93. BCU executive software.

Table 2-22. Software function sizing assumptions.

Function	Instruc- tions	Function	Instruc- tions
1. Internal times	10	9. Operator command processing	10
2. Interrupt to command	20	10. Discrete command	20 to 5
3. Read length	10	11. Verify operations	5
4. Compare two values	4	12. Limit switch check	20
5. Logical decision	100	13. Command to stop	5
6. Control and monitor loop	50	14. Command to go	5
7. Flag operator	10	15. Slow drive sensing	50
8. Pause	50	16. Weld check (I, V, Time)	50

forming operations, (3) assuming that the material is maintained at the 70°F launch temperature, and (4) reduction in the heating strip areas by using a 12 mm bend radius instead of 15 mm.

Current power and energy requirements are estimated to be approximately equal to 2 kW average (3.2 kW peak) and 160.5 k joules/bay of energy, respectively. These values represent the sum of the four groups of beam builder power users as shown in Table 2-26. The greatest power user function was the cap heating sections (at 1318 watts), which represents 66% of the total energy requirement. This value is a function of strip length and width, and coefficient of heating (346.57 J/cm) of the total energy requirement. Next high power use was for subsystem controls, motors, and actuators, at 362 watts average, representing 18% of the energy. This value was determined by running the total energy required by all controls/actuators during one bay length and dividing by 80 seconds. A significant safety factor of 4.7 was included to account for friction/acceleration/conversion losses over basic values calculated for mechanism operations. Peak power values were obtained by identifying and summing the larger simultaneous user functions.

The third ranked power user (at 13%) was the ultrasonic weld operations. This function was based on six sequential 4-second weld operations per bay at 900 watts each. The lowest power use at 58 W average (3%) is for operation of the thermal control subsystem pump/motors.

2.2.3.5 Beam Builder Avionics Packaging/Arrangement. Figure 2-94 indicates the tunnel region configuration of the beam builder forming section support structure. The end view is taken from the cap material storage canister end of the structure. Package arrangement about the periphery of the tunnel is indicated in this view.

Table 2-23. ACU software sizing estimates.

Assembly Control Unit Software	Size Instruct.	Period (Rate)	Inst. Loop Size	Speed KOPS (Peak)
Executive Software				
Process Control				
● Interrupt Handler	200	(10/sec)	200	2.0
● Status Monitor	100	(1/sec)	100	0.1
● Scheduler	200	(100/sec)	200	20.0
● Task Controllers	400	(80/sec)	400	0.005
Peripheral Control				
● Process Timing	100	(10/sec)	100	1.0
● Command Bus	20	(20/sec)	20	0.4
● Monitor Bus	20	(100/sec)	20	2.0
● Communication Bus (with Orbiter)	50	(1/10 sec)	50	0.005
● I/O decoder (Orbiter)	300	(1/10 sec)	300	0.03
● Communication Bus (to BCU)	50	(1/10 sec)	50	0.005
Software Task Modules				
Assembly Jig Setup				
● Setup	90	189 sec	10030	0.053 (0.667)
● EVA Support Mech.	115	213 sec	6055	0.029 (0.200)
Beam Builder Control				
● Latch/Unlatch	30	3 sec	630	0.210
● Position B/B to Long. Loc. No. 1	120	390 sec	10240	0.026
● Position B/B to Long. Loc. No. X	30	180 sec	4210	0.023
● Cmd to Cross Beam Pos.	30	120 sec	3010	0.025
● Cmd to Stowage Pos.	30	300 sec	6410	0.021
Longitudinal Beam Handling				
● Deploy Beam Retention Mech.	40	180 sec	8420	0.047
● Clamp Longitudinal Beam X	40	30 sec	1220	0.041
● Synchronous Clamp	160	30 sec	4880	0.162
● Synchronous Guide	160	30 sec	4880	0.162
● Synchronous to Stowage	160	180 sec	4880	0.027
● Drive no. X to first weld position	39	—	305/sec	0.305
● Drive Platform to Position XXXX	120	—	1240/sec	1.240
Cross Beam Assembly				
● Deploy Holding Mech.	30	120 sec	3010	0.020
● Position Cross Beam	90	15 sec	630	0.042
● Return to X-Beam Position	90	15 sec	630	0.042
● Return to Stowage Position	30	120 sec	3010	0.026
● Weld Cross Beam	309	77.3 sec	68340	0.884 (5.8)
Total Instructions	3153	Peak KOPS (Executive + Peak Task)		31.35

Table 2-24. BCU software sizing estimates.

Beam Control Unit Software	Size Instruct.	Period (Rate)	Inst. Loop Size	Speed KOPS
Executive Software				
Process Control				
● Interrupt Handler	200	(10/sec)	200	2.0
● Status Monitor	100	(1/sec)	100	0.1
● Scheduler	200	(100/sec)	200	20.0
● Task Controllers	300	(40/sec)	300	0.007
Peripheral Control				
● Process Timing	100	(10/sec)	100	1.0
● Command Bus	20	(20/sec)	20	0.4
● Monitor Bus	20	(100/sec)	20	2.0
● Communication Bus	50	(1/10 sec)	50	0.005
● I/O Decoder	300	(1/10 sec)	300	0.03
Software Task Modules				
Cap Subsystem Control				
● Heater Control	50	.1 sec	50	0.5
● Platen Control	40	80 sec	60	0.08
● Alignment Control	372	40 sec	372	0.09
● Final Position Control	192	3 sec	19200	6.4
● Beam Length Control	105	80 sec		0.001
Cross-Member Control				
● Heater Control	50	.1 sec	50	0.5
● Platen Control	40	80 sec	60	0.08
● Length Control	192	40 sec	19200	0.48
Assembly Control				
● Cross-Member Lateral	35	4 sec	6045	1.51
● Cross-Member Vertical	30	1 sec	6030	6.03
● Cross-Member Return	30	5 sec	6030	1.20
● Tension Cord Control	80	(10/sec)	20	0.40
● Weld Head Control	60	1 sec	4650	4.65
● Weld Process Control	85	1 sec	4650	4.65
TOTAL INSTRUCTIONS	2651			52.11

Table 2-25. Early beam builder power requirements.

Process/Bay	Energy (KJ/Bay)	Avg Pwr (W)	Peak Power (W)	Energy
Cap Heating/Forming*	336.3	4204.	3876.1 655.2 <u>4531.3</u>	70.3%
Cross-Member Heating/Forming*	106.9	1336.	973.33 724.9 <u>1698.</u>	22.3%
Welding	21.6	270.	900.	4.5%
Subsystem Assembly & Control	13.6	170.	368	2.9%
Totals/Bay	478.4	5980.	7497.3	100%

*Heating values based on pseudoisotropic material.

Table 2-26. Baseline beam builder power & energy requirements.

Process/Bay	Energy (KJ/Bay)	Avg Pwr (W)	Peak Power (W)	Energy
Cap Heating/Forming	105.4	1318.	1215 205 <u>1420</u>	66%
Cooling	4.6	58.	58	3%
Welding	21.6	270.	900	13%
Subsystem Assembly & Control	28.9	362.	861	18%
Totals/Bay	160.5	2008.	3239	100%

ORIGINAL PAGE IS
OF POOR QUALITY

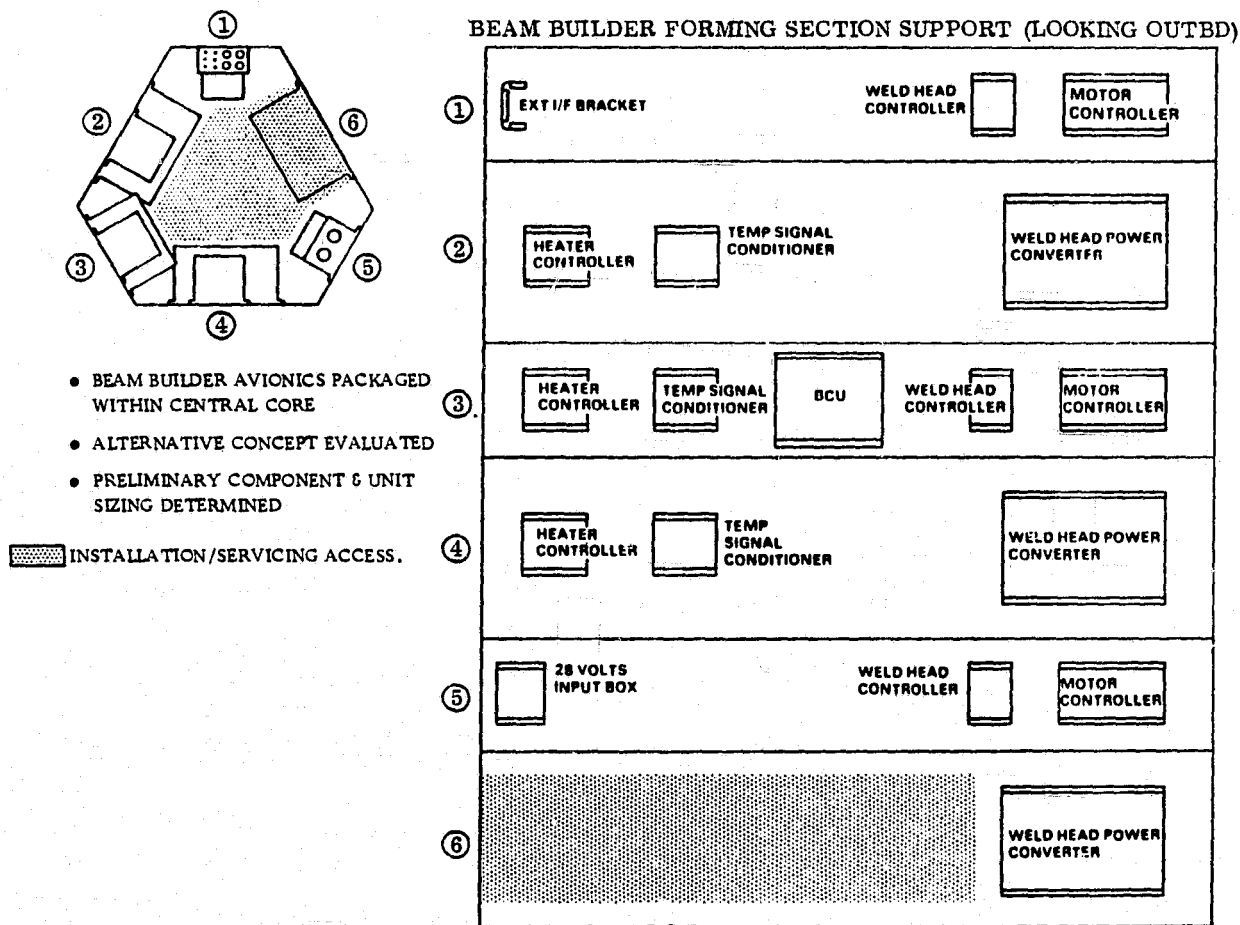


Figure 2-94. Control avionics packaging configuration.

Packages are distributed over the full length of five of the six surfaces of the tunnel. The sixth surface is clear over all of its length except at the farthest end. A flat surface development of the tunnel surfaces illustrates the distribution of the packages. The development starts (top of figure) with the surface supporting the external interface bracket, and continues counterclockwise around the tunnel to the surface supporting the external 28-volt input box. The bottommost surface illustrated here is that which was earlier noted as clear over most of its length. This surface provides for technician access to all packages and their related harnessing.

The packages listed in Table 2-27 are the total complement required for support of the beam builder. As indicated, these consist of:

- a. one external interface bracket
- b. three weld head controller packages
- c. three motor controller packages
- d. three heater control packages

Table 2-27. Beam builder equipment list and characteristics.

Item	Component	Description	Weight Per (lb)	Voltage	Qty (Net)	Remarks
<u>Heater Controls</u>						
1	Heater Element - Short		1.0	28 VDC	6	Cap Middle Strip
2	Heater Element - Short		1.0	28 VDC	12	Cap Edge Strips (2)
3	Heater Element - Long		1.5	28 VDC	6	Cap Middle Strip
4	Heater Element - Long		1.5	28 VDC	12	Cap Edge Strips (2)
5	Heater Element - Forming		1.0	28 VDC	6	Cap Middle Strip
6	Heater Element - Forming		1.0	28 VDC	12	Cap Edge Strips (2)
7	Heater Control Package	Solid State Relay	2.0	5 VDC	3	Each Pkg: 12 Switch
8	Infrared Temp. Sensor	TO-5 Can	0.2		36	
9	Ambient Temp. Sensor	Resistance	0.3		12	
10	Temp. Sig. Cond. Pkg		20.0	5 ± 15 VDC	3	
<u>Platen Controls</u>						
11	Inside Platen Solenoid	Solenoid	0.5	28 VDC	6	Control from BCU
12	Outside Platen Solenoid	Solenoid	0.5	28 VDC	12	Control from BCU
13	Open-Closed Sensor	Hall Effect Device	0.2	5 VDC	12	
<u>GTP Cap Drive Motor Controls</u>						
14	Drive Motor	Brushless DC	1.0	TBD	6	
15	Motor Travel Sensor		0.5		3	
16	Motor Controller Package		2.0		3	Includes 28 V-to-DC (TBD) Converter
<u>Beam Termination</u>						
17	Cutoff Drive Motor	Brushless DC	1.0	TBD	6	Controllers: Part of Item 16
18	Open-Closed Sensor	Hall Effect Device	0.2	5 VDC	12	
<u>Cross-Member Positioner</u>						
19	Fingergrip Actuator	Solenoid	0.5	28 VDC	6	
20	Grab Positioner Sensor	Hall Effect Device	0.2	5 VDC	6	
21	Retainer Actuator Sensor	Limit Switch	0.3	5 VDC	6	
22	Fingergrip Sensor	Hall Effect Device	0.2	5 VDC	6	
23	Belt Drive Motor	Stepper	2.0	TBD	6	Controllers: Part of Item 16
24	Positioner Motor	Brushless DC	1.0	TBD	2	Controllers: Part of Item 16
<u>Beam Tension Cord Control</u>						
25	Tension Cord Drive Motor (Outside)	Brushless DC	1.0	TBD	2	Controllers: Part of Item 16
26	Tension Cord Drive Motor (Inside)	Brushless DC	1.0	TBD	2	Controllers: Part of Item 16
27	Position Sensors	Hall Effect Device	0.2	5 VDC	36	3 per end × 2 ends × 3 sides × ± carriers
<u>Weld Control</u>						
28	Weld Heads	Ultrasonic	10.0		6	
29	Position Motor	Brushless DC	1.0	TBD	6	Controllers: Part of Item 16
30	Power Converter Package	28 V-to-20 KHz 2 channel	50.0	28 VDC	3	

Table 2-27. Beam builder equipment list and characteristics (Concl'd)

Item	Component	Description	Weight Per (lb)	Voltage	Qty (Net)	Remarks
31	Weld Head Controller Pkg	2 channel	15.0	TBD	3	Cam Drive; Controller: Item 16
32	Anvil Actuator Motor	Brushless DC	1.0	TBD	1	
33	Anvil Position Sensor	Limit Switch	0.3	5 VDC	3	3 Positions Per
34	Weld Head Position Sensor	Hall Effect Device	0.2	5 VDC	18	
35	Other 28V Source Interface Box		10.0	10 VDC	1	Transfer Switch; Distribution
36	BCU		38.0	28 VDC	1	System Controller: Processor, Memory, Discrete I/O, Data MUX, Shuttle Control Interface

- e. three temperature signal conditioner packages
- f. three weld head power converter packages
- g. one BCU package
- h. one 28-volt input box.

The external interface bracket provides for entry to the beam builder of electrical control and monitor functions from the Shuttle Orbiter mission specialist station.

The weld head controller package works in conjunction with its associated weld head power converter packages to activate and monitor weld head operation. Each two-package set supports two welders.

The motor controller package provides drive circuits for operation of applicable brushless DC and stepper drive motors. Each package can support up to 12 motors.

Each heater control package provides voltage regulation and power switching circuits to support a related cap member's infrared and ambient temperature sensors.

The 28-volt input box provides an input interface and transfer switch capability for distribution to beam builder elements of Orbiter-provided 28 volts DC excitation power.

The BCU consists of the system processor, supporting memory, and input/output (I/O) elements for data transfer. This unit controls the operation of all other packages described above. It also provides for monitoring of all discrete sensors, and for activation of all discrete control functions (solenoids, etc.). Finally, it provides the logical interface with the Shuttle Orbiter mission specialist station.

Figure 2-95 is an interconnect diagram relating the interfaces between the various discrete packages and other elements of the beam builder.

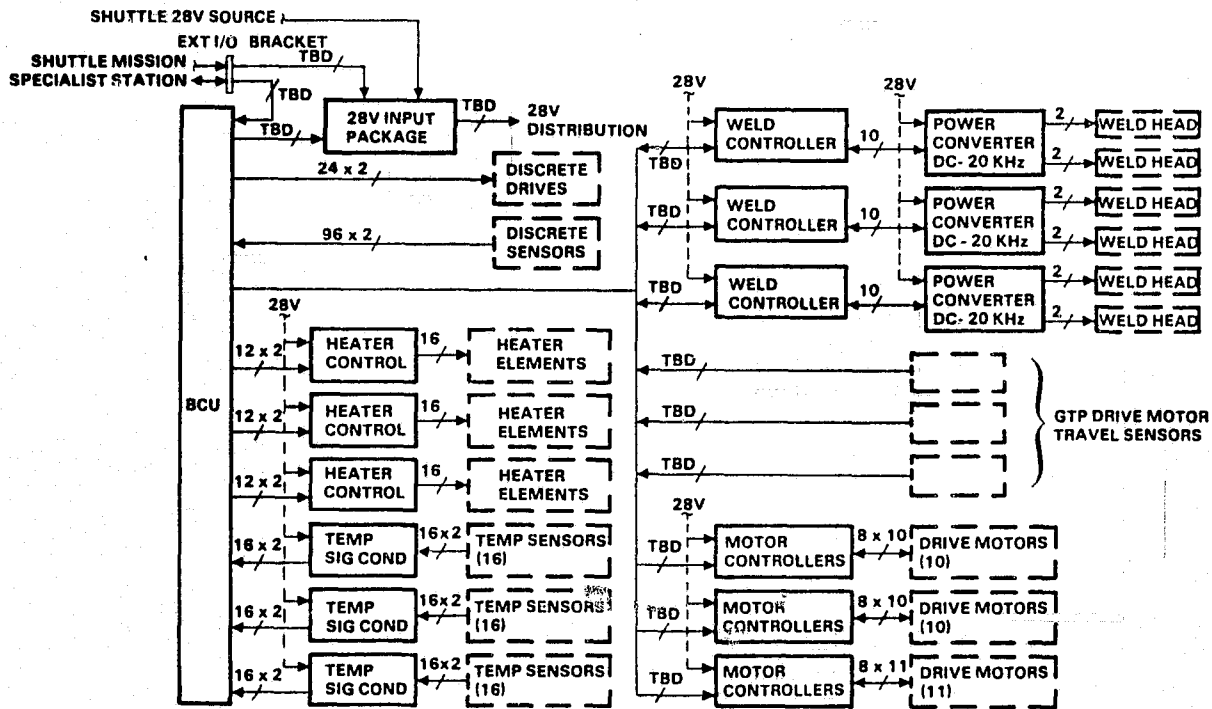


Figure 2-95. Beam builder avionics interconnect diagram.

2.3 ALTERNATIVE BEAM CONCEPT

Soon after receipt of authority to proceed with this study, an additional task was added, at NASA request, to investigate the applicability of an alternative "geodetic" beam concept to large space structure fabrication and assembly. This beam concept exhibits a circular cross section formed by an open grid system of continuous elements arranged longitudinally and in counterwound spirals. This grid is similar to the $0^\circ/\pm 60^\circ$ pattern shown in Figure 2-96, which illustrates three metallic mesh tube specimens produced and evaluated in a 1968 Convair lightweight structures program. The $0^\circ/\pm 60^\circ$ pattern was adopted in the current assessment since elements in all three "directions" are continuous and can, therefore, be fed from either rolled or coiled compact-storage equipment into an automated fabrication machine capable of producing a continuous member of great length.

Task effort was divided into three areas: analysis of structural efficiency, design of the beam and beam intersection concepts, and preliminary conceptual design of an automated fabricator. These topics are discussed in the following sections.

The baseline geodetic beam geometry and material were selected and compared with those of a corresponding triangular beam per the flow of Figure 2-97. Criteria, ground rules, and assumptions governing task conduct, shown in heavy boxes in Figure 2-97 and summarized below, were either provided directly by NASA or coordinated prior to adoption.

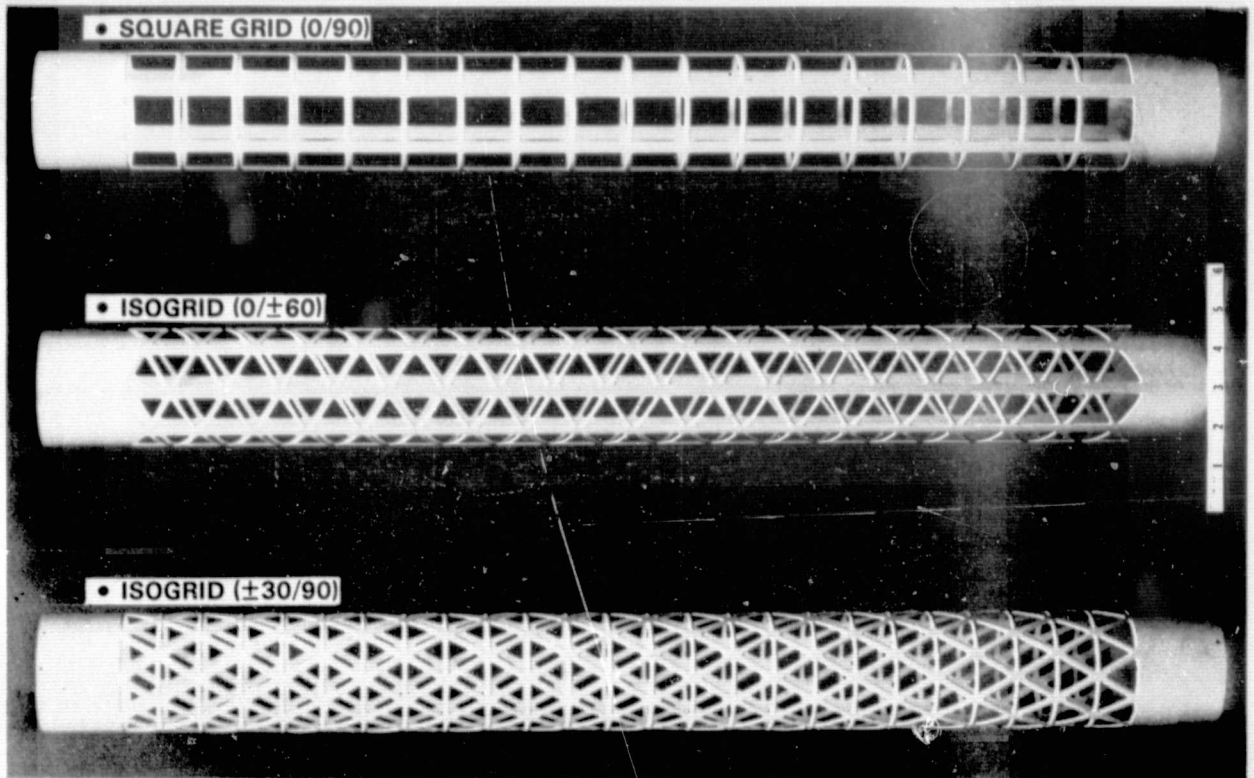


Figure 2-96. Mesh tube concepts.

2.3.1 STRUCTURAL EFFICIENCY ANALYSIS

2.3.1.1 Criteria. The NASA-provided design criteria specified three columns, with L/ρ of 100, 150, and 200, and a radius which yields a cylinder of perimeter equal to that of the baseline triangular beam. The early baseline triangular beam geometry shown in Figure 2-6 was used for this task. The geometry has since been revised, as discussed in Section 2.1.1.

Several possibilities existed for choosing a size relationship between the geodetic beam and the triangular beam for comparison. Table 2-28 lists several possible geometric relationships between the radius of the geodetic circular cylinder and the triangular cross section.

The equal perimeter option was specified for this task. It was later found, however, that only when the circle circumscribes the triangle will the lengths of two columns be equal for a given L/ρ . Consequently, using the specified L/ρ 's for comparison results in columns of unequal lengths.

- Geodetic Beam
 - Optimize for $L/\rho = 100, 150, 200$
 - Diameter: Equal perimeter with baseline triangular
 - Grid: Equilateral triangles: 0 ± 60 orientation; 12 longitudinals; assumed no nodal reinforcement
 - Elements: Square; all identical
 - Material: Unidirectional graphite; maximum E

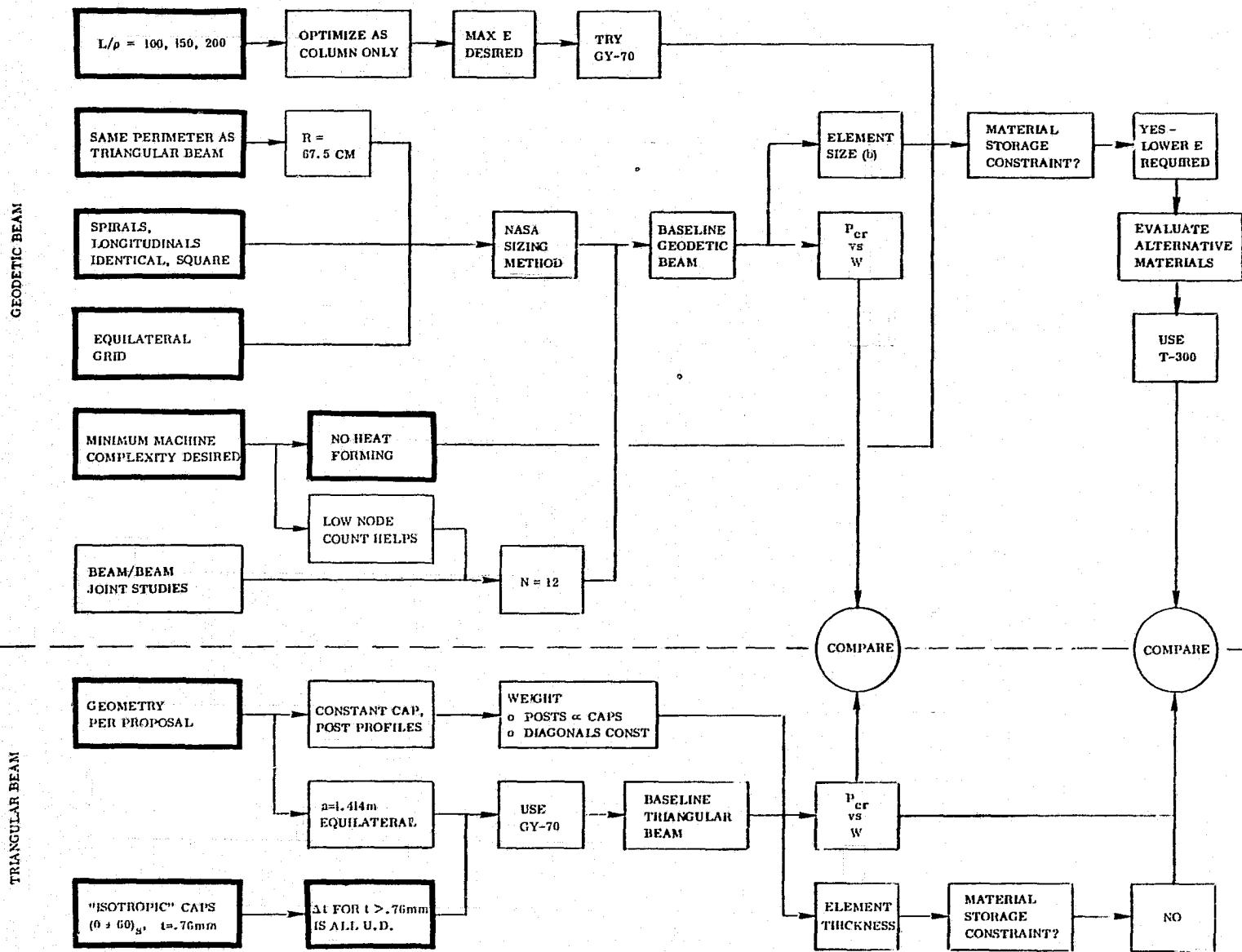


Figure 2-97. Task flow.

- Fabrication Machine
 - Feasible concept
 - No heat forming
- Triangular Beam
 - Arrangement: Study baseline
 - Material: Pseudoisotropic plus all unidirectional for $t > 0.762$ mm; maximum E

Table 2-28. Options for column size relationship.

No.	Option	Cylinder Radius (m)
1	Circle circumscribes the triangle	0.8164
2	Circle inscribed inside triangle	0.4082
3	Circle and triangle have equal perimeter	0.6751
4	Circle and triangle inclose equal areas	0.5250
5	Circle and triangle have equal perimeter line integrals	0.6082

Another option, not listed above, is to let the radius of the cylinder become one of the variables in the weight optimization scheme. It was discovered at the end of the study that, for a given load and length, allowing the radius to be a design variable yields a geodetic column of lighter weight than when preselecting a given radius and L/ρ , as specified for this task. The study results reported here are based on the original criteria, and have not been revised to reflect subsequent findings.

Assuming the geodetic structure acts as a column, the minimum weight design exists when the overall buckling stress of the total column, of length L , equals the buckling stress of an individual bay element (of the N longitudinals) where only the longitudinals react the axial load.

2.3.1.2 Derivation of Optimization Expressions. When the design criteria are specified in terms of a given column slenderness ratio, L/ρ , and radius, R , the derivation of the governing expressions for an optimum column follows from simple strength of materials considerations. For this study, the cross sections of all elements in the beam were specified to be square, $b \times b$. If there are N longitudinals, the elements at any given cross section of the column can support an axial compressive force of:

$$P_{CR} = N \frac{\pi^2 E I_e}{(a')^2}$$

where E = Modulus of elasticity

$$I_e = \text{element moment of inertia} = \frac{b^4}{12}$$

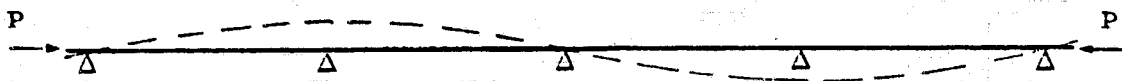
$$a' = \text{effective element length} = \frac{a}{\sqrt{c}} \text{ where } c = \text{end fixity}$$

ORIGINAL PAGE IS
OF POOR QUALITY

The end fixity of the individual column element is a function of the rotational constraint provided by the crossover helical members. If they provide little or no rotational constraint, the longitudinal element will buckle between supports as shown below:



or buckle over the constraints if the constraint is not sufficient:

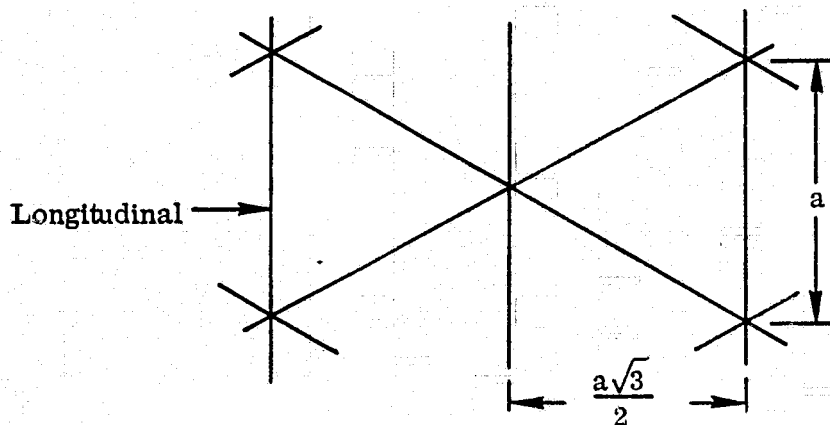


If complete fixity is assumed, the buckle pattern will exhibit zero slope at the nodes:



As in most structural systems, the true fixity is somewhere in between the two extremes. In a report, "A Cylindrical Structure Made With Continuous Rods", NASA-JSC, dated Feb 1977, tests of a similar beam configuration were reported. The results showed an end fixity coefficient of 1.78. This is equivalent to using the Euler column formula with an effective element length of three-quarters of the actual element length.

$$a' = \frac{a}{\sqrt{c}} = \frac{a}{\sqrt{1.78}} = 0.75a$$



The end fixity coefficient is based on one test where the members were round aluminum rods joined with epoxy because the joints could not be successfully made by welding. To properly verify the value for end fixity, the correct joint configuration and material should be tested. A more conservative and correct approach at this time would be to assume pinned joints for predesign. The two assumptions will be compared later for the impact on the weight of the column. Both sets of sizing expressions are developed below, one where $a' = 0.75a$ and the other where $a' = a$.

For $a' = 0.75a$:

$$P_{CR} = N \frac{\pi^2 EI_e}{(a')^2} = N \frac{\pi^2 E}{(0.75a)^2} \left(\frac{b^4}{12} \right) = \frac{4N\pi^2 Eb^4}{27 a^2}$$

Since $a = \frac{4\pi R}{\sqrt{3}N}$

the expression for P_{CR} for an element becomes

$$P_{CR} = \frac{N^3 Eb^4}{36 R^2}$$

Considering the entire column as simply supported, the critical load is

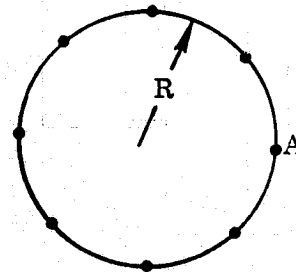
$$P_{CR} = \frac{\pi^2 EI_c}{L_c^2}$$

where $L_c =$ total column length

$I_c =$ column moment of inertia

For N areas evenly spaced on a radius, the area moment of inertia is:

$$\begin{aligned} I_c &= \frac{\sum AR^2}{2} \\ &= \frac{Nb^2 R^2}{2} \end{aligned}$$



Thus, P_{CR} for the column becomes

$$P_{CR} = \frac{\pi^2 ENb^2 R^2}{2L_c^2}$$

Equating the column critical load with the element critical load yields an overall minimum weight configuration for a given R and L .

$$P_{CRELEM} = P_{CRColumn}$$

$$\frac{N^3 Eb^4}{36R^2} = \frac{\pi^2 ENb^2 R^2}{2L_c^2}$$

Solving for b^2 :

$$b^2 = \frac{18\pi^2 R^4}{N^2 L_c^2}$$

Substituting this value into either expression for P_{CR} yields:

$$P_{CR} = \frac{9\pi^4 ER^6}{NL_c^4} \quad (\text{for } C = 1.78)$$

In terms of the column slenderness ratio, S_R , the critical buckling load can be expressed as:

$$P_{CR} = \frac{36\pi^4 ER^2}{NS_R^4}$$

$$b^2 = \frac{36\pi^2 R^2}{N^2 S_R^2}$$

where

$$S_R = L/\rho = L\sqrt{\frac{I}{A}}$$

$$I = Nb^2 R^2; A = Nb^2$$

$$\sqrt{\frac{I}{A}} = \frac{R}{\sqrt{2}}$$

$$L_c = \frac{S_R R}{\sqrt{2}}$$

The weight per unit length of the basic column is:

$$w = 3Nb^2\rho$$

where ρ = material density

For $a' = a$: (pin ended elements)

$$P_{CR} = \frac{16\pi^4 ER^6}{NL_c^4}$$

or
$$P_{CR} = \frac{64\pi^4 ER^2}{NS_R^4}$$

$$b^2 = \frac{64\pi^2 R^2}{N^2 S_R^2}$$

The element size, b , is independent of the material and can be calculated at this point for the three given S_R 's, $R = 0.675$ m and $N = 12$. The resulting values are listed in Table 2-29.

Table 2-29. Geodetic column element size.

S_R	Element Size, b (cm)	
	$C = 1$	$C = 1.78$
100	1.414	1.060
150	0.943	0.707
200	0.707	0.530

2.3.1.3 Material and Storage Considerations. To determine the column's critical

load, the material characteristics must be known (specifically the modulus of elasticity, E).

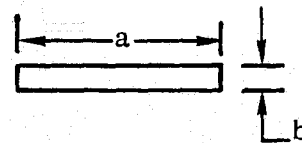
The material choices for the geodetic column were restricted to graphite/polysulfone composites from the start. Since the primary mode of failure is column buckling, choosing the material with the highest modulus of elasticity is indicated. Thus, the initial column sizing was done with GY-70 fiber. But, as the study progressed and the beam fabricator concept was being developed, material storage became an issue. The longitudinals must be unstressed in the deployed or straight position, therefore, they must be wrapped onto reels for transport into orbit. Heating of the material prior to storage, wrapping into a tight radius for reel storage, and then reheating in orbit as the rod is being deployed would be difficult without a cross section geometry change of the rod. Because the graphite fibers do not yield, the fibers on the inner radius of the square rod could not extend nor could the fibers on the outer radius contract as the rod is being straightened or curved when the matrix is heated.

The minimum hub size on which the rod material can be wrapped is a function of the rod cross-sectional geometry and allowable strength of the material. Taking the general shape of a rectangle and by using simple strength of material equations, the governing expression can be derived:

From beam bending theory:

$$M = \frac{EI}{R}$$

$$I = \frac{1}{12} ab^3$$



or

$$M = \frac{Eab^3}{12R}$$

The stress for pure bending in the rectangle is:

$$\sigma_B = \frac{6M}{ab^2}$$

or

$$M = \frac{ab^2\sigma_B}{6}$$

Equating the two expressions for M and solving for R gives:

$$R = \frac{Eb}{2\sigma_B}$$

or

$$D = 2R = \frac{b}{\bar{\epsilon}}$$

where $\bar{\epsilon}$ equals the allowable safe strain of the material.

Table 2-30 is a summary of representative candidate graphite/polysulfone materials and their pertinent material properties, at a typical 57 percent fiber volume content.

Table 2-30. Candidate graphite/polysulfone materials.

Property	AS/P1700	GY-70/P1700	HMS/P1700	T300/P1700	VSB-32T/T1700
E_{11} (GN/m ²)	112.39	279.93	205.47	131.00	197.88
ϵ_{11c} ($\mu\text{m}/\text{m}$)	-5896.	-2350.	-4300.	-7750.	-4000.
ϵ_{11t} ($\mu\text{m}/\text{m}$)	11534.	2350.	4300.	7750.	4000.
α ($\mu\text{m}/\text{m}/^\circ\text{K}$)	-0.0108	-0.9108	-0.8028	-0.4500	-0.7722
ρ (kg/m ²)	1522.4	1660.8	1605.4	1522.4	1660.8

The strains listed in Table 2-30 are ultimate or strains at failure. For this task, an allowable safe strain, $\bar{\epsilon}$, for prolonged storage was assumed to be one-half of the failure strain.

Combining Tables 2-29 and 2-30 produces a matrix table showing the minimum diameter that can be formed for a particular element size and material combination. The minimum diameter could be either the hub diameter of the current storage reel, 1.372 m, or twice the radius of curvature, 0.808 m, of the material as the axial members are being turned from the storage reels into the feed guide of the fabricator (Section 2.3.3).

For the baseline geodetic beam ($N = 12$ and $R = 0.6751$ m), Table 2-31 shows that several material/ S_R combinations are not practical because a storage reel could either not fit into the Shuttle bay (which is 4.572 m diameter) or the hub size would be too large to store an adequate amount of material onto the reel to fabricate the baseline total column length (914 m). GY-70, VSB-32T, and HMS can, therefore, be eliminated as candidate materials and, since AS had a lower modulus of elasticity than T300, T300 is the logical choice.

Figure 2-98 is a continuous plot of minimum diameter of the candidate fiber material versus element size.

Table 2-31. Minimum coil diameter for candidate materials.

S _R / End Fixity	Coil Diameter, m				
	Material Candidate				
	GY-70/P1700	VSB-32T/P1700	HMS/P1700	AS/P1700	T300/P1700
100/1.00	12.03	7.07	6.58	4.80	3.65
150/1.00	8.02	4.71	4.38	3.20	2.43
200/1.00	6.02	3.54	3.28	2.40	1.82
100/1.78	9.03	5.30	4.93	3.60	2.74
150/1.78	6.02	3.54	3.28	2.40	1.82
200/1.78	4.51	2.66	2.47	1.80	1.37

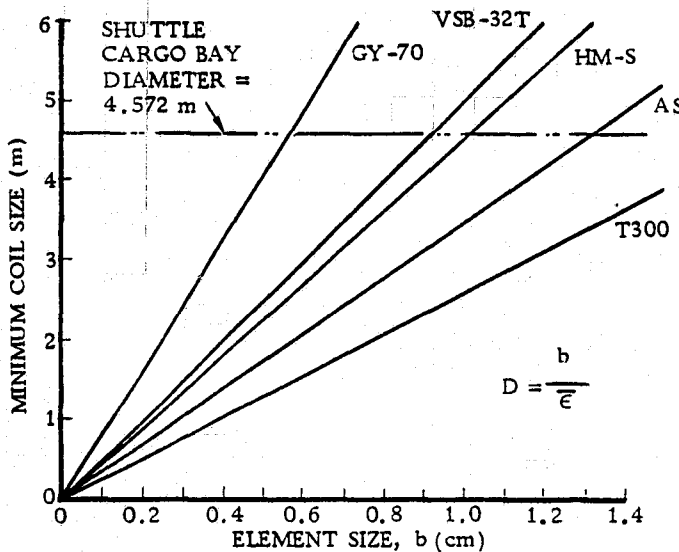
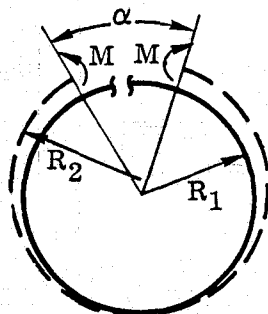


Figure 2-98. Minimum coil diameter vs. element size for candidate fiber materials.



The baseline beam builder has the helical members of the geodetic beam stacked concentrically on four levels such that, when the members are peeled off the storage drums, they will be stress free in the completed beam configuration. For the helical members to be stored concentrically, the diameter of the outer storage drum must be increased. To determine the resulting bending stress, consider the increase in diameter to be equivalent to opening a cut ring as shown below:

For the particular case to be considered:

$$R_1 = 1.5646 \text{ m}$$

$$R_2 = 1.676 \text{ m}$$

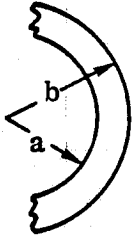
The change in circumference is:

$$\Delta C = \pi (1.6764) - \pi (1.5646) = 0.3505 \text{ m}$$

$$\text{Then } \alpha = \frac{\Delta C}{R_2} = \frac{0.3505}{0.8382} = 0.418$$

The bending moment to open the ring is

$$M = \frac{\alpha E}{8\pi} \left(\frac{4a^2b^2 (\ln b/a)^2 - (b^2 - a^2)^2}{2(b^2 - a^2)} \right)$$



For the baseline geodetic beam

$$t = 0.530 \text{ cm} \quad E = 131.00 \text{ GN/m}^2$$

$$a = 0.8382 - 0.0053 = 0.8329 \text{ m}$$

$$b = 0.08382 \text{ m (Ref., Sechler, Elasticity in Engineering, p. 148)}$$

Substituting gives

$$M = 6.485 \text{ Nm}$$

The stresses are:

$$\sigma_r = \frac{4M}{K} \left(\frac{a^2b^2}{r^2} \ln \frac{b}{a} - a^2 \ln \frac{r}{a} - b^2 \log \frac{b}{r} \right)$$

$$\sigma_\theta = \frac{4M}{K} \left(\frac{a^2b^2}{r^2} \ln \frac{b}{a} - a^2 \ln \frac{r}{a} - b^2 \ln \frac{b}{r} + b^2 - a^2 \right)$$

$$\tau_{r\theta} = 0$$

In which

$$K = 4a^2b^2 (\ln \frac{b}{a})^2 - (b^2 - a^2)^2 = 1.0696 \times 10^{-9} \text{ m}^4$$

$$@r = a$$

$$\sigma_r = 0$$

$$\sigma_\theta = 5.45 \times 10^7 \text{ N/m}^2$$

$$@r = b$$

$$\sigma_r = 0$$

$$\sigma_\theta = 5.42 \times 10^7 \text{ N/m}^2$$

For the baseline material T300/P-1600 at 57% fiber volume

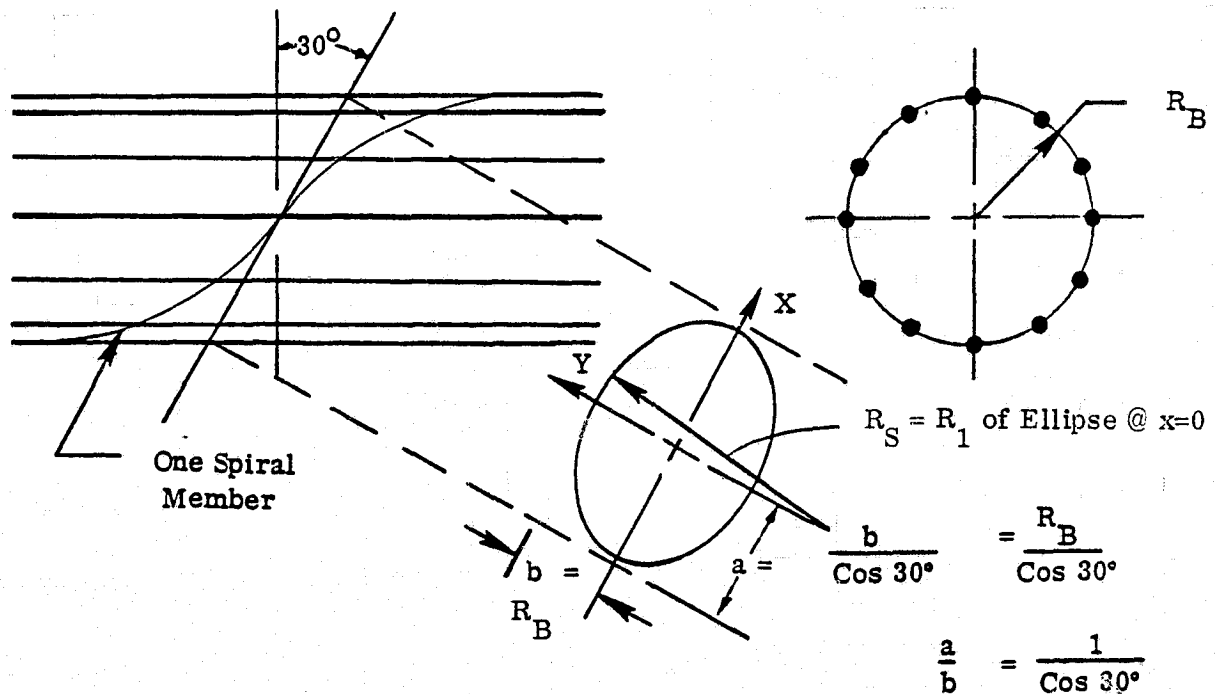
$$F_{tu} = 101.4 \times 10^7 \text{ N/m}^2$$

Thus the margin of safety is:

$$\text{M.S.} = \frac{101.4 \times 10^7}{1.4 (5.45 \times 10^7)} - 1 = + \text{Large (Ult)}$$

where the factor of safety = 1.40.

If the helical members are not preformed to the correct radii but are stored straight (like the longitudinals), bending stresses will be created as the helical members are flexed to their instantaneous radius in the assembled beam. For reel storage, the helical members would be constrained to the same minimum diameter hub as the longitudinals. The instantaneous bend radius, R_S , of the helical members can be expressed in terms of the beam radius as derived below:



$$R_S = R_1 = \frac{(a^4 - x^2(a^2 - b^2))^{3/2}}{a^4 b}$$

@ $x = 0$

$$R_S = \frac{(a^4)^{3/2}}{a^4 b} = \frac{a^2}{b}$$

$$R_S = \frac{R_B}{\cos 30^\circ} \left(\frac{1}{\cos 30^\circ} \right) \rightarrow R_S = \frac{4}{3} R_B$$

ORIGINAL PAGE IS
OF POOR QUALITY

For the baseline configuration where $R_B = 0.6751$ m, the instantaneous bend radius would be:

$$\begin{aligned} R_S &= \frac{4}{3}R_B \\ &= \frac{4}{3}(0.6751) \\ &= 0.900 \text{ m} \end{aligned}$$

For the baseline configuration, the resulting bending strain is:

$$\begin{aligned} \epsilon &= \pm \frac{t}{2R_S} \\ &= \pm \frac{0.0053}{2(0.900)} \\ &= \pm 2944 \mu\text{m/m} \end{aligned}$$

The safe allowable strain for T300/P1700 graphite/polysulfone is:

$$\bar{\epsilon} = \pm 3875 \mu\text{m/m}$$

Since the long term effect of built-in stress corresponding to this strain magnitude is not known (particularly at the nodal joints), a non-prestressed approach was adopted.

2.3.1.4 Sizing of Baseline Geodetic Column. With T300/P1700 chosen as the appropriate material, the load carrying capability of the baseline geodetic column can be calculated. For end fixity $C = 1.78$:

$$\begin{aligned} P_{CR} &= \frac{36\pi^4 ER^2}{NS_R^4} \\ &= \frac{36\pi^4 (131.0 \times 10^9) (0.6751)^2}{12S_R^4} \\ &= \frac{1.7911 \times 10^{11}}{S_R^4} \end{aligned}$$

For end fixity $C = 1.00$:

$$\begin{aligned} P_{CR} &= \frac{64\pi^4 ER^2}{NS_R^4} \\ &= \frac{3.1842 \times 10^{11}}{S_R^4} \end{aligned}$$

The weight per unit length is the same: $W = 3Nb^2\rho$.

C-3

Table 2-32 is a summary of the baseline beam characteristics.

Table 2-32. Summary of baseline geodetic beam characteristics.

S_R L/ρ	N	End Fixity	R m	b cm	E N/m^2	L m	P_{CR} KN	W kg/m
100	12	1.00	0.6751	1.414	13.1×10^{10}	47.74	310.2	10.96
150		1.00		0.943		71.61	61.3	4.87
200		1.00		0.707		95.48	19.4	2.74
100		1.78		1.060		57.73	174.5	6.16
150		1.78		0.707		85.59	34.5	2.74
200	12	1.78	0.6751	0.530	13.1×10^{10}	95.48	10.9	1.54

The last entry in the table is the baseline geodetic beam used for the beam builder design.

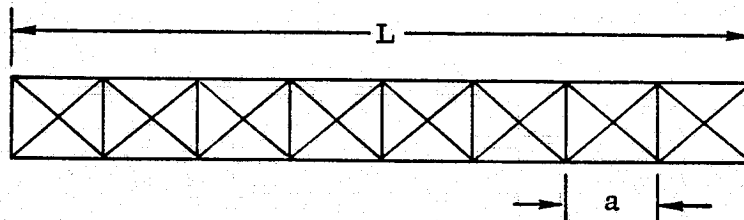
Another approach to presenting the design data of the geodetic beam is to plot P_{CR} vs. w , holding the radius constant but varying N . This approach is discussed in Section 2.3.1.8.

2.3.1.5 Triangular Beam Sizing. The triangular beam configuration used for comparison in this study is from the original SSAFE proposal. Since this task was completed, several changes have been made to the triangular beam concept. These changes have not been incorporated into this analysis.

Figure 2-6 shows the basic overall geometry of one bay for the triangular beam used for this study. The spacing between cross-members was maintained at 1.434 m for all loads even though this limits the optimization parameters. This spacing allows for convenient cross beam attachment. For optimum design, the spacing would be such that the column buckling/crippling stress of the caps between supports would equal the overall Euler column buckling stress of the beam. It is assumed for this study that the cap cross section for a given cap area, A' , can be configured to provide adequate local buckling strength between supports such that Euler buckling is critical.

The weight of the triangular beam is the sum of the caps, cross-members, and diagonal cords.

$$W_{TOT} = W_{CAPS} + W_{POST} + W_{DIAGONALS}$$



$$W_{CAPS} = 3 A' L \rho; \rho = \text{Material Density}$$

In determining the weight of the cross-members or posts, the developed length of the post material in the proposal will be used, but the thickness will be set equal to that computed for the cap.

$$W_{\text{POSTS}} = X_{\text{TOT}} \cdot A_p \cdot l_p \cdot \rho$$

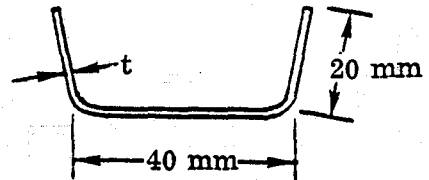
where

$$X_{\text{TOT}} = \left(\frac{L}{a} + 1 \right) 3$$

$$A_p = d \cdot t$$

$$l_p = 1 - 0.01358 = 1.4004 \text{ m}$$

$$\rho = 1743.84 \text{ kg/m}^3$$



$$d = 7.62 \text{ cm}$$

thus

$$W_{\text{POSTS}} = X_{\text{TOT}} (186.086) t$$

The total length of the diagonals in a beam of length L is:

$$D = \left(\sqrt{a^2 + (1 - 0.01358)^2} \right) \frac{6L}{a}$$

$$= 8.3268 L$$

The weight per meter of cord is

$$\bar{p} = 0.004145 \text{ kg/m} \quad (\text{KEVLAR density} = 1.38 \text{ g/cc})^*$$

Thus, the weight of the cord in the beam of length L is:

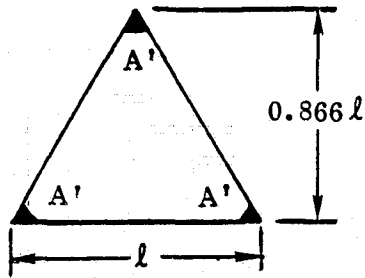
$$W = D \cdot \bar{p}$$

$$= 0.02317L \text{ kg}$$

For the sizing equations of the triangular beam, assume the required P_{CR} and S_{R} (L/ρ) are known. Since NASA asked for comparisons at special values of S_{R} , the sizing equations will be expressed in terms of S_{R} .

ORIGINAL PAGE IS
OF POOR QUALITY

*Data not updated to reflect later change to S-glass/polysulfone cord. Weight change negligible.



The area moment of inertia is:

$$I = 2A' \left(\frac{1}{3} (0.866 l) \right)^2 + A' \frac{2}{3} \left((0.866 l) \right)^2$$

$$= \frac{A' l^2}{2}$$

$$A = 3A'$$

$$\rho = \sqrt{\frac{I}{A}} = \sqrt{\frac{A' l^2}{2 \cdot 3A'}} = \frac{l\sqrt{6}}{6}$$

If given $S_R = \frac{L}{\rho}$ where L = total length of beam, then L can be expressed as:

$$L = S_R \rho = S_R \frac{l\sqrt{6}}{6}$$

Using pin-ended Euler column formula substitute in the above expressions:

$$P_{CR} = \frac{\pi^2 EI}{L^2}$$

$$= \frac{\pi^2 EA' l^2 \cdot 36}{2 S_R^2 l^2 \cdot 6}$$

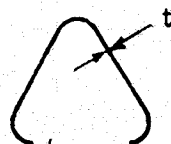
$$= \frac{3\pi^2 EA'}{S_R^2}$$

So, for a given S_R and P_{CR} , the cap area A' is:

$$A' = \frac{P_{CR} S_R^2}{3\pi^2 E}$$

The initial analysis of the cap compressive strength showed the cap to have more than adequate strength in column buckling between posts to develop the overall column strength of the beam. This is due to the short spacing between posts.

For this study, the cap cross-sectional geometry was held constant per the proposed configuration, allowing the thickness to vary in order to arrive at the proper A' .



Perimeter = D

The baseline material is GY-70/polysulfone graphite thermoplastic with a laminate layup of $(\pm 60, 0)_S$ or $t = 0.762$ mm. For the proposal, the material properties used were:

$$E_X = 8.687 \times 10^7 \text{ kN/m}^2$$

$$E_Y = 8.687 \times 10^7 \text{ kN/m}^2$$

$$\nu = 0.30$$

$$G_{XY} = 3.344 \times 10^7 \text{ kN/m}^2$$

For thicknesses requiring more than the 6 plies of the baseline, the additional thickness was achieved by adding unidirectional (0°) plies to the middle of the laminate, $(\pm 60, 0_N)_S$. Figure 2-99 is a plot of the elastic modulus in the cap longitudinal direction versus the laminate thickness as a result of adding unidirectional plies.

English units are used as well as SI in Figure 2-99 for clarity because the coefficients of the best fit polynomial were computed in English units.

Since the modulus is now a function of t , the basic sizing expression for the triangular beam cap must be modified to:

$$A' = \frac{P_{CR} S_R^2}{3\pi^2 E(t)}$$

Using the Hewlett-Packard 9830 desk computer, a cubic best fit was made of the elastic modulus versus laminate thickness curve in Figure 2-99 to find $E(t)$. For the relationship:

$$E(t) = B_0 + B_1 t + B_2 t^2 + B_3 t^3$$

the coefficients are:

$$B_0 = -4.3875 \times 10^6$$

$$B_1 = 7.2915 \times 10^8$$

$$B_2 = -5.1203 \times 10^9$$

$$B_3 = 1.1298 \times 10^{10}$$

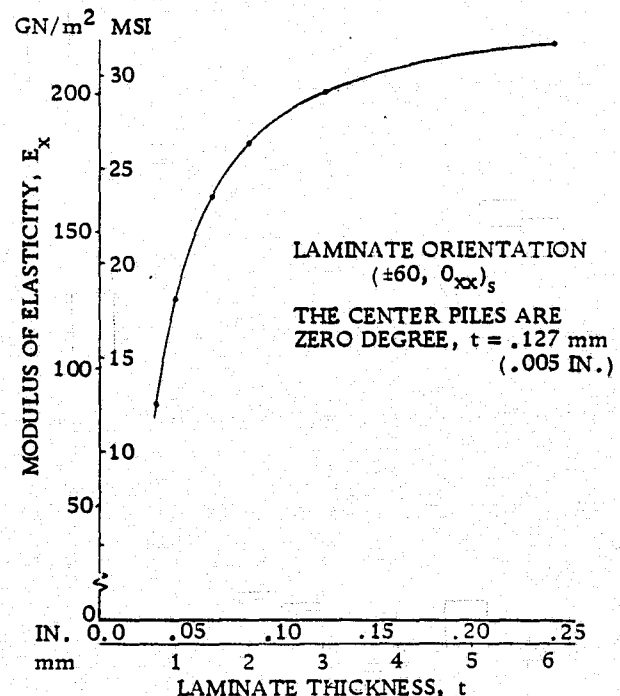


Figure 2-99. Modulus vs. laminate thickness.

If D is the developed length of the cap, then $A' = D \cdot t$. For the baseline, $D = 18.364$ cm (7.23 in). The sizing expression becomes:

$$Dt = \frac{P_{CR} S_R^2}{3\pi^2 E(t)}$$

or, substituting the cubic expression for $E(t)$, the sizing expression can be solved for t for a given P_{CR} and S_R :

$$B_3 t^4 + B_2 t^3 + B_1 t^2 + B_0 t - \frac{P_{CR} S_R^2}{3\pi^2 D} = 0$$

Knowing t , $E(t)$ and A' can be computed, and then the weight of the triangular beam for specific values of P_{CR} and S_R can be determined.

2.3.1.6 Beam Comparison. A polynomial regression program on the Hewlett-Packard 9810A was used to solve the above 4th order polynomial in t . For purposes of a direct comparison, the critical loads found for the geodetic beam for the given L/ρ 's, $R = 0.6571$ m, fixity and $N = 12$ were used.

(Note: Per Section 2.3.1.1, the two beams are not of equal length for a given S_R if they are of equal perimeter. Only when the geodetic beam circumscribes the triangle will the two be equal in length for a given S_R .)

From Table 2-33, for the $S_R = 200/\text{Fixity} = 1.78$ baseline geodetic beam configuration, the equivalent triangular beam weighs:

$$\frac{1.540}{1.115} - 1 \quad 100\% = 38\% \text{ less and is}$$

$$\frac{115.59}{95.48} - 1 \quad 100\% = 21.1\% \text{ longer}$$

The details of the triangular beam sizing are shown in Table 2-34. End fixity refers to the assumption for end fixity of a single longitudinal bay length element in the geodetic beam. The last entry in the table corresponds to the S_R and end fixity for the geodetic beam baseline configuration used for the machine design.

Due to the thin gage of the cap and post material in the triangular beam concept, there is no coilability problem for storage as in the geodetic beam.

Table 2-33. Geodetic vs. triangular beam comparison.

S_R (L/ ρ)	End Fixity	Geodetic Beam			Triangular Beam		
		L m	P_{CR} kN	W kg/m	L m	P_{CR} kN	W kg/m
100	1.00	47.74	310.2	10.96	57.73	310.2	3.843
150	1.00	71.61	61.3	4.87	86.59	61.3	2.095
200	1.00	95.48	19.4	2.74	115.46	19.4	1.502
100	1.78	47.74	174.5	6.16	57.73	174.5	2.448
150	1.78	85.59	34.5	2.74	86.59	34.5	1.502
200	1.78	95.48	10.9	1.54	115.59	10.9	1.115

Table 2-34. Triangular beam weight breakdown.

S_R (L/ ρ)	End Fixity	L m	P_{CR} kN	t cm	E GN/m ²	CAPS kg	POSTS kg	DIAGO- NALS kg	W kg/m
100	1.00	57.73	310.2	0.286	199.5	158.62	61.85	1.308	3.843
150	1.00	86.59	61.3	0.155	163.0	112.94	43.79	1.714	2.095
200	1.00	115.45	19.4	0.111	128.5	123.14	47.44	2.617	1.502
100	1.78	57.73	174.5	0.182	177.2	100.71	39.27	1.308	2.448
150	1.78	86.59	34.5	0.111	128.5	92.35	35.73	1.963	1.502
200	1.78	115.45	10.9	0.082	97.9	90.99	35.05	2.617	1.115

2.3.1.7 Effects of End Fixity Assumption for Geodetic Column. Comparing the results in Table 2-34 between the end fixity assumptions indicates the significance of this factor. For a more direct comparison of the geodetic beam weight between the assumptions, a ratio was derived using the original sizing expressions. For this comparison, the axial loads, length, material, and N are equal, leaving the radius, R, to be a variable. If the subscript p designates pinned and f designates fixed, then:

$$\frac{W_p}{W_f} = \frac{3Nb_p^2\rho}{3Nb_f^2\rho} = \frac{b_p^2}{b_f^2}$$

ORIGINAL PAGE IS
OF POOR QUALITY

$$\frac{b_p^2}{b_f^2} = \frac{\left(\frac{32\pi^2 R_p^4}{N^2 L^2} \right)}{\left(\frac{18\pi^2 R_f^4}{N^2 L^2} \right)} = \frac{32}{18} \frac{R_p^4}{R_f^4}$$

$$\frac{R_p^6}{R_f^6} = \frac{\left(\frac{P_{CR} N L^4}{16\pi^4 E} \right)}{\left(\frac{P_{CR} N L^4}{9\pi^4 E} \right)} = \frac{9}{16} = 0.5625 = (0.90856)^6$$

$$\frac{R_p^4}{R_f^4} = 0.68142$$

Thus, substituting back into the expression for the weight ratio:

$$\begin{aligned} \frac{W_p}{W_f} &= \frac{32}{18} = (0.68142) \\ &= 1.213 \end{aligned}$$

Thus, for a geodetic column of equal length, critical load, material, and N, but with one assuming pin-ended longitudinal elements and the other assuming an end fixity $C = 1.78$, the weight increase for the pin-ended assumption is 21.3%. Since the end fixity coefficient $C = 1.78$ was the result of one test of one configuration, the use of this coefficient for all configurations is questionable. Further testing with several configurations would be desirable to verify the use of an end fixity coefficient greater than 1.0 (pinned) and to determine a statistically justified value.

2.3.1.8 Alternate Comparison. As mentioned in Section 2.3.1.4, a more general way to present the data for comparing the geodetic column with the triangular column is to plot P_{CR} versus weight per unit length (w), allowing the number of longitudinals to vary. To reduce the number variable involved, again the specific relationship between column cross section is held constant where the perimeters of the geodetic and triangular columns are equal. For this comparison, an $L/\rho = 200$ is used.

For the geodetic column using the sizing expressions for end fixity of $C = 1.78$, or

$$P_{CR} = \frac{36\pi^4 ER^2}{NS_R^4}$$

$$b^2 = \frac{36\pi^2 R^2}{N^2 S_R^2}$$

$$w = 3NB^2\rho$$

where

$$E = 13.1 \times 10^{10} \text{ N/m}^2$$

$$\rho = 1552.4 \text{ kg/m}^3$$

$$R = 0.6751 \text{ m}$$

$$S_R = 200$$

$$N = \text{variable}$$

Thus,

$$P_{CR} = \frac{36\pi^4 (13.1 \times 10^{10}) (0.6751)^2}{N (200)^4}$$

$$= \frac{130854.8}{N} \text{ (N)}$$

$$b = \frac{0.06363}{N} \text{ (m)}$$

$$W = 3N \left(\frac{0.06363}{2} \right)^2 (1552.4)$$

$$= \frac{18.4896}{N} \text{ (kg/m)}$$

Thus, the results are linear with the inverse of N , the number of longitudinals. The plot of P_{CR} versus W is shown in Figure 2-100.

For the triangular column, several points must be calculated because the sizing is not linear. Using the expressions developed, starting in Section 2.3.1.5, Table 2-35 was developed and plotted in Figure 2-100.

Table 2-35. Triangular beam weight summary.

P_{CR} N	S_R (L/ ρ)	L m	t cm	E GN/m ²	A cm ²	CAPS kg	POSTS kg	DIAGONALS kg	W kg/m
29784	200	115.45	0.1422	154.4	2.612	157.8	60.7	2.62	1.9157
23828			0.1247	140.7	2.290	138.3	53.3		1.6824
19856			0.1123	129.6	2.062	124.5	48.0		1.5169
14891			0.0963	113.8	1.768	105.8	41.1		1.3038
11912			0.0859	102.0	1.577	95.2	36.7		1.1654
7940			0.0701	83.4	1.287	77.7	29.9		0.9554
3972			0.0511	57.2	0.937	56.6	21.8		0.7020
3309			0.0472	51.7	0.868	52.4	20.2		0.6515
890			0.0290	22.8	0.532	32.1	12.4		0.4079
445	200	115.45	0.0239	13.7	0.438	26.5	10.2	2.62	0.3400

Figure 2-100 is a graphical comparison of the triangular beam and the geodetic beam acting as columns. The triangular beam shows a distinct weight advantage over the geodetic column for high loads. At the geodetic baseline of $N = 12$, the triangular beam has a 38.1% weight advantage. The cutoff shown for the triangular beam corresponds to the baseline minimum thickness for the cap materials (6 plies) resulting in a balanced pseudoisotropic lay-up of $(\pm 60, 0)_S$. Where this cutoff intersects the curve for the geodetic beam, $N = 18$, is the point at which the geodetic column becomes more structurally efficient than the triangular column. Thus, the geodetic concept is lighter than the triangular column when sized for axial loads of 7270 N or less.

2.3.1.9 Alternate Failure Mode of Geodetic Column. The alternate failure mode of the geodetic beam as a column is in general shell buckling or instability. From the Isogrid Design Handbook, NASA CR-124075, Equation 4.9.8, the critical load is:

$$N_{CR} = \frac{0.612 \gamma \pi E b^3}{R h}$$

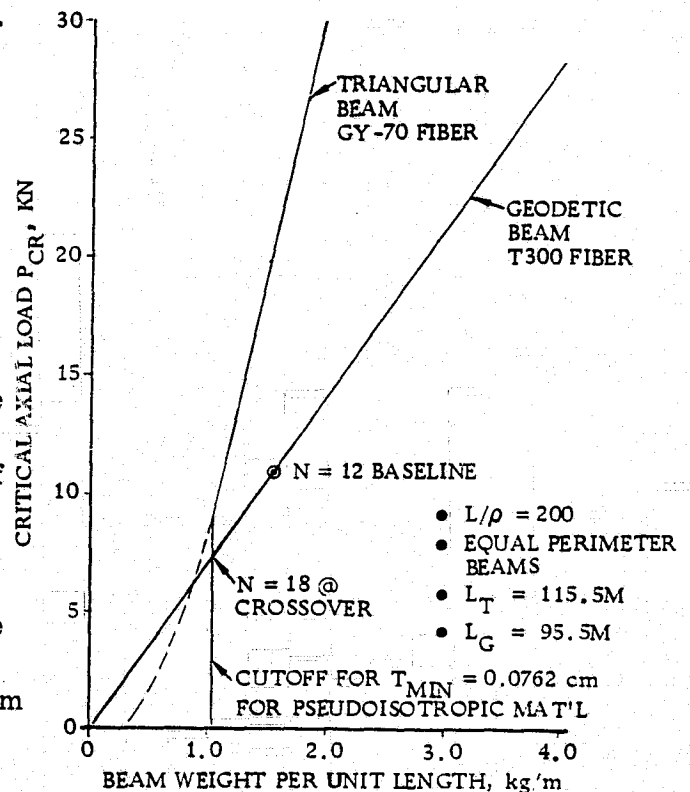


Figure 2-100. Critical axial load vs. unit weight.

where the cross section of the longitudinals is $b \times b$. The term h can be expressed in terms of R and N simply as:

$$h = \frac{2\pi R}{N}$$

So the expression for the critical load becomes:

$$\begin{aligned} N_{CR} &= \frac{0.612 \gamma N e b^3}{2\pi R^2} \\ &= \frac{0.0974 \gamma E N b^3}{R^2} \end{aligned}$$

The term γ is the knockdown or correction factor for isotropic cylinders in axial compression. NASA SP-8007 gives:

$$\gamma = 1 - 0.901(1 - e^{-\phi})$$

where

$$\phi = \frac{1}{16} \sqrt{\frac{R}{b}} \quad \text{for} \left(\frac{R}{b} < 1500 \right)$$

This expression should be used with caution for cylinders with length-to-radius ratios greater than about 5 since the correlation has not been verified by experiment in this range. For the baseline geodetic beam in this study:

$$\frac{R}{b} = \frac{0.6751}{0.0053} = 127$$

and

$$\frac{L}{R} = \frac{95.5}{0.6751} = 141$$

The L/R ratio is clearly out of the range recommended by NASA SP-8007 for use of these expressions for γ and, therefore, should be verified by test. However, lacking other relationships they were used for the general instability check.

Substituting into the expression for γ gives:

$$\gamma = 0.544$$

so the critical buckling load becomes:

$$\begin{aligned} N_{CR} &= \frac{0.0974(0.544)(13.1 \times 10^{10})(0.00531)^3(12)}{(0.6751)^2} \\ &= 27.4 \text{ kN/m} \end{aligned}$$

ORIGINAL PAGE IS
OF POOR QUALITY

The applied critical load that would cause simultaneous overall Euler column failure and element Euler column failure for the baseline beam is:

$$N_x = \frac{P}{2\pi R} = \frac{10.9}{2\pi(0.6751)}$$

$$= 2.57 \text{ kN/m}$$

Thus, constraining the radius to bear a specific relationship to the triangular beam precludes optimization of the geodetic column to all three failure modes.

2.3.2 BEAM DESIGN. The baseline geodetic beam configuration and arrangement was developed per Figure 2-97, and is shown in Figure 2-101. The selection of 12 longitudinal elements ($N = 12$) was influenced primarily by: (1) the desire for minimum fabricator complexity (maximum reliability); and (2) compatibility of the nodal geometry with in-plane beam joints.

The latter issue is of concern since the circular cross section is incompatible with the lap joint intersection concept used in triangular beam assemblies. To address this issue, several concept sketches, similar to Figure 2-102, were prepared for node count, $N \geq 6$. The lowest N for which reasonably close nodal alignment occurred was 12 and, consequently, this value was adopted.

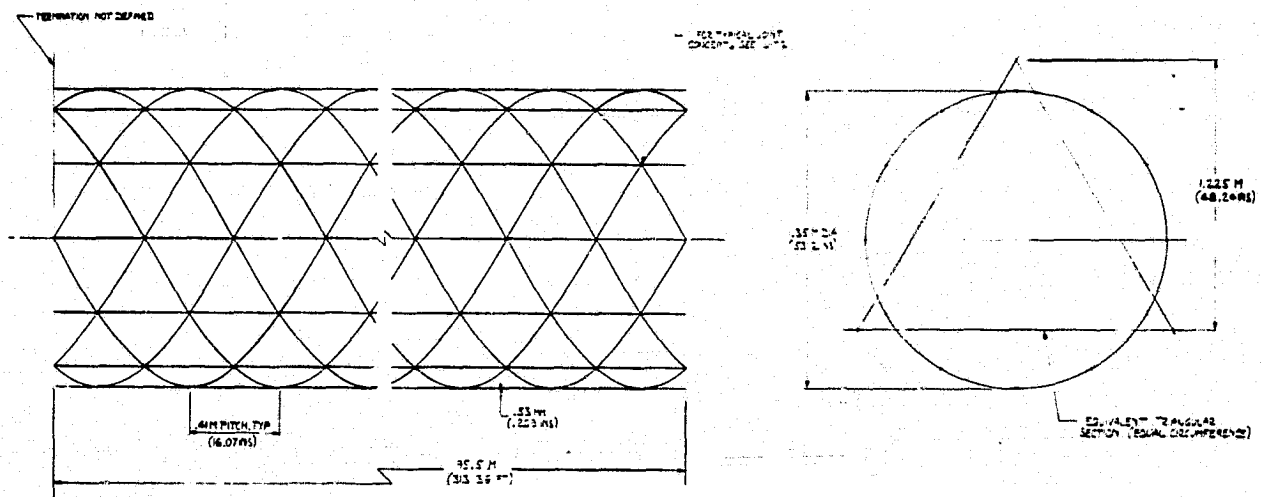


Figure 2-101. Cylindrical geodetic beam.

Several concepts were developed for the typical 3-element joint within the geodetic beam. These are shown in Figure 2-103 and discussed in the following paragraphs.

- a. **Concept 1.** A simple "crossover" arrangement of the three structural elements. This concept exhibits extreme simplicity with no forming requirements, but the offset dimension (y) of both diagonal elements, from the node point results in

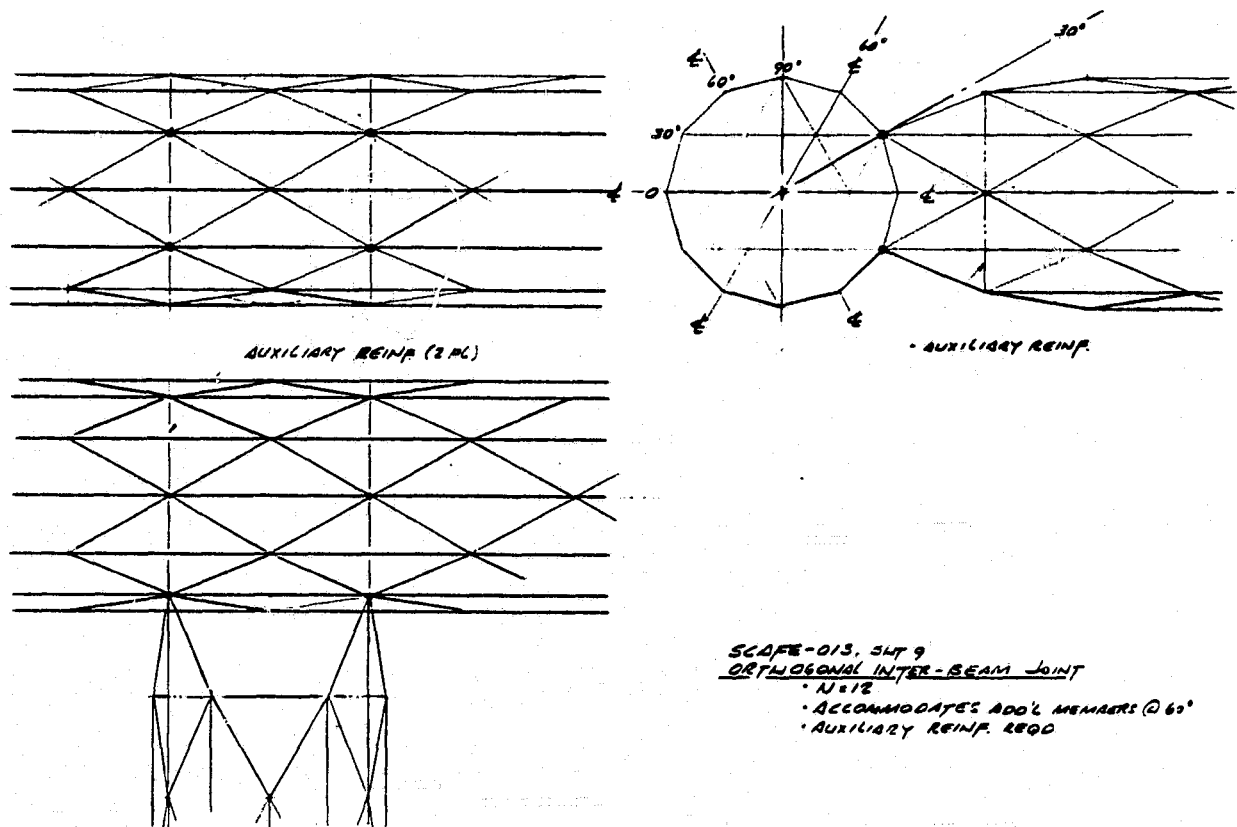


Figure 2-102. In-plane beam/beam joint concept.

"rolling" of the longitudinal element, and tends to promote "peeling" separation of the joints. The offset also produces bending in the diagonals and twisting of the longitudinals.

- b. Concept 2. Same as concept 1, except that elements are aligned to the common node point and, therefore, feel no bending in their straight sections. However, the tendency to roll the longitudinal element and peel the two bonded interfaces is still present. This effect can be reduced by the optional addition of the two vertical splicing pieces, but this presents a significant manipulation problem. The rather severe forming required for this concept suggests significant energy requirement and the effect of fiber displacement must be studied.
- c. Concept 3. Here the three structural elements are notched to one-third their thickness. Compared to the preceding concepts, this reduces the offset (y) of the bonded interfaces by a factor of three, thereby significantly reducing rolling and peeling effects. The joint design is clean and efficient, and no forming is required. The notches are cut before launch and must be accurate if used to aid joint location or could be broad, as shown, to avoid tolerance buildup.
- d. Concept 4. Similar to concept 3, except that local thickness reduction is achieved by in-space heating and forming instead of notching before launch. The possibility

of fiber breakage during forming requires study although loss of a percentage of the fibers may be acceptable. Again, the tendency towards peeling, bending, and twisting results from the moderate offset of the bonded interfaces, which, incidentally, are larger than in the preceding concepts.

- e. Concept 5. Same as concept 4, except that strength and stiffness are increased by addition of annular shear rings.
- f. Concept 6. Similar to concepts 4 and 5, except that all elements are discontinuous, spade-ended, and butt-jointed with two shear plates effecting the splice. Such spade-end forming and trimming can be performed before launch, or alternatively, the elements can be stack stowed as plain (unspaded) components with the spading performed in situ during the joint splicing process.

Element manipulation and positioning, and general dimensional control are significant problems, but the joint is clean and efficient.

- g. Concept 7. A conventional fitted butt joint, in which the longitudinal element is plain, continuous, and straight, while the diagonal elements are straight and unformed but are discontinuous and end cropped as shown. The joint is unified by the two shear splice plates. The joint is clean and efficient but the end profiling and element manipulation are significant problems.
- h. Concept 8. Similar to concept 7, except: all elements are continuous; longitudinal element is straight and plain with no forming or notching, and its section is wedge-shaped to provide interfaces normal to the diagonal elements; diagonal elements are continuous and are notched alternatively on their right and left flanks. On assembly, the diagonal element is formed at the notch to an angle of 60° so that the element assumes a continuous zigzag shape. In so doing, the notch itself becomes straight, providing a flat face for bonding to the longitudinal elements.

In this concept, each of the 12 diagonal elements zigzag within the same pair of longitudinal elements, thus avoiding the problems associated with overlapping and spiralling. The energy required to form at the notches is minimal. The splicing cap plates increase the strength of the joint but should be considered optional.

Although potentially unsatisfactory due to joint eccentricity effects, Concept 1 was selected as the baseline since data justifying its rejection are not available. Consequently, the fabrication concept is perhaps optimistically simplified and beam weights include no allowance for auxiliary splice provisions.

2.3.3 BEAM FABRICATOR. The fabrication machine is a non-optimized, feasible point design concept in which heat forming was avoided due to likely fiber inextensibility constraints (i.e., breakage or buckling) associated with forming bends and/or local flat areas in material as thick as the baseline element.

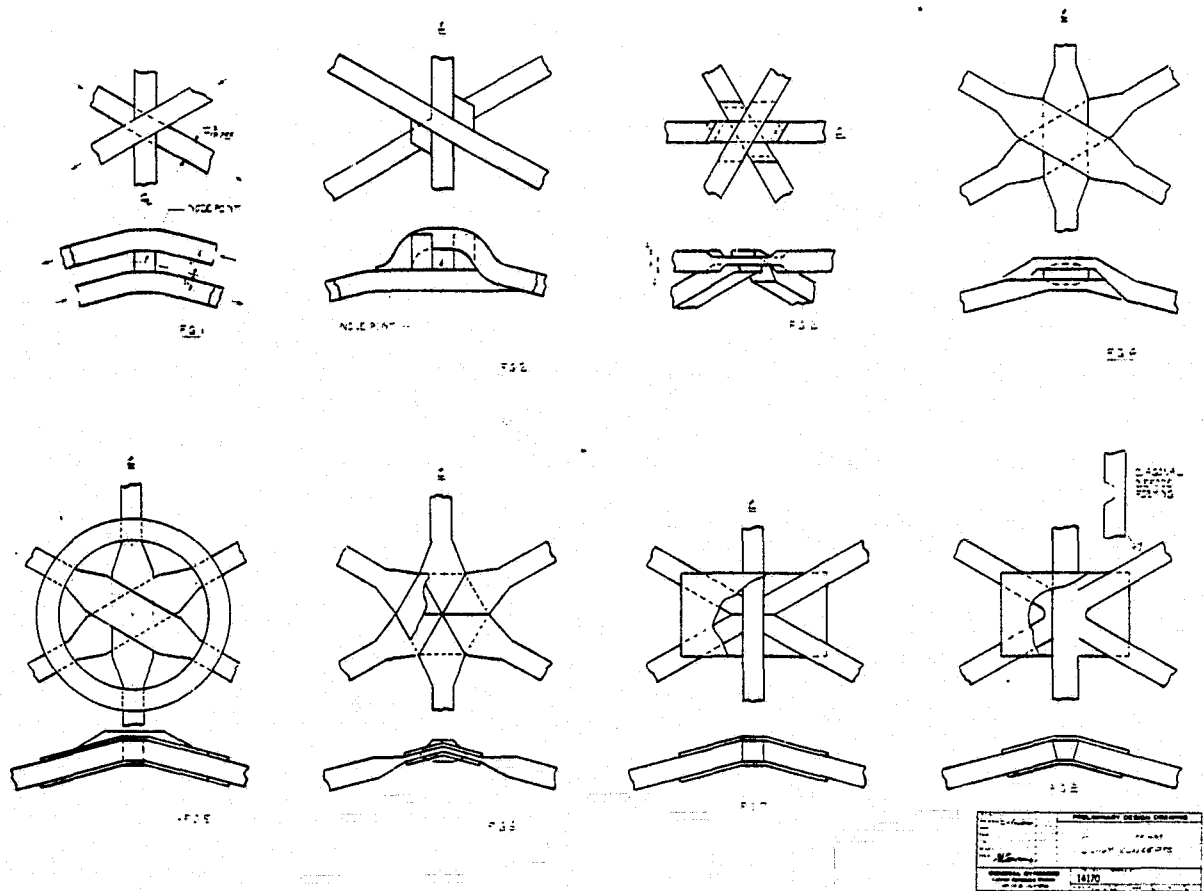


Figure 2-103. Geodetic beam joint concepts.

The fabricator concept is shown in Figure 2-104, and satisfies the following ground rules/requirements:

- Compatible with Shuttle cargo bay envelope (including OMS kit)
- Fabricate baseline ($N = 12$) beam concept
- Store continuous structural elements in dispensable form
- Provide joint capability at element nodal intersections
- Provide proportional element feed for beam continuity
- Incorporate provision for beam length cutoff with minimal fabrication debris
- Fabricate same beam length as triangular system (914 m)

Fabricator details are shown in Figures 2-105 and 2-106 and are based on the considerations discussed in the following sections.

2.3.3.1 Material Storage. The twelve axial members are radially coiled, six abreast, in two spools. The twelve helical members are helically preformed, compressed to solid height, and stacked in four separately supported concentric levels. The selection of T-300 graphite fiber for the beam elements resulted from the investigation of raw stock storage considerations discussed in Section 2.3.1. The two corresponding longitudinal element storage spools require 2.81 m O.D. each to accommodate six adjacent 931 m coils of material. (An additional 17 m of material, above the 914 m requirement, is provided for machine priming, checkout, and residual allowance.)

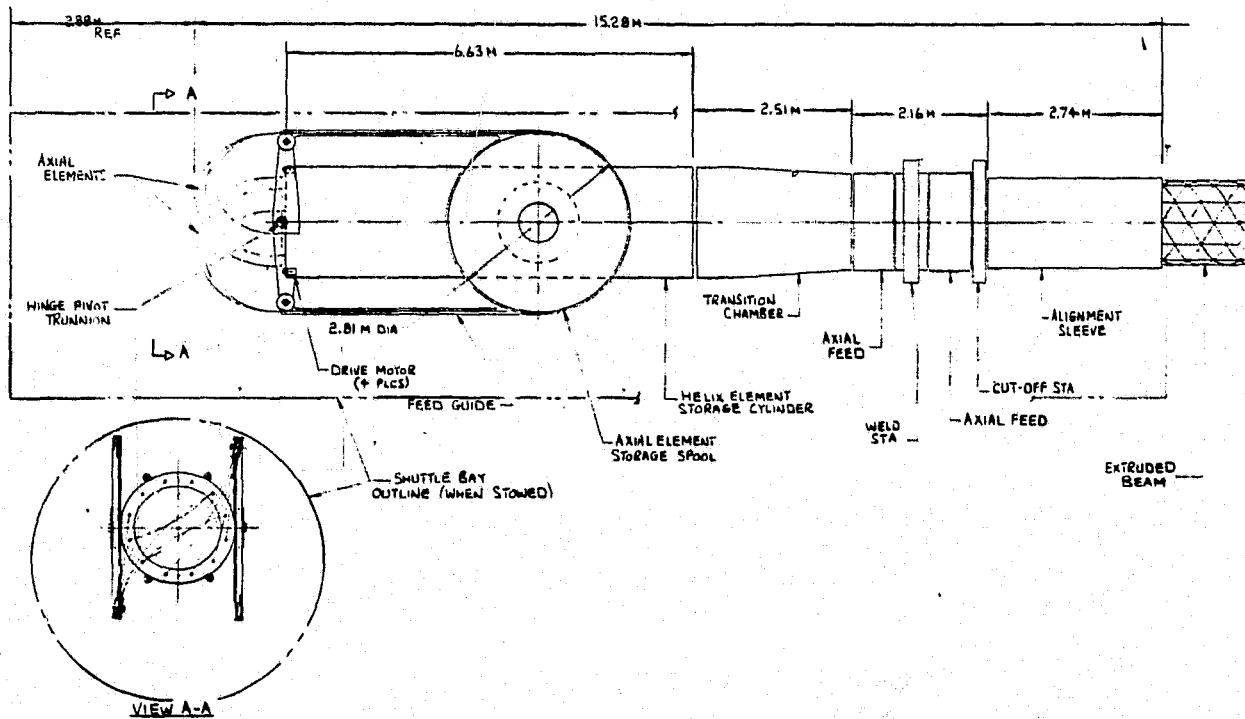


Figure 2-104. Beam fabricator concept.

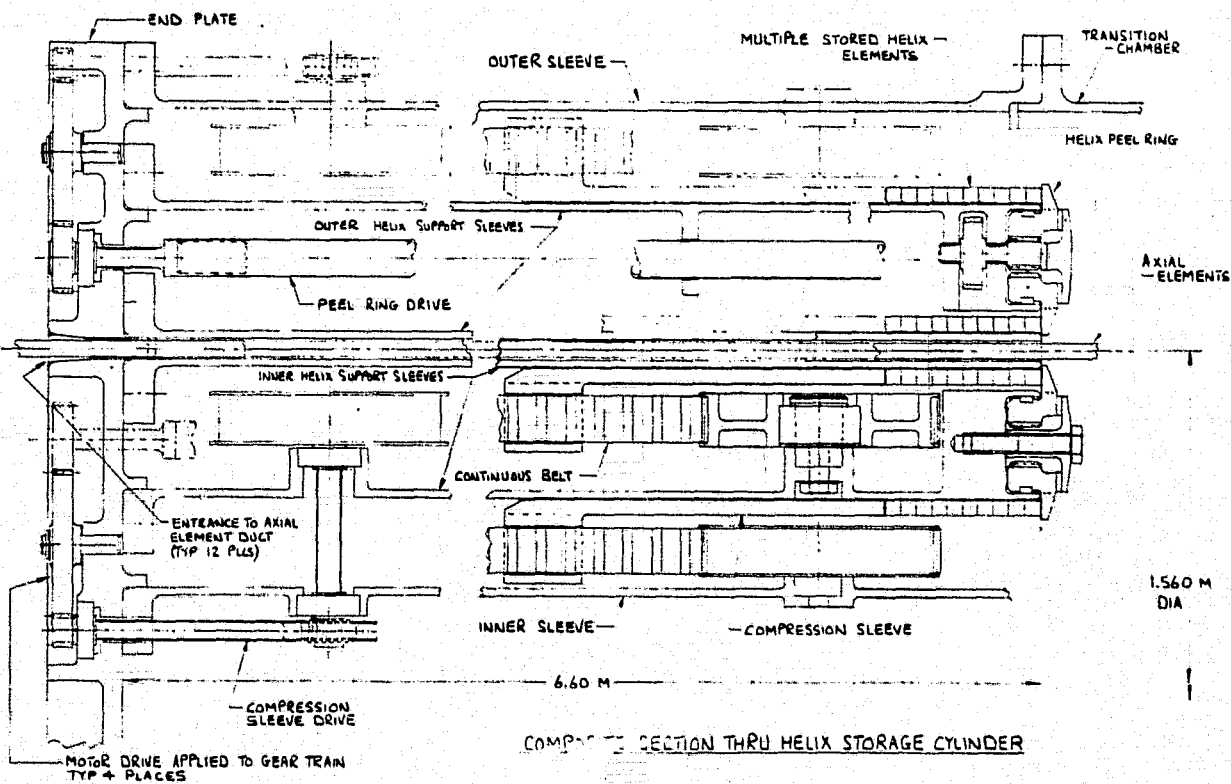
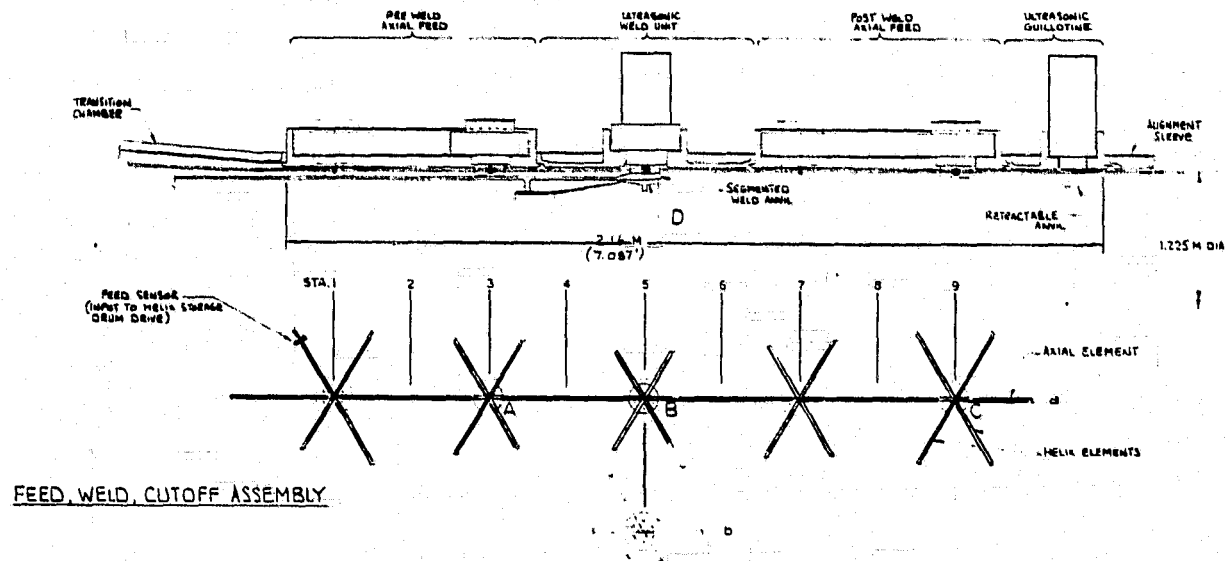


Figure 2-105. Helix element storage cylinder detail.



FEED, WELD, CUTOFF ASSEMBLY

OPERATIONAL SEQUENCE		STAGE													REPEAT CYCLE
		I	II	III	IV	V	VI	VII	VIII	IX	X	XI	XII	XIII	
PRE WELD AXIAL FEED	JAW A	OPENS & RETRACTS	SLIDES FROM STA 3 TO STA 1	EXTENDS & CLOSES				FEEDS FROM STA 1 TO STA 2						FEEDS FROM STA 2 TO STA 3	
SONIC WELD UNIT	JAW B	OPENS & RETRACTS	ROTATES FROM ELEM. A TO D					EXTENDS & CLOSES	WELDS	OPENS & RETRACTS	ROTATES FROM ELEM. D TO A	EXTENDS & CLOSES	WELDS		
POST WELD AXIAL FEED	JAW C				OPENS & RETRACTS	SLIDES FROM STA 9 TO STA 7	EXTENDS & CLOSES	FEEDS FROM STA 7 TO STA 8						FEEDS FROM STA 8 TO STA 9	
SPREADER SLEEVE	D	EXTENDS							RETRACTS	EXTENDS				RETRACTS	

TYP FOR 4 COUNTERFENCIAL STATIONS

Figure 2-106. Feed/weld/cutoff assembly.

The counter-spiralling helix members require a different storage approach to accommodate their greater length (1828 m + 17 m allowance) and to achieve a stress-free configuration when integrated into the beam. Therefore, the helix elements will be preformed in the manufacturing stage to their individual beam profiles and compressed solid (coil-spring fashion) for storage. This storage compression incurs very little stress within the members since the uniaxial material is torsionally flexible. However, due to the total quantity of material involved (six helical elements in each direction), it is necessary to concentrically stack these compressed coils in radial disposition (i.e., two layers of three parallel right-hand wound elements over two layers of three parallel left-hand wound elements), with suitable support sleeves for layer separation.

2.3.3.2 Material Feed. Motor-driven spools containing axial material are activated by microswitch sensors positioned at the member loop area. Helical material is peel ring fed when activated by microswitch sensors within the transition chamber.

2.3.3.3 Pre Feed Orientation. Helical material enters the transition chamber from the peel rings and contracts into respective internal and external contact with axial members preparatory to entering the preweld feed unit.

2.3.3.4 Beam Feed. Two powered beam feed units (one each side of the weld station) initiate linear extension of beam.

Because uniformity of the beam is dependent upon close repetitive tolerance between intersectional nodes, a simple friction drive of elements is not practical. Therefore, the feed system is composed of a series of axially reciprocating intersection-grasping jaws. Element intersections are grasped prior to, during, and after joining. Jaw feed prior to welding aligns only the intersection of the helical elements along the path of the axial elements. Jaw alignment hold at the welding head is positioned relative to the post-weld feed jaws to maintain correct node pitch sequencing. Post weld feed jaws provide linear expulsion of beam by driving the now rigidly fixed intersections. The operational sequence is also shown on Figure 2-106.

2.3.3.5 Welding. Six ultrasonic weld heads, supported on a ring, reciprocating through 30° about the beam axis to cover all twelve axial members, grasp the node intersections for alignment during weld. A segmented weld anvil is internally expanded by a spreader sleeve in sequence with the weld operation.

Ultrasonic welding was selected for element joining since it does not degrade the element interfaces, require contour deviation for added cross section, nor require additional components or complicated manipulation. The element fibers, both axial and helical, remain continuous with joining accomplished by fusion of the resin matrix without the production of debris, nor fiber displacement or breakage.

2.3.3.6 Beam Straightness. An external alignment sleeve is provided for beam stabilization beyond the post-weld feed unit.

2.3.3.7 Beam Cutoff. Six ultrasonic guillotines, orientated similar to weld units, perform cutoff of beam members midway between the circumferentially staggered nodal intersections. Cutoff in this manner provides element material beyond each welded intersection for attachment to a closure ring and does not produce waste or debris.

3

FLIGHT EXPERIMENT INTEGRATION

This section describes how the selected system design (Section 2) will meet the SCAFE program requirements to develop and demonstrate:

- a. The techniques, processes, and equipment required for automatic fabrication and assembly of structural elements in space using shuttle as a launch vehicle and construction base.
- b. Additional construction/systems/operational techniques, processes, and equipment to provide further risk reduction benefits to future large space systems.

The discussion includes: (1) mission requirements and guidelines, (2) the construction experiment objectives and accomplishments, (3) the structural and thermal tests and attendant instrumentation required to check induced platform response against predicted behavior, (4) the free flight scientific experiments which will be performed after platform separation and return of the shuttle to earth, (5) additional application missions which can take advantage of the platform while in orbit and through an optional revisit mission, (6) the mission and ground operations including the required crew EVA activities, and (7) the requirements for interfacing and providing compatibility with the Orbiter.

3.1 MISSION REQUIREMENTS AND GUIDELINES

The following mission guidelines were used to help define the baseline mission:

- a. The space construction experiment shall be compatible with the operational Space Transportation System (STS). Specific considerations are Orbiter landing center of gravity constraints, Orbiter payload bay envelope, payload bay accommodations, STS performance capability and STS launch turnaround.
- b. The experiment shall be constructed and operated with one STS flight. In addition, the flight will carry experiment equipment and subsystems to perform appropriate applications experiments after platform separation.
- c. Revisit, as a mission option, would occur within three months.
- d. Crew EVA capability in support of space construction experiment will be provided by the nominal four-person crew of the STS.
- e. On-orbit dynamic and thermal response tests will be required as part of the orbital experiment. In addition, a separation and recapture test will be performed as a prelude to an optional revisit flight.
- f. Launch is assumed to take place in mid 1982.

During the course of the study it became apparent that a nominal seven-day mission would accomplish all shuttle attached mission objectives. In order to be cost effective, we concluded that, if additional mission time is required, an extended mission duration should be used as opposed to a dedicated revisit flight.

Figure 3-1 depicts the total top level operational flow for the SCAFE program. The contractor will design, manufacture, and test the structural experiment equipment along with the structural test instrumentation. This equipment will be integrated and checked out with the applications experiment equipment at JSC and then shipped to KSC for launch site operations and launch. During flight the Orbiter crew initiates each operational or test phase and controls Orbiter maneuvers, and the RMS. Executive control and monitor of the beam fabrication on-orbit operation is provided via the Orbiter RF command link to ground controllers at the Payload Operations Control Center (POCC) which is co-located with Mission Control Center Houston (MCC-H). MCC-H provides Orbiter and overall mission control.

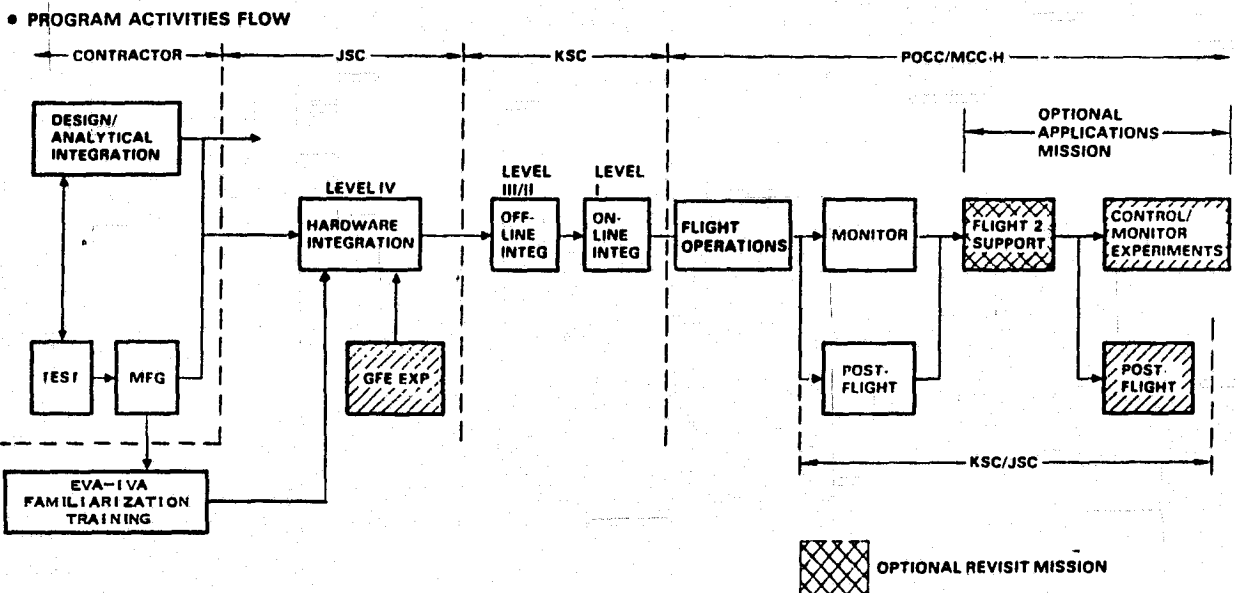


Figure 3-1. SCAFE program top level activities.

3.1.1 ORBITAL ALTITUDE AND INCLINATION. Analysis has shown that the experiment can be conducted in orbit inclinations from 28.5 to 57 degrees. However, 28.5 degrees is the most acceptable because payload capability is higher, as shown on Figure 3-2. For orbital altitude, Figure 3-3 shows that, below approximately 555 km, the orbital lifetime of a representative platform drops off rather sharply. This would make it undesirable to carry out applications experiments after the first flight and preclude time for an optional revisit mission to carry out additional applications experiments. Altitudes above 650 km (350 n. mi.) at 28.5 degrees would require an additional OMS kit, further reducing payload available (see Figure 3.2). Therefore, a 555 km orbit altitude was chosen.

Figure 3-4 illustrates the geometry of the SCAFE orbit at the guideline launch date/time.

3.1.2 FABRICATION ORIENTATION.
 During SCAFEDS proposal preparation, various fabrication orientation options were developed and evaluated to support selection of a proposal baseline.

Three candidate orientation families shown in Figure 3-5 were evaluated with respect to their then-identified advantages/disadvantages, and the constant Earth-fixed approach was selected.

However, within the Earth-fixed family several options exist for orientation of system coordinate axes with respect to both the Earth and the orbit plane. The free platform is stable if oriented in-plane with its long axis radial and separation from the Orbiter in that orientation is desirable. Consequently, a reference orientation satisfying this condition was selected and is shown in Figure 3-6.

However, the final orientation selection required system mass properties and stability/control analyses plus consideration of several other factors including viewing/illumination, potential thermal constraints on either the Orbiter or the platform, and communication capability. These studies are discussed in the following subsections. The result of the combined evaluation was the selection of the reference orientation as the preferred attitude for SCAFE fabrication assembly, and test.

3.1.2.1 Stability-Control and Mass Properties Considerations. At any mission time the Orbiter/platform system will exhibit a discrete set of inertias and will remain stable if its principal axes are oriented per Figure 3-7.

In the SCAFE fabrication/assembly/test/separation sequence significant inertia changes occur about the roll (X) and yaw (Z) axes such that the stable attitude changes with mission event. This is discussed in detail in Section 4.1 and illustrated in Figure 4-4. Therefore, it was necessary to reconsider the varying-attitude option

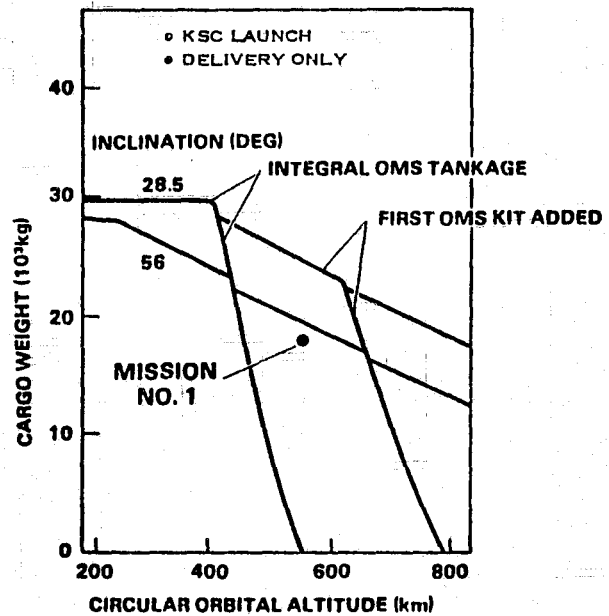


Figure 3-2. Cargo weight vs. altitude.

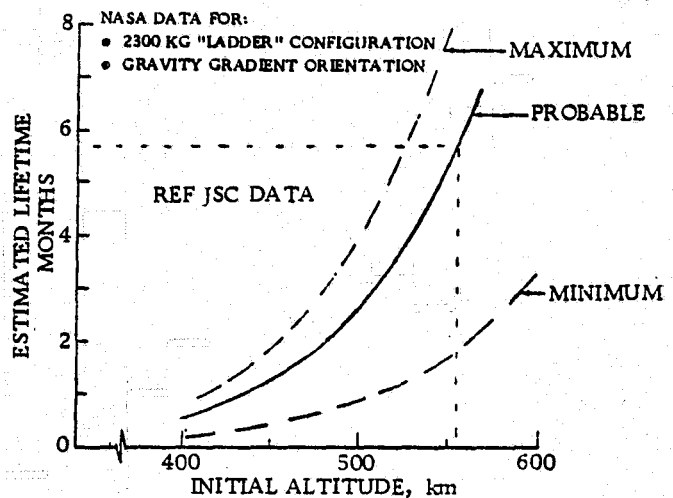


Figure 3-3. Orbit lifetime.

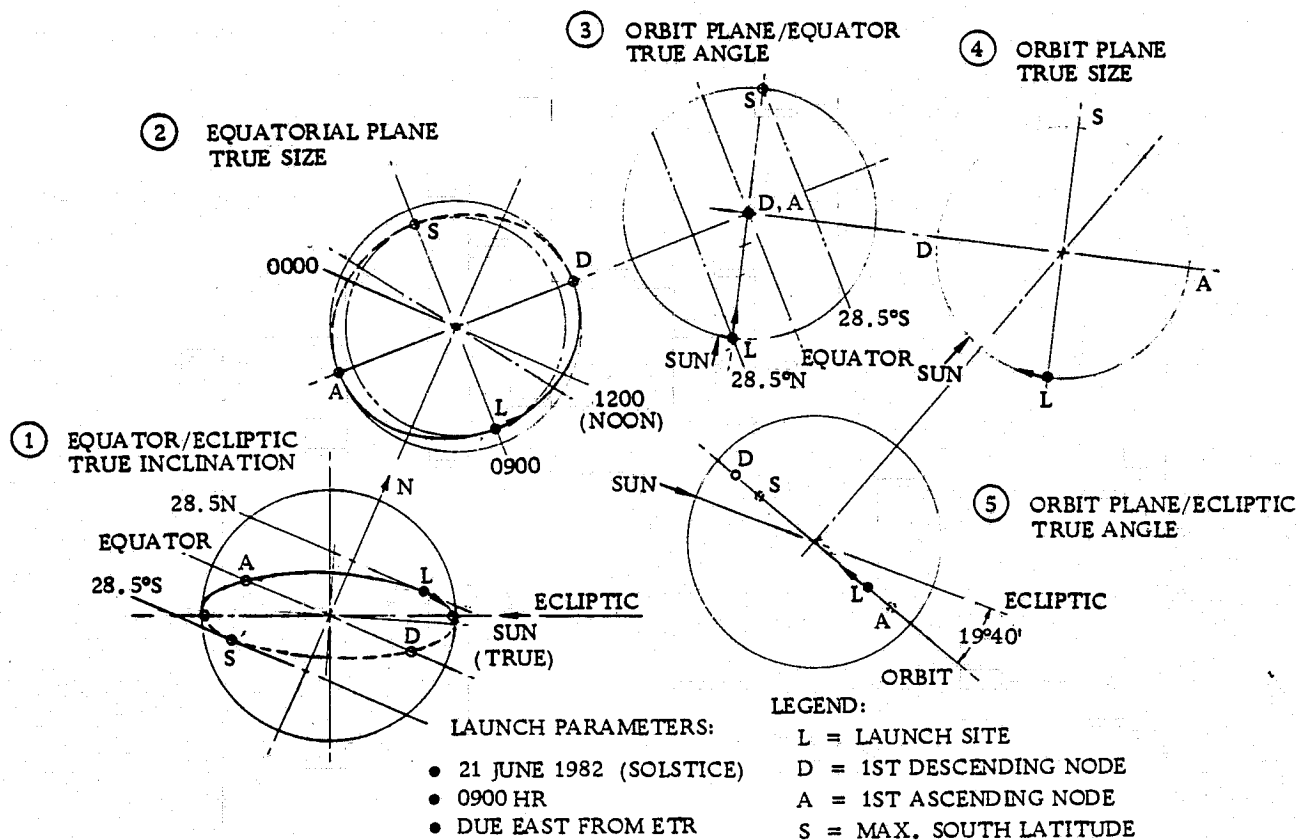


Figure 3-4. Graphical determination of SCAFE orbit geometry.

<p>EARTH FIXED</p>	<p>INERTIALLY FIXED</p>	<p>VARYING ATTITUDE</p>
<ul style="list-style-type: none"> • MINIMIZE ENVIRONMENTAL TORQUES • STABLE RELEASE ATTITUDE • REDUCED COMMUNICATION PROBLEMS • ELIMINATES ORBITER MANEUVERING • REDUCED BEAM LOADS 	<ul style="list-style-type: none"> • CYCLIC ENVIRONMENTAL TORQUES • OMNIDIRECTIONAL COMMUNICATIONS REQUIRED • ORBITER MANEUVERING REQUIRED • LOW MANEUVERING RATES REQUIRED 	<ul style="list-style-type: none"> • ORIENTATION OPTIMIZED MISSION PHASE • ENVIRONMENTAL TORQUES • ORBITER MANEUVERING REQUIRED • LOW MANEUVERING RATES REQUIRED

Figure 3-5. Candidate orientation families.

(Figure 3-5) as a possible orientation candidate. To operate in this mode, requires attitude control maneuvers to realign the system as the principal inertia relationships change, but presumably permits the VRCS to operate in a rate damping mode once the stable gravity gradient attitude is achieved. This is expected to result in reduced propellant consumption and low beam/platform structural response due to the long periods of widely spaced, very-short duration firings characteristic of rate mode operation. Stability and control analyses were conducted (Section 4.2.1.1) to determine system characteristics in the sequential-gravity-gradient attitude mode. These analyses indicated that closed loop attitude control was still necessary about certain axes. Also, mass properties data showed that none of the successive gravity gradient orientations would result in platform orientation in the desired post-separation stable position without further attitude control maneuvering. Consequently, the anticipated propellant consumption and dynamic response advantages were challenged.

Stability/Control analyses, discussed in Sections 4.2.1.2 and 4.2.1.3, were also conducted on the reference orientation of Figure 3-6. Duty cycles were developed for closed-loop attitude control with arbitrarily selected, $\pm 1^\circ$ and $\pm 5^\circ$ attitude error limits. The $\pm 1^\circ$ duty cycles required the highest frequency impulse/time histories so these were conservatively used as forcing functions in dynamic response analyses (Section 4.3).

These analyses indicated very low loads and deflections in the fabricated structure. A preliminary RCS consumption analysis also indicated a small propellant requirement for stabilization and control. Furthermore, examination of the phase plane plots (Figure 3-8) resulting from these analyses also indicated that in the reference

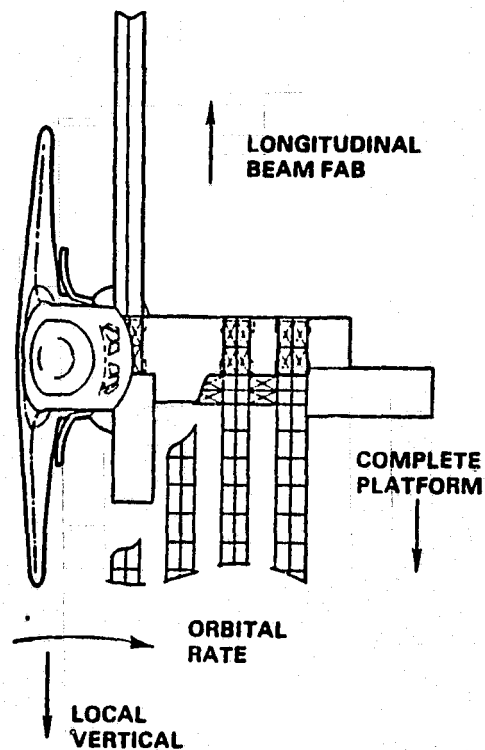


Figure 3-6. Reference fabrication orientation.

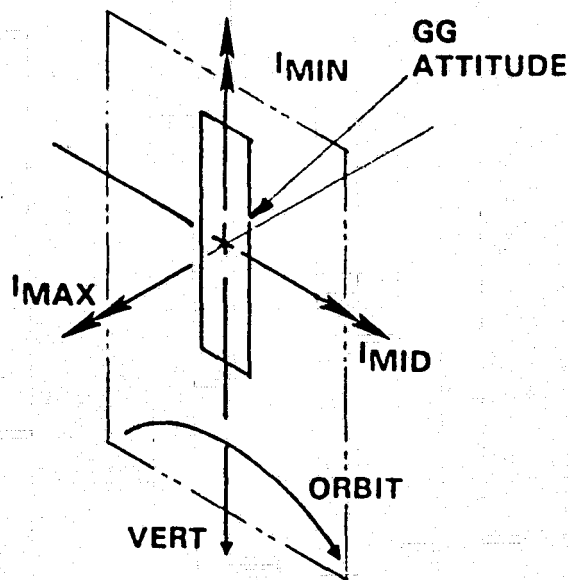


Figure 3-7. Stable axis orientation.

orientation the system exhibited a stable oscillation about both the yaw and roll (highest inertia) axes within $\pm 10^\circ$ attitude error limits. Consequently, the system, in the reference orientation, could be operated in the rate damping mode about two axes after all with closed-loop attitude control required only about the pitch axis. Since no specific attitude error limit has yet been identified, the reference orientation was preferred from a stability/control point of view.

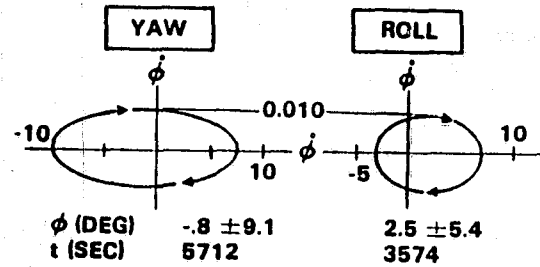


Figure 3-8. Phase planes for rate-mode VRCS operation.

3.1.2.2 Viewing/Illumination Considerations. The principal requirement here is that the selected orientation should minimize (and preferably avoid) back lighting the platform (by either direct or Earth-reflected sunlight) since this severely impairs direct viewing from the aft facing cabin windows. Consequently, orientations in which the Orbiter +X (aft) axis points toward either the Sun or the Earth should be avoided. Since the mission orbit has a low inclination with respect to the ecliptic ($\sim 20^\circ$) this can be achieved by orienting the Orbiter longitudinal (X) axis essentially normal to the orbit plane. This condition is provided by the reference orientation. However, an alternative orientation, in which the Orbiter leads the platform along the flight path also satisfies this requirement.

From the above, the oscillation in yaw for rate mode operations of the VRCS is $-0.8^\circ \pm 9.1^\circ$. This results in a slight sunward viewing component (9.9° max) from the aft cabin windows as shown in Figure 3-9. However, the corresponding roll oscillation has a 1° bias, due to drag effects, which constrains the sunward component from the top windows to 1.9° max, as shown, and favors the reference orientation. Although no strong discriminator exists between the two, the reference orientation is preferred for viewing/illumination.

3.1.2.3 Thermal Considerations. Space heating analyses were conducted for the reference orientation (Section 4.5) and indicate very small structural distortion and

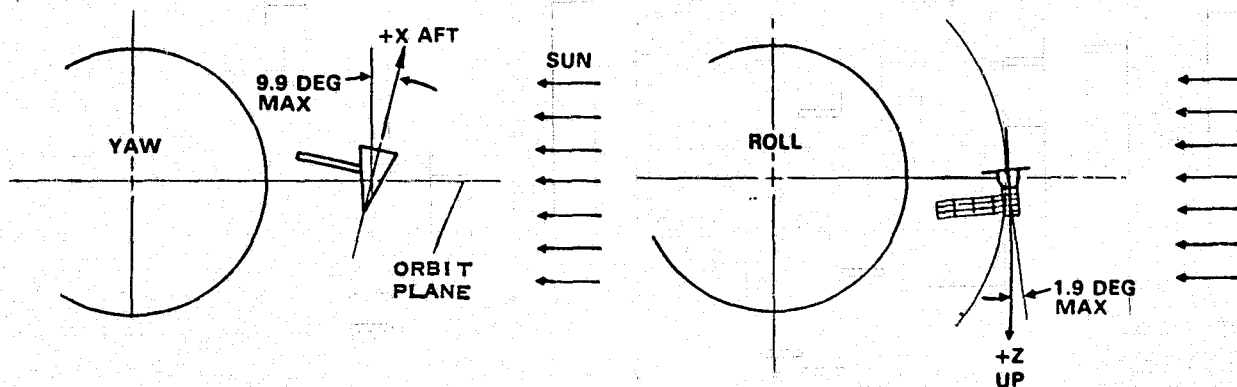


Figure 3-9. Sunward viewing due to attitude oscillation.

relatively small temperature excursions, with peaks well within the maximum use temperature for the composite structural materials. Consequently, there are no thermal constraints on platform orientation.

Furthermore, the Orbiter is required (per JSC07700) to permit sustained freedom of orientation, including continued full sun normal to the radiators, for orbit inclinations less than 55°. Since the baseline SCAFE orbit inclination is 28.5°, there is also no thermal constraint on Orbit orientation. The reference orientation is, therefore, satisfactory in terms of thermal consideration.

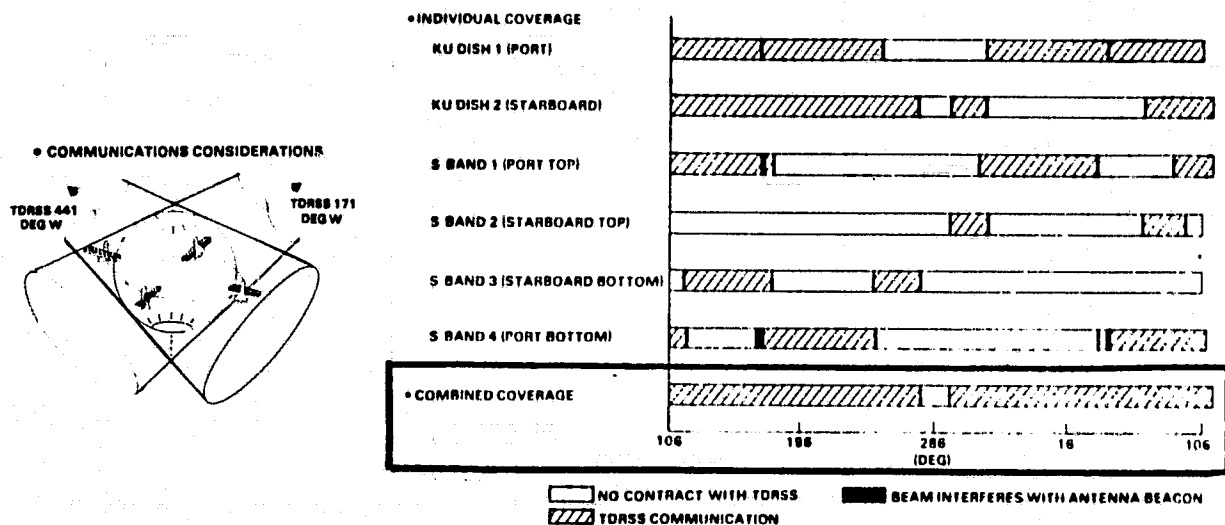
3.1.2.4 Communications Considerations. SCAFE communication requirements were examined for impact on the Orbiter/beam fabrication and assembly operations. In this task, we first examined the communication requirements for the SCAFE. The Orbiter communication system was then compared against these requirements to drive out any differences. The results indicate that SCAFE/Orbiter RF communication operations will have no major impact on SCAFE fabrication and test operations. These results are discussed in greater detail below.

A required data rate of the order of 15 kbps has been estimated for the beam builder experiment. This estimate is broken down into subsystem requirements in Table 3-1.

A link analysis indicates that this data rate can be easily achieved on both the S-band and Ku-band multiple-access TDRSS links. The communication link can only be achieved, however, if an antenna link with a TDRS is possible. Figure 3-10 shows the SCAFE/Orbiter and TDRSS coverage relationship. This link will be restricted by the directionality of the S-band antennas, by interference of the Orbiter structure with the antenna beacons, and interference of the large beam structures with the antenna beacons. The antenna coverage that the Orbiter will have with TDRSS has been

Table 3-1. Platform data rates for dynamics, deformation, and docking experiments.

Sensor	Quantity	Accuracy bits	Sampling Rate samples/sec	Data Rate bits/sec
Temperature Probes	102	8	0.1	82
Laser Beacon Detector Array	30	32	15	4800
Time	10	24	15	3600
Accelerometers	6	8	100	4800



RESULTS

- 70 deg no coverage zone using port side ku-band antenna
- 18 deg no coverage zone using port & starboard antennas
- 18 deg no coverage zone using switched s-band antennas

CONCLUSION

- No significant SCAFE impacts - combined coverage of 342°

Figure 3-10. Orbiter-TDRS antenna coverage.

analyzed. The results of this analysis are also diagrammed in Figure 3-10. Ku band coverage with the steerable disk on the port side of the Orbiter is blocked by the Orbiter body over a 70° arc centered about the TDRSS "no coverage zone" and, for a short period, when the large beam structure interferes with the antenna beacon. Analysis also indicates that the addition of a similar steerable Ku-band antenna on the starboard side of the Orbiter would reduce the no coverage area about the TDRSS "no coverage zone" to 18°.

TDRSS coverage with the four Orbiter S-band antennas, which are located on the 45° bisectors of the Orbiter pitch and yaw axes, can be achieved except over an 18° arc centered about the TDRSS "no coverage zone". The antennas must be switched at least six times during an orbit however, since the coverage of each antenna is broken up into several regions.

Our communications with Johnson Space Center personnel indicate that NASA has not specified operational requirements for the Orbiter communication link. Since our results indicate that TDRSS antenna coverage will not be significantly impacted by the large beam structure we anticipate that the Orbiter-TDRSS link will meet the requirements of the SCAFE mission without imposing special constraints on SCAFE construction orientation or techniques.

3.2 FABRICATION AND CONSTRUCTION EXPERIMENT REQUIREMENTS

The techniques, processes, and equipment which are developed for the fabrication and assembly of this test platform shall provide the technology base to be applied for the production of operational large structures that are fabricated in space.

The following paragraphs delineate the given and derived requirements for the construction experiment. Section 2 describes the design of the resulting system and the remainder of this Section 3 describes the operation and design verification activities. The basic fabrication and construction techniques required to be developed and proven in the on-orbit experiment operation are:

- a. Construction material verification
- b. Basic truss element fabrication
 1. Joints & joining
 2. Material forming
- c. Multiple truss element assembly
- d. Large structure handling
- e. Equipment/component installation
- f. Manned orbital operations
 1. IVA
 - (a) Construction monitor/control
 - (b) Vehicle stability & control
 2. EVA
 - (a) Equipment handling/installation
 - (b) Repair demonstration

ORIGINAL PAGE IS
OF POOR QUALITY

3.2.1 NASA DESIGN GUIDELINES/REQUIREMENTS. The following design requirements were established by NASA for this study:

- a. The initial design concept for the space construction experiment shall be as shown in Figures 3-11 and 3-12. The platform shall consist of four longitudinal trusses, approximately 200 m long, joined by nine crossmember trusses, approximately 10.5 m long.
- b. Primary emphasis shall be on thermoplastic composite materials for truss materials.
- c. The basic truss cross section shall be triangular with continuous caps.
- d. The basic truss size shall not be less than one meter deep.
- e. Truss fabrication shall be accomplished with automatic construction equipment (beam builder) in orbit from preprocessed stock material. The objective of preprocessed stock material is to complete as much as possible of the truss fabrication process on the ground while retaining a dense package of material

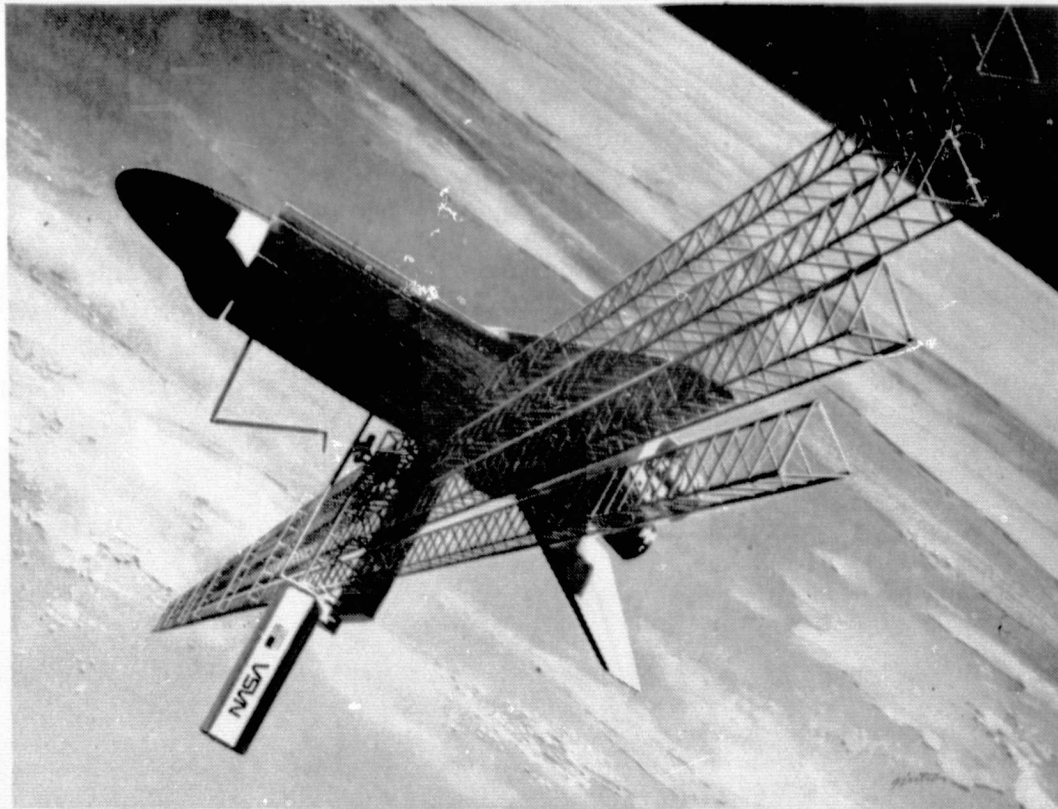


Figure 3-11. Baseline system concept.

for launch.

- f. Truss fabrication shall be a continuous process with appropriate lengths cut off (minimizing debris) to use as construction elements.
- g. Handling of individual trusses shall be reduced by orienting the beam builder to produce the truss in situ.
- h. EVA capability of the crew shall be used to perform assembly operations which would be difficult or costly to automate.
- i. The concept for the beam builder shall be compatible with scale up to a larger machine for fabrication of the larger (approximately 10 meter) trusses necessary for the future large space platforms.

3.2.2 DERIVED PERFORMANCE REQUIREMENTS. The following performance requirements have been derived from analysis to satisfy the NASA-stated guidelines and to essentially maximize the automatic construction process where cost effective, and leave the attachment of subsystems and instrumentation to the platform and repair work (real or simulated) for the crew to do on EVA where they can better use their unique capabilities.

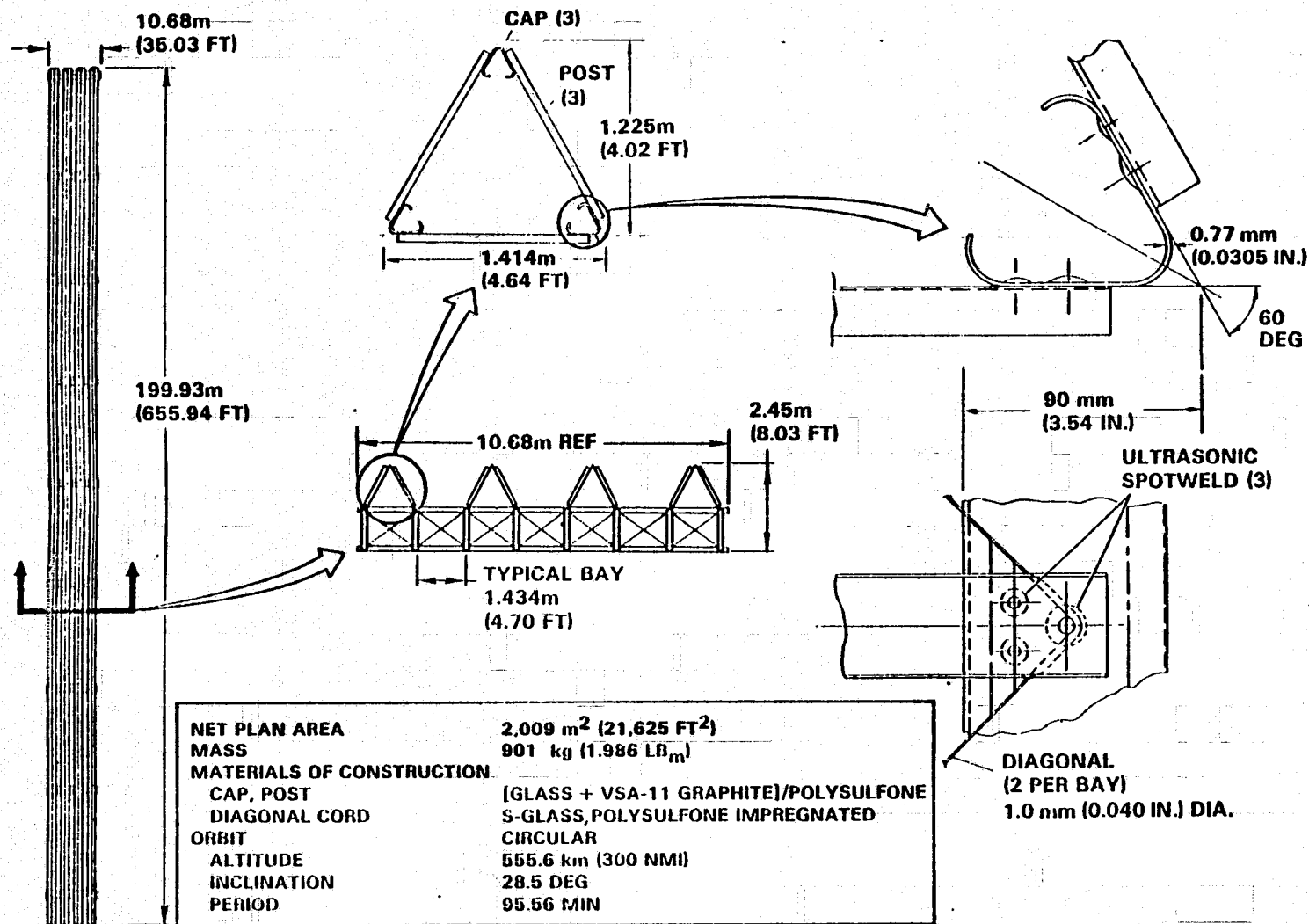


Figure 3-12. Initial platform baseline.

- a. Ascent to Orbit
 - 1. SCAFE equipment shall be inactive during ascent, requiring only mechanical support and caution and warning support from the Orbiter.
 - 2. SCAFE equipment shall provide equipment stowage locks.
- b. Activation and Checkout. Provisions shall be made for activation and checkout of SCAFE equipment to determine satisfactory performance prior to fabrication/assembly operations, tests, and platform separation.
- c. Deployment
 - 1. Provisions shall be made for deployment of the SCAFE equipment from the stored position in the Orbiter bay to the operating position.
 - 2. Provisions for power, data, command/control, and thermal resources shall be made for equipment in the deployed position.
- d. Attached Engineering Evaluation/Operations
 - 1. Provisions shall be made to evaluate platform distortion and dynamic response.
 - 2. Provisions shall be made for the installation of engineering instrumentation.
 - 3. Provisions shall be made for activation and checkout of installed engineering instrumentation while attached to the Orbiter.
 - 4. SCAFE equipment shall be compatible with natural or induced loads occurring during all phases of Orbiter-attached operation.
- e. Subsystem Installation/Checkout
 - 1. Provisions for subsystem installation, wiring, etc., shall be made on the platform structure.
 - 2. Provisions shall be made for activation and checkout of installed subsystems while attached to the Orbiter.
- f. Scientific Experiment Installation/Checkout
 - 1. Provisions for the installation of scientific experiment equipment shall be made.
 - 2. Provisions shall be made for activation and checkout of installed scientific equipment while attached to the Orbiter.
- g. Separation. Provisions shall be made to grapple the platform with the Orbiter RMS, and separate the platform from the assembly jig and the manipulator arm.
- h. Platform Retrieval. Provisions shall be made to recapture the platform with the RMS during the flight and reattach it to the assembly jig in a manner that it can be translated back and forth by the jig.
- i. Free-flying Mode
 - 1. Provisions shall be made to evaluate platform engineering characteristics and scientific experiments while in the free-flying mode.

2. Attitude control shall be provided by gravity gradient orientation, employing a passive damper, if required.
- j. Descent. Performance requirements for descent shall be in accordance with the ascent requirements.

3.2.3 DERIVED GROUND OPERATIONS GUIDELINES/REQUIREMENTS. The following guidelines have been derived for the SCAFE ground operations:

- a. Installation and interface verification of the SCAFE equipment in the Orbiter shall be accomplished in no longer than 14.5 hours.
- b. Experiments should minimize operation on the ground, except to verify interfaces with the Orbiter or to satisfy launch site safety and compatibility requirements.
- c. Experiment-to-Orbiter compatibility testing should be planned to address only unique requirements.
- d. Launch site ground checkout requirements for the SCAFE should be included in design and test of experiment software and checkout procedures.
- e. The experiment shall be designed to require no physical access on the launch pad unless it is absolutely necessary to achieve experiment objectives.
- f. Removal of the SCAFE equipment from the Orbiter shall be accomplished in no longer than 3 hours.

3.2.4 DERIVED BEAM BUILDER AND ASSEMBLY JIG FUNCTIONAL REQUIREMENTS. The following functional requirements have been derived throughout the study to drive the beam builder and assembly jig design toward one that is the most adaptable to large space construction, compatible with the STS, and optimized for complexity versus risk/cost.

3.2.4.1 Beam Builder.

- a. Provisions shall be made to provide supports and positioning mechanisms for the beam builder to the assembly jig during ascent and descent, and during the process of making longitudinal beams and cross beams.
- b. Provisions shall be made to automatically fabricate three triangular shaped beam caps simultaneously from flat strips of graphite-glass/thermoplastic material contained in storage reels.
- c. Provisions shall be made to cyclic-feed the caps using drive members on each cap forming section to position them for attachment to the posts and diagonal cords.
- d. Provisions shall be made for an independent cooling system to reject the residual heat from forming the caps.

- e. Beam posts shall be preformed and precut on the ground and stored on the beam builder. Automatic handling and positioning mechanisms shall be provided on the beam builder for the posts (cross-members) to be attached to the caps.
- f. Provisions shall be made for a diagonal cord storage, feed tensioner, and pleyer mechanism to automatically position the cord for attachment to the caps and cross-members.
- g. Provisions shall be made for an automatic welding mechanism to weld the caps, cross-members, and diagonal cords together in the designated place.
- h. Provisions shall be made for a mechanism which will cut off finished lengths of beams.
- i. Provisions shall be made to provide a control system with the terminal in the Orbiter to automatically and remotely control, through astronaut direction, the functions previously described.
- j. The design of the beam builder and support equipment shall provide for: (1) equipment accessibility, (2) rapid fault isolation, (3) ease of remove/replace activities, and (4) maximum possible use of standard tools and test equipment.

3.2.4.2 Assembly Jig

- a. The assembly jig shall be designed such that it will fit in the available cargo bay space within one continuous section for SSAFE application without any folding or extension mechanism to make it wider.
- b. Provisions shall be made to support the assembly jig in the cargo bay during launch and ascent, and to remotely deploy the jig out of the cargo bay on orbit to perform the construction experiment, and to reposition it in the cargo bay for descent.
- c. Provisions shall be made to support the beam builder and instrumentation/support subsystem package during the launch and ascent phases, and position and support it during the longitudinal beam building operation.
- d. Provisions shall be made to automatically retain and guide the longitudinal beams and platform during construction.
- e. Provisions shall be made to provide an automatic welding mechanism to attach the beam caps, ports, and diagonal cords.
- f. Provisions shall be made to automatically reposition the beam builder from the longitudinal beam building position 90° in order that the cross beams may be constructed and attached.
- g. Provisions shall be made to automatically retain and guide the cross beams during construction.

- h. Provisions shall be made to translate the completed longitudinal beams from one end to the other to attach the cross beams and also the completed platform to attach instrumentation and support subsystem.
- i. Provisions shall be made to provide for an EVA support mechanism for crewmen and means to translate the supported crewmen to various work positions.
- j. Provisions shall be made to provide platform remote release and reattach mechanisms.
- k. Provisions shall be made to provide a control system with the terminal in the Orbiter to automatically and remotely control, through astronaut direction, the functions previously described.
- l. The design of the assembly jig and support equipment shall provide for:
 - (1) equipment assessability, (2) rapid fault isolation, (3) ease of remove/replace activities, and (4) maximum possible use of standard tools and test equipment.

3.3 STRUCTURAL TEST DESCRIPTION

This section identifies the structural tests to be performed to correlate the actual behavior of the platform in space with the predicted behavior from analysis, lists the instrumentation needed, and describes the operations of the tests.

3.3.1 FIRST BEAM DYNAMICS EXPERIMENT

3.3.1.1 Requirements. The purpose of the first beam dynamics experiment is to measure the response of a single beam to the dynamic loads imposed upon it by the beam builder, assembly jig, and Orbiter, plus variable loads from a vibrator assembly. The actual response on orbit will be compared to the analytically predicted response to see how closely they match and to see if any changes in the experiment protocol should be instigated if the data are significantly different. The analysis of the resultant beam responses will provide data for improved models for accurate prediction of dynamic response of beams and larger structures composed of beams of the same type, constructed in orbit for future operations.

The primary requirements are to provide data on the response of the beam to the construction environment to an accuracy of 14% and data on the response to loads induced additional to the construction environment to an accuracy of 14%. The additional loads imposed must excite all the important modes to an amplitude that can be measured to the desired accuracy. Data on the imposed loads are required from the Orbiter. This includes data on all thruster firings during the experiment and attitude/attitude rates from the Orbiter guidance system.

3.3.1.2 Description. The system diagram of the experiment equipment with interfaces to the Orbiter and beam builder is shown in Figure 3-13.

3.3.1.2.1 Instruments. The instruments required include two accelerometers mounted in an instrument package and attached to the end of the beam in the beam builder on the ground, a TV camera with a zoom lens and light mounted inside the beam builder, plus the Orbiter inertial measurement unit and Orbiter TV system including TV camera located on the remote manipulator.

Built-in strain gages were also considered, but not added to our instrumentation because the expected accuracy would not approach the other instrumentation (such as the laser beacon used on the complete platform experiment) and the values for strain derived from measuring deflection and dynamic response.

3.3.1.2.2 Equipment List. Table 3-2 is the list of experiment instrumentation required for this activity.

3.3.1.3 Operation. The instrument package equipped as in Figure 3-13 will be attached to the end of the beam in the beam builder while the beam builder is on the ground. The package will be commanded ON by an RF link to the Orbiter or manually by a crew member during the first EVA. Data from the accelerometers will be telemetered to the Orbiter continuously as long as the batteries last.

When the first beam is completed, a crew member will command a selected attitude rate (typically 0.01 degree/second) in yaw with the hand controller for the vernier attitude control system. This impulse will cause the beam to oscillate at a low frequency (typically 2 cycles per minute). After the oscillations die down (5 to 10 minutes), the crew member will command an attitude rate about the Orbiter roll axis. During this time personnel on the ground and other crew members will be observing

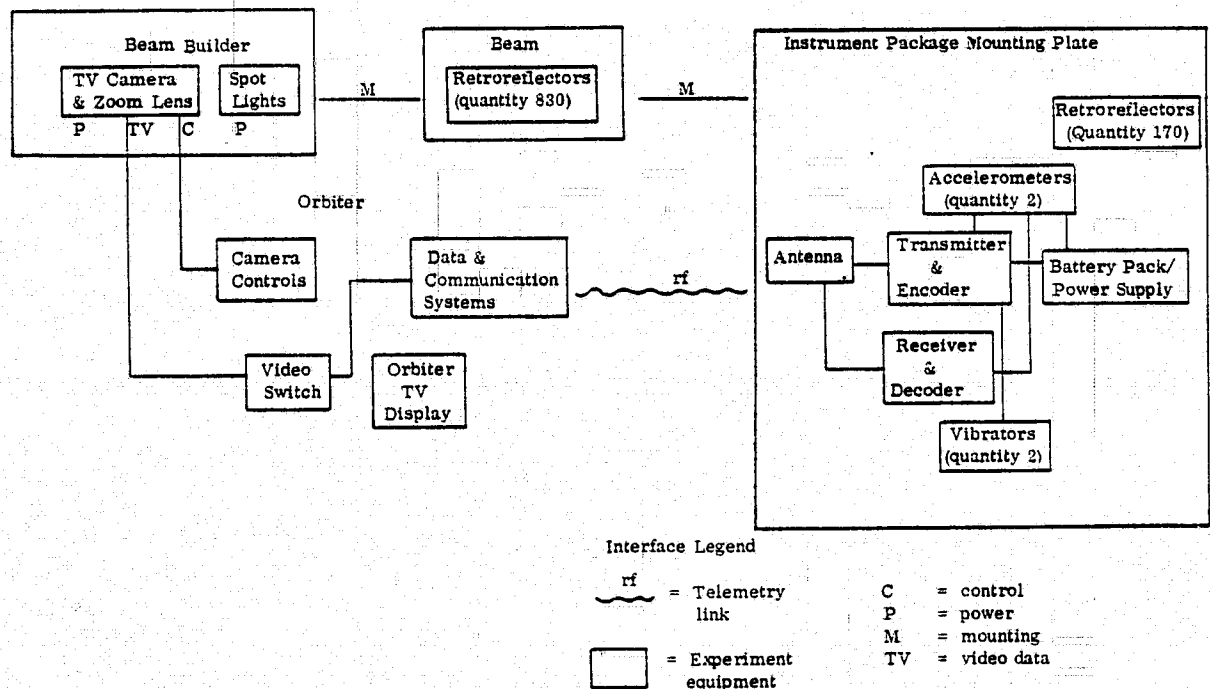


Figure 3-13. First beam dynamics experiment system diagram.

Table 3-2. Equipment list.

Name	Characteristics/Requirements
Accelerometers* (quantity 2)	0.005 m/sec ² (0.0005g) rms noise level or better; frequency response 0.03 to 150 Hz; amplitude linearity $\pm 1\%$ to 3 m/sec ² (0.3g); peak power requirement 15 watts; mass < 0.5 kg (weight less than 1.1 pound).
TV Camera & Zoom Lens	Orbiter compatible; 200-line resolution; zoom lens; field of view 0.0075 radian (0.43 degree) to 0.075 radian (4.3 degree); maximum size envelope 0.4m \times 0.2m \times 0.2m; mass < 10 kg; power requirement < 20 watts
Spot Light	Size envelope 0.1m diameter \times 0.1m; power 40 watts
Retroreflectors* (quantity 1000)	Mount on beam cross-members and instrument package mounting plate; size < 1 cm diameter; mass less than 0.005 kg each
Vibrators* (quantity 2)	Includes programmer
Transmitter & Encoder*	Orbiter compatible; 1 watt output effective radiated power; encodes 5 to 10 measurements
Receiver & Command Decoder*	Orbiter compatible; 50-command capability
Battery Pack/Power Supply*	Sized to provide power to accelerometers, vibrators, transmitter, and receiver & command decoder for life of experiment. Compatible with subsystem rack power for further experiments after first beam experiment is complete.
Instrument Package Mounting Plate*	Flat triangular mounting plate attaches to 3 beam cross-members and mounts accelerometers, vibrators, transmitter, receiver & command decoder, battery pack/power supply antenna, and an array of retroreflectors. Size 1.4 m sided triangle, 0.001 m thick & stiffeners and attachments to beam cross members.
Transmit/Receive Antenna*	Monopole antenna
Camera Controls	Control zoom lens focus, zoom, iris. 3-position momentary switches.

*Included in Instrument Package

the motions of the beam with a TV system. One TV camera equipped with a zoom lens will be located in the beam builder and will look out into the inside of the beam. It will be equipped with a light to illuminate the beam. The two initial firings of the vernier rockets will provide an opportunity to make sure the communication links from instrument package to Orbiter to ground operations center are good and that the experiment is providing good quality data.

If the experiment is going as desired, a crew member can set the deadband on the Orbiter attitude control system so that beam oscillations will have time to damp out between thruster firings. This completes flight crew participation in the first part of the experiment. The second part of the experiment is controlled excitation of the beam, with vibrators. Upon receipt of an rf command from the Orbiter, the vibrators will turn on and begin a slow scan in frequency. One vibrator will operate at a constant frequency, 300 Hz for example, while the other vibrator will slowly change its frequency. The beat frequency difference between the two vibrators will excite different modes in the beam, permitting natural frequencies, mode shapes, and resonant responses to be determined.

3.3.2 COMPLETE PLATFORM DYNAMICS EXPERIMENT

3.3.2.1 Requirements. The purpose of the complete platform dynamics experiment is to provide on-orbit data on dynamic responses of space structures and compare these to the analytically predicted response to see how closely they match. The analytical models will be updated and used to design efficient, economical, large space structures to be constructed in orbit, and to predict their performance under various loads.

In order to understand the requirements for the accuracy of the deflection measurement, an understanding of the operational tolerances is needed. This paragraph explains the reason for the deflection accuracy chosen. One use of future structures is for microwave transmission and reception. At a frequency of 3 GHz (wavelength 10 cm), a lens has a contour tolerance of 2.5 cm. To measure this much deflection at 10% accuracy implies 2.5 mm resolution in the measurements. The highest expected frequency of interest in the platform bending modes is about 1.5 Hz. To track the movements of the platform accurately requires a sampling rate of 15 Hz. The number of points needed to determine the shape of the platform is 10 for the low frequency modes of interest. From these basic requirements to use future platforms for microwave transmission, the derived requirements are to monitor the position of 10 representative points on the platform at a rate of 15 samples per second with an accuracy of 2.5 mm. From the dynamics analysis (Section 4.3), the expected maximum peak-to-peak deflection amplitude is approximately one meter. With 2.5 mm resolution elements, 400 elements are needed, or the 2.5 mm accuracy corresponds to 0.25% of full scale for a one meter range.

The experiment requires input forces and torques with related attitude and attitude rate data from the Orbiter, similar to the single beam experiment. During

the free-flying portion of the experiment, controllable excitation forces from vibrators are required to excite the various modes of interest.

3.3.2.2 Experiment Description. The system diagram of the experiment equipment with interfaces to the Orbiter, beam builder, platform, grapple fixture, and sub-systems rack is shown in Figure 3-14. The heart of the experiment is the laser beacon and detector array, shown in conceptual form in Figure 3-15.

3.3.2.2.1 Instruments. The instruments required include four accelerometers, one laser beacon with associated 400 element detector array, plus the Orbiter inertial measurement unit.

The laser beacon and detector array scan 15 times per second and measure the platform shape as located by 10 individual retroreflectors. This arrangement is reasonably straightforward electronically and keeps the instrumentation relatively simple and compact. To attain the desired accuracy imposes a stringent mechanical requirement, however, of less than 10^{-5} radian wobble in the shaft which turns the assembly at 15 revolutions per second. An alternative arrangement that is mechanically less demanding is to use 10 linear detector arrays in place of the retroreflectors. This alternative requires less sensitivity from the detectors but is more complex electronically and requires wiring to the ends of the platform. A design/cost trade-off study of these alternatives is recommended in a later program phase.

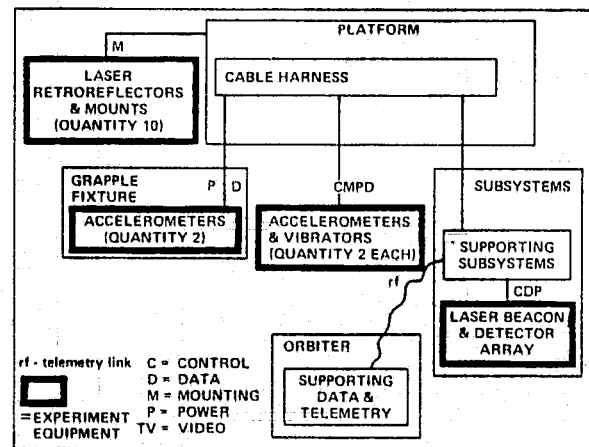


Figure 3-14. Platform dynamics experiment system diagram.

3.3.2.2.2 Equipment List. Table 3-3 is the list of equipment required for the complete platform dynamics experiment.

3.3.2.3 Experiment Operations.

3.3.2.3.1 Equipment Installation. The equipment is installed by the mission specialist during the subsystem component and instrumentation installation EVA on Day 3. The mission specialist will mount the laser beacon and detector array on the same cross beam as the subsystems rack and connect them together with a power command and data cable. The two accelerometers attached to the grapple fixture also require attachment of a power and data cable. The two accelerometers attached to the platform at the opposite end from the subsystems rack require that the mission specialist fasten them to the structure and attach the power and data cable. The mission specialist also will attach the 10 laser retroreflectors and mounts to the ends of the selected cross beams.

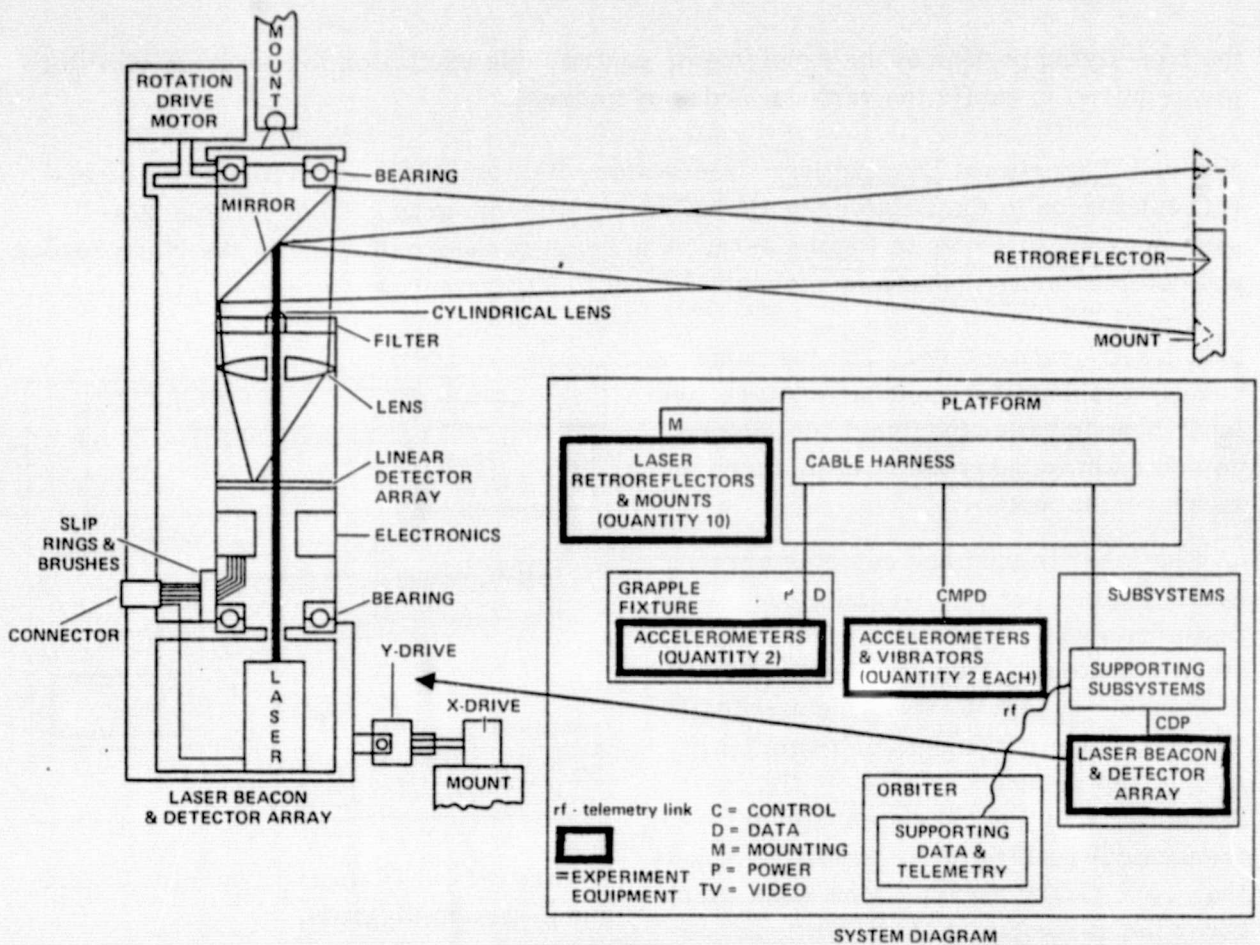


Figure 3-15. Laser beacon, detector array concept.

Table 3-3. Equipment list.

Name	Characteristics/Requirements
Laser Beacon & Detector Array	Fifteen revolutions per second scan rate, determines position of retroreflector to accuracy of 2.5 mm at distance of 200 m. Detector array instantaneous field of view 1.25×10^{-5} radians $\times 5 \times 10^3$ radians. Rotation wobble less than 10^{-5} radians; remote control alignment of mounting through x and y direction drive motors to accuracy of 10^{-4} radians.
Laser Retroreflectors & Mounts (quantity 10)	Position 5 mm or smaller diameter retroreflector 1 meter above platform; thermal and mechanical oscillations of mount less than 1 mm relative to platform.

3.3.2.3.2 Checkout and Alignment. The only alignment of importance is the adjustment of the laser beacon rotation vector so that the laser beacon will light the retroreflectors. The laser beam is 25 mm high where it intersects the nearest laser retroreflector mounts and 1 m high where it intersects those farthest away. The alignment accuracy required is 10^{-4} radians. The alignment procedure is to start the beacon and look at the detector output to see if any signal is being returned from the retroreflectors. See Figure 3-15. If any retroreflectors are in view, adjust the rotation vector direction to put the reflected beam from one retroreflector on the middle of the detector array. Then adjust the appropriate X or Y drive position to bring the other retroreflectors into the laser beacon field-of-view. When the detector array is sensing all the retroreflectors, adjust the X and Y drive so that one near retroreflector and one far retroreflector signal are coming from the middle of the detector array. If no signal is received from any retroreflectors at first, the X-drive should be slowly scanned through its range.

The rest of the checkout is an end-to-end communications check to make sure the data received at the ground control center is good and that all the instrumentation is operating properly.

3.3.2.3.3 Operation. The platform will be excited in its various dynamic modes in the same way as in the first beam dynamics experiment using the Orbiter vernier thrusters and also with the vibrators located on the instrument package. Data from the instruments will be telemetered to the Orbiter and to the ground from the subsystems rack.

The experiment will continue whenever it is convenient to operate the vibrators and laser beacon and detector array. The operation will be on a noninterference basis with other experiments and Orbiter operations, including operation in the free-flying mode up to three weeks after platform separation.

3.3.3 THERMAL EFFECTS TEST

3.3.3.1 Requirements. The purpose of the thermal deflection experiment is to provide data on temperature variations in different parts of the platform structure and on any deformation of the structure caused by the temperature difference. These data will be compared to analytical predictions and will be used to improve computer models of the thermal behavior of future space structures.

The experiment requires temperature measurements at 51 locations on the platform to an accuracy $\pm 5.50^\circ\text{K}$ over a range from 155°K to 283°K . The experiment also requires measurement of deflections of the structure to an accuracy of 2.5 mm. In order to produce significant temperature differences in the structure, such as would be expected in future space platforms, it is necessary to deploy a sun shade over part of the platform. Figure 3-16 shows the locations of the sun shade and temperature sensors. The setup operation requires a crewman to attach the sunshade and temperature sensors to the platform during an EVA.

3.3.3.2 Description. The system diagram of the experiment equipment with interfaces to the platform and subsystems rack is shown in Figure 3-17. The laser beacon & detector array and laser retroreflectors are used in the complete platform dynamics experiment, described in Section 3.3.2. The experiment concept is to cause an unsymmetrical temperature distribution in the platform by using a sunshade, and then measure the temperature pattern and distortion of the platform.

3.3.3.2.1 Instruments. The main instrumentation added to the platform for the experiment is the temperature sensor unit, shown in Figure 3-18. There are 51 units, each of which has two temperature probes. The units are mounted in triplets; each of the seventeen locations indicated in Figure 3-16 will receive three units, one in each of the three caps in the beam.

We considered building the temperature sensors into the cross-members on the ground to reduce the extravehicular activity workload. This approach was rejected because beam cap (not cross-member) temperatures are needed to understand the deflections due to temperature differences.

3.3.3.2.2 Equipment List. Table 3-4 is the list of equipment required for the thermal deflection experiment.

3.3.3.3 Operations

3.3.3.3.1 Equipment Installation. The laser beacon and detector array, laser retroreflectors and mounts installations are described in Section 3.3.2. The temperature sensors are attached to the beam caps during the wiring harness installation. This is an extravehicular activity task.

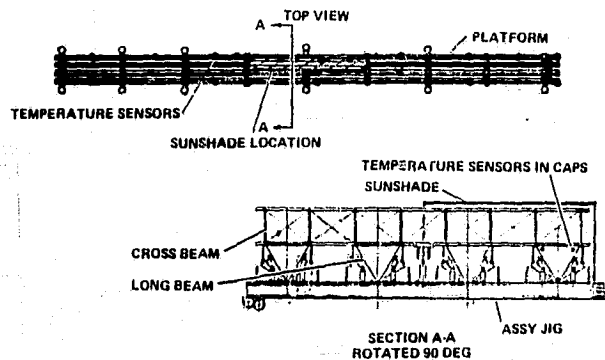


Figure 3-16. Location of sun shade and temperature sensors.

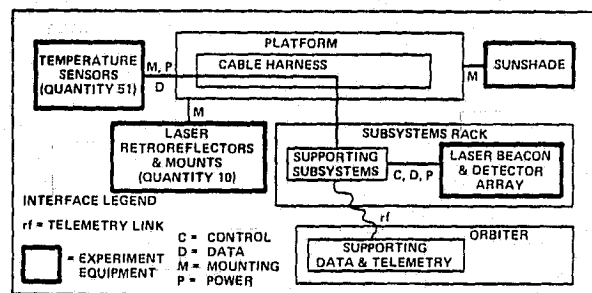


Figure 3-17. Thermal deflection experiment system diagram.

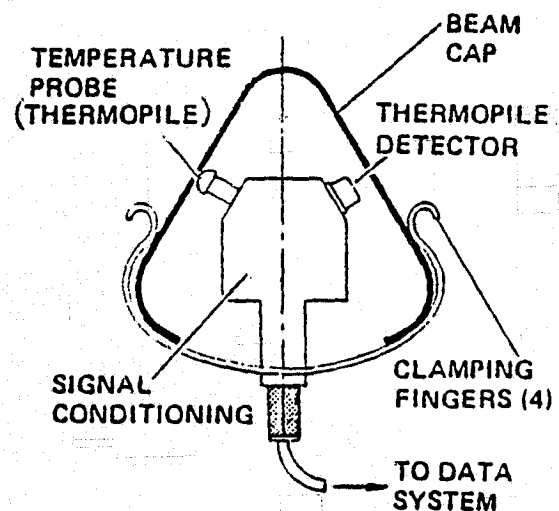


Figure 3-18. Beam cap temperature measurements.

Table 3-4. Equipment list.

Name	Characteristics/Requirements
Sun Shade	Foil-fabric shade with mounts to attach to cross beams.
Temperature Sensors (quantity 51)	Measure temperature on two inner surfaces of cap over range of 155 to 283°K with accuracy $\pm 5.5^\circ\text{K}$. Clip mount to cap.
Laser Beacon & Detector Array	See complete platform dynamics experiment (Section 3.3.2).
Laser Retroreflectors & Mounts	" " " " "

The sunshade is installed after the temperature sensors because it will cover part of the beams where the temperature sensors are located. The crewman will attach the sunshade mounts to one cross beam, unroll the sunshade to the next cross beam, attach more mounts, and unroll the sunshade to the next cross beam, where he will attach the rest of the mounts.

3.3.3.3.2 Operation. The equipment will be checked for proper operation from the Orbiter and from the ground operations center center. See Section 3.3.2 for laser beacon alignment. Temperature measurements will be made continually at a low sampling rate of approximately 10 seconds to read out the 102 measurements. The deflection experiment will primarily be a daylight operation. As the platform heats unevenly on the day side of the orbit, the laser beacon & detector array will measure the deflection of the platform. It will be easier to analyze the data if other disturbing forces on the platform are minimized during this time. The experiment will start from the time the subsystems rack telemetry begins to transmit temperature measurements and continue during the Orbiter stay and also during the free-flight time after the Orbiter returns to earth.

3.3.4 SEPARATION/RECAPTURE DEMONSTRATION

3.3.4.1 Requirements. During this demonstration the crew will separate the platform from the assembly jig, separate the platform from the remote manipulator system, and move the Orbiter away from the platform. The requirement is safe separation, with measurement of the undocking loads to an accuracy of 10%. After separation, the platform rendezvous and tracking transponders should be checked for proper operation during an Orbiter flyaround.

The recapture demonstration will show that the platform can be attached to the remote manipulator, placed into the assembly jig, locked down, and moved by the assembly jig along the platform axis. The requirements are safe docking,

measurement of the docking loads to an accuracy of 10%, and movement of the platform by the assembly jig in a reasonable length of time. For this demonstration, safe docking means that the platform touches only the remote manipulator and the assembly jig, and the loads are within the specified limits.

This demonstration will provide important information for an optional second mission, when additional applications experiments may be attached to the platform, and future missions where larger structures are assembled.

3.3.4.2 Platform Grapple Fitting. The grapple fitting used for platform separation and recovery is part of the SPAR Aerospace Products capture mechanism concept illustrated in Figure 3-19. The grapple fitting will be attached to a special support which can be attached to the face of a beam by EVA during platform equipment installation. The support will be attached to the face of the caps in the two center longitudinal beams such that the grapple fitting lies in the center of the platform as close to the center of mass as is practicable.

Two accelerometer packages are mounted on the grapple fitting support near the fitting. These instruments measure the loads experienced at the fitting during capture, translation, and release of the platform.

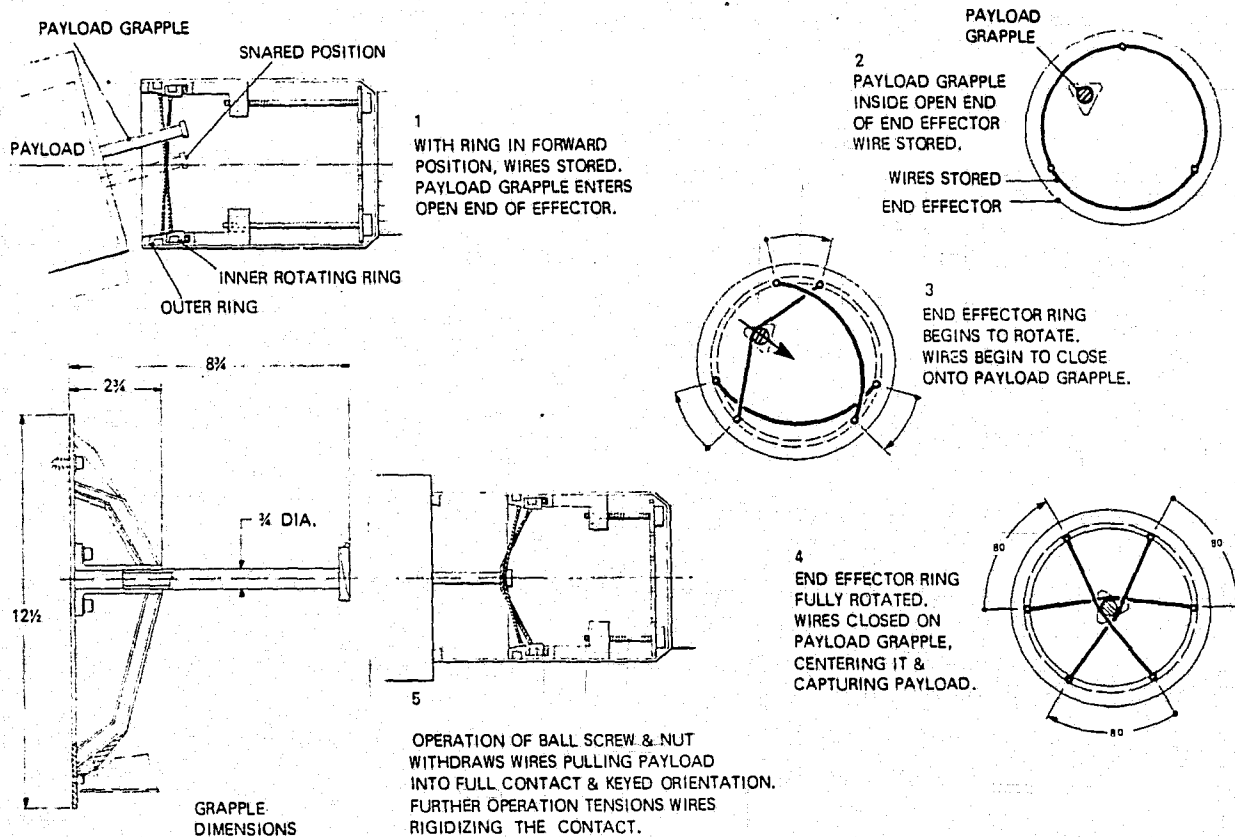


Figure 3-19. End effector/grapple fitting capture and rigidize sequence.

3.3.4.3 Sequence. The following sequence will be performed for the demonstration. The platform is positioned with its center-of-mass near the support plane of the RMS. The grapple fitting is located near the platform center-of-mass such that the remote manipulator is within easy reach of the grapple fitting. Figure 3-20 shows the position of the platform in the jig and the reach envelope of the RMS support plane the grapple fitting. Next, the platform subsystems and accelerometers are turned on so that data can be transmitted to the Orbiter and ground control center. The six accelerometers will measure the acceleration experienced by the platform during the separation operation. The Orbiter inertial measurement unit will supply additional data needed for the demonstration.

A crewman will guide the remote manipulator end-effector to the grapple fixture and capture it. See diagram Figure 3-19. Next, the platform will be released from the assembly jig. Then the platform will be pulled away from the assembly jig with the remote manipulator. When a safe clearance distance is reached the platform will be released from the remote manipulator and then a crewman will move the Orbiter away from the platform using vernier thrusters. The platform will be aligned with the long axis along the local gravity vector and with a rotation period equal to the orbital period so that the long axis remains aligned with the local gravity vector. After separation the Orbiter will fly around the platform to check the antenna patterns from the tracking and rendezvous transponders and to determine the impact of the Orbiter attitude control and maneuvering thrusters on the platform. The impact of the exhaust gases from these thrusters may cause unwanted attitude rates in the platform.

The recapture sequence is as follows:

- a. The Orbiter will be maneuvered in a position where the platform grapple fixture can be reached with the remote manipulator and attached.
- b. The platform will be pulled closer to the Orbiter and put in position close to the assembly jig.
- c. The remote manipulator will be used to push the platform into the guides on the assembly jig and the platform will be attached to the assembly jig with the retention mechanism.

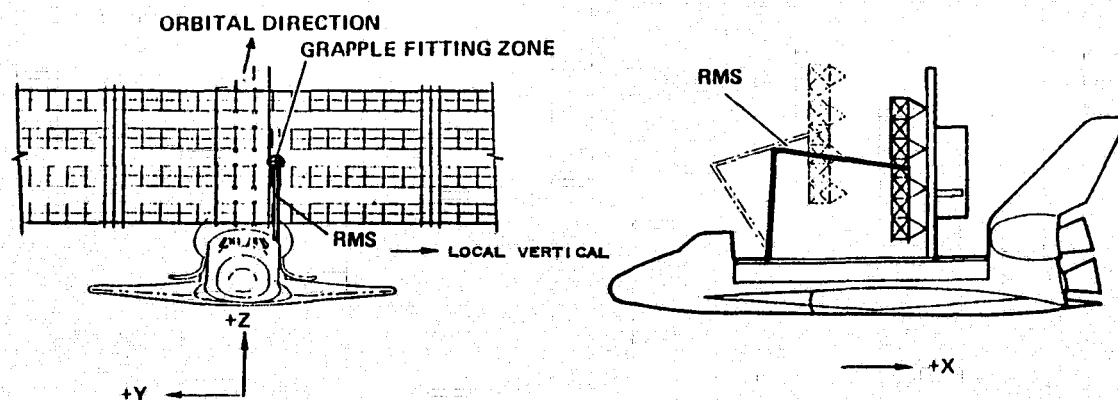


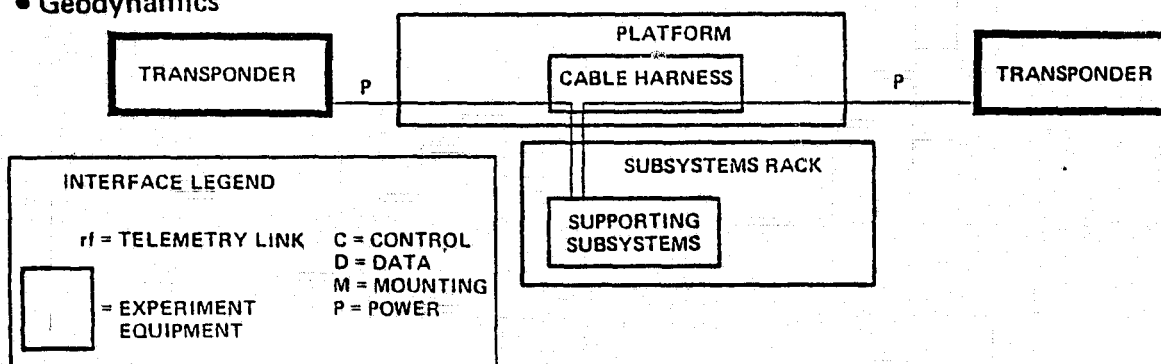
Figure 3-20. RMS/grapple fitting relationship.

- d. The last step in the demonstration is to move the platform along the assembly jig to show they are once more properly mated.

3.4 POST SEPARATION EXPERIMENTS

Two experiments previously identified and defined by JSC have been chosen as examples of scientific experiments that can be installed on the platform after it has been fabricated on a single Orbiter mission and performed using the platform in the free-flying mode after the Orbiter returns to earth. The two experiments are very briefly described in the following paragraphs. Systems diagrams for each are shown in Figure 3-21. An in-depth investigation and analysis of candidate scientific experiments to be performed with the platform should be undertaken in future study activities to identify experiments that would be cost effective and the requirements of these experiments on platform subsystems.

• Geodynamics



• Atmospheric Composition

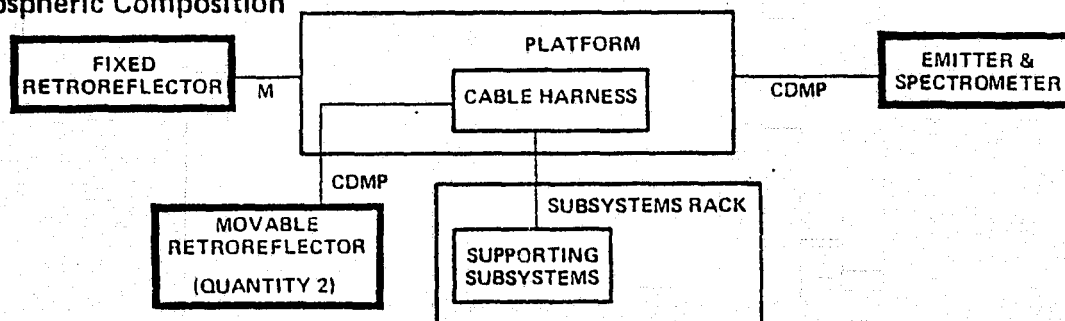


Figure 3-21. Scientific experiments system diagrams.

3.4.1 GEODYNAMIC EXPERIMENT. The objective of the experiment is to map anomalies in the earth's gravity field to obtain data on internal mass distribution of the earth. The approach is to use doppler frequency shift of communications from the platform, in a stabilized gravity gradient attitude and with transponders at each end 200 meters apart, to the TDRSS, and from the platform to the ground tracking stations to detect platform acceleration caused by lateral variations in the gravity field over density anomalies in the earth's structure.

Two S-band transponders with a total weight of 60 kg are required. Their peak power requirement is 100 W. The equipment is installed and connected during the EVA activities on the third day as described later.

Performance of the experiment, after platform separation from the Orbiter, will alternate (for only a short time) with the atmospheric composition experiment and then with the platform dynamics/thermal deflection experiment until a possible optional revisit mission.

3.4.2 ATMOSPHERIC COMPOSITION EXPERIMENT. The objective of the experiment is to measure the composition and density of the atmosphere at the orbital altitudes of the platform. The approach is to transmit resonance gas radiation sources excited by microwaves through a known path and measure the absorption by spectrometer to determine the composition and density. The radiation source and spectrometer are placed at the end of the platform where the subsystems are located. Reflectors are positioned at various distances along the platform to obtain different path lengths for comparison. Movable reflectors are placed near the radiation source and fixed reflectors away from the source and at the end of the platform so that the maximum path length is approximately 400 m.

The following experiment equipment is required.

Radiation Source and Spectrometer	100 kg
Fixed Reflector	5 kg
Movable Reflectors (2)	<u>20 kg</u>
Total	135 kg

The peak power is 150W.

The experiment is planned to be performed just before the Orbiter separates from the platform and returns to earth and, for a short time, after the Orbiter separates and leaves, in order to measure the dissipation rate of the propellant cloud and contamination in the vicinity of the Orbiter. The same procedure will be followed if there is a second, optional revisit mission.

Later in the orbital mission, after all the other applications experiments have been performed, in order to null out the effect of orientation relative to the flight path, the platform will be rotated slowly during experiment data acquisition. In addition, data will continue to be collected to obtain composition and density variation as the orbit decays and the platform enters the atmosphere.

3.5 FUTURE APPLICATIONS

The purpose of a space structure is to position useful elements of some system, subsystem, or experiment equipment. From a structural viewpoint, the required positioning accuracy is one useful distinction among the various uses of the structure. This positioning accuracy has two aspects. One is the relative position of different elements on the platform, and the other is the position relative to the orbit, earth,

sun, inertial space, a satellite, or space probe. The relative position on the platform requires structural dimensional accuracy, while the others require accuracy in attitude control for the entire platform or pointing mounts. Two extreme examples are an exposure facility which mounts samples to be exposed to the space environment, and a deep space tracking antenna for a relay satellite. The exposure facility has no relative position accuracy requirements between elements and practically no attitude requirements on the platform. Exposure type experiments could be performed on the platform with no additional subsystems. However, the exposed samples are to be returned to earth for analysis, so this use of the platform must be done before the final visit of the Orbiter to the platform. Figure 3-22 gives a relative idea of the requirements imposed by various future operational applications. The MOBCOMSAT is a communication satellite with several large expandable antennas to be used for traffic control and communication to mobile users.

Most applications of large structures require some pointing capability in addition to gravity gradient stabilization. Some of the applications require somewhat expensive solar cell arrays, antennas, and larger transmitters. To get a reasonable return on the total investment from these requires the addition of three-axis stabilization capability to the platform subsystems, and the addition of propulsion to maintain the orbit or, preferably, boost the platform to a higher orbit.

The scientific experiments described in the previous section are just representative of additional experiments that can be carried up on the first flight and performed along

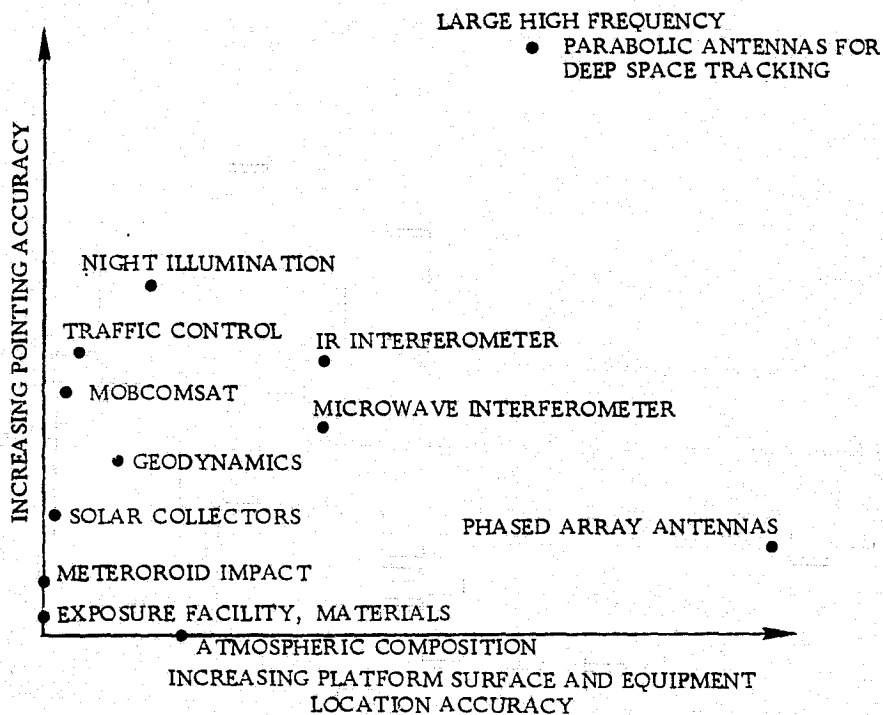


Figure 3-22. Position accuracy relative requirements for future applications of platform.

with the structural response tests while attached to the orbiter and during the free flight mode after the orbiter returns to earth. These activities may not represent the most cost-effective use of the platform to run precursor operations leading up to the operational missions identified in Figure 3-22. In addition, no work was done in looking at what additional experiments would be desirable to perform on an optional revisit mission, including raising the platform orbit for longer orbital life. The overall application of the platform as a total system should be studied and optimized by driving out those experiments and operations which will pave the way for future operational missions in the most cost-effective manner.

Table 3-5 lists some of the additional experiments and operations which should be considered in an overall system study of the platform and its applications in the follow-on study in order to optimize its effectiveness to develop the capability to perform future operational missions. The activities identified in Table 3-5 should be considered for inclusion in the first mission, a second or possibly third revisit mission, and for the free-flying operation when the Orbiter isn't attached to the platform. Many of these activities in the free-flying mode will require additional attitude control, measurement, propulsion, and avionics capabilities that have not been considered in this study.

3.6 MISSION OPERATIONS

This section describes: (1) the recommended mission profile for the SCAFE while attached to the orbiter, (2) the experiment timelines both while attached to the orbiter and during free flight after the orbiter returns to earth, (3) the requirements for the supporting subsystems, (4) the EVA activity required to install experiment instrumentation and supporting subsystems, (5) the ground operations to prepare the SCAFE equipment for flight, and (6) mission options leading to a conclusion that the SCAFE can be accomplished in a very cost-effective manner in one flight along with several applications experiments and that an optional revisit mission with additional applications experiments should be able to be accomplished effectively.

3.6.1 MISSION PROFILE. Figure 3-23 shows the mission profile for the Orbiter portion of the SCAFE to satisfy the requirements discussed at the beginning of Section 3. Figure 3-24 indicates the SCAFE equipment stowed in the cargo bay for launch. The assembly jig is supported from a short cradle and a forward cargo bay mount. The beam builder is supported on the assembly jig, and the supporting subsystem and experiment instrumentation packages are supported off the cradle.

During ascent (or reentry) to the delivery orbit, the SCAFE equipment is inactive, requiring only mechanical and caution and warning support from the Orbiter. The nominal mission is seven days long. The Orbiter crew initiates each operational or test phase and controls Orbiter maneuvers and RMS operations. Before the start and during the initial phase of the beam building experiment, an EVA operation is performed to make sure the equipment is functioning properly.

Table 3-5. Potential future SCAFE platform activities and uses.

-
- I. Large Structure Characteristics/Tests/Demonstration Missions
- A. Structural rigidity, shape, flatness
 - 1. Test thin mylar material deflection/bowing for unrigidized surfaces (gravity, drag, solar pressure deflections).
 - 2. Demonstrate/test capability to measure flatness and curvature.
 - 3. Demonstrate/test capability to adjust flatness and curvature.
 - B. Structural Dynamics
 - 1. Docking dynamics with impact at different velocities.
 - 2. Dynamics and damage assessment with object impacts.
 - 3. Dynamics and damage assessment of ACS velocity jet on beams/planar surface.
 - 4. Dynamics with astronauts moving along beams.
 - 5. Dynamics with on-board control system.
 - C. Interactions of Gravity/Drag Solar Pressure
 - 1. Gravity gradient of large open structures with and without unsymmetrical c.g. locations.
 - 2. Drag impact of large open structures.
 - 3. Interaction of gravity, drag, and solar pressure on attitude and ACS requirements.
 - D. Operations
 - 1. Demonstrate capability to add structure/attachment points to existing beams.
 - 2. Demonstrate and test additional mounting and wiring techniques for open beams in space.
 - 3. Test different open beam colors in space for visibility and thermal desirability.
 - 4. Demonstrate and test various methods to deploy surfaces on open beams.
 - 5. Demonstrate techniques and test visual aids for docking with a large open beam structure.
 - E. Multiple Services
 - 1. Evaluate electromagnetic interference with several antennas located on the same platform.
 - 2. Test effect of manned operations on one end of platform with scientific testing/operations being performed elsewhere on the platform.
- II. Materials Test Bed Missions (test structural, thermal, electrical decay vs. exposure time)
- 1. Composite materials
 - 2. Metals/Alloys
 - 3. Thermal Shields
 - 4. Solar Cells
- III. Demonstration Missions
- 1. Use of trim tabs to supplement attitude control.
 - 2. Mounting of solar cells on large structures.

Table 3-5. Potential future SCAFE platform activities and uses. (Concl'd)

3. Night illumination platform demonstration.
4. Multiple (public) services mounting platform.
5. Microwave transmission.
6. Platform for mounting SEPS demonstration components.
7. Radiometer platform.
8. Solar collector panel for solar power module/satellite.
9. Solar cell annealing procedures for deployed panels.

IV. Direct Measurement Missions

1. Atmosphere density determination (use maximum drag configuration).
2. Interaction of drag/gravity/solar pressure on attitude, trajectory.
3. Impact determination of meteorites (meteorite shower) as function of time and size.

During the beam building operation the equipment operates automatically under the control of the experiment computer. When the first beam is finished a dynamic response test will be conducted to determine its characteristics and fed back to the ground to compare with the predicted behavior. This will help predict the characteristics and behavior of the completed platform. The remainder of the platform will be completed by the middle of the third day. During this time the crew will monitor the operation at the aft flight deck and observe directly and with TV. During the afternoon

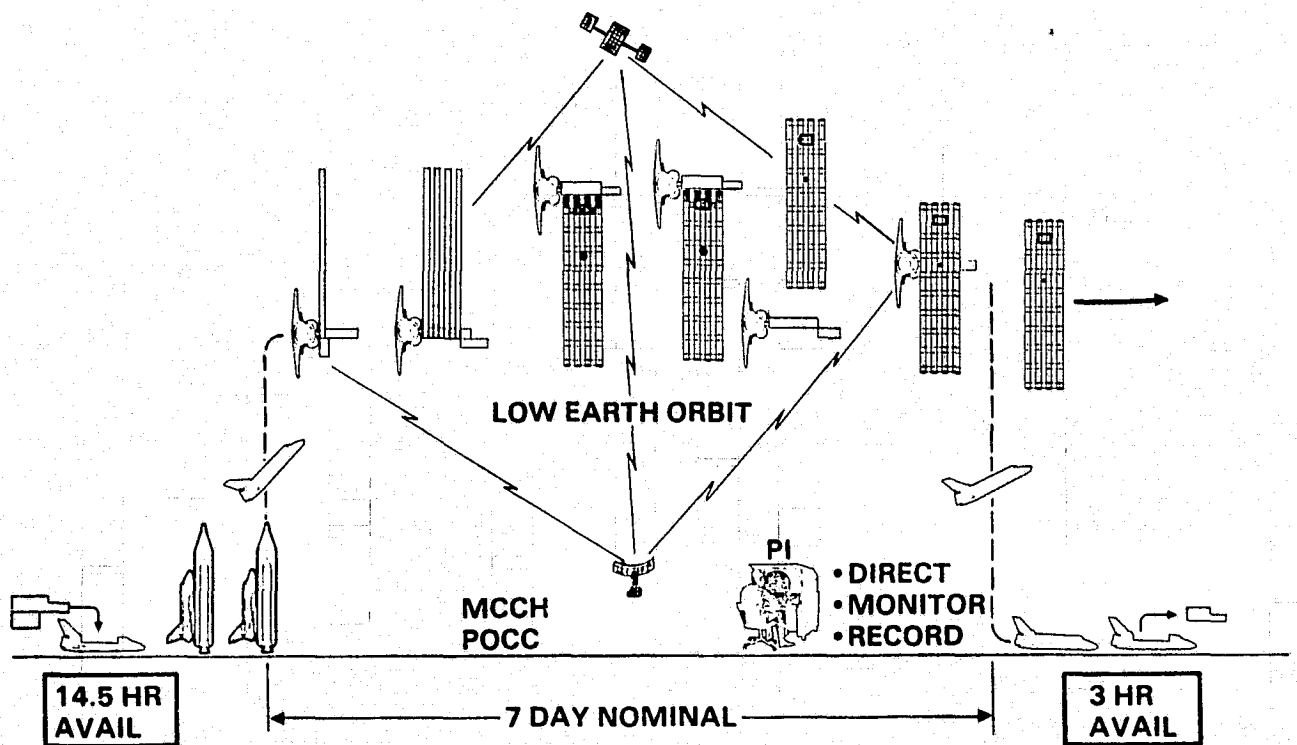


Figure 3-23. SCAFE flight profile.

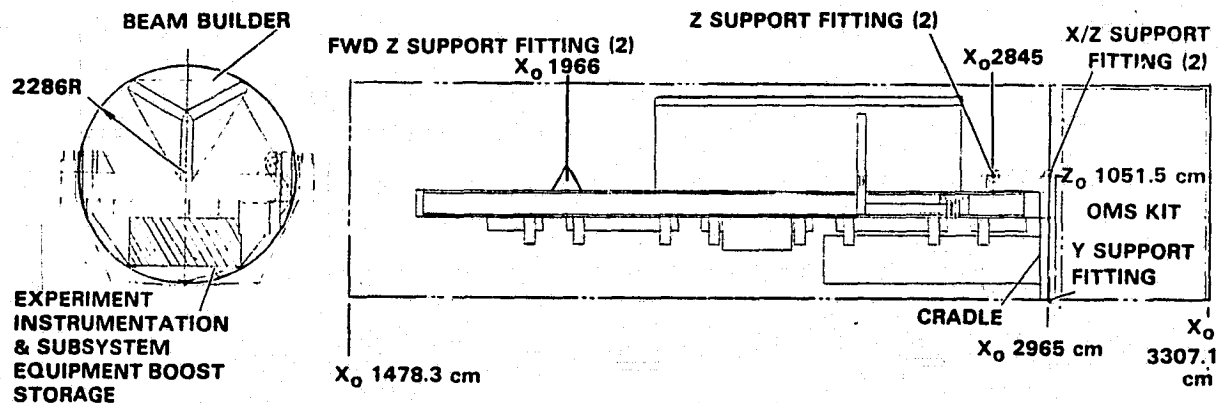


Figure 3-24. SCAPE stowage concept.

of the third day, another EVA is performed to install the test instrumentation, the subsystems, and the free flight experiment equipment. On the fourth day, the dynamic response and thermal deflection experiments will be checked out and performed. During the morning of the fifth day, the separation and recapture demonstration experiment will be conducted. The dynamic response and thermal deflection tests will resume on the afternoon of the fifth day. On the sixth day, another EVA operation will be performed to simulate repair which might occur on operational platforms. The seventh day will be used for releasing the platform ready to perform the free-flying scientific experiments (geodynamics and atmospheric composition) and to continue the dynamic response and thermal deflection experiment, closeout activity, and reentry.

Executive control and monitor of the beam fabrication on-orbit operation is provided via the orbiter RF command link by ground controllers at the Payload Operations Control Center (POCC) which is co-located with Mission Control Center-Houston (MCC-H). MCC-H provides Orbiter and overall mission control.

Figure 3-25 shows the various positions of the beams and platform during the successive operations. Upon system deployment from the stowed position, the beam builder, moving to successive positions along the shuttle-attached assembly jig, automatically fabricates four triangular beams, each 200 meters long in the first two days on orbit. Retention of the completed beams is provided by the assembly jig.

The beam builder then moves to the position shown for the third day and fabricates the first of nine shorter, but otherwise identical, cross beams. After cross beam attachment, the partially completed assembly is automatically transported across the face of the assembly jig to the next cross beam location, where another cross beam is fabricated and installed. This process repeats until the "ladder" platform assembly is complete.

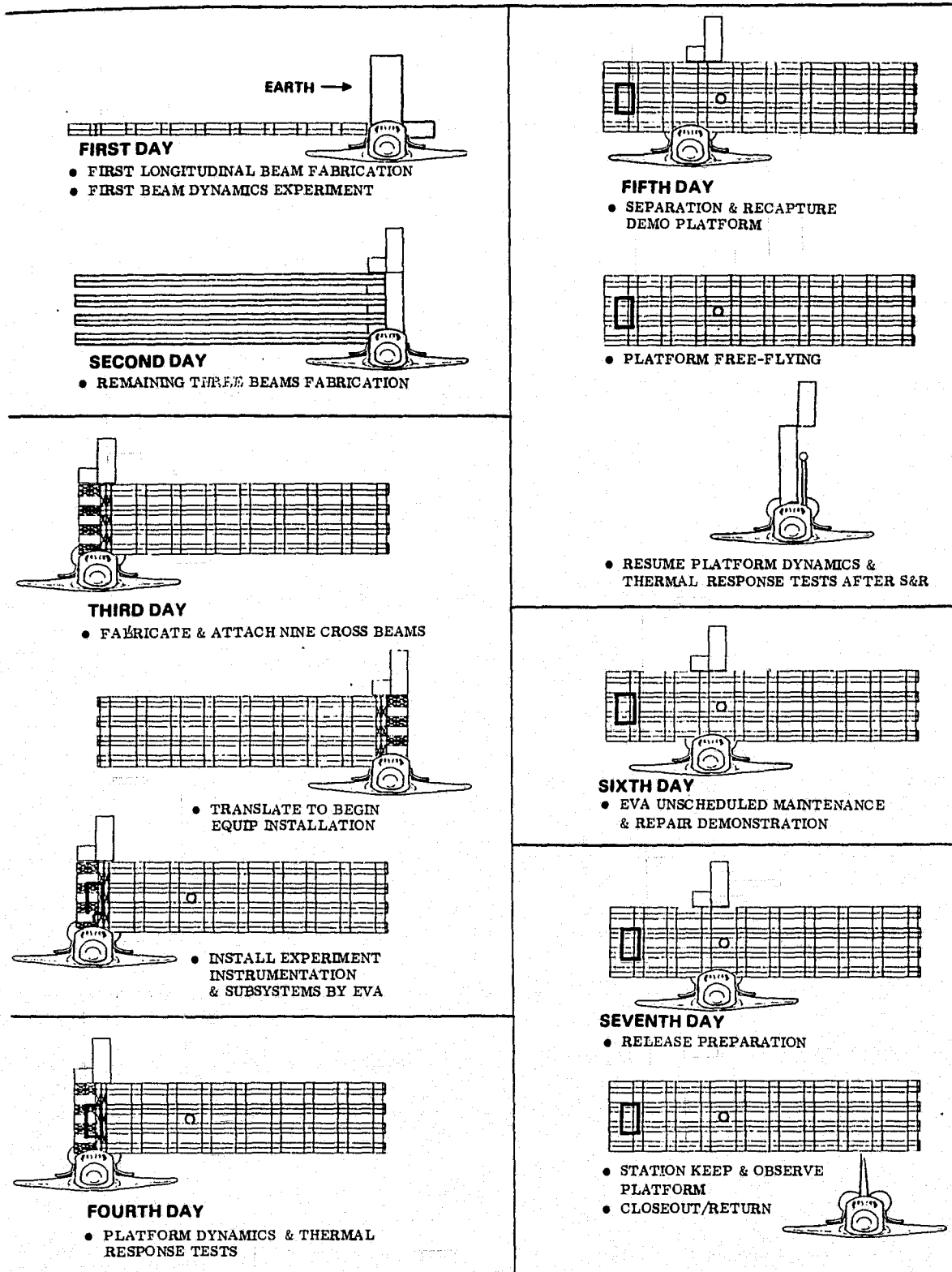


Figure 3-25. Beam/platform/Orbiter positions.

Section 3.6.2 presents experiment timelines and Section 3.6.4 discusses the EVA activity. Figure 3-26 shows the general arrangement of the equipment on the platform in the free-flying configuration. Figure 3-27 shows the subsystem installation, details of which will be discussed in a following section. The instrumentation installation details are shown in Section 3.6.4.

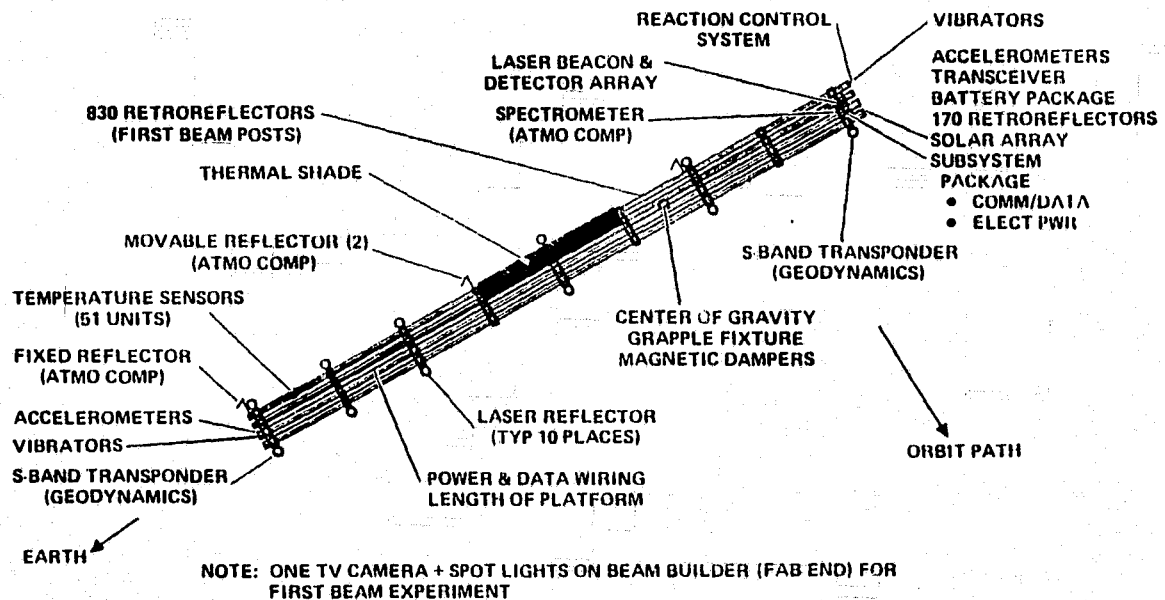


Figure 3-26. Platform equipment general arrangement.
(Experiment plus Subsystems)

The orientation of the platform in the free-flying mode is in the plane of the orbit aligned with the local vertical with the subsystem end pointed away from earth so that the solar arrays are pointed toward the sun.

Figure 3-28 indicates the SCAFE program mission profile. All the objectives of the SCAFE can be met during the first Orbiter flight and within the next 45 days of free flight. In addition, the equipment for the geodynamics and atmospheric composition experiments can be installed on the platform on the first flight. The atmospheric composition experiment will be performed for a short time after the shuttle departs and the monitoring and testing of the platform and the geodynamics experiment will be performed alternately during the first 45 days of free flight. At that time, an optional revisit mission by the Orbiter can bring up additional applications experiment equipment. This would be a cost-effective use of the platform. If this happened, these experiments could be run for about 45 days before the platform would have to be spun up to perform the second part of the atmospheric composition experiment. This should be plenty of time to accomplish additional meaningful experiments, taking advantage of the platform already in orbit. If there is no second flight, the second part of the atmospheric composition experiment can begin as soon as the platform and geodynamics experiments are concluded.

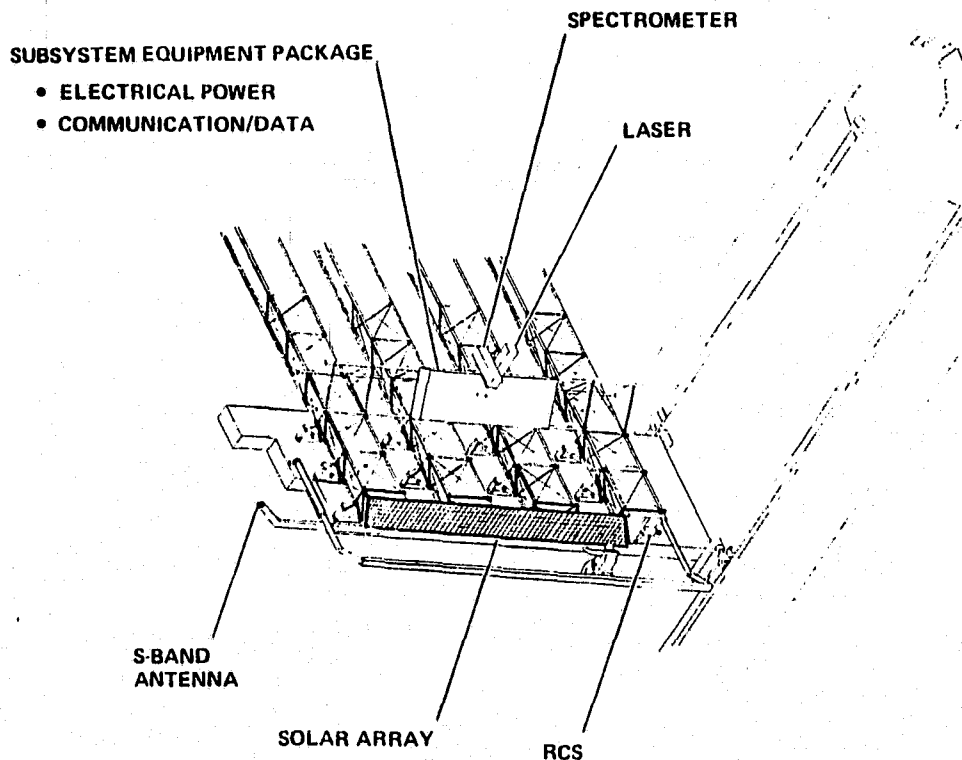


Figure 3-27. Subsystem installation.

3.6.2 EXPERIMENTS TIMELINE. Figure 3-29 defines the timeline for structural response and separation/recapture experiments previously discussed while the platform is attached to the Orbiter. It also indicates the period of checkout for the scientific experiments before free flight of the platform and the atmospheric composition experiment time while attached to the Orbiter and just after separation. The crew activities including EVA to go along with the experiments are described in Section 3.6.4.

Figure 3-30 gives the overall mission experiment timeline for the proposed six months including an optional revisit mission to bring up additional applications experiments to attach to the platform. There would be several days available to perform some of these experiments attached to the Orbiter and approximately 45 days to perform them with the platform free flying before it is spun up for the final portion of the atmospheric composition experiment, which goes on until the platform orbit decays and the platform enters the atmosphere. It appears that, after the second Orbiter mission, boosting the platform to a higher orbit to increase its life may be cost-effective. This is something that should be analyzed in the next study phase.

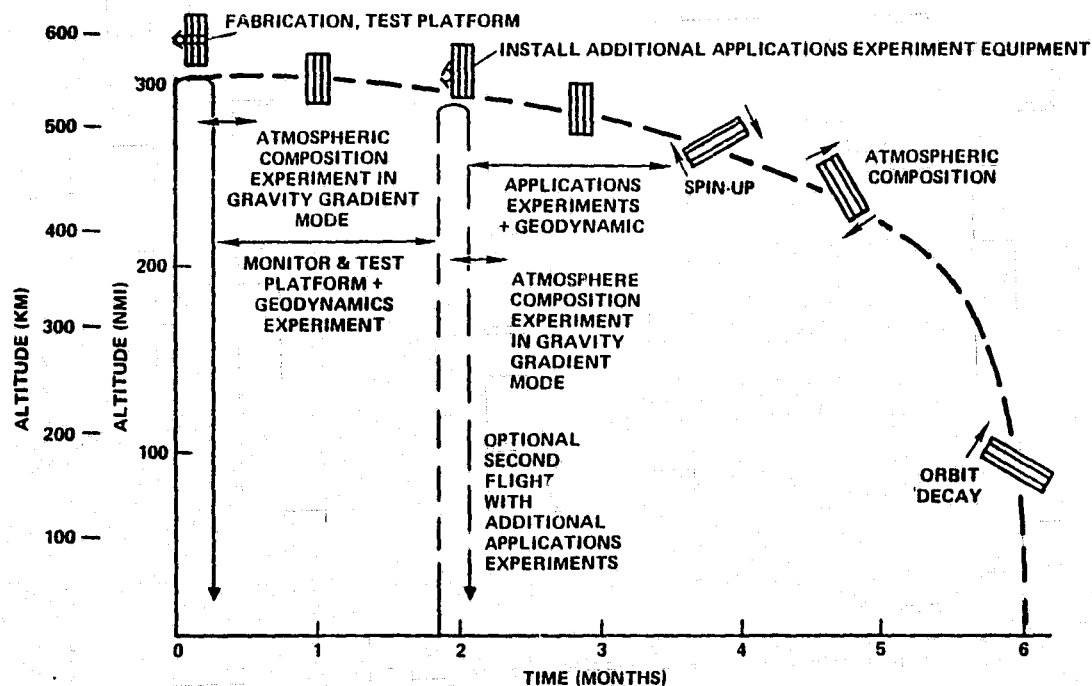


Figure 3-28. SCAFE program mission profile.

3.6.3 SUPPORTING SUBSYSTEMS. The requirements and the initial selection of subsystems for the SCAFE dynamic response/thermal deflection experiments and to support the representative applications experiments are described in this section. The selected subsystems will be composed of standard spacecraft parts to minimize cost.

3.6.3.1 Electrical Power. Figure 3-31 shows the installation of the solar array at the end of the platform. This approach was proposed previously by JSC and the subsystem has not been analyzed in any depth nor have trade-offs been performed to see if it is the optimum way to go, because the applications experiments which are to be run on the beam are only representative. Their requirements have not been derived in detail. The area shown on the figure was previously determined to be adequate for the atmospheric composition experiment. (The rationale will be summarized below.) We only checked to see that, with the original assumptions of energy available from this arrangement, the requirements for the structural response/thermal deflection experiments can be met. Future study activity should investigate an optimum power generation system, taking into account the inefficiency of the solar array system on the end of the beam with its intermittent exposure to sunlight during the orbit and the added payload capability available for batteries. In addition, the detailed experiment requirements and the number of times the experiments need to be conducted should be a part of the system analysis.

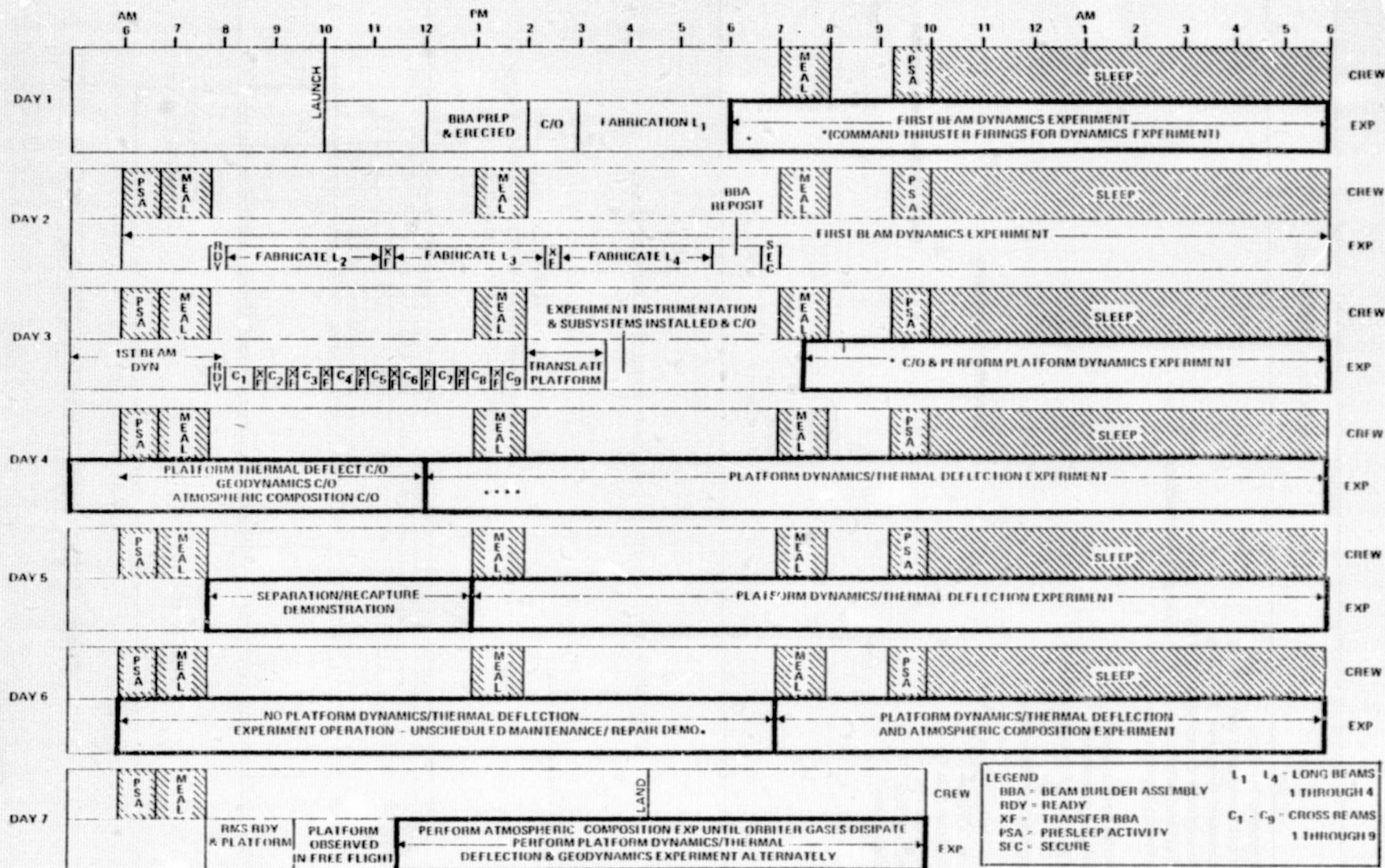


Figure 3-29. Experiment timeline.

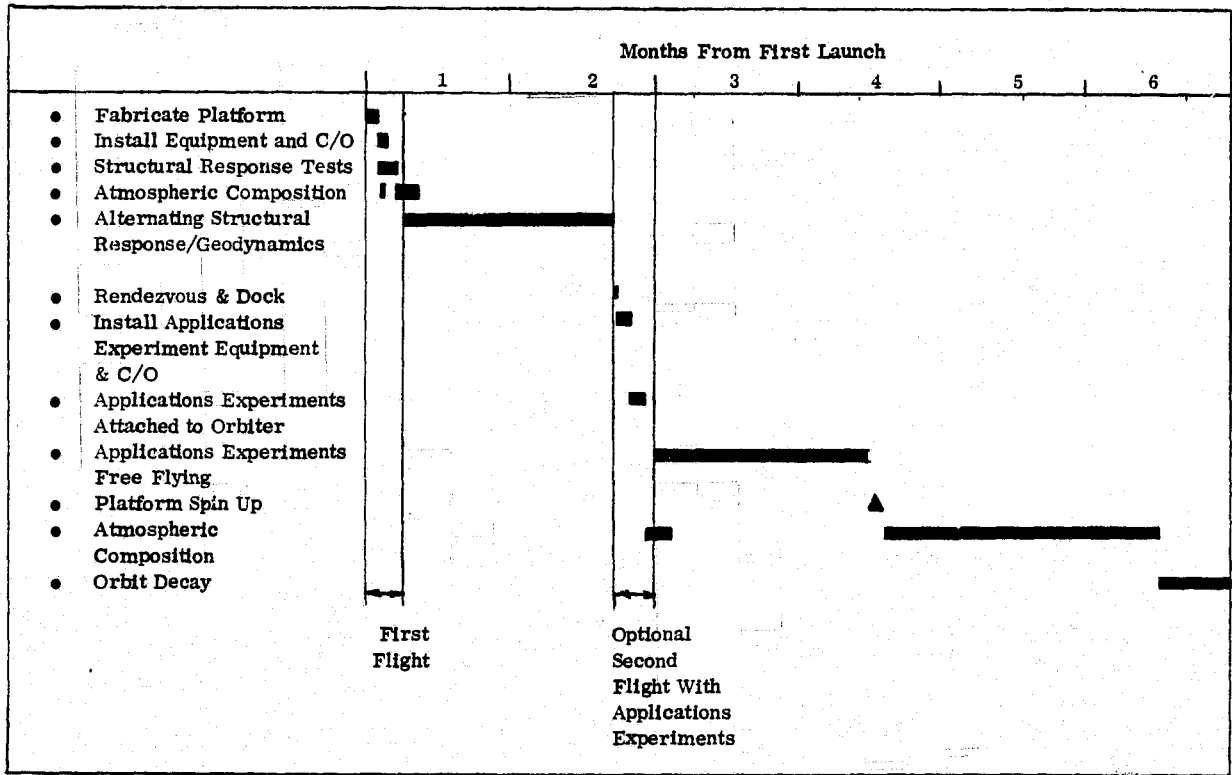


Figure 3-30. Overall mission experiment timeline.

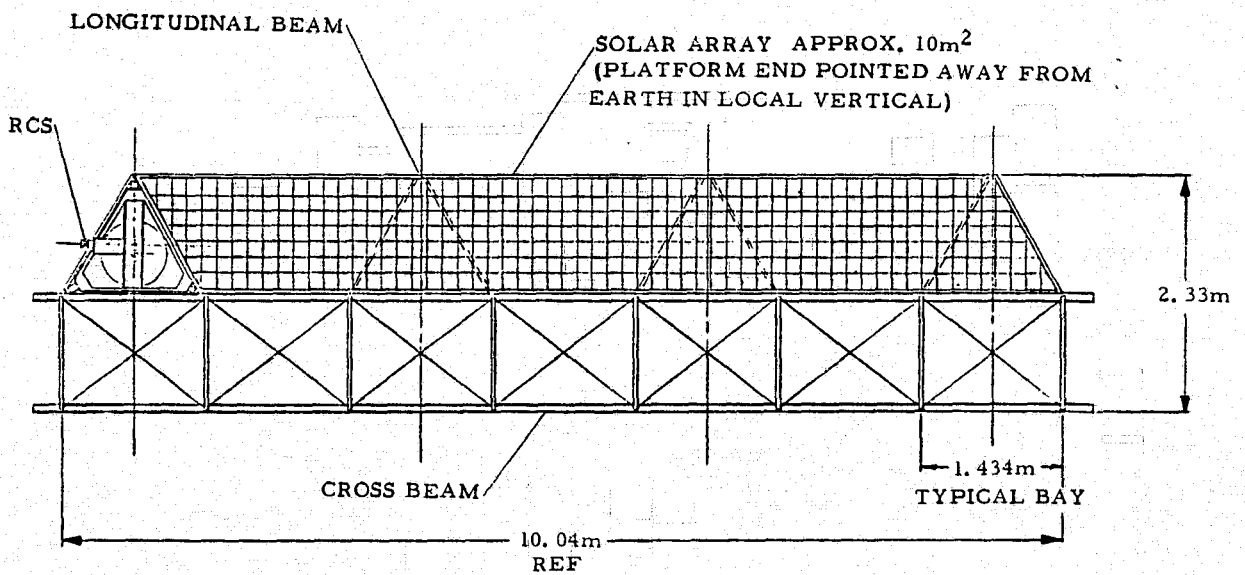
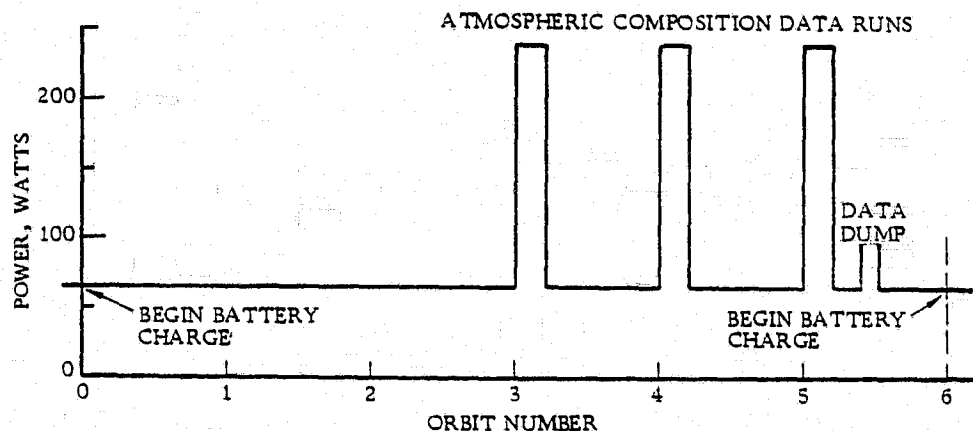


Figure 3-31. Solar array installation.

JSC analysis had determined that, in a gravity stabilized mode, the energy per orbit including battery charging losses at $\beta = 53^\circ$ (worst case) was 284 W-h. With the platform rotating in orbit, the energy available per orbit is 135 W-h minimum. Figure 3-32 shows the power profile-limiting case for the atmospheric composition experiment. The proposed approach is to begin battery charging about three orbits ahead of start of the atmospheric composition experiment runs. The batteries would then have sufficient reserve to supply the power needed for the experiment. The geodynamic experiment power requirements are less than the atmospheric composition requirements, therefore, it can also be accommodated.



NASA DATA:

- PLATFORM ROTATING IN ORBIT PLANE
- SUB-ORBIT PLANE ANGLE = 53° (WORST CASE)
- SOLAR CELL AREA = 9.7 m^2
- BATTERY WEIGHT = 93 kg
- 3-FOR-2 BATTERY REDUNDANCY

Figure 3-32. Power profile-limiting case.

Figure 3-33 shows the power requirements for the platform dynamics/thermal deflection experiment data runs. It is assumed that the laser motor is running all the time and that the vibrators have a narrowed down frequency range (selected while attached to the Orbiter). The MMS communication and data handling subsystem is considered to be in a standby mode all the time, requiring about 100 watts. The communication system, when transmitting, the vibrators, and the laser system peak out at about 230 watts. The vibrators need to be on for about a quarter of an hour and the laser measurement system for about one half hour. The total energy required is well within the output of the solar array as determined by JSC.

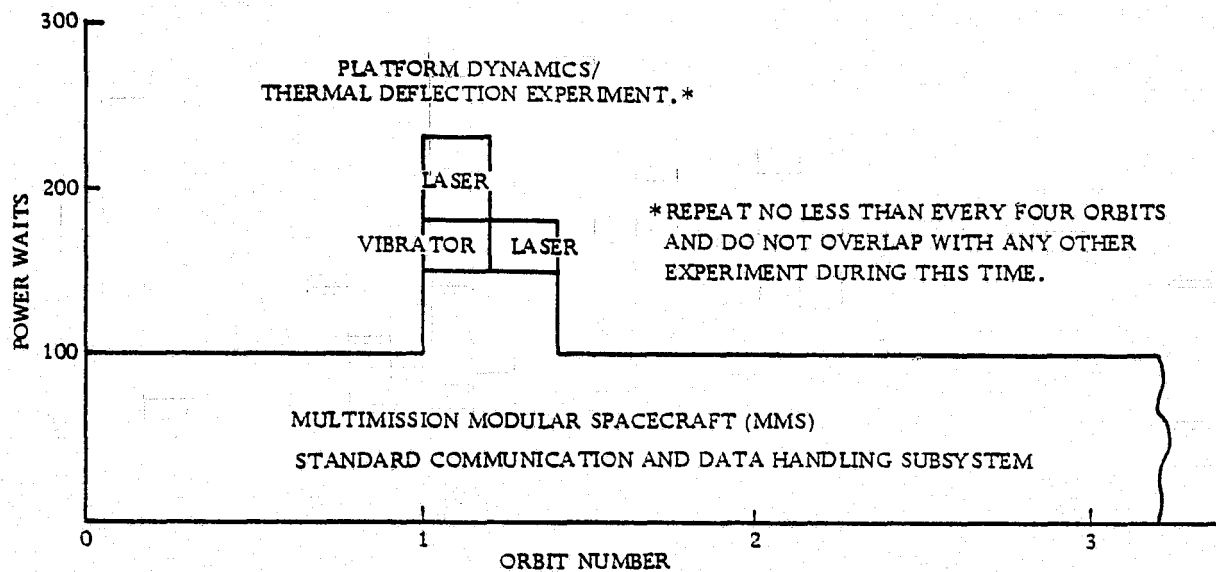


Figure 3-33. Platform dynamics/thermal deflection experiments power requirements.

3.6.3.2 Platform Avionics. The platform will require a capability to: (1) receive, decode, and distribute commands to platform and experiments; (2) collect, code, and transmit experiment and platform data; and (3) provide on-orbit control and monitoring of platform and experiment functions as required. The baseline equipment adopted for these functions is to use a multimission spacecraft communication and data handling module. This equipment includes the transponders, data processor, and data bus system for distribution of command and acquisition of data. Although this baseline capability exceeds the current capability requirements, it is felt that it is a good choice because it: (1) is standard NASA equipment, (2) provides for addition of other SCAFE platform and experiment function, (3) will be developed, tested, and in production during the experiment time frame.

3.6.3.3 Attitude Control. While the platform is free flying in the gravity gradient stabilized mode with its long axis vertical, magnetic dampers have been added to the structure (54 kg) to reduce oscillations due to separation from the Orbiter and the environment. The requirements are derived in Section 4.2.

The gravity gradient mode will be used until it is time to spin up the platform for the final portion of the atmospheric composition experiment. Previous analysis by JSC of the experiment requirements indicated that a rotation rate of about 1/15 rpm about the maximum moment of inertia axis is preferred. Also, the rotation axis should be placed perpendicular to the orbit plane for best stability. JSC determined that the

spinup could best be accomplished by cold gas thrusters at one end of the platform (Figure 3-26) using less than 2.5 kg of propellant.

Table 3-6 indicates the subsystem components selected by JSC to perform the required spinup for the experiment.

Table 3-6. Attitude control system.

Component	Mass kg (lb)	
Magnetic Damper	54	(119)
Thrusters, Valves, and Plumbing	21	(46)
Propellant and Tanks	39	(86)
Control Electronics	20	(44)
Horizon Sensors	10	(22)
Mounting	10	(22)
Total	154	(339)

3.6.4 EVA. Figure 3-34 depicts the crew activities scheduled to take place during the seven-day flight. The EVA activities are highlighted in the figure and are identified and described in the following paragraphs.

Day 1 EVA, 2.5 hours (5 manhours), will be used to visually inspect the beam-builder equipment to verify that it is in the proper configuration prior to starting automatic beam fabrication. Day 1 EVA will also be used to prepare the experiment equipment for installation on the third day. The smaller equipment items will be moved from the Orbiter bay and tethered to the EVA carriage. The subsystem unit to be installed on the end of the platform will remain stowed in the Orbiter bay until the third day of the mission.

Day 1 EVA will be performed by the mission specialist (MS), wearing his extra-vehicular mobility unit (EMU), and the pilot (PLT), wearing his EMU and a manned maneuvering unit (MMU) (Figure 3-35). The MS will translate to and from work positions using combinations of Orbiter-provided handrails and pre-positioned remote manipulator system (RMS). The PLT will translate to and from his work positions with his MMU.

The MS will exit the airlock and translate to the erected and locked beam builder and start his visual checks. The PLT will exit the airlock and translate to the MMU station, don and check out his MMU, and translate to the beam builder assembly to assist the MS. When the checkout of the beam builder assembly, EVA bridge, and carriage are complete, the PLT will translate to the experiment stowage area. He will unstow preselected components and transfer them to the MS for tethering in pre-selected locations on the bridge assembly, for installation on Day 3.

Day 3 EVA, 3.5 hours (7 manhours) will be used to install the experiment equipment. This will be accomplished by translating the platform to preselected positions

3-42

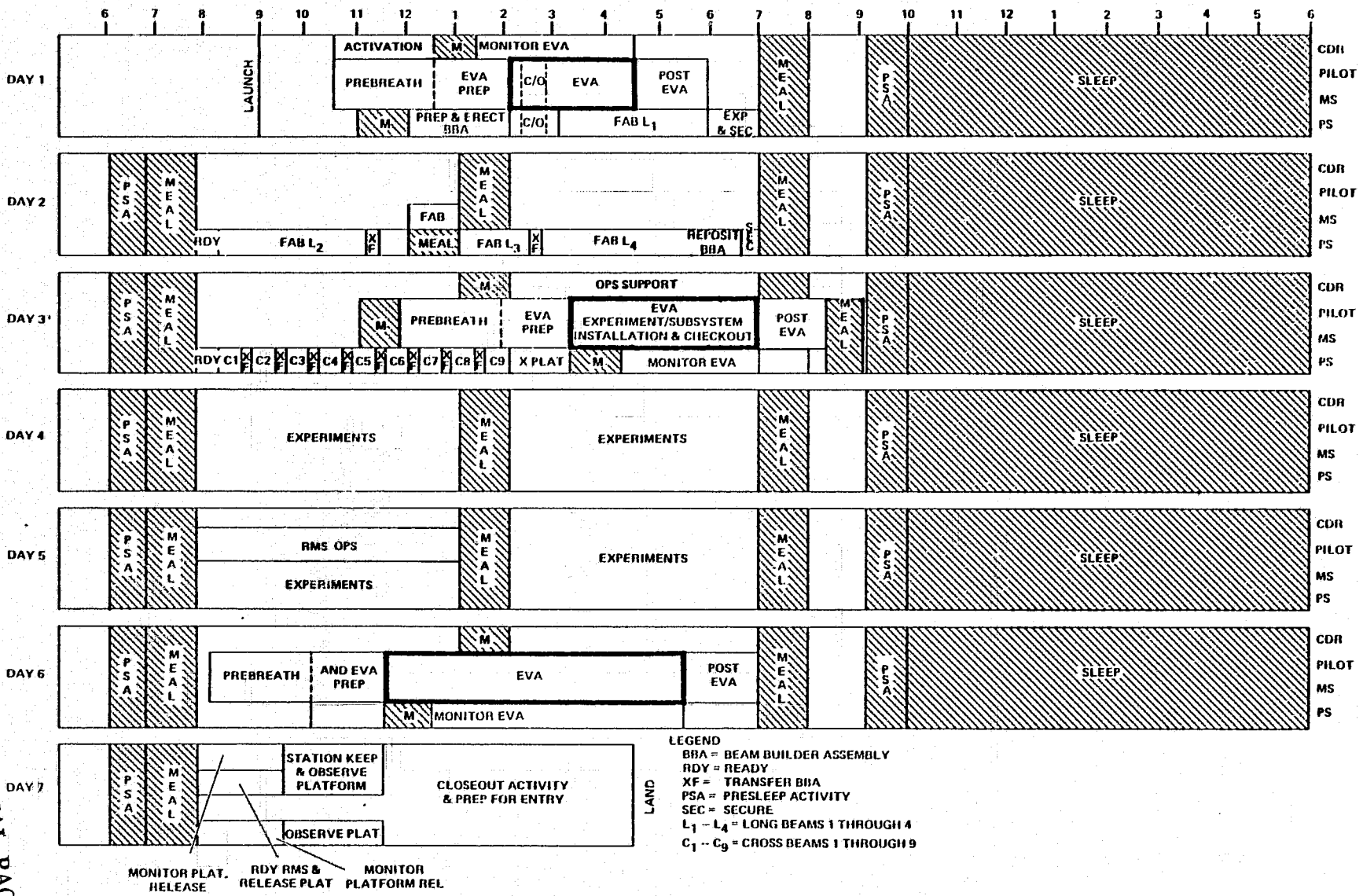


Figure 3-34. Crew activities.

ORIGINAL PAGE IS
OF POOR QUALITY

under the MS, who will be restrained in the EVA carriage work stations as shown in Figure 3-36. The experiment instrumentation/subsystem/components to be installed are listed in Tables 3-7 and 3-8. Their locations on the platform are shown in Figures 3-26 and 3-27. Specific details of instrumentation/subsystem/component installation are shown in Figure 3-37 and 3-38. Hardwiring will be accomplished by the MS and PLT pushing wiring shuttles through the long beams. The wiring shuttle concept is shown in Figure 3-39.

Day 3 EVA will be performed by the MS and PLT. The EMU and MMU setup will be the same as for Day 1.

Day 6 EVA, 6 hours (12 manhours), will be used to demonstrate unscheduled maintenance on the platform. Un-scheduled maintenance tasks will include:

- a. Platform Repairs
 - Cap Repair
 - Cord Repair
- b. Beam Builder Repairs
 - Remove and replace cap-forming reel
 - Remove and replace cord reel
 - Remove and replace spot welder head
 - Remove and replace roll-trusion head

Day 6 EVA will be performed by the MS and PLT wearing EMUs and MMUs. MMUs were selected for their utility as work stations as well as their capability to translate along the beam without physically touching it. Figure 3-40 illustrates MMU-supported platform repair activity. Figure 3-41 is a time line of Day 6 EVA.

In the event that all of the experiments cannot be performed in the normal seven-day mission a few days extension could be tolerated by the crew provided that extended EVA are not planned for consecutive days. Table 3-9 shows crew equipment and consumables charged to the payload for normal and extended sortie missions.



- MMU PROVISIONS
- ASTRONAUT TRANSLATION TO SPECIFIED POSITION ON PLATFORM
 - REMOTE WORK STATION
 - SAFETY BACKUP (RESCUE)

Figure 3-35. Astronaut wearing MMU.

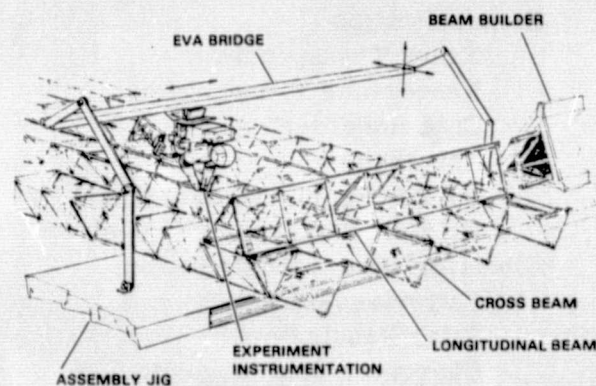


Figure 3-36. EVA work station.

Table 3-7. On-orbit experiment instrumentation.

ITEM	REQUIREMENT
Structural Response	
Instrumentation	
Sunshades	2
Accelerometers	5
Temperature Probes	51
Retro Reflectors (Installed on ground)	(1000)
Laser	1
TV Camera	1
Controls and Displays (In orbiter on ground)	(x)
Laser Retro Reflectors	10
Vibrators	2
Geodynamics	
S-Band Transponder *	2
Atmospheric Composition	
Spectrometer and Radiation Source *	1
Fixed Reflector *	1
Movable Reflectors *	

* Scientific Experiment - GFE x Quantity to be done

Table 3-8. On-orbit structural fabrication equipment support subsystems.

ITEM	REQUIREMENT
Spares for Simulated Repair	x
Platform Subsystems	x
Communication	
Track Transponder	1
Rendezvous Transponder	1
Data Recorder	1
Antennas	x
RF Downlink (Telemetry package)	1
RF Uplink (Telemetry receiver)	1
Electrical Power/Distribution	
Batteries (secondary) *	x
Solar Panels *	x
Charge Central/Regulators *	x
Interconnecting Wiring	x
Attitude Control *	
Thrusters (cold gas), Valves, and Plumbing	x
Propellant Tanks	x
Control Electronics	x
Horizon Sensors	x
Magnetic Dampers	x
Grapple Fixture	1

* Scientific Experiment Support - GFE x Quantity to be determined

ORIGINAL PAGE IS
OF POOR QUALITY

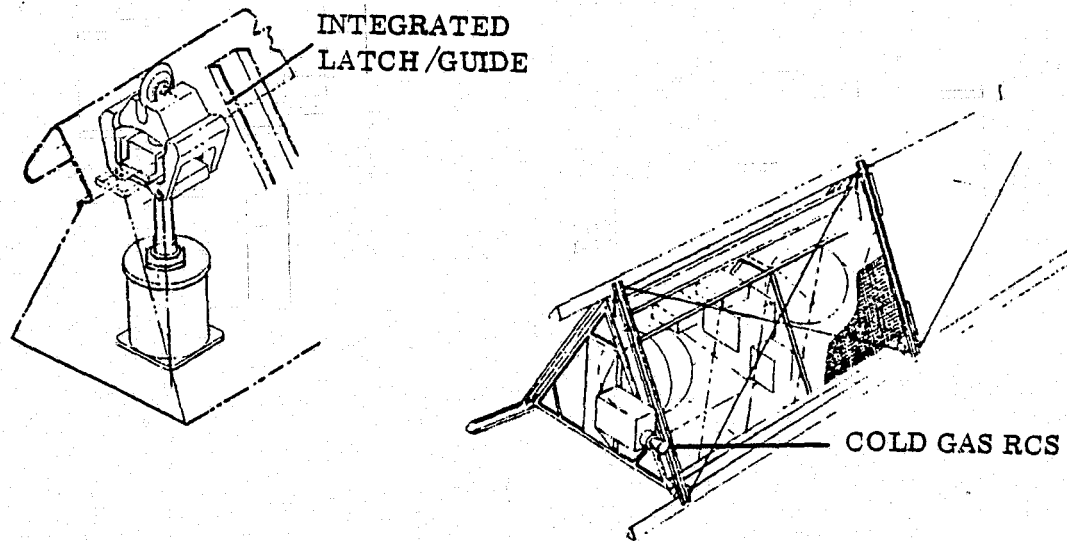


Figure 3-37. Equipment module installation.

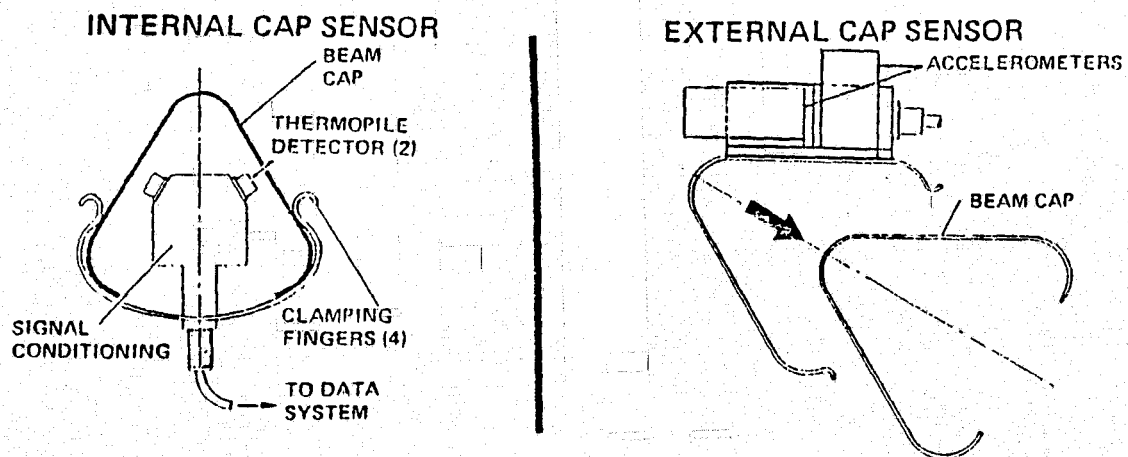


Figure 3-38. Instrument installation concepts.

ORIGINAL PAGE IS
OF POOR QUALITY

3.6.5 GROUND OPERATIONS. Figure 3-1 shows the top level operational flow for the SCAPE program and depicts the three major ground activities and locations where these are proposed to take place. Factory acceptance testing will take place at the contractor's facilities. Equipment integration, referred to as Level IV integration, of the structural experiment equipment and instrumentation, scientific experiment equipment, and supporting subsystems will take place at JSC. Launch site operations, including Levels III/II/I integration, will take place at KSC.

During factory acceptance testing, a section of beam will be constructed under ambient conditions to check the end-to-end

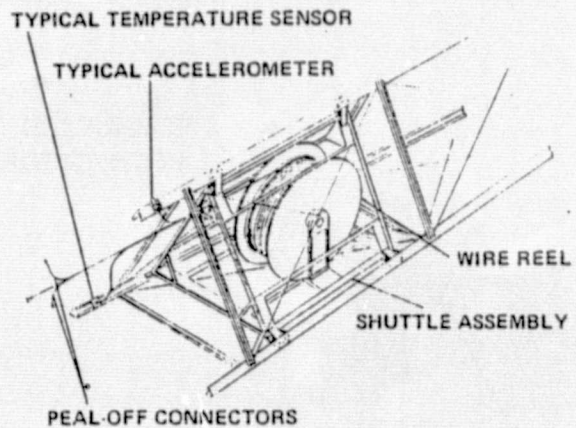


Figure 3-39. Wiring shuttle concept.

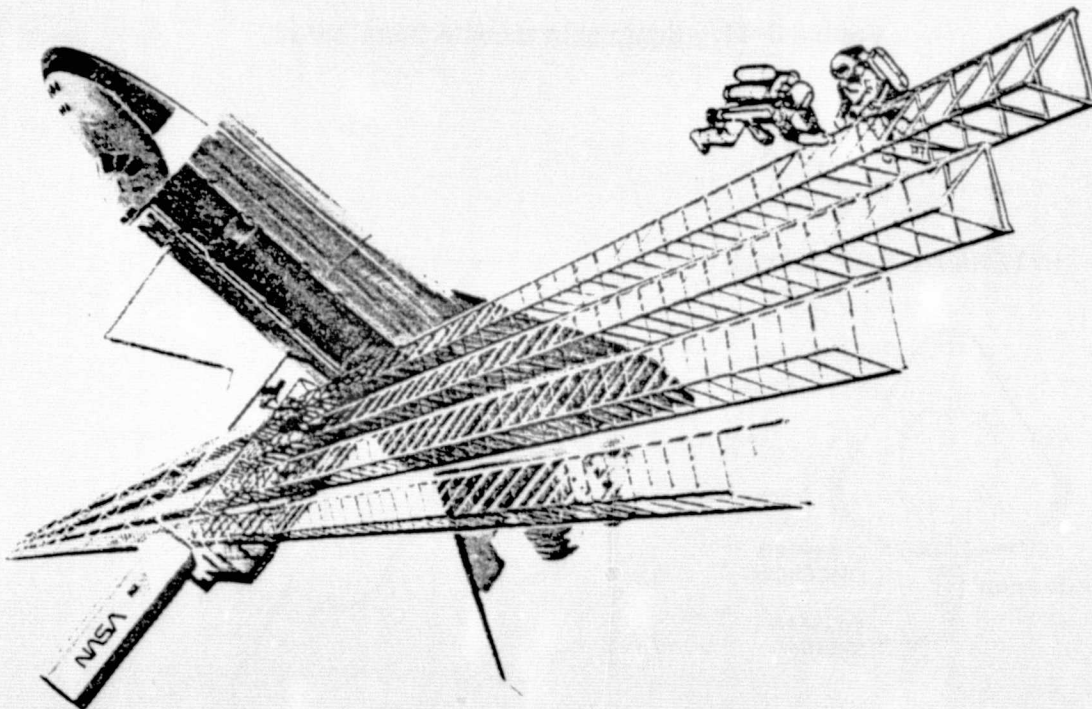


Figure 3-40. Platform repair using MMU.

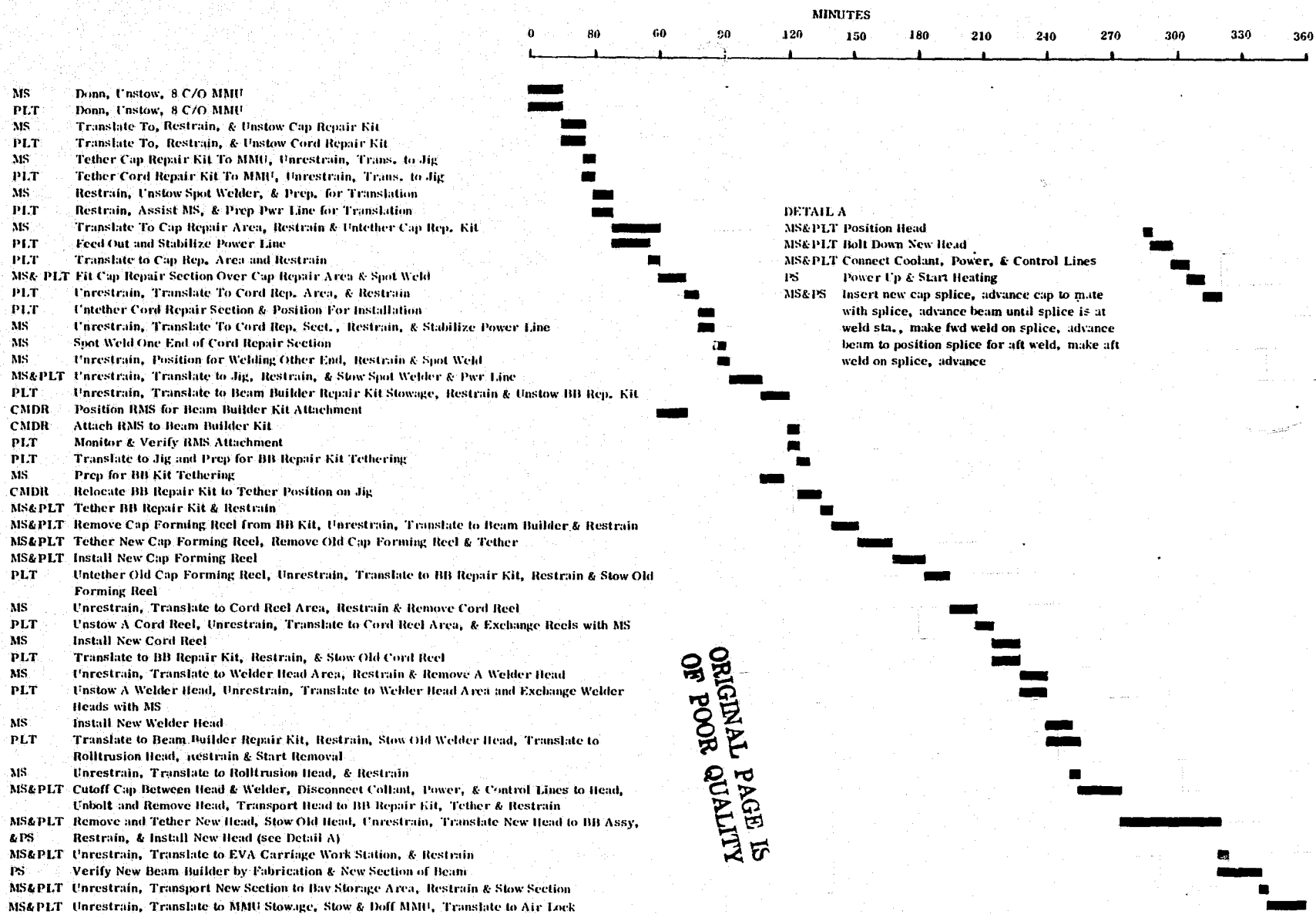


Figure 3-41. Timeline Day 6 EVA activity.

Table 3-9. Extended mission crew provisions.

Item	Weight (kg)	Payload Chargeability
Orbiter		
Food	1.51	Per Manday Above Baseline of 28 Mandays
LiOH Canisters	1.45	
Stowage Containers	12.95	Per Mission Day Above 7
Flight Operations Equipment	1.18	
Hygiene Equipment	1.27	
Crew Provisions	2.90	
Miscellaneous	0.15	
Cryogenic O₂ Plus System Hdw	729.	
GN₂ Plus System Hdw	64.9	Above 10.5 Days — To 14 Days
Airlock Repressurization		
O ₂	1.2	Per Repressurization
GN ₂	3.9	Orbiter Baseline (24 MH)
Extravehicular Maneuvering Unit		
Recharge		
O ₂	.72	Per EVA Above Orbiter
H ₂ O	4.5	Baseline (24 MH)
Back Pack LiOH Cartridges	2.5	One Per Crewman Per EVA Over Two
Prebreath LiOH Cartridges	1.8	One Per Crewman Per Prebreath Over Two
MMU Recharge GN₂	3.0	Each MMU Recharge

functional capability of the beam builder, including its alignment accuracy. Sections of dummy beams will be translated through the assembly jig to check the translation mechanism and position sensing indicator along with positioning and retracting the retention and guide mechanisms. After factory checkout, the completed beam builder, assembly jig, experiment instrumentation, and Orbiter aft flight deck (AFD) SCAFE control and monitoring equipment will be delivered to JSC for Level IV integration. Level IV tasks consist of installation of the above equipment and the GFE experiment subsystems and instrumentation, interface verification testing, and checkout activities. Typical tasks are: (1) fabricating a short length of beam in a vacuum chamber for final check prior to flight, (2) fabricating two bays of the beam to prime the beam builder for flight, (3) installing equipment and instrumentation packages on the assembly jig and cradle, (4) test and checkout of the subsystems integration, (5) electrical and data interface proofing, and (6) software checkout with Orbiter GPC simulation, etc. A preliminary Level IV integration flow diagram is shown in Figure 3-42. The corresponding requirements are summarized in Table 3-10.

Subsequently, the flight unit will be delivered to KSC for off-line integration with Orbiter simulation equipment and with on-line Orbiter equipment. The SCAFE equipment will be installed with the Orbiter in the horizontal position in the Orbiter Processing Facility. It will not require special environmental monitoring or control during any ground operations phase, nor time-critical prelaunch access at the pad. Payload handling in the vertical position is not planned; however, it is not precluded by design. A preliminary Level III/II flow diagram is shown in Figure 3-43. The requirements for Level III/II integration are given in Table 3-11 and for Level I in Table 3-12.

Post mission analysis of the on-orbit test data and the free flight test data being received will take place at JSC. In addition, post mission inspection of the beam builder and assembly jig will be performed. Any required refurbishment for an optional revisit applications flight for the assembly jig and the beam builder, if required, will be performed at JSC.

3.6.6 MISSION OPTIONS. Analysis of the SCAFE payload weight, on-orbit construction time, dynamic and thermal response test time, EVA equipment installation and platform unscheduled maintenance demonstration time, and time for a platform separation and recapture test has shown that the required equipment weight is well within the Orbiter payload capability and the Orbiter-attached time conservatively allocated to the above tasks falls well within the nominal seven-day shuttle mission. Some structural experiments can continue in the free flight mode as long as desired. As far as accomplishing all the SCAFE objectives, one seven-day mission is all that is required.

This report has indicated that there is excess payload capability available for additional applications experiments. Two experiments (described earlier) were chosen as representative of additional scientific experiments that may be transported to orbit on the SCAFE mission, set up after the platform has been fabricated, and performed during free flight after the Orbiter has returned to earth. This makes cost-

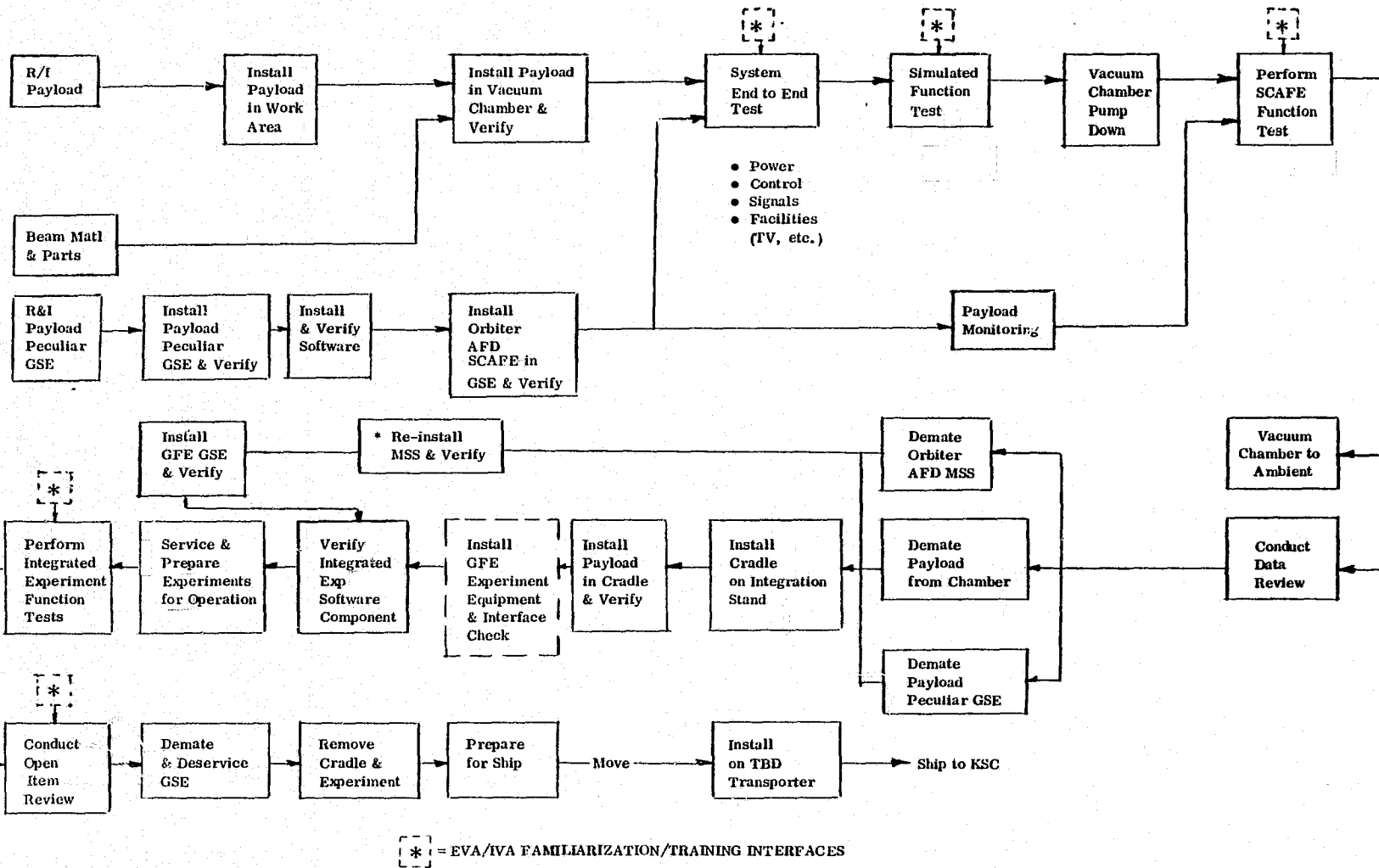


Figure 3-42. Preliminary Level IV integration flow diagram.

Table 3-10. Level IV integration requirements summary.

Function	Experiment Requirements
Install payload in vacuum chamber and verify	Install beam builder
System end-to-end check	Check beam builder and assy jig to AFD equipment to power controls, signals, and monitoring equipment such as TV cameras, etc.
Perform SCAFE function test	Verify beam builder can fabricate acceptable beam under simulated space conditions and prime beam builder.
Demate payload from vacuum chamber	Remove beam builder from vacuum chamber primed for space operation.
Install payload in cradle and verify	Integrate structural experiment equipment with cradle. <ul style="list-style-type: none"> ● Beam Builder ● Assembly Jig ● Structural Exp. Subsystem ● Structural Exp. Instrm. Pkg.
Reinstall MSS	Experiment control, CRT, keyboard, C&W
Load software and verify load	Loader, compilers
Install GFE experiment equipment and interface check	Orbiter GPC software. GFE software
Verify integrated experiment software compatibility	Experiment C/D and control
Service & prepare experiments for operation	Fill & bleed coolant loop Prepare TV, film camera, laser, Load tape recorders & film cameras Load EVA equipment & check access
Perform integrated experiment function tests	Crew command/control interfaces, mission sequence simulation and MSS training.

Table 3-11. Level III/II off-line integration requirements.*

-
- Install payload equipment in CITE test stand
 - Install experiment equipment in simulated AFD
 - Install experiment GSE
 - Connect and verify GSE-to-Experiment interfaces
 - Service and prepare payload for operation
 - Load
 - Spares for simulated repair
 - Recorder tape reels (data & video)
 - Camera magazines
 - Packaged laser reflectors with brackets
 - Packaged accelerometers & temperature sensors
 - Portable weld unit
 - Service
 - Fill and bleed coolant loop and cold gas tanks and activate batteries
 - Power-up tests
 - Load experiment flight software and verify load
 - Perform mission sequence simulation
 - Reservice experiment equipment for flight
 - Remove payload from test stand and GSE and move to Orbiter processing facility
-

* Conducted in the Operations and Checkout Building

Table 3-12. Level I on-line integration requirements.

-
- Install payload equipment in Orbiter payload bay
 - Install experiment equipment at Orbiter AFD MSS & on-orbit station
 - Connect and verify Orbiter-to-payload interfaces
 - Prepare for Orbiter integrated tests including:
 - Load exp. flight software and verify load
 - Verify uplink commands and downlink data flow (Note 2)
 - Verify communications network (TDRSS & POCC) (Note 2)
 - Perform Orbiter integrated tests
 - Payload final servicing including:
 - Verify launch locks
 - Remove lens covers from TV/cameras
 - Stow equipment in orbiter cabin
-

- Notes:
1. Time, access resources, and operations are assumed to be shared with potential secondary payload equipment
 2. Extent of payload participation TBD

ORIGINAL PAGE IS
OF POOR QUALITY

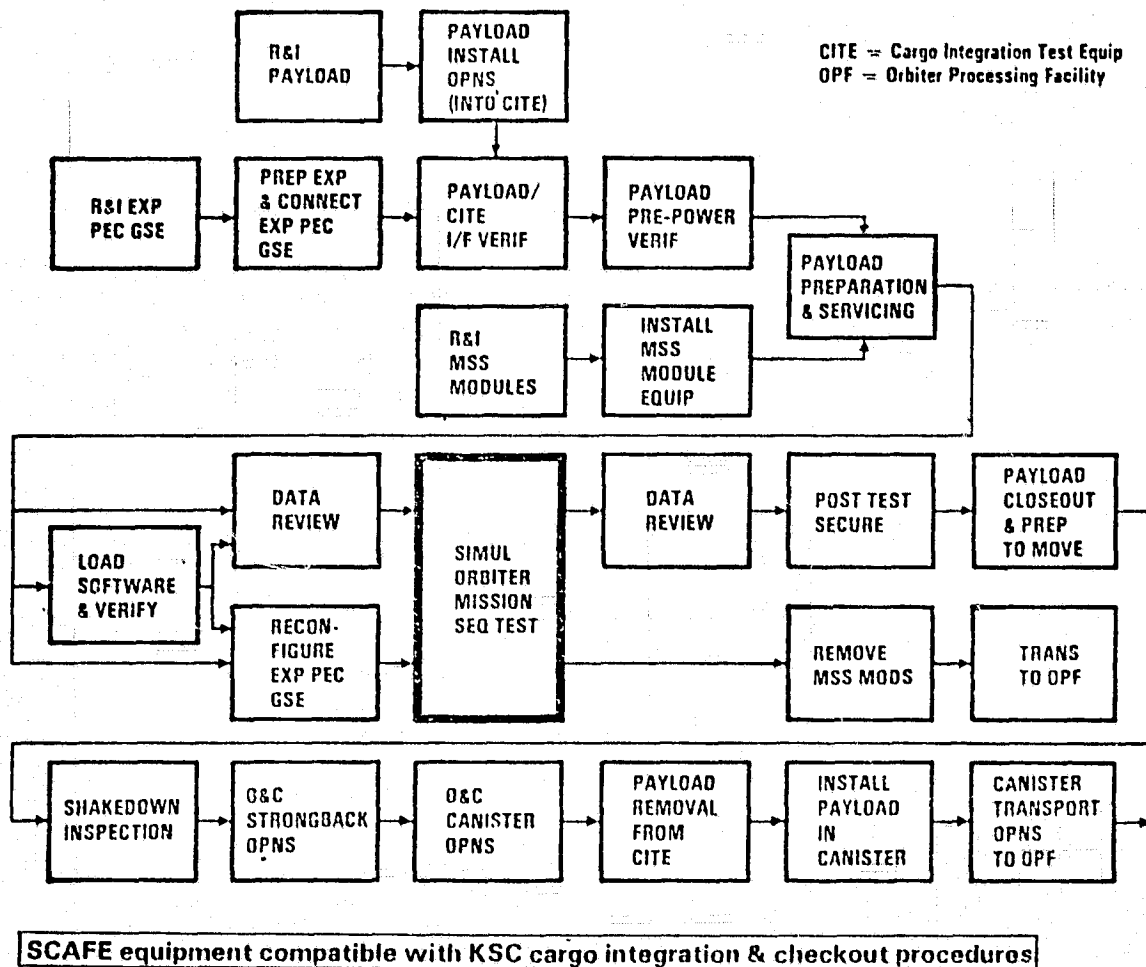


Figure 3-43. Preliminary Level III/II payload integration flow diagram.

effective use of the platform after the fabrication process and the response tests have been accomplished. The selected applications experiment equipment falls well within the net payload capability of the Orbiter and, in fact, there is some additional volume and weight available for larger applications experiments or additional ones. In Section 3.6.4 it was shown that we allowed 3.5 hours of EVA on Day 3 to install the structural and thermal response experiment along with the grapple fitting. In addition, the installation of the applications experiment equipment was also included in this 3.5 hours. Since all of this equipment is installed at the assembly jig using the EVA bridge for support, this appears to be enough time. If it is found in the next phase of the study that more time than the 3.5 hours is required to perform these combined tasks, several alternatives present themselves: (1) additional EVA time can be taken on Day 6 to install applications experiment equipment and less time can be

spent on platform unscheduled maintenance demonstration, (2) a revisit mission can be performed within two months of the first mission to carry up and install the additional equipment, or (3) the first mission applications experiment can be extended for a day or two to provide the required time for installing all the applications experiment equipment.

Approach number one reduces the time to be spent for contingencies or demonstration of the SSAFE experiment and is not recommended.

Approach number two is not cost-effective at all. An optional revisit should be planned to take up additional experiment equipment that can't be accommodated within the payload capability of the first mission. To pay additional shuttle user fees to carry up and install equipment that can be accommodated on the first flight is not cost-effective.

Approach three is the recommended approach. Table 3-9 shows that for an additional one-day mission time with an extra EVA the weight of consumables is approximately 110 kg. The EVA schedule can be changed to have EVA on the fifth and seventh days and return to earth on the eighth day so the groundrule of no EVA on consecutive days can be observed.

The additional RCS propellant for the Orbiter would also be very small. During EVA, approximately 13 kg of propellant will be used and only around 6 kg of propellant is needed for each additional day on orbit. This is well within the propellant capacity carried by the Orbiter. In addition, the electrical energy required from the Orbiter is well below the allowable for a nominal 7-day mission, so no additional energy kits would be required for a 1- or 2-day mission extension. The extra day or two on orbit shouldn't impact the Orbiter turnaround schedule too drastically, especially if the experiments can be accomplished in a more cost-effective manner.

3.7 ORBITER COMPATIBILITY/INTERFACES

The SSAFE equipment and mission operations were developed for compatibility with known Orbiter characteristics/payload accommodations and physical/functional interface requirements. Specific areas of concern were: mass properties, structural supports, RMS utilization, subsystems interfaces, viewing/illumination, and aft cabin provisions. These topics are addressed in the following sections.

3.7.1 MASS PROPERTIES. Total system weight and the center of gravity were compared with Orbiter limits for the boost, abort, and normal entry flight modes. Figure 3-44 illustrates the stowage arrangement in the Orbiter cargo bay and indicates system weight and longitudinal (x-axis) cg versus Orbiter limits for the three flight modes of concern. Figure 3-45 provides similar data for each flight mode with respect to the vertical (Z-axis) limits. In all cases the SSAFE equipment complies with Orbiter maximum weight and cg position constraints.

3.7.2 STRUCTURAL SUPPORTS. The detailed arrangement of SCAFE equipment within the cargo bay is shown on Figure 2-71 in conjunction with the discussion of Flight Support Subsystems in Section 2.2.2.6.1. Mass properties of all SCAFE equipment are discussed in Section 4.1.

The locations selected for structural support within the cargo bay are summarized in Table 3-13.

The aft X/Z support point (No. 296) was selected to provide: maximum jig length with reasonable pivot diameter and deployment clearance from the OMS kit; coplanar longeron and keel fittings for cradle simplicity; high load capability; and a payload deployment trunnion. The cradle stabilizing support point (No. 284) permits sufficient span to react cradle/stowed equipment pitching moments while minimizing the length of clearance "notch" on the +Y side of the jig (which, in turn, influences the vertical coordinate of the Beam No. 1 RGM). It also provides high load capability (though not mandatory) and a payload deployment trunnion. The use of latching trunnions at the two cradle/cargo bay longeron support stations aids system emergency jettison in the event of critical malfunction. The jig stabilizing support point (No. 196) was selected: to provide high load capability (within the available set of supports between the fuselage frames at X_0 1905 and 2049.8); to reduce the X-axis bending span of the jig in the interest of minimizing Z-axis dynamic response without concentrating excessive beam builder inertia reactions on the lower capability forward Z-supports; and to provide mandatory latching trunnions to permit jig tilt-up to the fabrication position.

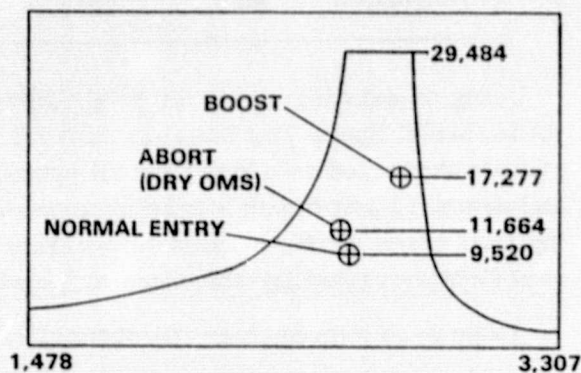
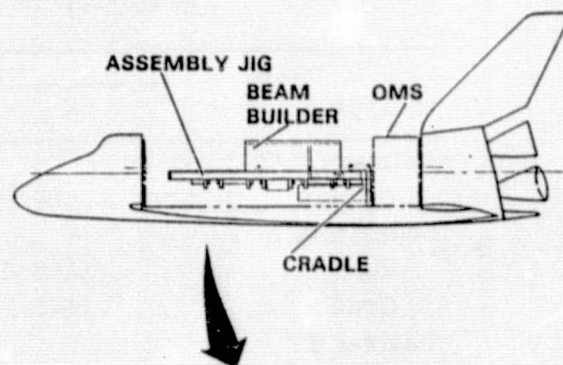


Figure 3-44. Weight/ X_{cg} compatibility.

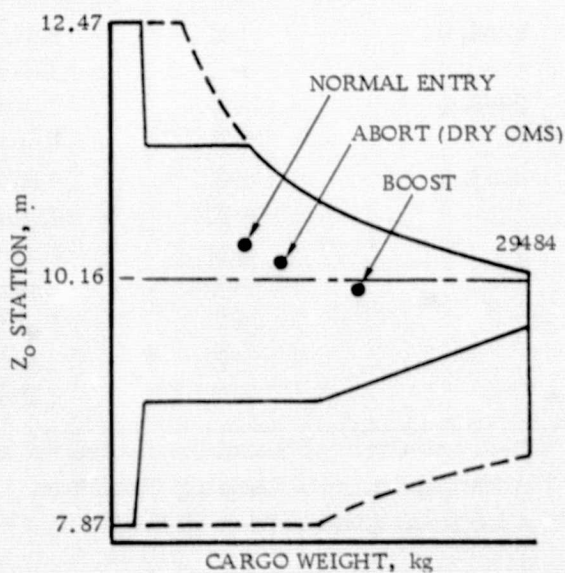


Figure 3-45. Weight/ Z_{cg} compatibility.

Table 3-13. Selected support locations.

Type	Location (cm)		
	X _o	Y _o	Z _o
Primary X/Z			
Cradle	2964.9	± 238.8	1051.6
Stabilizing Z			
Jig	1966.0	± 238.8	1051.6
Cradle	2845.1	± 238.8	1051.6
Lateral Y			
Cradle	2964.9	0.0	774.7

Using an existing computer program developed for the specific purpose in earlier NASA/MSFC Space Tug Studies, support reactions were computed, for the mass system supported as above, for all perturbations and combinations of Orbiter ascent and descent limit linear + angular accelerations. Maximum values and the governing load cases were provided as program output. These were compared with current Orbiter capability and found to lie within Orbiter limits in all cases.

Table 3-14 summarizes the support reaction comparison.

Table 3-14. Support reaction compatibility.

Station, X _o (cm)	Reaction Component	Governing Condition *	Reaction Magnitude (KN)	Orbiter Capability (KN)
1966.0	+Z	Entry: Pitch	+66.3	+278.9
	-Z	Liftoff	-36.5	-338.0 (-302.0)**
2845.1	+Z	Liftoff	+79.2	+443.9
	-Z	Entry: Pitch	-37.8	-467.0 (-468.8)**
2964.9	+X	Liftoff	+103.6	+533.8 (+185.0)***
	-X	Liftoff	-247.8	-533.8
	+X	Entry: Yaw	+208.6	+338.0
	-X	Entry: Yaw	-136.6	-338.0
	±Y	Entry: Yaw	±147.2	±459.0
	+Z	Landing	+106.3	+519.5
	-Z	Liftoff	-93.9	-631.6 (-462.1)**

* Descent-Critical Reactions Based on Mass Properties for Prefabrication Abort.

** Additional Limit, Landing Condition.

*** Additional Limit, Post SRB-Staging Condition.

3.7.3 REMOTE MANIPULATOR SYSTEM (RMS). The RMS is used for several functions during the mission. The capabilities of the RMS that were considered are as described in Space Shuttle Systems Payload Accommodations, JSC 07700, Vol XIV.

The RMS is used to help transfer the mission specialist and equipment to and from work positions on the assembly jig during EVA operation. This is described in Section 3.6.4.

The attached light on the RMS is used to supply additional lighting at the work area and the attached closed circuit TV camera is used to aid in equipment transfer and attachment as described in Section 3.7.5.

In addition, the RMS is used to separate the platform from the assembly jig, let the platform free fly, reacquire the platform by the grapple fixture, and reattach it to the assembly jig as a demonstration of a docking operation for an optional revisit mission. The RMS is also used to separate the Orbiter from the platform prior to returning to earth. Section 3.3.4 describes the separation/recapture demonstration.

3.7.4 SUBSYSTEM INTERFACES. The Orbiter to assembly jig and beam builder interface configuration has been determined as shown in Figure 3-46. In this configuration all executive control and monitoring of beam builder and assembly jig operations are performed using the Orbiter general purpose computer and associated data bus network. Data display and command initiation would be accomplished via the Orbiter multifunction control and display system (MCDS) or via SCAFE control panels. SCAFE control panels would be used for functions requiring quick reaction or location near viewing areas and would interface with the GPC via the Orbiter payload MDM. At the assembly jig the main control and monitor interface with the Orbiter would be performed using redundant MDM data bus interface modules. These units will interface with the Orbiter data bus couplers located in the cargo bay. In addition, separate hardwired caution and warning signals and safing commands are shown interfacing with the Orbiter via the payload MDM located in the Orbiter cabin. Only two C&W signals have been identified: (1) beam builder main power arm/safe switch and (2) aft assembly jig release latch arm/safe switch. A final set of interfaces has been indicated to accommodate video signal data from TV monitors which may be located in the assembly jig or within the beam builder. Power from the Orbiter is shown to be supplied via the payload power interface at Station X₀ 1765. Redundant power umbilicals will be used for this purpose.

Orbiter payload support equipment has been assessed with the result that no major incompatibilities have been identified. Control panels for power, lighting, and deployment control would be located in payload-dedicated areas of the MSS and on-orbit stations (OOS). Additional SCAFE-provided TV monitors and their controls are also shown in the payload portion of the MSS. Further analysis will determine if a video data switching unit is required or if Orbiter capability is sufficient for control of SCAFE video cameras, receiving of their data, and its routing among MSS monitors, Orbiter recorders, or retransmission to ground. It should also be noted that the payload specialist station volume has been reserved for control and monitor equip-

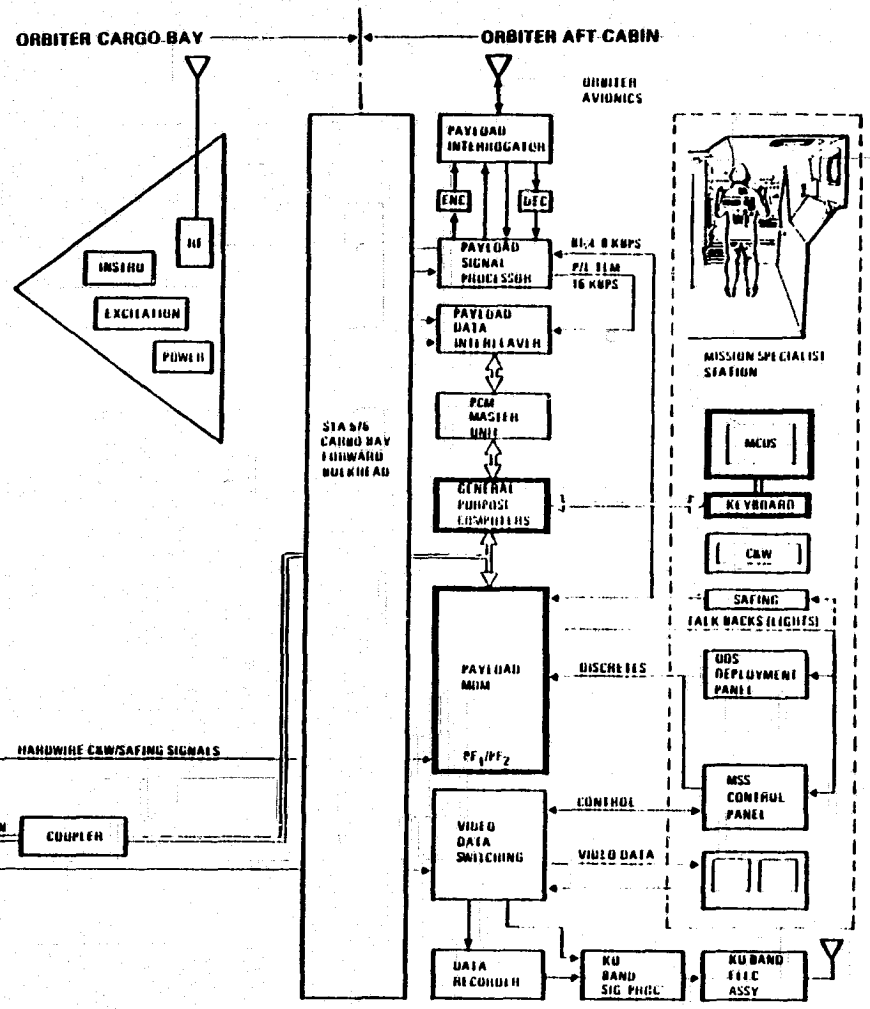
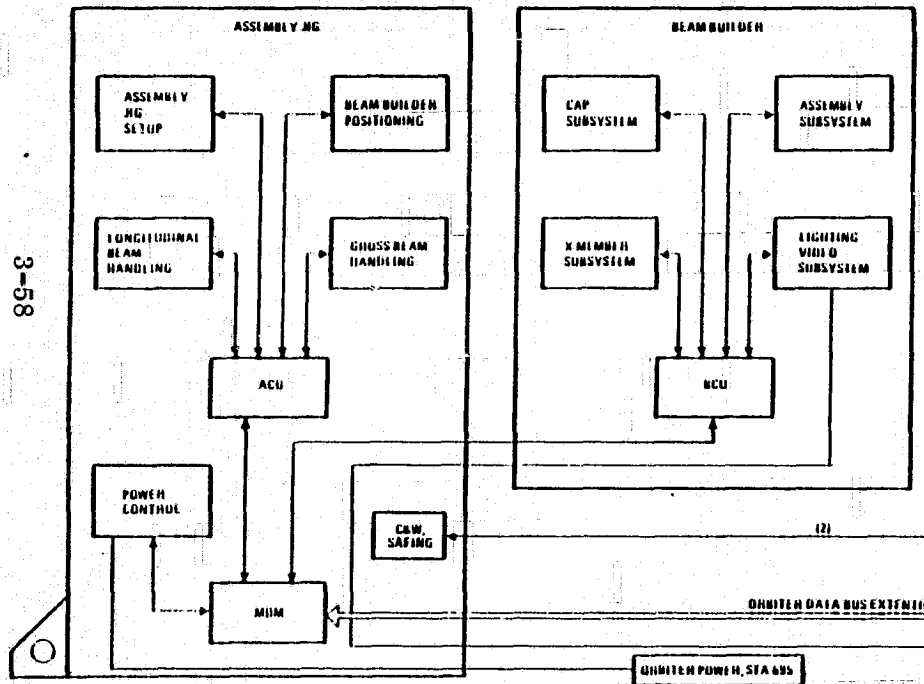


Figure 3-46. Baseline Orbiter interface block diagram.



3-58

ORIGINAL PAGE IS
OF POOR QUALITY

ment associated with instrumentation located on the beam or assembled platform.

The Orbiter GPC and associated software system was investigated to determine its compatibility with the SCAFE. In addition, preliminary concepts for SCAFE support by the Orbiter data management system were defined. Figure 3-47 shows the Orbiter data processing system and its hardware/software environment from the viewpoint of the SCAFE payload user. The Orbiter's five GPCs are shown in the center with multiple layers of Orbiter software and hardware acting to interface, isolate, buffer, and protect the payload application software from actual GPC and Orbiter/payload support avionics hardware. This peripheral support equipment includes: (1) the ground checkout and control functions such as LPS; (2) payload data gathering equipment (PCM MU, PDI, P/L MDM); (3) payload command generation equipment (P/L MDM, PSP, PI); (4) operator interface equipment (DEU, CRT & keyboard, C&W/safing panels, and payload control panels); and (5) the Orbiter mass memory units used for storing software programs and data.

The major Orbiter GPC software structures are the flight computer operating system (FCOS), the user interface (UI) software, and the actual software applications programs. The FCOS performs executive type software management tasks and also controls GPC physical input/output functions through the use of flight environment/GSE interface software and the input/output processor (IOP), which drive the Orbiter DPS data bus network.

The user interface software acts as a buffer to the FCOS and links applications software to systems software. Systems services for control of interfaces include GSE support software, downlink/uplink support software, and display and control software.

The application software is the actual GPS software system user because it is the working level programs that initiate the command/monitor activities required to fly the Orbiter and operate payloads functions. This software is divided into two functional groups called major functions, which are mission phase dependent and interface with the GPC via the user interface software. These major functions are: (1) GN&C and (2) systems management (SM). An additional function exists for payload management but is currently integrated into both GN&C and SM major functions. Each major function consists of control segments made up of four types of software structures: (1) operational sequences (OPS), (2) principal functions, (3) specialist functions (SPEC), and (4) display functions (DISP). The OPS type functions can be thought of as representing the complete set of software required during any specific mission phase, and the other three software structures are subsets of each OPS.

Four high level type OPS functions that have been identified for the SCAFE payload management function are shown in Figure 3-48. Within each of these are sub-level OPS for each task type identified.

The Orbiter positioning function contains an idle mode, a fabrication mode, and a test mode. This function exercises (automatically or via crew input) control over the Orbiter/SCAFE attitude, rates, and accelerations during each operational phase

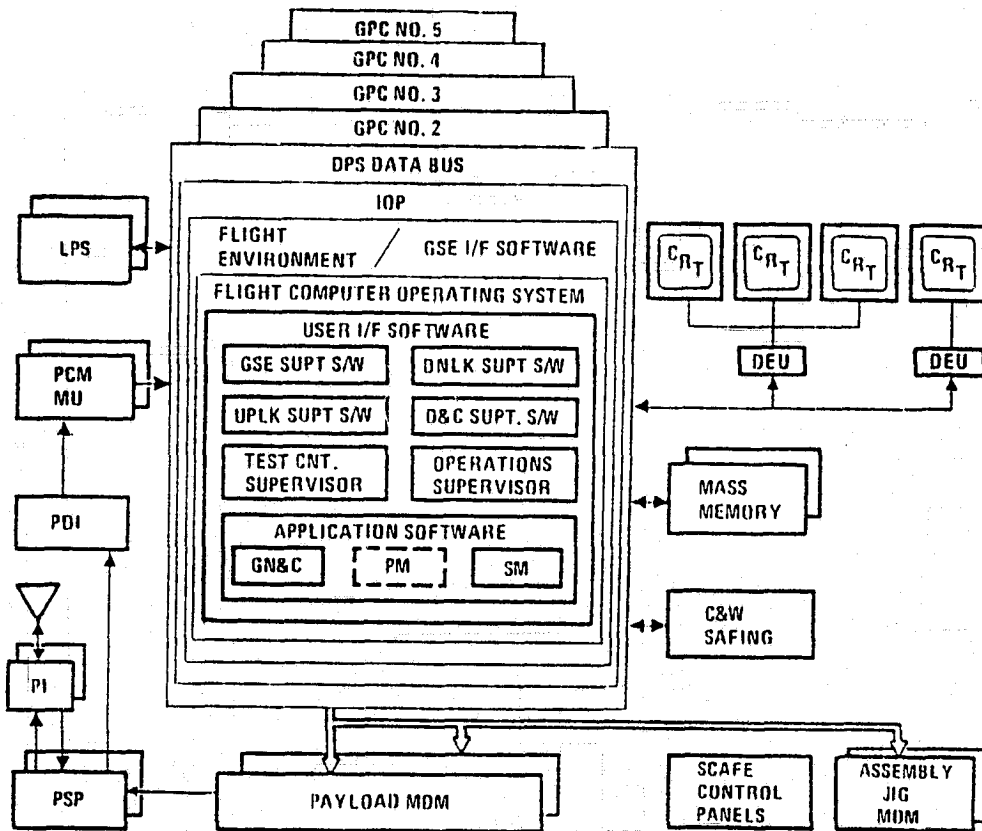


Figure 3-47. Orbiter software system block diagram.

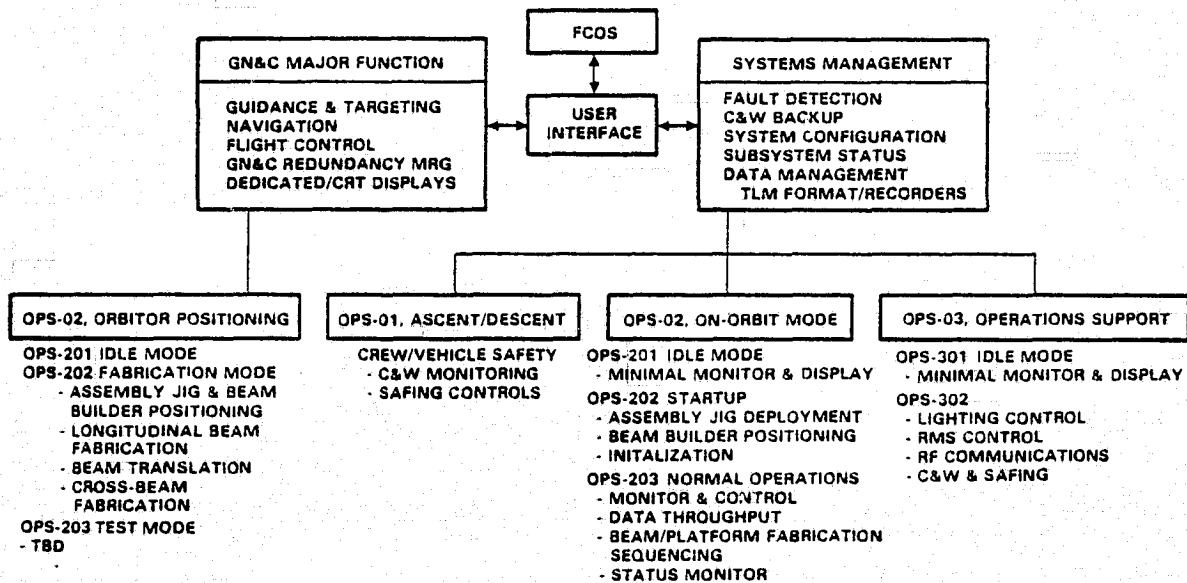


Figure 3-48. SCAPE major function support software.

of SCAFE. Orbiter capabilities in this area appear adequate for SCAFE, except for limitations on numbers of payload inertia matrices allowed. Six are currently allowed, and preliminary estimates for SCAFE indicate at least nine are required.

The ascent/descent mode is minimal for SCAFE since all power is shut down and only the two C&W arm/safe switch positions need be monitored.

The on-orbit mode contains an idle mode, a start-up mode, and a normal operating mode. These modes are responsible for effecting the executive command and monitoring functions associated with assembly jig and beam builder operations.

The operations support function provides normal payload services to SCAFE such as RMS control, data downlinking, and command throughout services.

The software functions to support SCAFE were further investigated to determine requirements for specific software functional capabilities and their current development status. These functions are summarized in Table 3-15. Results indicate that Orbiter capability does or will exist for most desired functions. The sequencing function required for executive control/monitor of beam builder functions appears to be least developed of those identified since it is currently in the concept definition phase. In addition to those functions shown, capability to communicate with SCAFE on-board avionics during its test phase when in the detached mode is expected to be required. These, however, should involve the use of standard software for receiving data and transmitting commands via the PSP unit.

Table 3-15. SCAFE control/monitor software capabilities.

SOFTWARE FUNCTION	PURPOSE	ORBITER CAPABILITY	STATUS
EXECUTIVE CONTROL/MONITOR	SEQUENCING OF MDM COMMAND/INPUT DATA	YES	CONCEPTUAL
MDM OUTPUT	EFFECT SPECIFIED P/L OUTPUT SIGNAL	YES	PLANNED
MDM INPUT	READ/RETRIEVE SPECIFIED P/L MDM SIGNAL INPUT	YES	PLANNED
READ DISPLAY	RETRIEVE DATA FROM KNOWN CRT REGION	YES	YES
WRITE DISPLAY	WRITE ON SELECTED CRT DISPLAY LOCATION	YES	YES
LIMIT SENSING	CHECK OF DATA, ANNUNCIATION OF SPECIFIED LIMITS	YES	PLANNED
TIME	PROVIDE PAYLOAD S/W ACCESS TO DATE, TIME CLOCKS	TBD	TBD
TIME DELAY	CAUSE SPECIFIED REAL-TIME DELAY BETWEEN PROGRAM STEPS	TBD	CONCEPTUAL
STATUS MONITOR	MONITOR SYSTEM CONFIGURATION/STATUS	YES	TBD
AUTO ROTATION	TWO MODES MANEUVER-TRACK, ATTITUDE HOLD	YES	TBD
MANUAL ROTATION	ATTITUDE CONTROL	YES	TBD
TABLE MAINTENANCE	CAPABILITY TO STORE, RETRIEVE, UPDATE DATA IN MEMORY	YES	TBD

3.7.5 AFT CABIN VIEWING/ILLUMINATION. Visual observation of SCAFE operations from the Orbiter aft cabin has been investigated using data from JSC 07700, SL-I-0015 (Baseline Shuttle Vehicle/Cargo Standard Interface Specification) and Orbiter cargo bay lighting analysis, on aft cabin viewing angles, cargo bay illumination capabilities, and cargo bay video monitors. The results are discussed in the following sections.

3.7.5.1 Aft Cabin Viewing. Initial viewing angle analysis data (Figure 3-49) indicate that the visibility looking aft through the cargo bay and overhead windows appears to have blind areas. When measured from the given design eye points and using the given angles for field of vision: (1) the lower three longitudinal beam fabrication operations and their respective attachment to the cross beams are within view of the Orbiter crew via the cargo bay, facing windows, (2) the upper portion of the beam builder is also within view through the aft cabin roof window during cross beam fabrication, but (3) the fourth longitudinal beam fabrication and the early portions of cross beam fabrication operation are out of view because they fall within the blind spot between the two groups of windows. In addition, viewing of the platform in the Y directions is limited to that area within approximately 10 meters of the Orbiter centerline (about 7 bay lengths).

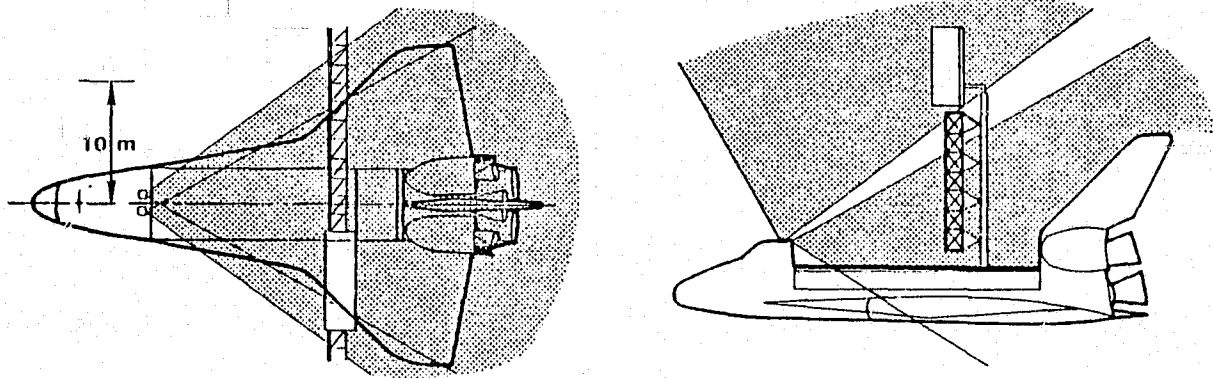


Figure 3-49. Aft cabin viewing with fixed eye positions (JSC 07700).

However, in actuality the observers eye does not remain fixed at any given point and the FOV changes considerably with slight movement of the eye point. Figure 3-50 demonstrates the increase in FOV with slight movement of the eye point looking aft (two inches down) and looking through the overhead windows (four inches forward). As is apparent, the blind spots are in effect eliminated by these slight head/eye movements, which are easily accomplished in the aft Orbiter environment.

3.7.5.2 Illumination. An analysis was also performed of SCAFE illumination level resulting from use of standard Orbiter cargo bay and rendezvous lighting provisions. For this analysis, direct illumination of two assembly jig locations was estimated using lighting data and lamp positions from JSC-07700 and SLI-0015.

Results of the SCAFE illumination levels analysis, indicate that Orbiter cargo bay lighting does not provide sufficient illumination to allow adequate monitoring of the assembly jib/beam builder operations and functions. Refer to Figure 3-51.

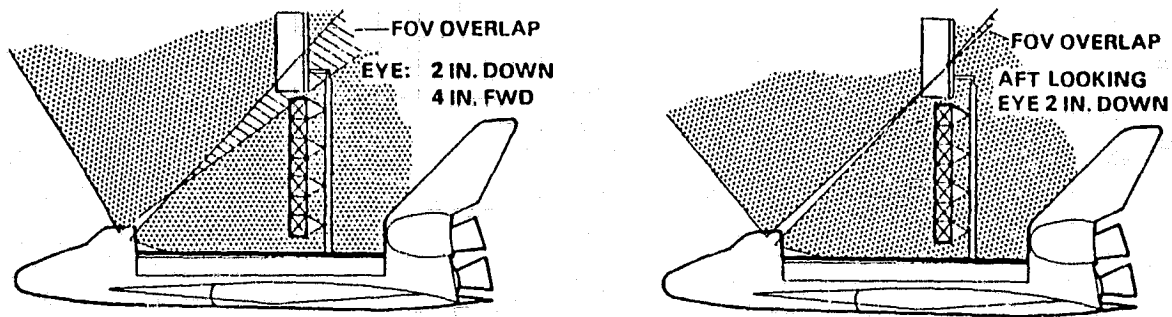


Figure 3-50. Aft cabin viewing with normal eye/head movement.

At position one, corresponding to the lowest longitudinal beam position near the assembly jig/beam builder interface, an illumination level of 15.1 lx (1.4 foot candle) was possible, and an illumination of 3.2 lx (0.3 foot candle) was available at the fourth longitudinal beam position directly above. Beam builder/assembly jig lighting levels recommended are: (1) 215 lx (20 foot candle) for general monitoring, (2) 538-1076 lx (50-100 foot candle) for detailed monitoring or inspection, and (3) 323-1076 lx (30-100 foot candle) for EVA operation and associated equipment attachment. Use of the spot-light-equipped RMS, however, provides approximately 538 lx (50 foot candle) illumination at a distance of 1.5m and 1076 lx (100 foot candles) at 0.5m. Thus, this capability meets recommended illumination levels for inspection-type activities.

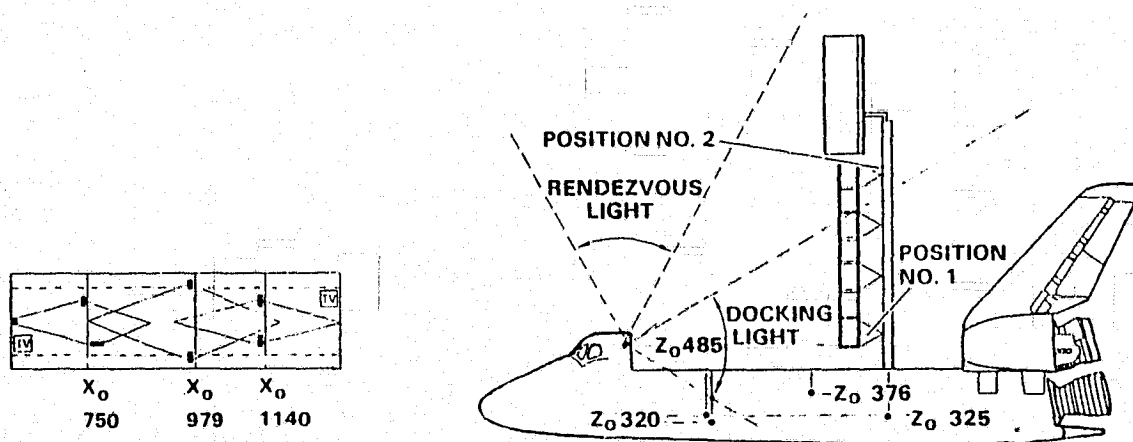
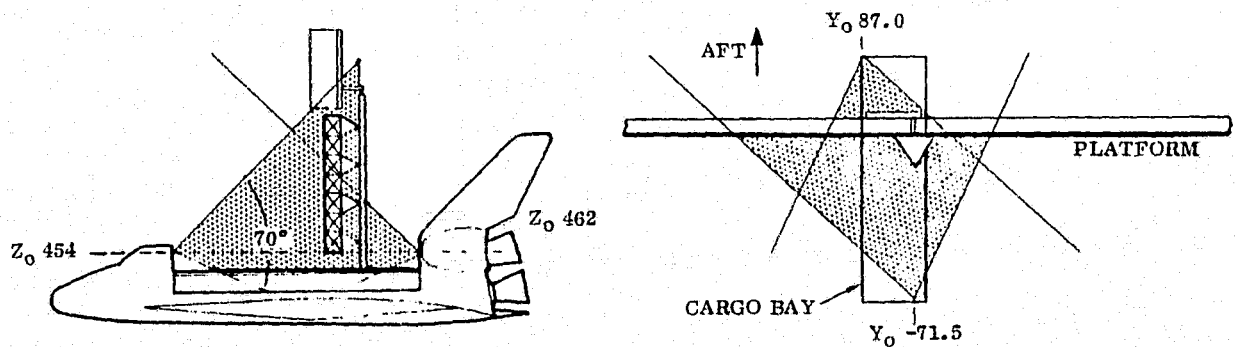


Figure 3-51. SCAFE illumination.

3.7.5.3 Cargo Bay Video Monitors. The Orbiter's CCTV cameras' fields-of-view (FOV) cover most of the forward-facing surface areas of the SCAFE platform and equipment. See Figure 3-52. The aft side, however, falls only within the FOV of the aft bay camera. It cannot be viewed via the RMS camera. This allows viewing of an area of less than one-third of the assembly jig and beam builder's (stowed position) height, and less than six meters in width.

To provide the capability of viewing the SCAFE apparatus over its full height, another camera may be installed at the aft end of the bay as shown in Figure 3-53. Its location may be the same as that of the camera already provided. But on the opposite side of the bay. It should, however, be aimed with its initial centered line-of-sight set at an angle approximately 32-deg. above the Orbiter's horizontal reference plane. (The camera's FOV is assumed to be 30-deg. vertical with an elevation select range of -10-deg. to +30-deg.) This camera would increase the visible area to a width of eight meters. (An FOV of 40-deg. horizontal is assumed, with pan select range of 20-deg. inboard to 10-deg. outboard.)

Cameras should also be provided to facilitate TV monitoring of the EVA operations, such as the unscheduled repairs to be performed. During such activities the view from the bay cameras may be blocked by the bodies of the astronauts and/or by the structure/equipment. An RMS-mounted CCTV camera can provide both close-up and far-field viewing, as shown in Figure 3-54.



PLANE	FOV		
	LENS	PAN	TOTAL
VERT	30°	30° UP 10° DN	70°
HORIZ	40°	10° OUTBD 20° INBD	70°

ORIGINAL PAGE IS
OF POOR QUALITY

Figure 3-52. Locations and FOVs of Orbiter CCTV cameras.

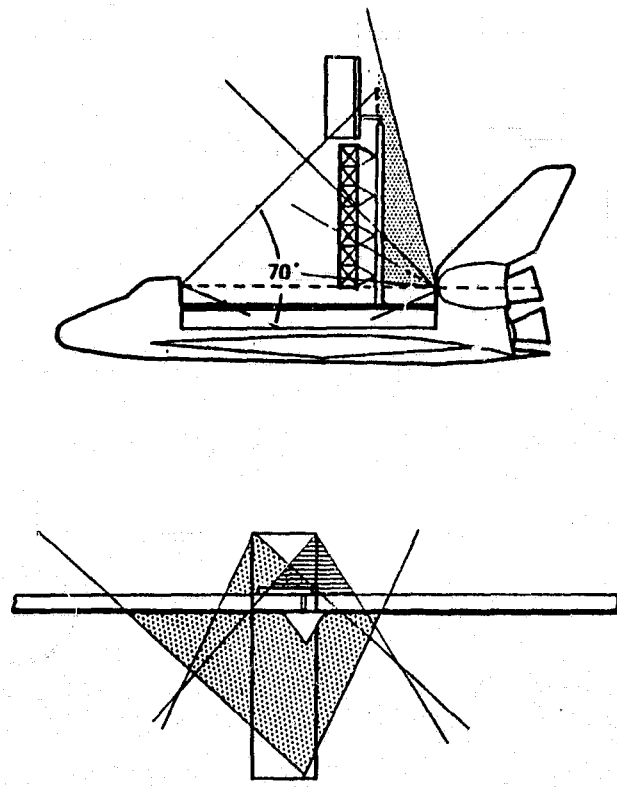


Figure 3-53. FOV with two TV cameras at aft end of cargo bay.

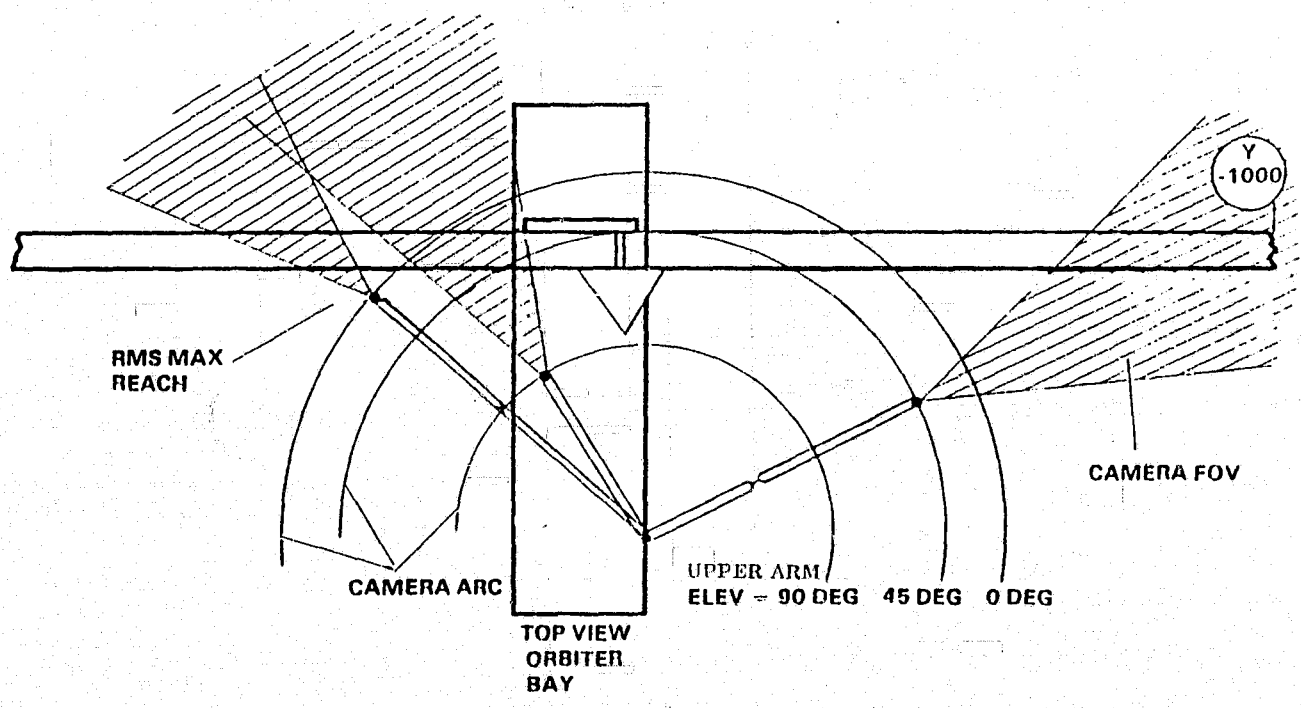


Figure 3-54. Orbiter/RMS CCTV viewing.

It would be undesirable to have the RMS independently manipulated in close vicinity to the crew member during performance of EVA tasks, in order to utilize the RMS cameras for close-up viewing. Therefore, cameras might also be installed on the manned maneuvering unit (MMU) to facilitate local viewing of EVA operations, outside of either the range or FOV of the various Orbiter-attached cameras.

Each of the camera installations recommended should have associated camera lighting provided. Lights mounted on the support beam and on the individual MMUs should be adequate to meet all of the illumination requirements related to EVA operations. The nature of the cameras and associated lighting required, and the controls is a matter for further study.

Another camera will also be required for the beam dynamics experiment. This camera should be mounted on the beam builder, viewing down the lengthwise axis of the beam. Camera lighting will again be required. Necessary levels of illumination must be defined to determine the nature of the lighting requirements.

3.7.6 SCAFE AFT STATION CONTROL/DISPLAY PROVISIONS. The following is an evaluation of the controls and displays needed at the aft station, and their locations with respect to IVA interfaces. Consideration has been given to coordination with Orbiter operations, EVA activities, and RMS operation. Required controls/displays have been identified based on the information available about the nature of the operations and experiments to be performed. Their locations are recommended with consideration given to functional grouping, accessibility, and operability, within the constraints imposed by the system's space available for payload controls/displays. Figure 3-55 shows panel locations and identifies recommended control/display details.

3.7.6.1 Mission Station CRT and Keyboard (Panel R-12). The mission station CRT and keyboard ("CRT No. 4") will be used for:

- a. Control of assembly jig and beam builder operation.
- b. Control required for conduct of experiments.
- c. Display of data from experiments.

3.7.6.2 SCAFE Master Control Panel (Panel R-11). The SCAFE master should be located on panel R-11 to be functionally grouped with the mission station keyboard and the associated TV monitor displays. This control panel consists of:

- a. PAYLOAD AFT LATCH CONTROL — LATCH ARM BUTTON. This should be a lighted push-button with a transparent guard. The lighted button will indicate that the latch is armed.
- b. PAYLOAD AFT LATCH CONTROL — LATCH RELEASE BUTTON. This should be the same as the arm button, indicating that the latch release is activated when the button is illuminated.

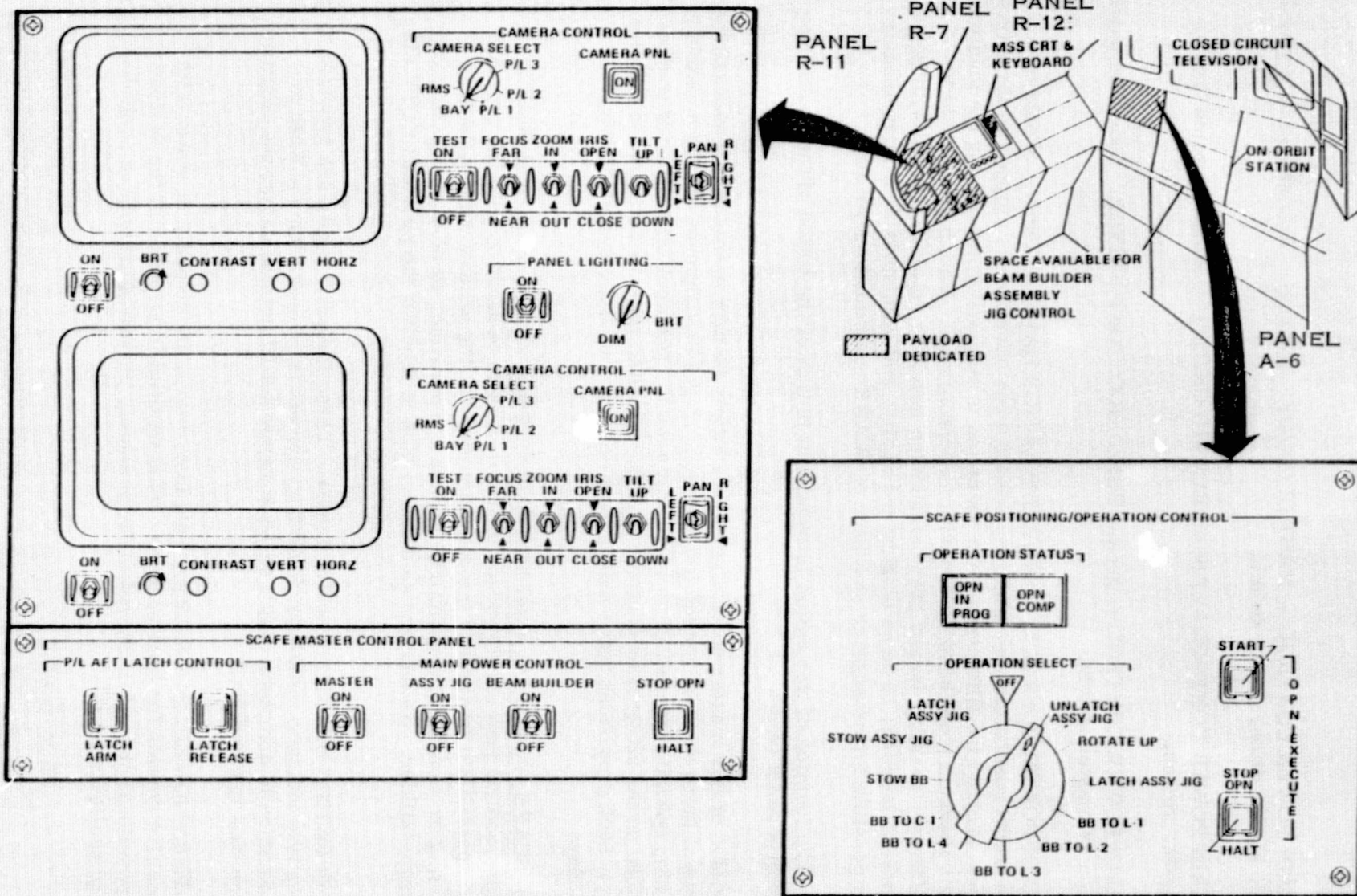


Figure 3-55. IVA payload support displays and controls.

- c. MAIN POWER CONTROL — MASTER ON/OFF SWITCH. This should be a guarded, two-position, on/off switch.
- d. MAIN POWER CONTROL — ASSEMBLY JIG ON/OFF. Should be same type as master switch.
- e. MAIN POWER CONTROL — BEAM BUILDER ON/OFF SWITCH. Should be same type as master switch.
- f. MAIN POWER CONTROL — STOP OPERATION HALT BUTTON. Should be a recessed pushbutton which will illuminate when operation is stopped by its activation. Should also illuminate when operation is stopped by depressing the identical halt pushbutton on the SSAFE position control panel. This button should be different, possibly larger than neighboring switches, clearly marked with large lettered labeling, to be as quickly and easily, and unmistakably distinguishable as possible for emergency shutdown of SSAFE equipment operations.

The function of this button is redundant to that of the button of the positioning control panel (A-6).

Provision of this master control panel is a safety feature in that it will necessitate activation of more than one switch to initiate any SSAFE equipment operation (except for the stop operation button) or to release the latch. (Another latch release control is provided on the aft Orbiter control panel (A-6). Both must be activated to affect a release.) Such provisions make inadvertent operation of these systems almost impossible.

3.7.6.3 SSAFE Positioning/Operation Control Panel (Panel A-6). The SSAFE positioning control panel is provided on the aft console to allow the SSAFE operator (payload specialists) to observe the operation through the window while selecting, and starting or stopping the appropriate phase of operation, or positioning the assembly jig or beam builder. Its location also allows him to monitor the provided CCTV displays.

- a. OPERATION STATUS Indicator Lights. These indicator lights are provided to give positive indication when the SSAFE equipment is in operation and when an operation is complete. "OPN COMP" should not illuminate unless the operation selected is complete.)
- b. OPERATION SELECT Switch. This is a rotary, multi-position switch with positive detents for each position. This facilitates selection of the desired operational phase for control of the assembly jig and beam builder positions and configurations.

- c. OPN EXECUTE — START BUTTON. This is a pushbutton with a hinged transparent guard, which illuminates when SCAFE equipment is in operation. It is guarded to prevent inadvertent initiation of equipment operation. It is lighted to provide positive indication that the SCAFE equipment is in fact in operation. It also provides redundancy for the operation status indicator - "OPN IN PROG" light.
- d. OPN EXECUTE — STOP OPN - HALT BUTTON. This is a recessed pushbutton, which illuminates when the operation is stopped for other than a completed operation (it should not illuminate when the operation is stopped because an operation is complete). It should be highly visible and easily distinguishable, for emergency shutdown of SCAFE equipment operation. This button should also be identical and redundant to the HALT button on the SCAFE master control panel.

3.7.6.4 Payload TV Monitor Displays and Display Controls (Panel R-11). Two TV monitors are provided to allow the SCAFE equipment operator to monitor views of the operation as seen from payload-dedicated cameras. They are located at the mission station to facilitate viewing while controlling operations from the mission station keyboard. They will also allow for viewing from up to four camera positions simultaneously when used in conjunction with the provided CCTV displays (useful for example to meet the individual, simultaneous viewing requirements of two crew members, such as commander and payload specialist.)

3.7.6.4.1 Display Controls. Controls required for the displays include:

- a. ON/OFF SWITCH. This should be a guarded, two-position switch.
- b. BRT-BRIGHTNESS CONTROL KNOB. This should be a round knob, labelled with an arrow to indicate clockwise direction for increased brightness.
- c. CONTRAST CONTROL KNOB. Should be a round knob.
- d. VERT-VERTICAL HOLD CONTROL. Should be a round knob.
- e. HORZ-HORIZONTAL HOLD CONTROL. Should be a round knob.

3.7.6.4.2 Payload Camera Controls (Panel R-11). Two sets of payload camera controls are provided where they are needed - adjacent to the associated TV displays grouped under CAMERA CONTROL. They include:

- a. CAMERA SELECT Rotary Switch. The switch should have positive detents at each selectable position. It provides for selection of any camera view available and switches the camera controls to operate the selected camera.
- b. CAMERA PWR ON Pushbutton. This is a recessed push button switch, which illuminates when the selected camera is operating. The illuminated button provides an indication that the camera is operating when the video display is off.

c. Camera Controls Include:

1. TEST - ON/OFF Switch (two-position)
2. FOCUS - FAR/NEAR Switch (two-position, momentary - contact switch)
3. ZOOM - IN/OUT Switch (two-position, momentary - contact switch)
4. IRIS - OPEN/CLOSE Switch (two-position, momentary - contact switch)
5. TILT - UP/DOWN Switch (two-position, momentary - contact switch)
6. PAN - LEFT/RIGHT Switch (two - position, momentary - contact switch)

3.7.6.4.3 PANEL LIGHTING Controls. These are provided for individual control of panel R-11 lighting (Integrally illuminated)

- a. Two-position ON/OFF switch.
- b. DIM-BRT control - blade knob with pointer.

3.7.6.5 TV Camera Lighting Controls (Panel R-7). The necessary flood or camera light controls should be provided at the mission station in the vicinity of the TV monitors. Panel R-7 would facilitate ease of accessibility and would be adjacent to the TV Monitors. The controls should include on/off switches and rheostat control knobs (blade knob with pointer) to control levels of illumination, for each set of lights.

3.7.6.5 Re-evaluation of Station Control/Display Provisions. It has been assumed that the mission station keyboard will be adequate for control of the automated platform fabrication operations, all SSAFE equipment operation (when used in conjunction with the other SSAFE controls), and the experiment related operations. The CRT will, in turn, be adequate to provide the information and data required for the same. This should be reexamined when the exact nature of all of the operations and experiments have been further defined. It is possible, for example, that an additional display may be required, or desirable, to display accelerometer data, which cannot be displayed on the mission CRT. However, should requirements be revealed for additional controls/displays, considerable space is available at the payload station (panels L-10, L-11, and L-12) or on the aft console (panels A-6 and A-7).

Another IVA interface which should be reevaluated when the nature of the operations is further defined, is the use of the RMS. As presently conceived, there are no discrepancies in control/display design with respect to IVA interfaces. This could change, however, with development of additional uses of RMS or other additional crew requirements not yet defined.

The overall layout of the aft flight deck controls/displays has been evaluated with respect to simultaneous task performance by two or more crew members. No conflicts appear to exist with the recommended layout as shown in Table 3-16.

An important consideration, which should not be overlooked in the design of the crew stations, is the requirement for hand holds and foot restraints. All controls/displays should also be designed to meet the man/system requirements for weightless environments as set forth in the Marshall Space Flight Center Design Standard 512A.

Table 3-16. Summary of simultaneous task/work station analysis

Operation	IVA Crew Members Controlling Opn.	Control Panel Used	Simultaneous Operations	Conflicts
Docking/Station Keeping	Cmdr.	Fore Flt. Deck/ Aft Orbiter	None	None
Platform Fabrication	Payload Spec.	Mission Sta. (left aft & aft)	Prebreath EVA Prep	None
Experiments	Payload Spec.	Mission Sta. (left aft & aft)	None	None
RMS Operations	Cmdr.	Aft Orbiter (RMS Panel)	EVA	None
Platform Repair	Cmdr. Payload Spec.	Aft Orbiter (RMS Pnl) Mission Sta (Left Aft)	Control of Beam Build- er Equip.; RMS Control	None None
Platform Release	Cmdr. Payload Spec.	Aft Orbiter (RMS Pnl) Mission Sta. (Left Aft)	Control of platform movement (Keyboard); RMS Control	None None
Platform Retrieval	(Same as Docking & RMS Operations)			None

3.7.7 ORBITER RCS PROPELLANT REQUIREMENTS. Orbiter RCS propellant requirements were calculated during: (1) platform construction; (2) Orbiter-attached test/experiment periods; and (3) crew meal/rest periods. Propellant usage was not calculated during: (1) the first three and last five mission hours (since these are dedicated to non-SCAFE STS mission activities); and (2) the five-hour separation/recepture demonstration period. The latter interval was omitted since specific Orbiter maneuvers, if any, are undefined. For example, if an Orbiter fly-around is planned (as suggested in Section 3.3), delta-velocity and attitude time histories must be developed. On the other hand, if the Orbiter is held in a fixed position relative to the platform, RCS propellant usage would be less than 1.8 kg/hr (based on data in Reference 1, page 3-3 and Reference 2, Amendment 63, page 4.3.2-1).

The expected RCS propellant usage is tabulated as a function of time from launch in Table 3-17.

Reference 1 gives the total RCS propellant quantity for an on-orbit operation as 1814 kg. This leaves 1611 kg for the experiments and observations with the Orbiter and beam separated.

The method used to compute the propellant consumption was based on the following data and analysis. The vernier thruster data used in the analyses were obtained from Reference 2.

- a. Nominal vacuum impulse - 260 sec (Amendment 63)
- b. Vacuum thrust - 111 Newtons (Amendment 42)

The duty cycles calculated in Section 4.3 were used to calculate the control impulse per hour required in the attitude mode. The impulse rate with a single beam built (phase 2) and the entire platform (phase 3) was used to estimate at other times. After the platform is built, the Orbiter/beam is allowed to operate in a rate mode in roll and yaw, with pitch in an attitude mode. The pitch impulse rate used during this period is calculated from the pitch duty cycle with the beam built and extended toward the earth. The yaw and roll duty cycles assume a gravity gradient stabilized mode with a maximum rate of 0.01 deg/sec. During each cycle, it is assumed there will be one minimum firing to reduce momentum in roll and yaw. The firing will be longer than the minimum firing to reduce momentum in roll and yaw. The firing will be longer than the minimum time of 0.04 seconds so that there will be torque around one axis during the combined thruster firings. In yaw the minimum impulse is three thruster for 0.08 seconds and two for 0.04 seconds. In roll the minimum impulse is two thrusters for 0.240 seconds and one for 0.16 seconds.

In the attitude mode, the phase 1 impulse was used until L + 22, the average of phase 1 and phase 3 from L + 23 to L + 47. After L + 47, the phase 3 impulse was used.

The references used in the above analysis were:

- a. Reference 1 - JSC 07700 Vol. XIV
- b. Reference 2 - Shuttle Operational Data Book
JCS 08934 Vol I Rev A

Table 3-17. RCS propellant usage.

<u>TIME FROM LAUNCH, HOURS</u>	<u>VERNIER RCS DEADBANDS</u>	<u>PROPELLANT, KG</u>
L + 3 to L + 23	Attitude mode all axes 5.0 deg 0.01 deg/sec	29.3
L + 8 and L + 11	2 manual yaw pulses	0.5
L + 23 to L + 34	Attitude mode all axes 5.0 deg 0.01 deg/sec	35.5
L + 34 to L + 47	Attitude mode pitch axis 5.0 deg 0.01 deg/sec Rate mode yaw/roll axes 0.01 deg/sec	3-7
L + 47 to L + 61	Attitude mode all axes 5.0 deg 0.01 deg/sec	69.8
L + 51	1 Manual yaw pulse	.8
L + 61 to L + 74	Attitude mode pitch axis 5.0 deg 0.01 deg/sec Rate mode yaw/roll axes 0.01 deg/sec	3.7
L + 74 to L + 82	Attitude mode all axes 5.0 deg 0.01 deg/sec	39.8
L + 74	4 Manual yaw pulses	3.2
L + 82 to L + 95	Attitude mode pitch axis 5.0 deg 0.01 deg/sec Rate mode yaw/roll axes	3.7
L + 95 to L + 100	Separation/recapture Demonstration	TBD
L + 100 to L + 146	Attitude mode pitch axis 5.0 deg 0.01 deg/sec Rate mode yaw/roll axes 0.01 deg/sec	13
TOTAL PROPELLANT		203

4

ANALYSES

System design and flight experiment integration tasks (Sections 2 and 3) were supported by an integrated series of technical analyses conducted in five disciplines: mass properties, stability and control, structural dynamics, stress, and thermodynamics.

Three integrated groups of analyses comprised the majority of study analytical effort. Structural/mechanical evaluation of the combined Shuttle, fabrication system, and platform structure required the greatest analytical integration as illustrated in Figure 4-1. In addition, structural/mechanical evaluation of the free-flying platform involved the task flow of Figure 4-2 and thermal analyses were conducted and coordinated with tasks in other disciplines as shown in Figure 4-3. Activities in each discipline area are discussed in the following subsections.

4.1 MASS PROPERTIES

Mass properties analyses were conducted to: support stability/control and dynamic response analyses; evaluate SCAFE system orbiter compatibility; and, at Part II conclusion, to document the characteristics of the selected concept preliminary design. The analysis support and final summary activities are discussed in the subsections below. Results of the Orbiter compatibility investigation are documented in Section 3.7.1.

4.1.1 PRELIMINARY ANALYSES. Data supplied for use in stability and control analyses and subsequent structural dynamics analyses is summarized in Figure 4-4. SCAFE structure and fabrication system elements are shown relative to the Orbiter cargo bay, OMS kit, and Orbiter c.g. Specific geometry was initially based on the Part I coordinates of system elements. Beam builder and assembly jig mass properties were taken from the Convair proposal, while beam mass properties reflected the Part I geometry and laminate.

In the operational orientation, the three mission phases shown were of interest in determination of duty cycle requirements for the Orbiter VRCS: (1) equipment deployed, just prior to fabrication start; (2-1) beam No. 1 complete; and (3) platform fabrication and assembly complete. The c.g. and inertia data for these are shown in the upper "Total System" table as used for preliminary VRCS duty cycle analysis (Section 4.2). The most dramatic variations occur in roll and yaw inertias as fabrication progresses. As Part II design progressed, final coordinates were chosen for the system elements and the resulting updated data (lower table) were supplied for the final VRCS duty cycle analysis.

4.1.2 FINAL ANALYSES. Upon completion of the platform, fabrication equipment, and subsystem design tasks, final mass properties were developed. These are

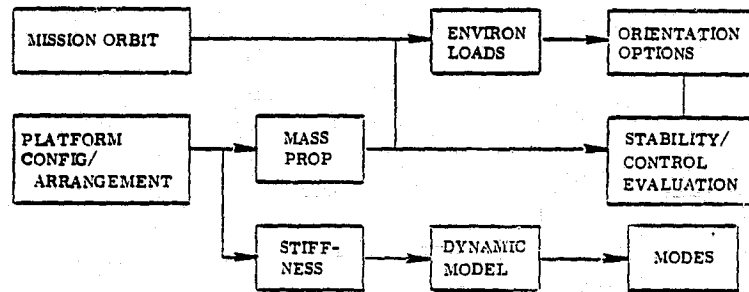
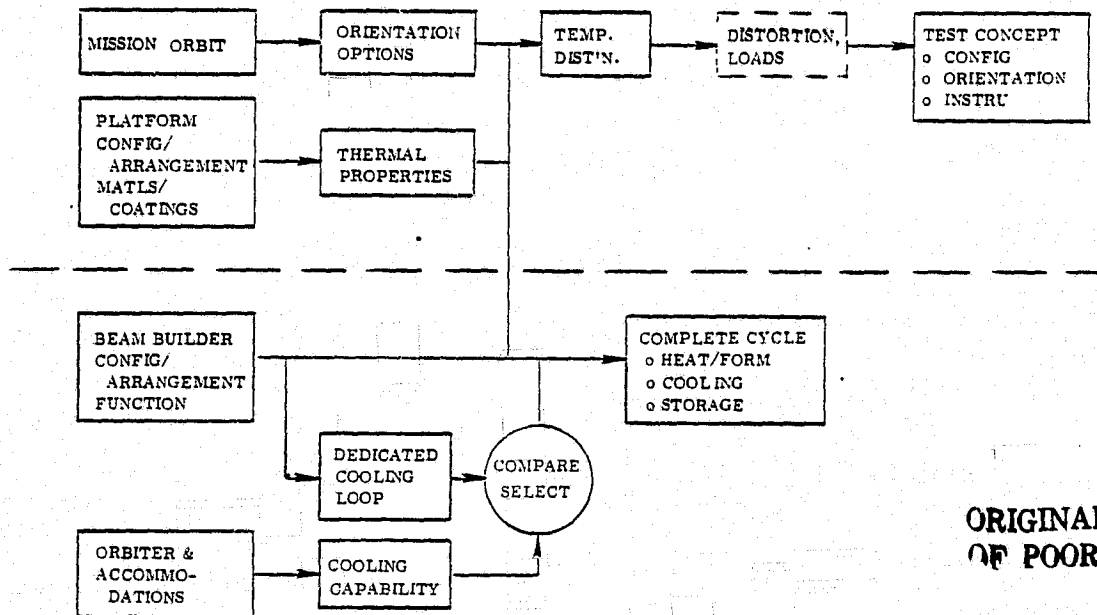


Figure 4-2. Structural/mechanical evaluation task flow of free-flying platform.



ORIGINAL PAGE IS
OF POOR QUALITY

Figure 4-3. Thermal evaluation task flow.

presented for the beam builder, assembly jig, and free platform (with equipment) in Tables 4-1, 4-2, and 4-3, respectively.

In addition, the system mass properties were determined for each discrete-configuration mission event from post-boost stowed to preentry stowed. These data are shown in Table 4-4 and selected items are also plotted vs. event in Figure 4-5.

Table 4-1. Beam builder weight summary.

Item	Weight - kg (lb)	
Basic Structure	660.3	(1456)
Cap Forming Machine Assy (3)	532.0	(1173)
Cap Material - Stored (3)	786.4	(1734)
Cross Member Positioner (3)	37.6	(83)
Cross Member Clip & Feed Mechanism (3)	762.8	(1682)
Cross Member Material Stored (3)	239.5	(528)
Cord Tensioner Mechanism (6)	177.3	(391)
Cord Plyer Mechanism (2 Stations)	153.7	(339)
Beam Welding Mechanism (3)	80.7	(178)
Beam Builder Cutoff Mechanism (3)	68.0	(150)
Beam Builder/Assy Jig Latch Mechanism	62.6	(138)
Cooling System (Panel)	7.3	(16)
Handler Arm Fitting & Mechanism	49.9	(110)
Total Beam Builder	3618.1	(7978)

Table 4-2. Assembly jig weight summary.

Item	Weight - kg (lb)	
Basic Assy Jig Structure	1585.5	(3496)
Cross Beam Positioner Mechanism	30.8	(68)
Weld Head Assy & Mechanism (8 Locations)	60.3	(133)
Rotating Mechanism	22.7	(50)
EVA Linkage & Mechanism	47.6	(105)
Retention & Guide Mechanism (12 Locations)	590.5	(1302)
Drive Shaft & Motor Mechanism	272.1	(600)
Gear Rack	14.5	(32)
Guide Way Support	172.3	(380)
Umbilical Guide & Track	38.5	(85)
Umbilical Wire & Return Spring Mechanism	192.3	(424)
Total	3371.8	(7435)

Table 4-3. Free platform/equipment mass properties.

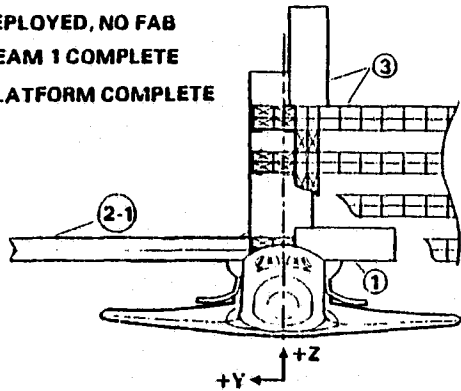
Item	Weight, kg	Center of Gravity, Meters			Moments of Inertia kg - m ² x 1000			Products of Inertia kg - m ²		
		X	Y	Z	IXX (Roll)	IYY (Pitch)	IZZ (Yaw)	IXY	IXZ	IYZ
A. Long Beams (4)	888.9	28.0	-97.5	16.7	2,971	9.5	2,862	0	0	0
B. Long Beams + Cross Beams (9)	996.6	27.9	-97.7	16.8	3,400	10.6	3,390	116.1	-1.2	-2.2
C. Equipment + L/B + C/B	2143.6	28.0	-82.8	16.8	9,463	18.3	9,446	-548	-346	46,854
1. Struct. Resp. Instr.	102.0	28.3	-49.6	16.8	404	.4	404	-1624	0	0
2. Scientific Experiments	194.6	28.1	-55.3	15.5	1,214	1.2	1,212	-798	-53.9	11,178
3. Communications	85.3	28.5	-28.3	15.2	441	.4	440	336	40.3	7,076
4. Electrical Power	441.7	27.9	-.6	18.1	4.1	2.8	1.5	-201	-180	1,257
5. Attitude Control	153.7	27.9	-22.5	16.4	143.9	.4	143.5	-534	-9.4	-1367
6. Wiring	119.7	28.0	-97.5	16.8	400	1.1	399	0	0	0
7. Grappling Fixture	49.9	28.0	-73.1	16.8	34.4	34.4	19.3	0	0	0

Table 4-4. Orbiter/SCAFE mass properties with mission phase.

Mission Event	Weight kg	Center of Gravity Meters			Moments of Inertia, kg - m ² x 1000			Products of Inertia, kg - m ²		
		X	Y	Z	IXX (Roll)	IYY (Pitch)	IZZ (Yaw)	IXY	IXZ	IYZ
A. Orbiter W/BB-Jig Stowed	94088	28.4	.0	9.7	1,174	8,628	8,974	-2,379	363,603	-7,874
B. Orbiter W/BB-Jig Deployed	94088	28.8	-.2	10.0	1,594	8,632	8,871	15,459	391,757	-82,089
C. Orbiter One Beam Out	94088	28.8	.0	10.0	4,491	8,632	11,768	-4,007	391,734	-1,938
D. Orbiter Two Beam Out	94088	28.8	.3	10.1	7,470	8,723	14,655	-23,378	384,105	86,474
E. Orbiter Three Beam Out	94088	28.8	.5	10.2	10,479	8,860	17,528	-42,868	376,967	240,022
F. Orbiter Four Beam Out	94088	28.8	.8	10.3	13,515	9,034	20,390	-62,299	370,246	478,821
G. Orbiter Four, B/B to C/M Pos.	94088	28.8	.9	10.4	13,757	9,372	20,305	-63,858	323,133	558,205
H. Orbiter One B/B to C/M Pos.	94088	28.8	.9	10.4	13,573	9,369	20,125	-63,145	323,399	551,963
I. Orbiter Two B/B to C/M Pos.	94088	28.8	.7	10.4	9,898	9,365	16,453	-45,846	323,665	394,716
J. Orbiter Three B/B to C/M Pos.	94088	28.8	.4	10.4	7,292	9,361	13,851	-28,088	323,931	235,546
K. Orbiter Four B/B to C/M Pos.	94088	28.8	.2	10.4	5,769	9,357	12,332	-9,871	324,197	74,453
L. Orbiter Five B/B to C/M Pos.	94088	28.8	-.1	10.4	5,343	9,353	11,911	8,805	324,462	-88,565
M. Orbiter Six B/B to C/M Pos.	94088	28.8	-.3	10.4	6,028	9,349	12,600	27,939	324,728	-253,510
N. Orbiter Seven B/B to C/M Pos.	94088	28.8	-.6	10.4	7,812	9,345	14,388	47,322	324,994	-418,434
O. Orbiter Eight B/B to C/M Pos.	94088	28.8	-.8	10.4	10,748	9,341	17,327	67,374	325,260	-587,236
P. Orbiter Nine B/B to C/M Pos.	94088	28.8	-1.1	10.4	14,887	9,337	21,471	88,096	325,526	-759,919
Q. Orbiter Eq/Plat Moved to C/G	94088	28.8	-.1	10.5	11,573	9,387	18,103	7,080	318,057	-119,741
R. Orbiter Eq/Plat Released/Orb	91944	28.8	0	10.4	2,009	9,280	8,643	3,341	329,214	-39,287
S. Orbiter B/B + A/J Stowed	91944	28.5	0	9.7	1,101	8,576	8,834	-3,533	376,871	25,307

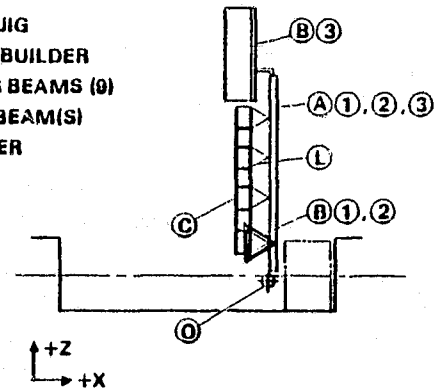
• PHASE

- ① DEPLOYED, NO FAB
- ②-1 BEAM 1 COMPLETE
- ③ PLATFORM COMPLETE



• ITEM

- Ⓐ ASSY JIG
- Ⓑ BEAM BUILDER
- Ⓒ CROSS BEAMS (0)
- Ⓓ LONG BEAM(S)
- Ⓔ ORBITER



W = 90,624 kg

Item	Phase	Wt (kg)	CG (cm)		
			X	Y	Z
A	All	1856	2876.1	-76.2	1661.2
B	1	2609	2800.4	-569.0	1251.2
	2-1	2387	2800.7	-558.5	1251.8
	3	1612	2717.6	-149.6	2525.2
L	2-1	222	2797.5	9887.3	1244.6
	3	889	2797.5	-9758.8	1674.8
C	3	108	2718.8	-9902.1	1674.8
L+C	3	997	2738.9	-9774.4	1674.8
0	All	86159	2869-1	0.6	961.0

• Preliminary VRCS Analysis

Phase	Center of Gravity (cm)			Moment of Inertia (10 ⁶ kg - m ²)		
	X	Y	Z	I _{xx} (Roll)	I _{yy} (Pitch)	I _{zz} (Yaw)
1	2889.0	-14.7	981.5	1.432	8.687	9.009
2	2889.0	7.6	981.5	4.073	8.687	11.651
3	2887.5	-97.5	1005.6	14.106	9.072	21.307

• Final VRCS Analysis

Phase	Center of Gravity (cm)			Moment of Inertia (10 ⁶ kg - m ²)		
	X	Y	Z	I _{xx} (Roll)	I _{yy} (Pitch)	I _{zz} (Yaw)
1	2867.3	-17.4	983.6	1.422	8.622	8.942
2-1	2867.3	8.5	983.6	4.326	8.622	11.846
3	2865.7	-111.5	1010.8	14.494	9.045	21.596

Figure 4-4. Mass properties for analyses.

to highlight the significant variations (particularly in lateral (y) c.g. and both roll and yaw axis inertia) during the nominal mission. Inertia crossovers indicate the change of gravity gradient attitude of the total system, as discussed in Section 4.2. Durations of each event were determined from the mission timelines (Section 3.6.2) and used to compute RCS propellant expenditures (Section 3.7.7).

4.2 STABILITY AND CONTROL

The stability and control analysis is comprised of two parts: (1) the Orbiter control during fabrication of the beams and platform; and (2) the free flight mode of the completed platform.

4.2.1 ORBITER/PLATFORM RESPONSE. The Orbiter/platform response was analyzed in three phases. First, the frequencies and amplitudes for a rate-damped, gravity-stabilized mode were determined. Second, duty cycles were calculated for a baseline construction orientation using preliminary mass properties and with an assumed control logic which fired thrusters to give a net torque in only one axis while

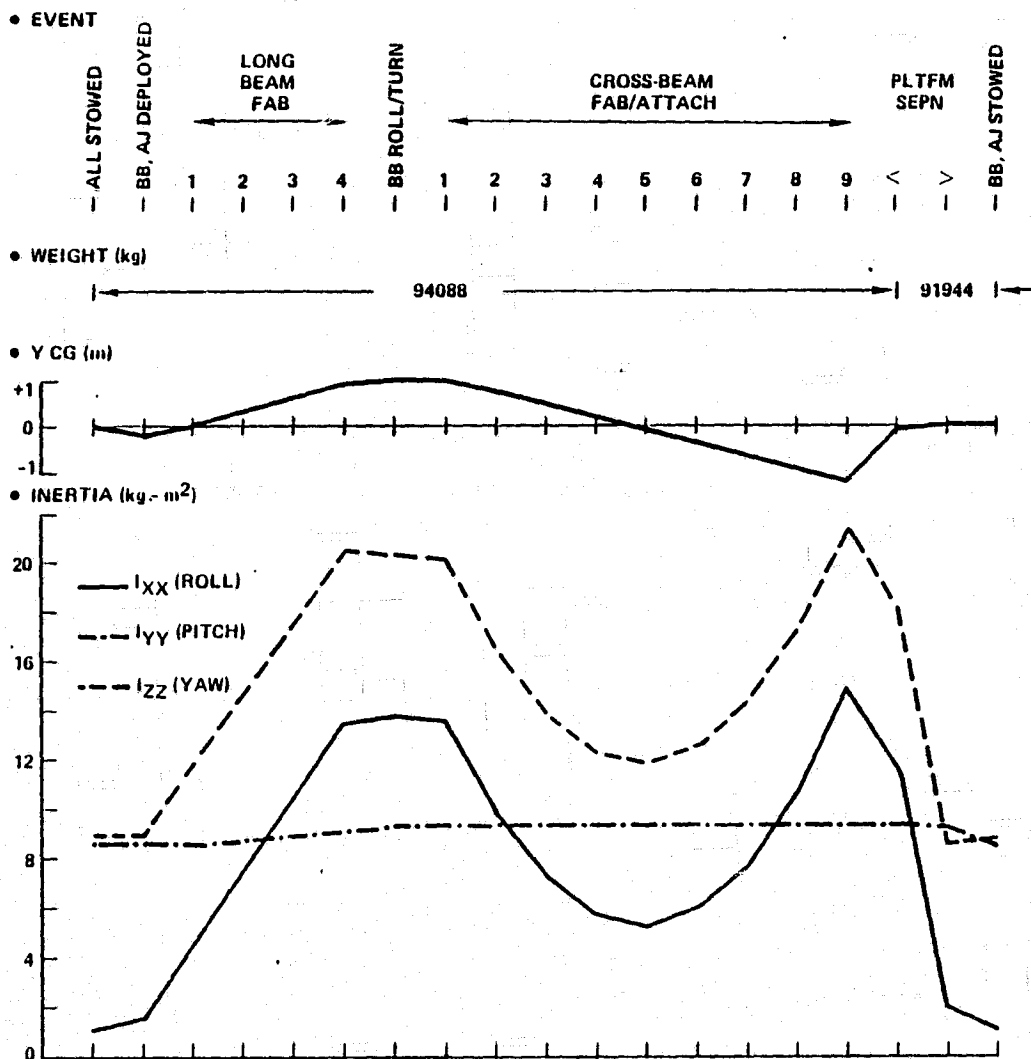


Figure 4-5. Mass properties variation with mission event.

minimizing On-time for each control pulse. Third, the duty cycles were recalculated using revised mass properties, including the effects of environmental torques, and using the vernier RCS control logic as presented in Reference 1*.

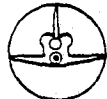
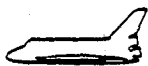
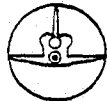
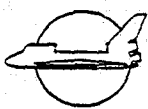
4.2.1.1 Gravity Gradient Stabilization. The possibility of using a gravity gradient mode during the construction was investigated. The Orbiter vernier RCS would be

Reference 1*. Space Shuttle Orbiter Orbital Flight Test, LEVEL C, Functional Sub-system Software Requirements; Guidance, Navigation and Control; Part C, Flight Control On Orbit; SD76-SH-0009, 1 June 1977.

C-4

operated in a rate mode with the rate deadband set to keep variation in rate about an orbit-fixed axis system to within ± 0.01 deg/sec. The mass properties and Orbiter coordinate system shown in Figure 4-4 were used for this analysis. The Orbiter orientation, limit cycle frequencies, and maximum attitudes are given in Table 4-5 for three construction phases. The illustrations show which axis of the Orbiter is perpendicular to the orbit plane (POP) for each phase. If the maximum attitudes shown in Table 4-5 were too large, closed-loop attitude control would still be required. The disadvantages of maneuvering from one attitude to another and, finally, to the stable platform separation attitude (X-POP, Y-NADIR) outweigh the theoretical advantages of reduced beam excitation and reduced propellant consumption. Therefore, the baseline orientation for the duty cycle analysis was that which provided a stable platform orientation after separation. This orientation still allows for rate stabilization in yaw and roll with maximum attitude errors less than ± 10 degrees.

Table 4-5. Gravity gradient stabilization.

Phase Axis	Orientation	Maximum Attitude, deg	Frequency, rad/sec
1	Z-POP, X-NADIR		
Pitch		± 4.9	2.04×10^{-3}
Yaw		± 5.9	1.70×10^{-3}
Roll		± 19.3	5.2×10^{-4}
2-1	Z-POP, X-NADIR		
Pitch		± 4.9	2.04×10^{-3}
Yaw		± 8.78	1.14×10^{-3}
Roll		± 10.6	9.4×10^{-2}
3	Z-POP, Y-NADIR		
Pitch		± 14.6	6.85×10^{-4}
Yaw		± 10.5	9.5×10^{-4}
Roll		± 4.9	2.03×10^{-3}

4.2.1.2 Preliminary Duty Cycle Analysis. The preliminary duty cycle analysis was performed using the mass properties in Figure 4-4. Three phases of platform construction were analyzed. In Phase 1, the beam builder was deployed and was ready to start building the first beam. In Phase 2-1, the first beam had just been completed. In Phase 3, the last cross beam had been built and attached. The VRCS duty cycles were calculated in Orbiter pitch, yaw, and roll axes for each of the three phases. The assumption used for the calculations were:

- a. Vernier RCS thrusters are used for control.
- b. No failed RCS thrusters.
- c. Control logic fires thrusters to give a net torque in one axis during On-time.

- d. Maximum attitude rate is ± 0.01 deg/sec (Orbiter maximum per JSC 07700).
- e. Disturbance torques are from gravitation and gyroscopic forces. Others (drag, solar pressure, etc.) at least an order of magnitude less.

Figure 4-6 parametrically illustrates roll axis duty cycles for Phase 3 for two values of maximum attitude error. The pulse-time histories in roll are given in Table 4-6 for both error values to permit comparison of requirements for the three construction phases.

Tables 4-7 and 4-8 give the pitch and yaw duty cycles, respectively, for construction Phases 2-1 and 3.

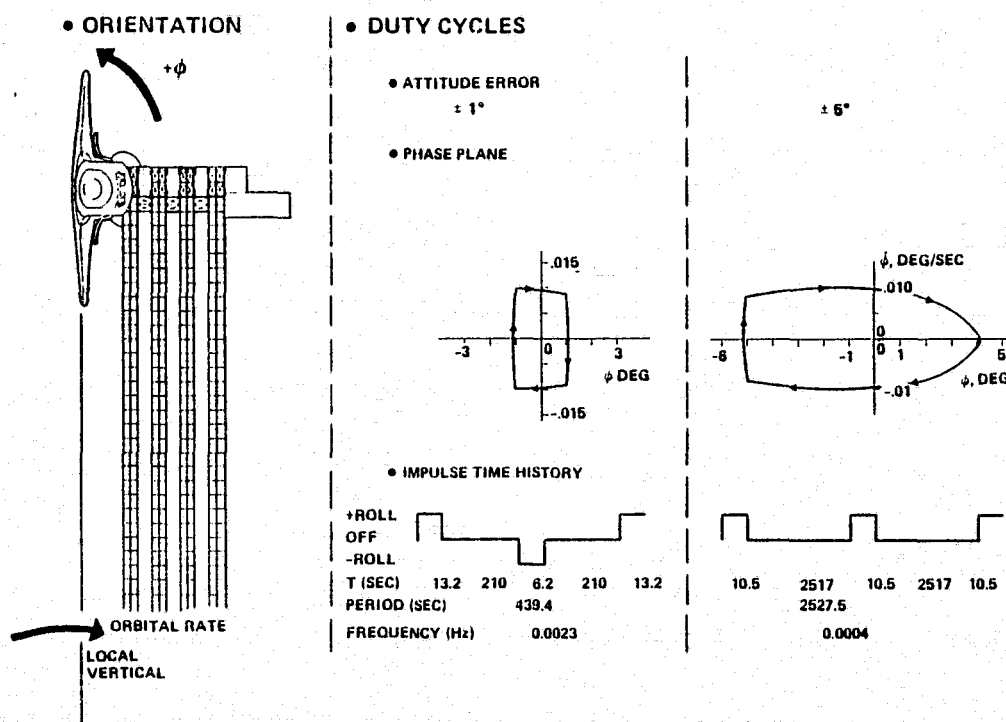


Figure 4-6. Orbiter VRCS operation.

4.2.1.3 VRCS Thruster Operation. The preliminary duty cycles calculated in Section 4.2.1.1 assumed an RCS system in which the thrusters would fire to minimize the impulse required while still providing a torque about one axis at a time. Revised duty cycles were calculated and are presented here using the VRCS logic in Reference 1. Figure 4-7 shows the location of the VRCS thrusters

Table 4-6. Roll duty cycles.

Maximum Attitude Error	Construction Phase	Time (sec)				
		+Roll	Off	-Roll	Off	+Roll
± 1 Deg	1	0.93	217	0.65	217	0.93
	2-1	2.9	201	3.0	201	2.9
	3	13.2	210	6.2	210	13.2
± 5 Deg	1	0.92	2420	—	—	0.92
	2-1	1.7	1165	1.8	1165	1.7
	3	10.5	2517	—	—	10.5

Table 4-7. Pitch duty cycles.

Maximum Error	Construction Phase	Time (sec)				
		+Pitch	Off	-Pitch	Off	+Pitch
± 1 Deg	2-1	0.87	211	1.2	211	0.87
	3	1.2	208	1.6	208	1.2
± 5 Deg	2-1	0.87	1470	1.2	1470	1.2
	3	1.2	1370	1.6	1370	1.6

Table 4-8. Yaw duty cycles.

Maximum Error	Construction Phase	Time (sec)				
		+Yaw	Off	-Yaw	Off	+Yaw
± 1 Deg	2-1	1.65	201	1.64	201	1.65
	3	3.4	203	5.4	202	3.4
± 5 Deg	2-1	1.65	1230	1.64	1230	1.65
	3	3.2	1063	5.2	1063	3.2

Reference 1: Space Shuttle Orbiter Orbiter Flight Test, LEVEL C, Functional Subsystem Software Requirements; Guidance, Navigation and Control; Part C, Flight Control On Orbit; SD76-SH-0009, 1 June 1977.

● THRUSTER ARRANGEMENT

● IMPULSE TIME HISTORY

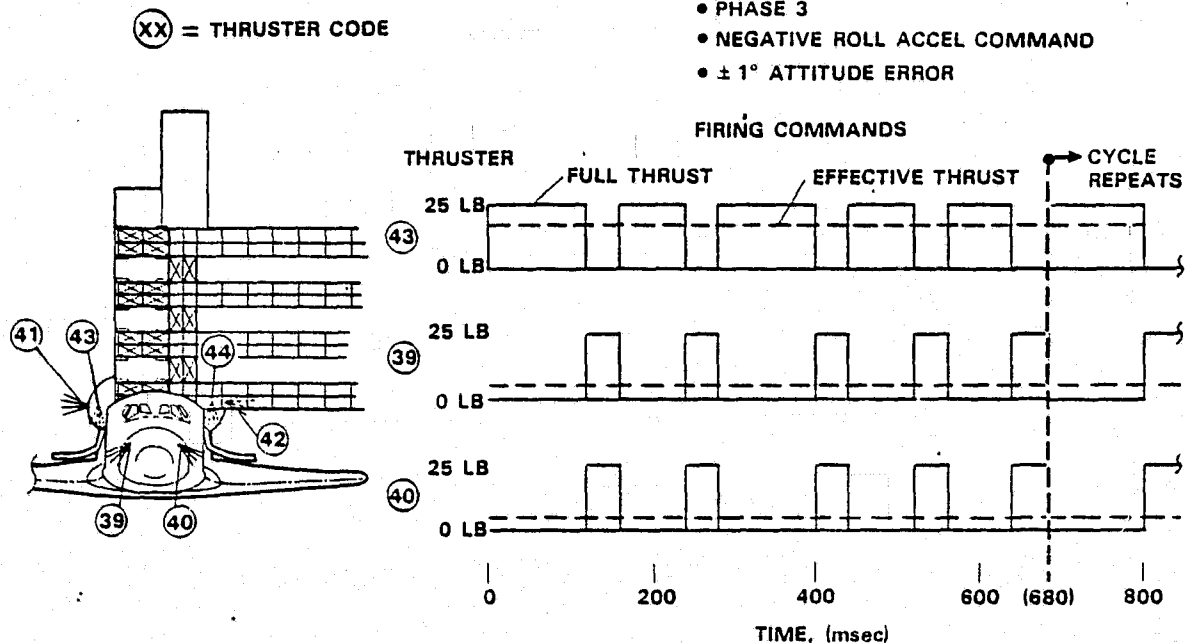


Figure 4-7. VRCS thruster operational details.

and the pulse time history for a negative roll command during phase 3, using the Orbiter VRCS logic from Reference 1.

The operation of the Orbiter VRCS is such that, during a command to change rate in a given axis, the cross coupling into another axis is balanced out. A negative roll command will fire thruster 43. The net pitch acceleration will be four times the roll acceleration. To prevent a change in pitch rate, the two vernier nose thrusters are turned On and the aft thruster, providing the roll correction, is turned Off. For normal operation after a roll command of 80 to 120 ms, a positive pitch command is output to the vernier thruster firing logic. For the control accelerations with the platform completed, the positive pitch command and negative roll command will only fire thrusters 39 and 40. The net result is a longer roll pulse and an on/off cycling of the thruster during a given command control pulse. As shown in Figure 4-7, the beam response can be determined by applying a steady pulse during the commanded On-time at a reduced (i. e., effective) thrust level. With constant total effective impulse, beam response was reduced about three percent below the values obtained with cyclic thrusting.

The basic Orbiter VRCS logic and thruster locations were designed for a vehicle with the center of gravity close to the XY plane, the pitch and yaw inertias about the same, and the roll inertia about 10 percent of the pitch/yaw inertia. The control acceleration in each axis will then be no greater than two to one. A look at the

revised mass properties, Figure 4-4, shows that this condition is violated as the beams and platform are built.

The control accelerations for each VRCS thruster are given in Table 4-9. The revised mass properties shown in Figure 4-4 were used for the calculations. For the same negative roll command during case 1, thrusters 39, 43, and 41 would fire. The resulting roll correction time will be short since the average roll acceleration will be as great as the pitch or yaw accelerations.

Table 4-9. Thruster control accelerations.

Thruster	Control Acceleration, deg/sec ²		
	Pitch	Yaw	Roll
Case 1			
39	0.0115	0.00957	0.00374
40	0.0115	0.00957	0.00188
41	0.0	0.00786	0.00817
42	0.0	0.00786	0.00817
43	0.0082	0.0	0.0142
44	0.0082	0.0	0.0126
Case 2			
39	0.0116	0.00722	0.000727
40	0.0116	0.00722	0.000907
41	0.0	0.00599	0.00269
42	0.0	0.00599	0.00269
43	0.0082	0.0	0.00429
44	0.0082	0.0	0.00454
Case 3			
39	0.0110	0.00395	0.000293
40	0.0110	0.00395	0.000458
41	0.0	0.00327	0.000680
42	0.0	0.00327	0.000680
43	0.00782	0.0	0.001807
44	0.00782	0.0	0.000825

In Section 4.2.1.2 the pulse time histories for pitch, yaw, and roll corrections using preliminary mass properties were presented. The thrusters that fired during the pulse and their effective thrust are given in Tables 4-10 and 4-11. The thruster data using the Orbiter VRCS logic is also given in this table. The thrust factor times the nominal thrust gives the effective thrust during a commanded change in rate for a given axis. The thrust factor also represents the fraction of time a given thruster is On during the period rate is being changed. In Section 4.2.1.4 the pulse histories were developed using the revised mass properties and the Orbiter VRCS logic. During Phase 3, when pitch and yaw pulses are called for, the roll rate is not zero when the

Table 4-10. Case 2 thrust factors.

Pulse Axis	Logic	Thruster Number & Thrust Factor					
		39	40	41	42	43	44
+ Pitch	Preliminary	1.0	1.0	0.0	0.0	.04	0.0
	Orbiter VRCS	1.0	.99	.01	0.0	0.0	0.0
- Pitch	Preliminary	0.0	0.0	0.0	0.0	1.0	.95
	Orbiter VRCS	0.0	0.0	0.0	0.0	1.0	.95
+ Yaw	Preliminary	0.0	.36	1.0	0.0	0.0	.60
	Orbiter VRCS	0.0	.5	.7	0.0	.2	.5
- Yaw	Preliminary	.37	0.0	0.0	1.0	.54	0.0
	Orbiter VRCS	.49	0.0	0.0	.66	.51	.34
+ Roll	Preliminary	0.0	.69	0.0	0.86	0.0	1.0
	Orbiter VRCS	.26	.26	0.0	0.0	0.0	.74
- Roll	Preliminary	.69	0.0	.86	0.0	1.0	0.0
	Orbiter VRCS	.26	.26	0.0	0.0	.74	0.0

Table 4-11. Case 3 thrust factors.

Pulse Axis	Logic	Thruster Number & Thrust Factor					
		39	40	41	42	43	44
+ Pitch	Preliminary	1.0	1.0	0.0	0.0	0.0	.75
	Orbiter VRCS	1.0	1.0	0.0	0.0	0.0	0.0
- Pitch	Preliminary	0.0	0.0	0.0	0.0	.51	1.0
	Orbiter VRCS	0.0	0.0	0.0	0.0	1.0	1.0
+ Yaw	Preliminary	0.0	.69	.97	0.0	0.0	1.0
	Orbiter VRCS	0.0	.81	.81	.2	0.0	.92
- Yaw	Preliminary	.08	0.0	0.0	1.0	.3	0.0
	Orbiter VRCS	.6	.4	0.0	1.0	.4	0.0
+ Roll	Preliminary	0.0	.69	0.0	.86	0.0	1.0
	Orbiter VRCS	.25	0.0	.04	.64	0.0	.64
- Roll	Preliminary	.86	0.0	.86	0.0	1.0	0.0
	Orbiter VRCS	.29	.29	0.0	0.0	.71	0.0

primary axis command is satisfied. Therefore, a positive roll pulse will be called for using the thrust factors from the +roll pulse axis.

This is a result of operating the other VRCS logic out of the mass properties range for which it was designed. Normally, when a change in rate command for a given axis is finished, the rates in the other axes are equal to the rates before the command to within \pm the rate resulting for a minimum impulse firing.

4.2.1.4 Final Duty Cycle Analysis. The final duty cycle analysis was performed using the mass properties in Figure 4-4 and the VRCS logic from Reference 1.

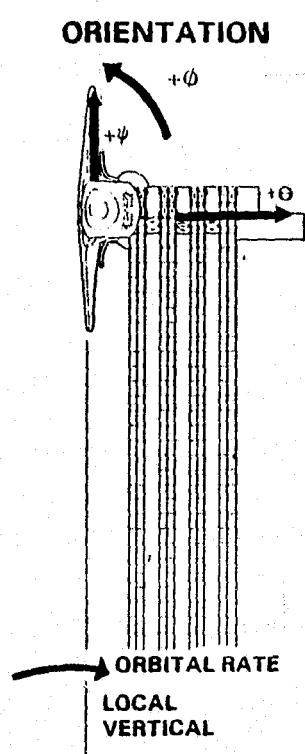
The VRCS duty cycles were calculated in Orbiter pitch, yaw, and roll for Phase 2-1 and Phase 3. In Phase 2-1 one beam was complete. In Phase 3 the platform was completed and the last cross beam had been attached. The following assumptions were used for the calculations:

- a. Only VRCS thrusters were used for control.
- b. No failed thrusters.
- c. Maximum attitude rate is ± 0.01 deg/sec.
- d. Disturbance torques are from gravity gradient and gyroscopic sources. The other disturbances (drag, solar pressure, etc.) are at least an order of magnitude less.

Figure 4-8 presents the maximum disturbance torques about the nominal position of the Orbiter and platform for the Phase 3 configuration, considering gravitational, gyroscopic, drag, solar, and magnetic forces. The torques resulting from small deviations from the nominal positions are given for the gravitational and gyroscopic forces.

The roll and yaw forces would restore the system to a trim position while the pitch torque is destabilizing and requires positive control to maintain system stability. Except for pitch, there is a stable trim position within 3 degrees of the local vertical and the Orbiter's pitch axis. Excluding the gravitational and gyroscopic torques, the largest environmental torque occurs in roll. This is the result of unbalanced drag forces on the Orbiter and platform. A roll trim angle of 0.46 degrees varying between 0.46 and 0.18 degrees during an orbit, will balance this torque. Therefore, except for a short period during the orbit, the assumptions as to disturbances were valid.

Figures 4-9 and 4-10 parametrically illustrate the roll duty cycles for two values of maximum attitude error for Phase 2-1 and Phase 3, respectively. The big difference can be seen in long roll pulse time in Phase 3 as a result of the low roll control torque relative to Phase 2-1, and the disturbed duty cycle resulting from a gravity gradient torque trying to put the center of gravity on the local vertical. The effect of the difference in the VRCS control logic can be seen by comparing the positive firing times in Figure 4-6 and Figure 4-10. The roll pulse times are increased by a factor of 2.5. By looking at the control accelerations and effective thruster-On-time



ENVIRONMENT	TORQUE, FT-LB		
	ROLL	PITCH	YAW
GRAVITY GRADIENT	$1.85-16.6 \sin 2 \phi$	$0.2+7.2 \sin 2 \theta$	$0.07+2.4 \sin 2 \psi$
GYROSCOPIC	0.0	$0.32-3.12 \sin 2 \theta$	$0.07 + 2.4 \sin 2 \psi$
DRAG	0.3	0.004	0.0
SOLAR PRESSURE	0.05	0.007	0.02
MAGNETIC FIELD	0.02	0.0	0.03

Figure 4-8. Environmental torques.

in Section 4.2.1.3 this would be expected. If propellant consumption should become a problem, modifications to the scaling in the Orbiter VRCS logic could reduce the firing times.

Time pulse histories for delta pitch rate, yaw rate, and roll rate commands are given in Tables 4-12, 4-13, and 4-14, respectively. The pulse time history tables were used to calculate propellant consumption during active VRCS periods. The tables of pulse time histories plus the tables in Section 4.2.1.4 can be used to determine a forcing function from which the beam and platform response can be determined. The actual thruster time histories were determined for all Phase 3 cases. A typical time history is shown in Figure 4-7 for negative roll acceleration command. This is the least complex of the thruster time histories. The actual time histories were used in the response analysis (Section 4.3) for Phase 3.

4.2.2 PLATFORM STABILITY DURING FREE FLIGHT MODE. The platform is to be released and then recaptured during the fifth day. Analysis was conducted to determine the platform response during this period with all platform systems installed. The response of the platform alone was analyzed first, then the passive damping

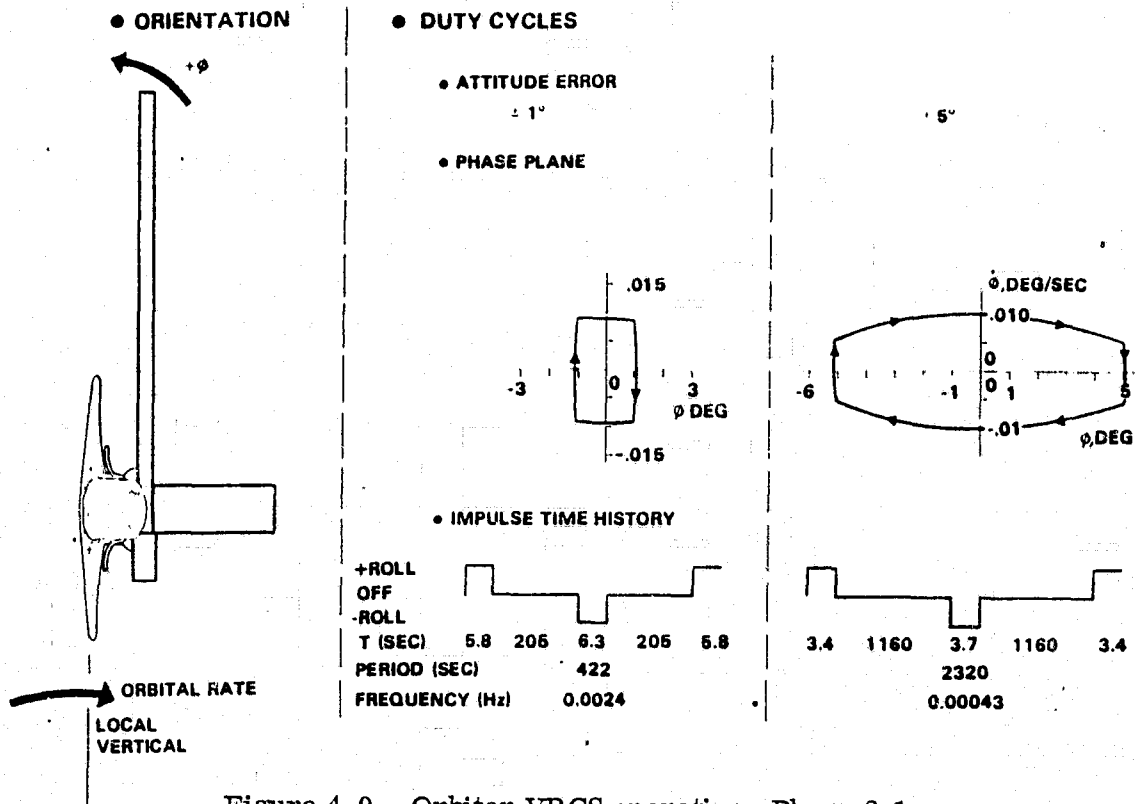


Figure 4-9. Orbiter VRCS operation, Phase 2-1.

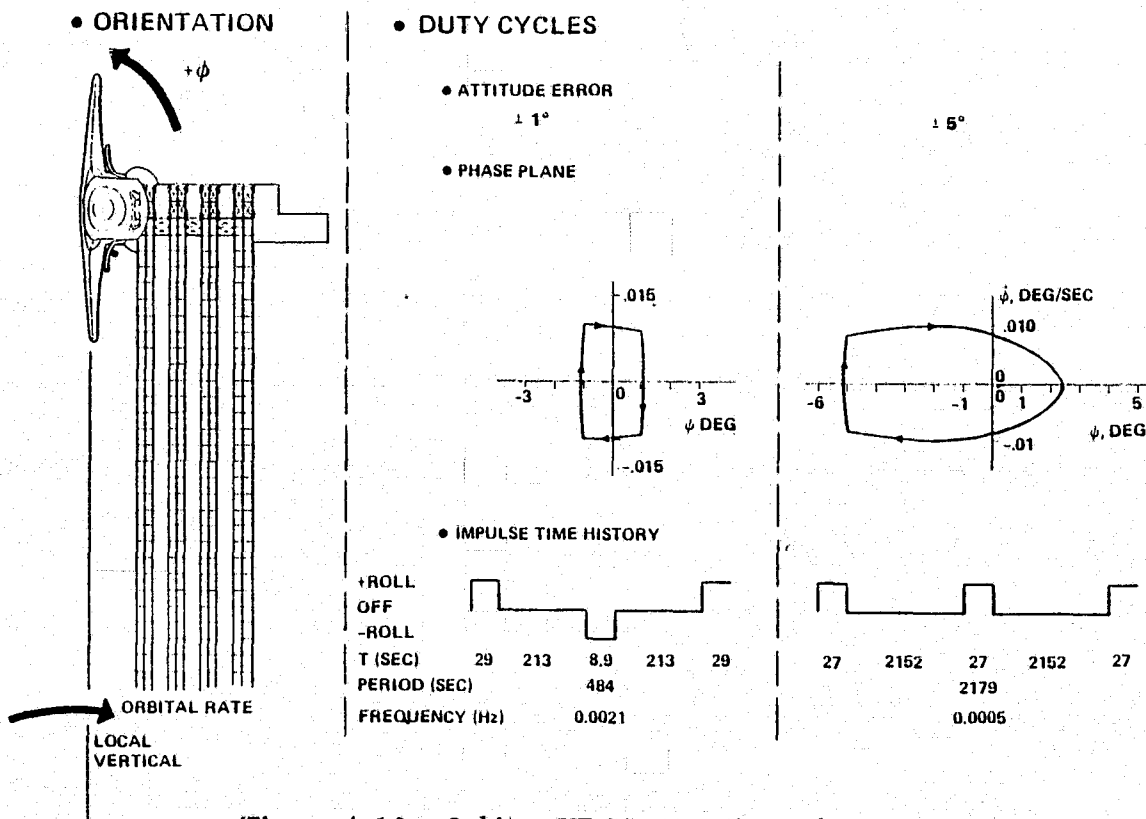


Figure 4-10. Orbiter VRCS operation, Phase 3.

Table 4-12. Final pitch duty cycles.

Maximum Error	Construction Phase	Time (Sec)							
		+ Pitch	+Roll	Off	- Pitch	+ Roll	Off	+ Pitch	+ Roll
± 1 Deg.	2-1	.87	--	208	1.2	--	208	.87	--
	3	.91	.98	200	1.2	1.6	204	.91	.98
± 5 Deg.	2-1	.77	--	1462	.76	--	1462	.77	--
	3	.91	.98	1366	.86	1.1	1369	.91	.98

Table 4-13. Final yaw duty cycles.

Maximum Error	Construction Phase	Time (Sec)						
		+ Yaw	+ Roll	Off	- Yaw	Off	+ Yaw	+ Roll
± 1 Deg.	2-1	2.6	--	201	2.7	201	2.6	--
	3	3.2	--	404	3.6	404	3.2	--
± 5 Deg.	2-1	2.6	--	1209	2.7	1209	2.6	--
	3	2.8	2.7	1065	2.8	1066	2.8	2.7

Table 4-14. Final roll duty cycles.

Maximum Error	Construction Phase	Time (Sec)				
		+ Roll	Off	- Roll	Off	+ Roll
± 1 Deg.	2-1	5.8	205	6.3	205	5.8
	3	27	213	8.9	213	29
± 5 Deg.	2-1	3.4	1160	3.7	1160	3.4
	3	27	2152	--	--	27

required for long term orbit stabilization was evaluated.

The mass properties of the platform with and without the systems installed are given in Figure 4-5. The position of the platform in free flight, the coordinate system, and the sense of pitch, yaw, and roll are given in Figure 4-11. Platform oscillations are shown in Table 4-15. The oscillations are about the trim position which is essentially 0° in pitch and roll and -6.1° in yaw. An initial condition of 0.01 deg/sec was assumed on separation from the Orbiter.

The environmental torques were calculated as a function of orbit position. The results are given in Table 4-16 for seven days after launch passing through the descending node.

The torques resulting from small deviations from the reference position are given for the gravitational and gyroscopic forces. The forces in all axes will restore the platform to a trim position. The disturbance forces are cyclic in nature and, except for yaw, the frequencies are separated from the beam natural frequencies. The amplification factors in pitch and roll are 2.4 and 2 for disturbances at orbit frequency. In yaw, the disturbance caused by drag will be cyclic due to the diurnal variation in atmospheric density. The amplification factor is 54.5 with a forcing function of ± 2.6 deg. The resulting oscillations would result in tumbling in yaw based on linear analysis. If it were desired to separate the bare platform and recapture it, a detailed analysis would be required to determine if platform rates remained within the recapture envelope of the Orbiter RMS.

The platform is planned to be released with full systems installed. By the positioning of the thermal shield with respect to the platform center of gravity the yaw stiffness can be increased. Table 4-17 shows the response and natural frequencies of the platform with all systems installed. There is a variation in natural frequency in yaw resulting from the diurnal variation in density. The effect of this variation is shown in the table along with the effect on oscillation amplitude.

The environmental torques were calculated for the full-up platform because some of the environmental torques have an effect on the stability of the platform and have an effect on oscillation amplitudes, as well as acting as a bias. The maximum torques will be given along with the minimum where appropriate. The variation in gravity

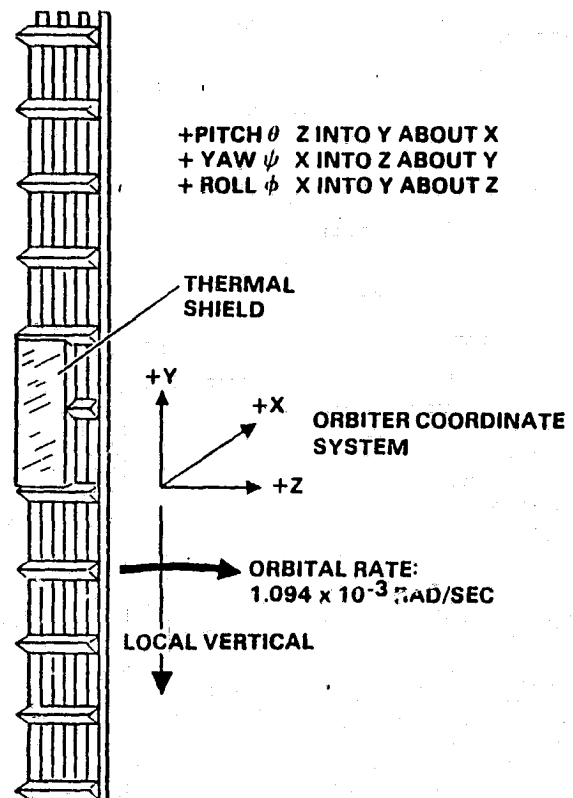


Figure 4-11. Platform stable release orientation.

Table 4-15. Bare platform response.

Axis	Oscillation frequency	Bias	Oscillation Amplitude
Pitch	1.886×10^{-3} Rad/Sec	0.0	± 5.3 Deg
Yaw	1.07×10^{-3} Rad/Sec	-6.1	± 9.3 Deg
Roll	2.18×10^{-3} Rad/Sec	0.0	± 4.6 Deg

Initial Rate each axis 0.01 Deg/Sec

Table 4-16. Bare platform environmental torques.

Environment	Torque, Nm		
	Roll	Pitch	Yaw
Gravity Gradient	$-6.1 \sin 2\theta$	$-6.1 \sin 2\theta$	0.0
Gyroscopic	$-2.1 \sin 2\theta$	0.0	$-6.1 \times 10^{-3} \sin 2\psi$
Drag	0.0	1.2×10^{-4}	-1.8×10^{-3}
Solar Pressure	1.4×10^{-5}	1.1×10^{-7}	-2×10^{-6}
Magnetic Field	-2.2×10^{-4}	-1.2×10^{-4}	0.0

Table 4-17. Platform response systems installed.

Axis	Oscillation Frequency	Bias	Oscillation Amplitude
Pitch	1.888×10^{-3} Rad/Sec	-0.22	± 5.3 Deg
Yaw	1.967×10^{-3} 1.475×10^{-3} } Rad/Sec	+2.18	± 5.08 ± 6.78 } Deg
Roll	2.186×10^{-3} Rad/Sec	0	± 4.57 Deg

(Initial Rate in each Axis 0.01 deg/sec)

gradient and gyroscopic torques are also given in Table 4-18.

The cyclic disturbance torques will result in oscillations of the platform exceeding the angles required to trim the disturbances. Because of the added stability in yaw provided by the thermal shield, the amplitudes will be within the capture range of the Orbiter during the three orbits the platform will be flying free. This assumes no damping, since the passive damping system, to be discussed later, has a time

Table 4-18. Platform with systems environmental torques.

Environment	Torque N-m		
	Roll	Pitch	Yaw
Gravity Gradient	$-17.3 \sin 2\theta$	$17.6 \sin 2\theta$	0.0
Gyroscopic	$-5.7 \sin 2\theta$	0.0	$1.1 \times 10^{-2} \sin 2\psi$
Drag	0.0	0.33 -0.13	$3.2 \times 10^{-3} - 5.2 \times 10^{-1} \sin 2\psi$ $1.3 \times 10^{-3} - 2.1 \times 10^{-1} \sin 2\psi$
Solar Pressure	-1.2×10^{-2}	± 0.037	$+1.0 \times 10^{-4}$
Magnetic Field	-4.6×10^{-5}	2.5×10^{-5}	0.0

constant of 12 orbits. Table 4-19 gives the expected oscillation amplitude, rate frequency and cause for the largest environmentally caused oscillation in each axis.

Table 4-19. Response to environment disturbance torques.

Axis	Amplitude	Rate	Frequency	Environment
Roll	±.54 Deg	$\pm 1.18 \times 10^{-3}$ Deg/Sec	2.188×10^{-3}	Solar
Pitch	±.157 Deg	$\pm 1.71 \times 10^{-4}$ Deg/Sec	1.09×10^{-3}	Drag
Yaw	±1.39 Deg	$\pm 1.51 \times 10^{-4}$ Deg/Sec	1.09×10^{-3}	Drag

The analysis of the full-up platform indicates that the Orbiter rates at separation, and the ability to release the platform at the trim position, will determine the oscillation amplitudes after platform release. Minimum trim will be required if the platform is released in the shadow of the Earth.

As part of the platform analysis, the requirements for a passive damper were determined. A magnetically anchored spherical eddy-current or viscous fluid damper may be used. The viscous damper will have a damping coefficient four times that of an eddy current damper for the same size and weight. This is based on two dampers built by General Electric and flown on the NRL satellite. Either damper will reduce the amplitude of platform oscillations to a steady state value at a rate dependent upon the damping coefficient and the system inertia level. Large damping values will rapidly reduce the oscillations but will result in a large steady-state error. To select a damping level, it will be necessary to trade off these two effects. A value was selected which will produce an exponential decay time constant of about 12 orbits. This value will result in a steady-state error of about 0.5 degree. The full-up platform would require a damper with a damping coefficient of 262 Newton-meter-second. This could be provided by one of the General Electric viscous dampers, used on the NRL satellite, for a total weight of 2.7 kg.

4.3 STRUCTURAL DYNAMICS

The structural dynamic characteristics of both a single beam and the complete platform, while attached to the Orbiter, have been determined. The analysis objective has been to evaluate the two ends of the beam building process, from which conclusions could be formulated about the general response characteristics at any time. Response of the beams was determined for the operation of the Orbiter VRCS. Parametric development of VRCS time histories for selected attitude error limits (± 1 , and $\pm 5^\circ$) is discussed in Section 4.2.1. Response analyses in the Orbiter-attached mode were conservatively based on VRCS duty cycles for $\pm 1^\circ$ maximum attitude error, since pulse frequencies are highest for this case and pulse durations are similar in both cases.

Tip deflection of the beams and root bending moments were found to be small for a single set of pitch, yaw, or roll pulses. The analyses revealed the need to consider the timing of succeeding pulses. The mode shapes and frequencies of a free platform have also been computed.

4.3.1 SINGLE BEAM ATTACHED TO ORBITER. This event is considered at the point when the first beam is complete but still attached to the beam builder. The beam is also attached to the assembly jig with rollers at two points.

4.3.1.1 Math Model. For the purpose of computing free-free mode shapes and frequencies, the Orbiter and a single completed beam were idealized into a finite element system. The beam was divided into twelve segments with six degrees of freedom permitted at each beam node point. The Orbiter, assembly jig, and beam builder were idealized as lumped masses with six degrees of freedom each, interconnected with elastic members. The beam was attached to the beam builder through springs representing the roller supports.

4.3.1.2 Modes. Rigid body and elastic modes were computed. Table 4-20 provides a list of the frequencies and a brief description of the predominant motion associated with each mode. The modes encompass bending, torsion, and longitudinal motion. Shapes of the first five free-free elastic modes have been plotted in Figure 4-12.

Selected modes including first, second, and third yaw and roll bending, were used in the response analysis.

4.3.1.3 Response. Transient analyses were conducted to determine beam tip elastic responses due to firing of the VRCS thrusters. Thruster combinations which produce Orbiter yaw, roll, and pitch were used in three separate analyses. Typical beam tip displacement and acceleration time histories due to a single roll pulse are presented in Figure 4-13. The maximum beam tip responses and clearance loss are given in Table 4-21. Note that cross coupling causes beam tip displacement in both the fore and aft and vertical direction due to any pulse type considered.

Beam tip response in the vertical direction will cause a loss of clearance between adjacent beams. Conservatively assuming that the response amplitudes for two or more beams are the same as for a single beam and that adjacent beams are

Table 4-20. Mode frequencies: Single beam and Orbiter.

No.	Freq (Hz)	Period (Sec)	Description
1*	0.0338	29.59	1ST YAW BENDING
2*	0.0512	19.53	1ST ROLL BENDING
3	0.1694	5.90	1ST TORSION
4*	0.2523	3.96	2ND YAW BENDING
5*	0.2527	3.96	2ND ROLL BENDING
6	0.5019	1.99	2ND TORSION
7*	0.7554	1.32	3RD YAW BENDING
8*	0.7555	1.32	3RD ROLL BENDING
9	0.8156	1.23	3RD TORSION
10	1.0988	0.91	4TH TORSION
11	1.1857	0.84	1ST LONGITUDINAL
12	1.3407	0.75	5TH TORSION
13	1.5063	0.66	4TH YAW BENDING
14	1.5064	0.66	4TH ROLL BENDING

* USED IN RESPONSE ANALYSIS

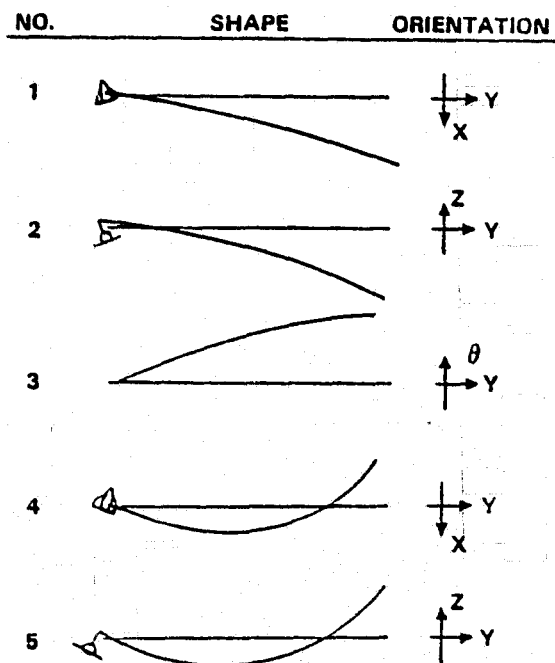


Figure 4-12. Mode shapes: single beam and Orbiter.

out of phase, net clearance between beams was computed to have a minimum value of 1.175 meters, as illustrated in Figure 4-14.

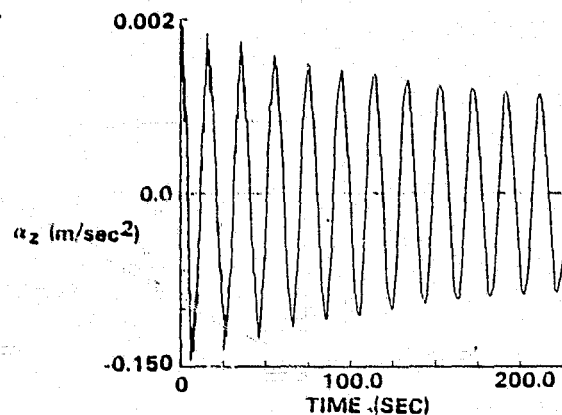
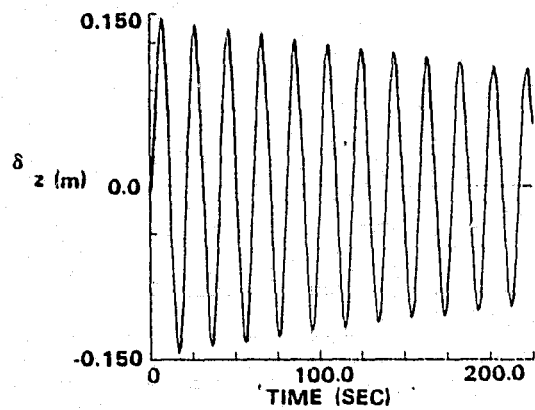


Figure 4-13. Dynamic response: single beam, roll pulse.

Beam root bending moments were determined for thruster combinations which produced Orbiter yaw, roll, and pitch in three separate analyses. The highest beam root bending moment and beam tip deflection is in the fore and aft direction due to a 1.06-second yaw pulse. Since there is no potential beam-to-beam interference in this direction, bending moment is the key item of interest. A time history of the root yaw bending moment due to a yaw pulse is shown in Figure 4-15.

Table 4-21. Displacement and clearance loss: single beam.

VRCS Pulse		Beam Tip Displacement (Meters)				Net Clearance Between Beams (Meters)
Type	Duration (Sec)	Fore & Aft		Vertical		
		Max +	Max -	Max +	Max -	
Yaw	1.06	.3035	-.3098	.1083	-.1154	1.300
Roll	4.61	.0335	-.0312	.1766	-.1729	<u>1.175</u>
Pitch	1.20	.0112	-.0117	.0170	-.0178	1.489

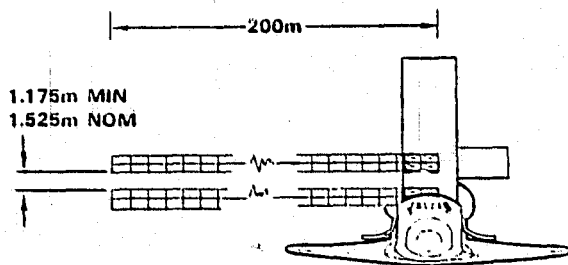


Figure 4-14. Clearance loss due to dynamic response.

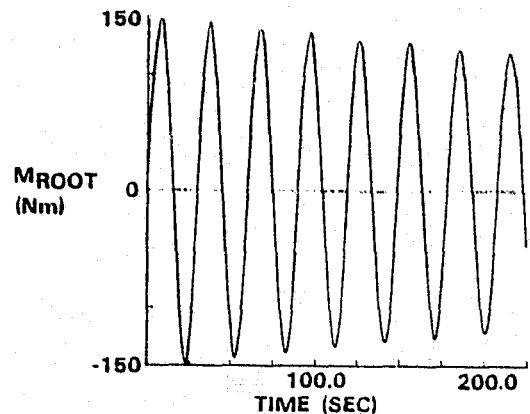


Figure 4-15. Beam root yaw bending moment.

4.3.1.4 Response Sensitivities, Phase 2-1. Response sensitivity studies were conducted to determine the effects of: (1) increasing the duration of a pulse, and (2) varying the start time of succeeding pulses.

Pulse length was increased to a time equal to the period of the mode producing the major response. Beam tip vertical displacement is presented in Figure 4-16 for a range of yaw and roll pulse lengths. Increasing roll produces a maximum vertical deflection of 0.25 meter. Increasing yaw pulse duration produces a maximum vertical response of 0.92 meter. Since 0.762 meter is the maximum allowable deflection which can occur before adjacent beams make contact, the maximum permissible yaw pulse length is approximately 10 seconds. The effect on maximum vertical response due to varying the timing of the next pulse is illustrated in Figure 4-17. After each pulse the beam is given a vibratory motion. This motion is either reduced or increased by succeeding pulses. The curve in Figure 4-17 represents the maximum vertical response after a second pulse. If the second pulse was started at 197 seconds, the resulting response would be 0.05 meter. If the second pulse came at 187 or 206 seconds, the responses add, giving a total of 0.30 meter. This illustrates the potential requirement for some type of structural feedback to the VRCS if narrow attitude error limits (requiring approximately 200 seconds between firings) must be maintained.

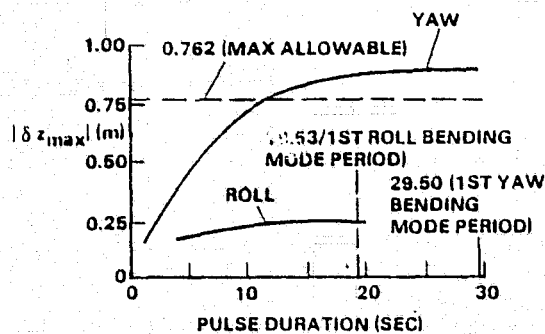


Figure 4-16. Beam tip response sensitivity to pulse duration.

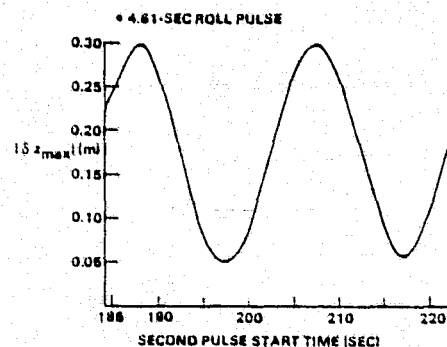


Figure 4-17. Beam tip response sensitivity to pulse timing.

4.3.2 COMPLETED PLATFORM ATTACHED TO ORBITER. This event is considered at the point when all four beams are complete and all nine cross beams have been attached. The platform is attached at one end to the assembly jig.

4.3.2.1 Math Model. For the purpose of computing free-free mode shapes and frequencies, the single beam math model was expanded to include the four longitudinal beams and the nine cross beams. Each cross beam was divided into three segments. Each longitudinal beam was attached to the assembly jig at three points. This attachment is stiffer than the two point attachment used previously for a single beam. The math model is illustrated in Figure 4-18. For the purpose of determining the model deflection at the VRCS thrusters, rigid beams were run from each thruster to the Orbiter c.g.

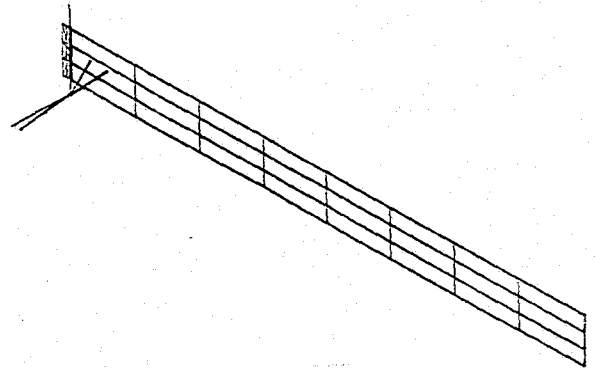


Figure 4-18. Math model: platform with Orbiter.

4.3.2.2 Modes. Rigid body and elastic modes were computed. Table 4-22 provides a list of the frequencies and a brief description of the predominant motion associated with each mode. The modes encompass platform bending, torsion, and longitudinal motion. Shapes of the first six free-free elastic modes have been plotted in Figure 4-19. The undeflected structure is shown by solid lines and the deflected structure by dashed lines. All fourteen elastic modes plus the six rigid body modes were used in the response analyses.

Table 4-22. Mode frequencies: platform and Orbiter.

Mode No.	Frequency Hz	Period Sec	Description
1	.07201	13.887	1st Torsion
2	.081072	12.335	1st Yaw Bending
3	.17204	5.8125	1st Roll Bending
4	.32802	3.0486	2nd Yaw Bending
5	.34095	2.9330	2nd Torsion
6	.44294	2.2576	2nd Roll Bending
7	.87626	1.1412	3rd Torsion
8	.87642	1.1410	3rd Yaw Bending
9	1.0811	.92498	3rd Roll Bending
10	1.1547	.86605	1st Longitudinal
11	1.6386	.61027	4th Torsion
12	1.6567	.60360	4th Yaw Bending
13	1.9020	.50455	4th Roll Bending
14	2.5972	.38504	5th Torsion

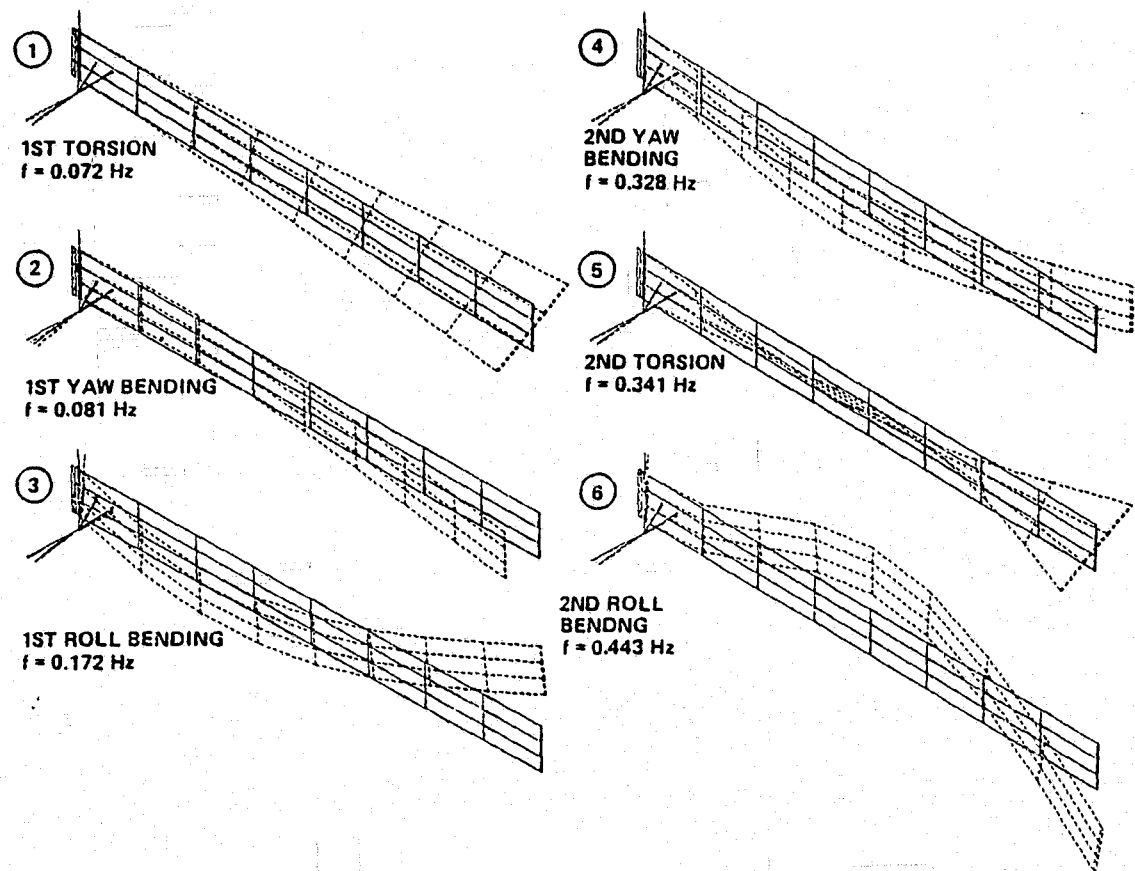


Figure 4-19. Mode shapes: platform and Orbiter.

4.3.2.3 Response. Transient analyses were conducted to determine the platform tip elastic responses and internal loads due to firing of the VRCS thrusters. The results are conservative since they are based on a duty cycle which maintains an attitude of $\pm 1^\circ$ in all three axes. (Reference Section 4.2.1.) Thruster combinations that produce Orbiter yaw, roll, and pitch were used in three separate analyses. A complete VRCS duty cycle was considered in each case. No attempt was made to adjust successive pulse start times to minimize response.

Typical platform tip displacement and acceleration time histories due to a single cycle of yaw pulses are presented in Figure 4-20. The maximum tip responses for all three types of pulses are given in Table 4-23. Beam 1 is the lower beam and beam 4 is the upper beam. Difference refers to the difference between beam 1 and 4. The platform is relatively stiff in the vertical direction compared to the fore and aft direction. This difference in stiffness is illustrated by the largest deflection occurring in the fore and aft direction. The time history response plots in Figure 4-20 illustrate the effect of starting time of the negative yaw pulse starting at 206 seconds. If the pulse started a half cycle (~ 6 sec) sooner or later, a cancelling effect would occur. The same principle applies to succeeding pulse cycles.

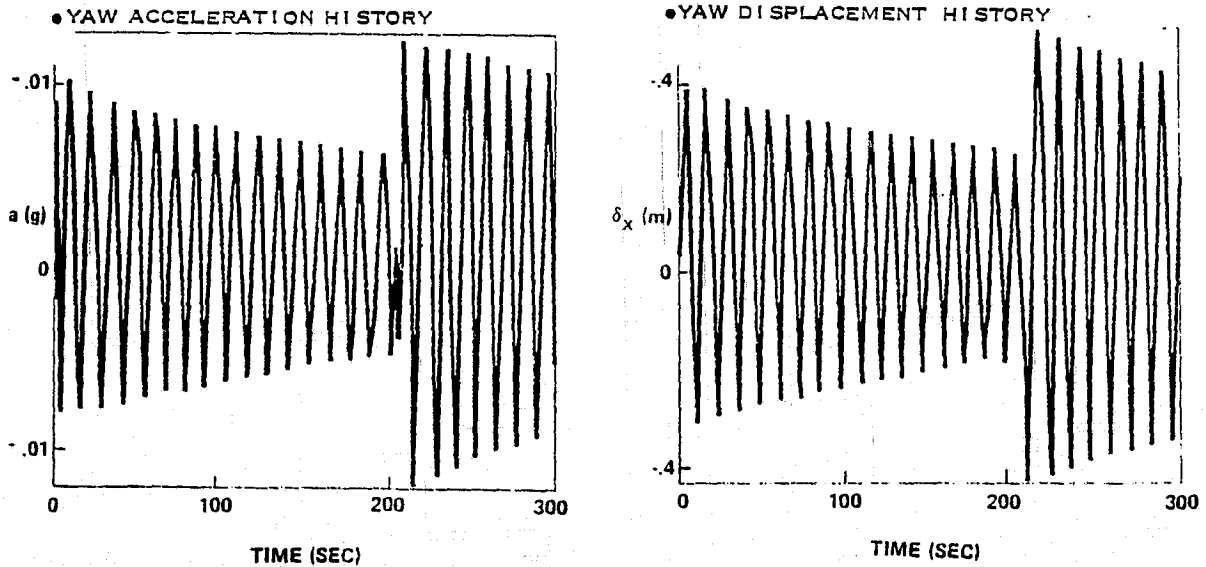


Figure 4-20. Platform tip response, yaw pulse.

Table 4-23. Platform tip displacements.

VCRS Pulse Type	Tip Displacement (Meters)							
	Beam 1				Beam 4		Difference	
	Fore & Aft		Vertical		Fore & Aft		Fore & Aft	
	Max+	Max-	Max+	Max-	Max+	Max-	Max+	Max-
Yaw	.4576	-.4583	.0273	-.0303	.4579	-.4587	.0048	-.0049
Roll	.1947	-.3314	.0042	-.0447	.1948	-.2307	.0014	-.0018
Pitch	.0890	-.0956	.0317	-.0329	.0920	-.1005	.0092	-.0091

The maximum loads developed in each of the four main beams were determined and are presented in Table 4-24. These root loads occur at the point where the beams attach to the assembly jig. The maximum moment and shear developed in a cross beam are also presented in Table 4-24.

4.3.3 FREE PLATFORM. Mode shapes and frequencies were computed for the platform separated from the Orbiter. The math model of the platform was extracted from the math model of the platform attached to the assembly jig and Orbiter. The mass used in the modal analysis was for a bare platform without instrumentation. Fourteen elastic modes were computed. Table 4-25 provides a list of the frequencies and a brief description of the predominant motion associated with each mode. Selected shapes of six free-free elastic modes have been plotted in Figure 4-21.

Table 4-24. Platform dynamic response loads.

Location	Description	Coord	Units	Pitch		Roll		Yaw		Maximum
Beam 1 Root	Yaw Bending Moment	170.6	Nm	154.359	- 176.912	349.799	- 295.478	697.425	- 644.265	697.425
	Roll Bending Moment	170.4	Nm	85.883	- 41.832	113.239	- 7.029	80.449	- 36.455	113.239
	Side Shear	170.1	N	4.102	- 2.276	2.946	- 2.088	5.051	- 7.823	7.823
	Vertical Shear	170.3	N	.771	- .489	.915	- .117	.641	- .366	.915
	Axial Load	170.2	N	13.655	- 17.258	18.106	- 15.396	13.433	- 12.562	18.106
	Torsion	170.5	Nm	.048	- .019	.084	- .018	.023	- .035	.048
Beam 2 Root	Yaw Bending Moment	171.6	Nm	157.082	- 180.003	359.417	- 295.249	697.948	- 643.795	697.948
	Roll Bending Moment	171.4	Nm	87.693	- 42.246	114.695	- 6.678	82.564	- 36.873	114.695
	Side Shear	171.1	N	4.458	- 2.417	3.221	- 2.073	5.335	- 3.142	5.335
	Vertical Shear	171.3	N	.396	- .636	.941	- .160	.650	- .542	.941
	Axial Load	171.2	N	5.049	- 5.221	6.154	- 5.103	4.477	- 3.870	6.154
	Torsion	171.5	Nm	.057	- .022	.028	- .021	.027	- .042	.057
Beam 3 Root	Yaw Bending Moment	172.5	Nm	189.806	- 183.205	346.981	- 295.593	698.583	- 643.418	698.583
	Roll Bending Moment	172.4	Nm	87.414	- 41.956	114.781	- 6.941	82.486	- 36.708	114.781
	Side Shear	172.1	N	4.815	- 2.562	3.478	- 2.136	5.643	- 3.507	5.643
	Vertical Shear	172.3	N	.902	- .643	.941	- .160	.633	- .502	.941
	Axial Load	172.2	N	6.001	- 4.833	6.040	- 6.746	4.174	- 3.937	6.040
	Torsion	172.5	Nm	.057	- .022	.028	- .021	.028	- .042	.057
Beam 4 Root	Yaw Bending Moment	173.6	Nm	162.501	- 186.370	347.168	- 295.85	699.008	- 642.858	699.008
	Roll Bending Moment	173.4	Nm	85.698	- 41.754	113.239	- 6.989	80.502	- 36.594	113.239
	Side Shear	173.1	N	5.104	- 2.660	3.694	- 2.217	5.825	- 3.674	5.825
	Vertical Shear	173.3	N	.768	- .456	.916	- .125	.648	- .352	.916
	Axial Load	173.2	N	17.984	- 13.189	15.566	- 18.899	12.886	- 13.019	18.899
	Torsion	173.5	Nm	.054	- .021	.027	- .020	.026	- .040	.054
Cross Beam At Node 113	Roll Bending Moment	113.4	Nm	3.948	- 4.124	4.987	- 5.370	3.784	- 3.198	5.370
	Lateral Shear	113.4	N	1.977	- 2.047	2.486	- 2.879	1.884	- 1.597	2.879
Cross Beam At Node 123	Roll Bending Moment	123.4	Nm	4.495	- 4.203	4.236	- 4.869	3.479	- 3.650	4.869
	Lateral Shear	123.4	N	2.253	- 2.067	2.118	- 2.438	1.737	- 1.831	2.438

Table 4-25. Mode frequencies: Free platform.

Mode No.	Frequency Hz	Period Sec	Description
1	.0815	12.2680	1st Torsion
2	.3081	3.2461	1st Yaw Bending
3	.3418	2.9255	2nd Torsion
4	.3854	2.5946	1st Roll Bending
5	.8160	1.2225	2nd Yaw Bending
6	.8325	1.2012	3rd Torsion
7	1.0068	.9933	2nd Roll Bending
8	1.5433	.6480	4th Torsion
9	1.5499	.6452	3rd Yaw Bending
10	2.2137	.4517	1st Longitudinal
11	2.4493	.4083	5th Torsion
12	2.4781	.4035	4th Yaw Bending
13	3.5207	.2840	6th Torsion
14	3.5719	.2800	5th Yaw Bending

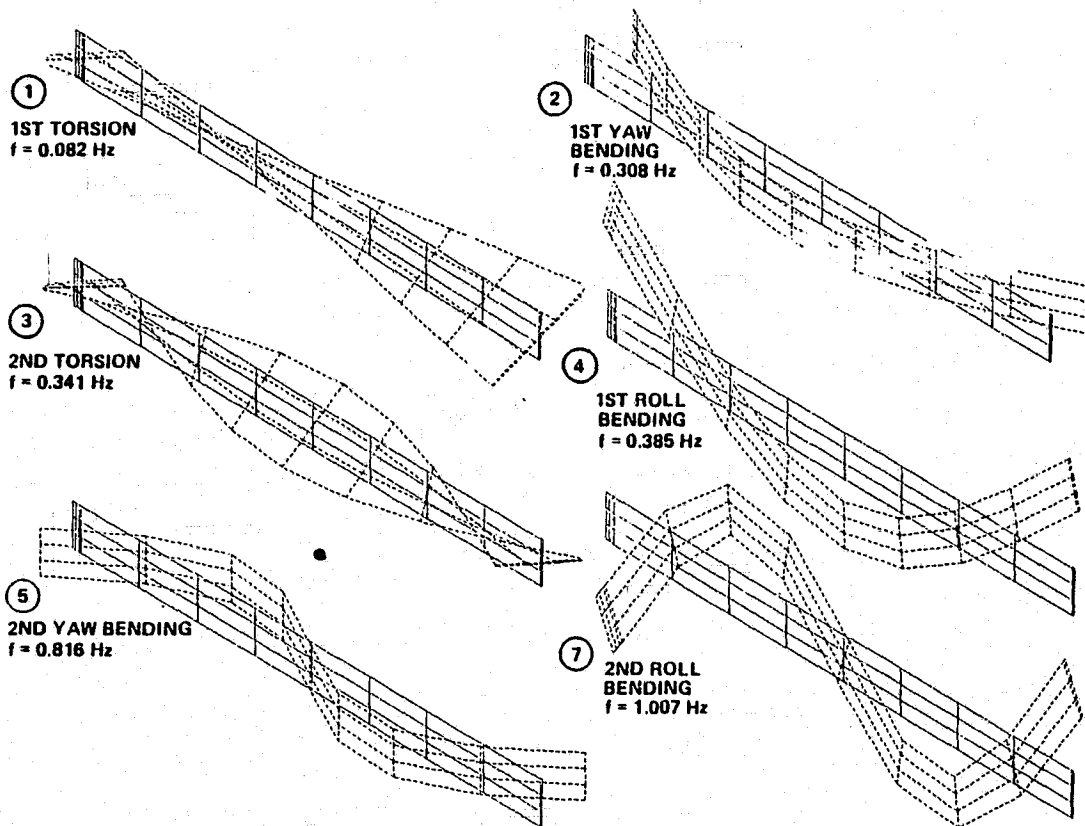


Figure 4-21. Mode shapes: free platform.

4.4 STRESS ANALYSIS

This section documents the preliminary stress analysis of the SCAFE beam and platform.

4.4.1 ELEMENT SECTION AND MATERIAL PROPERTIES.

4.4.1.1 Cap Member. The cross section of the SCAFE beam cap member is shown in Figure 4-22 with its section properties. The laminate configuration for the cap materials is VSA-11 (120/W-705₃/120). In words, this designation means that there are three inner plies of VSA-11 (Pitch) graphite/polysulfone in the form of a weave W-705 and one ply of 120 glass/polysulfone on each side of the laminate. All five laminae are oriented in the zero direction or along the axis of the cap. At the end of the study, the prepreg vendor

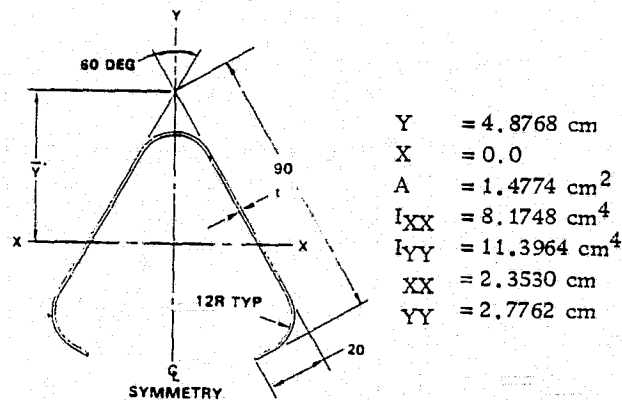


Figure 4-22. SCAFE beam cap geometry and section properties.

changed the woven tape configuration and type of pitch to VSB-32T/W704. The VSB-32T is a higher strength pitch fiber than the original VSA-11. For this analysis, the properties using VSA-11/W-705 will be used. The analytical predictions of the material properties in Table 4-26 are summarized from Table 2-13.

Table 4-26. Cap material properties, VSA-11 (120/W705₃/120).

E_x	=	143.14 GN/m ²	F_x^T	=	323.37 MN/m ²
E_y	=	9.17 GN/m ²	F_x^C	=	-323.37 MN/m ²
ν	=	0.20	F_y^T	=	50.33 MN/m ²
G	=	6.14 GN/m ²	F_y^C	=	-107.56 MN/m ²
α_x	=	0.380 $\mu\text{m}/\text{m}/^\circ\text{K}$	F_s	=	91.70 MN/m ²
α_y	=	20.000 $\mu\text{m}/\text{m}/^\circ\text{K}$			
t	=	0.0775 cm			
ρ	=	1772.0 kg/m ³			

Generally speaking, test results compare well with the predicted values of E_x and F_x^T , but there can be significantly large errors for the other values. An extensive test program to characterize the material when using composites is necessary, especially in this case for a hybrid. A further complication in predicting laminate properties is that to date the strength test properties have been lower than predicted and erratic for the pitch fibers.

4.4.1.2 Cross-Member. The cross section of the SCAFE beam cross member is shown in Figure 4-23 with its section properties. The dimensions shown are for the bare material only and do not include the T_1O_2 coating. The laminate configuration for the cross member material is VSA-11 (120/W-705 /120). The analytical predictions of the laminates material properties in Table 4-27 are summarized below from Table 2-13.

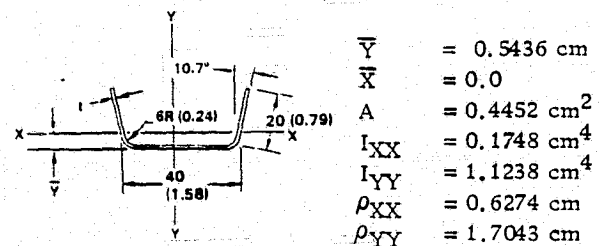


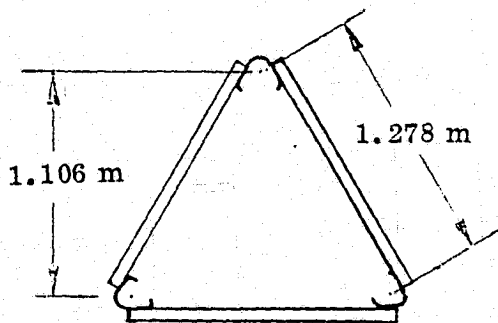
Figure 4-23. SCAFE cross-member geometry and section properties.

Table 4-27. Material properties, VSA-11(120/W705₂/120 cross member.

E_x	= 128.66 GN/m ²	F_x^T	= 291.65 MN/m ²
E_y	= 10.27 GN/m ²	F_x^C	= -291.65 MN/m ²
ν	= 0.190	F_y^T	= 55.85 MN/m ²
G	= 5.86 GN/m ²	F_y^C	= -119.97 MN/m ²
α_x	= -0.209 $\mu\text{m}/\text{m}/^\circ\text{k}$	F_s	= 88.25 MN/m ²
α_y	= 18.646 $\mu\text{m}/\text{m}/^\circ\text{k}$		
t	= 0.0584 cm		
ρ	= 1799 kg/m ³		

4.4.1.3 Diagonal Cords. The diagonal cords are made of S-glass/polysulfone with a nominal cord diameter of 0.1016 cm. The target modulus of elasticity is 41.27 GN/m² with a breaking strength of 667 N.

4.4.1.4 Beam Properties. The overall section properties for a single beam cross section are computed below using the projected VSA-11(120/W-705₃/120) materials properties:



$$E_{CAP} = 143.14 \text{ GN/m}^2$$

$$A_{CAP} = 1.4774 \text{ cm}^2$$

(Dimensions are between centroids)

ORIGINAL PAGE IS
OF POOR QUALITY

The axial stiffness is:

$$\begin{aligned}
 AE &= 3A_{CAP} E_{CAP} \\
 &= 3(1.4774 \times 10^{-4}) (143.14 \times 10^9) \\
 &= 63.44 \times 10^6 \text{ N} \\
 I &= \frac{A_{CAP} l^2}{2} \quad \text{where } l = 1.2775 \\
 &= \frac{1.4774 \times 10^{-4} (1.3082)^2}{2} \\
 &= 1.206 \times 10^{-4} \text{ m}^4
 \end{aligned}$$

The bending stiffness is:

$$\begin{aligned}
 EI &= (143.14 \times 10^9) (1.206 \times 10^{-4}) \\
 &= 17.26 \times 10^6 \text{ N-m}^2
 \end{aligned}$$

The torsional stiffness of the beam was determined with a small finite element model. The torsional stiffness of a bar can be expressed by the general equation

$$KG = \frac{T \ell}{\theta}$$

where K is a factor dependent on the form and dimensions of the cross section.

For a circular section, K is the polar moment of inertia J. For non-circular sections, K is less than J, and may be only a small fraction of J. For an open section

$$K = \frac{1}{3} \sum_{i=1}^n b_i t_i^3$$

where b is the element width and t is the thickness. For the SCAFE beam, the primary shear carrying members, the diagonal cords, do not conform to simple expressions for analysis, thus the finite element model. The equivalent KG can be calculated by applying a known torque to the cross section of beam length determining the resulting rotation and substituting into the expression for KG.

The general geometry of the model is shown in Figure 4-24. The model was one bay long, $l = 1.434\text{m}$.

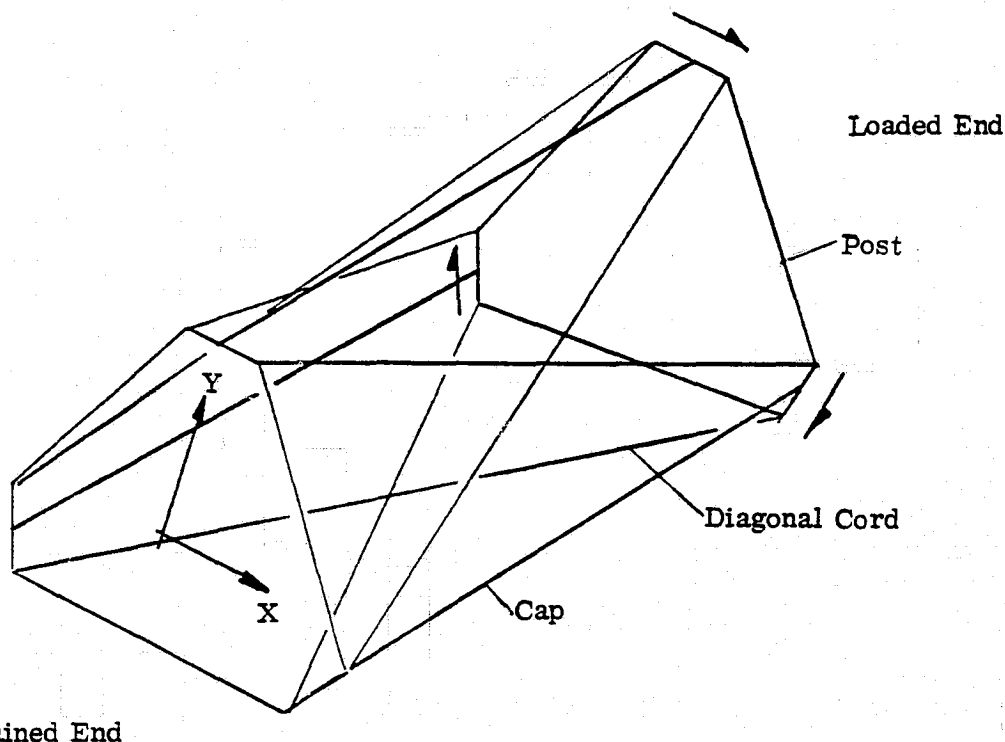


Figure 4-24. Finite element model for determining torsional constant.

The beam was subjected to an arbitrary torque as shown in Figure 4.25. The resulting rotation θ was

$$\theta = 0.1244 \text{ rad}$$

Therefore, the torsion constant becomes

$$\begin{aligned} KG &= \frac{Tl}{\theta} \\ &= \frac{(963.57)(1.434)}{0.1244} \\ &= 11110 \text{ N-m}^2 \end{aligned}$$

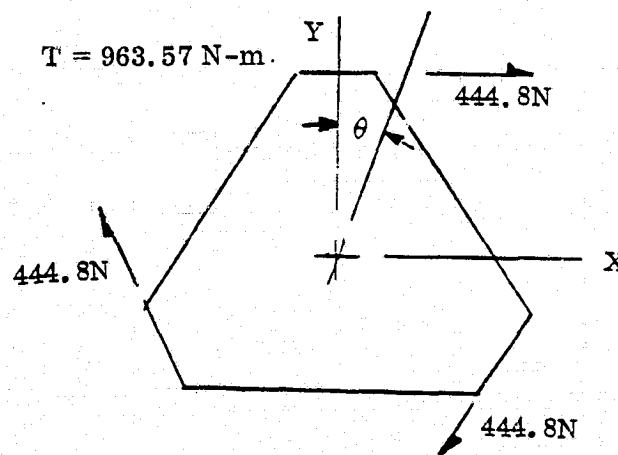


Figure 4-25. Torque applied to model.

Table 4-28 summarizes the beam stiffness properties.

Table 4-28. Beam stiffness properties.

A	=	4.4322 cm ²
I	=	1.206 × 10 ⁻⁴ m ⁴
AE	=	63.44 × 10 ⁶ N
EI	=	17.26 × 10 ⁶ N-m ²
KG	=	11.11 × 10 ³ N-m ²

ORIGINAL PAGE IS
OF POOR QUALITY

4.4.2 LOADS.

4.4.2.1 Preliminary Design Loads. To develop preliminary design loads for the SCAFE beam, a hopefully conservative approach was taken. Later analysis proved the assumption to be in fact conservative. The preliminary design loads are produced by assuming an Orbiter yaw maneuver with a single 200 m beam cantilevered from the beam builder as shown in Figure 4-26. The Orbiter VRCS rates used for this analysis are listed below (Ref. JSC07700, Vol. XIV, Table 3.12).

About X-X: (Roll)

$$\pm \ddot{\phi} = 0.00065 \text{ Rad/Sec}^2$$

About Y-Y: (Pitch)

$$+ \ddot{\theta} = +0.00042 \text{ Rad/Sec}^2$$

$$- \ddot{\theta} = -0.00030 \text{ Rad/Sec}^2$$

About Z-Z: (Yaw)

$$\pm \ddot{\Psi} = 0.00033 \text{ Rad/Sec}^2$$

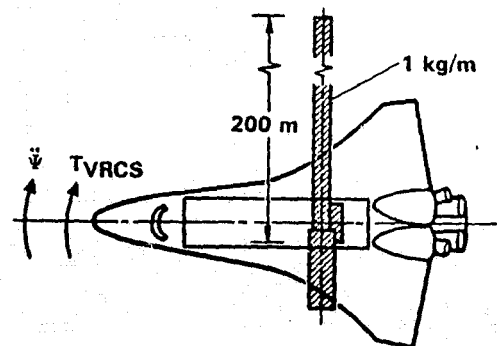


Figure 4-26. Orbiter/beam configuration.

The Orbiter mass properties used for this study are listed in Table 4-29.

Table 4-29. Orbiter Mass Properties.

Case	I _{XX} (10 ⁶ kg-m ²)	I _{YY} (10 ⁶ kg-m ²)	I _{ZZ} (10 ⁶ kg-m ²)	W _t (10 ³ kg)	X _{CG} (m)
1	1.0535	7.5913	7.9180	72.08	28.12
2	1.1741	8.4265	8.7858	82.42	28.80

Therefore the apparent VRCS torques from

$T = I \alpha$ are listed in Table 4-30.

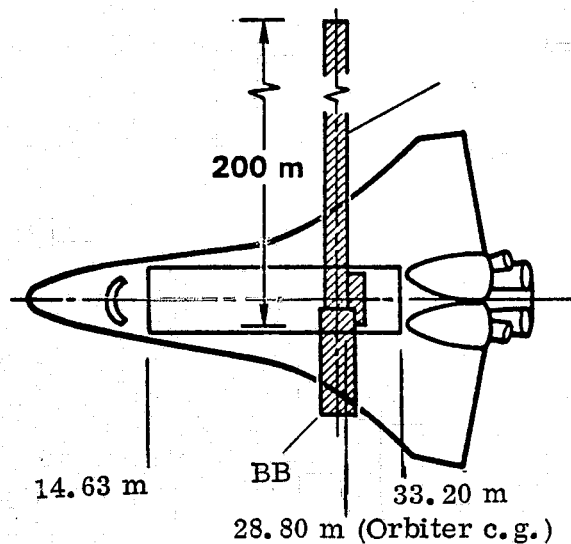
Table 4-30. Orbiter VRCS Torques.

Case	T_{XX} Nm	$+T_{YY}$ Nm	T_{ZZ} Nm
1	684.8	3188.2	2612.8
2	763.2	3538.9	2899.1

The Y-Y (pitch) loading does not introduce bending into the beam so the maximum torque is

$$T_{ZZ} = 2900 \text{ Nm}$$

The mass properties of the combined Orbiter/beams are computed below:



$$I_{ZZ} = 8.7858 \times 10^6 \text{ kg-m}^2$$

$$W_t = 82.42 \times 10^3 \text{ kg}$$

	W_t (kg)	X_{CG} (m)	$W_t \cdot X_{CG}$	Y_{CG} (m)	$W_t \cdot Y_{CG}$	I_o (kg-m ²)
Beam Builder	2475	28.400	70290	- 4.240	- 10494	11307.51
Assembly Jig	1856	29.845	55392.3	0.00	0	2321.06
Beam	200	28.400	5680	99.630	19926	666231.90
	4531		131362.3		9432	679860.47

$$\bar{X} = \frac{131362.3}{4531}$$

$$= 28.99 \text{ m}$$

$$\bar{Y} = \frac{9432}{4531}$$

$$= 2.08 \text{ m}$$

The mass moment of inertia of the SCAFE hardware and beam about its own center of gravity is

$$I_{X/Y} = I_o + \sum W_t \Delta \bar{X}^2 + \sum W_t \Delta \bar{Y}^2$$

$$= 2.690 \times 10^6 \text{ kg-m}^2$$

$$W_t = 4531 \text{ kg}$$

For the total system, Orbiter plus SCAFE hardware, the corresponding values are

$$W = 82420 + 4531 = 86951 \text{ kg}$$

$$\bar{X} = 28.81 \text{ m}$$

$$\bar{Y} = 0.109 \text{ m}$$

$$I = \sum I_o + \sum_i (W_t \Delta \bar{X}^2 + W_t \Delta \bar{Y}^2)$$

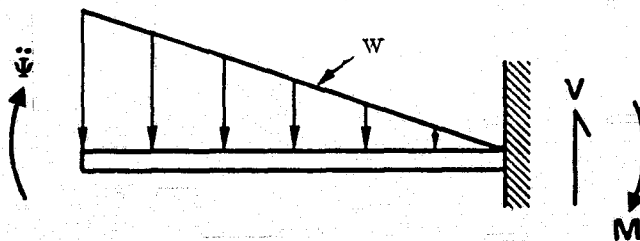
$$\ddot{\Psi} = 11.494 \times 10^6 \text{ kg-m}^2$$

The resulting acceleration on the combined structure is

$$\ddot{\Psi} = T/I = \frac{2900}{11.494 \times 10^6}$$

$$= 2.523 \times 10^{-4} \text{ Rad/Sec}^2$$

The resulting moment at the base of the beam can now be computed assuming the acceleration is steady-state or "pinwheeling".



$$w = \rho \ddot{\Psi} (200 - X)$$

$$\rho = 1.0 \text{ kg/m} = 1.0 \text{ NSec}^2/\text{m}^2$$

$$w_{AVG} = \frac{1}{2} (1.0) (2.523 \times 10^{-4}) (200)$$

$$= 0.02546 \text{ N/m}$$

$$W = Lw_{AVG} = 5.0918 \text{ N}$$

$$M = \frac{2}{3} WL = 678.6 \text{ N m}$$

Conservatively assuming that a dynamic magnification factor of 2.0 should be included to account for the effects of initial load application, the loads in Table 4-31 result.

Table 4-31. Preliminary single beam design loads.

	Steady	Dynamic
V(N)	5.09	10.18
M (Nm)	678.6	1357.2

The assembly jig provides a two-bay support to react the shear and bending moment as shown in Figure 4-27.

Solving the statics problems for internal loads gives the distribution in one fact of the beam as shown in Figure 4-28. Internal loads in the beam posts and diagonals are strongly influenced by the beam to assembly jig support configuration (especially the span over which the cantilever bending moment is reacted). The baseline beam builder/assembly jig configuration supports the beam over a 2.868 m span (2 bays). This length was selected as the best compromise between assembly jig size and complexity and beam loads.

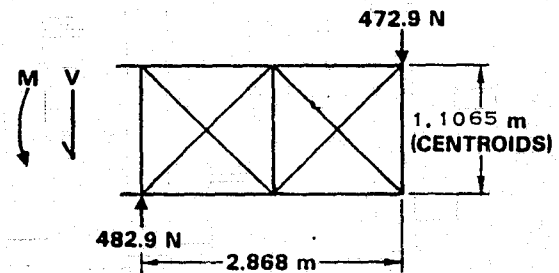


Figure 4-27. Preliminary beam limit reaction loads on jig.

Maximum design loads in the beam elements are:

Cap	±	590.3N	
Post	-	278.8N	(Limit)
Diagonal	+	402.1N	

ORIGINAL PAGE IS
OF POOR QUALITY

4.4.2.2 Final Design Loads. Transient analyses were conducted, to determine the elastic responses due to firing of VRCS thrusters, details of which are in Section 4.3.1. The analysis showed that the maximum bending moment at the root of a single

beam is 150 Nm. This compares to a hand-solution value of 1357 Nm used for initial sizing.

An additional transient analysis was conducted in which the platform was completed but still attached to the Orbiter through the Assembly Jig. The analysis is also discussed in Section 4.3.1. The resulting maximum loads at the beam root are

$$M = 699.0 \text{ Nm}$$

$$V = 113.2 \text{ N} \quad (\text{Limit})$$

Again, these loads are lower than the initial sizing loads in Table 4-31.

The resulting ultimate internal loads are shown in Figure 4-29 for beam reactions in Figure 4-30 where the ultimate Factor of Safety = 1.40

The internal loads in Figure 4-30 are the maximum loads for a 200 m beam; those for shorter lengths are lower. The post and diagonal loads outside the assembly jig are small compared to the loads induced by reacting the beam bending moment and shear loads in Figure 4-30.

4.4.2.3 Platform. The loads at the cross beam and the four longitudinal beams are very low. From Table 4-24 in Section 4.3.2 the maximum shear and moment are shown in Figure 4-31.

Figure 4-32 shows the joint configuration in more detail. The interface moment and shear will be reacted over the pattern of ultrasonic spot welds at the four corners of the intersection between the cross beam and longitudinal beam. Using a shear strength of the ultrasonic weld to be (Test Values/3)

$$F_S = 10.34 \times 10^6 \text{ N/m}^2$$

and the combined area of the two spot welds to be

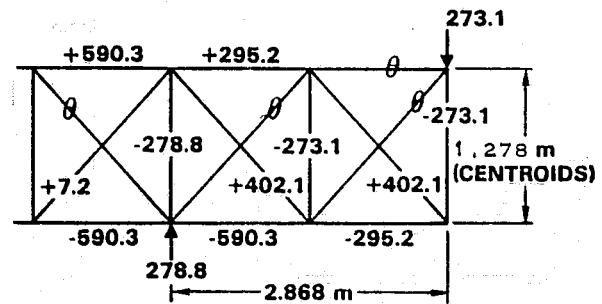


Figure 4-28. Preliminary internal limit loads in bay (N).

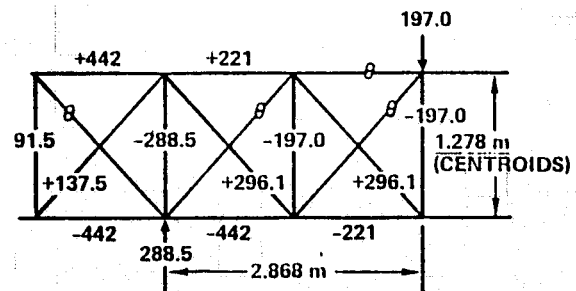


Figure 4-29. Final internal ultimate loads in bay (N).

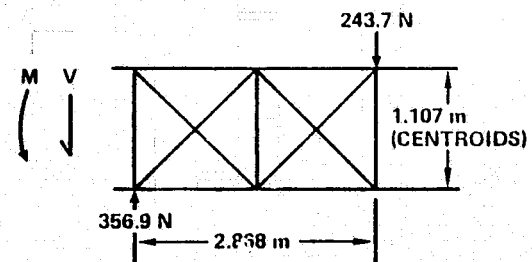


Figure 4-30. Final beam limit reactions loads on jig.

$$A = \frac{2 D^2}{4} = \frac{2 (.01)^2}{4}$$

$$= 1.571 \times 10^{-4} \text{ m}^2$$

the allowable shear load per joint is

$$P_S = F_S \cdot A$$

$$= (10.34 \times 10^6) (1.571 \times 10^{-4})$$

$$= 1624 \text{ N}$$

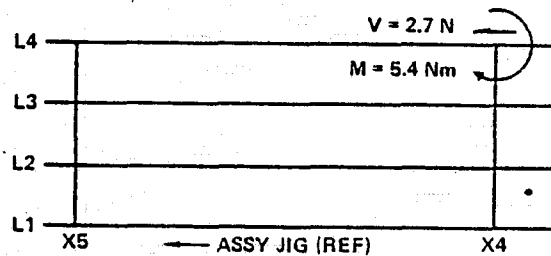


Figure 4-31. Maximum platform joint loads.

Figure 4-32 shows the joint configuration in more detail.

Analyzing the pattern as a typical rivet pattern and using an HP9830 program, the resulting loads per joint and margins are shown in Table 4-32.

Table 4-32. Maximum spotweld loads in platform.

M = 5.37 Nm VX = 2.679 N VY = 0 N
 XBAR = 0.631m YBAR = 0.631m

Weld	Location (m)		Force (N)			Moment (Nm)		M.S.
	X	Y	Allow	VX	VY	M-X	M-Y	
1	0.00	0.00	1624	1	0	1	-1	649.40
2	0.00	1.26	1624	1	0	-1	-1	1028.67
3	1.26	1.26	1624	1	0	-1	1	1028.67
4	1.26	0.00	1624	1	0	1	1	649.40

The spotweld loads are small as shown in the above margins.

4.4.3 PRELOAD IN DIAGONALS. The tension-only diagonal cords require preload to preclude slack and consequent shear stiffness degradation. Two effects contribute to determination of required preload: (1) differential beam cap/diagonal cord expansion due to thermal effects; and (2) shortening of adjacent caps due to beam bending. These effects are evaluated below and the resulting preload requirements are shown in Figure 4-33.

4.4.3.1 Thermal Effects. Assuming the baseline beam, a conservative analysis was performed using the worst case cap and cord temperature differences to predict cord preload requirements due to thermal effects. Beam parameters used in the analysis are summarized in Table 4-33.

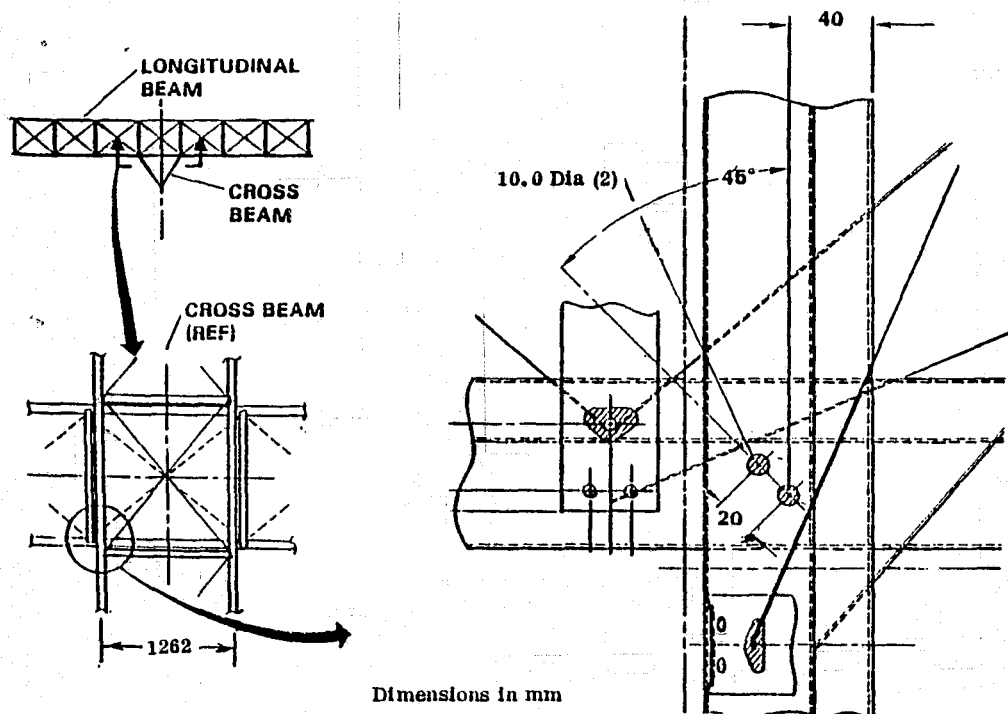


Figure 4-32. Details of longitudinal/cross beam joint.

CORD MATL	σ PRELOAD (MN/m ²)		
	THERMAL	BEAM BENDING	TOTAL
E GLASS	14.6	0.76	15.36
KEVLAR 29	10.2	0.66	10.86

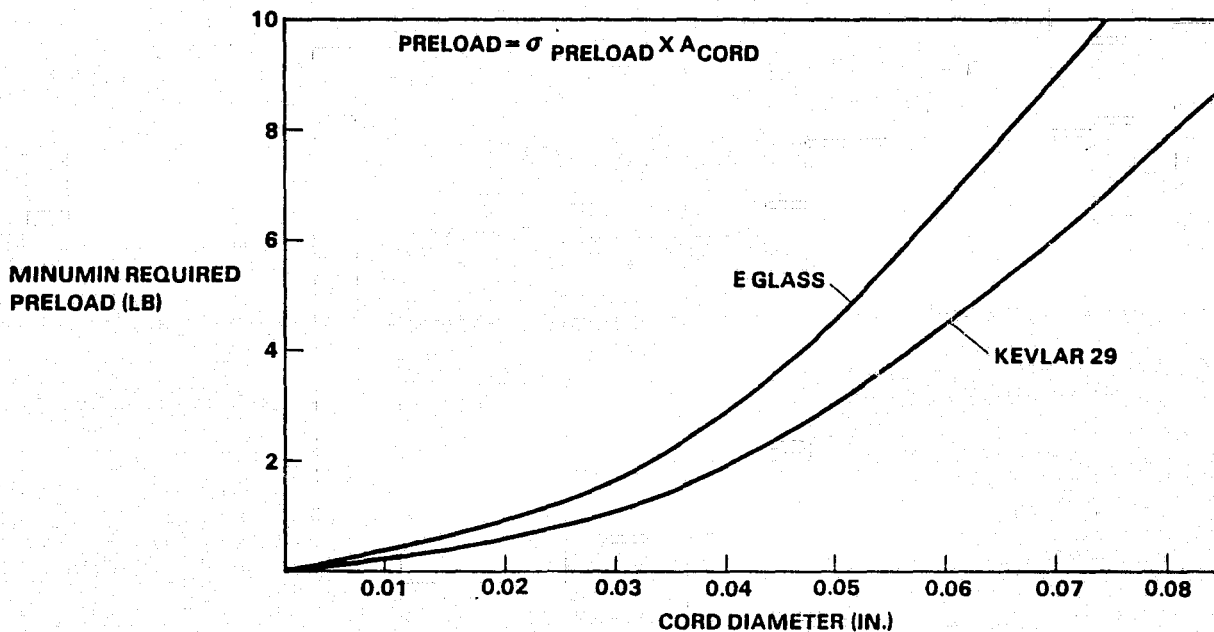


Figure 4-33. Minimum required preload in diagonals.

Table 4-33. Beam parameters.

Element	Material	E GN/m ²	α (μ m/m/K)	Assembly Temp. Range (K)	Operating Temp Range (K)
Cap & Posts	Graphite	137.9	-.36	294 to 366	194 to 278
Cord	E Glass	42.1	4.21	200 to 255	192 to 283
	Kevlar 29	36.5	3.38	200 to 255	192 to 283

Maximum preload is established by the temperature condition with minimum expansion of the beam caps and posts, and maximum expansion of the diagonal cords. For maximum preload

$$T_{\text{CAP}} = 278 - 294 = -16 \text{ K (min expansion)}$$

$$T_{\text{CORD}} = 283 - 200 = 83 \text{ K (max expansion)}$$

The changes in diagonal cord length due to these temperature changes are calculated below.

- a. Change in Cord Length Due to Thermal Expansion of Caps and Posts. Cord length change was calculated for the geometry of a typical beam bay shown in Figure 4-34.

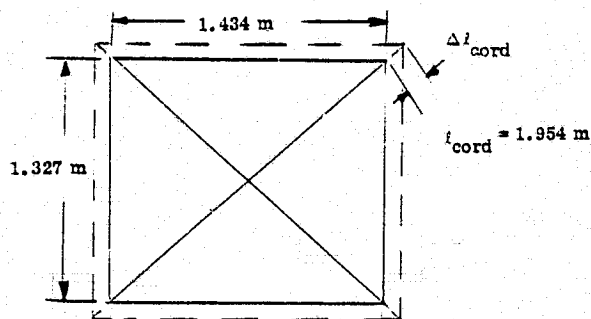


Figure 4-34. Typical beam geometry.

$$\text{Let } K = \frac{\text{bay length, } L}{\text{bay height, } H} = \frac{1.434}{1.32} = 1.0806$$

$$\begin{aligned} \text{then } \Delta l_{\text{CORD}} &= H \left[\sqrt{(K^2 + 1) (1 + \alpha_{\text{CAP}} \Delta T_{\text{CAP}})^2} - \sqrt{K^2 + 1} \right] \\ &= 1.327 \left[\sqrt{[(1.0806)^2 + 1] \left[1 - (.36 \times 10^{-6}) (-16) \right]^2} - \sqrt{(1.0806)^2 + 1} \right] \\ &= 11.25 \mu\text{m} \end{aligned}$$

b. Change in Cord Length Due to Thermal Expansion of Cord.

$$\begin{aligned}\Delta l_{\text{CORD}} &= l_{\text{CORD}} \alpha_{\text{CORD}} \Delta T_{\text{CORD}} \\ &= (1.954) (4.21 \times 10^{-6}) (83) = 682.71 \mu\text{m (E glass)} \\ &= (1.954) (3.38 \times 10^{-6}) (83) = 548.12 \mu\text{m (Kevlar 29)}\end{aligned}$$

The differential expansion requiring preload is:

$$\begin{aligned}\Delta l_{\text{CORD}} &= 682.71 - 11.25 = 671.46 \mu\text{m} = .067 \text{ cm (E Glass)} \\ &= 548.12 - 11.25 = 536.87 \mu\text{m} = .054 \text{ cm (Kevlar 29)}\end{aligned}$$

The required preload stress, $\sigma_{\text{CORD}} = E_{\text{CORD}} \epsilon_{\text{CORD}}$

$$\begin{aligned}\sigma_{\text{CORD}} &= (42.1 \frac{\text{GN}}{\text{m}^2}) (343.63 \frac{\mu\text{m}}{\text{m}}) = 14470 \frac{\text{kN}}{\text{m}^2} \text{ (E glass)} \\ &= (36.5 \frac{\text{GN}}{\text{m}^2}) (274.75 \frac{\mu\text{m}}{\text{m}}) = 10030 \frac{\text{kN}}{\text{m}^2} \text{ (Kevlar 29)}\end{aligned}$$

4.4.3.2 Beam Bending Effects. The maximum beam bending loads shown in Figure 4-35 were used to evaluate beam bending effects on diagonal cord preload.

M = 1356 Nm

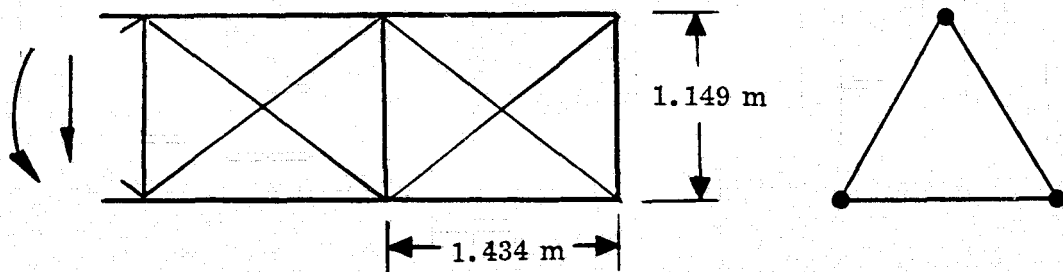


Figure 4-35. Beam bending loads.

The maximum applied bending moment of 1356 Nm produces a maximum cap compression loading of $\frac{1356}{2(1.149)} = 590 \text{ N}$

For a cap area of 1.48 cm^2 :

$$\sigma_{\text{CAP}} = 3986.5 \frac{\text{kN}}{\text{m}^2}$$

The resulting change in length of one bay is:

$$\Delta l_{\text{BAY}} = \frac{\sigma_{\text{CAP}} l_{\text{BAY}}}{E_{\text{CAP}}} = \frac{(3986.5 \text{ kN/m}^2)(1.434 \text{ m})}{137.9 \text{ GN/m}^2} = 41.45 \text{ } \mu\text{m}$$

The resulting change in cord length required to maintain cord tension is:

$$\Delta l_{\text{CORD}} = 30.42 \text{ } \mu\text{m} = .0030 \text{ cm}$$

and the preload stress is

$$\begin{aligned} \sigma_{\text{CORD}} &= E_{\text{CORD}} \epsilon_{\text{CORD}} \\ &= (42.1 \text{ GN/m}^2)(15.568 \text{ } \mu\text{m/m}) = 655 \text{ kN/m}^2 \text{ (E Glass)} \\ &= (36.5 \text{ GN/m}^2)(15.568 \text{ } \mu\text{m/m}) = 568 \text{ kN/m}^2 \text{ (Kevlar 29)} \end{aligned}$$

Total minimum preload required is the sum of the thermal and beam bending preload. Minimum required preload vs. cord diameter is shown in Figure 4-33. Actual preload in the cords should be higher than these minimum values to account for tolerances and manufacturing variations.

4.4.3.3 Effect of Diagonal Cord Preload Unbalance. Tolerances and manufacturing variations will cause unequal preloading between the diagonal cords. This cord preload unbalance produces bending and twisting distortions of the beams. To design a cord tensioning control system, it was necessary to establish the sensitivity of the beam distortions to preload unbalance. A parametric study was performed to evaluate beam tip deflection and twist as a function of cord preload unbalance.

- a. **Beam Torsion (Twist).** Assuming preload unbalance, ΔP in each panel such as to cause pure torsion of the beam, the unbalanced loading is shown in Figure 4-36.

$$\text{Beam twist} = \frac{TL}{JG}$$

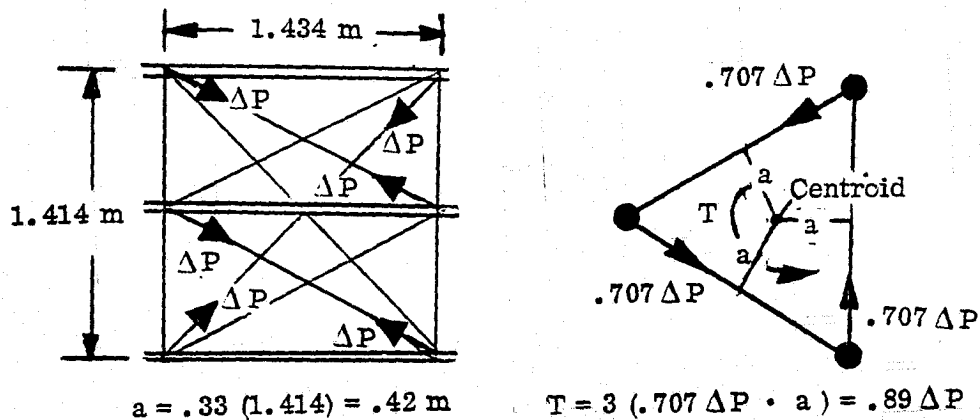


Figure 4-36. Beam torsion due to diagonal cord preload unbalance.

Conservatively assuming a constant error bias over the full beam length, and using a beam effective JG of 43 kNm^2 and a beam length of 200 m:

$$\text{Beam twist} = \frac{(.89 \Delta P) (200 \text{ m})}{43 \times 10^3 \text{ N m}^2} = 4.14 \times 10^{-3} \Delta P \text{ (radians)}$$

- b. Beam Bending (Deflection). Assuming preload unbalance, ΔP , in each panel such as to cause pure bending of the beam, the unbalanced loading is shown in Figure 4-37.

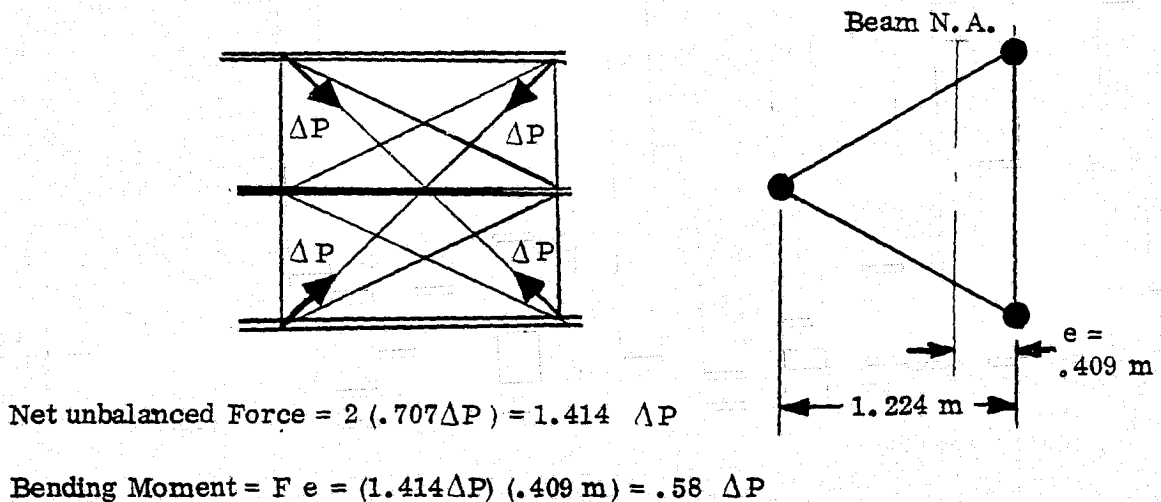


Figure 4-37. Beam bending due to diagonal cord preload unbalance.

Conservatively assuming a constant error bias over the full beam length, and using a beam effective EI of 9.95 MN m² and a cantilevered beam length of 200 m:

$$\begin{aligned} \text{Beam tip deflection} &= \frac{Ml^2}{2EI} \\ &= \frac{(.58 \Delta P)(200 \text{ m})^2}{2(9.95 \text{ MN m}^2)} = 1.17 \times 10^{-3} \Delta P \text{ (m)} \\ &= .117 \Delta P \text{ (cm)} \end{aligned}$$

Results of the study, shown in Figure 4-38, indicate that large preload unbalance (approximately of the same magnitude as the minimum required preload) can be tolerated without producing unacceptable beam distortion. A highly accurate method of controlling cord pretension is thus not required. This should permit the incorporation of a simple mechanical cord pretensioning control system in the beam builder design.

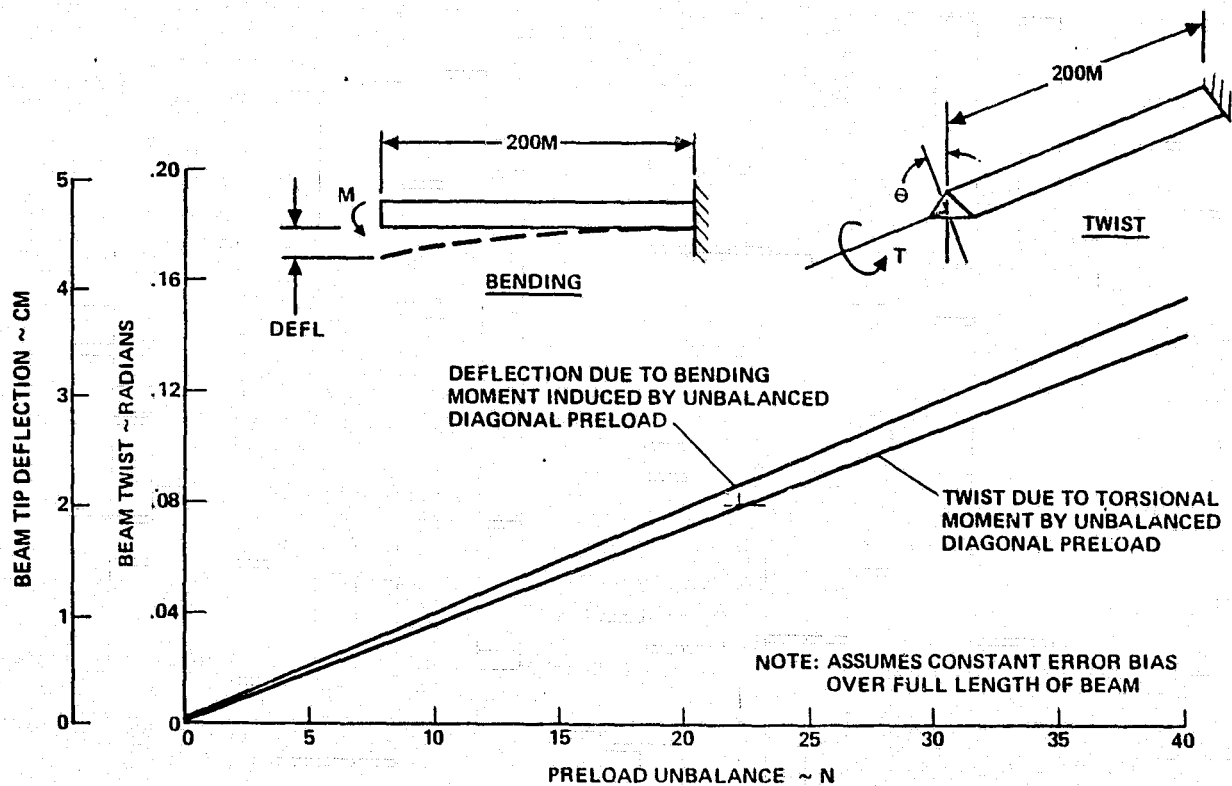


Figure 4-38. Beam distortion due to diagonal cord preload unbalance.

4.4.4 OPEN SECTION CAPS. The open section cap concept offers many advantages for LSS applications. However, there is concern that this concept may not be structurally adequate (yet simultaneously efficient) in large space structures applications

due to the reduction in axial load capability caused by the torsional instability failure mode. To evaluate the adequacy of the open cap concept, extensive analyses were conducted using both classical linear hand-solution techniques and nonlinear finite-difference solutions.

4.4.4.1 Classical Linear Instability Analysis. First, a classical linear instability was conducted to evaluate the compressive load carrying capability of two candidate cross sections, identical except for corner radii, shown in Figure 4-39. Crippling cutoffs, torsion-only load capability, and torsion/bending interaction characteristics, were determined for each. Curiously, the round-cornered option, although exhibiting considerably higher short column capability (as expected), exhibits a lesser capability than its counterpart in the medium and long column ranges. Since it appears, therefore, that sharper corners enhance column capability, radii in the baseline cap were revised downward from 15 mm to 12 mm.

The results of the analysis are presented in Figure 4-40. The plot shows the critical load versus column length for the two candidate cross sections using the baseline laminate VSA-11 (120/W-705₃/120). At the baseline post spacing of 1.434 m the sharp cornered cross section has a slightly higher failure load than the radiused cornered cross section, 2335 N versus 1846 N.

In any event, the capability of either shape exceeds the maximum cap load (conservatively given as 590.3 N) in the preliminary loads analysis by a factor greater than 3. Consequently, it appears that the open cap is fully adequate in the SSAFE application using the classical linear instability theory. The latter final loads analysis found the maximum cap limit load to be 316 N, showing an even larger margin.

The torsional instability is based on the theory presented by Timoshenko and Gere, "Theory of Elastic Stability", 2nd Ed., McGraw-Hill, New York, 1961. In calculating the warping function for the cap with rounded corners, the corners were idealized by a series of flats.

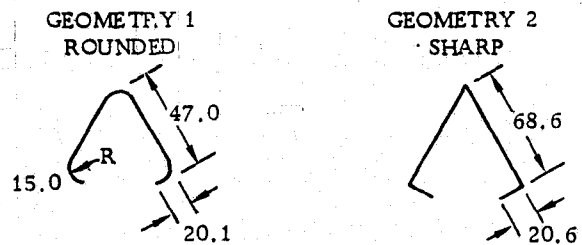


Figure 4-39. Cap geometry used for comparison.

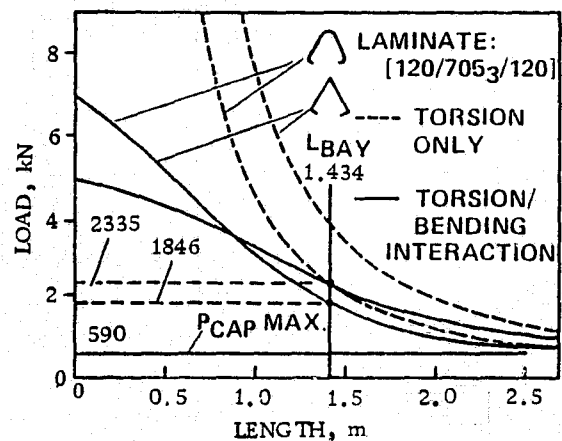


Figure 4-40. Column allowable for open section caps.

4.4.4.2 Nonlinear Analysis. The stability analysis was performed by use of a linear/nonlinear finite-difference computer code called STAGS (Structural Analysis of General Shells) where both bifurcation and nonlinear collapse analysis were performed.

The study considered the two candidate cross sections shown in Figure 4-39 and several candidate graphite/thermoplastic laminates for a compression member of specified length.

In general, the results of the analytical study indicated that local post buckling or general torsional instability or a combination of both govern the stability strength of the compression structure.

The analysis was conducted using company funds under an Independent Research and Development (IRAD) program. Figure 4-41 is a flow chart of the analysis task.

The candidate graphite/thermoplastic laminates are presented in Table 4-34. The lamina thickness and mechanical properties are shown in Table 4-35. There are just two classes of laminates considered:

- 120/ [VSA11 (W705)]_i/120
- HM-S/P-1700

Table 4-36 is a summary of the results from the STAGS solution.

Two geometries, of equal perimeter, one with rounded and one with sharp corners, were compared, initially using the same material. These runs showed that local buckling of the side flats occurred first. Therefore, the geometry with rounded corners proved best because of the post-buckling strength of its corners and the higher initial buckling stress of the narrower flat portions of the cross section.

After determining that the rounded corner cross section is best and local buckling dominates, various laminate layups and materials were investigated to determine the effects of material properties. The laminates fell into two groups: those with low shear modulus and those with high shear modulus. The pseudo-isotropic layup of HMS/P-1700 with the high shear modulus exhibited an initial buckling load almost three times as great as the baseline hybrid despite possessing a 50% lower axial modulus, thus, showing the desirability of high shear modulus for applications, other than SSAFE, where

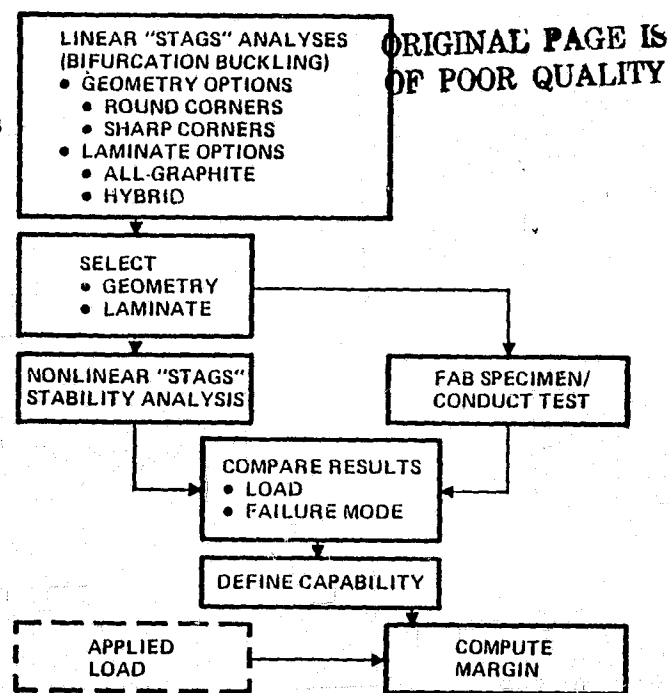


Figure 4-41. Flow chart of STAGS cap stability analysis.

Table 4-34. Candidate graphite/thermoplastic laminates.

LAMINATE	NUMBER PLIES	TOTAL THICKNESS (mm)
120/[VSA11 (W705)] ₃ /120	5	0.775
120/[VSA11 (W705)] ₂ /120	4	0.584
120/ VSA11 (W705)/120	3	0.394
HM-S/P-1700 [0 ₂ /90] _s	6	0.762
HM-S/P-1700 [0/90] _s	4	0.508
HM-S/P-1700 [±60/0] _s	6	0.762
HM-S/P-1700, t _{ply} = 0.0762 mm [±60/0] _s	6	0.457

Table 4-35. Lamina properties* for candidate graphite/thermoplastic laminates.

SYSTEM	PLY THICKNESS (cm)	E ₁₁ (GN/m ²)	E ₂₂ (GN/m ²)	G ₁₂ (GN/m ²)	ν ₁₂
120 GLASS/P-1700	0.0102	18.13	17.86	4.00	0.15
VSA11 (W705)	0.0191	187.54	5.99	6.89	0.25
HM-S/P-1700	0.0127	20.55	5.72	5.86	0.20

*(Ref., Lamina Properties, Table 2-7,)

Table 4-36. Results of STAGS stability analysis.

Geometry	Laminate		t (cm)	Stability Analysis		
	No.	Layup		Type	Failure Mode	P ^c (KN)
1	1	120/ [VSA11(W705)] ₃ /120	0.0775	Bifurcation	Local	2.540 ₁
				Nonlinear	Local	6.583 ₂
2	2	120/ [VSA11(W705)] ₂ /120	0.0584	Bifurcation	Torsion	16.902 ₃
				Bifurcation	Torsion	13.646 ₃
1	3	120/VSA11(W705)/120	0.0394	Bifurcation	Column	21.230
				Bifurcation	Local	.334
1	4	HM-S/P-1700 [0 ₂ /90] _S	0.0762	Bifurcation	Local	1.009 ₂
				Bifurcation	Torsion	10.648 ₂
1	5	HM-S/P-1700 [0/90] _S	0.0508	Bifurcation	Column	12.748
				Bifurcation	Local	.280 ₂
1	6	HM-S/P-1700 [±60/0] _S	0.0762	Bifurcation	Torsion	5.093 ₂
				Bifurcation	Column	5.102 ₂
1	7	HM-S/P-1700, t _{ply} = 0.00762 cm [±60/0] _S	0.0457	Bifurcation	Local	3.167 ₂
				Bifurcation	Torsion	15.790 ₂
1	7	HM-S/P-1700, t _{ply} = 0.00762 cm [±60/0] _S	0.0457	Bifurcation	Local	1.410 ₂
				Bifurcation	Torsion	8.709 ₂
1	7	HM-S/P-1700, t _{ply} = 0.00762 cm [±60/0] _S	0.0457	Bifurcation	Column	11.703 ₂
				Bifurcation	Local	6.761 ₂
1	7	HM-S/P-1700, t _{ply} = 0.00762 cm [±60/0] _S	0.0457	Bifurcation	Torsion	28.912 ₂
				Bifurcation	Column	16.369 ₂

1. Maximum nonlinear collapse load reached, not necessarily close to collapse.
2. Local buckling precluded; also, reduction in shortening stiffness precluded.
3. Local buckling precluded; extensional shortening stiffness reduced by 50% in flats.

ORIGINAL PAGE IS
OF POOR QUALITY

member loads demand maximum buckling strength.

Figure 4-42 is a plot of the load versus end shortening of the baseline cap geometry and material. The bifurcation points for both corner geometries are shown, showing the distinct advantage of the rounded corners. The buckling, or bifurcation, point occurred in the flat plate portion of the cross section. The post buckling strength of the rounded corner geometry is indicated by the nonlinear collapse solution. The slope change occurring near the linear bifurcation point indicates that there is an approximate 50% reduction in cap stiffness when the flats of the cross section buckle.

The maximum SSAFE load is also indicated in Figure 4-22 showing the large margin which the open triangular cap geometry has for this application. The nonlinear collapse solution was terminated at P_{CR} = 6583 N because this load was much greater than the maximum SSAFE load and the cost of the computer runs increases significantly when the solution nears general collapse.

Thus, the allowable compressive axial load on the baseline cap lies somewhere between the maximum load reach reached in the nonlinear solution and the torsional

buckling load determined by the linear bifurcation solution using 50% stiffness in the flats, or

$$6853 \text{ N} < P_{\text{FAILURE}} < 13646 \text{ N.}$$

Even using the lower bound as the allowable, P_{FAILURE} is 15 times the maximum SCAFE ultimate load of 441 N.

4.4.5 DIFFERENTIAL DRIVE EFFECTS.

To determine the spring rate or resistance of the SCAFE beam to a differential cap drive, a finite element model was prepared using Convair's version of Solid SAP. The model was constrained to represent the beam builder's support points as shown in Figure 4-43. Varying lengths of complete beam were considered and the analysis showed that the spring rate exhibited by the beam, while attempting to drive one cap a given length and holding the other two fixed, is constant at 29.95 KN/m.

The internal loads distribution is also independent of the length of beam out of the assembly jig are summarized in Figure 4-44. The loads shown are for a $\Delta L = 0.254 \text{ cm}$.

The stress levels in the elements of the beam can be checked for the arbitrary $L = 0.254 \text{ cm}$. The stress levels are linear with respect to ΔL .

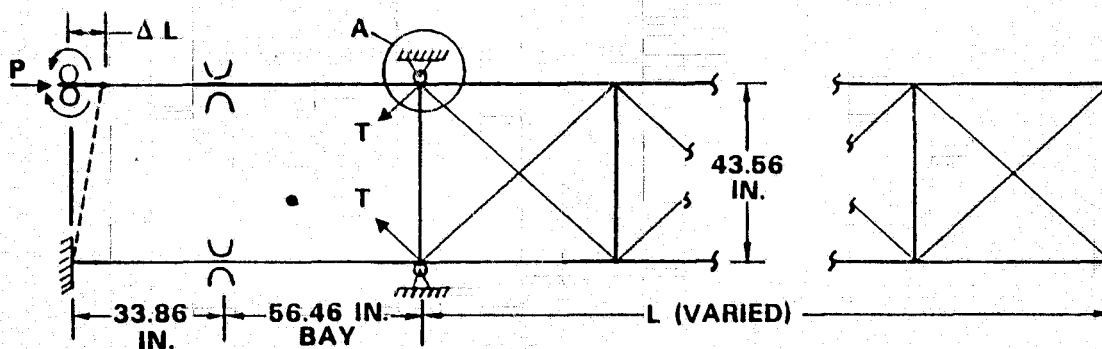


Figure 4-43. Finite element geometry for differential cap drive study.

a. Cap. The maximum loads from Figure 4-43 are:

$$P = 76.06 \text{ N}$$

$$M_x = 26.1 \text{ N-m}$$

At point A on the cross section,

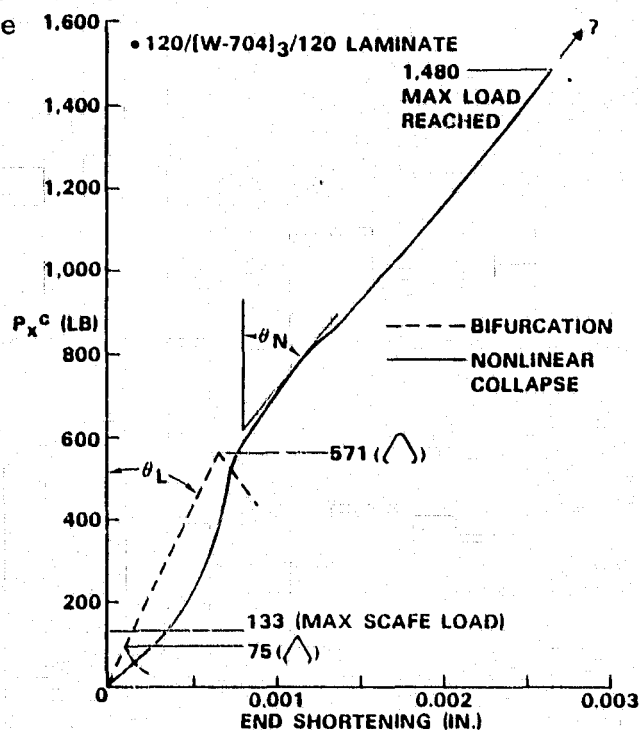


Figure 4-42. Post buckling load-displacement curve.

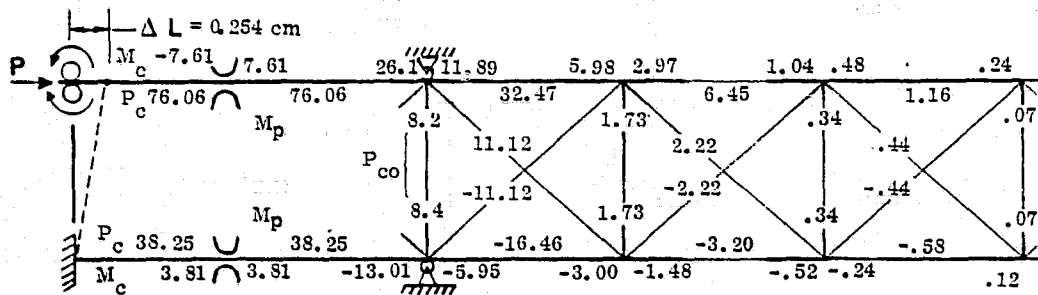
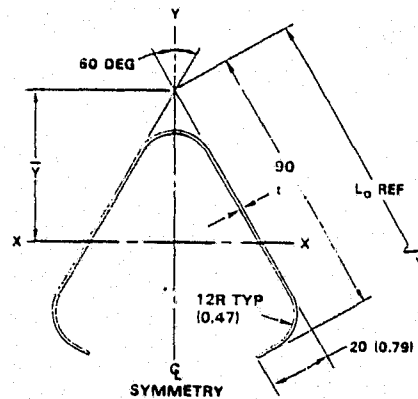


Figure 4-44. Internal load distribution for differential drive.

$$\sigma_A = \frac{26.1 (3.914 \times 10^{-2})}{8.1748 \times 10^{-8} \cdot 76.06} - 1.4774 \times 10^{-4} = 13.0 \text{ MN/m}^2$$



(Ref. Figure 4-22)

From the STAGS solution, the allowable load is greater than the local buckling stress or $P_{cr} > 6583\text{N}$. So, the allowable stress is at least

$$\sigma_{\text{allow}} \geq \frac{6583}{1.4774 \times 10^{-4}} = 44.56 \text{ MN/m}^2$$

Thus, the cap is good for a differential drive equal to:

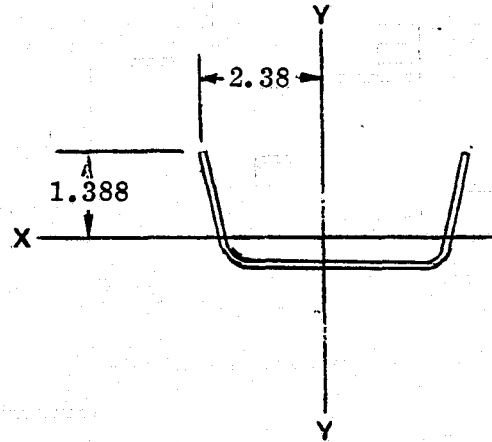
$$\Delta L = 0.254 \left(\frac{44.56}{13.0} \right) = 0.871 \text{ cm}$$

- b. Diagonal Cords. The diagonal cords are not critical in this case because of the extremely low loads.
- c. Cross-Member. The maximum bending moment in the cross-members is a side bending for the differential cap drive. For a $L = 0.25$ in the moment is:

$$M_y = 8.4 \text{ N m}$$

The bending stress is:

$$\begin{aligned} \sigma_b &= \pm \frac{M_y C}{I} \\ &= \pm \frac{8.4 (2.38 \times 10^{-2})}{1.1238 \times 10^{-8}} \\ &= \pm 17.75 \text{ MN/m}^2 \end{aligned}$$



The upstanding leg will be critical in crippling. For the post, the material is (120/W-704₂/120). The D matrix is

$$D = \begin{bmatrix} 1.0898 & .03985 & 0 \\ .03985 & .24721 & 0 \\ 0 & 0 & .07987 \end{bmatrix} \quad (\text{Ref. SQ-5 laminate analysis program})$$

F^{cr} = Buckling stress

$$= \frac{12 D_{66}}{b^2 t} + \frac{\pi^2 D_{11}}{L^2 t} \quad (\text{One edge free - one edge fixed})$$

Substituting

$$b = 2.006 \times 10^{-3} \text{ m}$$

$$t = 5.842 \times 10^{-5} \text{ m}$$

$$L = .122428 \text{ m}$$

Gives

$$F^{cr} = 4.08 \text{ MN/m}^2$$

So, the current post design will not buckle for a differential drive of

$$\Delta L = .254 \left(\frac{4.08}{17.75} \right) = .0584 \text{ cm}$$

ORIGINAL PAGE IS
OF POOR QUALITY

If a return flange were added to the post, the allowable stress of the upstanding leg could be raised to a fixed - fixed condition where the allowable buckling stress would become

$$F_{cr} = \frac{2 \pi^2}{t b^2} \left[\sqrt{D_{11} D_{22}} + D_{12} + 2D_{66} \right]$$

$$= 60.2 \text{ MN/m}^2$$

or

$$\Delta L = .254 \left(\frac{60.2}{17.75} \right) = .8614 \text{ cm}$$

Adding the return flange to the post cross section would be an easy design change and would also improve the feed mechanism in the clip used for dispensing the posts during beam construction.

The allowable twisting moment on the ultrasonic spot weld pattern is computed based on the geometry shown in Figure 4-45.

Tests of the spot weld indicate a typical strength in shear of 20.68 MN/m^2 for design use

$$F_s = 10.34 \text{ MN/m}^2$$

Thus, the allowable shear load on the .640 cm dia. spot welds is

$$P_s = \frac{\pi}{4} (.640 \times 10^{-2})^2 \times (10.34) \times 10^6 = 333.6 \text{ N}$$

At the cord attachment use half of the area involved, assuming there will not be a perfect weld:

$$P_s = (1.0 \times 10^{-4}) (10.34 \times 10^6) = 1032 \text{ N}$$

- d. Differential Cap Drive. Use an HP 9830 program to determine joint moment allowable.

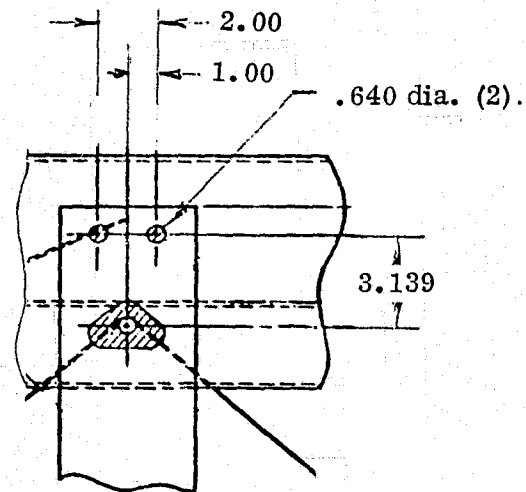


Figure 4-45. Spot weld geometry for cap/cross-member joint.

SPOTWELD PATTERN ANALYSIS

M = 838.46 Nm VX = 0 N VY = 13.34 N

XBAR = 1.233m YBAR = 0.000m

Weld	Location (m)		Force (N)			Moment (Nm)		M.S.
	X	Y	Allow	VX	VY	M-X	M-Y	
1	0.00	0.00	1032	0	8	0	-224	3.77
2	3.14	-1.00	334	0	3	59	112	1.59
3	3.14	1.00	334	0	3	-59	112	1.59

The allowable moment is

$$M_{allow} = (M.S. + 1) (M_{applied})$$

$$= (2.59) (8.4)$$

$$= 21.72 \text{ N-m}$$

The allowable ΔL differential drive for this weld pattern is:

$$\Delta L = \frac{21.72}{8.4} (.254) = .658 \text{ cm}$$

The weld pattern can be modified to match the capability of post in bending and is, therefore, not a limiting factor on the magnitude of ΔL per bay.

Thus, with the current beam configuration, except for the small change to the post, the buckling compression allowable of the cap is the limiting factor. The allowable ΔL per bay is

$$\Delta L = 0.871 \text{ cm}$$

4.4.6 THERMAL DISTORTION ANALYSIS. A worst case cap thermal condition was analyzed to determine tip end deflection. Assuming one beam (200m) attached to the Orbiter, a finite element model was used using beam elements for the caps and posts, and rod elements for the diagonals.

The preliminary material properties summarized in Table 4-26 were used.

Worst case thermal distortion would occur if there were cap-to-cap shadowing when any two caps are coplanar with incident space heating conditions as in Figure 4-46. Combining this with shuttle-beam shadowing results in maximum cap to cap temperature gradients.

The temperature distribution along the length of the three caps was input as grid temperatures at t = 23.9 minutes. The details of the temperature distribution are found in Section 4.5.2. A later thermal analysis also presented in Section 4.5.2 was

more realistic and did show the approach used for this distortion analysis to be very conservative.

4.4.6.1 Tip Deflections. Referring to Figure 4-46 the resulting tip deflections are:

$$\delta_x = -0.113\text{m}$$

$$\delta_y = -0.432\text{m}$$

$$\delta_z = 0.004\text{m}$$

In terms of beam closure or loss of clearance the distortion is

$$\begin{aligned} \delta_{\text{thermal}} &= -0.113 \sin 30^\circ - 0.432 \cos 30^\circ \\ &= -0.431\text{m} \end{aligned}$$

From the dynamics analysis (Figure 4-14) the worst loss of clearance occurs assuming that the beams are 180° out of phase or:

$$\delta_{\text{dynamics}} = \pm .175 \text{ m}$$

Figure 4-47 illustrates the effect of summing the loss of clearance due to both thermal distortion and dynamic response.

4.4.6.2 Internal Loads. The maximum resulting internal loads are very small and are summarized below per element: (limit loads)

a. Cord.

$$P = 53.8 \text{ N}$$

No compressive loads

b. Cap.

$$P = -76.95 \text{ N}$$

$$M = .41 \text{ Nm}$$

c. Post.

$$P = 93.4 \text{ N}$$

$$M = 0.06 \text{ Nm}$$

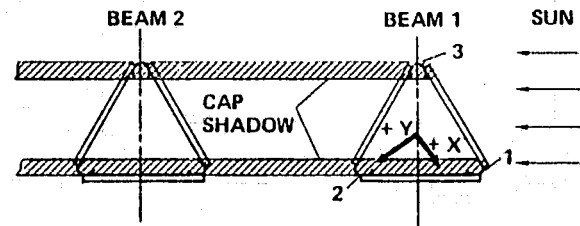


Figure 4-46. Worst case beam thermal loading.

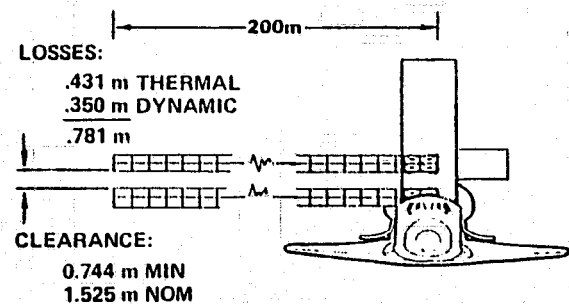


Figure 4-47. Beam tip clearance.

4.4.7 FINAL ANALYSIS. The calculation of the margins of safety for the various elements of the beam has been postponed to be presented in summary form at the end of this section. This was done in order to present only the most current allowables and loads to avoid confusion.

- a. Cap. The maximum cap load is the result of the final dynamic response analysis of the platform and can be found in Figure 4-29.

$$P_{\text{cap}} = 442 \text{ N (Ult)}$$

The allowable cap load is taken to be the lower bound collapse load resulting from the nonlinear analysis where P_{failure} was found to be between 6583 N and 13646 N. Thus, for the SCAFE application the cap margin of safety for axial compression is

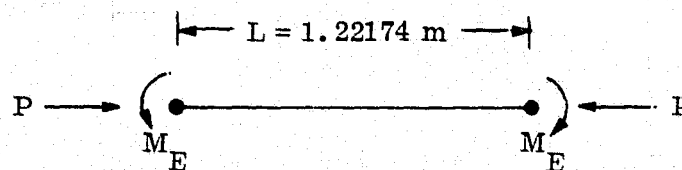
$$\text{M.S.} = \frac{6583}{442} - 1 = + \underline{\text{LARGE}} \text{ (Ult)}$$

- b. Post. The maximum post (or cross-member) load is again the result of the final dynamic response analysis of the platform and is shown in Figure 4-29.

$$P_{\text{post}} = -288.5 \text{ N (Ultimate)}$$

The post must be analyzed as a beam column because of the end moment created by the eccentricity between the post centroid and cap skin. The resulting end moment is

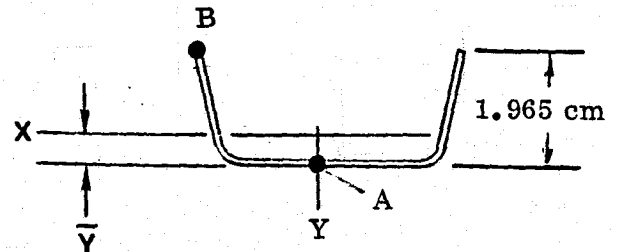
$$\begin{aligned} M_E &= P \cdot e \\ e &= X_{\text{post}} + \frac{t}{2} \text{ (cap)} \\ &= 5.842 \times 10^{-3} + \frac{7.747 \times 10^{-4}}{2} \\ &= 6.23 \times 10^{-3} \text{ m} \\ M_E &= (288.5) (6.23 \times 10^{-3}) \\ &= 1.80 \text{ Nm} \end{aligned}$$



Using the beam column analysis from Bruhn, p. A5.21, the maximum moment occurs at center span,

Where for the post

$$\begin{aligned}
 E &= 128.66 \text{ GN/m}^2 \\
 I &= 1.665 \times 10^{-9} \text{ m}^4 \\
 P &= 288.5 \text{ N} \\
 j &= .8617
 \end{aligned}$$



Therefore, the maximum moment is

$$M_{\max} = 2.37 \text{ Nm}$$

The resulting stress levels in the post can be computed using the section properties shown.

$$\begin{aligned}
 Y &= 0.5436 \text{ cm} \\
 A &= 0.4452 \text{ cm}^2 \\
 I_{xx} &= 0.17482 \text{ cm}^4
 \end{aligned}$$

At point B, the tensile stress is

$$\begin{aligned}
 f_t &= - \frac{288.5}{.4452 \times 10^{-4}} + \frac{2.37 (.01965 - .005436)}{.17482 \times 10^{-8}} \\
 &= 12.79 \times 10^6 \text{ N/m}^2 \text{ (Ult)}
 \end{aligned}$$

The tensile strength of the VSA - 11 (120/W-705₂/120) post material is

$$Ft_u = 291.65 \times 10^6 \text{ N/m}^2$$

Thus, the margin of safety is

$$M.S. = \frac{291.65 \times 10^6}{12.79 \times 10^6} - 1 = + \underline{\underline{\text{LARGE}}}$$

At point A, the compressive stress is:

$$f_c = - \frac{288.5}{.4452 \times 10^{-4}} - \frac{2.37 (.005436)}{.17482 \times 10^{-8}}$$

$$= -13.85 \times 10^6 \text{ N/m}^2 \text{ (Ultimate)}$$

The compressive strength of the flat plate at point A for buckling and crippling were computed using the SQ5 laminate analysis program.

$$F_{cr} = 15.05 \times 10^6 \text{ N/m}^2$$

$$F_{cc} = 36.36 \times 10^6 \text{ N/m}^2$$

The margin of safety using the buckling stress as the allowable is:

$$M.S. = \frac{15.05 \times 10^6}{13.85 \times 10^6} - 1 = \underline{\underline{+0.09}}$$

This condition exists only when the platform is complete and supported at one end by the assembly jig as a cantilever.

- c. Cord. The maximum cord load is from the final dynamic response analysis of the platform attached to the Orbiter from Figure 4-29 and is

$$P_{cord} = 296.1 \text{ N}$$

Add to this the preload, and the total cord load becomes

$$P_{preload} = 44.48 + 8.896$$

$$= 53.4 \text{ N}$$

$$P_{tot} = 296.1 + 53.4$$

$$= 350 \text{ N}$$

The cord material is not yet fully developed, but, the projected breaking strength is 667 N. So, the margin of safety is

$$M.S. = \frac{667}{350} - 1 = \underline{\underline{+0.90 \text{ (Ult)}}$$

Table 4-37 summarizes the minimum margins of safety of the SCAFE structure which include an ultimate factor of safety of 1.40. The critical mission event is with the completed platform attached to the Orbiter and loads being introduced by the Orbiter VRCS system.

4.5 THERMODYNAMICS

Thermal analysis objectives were: (1) determine the on-orbit beam builder heating/forming power and cooling requirements, and (2) perform a space heating study to obtain beam temperature distributions and time histories during the mission orbit.

4.5.1 BEAM BUILDER POWER AND COOLING REQUIREMENTS.

Minimum heating/forming power requirements were calculated for several different initial conditions, designs, and material variations while maintaining a 40-second run, 40-second pause machine operation. Also, an analysis of the cooling section was made to determine: (1) the maximum energy to be removed in order to cool the graphite/polysulfone laminate down below a structural use temperature of 394.3°K (250°F), and (2) the percentage of total Shuttle Orbiter cooling capacity needed to remove this energy.

4.5.1.1 Heating Forming Power Requirement. A summary history of all results concerning heating/forming power requirements is listed in Table 4-38. The minimum on-orbit power requirement has been steadily reduced throughout the SCAFED study. This is a direct result of the following changes:

Table 4-38. Heating/forming power requirement history.

VARIABLE	MILESTONE					
	PROPOSAL	PART I — MID	PART I — FINAL	NOW		
LAMINATE • MATERIAL • LAYUP	GRAPHITE (0±60) _s	GRAPHITE (0±60) _s	GRAPHITE/GLASS (0/90) _s	GRAPHITE/GLASS (0/90) _s		
FORMING SECTION LENGTH, (cm)	45	33.5	33.5	33.5		
BEND RADIUS (mm)	15	15	15	12		
STRIP TEMP (K)						
• INITIAL	255.4	255.4	255.4	255.4	294.3	310.9
• FINAL	533.2	491.5	491.5	491.5	491.5	491.5
REQUIRED POWER (w)						
• CROSS-MEMBERS	2,030	1,016	0	0	0	0
• CAPS	4,620	4,023	1,903	1,577	1,318	1,206
• TOTAL	6,650	5,039	1,903	1,577	1,318	1,206

LEGEND: — CHANGE — — SELECTED BASELINE

Table 4-37. Minimum margins of safety.

Structural Item	Factor of Safety (Ult.)	M. S.
CAP	1.40	+ Large
POST	1.40	+ .09
CORD	1.40	+ .90
LONG/ CROSS BEAM JOINT	1.40	+ LARGE

- a. Use of a graphite/glass ($0^\circ/\pm 90^\circ$) hybrid over an all-graphite ($0^\circ/\pm 60^\circ$) pseudo-isotropic laminate.
- b. Shortening of the forming section and reduction of the cap bend radius.
- c. Increase in initial, and reduction of final, laminate temperature.
- d. Ground prefabrication of cross-members.

The graphite/glass hybrid has a much lower thermal conductivity in the transverse direction than the pseudo-isotropic laminate. This reduces transverse energy losses between hot and cold areas during the heating and forming process. Shortening the forming section and reducing the cap bend radius decreases the total laminate area that must receive power input in the heating and forming sections, resulting in an energy saving. An increase in initial, and reduction in final, laminate temperature reduces the total ΔT required by the strip, further decreasing minimum power input. Finally, at the end of Part I of SCAFEDS, the decision was made to prefabricate cross-members on the ground, thereby eliminating any power requirement for on-orbit manufacture. The present baseline beam builder heating/forming power requirement is indicated in Table 4-38.

A 204.4 cm length (one bay length plus 30.5 cm at each end) of one half of a symmetrical cap strip was modeled by computer simulation through the 40-second run, 40-second pause beam builder heating/forming/cooling sequence. The model was subdivided into 20 longitudinal nodes \times 5 transverse nodes. The cross-member model was of a similar magnitude. However, cross-member thermal analysis is not discussed further as on-orbit fabrication was excluded from the selected baseline beam builder concept.

Heat is applied only to those areas of strip that are to be bent in the forming section (shaded areas in Figure 4-48). Figure 4-49 illustrates the time-temperature history of each heated longitudinal node (center and outboard heated node temperatures are the same) as a one bay length section of cap moves into the heating section.

A temperature "ramp" develops as the strip moves under the heaters during the first 40 seconds. The sloping temperature profile is then raised during the next 40 seconds until at 80 seconds the forward end is at the correct temperature and is ready to move into the forming section. Power input to the strip was adjusted to give the desired forming temperature (491.5°K) at the end of the 40-second pause.

High temperature gradients occur across the transverse direction of the strip. This is due to the localized heating plus low transverse thermal conductivity. Figure 4-50 shows the transverse temperature distribution for the all-graphite ($0^\circ/\pm 60^\circ$) plus the graphite/glass hybrid ($0^\circ/\pm 90^\circ$) laminates at the point where they enter the forming section. The energy savings through the use of the glass/graphite hybrid is readily apparent. The hybrid laminate has a much lower thermal conductivity in the transverse direction (Table 4-39), which significantly impedes energy flow from the locally heated portions of laminate to colder areas in between.

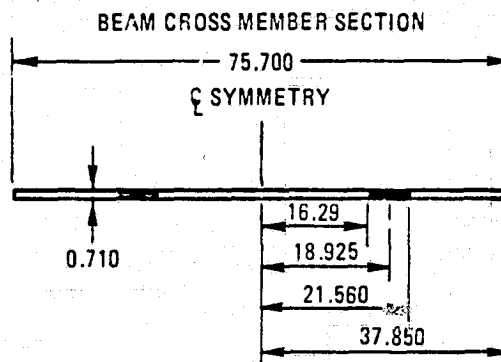
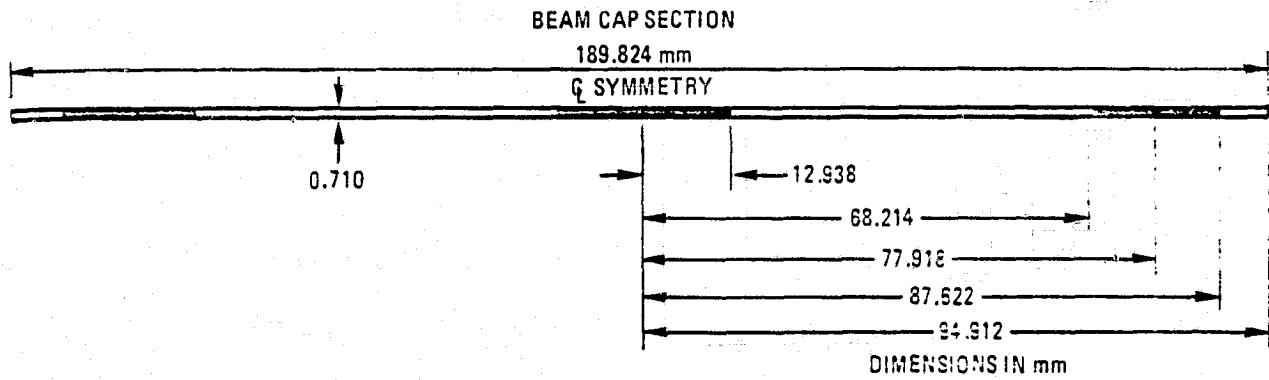
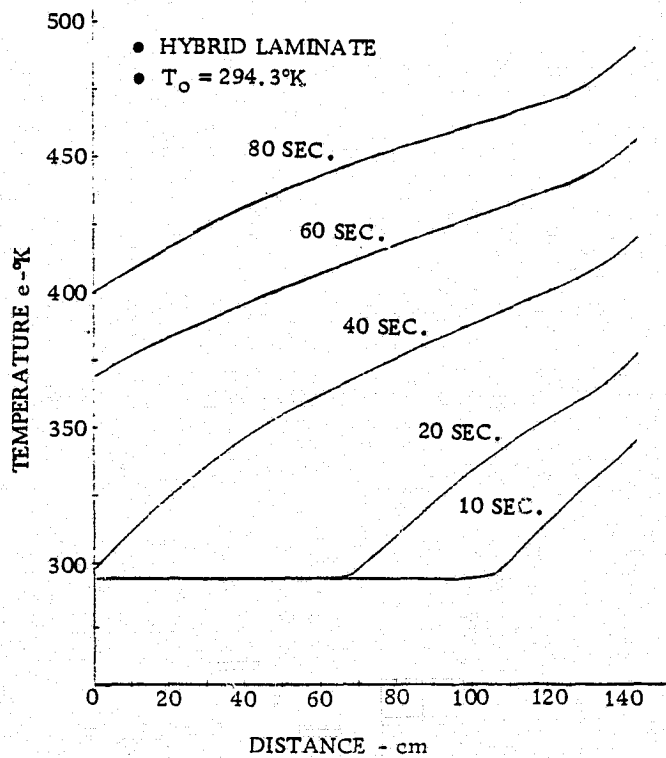


Figure 4-48. Beam cap strip material thermal model.



ORIGINAL PAGE IS
OF POOR QUALITY

Figure 4-49. Temperature vs. distance - longitudinal direction.

For the baseline laminate of Table 4-38, a minimum total of 422.0 watts is needed in the heating section for one cap. The cap is heated in three different areas, the center (120° bend) requires 171.7 watts with 125.2 watts needed at each of the out-board (90° bend) edge areas.

In the forming section, the same cap will require a minimum of 17.3 watts to maintain forming temperature. This input is needed to replace: (1) energy that is constantly moving across the strip into the colder areas, plus (2) longitudinal losses to the cooling section and area of the heating section not yet up to temperature. The center area must receive 6.9 watts while each of the edge areas requires 5.2 watts.

The assumption was made that 6% of all the energy in both heating and forming sections is absorbed in the reflectors. Argus International states that 6% reflector absorption is a typical value for focused infrared heating.

4.5.1.2 Cooling Requirements. After leaving the forming section, locally heated sections of beam cap are still at approximately 491.5°K (425°F). It is necessary to cool the beam cap down below the structural use temperature of 394.3°K (250°F) before cross-member attachment. The present configuration calls for aluminum platen cooling. Cooling by radiation to space plus intra-conduction between local hot and cold areas of beam cap was also analyzed. A one-bay length section of cap was modeled (same number of nodes as in heating/forming section) to simulate cooling.

Assuming a view factor to space of 0.5 and optical properties of $\alpha/\epsilon = 0.34/0.89$ (TiO₂ coating) it was found that radiation plus intra-conduction is not capable of cooling a one-bay length section of cap sufficiently in 80 seconds. Therefore, this type of cooling is not adequate for the present baseline beam builder rate of operation (40-second run, 40-second pause). Figure 4-51 illustrates the results of this analysis for the hybrid laminate. At $t = 0$, local areas of cap are still at the forming temperature. After 80 seconds of cooling, the amount of heat flow between hot and cold sections of strip is almost negligible (low transverse thermal conductivity) and the rate of radiation heat loss is not fast enough to cool the cap below structural use temperature.

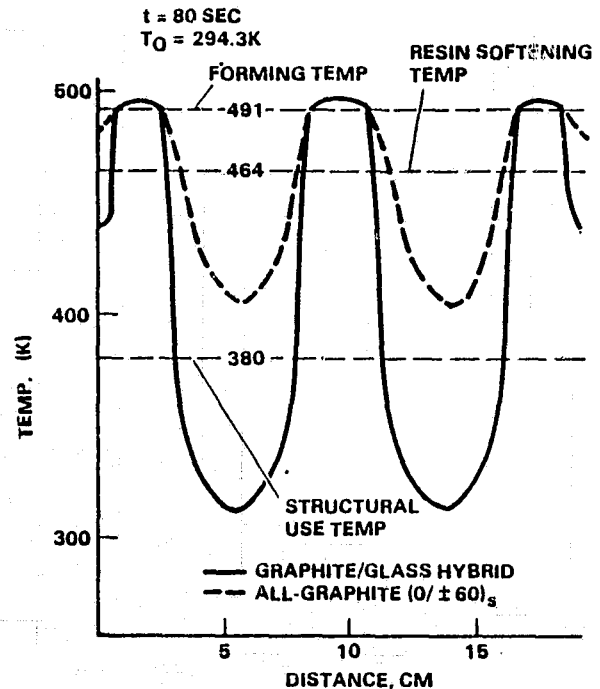


Figure 4-50. Transverse temperature vs. distance, two laminates.

Table 4-39. Estimated laminate thermal properties.

	Glass/Graphite Hybrid (0/±90)	All Graphite (0/±60)	Glass/Graphite Hybrid (0/±90)	All Graphite (0/±60)
Direction	K, watts/cm-°K	K, watts/cm-°K	C _p , watt-sec/g-°K	C _p , watt-sec/g-°K
Axial	.277 at 144.4 °K .912 at 328 °K	.277 at 144.4 °K .912 at 328 °K	.42 at 144.4 °K 1.25 at 422.2 °K	.42 at 144.4 °K 1.25 at 422.2 °K
Transverse	.0057 at 111.1 °K .0125 at 328 °K	.277 at 144.4 °K .912 at 328 °K		
Thickness	.0057 at 111.1 °K .0125 at 328 °K	.0057 at 111.1 °K .0125 at 328 °K		

Using the aluminum platen configuration, the computer model simulated 40 seconds of radiation (to the platens) as the cap moved out of the forming section and then conduction from cap to platen while in contact for the 40 second pause interval.

Figure 4-52 shows the cap transverse temperature distribution as it moves through the cooling process at t = 40 seconds where initial platen contact is made and at the end of the cooling process, t = 80 seconds.

This analysis was made with the following assumptions:

- Initial coolant temperature = 311°K (100°F)
- Final coolant temperature = 344.3°K (160°F)
- Contact coefficient between local hot sections of cap and platens:

$$h_{con} = 0.11 \text{ watts/cm}^2 - \text{°K} \text{ (200 BTU/hr - ft}^2 - \text{°F)}$$

- Contact coefficient

$$h_{con} = 0.014 \text{ watts/cm}^2 - \text{°K} \text{ (25 BTU/hr - ft}^2 - \text{°F)}$$

- Turbulent flow of coolant through inner platens.

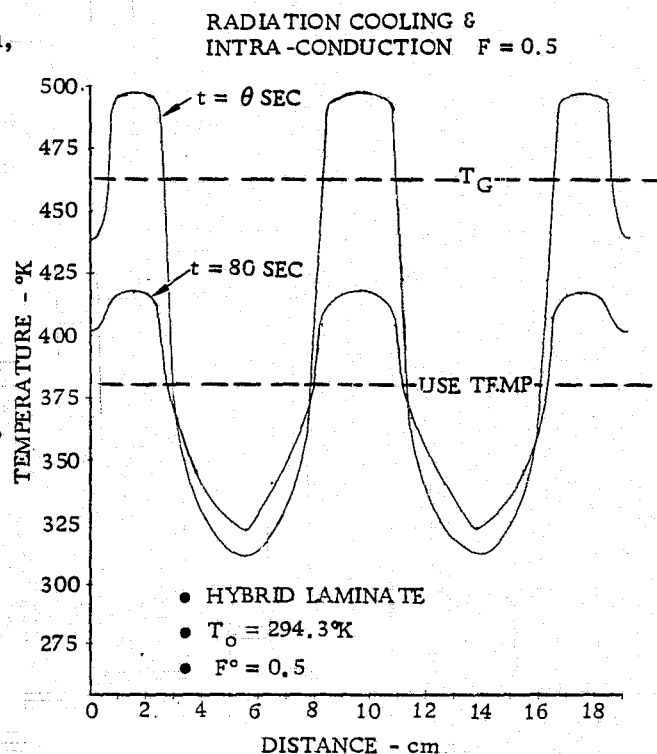


Figure 4-51. Transverse temperature vs. time, radiation/intra-conductive cooling.

ORIGINAL PAGE IS
OF POOR QUALITY

The transverse temperature distribution levels off after platen contact. For this analysis, based upon the above assumptions, the plates maintain an approximately stable temperature in the vicinity of 350°K (170°F). Energy is transferred from the platens into the local cold areas of cap. This energy is replaced in the platens with part of the energy stored in the local hot sections of cap and the remaining cap energy is removed by the coolant. This phenomenon results because the total indirect thermal resistance from local hot cap-to aluminum platen-to local cold cap is much smaller than the direct thermal resistance between hot and cold sections of cap. Also this indirect thermal resistance is of the same order of magnitude as the thermal resistance between cap and coolant. It should be noted that the assumptions for contact coefficients were chosen as being sufficiently conservative based upon Convair-developed information on thermal joint conduction in a vacuum.

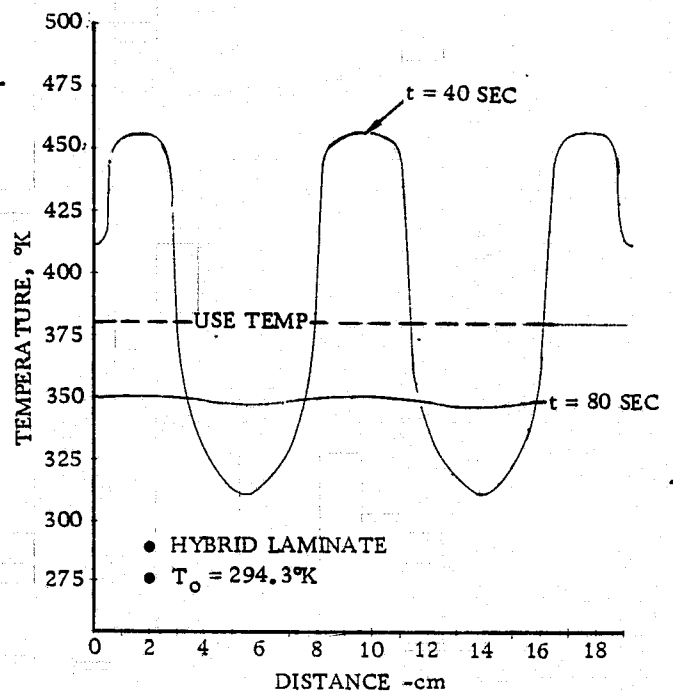


Figure 4-52. Transverse temperature vs. time, platen cooling.

Coolant temperatures used in the analysis were set at a high level because of a concurrent study to examine the feasibility of dumping waste heat from the cooling section back into the storage reels. Analysis revealed that a maximum 448 watts peak may be removed (for three caps) from the beam builder. This includes the peak heat removal from the cooling section plus the steady removal of heat from the heating/forming sections. Although this heat rate is small, it is greater than the heat loss from the insulated storage reels (approximately 170 watts for three reels).

However, a combination of poor view factors plus inadequate area on the perimeter of the reel canister prevents efficient heat transfer to the material. This idea, therefore, appears unfeasible especially when considering the small energy losses from the storage reels. Figure 4-53 illustrates the small reel energy loss by showing the storage reel bulk temperature vs time based upon the following assumptions.

- a. Initial temperature = 294.3°K (70°F)
- b. Reel is covered with 1.0 cm zer-o-cel insulation ($K = .020$ watts/m°K)
- c. Reel radiates only to free space, $\epsilon = 0.1$.
- d. Laminate thermal mass (wCp) = $250.6 \frac{\text{kw-sec}}{^\circ\text{K}}$

It should be noted the above assumptions would serve to make the curve of Figure 4-53 conservative.

The waste heat from the cooling system can be rejected from either an independent integral cooling system or through the orbiter cooling system. If an integral cooling system is used, the waste heat could be dissipated using a space radiator with effective area of 1.6m^2 . This is based upon peak waste heat dissipation from the cooling section (coolant bulk temperature = 327.6°K), worst case space heating to the radiator (100% solar plus 40% earth thermal radiation), and radiator optical properties of $\alpha/\epsilon = .11/.77$. Further analysis revealed that it is possible to have coolant temperatures as high as 355°K (inlet temp. = 333°K , outlet temp = 355°K) and still bring the beam cap down below the structural use temperature. Based upon the same previous assumptions, this would further reduce the required effective radiator area to 1.14m^2 .

On the other hand, the Orbiter can provide a 6300.0 watt heat rejection capability. Beam builder cooling would require approximately 7.1% of this capability at peak conditions.

4.5.1.3 Start-Up. At start-up, it is necessary to bring the material temperature up to approximately 491.5°K in the forming section and have a material temperature distribution approximating that at the end of the 40 second pause cycle during normal operation. (See Figure 4-49, $t = 80$.)

It is possible to create the correct temperature distribution in the heating section by placing two separate heating elements end-to-end within the heating section, each with the capability of turning on at different times. Figure 4-54 illustrates the heating element configuration, a workable timeline for start-up, plus the resulting temperature distribution across the heating and forming sections for one beam cap. This analysis assumes 40.0 watts of power input in the forming section per cap (only 17.2 watts required during steady-state operation) and accounts for conduction of heat underneath those portions of strip shadowed by the forming rollers.

4.5.2 SPACE HEATING. A space heating analysis was made using the Convair Vector Sweep program. This program has the capability of simulating virtually any type of space vehicle or structure. It can calculate the radiation view factors from any particular point or points of interest to space and all other emitters/receivers. In addition, the program can simulate any desired orbit, including maneuvers, and calculate the incident space heating plus shadowing that may occur.

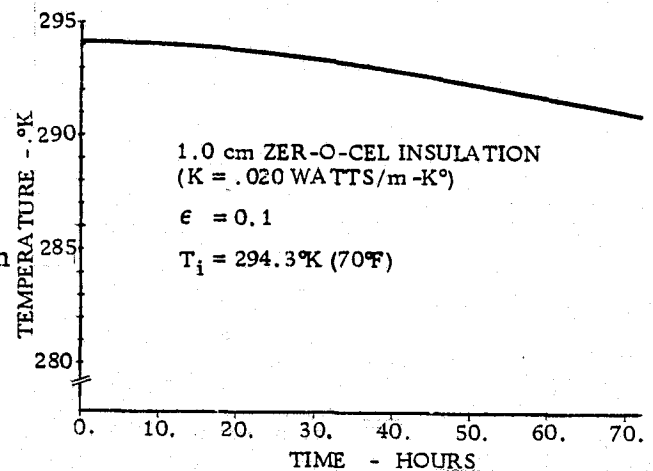


Figure 4-53. Temperature decay vs. time, insulated storage reel.

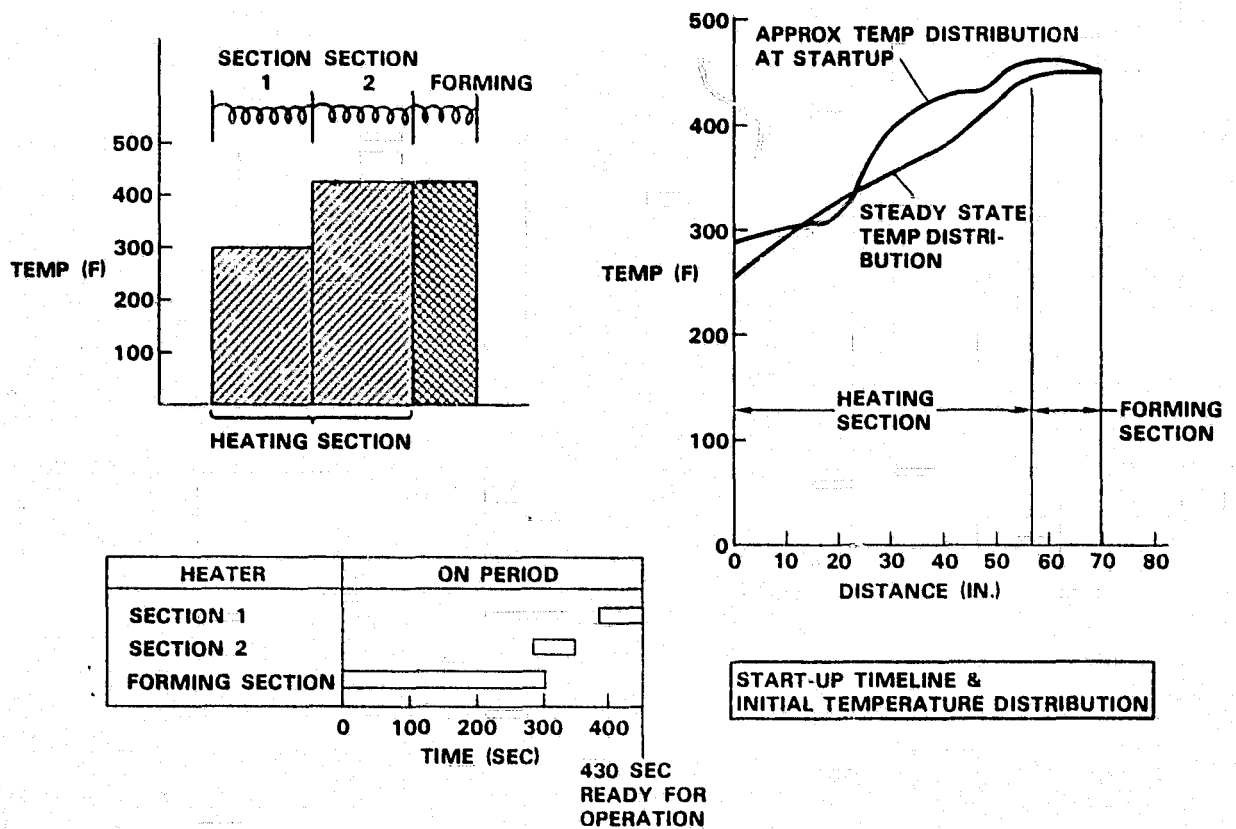


Figure 4-54. Start-up heating.

A preliminary space heating analysis was made in order to determine the beam time-temperature history for worst case space heating conditions. In this analysis, a 200-meter beam was put in a simulated orbit in the solar-ecliptic plane (555.6 km orbit, period = 95.6 minutes) such that one cap would always be shadowed by another.

One bay length of the beam was crudely modeled to calculate the radiation view factors to space. This model simulated only the beam caps and totally neglected cross-members. These results were extrapolated for the full length beam model to obtain incident space heating and temperatures versus time. An idealized shuttle was included in order to incorporate its potential shadowing effect.

Total shadowing of one cap by another gave the worst possible temperature gradient across the beam. Figure 4-55 shows beam cap temperatures versus time for the three caps plus their orbital orientation. These temperatures are averaged down the length of the beam and transversely across the cap. Actual temperature vs. length distributions, reflecting Orbiter shadowing effects, were obtained at 90° (23.9 minute) intervals along the orbit for each cap. For example, Figure 4-56 illustrates this time/temperature/length variation for cap No. 1 of Figure 4-55. The results of this analysis were used in determining the worst case beam thermal loading and distortion. (See Section 4.4.)

- MODEL
 - SINGLE 200M BEAM
 - IDEALIZED SHUTTLE
 - EARTH-FIXED ORIENTATION

- RESULTS
 - ORBIT PERIOD = 95,6 MIN
 - $\alpha/\epsilon = .34 / .89$
 - BEAM CAP AVERAGE TEMPERATURE VS TIME

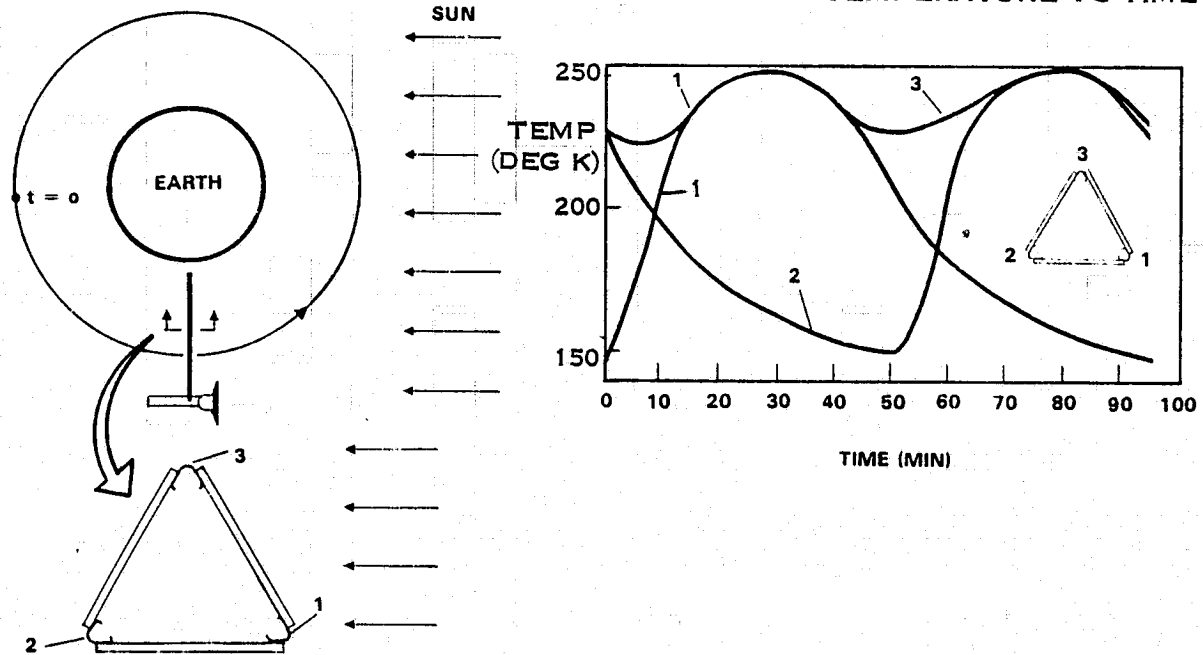


Figure 4-55. Preliminary space heating analysis.

In the preliminary space heating analysis, the simulated orbit was highly unrealistic. Beam cap to cap shadowing is a phenomenon that will not occur for extended periods of time.

A final analysis was conducted assuming a more realistic 9:00 AM ETR launch (555.6 km orbit, period 95.6 minutes) on 21 June 1982 with a 28.5° inclination to the equator. For the calculation of radiation view factors, one bay length of beam was modeled in great detail, including cross-members plus increased accuracy in the modeling of the caps. The results were again extrapolated for the 200-meter beam model, which included the shadowing effects of the shuttle. The estimated free pitch, yaw, and roll of the shuttle/beam configuration were also included in this

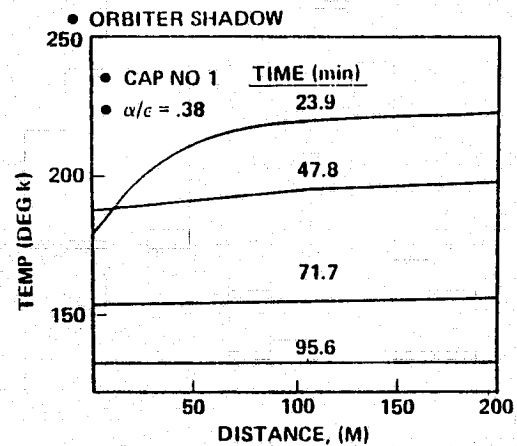


Figure 4-56. Axial temperature distribution, beam cap No. 1

analysis. Figure 4-57 gives the average cap temperatures and orientation for this particular orbit.

The increased modeling detail in the final analysis enabled a fairly accurate calculation of local temperatures across the beam caps. Local cap temperatures will reach a peak value of approximately 265.0°K with an approximate ΔT of 40.0°K across the cap at $t = 49$ minutes. Local minimum cap temperatures achieve a value of approximately 170.0°K with a ΔT of approximately 6.5°K across the cap at $t = 82.5$ minutes. The orbit period begins ($t = 0$) at the terminator moving eastward for the final analysis while for the preliminary analysis the orbit period begins on the back-side of the earth at the midnight position.

The final space heating analysis reveals a much smaller temperature difference cap to cap across the beam. This results in lower beam thermal loading and distortion than projected from the preliminary analysis (See section 4.4).

● MODEL

- SINGLE 200M BEAM
- IDEALIZED SHUTTLE
- EARTH-FIXED ORIENTATION
- ORBIT $i = 28.5$ DEG
- INCLUDES ATTITUDE OSCILLATIONS

● RESULTS

- $\alpha/\epsilon = 0.34/0.89$
- ORBIT PERIOD = 95.6 MINUTES

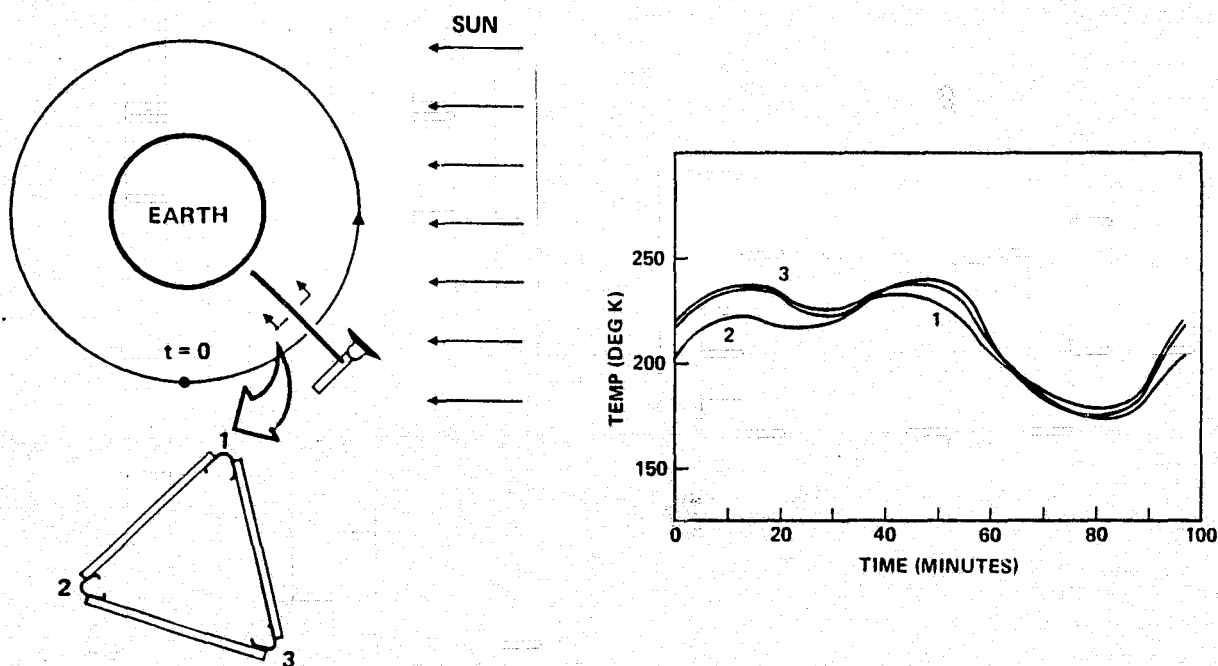


Figure 4-57. Updated space heating analysis.

5

PROGRAMMATICS

This section defines the more significant requirements and costs necessary to implement the definition, design, development, manufacture, and on-orbit operation of the SCAFE program. The program's objectives, guidelines, approach, and operations are described first to identify the elements that must be developed and the advances in the state of the art that must be accomplished during the development phase. A preliminary description of the development and qualification ground test program along with the attendant development schedule is presented to define the development plan. These data are used as the basis for the cost analysis which is presented for both the major work breakdown structure elements of the SCAFE program as well as by year.

5.1 PROGRAM DEFINITION FOR DEVELOPMENT PLAN AND COST ESTIMATION

The following is a summary of the flight and ground operations, the equipment required to carry them out, and an assessment of the advances in the state of the art for the equipment to meet the program objectives. These data are the basis for the development plan and cost analysis which follow.

5.1.1 OBJECTIVES AND GUIDELINES. The objectives of the SCAFE program are:

- a. To design, develop, and implement a Shuttle Orbiter compatible system that will fabricate and assemble a large, low density structural platform in low earth orbit.
- b. To develop fabrication and construction techniques which are applicable to future programs such as Orbital Construction Base and Solar Power Satellites.
- c. To provide a structural test platform from which design and performance data can be obtained.
- d. To use the resulting structure as a platform to mount appropriate experiments.

The following guidelines have been used for the definition of the orbital construction experiment mission:

- a. The on-orbit fabrication flight experiment will be a payload on a Shuttle flight in mid 1982.
- b. One Shuttle flight will be used for platform construction and verification testing. In addition, this flight will carry experiment and subsystems equipment to perform appropriate structural and application experiments after the Shuttle has returned to earth.

- c. On-orbit dynamics and thermal response tests will be required as part of the orbital experiment.
- d. A nominal seven-day mission will accomplish all Shuttle attached mission objectives. If additional mission time is required, an extended mission duration will be used as opposed to a second flight.
- e. Weight and volume will be available for additional Shuttle payloads but operations and timelines have not been constrained by any requirements imposed by these payloads.
- f. A revisit flight is optional to perform additional applications experiments but is not required to meet program objectives. A revisit flight should take place between two and three months after the first flight to be useful because of the orbital lifetime of the platform at the chosen altitude.

5.1.2 MISSION OPERATIONS SUMMARY. The mission profile for the SCAFE mission is shown in Figure 3-23. During ascent (or reentry from the delivery orbit) the SCAFE equipment is inactive, requiring only mechanical and caution and warning support from the Orbiter. The nominal mission is seven days long. The Orbiter crew initiates each operational or test phase and controls Orbiter maneuvers and RMS operations. Before the start and during the initial phase of the beam building experiment, an EVA operation is performed to make sure the equipment is functioning properly and to place instrumentation on the first beam. During the beam building operation the equipment operates automatically under the control of the experiment computer. When the first beam is finished a dynamic response test will be conducted to determine its characteristics and results fed back to the ground to compare with the predicted behavior. This will help predict the characteristics and behavior of the completed platform. The remainder of the platform will be completed by the middle of the third day. During this time the crew will monitor the operation at the aft flight deck and observe directly and with TV. During the afternoon of the third day, another EVA is performed to install the remaining test instrumentation, the subsystems, and the free flight experiment equipment. On the fourth day the dynamic response and thermal deflection experiments will be checked out and performed. During the morning of the fifth day the separation and recapture demonstration experiment will be conducted. The dynamic response and thermal deflection tests will resume on the afternoon of the fifth day. On the sixth day another EVA operation will be performed to simulate repair which might occur on operational platforms. The seventh day will be used for releasing the platform ready to perform the free flying scientific experiments (geodynamics and atmospheric composition), and to continue the dynamic response and thermal deflection experiment, closeout activity, and reentry.

Executive control and monitor of the beam fabrication on-orbit operation is provided via the Orbiter RF command link ground controllers at the Payload Operations Control Center (POCC) which is co-located with Mission Control Center - Houston (MCC-H). MCC-H provides Orbiter and overall mission control.

Tables 5-1, 5-2, and 5-3 list the flight characteristics, structural fabrication equipment, support subsystems, and experiment instrumentation for the flight. The equipment for the scientific experiments is considered to be GFE and does not pace the SCAFE development schedule, nor is it included in the total development cost. The platform configuration and characteristics are documented in Figure 5-1.

Table 5-1. Baseline mission characteristics.

<u>Mission</u>	<u>Characteristics</u>
Shuttle Flight (Extra payload capacity available)	1
Duration (Max.)	7 days
Launch Date (CY)	7/1/82
Delivery Orbit (Nominal)	28 1/2° Incl. 555 km, Circ.
<u>Mission Objectives</u>	
Fab & Assemble Struct Elements	x
Install Evaluation Instrumentation	x
Determine Platform Response - Dynamic/Thermal Separation	x
Recapture	x
Install Subsystem/Scientific Experiments	x
Conduct Scientific Experiments	(After Orbiter returns to Earth)
<u>Orbiter Support</u>	
Power	Baseline Orbiter
Thermal	Radiator Kit
EVA (Including tools)	Baseline Orbiter
RMS (1 provided in Baseline)	Baseline Orbiter
Structural Interface	Baseline Orbiter
AFD Control & Display	Baseline Orbiter
Crew (CMDR, Pilot, MS-1, PS-1)	4
OMS Kit	1
Guidance & Control	x
Communication Syst.	x
Data Management Syst.	x

Table 5-1. Baseline mission characteristics. (Concl'd)

<u>Experiments (Type)</u>	<u>Characteristics</u>
Structural Response/Deformation	Engineering *
Fabrication & Assembly Techniques	Engineering
Separation/Capture	Engineering
Atmospheric Composition/Density	Scientific
Geodynamics	Scientific
<u>Operations Support</u>	
Flight Operation	
TDRSS	x
POCC (Direction/Monitor)	x
MCC-H (Std. Orb/Msn Control)	x
Ground Operations	
Lch/Landing Site	KSC
Level IV	JSC
Off Line/On Line	KSC
Post Mission (Equipment)	JSC
Data Processing/Eval/Distribution	TBD

ORIGINAL PAGE IS
OF POOR QUALITY

*During the first orbiter flight and the free-flight time before a revisit mission.

5.1.3 GROUND OPERATIONS SUMMARY. During factory checkout, a section of beam will be constructed under ambient conditions to check the alignment of the beam builder. After factory checkout the completed beam builder, assembly jig, and sub-systems, along with the experiment instrumentation, will be delivered to JSC for Level IV integration consisting of installation, interface verification test, and check-out activities. Typical tasks are identified in Table 5-4. During Level IV integration, a short length of beam will be fabricated in a vacuum chamber for final check prior to flight. In addition, two bays of the beam must be constructed to prime the beam builder for flight. Subsequently, the flight units will be delivered to KSC for off-line integration with Orbiter simulation equipment and with on-line Orbiter equipment. The SSAFE equipment will be installed with the Orbiter in the horizontal position in the Orbiter Processing Facility. The SSAFE equipment will not require special environmental monitoring or control during any ground operations phase or time critical prelaunch access at the pad. Payload handling in the vertical position

Table 5-2. On-orbit structural fabrication equipment and scientific experiment support subsystems.

<u>Item</u>	<u>Devel. Test *</u>	<u>Flight</u>
Beam Builder	E/A Qual	1
Assembly Jig	E/A Qual	1
Platform Structure	TBD	≈ 1000 kg (2200) stowed
Spares for Simulated Repair	x	x
Platform Subsystems		x
Communication		
Track Transponder	E/A Qual	1
Rendezvous Transponder	↓	1
Data Recorder		1
Antennas		x
RF Downlink (Telemetry Pkg)		1
RF Uplink (Telemetry Rcvr)		1
Elect. Pwr/Dist		
Batteries (Secondary (1)	E/A Qual	x
Solar Panels (1)	↓	x
Charge Cntl/Regulators (1)		x
Interconnecting Wiring		x
Attitude Control (1)		
Thrusters (Cold Gas), Valves & Plumbing	E/A Qual	x
Propellant Tanks	↓	x
Control Electronics		x
Horizon Sensors		x
Magnetic Dampers		x

* E/A = Engineering article, Qual = Qualification

Table 5-2. On-orbit structural fabrication equipment and scientific experiment support subsystems. (Concl'd)

<u>Item</u>	<u>Devel. Test*</u>	<u>Flight</u>
Grapple Fixture	E/A Qual	1
Support Equipment		
Command/Cntl (AFD) (CRT, Keyboard)	TBD	Orbiter Baseline
Bay or Cabin Mounted [†]		
Sci Exp. Support Structure		x
Subsyst Support Structure		x
Elect I/F Equip		In Basic Equip.
Mech I/F Equip		
Fluid I/F Equip		
Software		Orbiter GPC I/F Exp. Peculiar
Manned Maneuvering Unit	-	2

*E/A = Engr. Article, Qual = Qualification
[†] Scientific Experiment Support - GFE
x = Quantity TBD

is not planned; however, it is not precluded by the design.

Post mission analysis of the on-orbit test data and the free flight test data being received will take place at JSC. In addition, post mission inspection of the beam builder and assembly jig will be performed. Any required refurbishment for an optional revisit applications flight for the assembly jig and the beam builder, if required, will be performed at JSC. Categories of experiment-peculiar GSE and unique facilities/special test equipment are identified in Tables 5-5 and 5-6, respectively. Equipment quantities are TBD.

5.1.4 TECHNOLOGY ADVANCEMENT. Technology for the SCAFE program is considered to be within the state of the art. Required technology for each SCAFE technique is identified in Table 5-7. Relative difficulty in demonstrating and verifying the technology is called out on the chart.

Table 5-3. On-orbit experiment instrumentation.

<u>Item</u>	<u>Devel. Test *</u>	<u>Flight</u>
Structural Response		
Instrumentation		
Sun Shades	E/A	2
Accelerometers	Qual	6
Temperature		x
Probes		
Retro Reflectors		1000
Laser Beacon and Detector Array		1
TV Camera		1
Controls & Displays (In Orbiter)		x
Laser Retro Reflectors		10
Vibrators		2
Geodynamics		
S-Band Transponder †	E/A Qual	2
Atmospheric Composition		
Spectrometer and Radiation † Source	E/A Qual	1
Fixed Reflector †		1
Movable Reflectors †		2

* E/A = Engineering article, Qual = Qualification

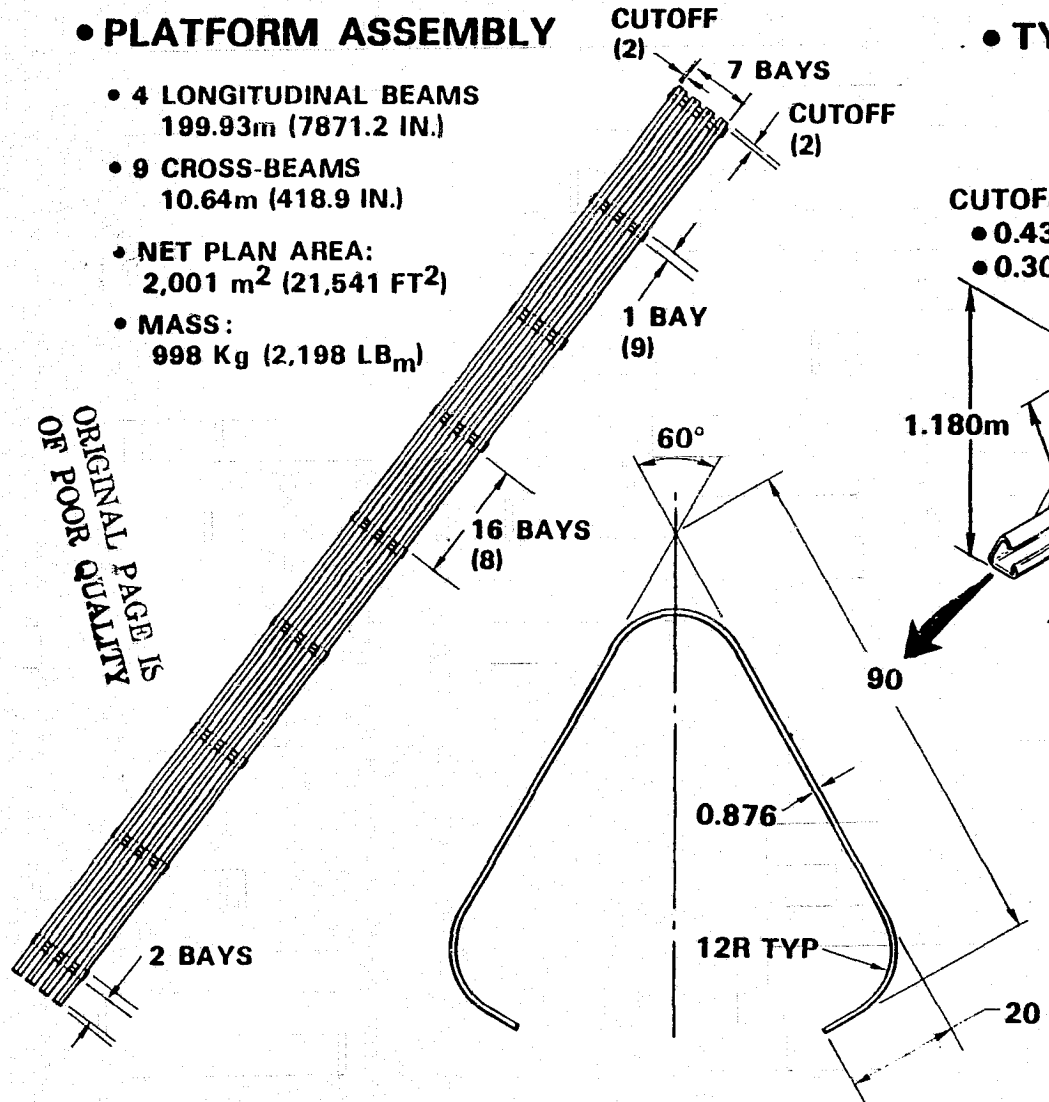
† Scientific Experiment, GFE

5-8

• PLATFORM ASSEMBLY

- 4 LONGITUDINAL BEAMS
199.93m (7871.2 IN.)
- 9 CROSS-BEAMS
10.64m (418.9 IN.)
- NET PLAN AREA:
2,001 m² (21,541 FT²)
- MASS:
998 Kg (2,198 LB_m)

ORIGINAL PAGE IS
OF POOR QUALITY



• TYPICAL BEAM

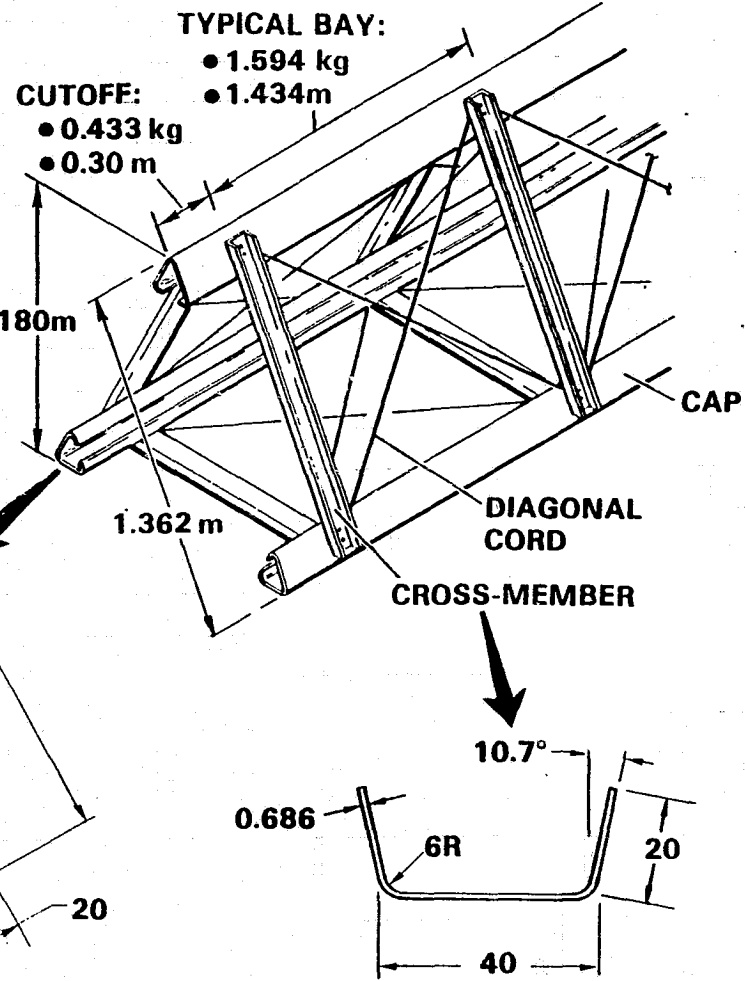


Figure 5-1. Platform characteristics.

Table 5-4. Typical Level IV integration tasks.

Integration Type*	Task	Reason
T & C/O	Produce beam segment in vacuum chamber	Functional checkout
T & C/O	Produce two bays with flight material	Prime fabrication system
I	Install equipment on assembly jig and cradle	1st time all together
T & C/O	Subsystem integration	" " "
T & C/O	Experiment Instrumentation C/O	" " "
V	Electrical, data interface	" " "
T & C/O	Software C/O with Orbiter GPC Simulation	" " "
T & C/O	Perform Combined Syst. Test	" " "

*V = Verification I = Installation T & C/O = Test & Checkout

Table 5-5. GSE - Experiment Peculiar

Item	Requirement
Handling & Transport	
Dollies	x
Shipping Containers	x
Slings	x
Servicing	
Thermal Fluid	x
Battery Fluids	x
Cold Gas	x
C/O & Maintenance	
Integration - Software	x
- Elect/Funct. C/O	Various
Auxiliary Power Supply	x
Ground Heat Exchanger	x
Special (Auxiliary)	TBD
Sim. /Trainers	
EVA Fixture (Support Boom)	x
Special EVA Tools	x
Exp. Peculiar RMS Tech (Uses Avail JSC Simulator)	x
Flight Opns, e. g., Docking	x
Mission Support	
POCC* Console & Computer & MCC-H I/F Equip.	Provided by POCC
POCC Software (e. g., Data Formatting)	"
Signal Format & Conversion Factors	Exp. Supp.

ORIGINAL PAGE IS OF POOR QUALITY

*POCC = Payload Operations Control Center x Required - Quantity TBD

Table 5-6. Unique facilities/special test equipment.

Item	Requirement
Design/Development - Fabrication	Clean Area (100,000 class)
- Test	Vacuum chamber
Integration	Clean Area (100,000 class)
Prelaunch	" "
Mission Support	None
Post Mission	None

Table 5-7. Preliminary technology demonstration assessment.

Technique	Technology	Rank
Verification of Construction	Resistance to environment	Low
Materials	- Vacuum	
- Graphite/Thermoplastic Composite	- Cosmic & Solar Radiation	
	- Thermal	
	Formability/Fabrication Characteristics	Low
	Structural Characteristics	Low
Joints/Joining	Welding	Medium
	Bonding	Low
Material Forming	Roll Forming	Low
Fabrication of Basic Truss Element	Automated Fabrication Machines	
	- Elect./Mech.	Medium
	- Electronic Controls	Low
	- Servomechanisms	High
	- Automatic Cable Tensioning Control	Low
	Automated Inspection & Quality Control	High
Assembly of Substructure (Multiple Truss Elements)	Assembly Jigs & Fixtures - Parts Handling	Medium
	Electronic Controls	Low
	Inspection & Quality Control	Medium
Handling of Large Structures	Manipulators	Medium
	Stabilization & Control Systems (Semi-Rigid Structure)	High
	Guidance Systems/Sensors	Medium

Table 5-7. Preliminary technology demonstration assessment. (Concl'd)

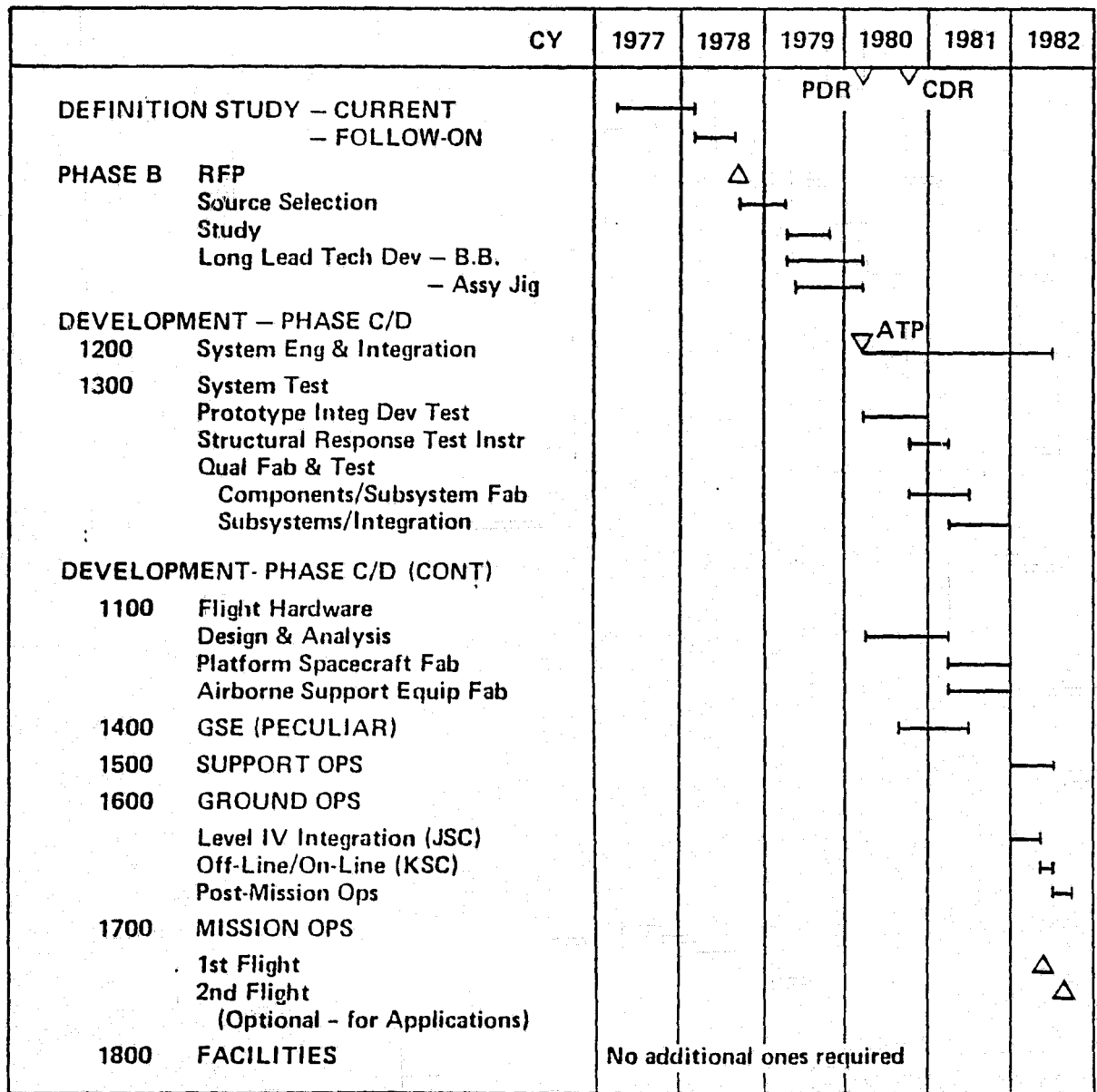
Technique	Technology	Rank
Attachment of Superstructure- Solar Arrays, Waveguides, Equipment Racks, etc.	Automated Machines (Special Purpose)	High
	Parts Handling Systems	Medium
	Automated Checkout Systems	High
Attitude Control/Maneuvering of Large Semi-Rigid Structure or Structural Sub-Assemblies	Guidance Systems	Medium
	Stabilization & Control Systems	High
	Propulsion Systems	Medium
Equipment - Individual Component Installation - Reflector, etc.	Parts Handling	Medium
	Assembly Jigs	Medium
	Automated/Semi-Automated Machines	High

5.2 PRELIMINARY DEVELOPMENT PLAN

A master development plan schedule has been generated for a launch date in mid-1982 and driven by the Engineering and Qualification Test requirements delineated below. The program can be accomplished with a minimum of risk to meet the scheduled launch date.

5.2.1 SCHEDULE. The preliminary SCAFE program schedule is shown in Figure 5-2. Schedule and durations are based on the following guidelines and assumptions:

- a. Launch date mid-1982 and WBS (Section 5.3).
- b. Follow-on SCAFE contract ending 1 Oct 1978.
- c. Source selection is an estimate of time to bid and select the Phase B contractor. The Phase B contractor is assumed to be selected to conduct the following development phase (Phase C/D) without a competitive bid.
- d. Follow-on contract produces the following products (as a minimum)
 - 1) Updated conceptual design of SCAFE
 - 2) Preliminary specification for beam builder and assembly jig subsystems
 - 3) Plans and costs for Phase B
- e. Phase B study produces the following products (as a minimum):
 - 1) Requirements in the form of specifications
 - 2) Definition of flight experiments
 - 3) A selected system predesign
 - 4) Plans and costs for development



*Post separation experiments instrumentation assumed to be GFE & not assumed in this schedule.

Figure 5-2. Preliminary SCAFE program development schedule.

- f. Included in Phase B is a prototype development program to be carried out before the start of Phase C/D on the subsystems for the beam builder and assembly jig.
- g. Phase C/D system engineering and integration includes definition of the integrated payload system and compatibilities with the STS, mission and flight operations, verification, software integration, reliability and safety analyses, and configuration management. Analytical integration starts at the same time as design analysis and concludes (for cost purposes) at the first flight (sustaining support may be required until program completion).
- h. Phase C/D design and analysis task is expected to reflect maximum utilization of existing equipment listed in the NASA Low Cost Program Office CASH catalog, as well as multi-use mission spacecraft equipment.
- i. Phase C/D prototype development equipment will be as near to final design as practical, including drives, controls, and sensors.

5.2.2 DEVELOPMENT & QUALIFICATION TEST PROGRAM. A preliminary estimate of SCAFE development and qualification testing is contained in Table 5-8. Key ground tests at the subsystem and system level are identified for development of mechanical and avionics equipment. Preliminary identification of component and subsystem qualification testing is included in Table 5-8. It is assumed that one engineering article will be adequate for design support testing and one ship set will be used for qualification.

Section IA in the table describes the development activity to take place during Phase B. This will only be on subsystem components. Section IB describes the development work which will be initiated with Phase C/D under WBS 1300 System Test, shown in Figure 5-2.

5.3 COST ANALYSIS

A cost analysis of the SCAFE has been conducted and the results are documented herein. This section includes the WBS, the cost analysis methodology and ground rules, program definition and assumptions, the program cost estimate, and annual funding requirements.

These data represent preliminary top level estimates that can only reflect the program definition work performed to date and, therefore, cannot be considered complete or final. They do, however, represent a reasonable estimate based on information available at this time and are applicable for planning purposes. As the program proceeds and more detailed definition of specific hardware becomes available, increased accuracy of individual cost element estimates can be determined.

5.3.1 WORK BREAKDOWN STRUCTURE. A preliminary work breakdown structure (WBS) for the SCAFE program is presented in Figure 5-3, which serves to identify all of the cost elements to be included in the cost analysis task. This WBS contains

Table 5-8. SCAFE development and qualification ground test program.

Type/Purpose	Test
I Development Engineering Test and Evaluation - Phase B	
A. <u>Components and Subsystems</u>	
1. <u>Beam Material Development</u>	
<ul style="list-style-type: none"> a. To determine the physical properties of the materials/composites used in the beam components. b. To determine the effects of the mission environments on the materials. c. To determine the process compatibility of the materials. 	<p>These tests will be performed on small samples in the materials lab to determine:</p> <ul style="list-style-type: none"> 1. Lamina/Laminates <ul style="list-style-type: none"> a. Graphite/P1700 lamina and glass/P1700 lamina <ul style="list-style-type: none"> . Strength - tension and compression (0°, 90°), μ . Moduli - 0°, 90°, $G_{x,y}$. Ultimate strains - tension and compression (0°, 90°) . Coefficient of thermal expansion: 0°, 90° at 144°, 200°, 256°, 311°K . Thickness (t) and density (ρ) . Thermal conductivity 0°, 90°, t . Effects of mission environments (including radiation, thermal cycling, vacuum) . Percentage of fiber volume b. Glass/Graphite/P1700 laminates Same as above plus flexural effects on strength, strain and creep in storage rolls 2. Coatings <ul style="list-style-type: none"> . Optical properties - α, ϵ . Forming and welding process compatibility . Environmental effects - consolidation and forming temperatures, vacuum, and radiation 3. Cord Tensile strength, modulus, ultimate strain, creep (in thermal vacuum) under maximum preload

ORIGINAL PAGE IS OF POOR QUALITY

Table 5-8. SCAFE development and qualification ground test program (continued).

Type/Purpose	Test
	<ul style="list-style-type: none"> • Flexural creep in storage roll • Diameter, density, conductivity, α, ϵ • Percentage of fiber volume • Environmental effects on properties
<p>2. Structural Development</p> <ul style="list-style-type: none"> a. To ascertain the physical properties of the beam components and complete beam. b. To verify the efficacy of the beam builder sections in terms of the physical properties of the fabricated components. 	<p>The test specimens will be formed on hard tooling; in the initial stages of development and as produced by the beam builder when available. Conventional structural laboratory loading, heating, instrumentation, recording, and data playback equipment will be used. The initial tests will be used to completely determine the component properties. (Verification of the production process during the later phases of the program will be achieved through an abridged version of the initial testing.)</p> <p>1. Cap Sections and Cross-members</p> <ul style="list-style-type: none"> • Crippling strength and initial buckling loads • Column strength and failure modes • Bending strength (about 2 axes) • Torsional stiffness <p>2. Joints</p> <ul style="list-style-type: none"> • Weld strength and associated machine schedules for each weld type/size • Cap/cross-member strength (shear and moment), failure modes • Cord retention strength (pull out from weld) • Cord preload retention during weld • Automated QA technique for welds

Table 5-8. SCAFE development and qualification ground test program (continued).

Type/Purpose	Test
<p>3. <u>Beam Building Components and Sub-Assemblies</u></p>	<p>3. Assembled Beam</p>
<p>a. Cap Forming Subsystem</p>	<ul style="list-style-type: none"> • Strength, stiffness in tension and compression, bending and torsion. • Dynamic response: Modal survey, damping coefficients, effect of shuttle environments (if return of beam segment from orbit is contemplated). • Thermal distortion - effect of solar heating in vacuum at various angles of incidence.
<ul style="list-style-type: none"> • Storage Canister <ul style="list-style-type: none"> • Determine shuttle environment effects on stored material. • Demonstrate ability of canister to correctly feed material from canister. 	<p>Expose canister with simulated stored material roll to shuttle accelerations and perform examination of material roll surfaces for damage.</p>
<ul style="list-style-type: none"> • Heating Section <ul style="list-style-type: none"> • Determine operating characteristics of heater, sensor, and reflector elements. • Determine effects of environment and life cycles on heater elements. • Determine heater productivity 	<p>Set up canister to automatically feed material in the normal run/pause mode under simulated zero g conditions. The canister will be laid on its side and the material supported on low-friction bearings as it is unrolled to reduce the effects of gravity. The unwinding behavior of the roll will be observed.</p>
	<p>Test manufactured prototype heaters under simulated space operating conditions. These tests will be performed in a thermo-vacuum chamber to measure heat rates, sensor and reflector cooling requirements, and effects of repeated life cycles. The section will be vibrated to measure effects on sensors and heaters. The manufacture of the prototype heater will serve as a pilot production for subsequent heaters.</p>

Table 5-8. SCAFE development and qualification ground test program (continued).

Type/Purpose	Test
<ul style="list-style-type: none"> • Complete Cap Forming Subsystem • Demonstrate ability to operate for long periods in a space environment • Demonstrate ability to withstand the effects of the shuttle environments. • Demonstrate ability to produce high quality cap sections. • Demonstrate accuracy of differential drive subsystems. 	<p>Tests will be performed in a thermo vacuum chamber, after initial checkout. The tests will be run in an automatic mode to produce cap sections. Measurements of power inputs, temperatures, drive speeds, and displacement will be made. The cap sections will be subjected to material testing to determine their physical and structural characteristics. Endurance tests will be conducted.</p> <p>The cap forming subsystem will be subjected to shuttle and ground vibration and shock, and examined for degradation.</p>
<p>b. Diagonal Cord Applicator Subsystem</p> <ul style="list-style-type: none"> • Demonstrate ability to operate for long periods in a space environment. • Demonstrate repeatability and accuracy of tensioner and pleyer positioner mechanism and controls. • Demonstrate satisfactory functioning of cord storage and feed mechanism and controls 	<p>A prototype cord plier and tensioner and a cord storage and feed mechanism and all necessary controls will be built and tested individually, then as a combined unit.</p> <p>Tests will be conducted to demonstrate ability to operate automatically in a thermo vacuum chamber. Instrumentation will measure power requirements, repeatable accuracy of the tensioner and positioner. The cord will be examined and tested for degradation caused by the mechanisms. The mechanisms will be examined for deterioration and lubrication problems.</p>
<p>c. Cross Member Subsystem</p> <ul style="list-style-type: none"> • Demonstrate ability to operate for long periods of time and function correctly. • Demonstrate mechanism and controls will correctly feed cross-members, extract cross-member, and position it consistently. 	<p>A breadboard cross-member subsystem and its controls will be fabricated and evaluated. Tests will be conducted to assure the mechanisms and controls will store, feed, and position a cross member. Visual examination will be made to measure possible degradation of the cross-members caused by the mechanisms. Measurements will be made to measure repeatability of cross-member positioning on caps. Power</p>

Table 5-8. SCAFE development and qualification ground test program (continued).

Type/Purpose	Test
<p>d. Ultrasonic Welding Sub-system</p> <ul style="list-style-type: none"> . Demonstrate ability to operate for long periods of time and function correctly in a space environment. . Demonstrate mechanisms and controls will correctly drive, position, and produce consistent welds. <p>e. Cutoff Mechanism</p> <ul style="list-style-type: none"> . Demonstrate ability to perform repeated cutoffs in space environment. 	<p>requirements and repeatability of controls will be measured.</p> <p>A prototype weld head and control mechanism, and a weld anvil mechanism will be constructed. Tests will be conducted to exercise the mechanisms and controls to assure drive mechanisms will position the anvil and welding head in the correct position based on position sensor feedback. Measurements will be made of drive speed, power required, and control and sensor parameters. The welding process will be investigated using beam component specimens to determine the efficiency of the pressure and power sensors in the feedback control loop. The weld samples will be examined by NDT and strength tests to determine the correct power and pressure settings and to verify the consistency of the welding process. The welder will be demonstrated in a thermal vacuum chamber to show long life repeatability and consistent weld quality.</p> <p>A prototype beam cutoff mechanism will be fabricated and evaluated. Tests will be conducted to verify the ability of the shears and drive mechanism to provide clean, repetitive cutoff of pieces from a length of beam cap in a thermal vacuum chamber.</p>
<p>4. <u>Assembly Jig Components and Sub-Assemblies</u></p> <p>a. Longitudinal Beam Handling Mechanism.</p> <ul style="list-style-type: none"> . Determine operating characteristics of three-position retention and guide mechanism. 	<p>A prototype of a three-station retention and guide mechanism (RGM) and platform drive mechanism and controls will be fabricated and tested. A fabricated beam will be used to demonstrate the mechanisms. Tests will be conducted to assure the measurements and controls</p>

ORIGINAL PAGE IS
OF POOR QUALITY

Table 5-8. SCAFE development and qualification ground test program (continued).

Type/Purpose	Test
<ul style="list-style-type: none"> . Determine operating characteristics of the platform drive mechanism and its controls. 	<p>will perform their desired functions. Measurements and observations will confirm the behavior of the RGM during retention and step-through, as well as the platform drive mechanism positioning and synchronization accuracy.</p>
<p>b. Platform Assembly Subsystem</p> <ul style="list-style-type: none"> . Demonstrate mechanism will function satisfactorily for long periods of time and function correctly drive, position, and produce consistent welds. 	<p>A prototype control arm and drive, bridge assembly, carriage and drive, personnel carrier and drive, and necessary controls will be constructed. These will be operated in the remote and manual mode to evaluate their behavior in terms of functional behavior and positioning accuracy. Measurements will be made of power requirements, position, velocity. Visual examination will be made of function and wear.</p> <p>A prototype weld head and control mechanism and weld anvil mechanism will be constructed. They will be tested in a manner similar to I-A-3-d above.</p>
<p>c. EVA Bridge Subsystem</p> <ul style="list-style-type: none"> . Demonstrate mechanism will function satisfactorily under manual and remote controls. . Demonstrate compatibility with astronaut control. 	<p>The equipment will be operated in the man-machine loop under space constraints for training. and to determine the suitability of the equipment for EVA use.</p>
<p>5. <u>Prototype Avionics System</u></p>	
<p>a. Beam Builder & Assembly Jig Controls</p> <ul style="list-style-type: none"> . To assist in the development and the choice of the control system components, and system design. 	<p>The development will include computer simulations, hybrid hardware/computer tests, and breadboard mockups of the controls system. These tests will progress to the point that prototype control units can be fabricated and demonstrated.</p>

Table 5-8. SCAFE development and qualification ground test program (continued).

Type/Purpose	Test
<ul style="list-style-type: none"> To demonstrate the feasibility of the control system (ACU, BCU, and software) 	<p>The off-the-shelf hardware will require validation testing, but entirely new hardware should be demonstrated under the Space Shuttle induced and space natural environments.</p>
<p>b. <u>Prototype Platform Avionics Equipment</u></p>	<p>The hardware will be available for use in the beam builder and assembly jig prototype tests above, so that it can actually be used to control the beam building processes automatically.</p>
<ul style="list-style-type: none"> To assist in the development and the choice of platform avionic system components, and the system design. To demonstrate the feasibility of the control avionics. 	<p>The testing will be as described under 5-a test above.</p> <p>The equipment to be tested will be as follows:</p> <ol style="list-style-type: none"> 1. Communications - Data recorder, antennas, instrumentation, RF links 2. Data management 3. TV 4. Electrical power distribution - batteries, solar panels, charge controls/regulators, wiring.* 5. Attitude control - thrusters, propellant tanks, control electronics, horizon sensors, CMG (if required)* 6. Software 7. Dynamics experiment instrumentation - 6 accelerometers, laser beacon and detector array, TV camera, and spotlight
<p>B. <u>Integrated System Tests Phase C/D</u></p>	<p>* Scientific support equipment will be GFE.</p>
<p>1. <u>Beam Builder</u></p>	<p>The beam builder will be assembled from the hardware developed and used for the systems tests of I-A-3 and I-A-5. In addition, the beam builder structural</p>

ORIGINAL PAGE IS
OF POOR QUALITY

Table 5-8. SCAFE development and qualification ground test program (continued).

Type/Purpose	Test
	<p>assembly will be provided, or simulated. These are the spider, forming section, and support beam assemblies. All necessary controls, software, and power will be provided. Necessary instrumentation to monitor the performance of the beam builder will be installed. Since the critical components will have been already tested in a thermal vacuum chamber, the beam builder tests will be run at ambient conditions. This may necessitate local temperature conditioning on the cap forming subsystem.</p> <p>The beam builder will be operated in an automatic mode and complete beams fabricated. The beams will be physically tested as a determination of the beam builder effectiveness.</p>
<p>2. <u>Beam Assembly</u></p> <ul style="list-style-type: none"> ● To determine the structural and dynamic characteristics of the platform beam joints. 	<p>A main beam and a cross beam will be welded together by the assembly jig welding process.</p> <p>The section will be supported so as to allow the introduction of design loads into the joint to determine joint strength and deflection.</p> <p>The section will be supported on shock cords and instrumented with accelerometers to determine the damping. This will be compared to that of the tests on the single beam to determine the joint effect.</p>
<p>3. <u>Assembly Jig</u></p>	<p>No integrated system tests will be performed prior to the qualification test program.</p>

II Qualification - Phase C/D

A. Components

1. Mechanical

Table 5-8. SCAFE development and qualification ground test program (continued).

Type/Purpose	Test
2. <u>Electrical</u>	
3. <u>Avionics</u>	
4. <u>Structural</u>	
To verify suitability of production parts to perform satisfactorily in a space environment.	Components should be qualified to satisfy the environments anticipated during ground handling, Shuttle transportation, deployment and assembly, and on-orbit. The tests to be <u>considered</u> are functional, thermal-vacuum, thermal cycling, pyro shock, acceleration, humidity, pressure, leak, EMC, life, and other special tests.
B. <u>Subsystems/Assemblies</u>	
1. <u>Beam Builder</u>	
To qualify the beam builder:	
<ul style="list-style-type: none"> ● To operate as an automated mechanism. ● To manufacture beams meeting the design specification. 	The beam builder will be tested in its entirety in a one-g environment to ensure it operates correctly as a mechanism. Following a successful checkout, it will be installed in a vacuum chamber and operated. The tests will include measurement of power requirements, fabrication speed, etc. It is assumed the component tests will have qualified the components so that the demonstration of function will suffice for qualification. It may be desirable to perform some modal and structural tests to yield data for analysis of suitability to meet the Shuttle and other specification requirements. The testing will be in the automatic mode so as to demonstrate the control system assemblies.
	The beams produced will be tested to ensure they will meet the design specifications.
2. <u>Assembly Jig</u>	
To qualify the assembly jig as an automated mechanism	Testing will be in the same manner as II-B-1 above. The beams and cross-members will be welded to demonstrate that process.

ORIGINAL PAGE IS
OF POOR QUALITY

Table 5-8. SCAFE development and qualification ground test program. (Concluded)

Type/Purpose	Test
<p>3. <u>Platform Avionics</u> To qualify the platform avionics system.</p>	<p>Tests will be in a generally similar manner as II-B-1 above.</p>
<p>4. <u>Grappler Assembly</u> To qualify a grappler assembly.</p>	<p>The testing will be a structural evaluation. Components will have been tested under II-A above.</p>

all of the hardware and tasks associated with program development and test, fabrication of the flight hardware, and operations activities incurred during the first flight. It is assumed that the Shuttle user charge includes all Shuttle-related activities such as on-line payload installation (OPF), MOC activities, flight crew costs, and other common ground operations/mission operations and activities. Shuttle-related services such as OMS kits, RMS, etc., and other optional services are added to the Shuttle charge for the basic transportation. Potential user charges for tracking and data acquisition (TDRSS, etc.) are carried as a separate program level item.

5.3.2 COST ANALYSIS

5.3.2.1 Approach and Methodology. The economic analysis approach and cost estimating methodology are discussed in this section.

Initially a cost-related work breakdown structure, discussed above, was developed that includes all elements chargeable to the SCAFE program for each of the program phases, namely, development, production, and operations. This cost WBS then sets the format for the estimating model, the individual cost estimating relationships (CERs), cost factors, or specific point estimate requirements, and finally the cost estimate output itself.

Cost estimates are then made for each element either at the breakdown level shown in the WBS or, in certain cases, one level low. These estimates are then accumulated to provide the cost for each program phase.

The estimating methodology varies with the cost element and with the historical data or vendor quotes available, etc. For new non-off-the-shelf hardware parametric CERs are used. These CERs have been derived for various categories of hardware and many subcategories representing differing levels of complexity. They are derived from available historical cost data or detailed estimating information and related cost to a specific driving parameter such as weight, area, power output, etc. For example, the various SCAFE structural items, mechanisms, control systems, etc., were estimated using CERs.

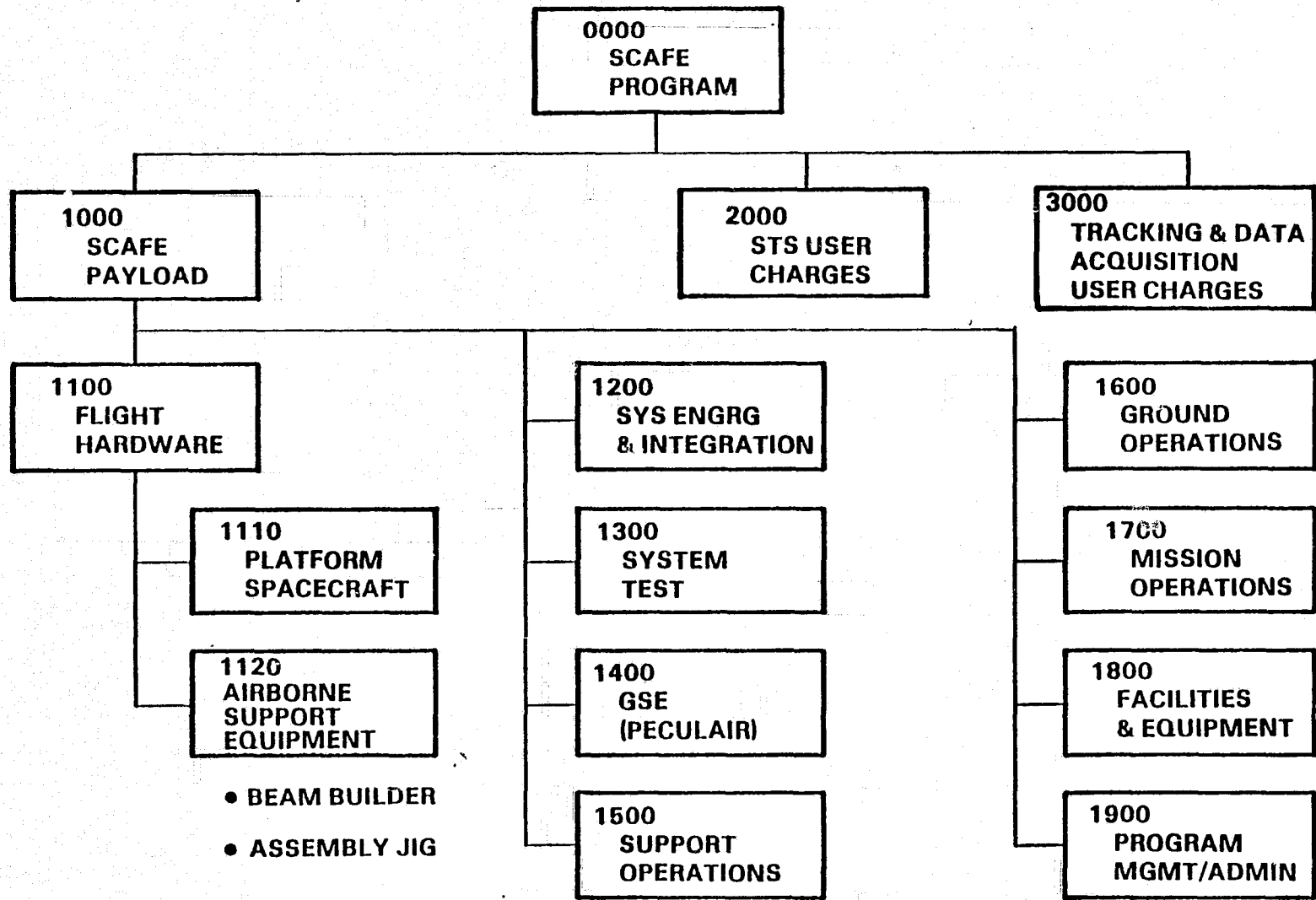


Figure 5-3. Work breakdown structure.

Point estimates were used for specific pieces of equipment where the definition data were sufficiently detailed or the hardware item was existing equipment and cost data were available. Certain electronic equipment and instrumentation were estimated in this manner. Another example of point estimates are several task areas in ground and mission operations where manloading estimates were made and converted to cost.

The remaining "floating item" cost elements, such as, system engineering and integration, program management, etc., are estimated using cost factors consisting of appropriate percentages of the applicable related program effort.

5.3.2.2 Ground Rules and Assumptions. The following general ground rules and assumptions were used in estimating the SCAFE program costs presented herein. Specific assumptions and definitions for individual cost elements are discussed in Program Definition and Assumptions (Section 5.3.2.3).

- a. Costs are estimated in current/constant FY 1977 dollars.
- b. Costs are estimated for nonrecurring, recurring production, and recurring operation phases. The costs include all SCAFE payload-related cost incurred from the start of Phase C/D (Development Phase) through the first launch of the SCAFE including three months of experiment orbital monitoring and data acquisition.
- c. Phase B study costs and pre-Phase C/D funding requirements for selected, long lead technology development are included as program development costs.
- d. The estimates presented represent total cost to the customer; however, NASA IMS and Program Office support (salaries, travel, etc.) and prime contractor fee are excluded.
- e. Flight 2 costs, GFE experiment costs, and post flight SCAFE refurbishment are not included at this time.
- f. The flight will occur in 1982.
- g. The Shuttle user charge will be included in the estimate.
- h. The SCAFE program estimated is defined in Section 5.1. The SCAFE is described in Section 2.
- i. These cost data are provided for planning purposes only.

5.3.2.3 Cost Definition and Assumptions. Cost estimates have been made for the complete SCAFE program, specifically, the nonrecurring or development phase, the production phase (unit flight hardware cost), and the operations phase including the experiment flight test. These estimates represent total cost to customer incurred by the overall program not just SCAFE prime contractor costs.

The nonrecurring development or DDT&E phase includes all of the one-time tasks and hardware to design and test the SCAFE experiment. It includes the design and analysis for all ground and flight hardware including structural analysis, stress, dynamics, thermal, mass properties, etc. This phase also includes all software development. The nonrecurring category also includes all component development and test through component qualification as well as all component development test hardware. In addition, this phase includes: system engineering and integration;

system level test hardware and (engineering test prototype and qualification article) and system test; GSE design, development, test and manufacture; facilities; and lastly, overall program management and administration.

The production phase (unit cost estimate) includes all tasks and hardware necessary to fabricate one complete set of flight hardware equipment. It includes all material and component procurement, parts fabrication, subassembly, and final assembly. In addition, this category includes the required quality control/inspection task, an acceptance test procedure for sell-off to the customer, and program management and administration activities accomplished during the manufacturing phase.

The operations phase includes all preparation launch and on-orbit operations associated with the SCAFE experiment. It includes all ground operations, Shuttle system integration (including post-mission activities) and the mission operations (ground) activities themselves including mission control, data handling, support, etc., together with program management and administration during the operations period.

Each of the individual cost elements is discussed below.

1000 SCAFE Program

This summary cost element includes all labor, hardware, and services necessary for the engineering development, production of the flight article, and the first flight operations of the SCAFE. The development phase, in addition to the design, development, and test activities, includes the fabrication of a non-flight engineering test prototype, a flight configuration qualification article refurbishable to a flight backup unit, and all necessary GSE. The production cost includes the fabrication and acceptance test of the primary flight unit. The operation phase includes the preparation, integration, and installation of the SCAFE flight unit into the STS Orbiter, the on-orbit beam construction operations, the return, removal and disposition of the SCAFE equipment, and the on-orbit test and monitoring of the free-flying space platform for 3 months. The revisit flight and all GFE experiments and equipment are excluded.

It is assumed for this estimate that maximum use is made of developed available off-the-shelf components for both the platform spacecraft and the beam builder and assembly jig. The only component development costs incurred are those of the truly unique new designs required. System (or subsystem) level design, analysis, and test are included in all cases however.

1100 Flight Hardware

This element includes all labor, materials, and services necessary for the platform spacecraft (WBS 1110) and the airborne support equipment (WBS 1120), which includes the beam builder and assembly jig. Costs are not included in this estimate for subsequent flights (Flight 2 - WBS 1130) or for GFE Experiments and equipment (WBS 1140).

1110 Platform Spacecraft

This element includes the platform structure or beam itself, together with such subsystems as are assembled to the beam and remain in orbit when the Orbiter returns to earth. These subsystems include communications/data management, electrical power, attitude control and stabilization, and rendezvous and docking.

1111 Beam Structure

The beam structure unit cost consists of the composite material (hybrid laminate with fabric of pitch fiber VSB-32T and polysulfone P1700 resin and glass fiber) used in the cap forming machine, the preformed composite cross-members, miscellaneous hardware such as the "docking" fixture for the manipulator, and equipment attachment provisions.

No beam structure fabrication or assembly labor costs are included for the on-orbit fabrication by the flight crew during flight operations. The composite cross-members and the miscellaneous hardware such as alignment sensor reflectors are fabricated on the ground.

Material development and production nonrecurring costs are also included.

1112 Communications/Data Management

The communications/data management subsystem installed in the free-flying platform will consist of standardized off-the-shelf components, such as an applicable standard MMS CDHS module. This equipment will include a computer, a telemetry transceiver/tracking transponder, and a data recorder and auxiliary interface equipment. In addition, unique antennas tailored to the free-flying configuration will be necessary.

1113 Electrical Power

An electrical power system is required to provide power for the structural response instrumentation and the communications/data handling system (as well as other GFE experiment equipment). It consists of a solar array and secondary batteries, and charge controllers and power conditioning (voltage regulators). In addition, all wiring and cable harnesses are also included in this cost element.

It should be noted that this subsystem is sized to include the capability of also providing power for the GFE experiments and full subsystem costs are included.

1114 Attitude Control Subsystem

The majority of the active attitude control system is considered to be GFE and required for the GFE experiments and is not defined at this time. Only the passive elements, specifically the magnetic dampers, are required for the structural response tests and, therefore are the only costs included herein.

1115 Rendezvous and Docking

The rendezvous and docking subsystem for the free-flying platform consists of a rendezvous transponder and a "docking" grapppling fixture for use by the RMS. This latter item is included under the beam structure/mechanical cost element.

1116 Experiments/Instrumentation

This element includes the components and equipment on the free-flying platform necessary to conduct the planned structural response experiments and measurements. These items include a sun shade, accelerometers, temperature sensors, reflectors, laser reflectors, laser beacon and detector array, vibrators, and Orbiter-to-beam telemetry transceiver and battery pack. Certain other proposed experiments are assumed to be GFE and not included in the current estimate, however, a cost element (WBS 1140) is provided but not estimated at this time because of lack of definition.

1120 Airborne Support Equipment (Flight 1)

This cost element includes the beam builder and the assembly jig, the necessary controls and displays (located in the aft flight deck), the software required by the beam builder and assembly jig, and all other flight support equipment (FSE) or interface hardware necessary to interface with the Orbiter or other STS systems.

1121 Beam Builder

This cost element includes the basic structure of the beam builder, all mechanical and mechanism hardware, process controls, sensors and instrumentation, wiring (cables and harnesses), and the system control computer. It includes the basic structure, the cap forming machine subsystem, the coolant subsystems, the cross-member subsystem, the diagonal cord application subsystem, the beam welding subsystem, the beam support subsystem, the beam cutoff subsystem, and the beam support subsystem.

1122 Assembly Jig

This cost element includes the basic structure of the assembly jig, all mechanical and mechanism hardware, all machine and process controls, sensors and instrumentation, all wiring (cables and harness), and the system control computer. It includes the basic structure, the beam builder positioning subsystem, flight support subsystem, longitudinal beam handling subsystem, the cross-beam handling subsystem, the platform assembly subsystem, and the EVA support subsystem.

Equipment associated with experiments and performance test instrumentation (WBS 1124) are excluded from this cost element.

1123 Controls and Displays

The SCAFE will use Orbiter baseline aft flight deck control and display equipment, including the CRT and keyboard at the MSS and RMS, and TV controls and displays at the OOS. In addition, redundant SCAFE control panels (2), redundant SCAFE positioning panels (2), and 2 additional SCAFE TV (CRT) displays will be required.

1124 Software

Software is required for (1) the beam builder, (2) the assembly jig, and (3) SCAFE/Orbiter interface. The POCC software required during the mission operations phase is included in WBS 1740. Software for the beam builder and assembly jig is estimated at 4000 instruction words each. A preliminary estimate for the Orbiter interface is approximately 10,000 words. Total flight software is, therefore, estimated at 18,000 words.

1125 Flight Support Equipment/Interface Hardware

The Flight Support Equipment (FSE) and Interface Hardware (IFHW) cost element includes all equipment items necessary for interface between the SCAFE experiment itself and the Orbiter payload bay, aft flight deck, and all associated systems. The principal interface hardware identified at this time is the experiment support cradle and deployment mechanism. It is assumed that any other interface hardware requirements will be satisfied by the basic design and only a minimum of additional interface equipment will be required.

STS/Orbiter FSE such as EVA aids, MMU, etc., are excluded from this element and included in WBS 2000.

1126 Experiments/Instrumentation

This cost element includes the components and equipment on the beam builder and assembly jig necessary to conduct the planned structural response experiments and measurements. These equipment items include a fixed black and white TV camera with a zoom lens and a spotlight illumination source. A small development allowance is included but the principal experiment design and development cost is carried in WBS 1116.

1130 Flight 2 Hardware

All hardware, labor, and services required for Flight 2, a revisit to the free-flying platform, is excluded from the current estimate.

1140 GFE Experiments/Equipment

Several GFE experiments and supporting hardware are being considered for inclusion in the free-flying platform for Flight 1. They include a geodynamics experiment, an atmosphere composition source, and an active attitude control system. Costs for these items are excluded from the current estimate because

of lack of definition.

1200 System Engineering and Integration

This cost element includes all labor, hardware, and services necessary for system engineering and integration (SE&I) during the development phase of the program.

The system engineering and integration (SE&I) activities include the overall integration activities during the SCAFE development phase, the integration into the STS system (analytical integration), and product assurance functions.

1210 System Engineering

This element includes all system level engineering and integration to ensure that all subsystems and all other aspects of the total experiment are compatible and properly integrated. This activity includes ensuring compatibility of the experiment equipment itself, sometimes termed "Level V" integration. Any required sustaining engineering activities required during the production phase are assumed to be satisfied by system engineering activities during the concurrent development phase.

1220 System Integration/Analytical Integration

This element is defined as those tasks necessary to ensure the compatibility of the SCAFE with all components of the STS system and other external systems the experiment must interact with. It includes such activities as mission planning analysis, flight operations analysis, ground operations analysis, Orbiter/payload integration analysis, and experiment requirements analysis.

1230 Product Assurance

This cost element includes the functions of quality assurance, reliability, safety, and parts-material-processes (PMP) control.

1300 System Test

This cost element includes all labor, test articles and other hardware, and services necessary to accomplish the all-up system level testing activities. The category excludes lower level subsystem and component development testing included under the individual hardware development elements.

The program development phase includes two complete test articles, a prototype breadboard engineering test prototype and a flight configuration qualification test article. The preparation for and conduct of the various system level development and qualification tests are included under system test operations, test support, and test software. Test article refurbishment is provided for updating the configuration of the qualification article to a flight backup unit.

Also included is acceptance test of the production flight unit as a production (unit) cost.

1310 Engineering Test Prototype

This complete test article is a prototype breadboard using prototype subsystems and components which will be functionally accurate but will not be flight rated. This test article will be used for all early development testing and feasibility demonstration of the basic function and processes of the SCAFE.

1320 Qualification/Test Article

This complete test article will be made up of flight qualified subsystems and components and will be used to accomplish the system level flight qualification testing. A portion of this testing will be conducted in the thermal vacuum chamber at JSC (Space Environment Simulation Chamber A).

1330 System Test Operations

This element includes system level test activities associated with both the engineering test prototype beam builder/assembly jig as well as the qualification flight article during the development phase. Individual component or subsystem testing is excluded and included under the nonrecurring cost elements for the beam builder (WBS1121) and assembly jig (WBS 1122). This element also includes the costs of the test operations associated with thermal vacuum testing of the qualification article in the JSC environmental simulation chamber. For the purposes of this estimate, user charges for use of the JSC facility are excluded and TBD.

A minimum allowance is also made for engineering analysis support during the three month period following platform fabrication and Orbiter return when the platform is free flying and is being monitored.

This element includes preparation of test planning and procedures, test preparation, the test operations themselves, and test analysis, evaluation, and documentation.

1340 Test Software

In addition to the beam builder and assembly jig process control software, an allowance estimate of 500 words of ground test software is made for interface functions, etc., during development system level tests, thermal vacuum tests, etc.

1350 Test Article Refurbishment

This element includes all of the maintenance and refurbishment necessary to convert the qualification article, after all system testing is completed, to flight article configuration for use as a flight backup payload. It includes all maintenance, configuration conversions or update, parts replacement and repair, calibration, test and checkout, etc.

1360 Test Support

The test support category includes all tasks and hardware necessary for the direct support of the system level test operations. It includes such items as design, fabrication, and installation of instrumentation, special test fixtures, instrument calibration, and all other supporting equipment and services not accounted for in other cost elements.

1370 Acceptance Test

This cost element includes the activities for the test and checkout of the flight article necessary to satisfy NASA acceptance procedures. This item is included as a production phase cost.

1400 Ground Support Equipment (GSE)

This cost element includes all hardware, labor, and services required to define, design, develop, test, and fabricate new or modified ground support equipment for the SCAFE program. This element includes deliverable GSE for support of the flight experiment through its lifetime. It includes all necessary unique handling, shipping, and transportation equipment, servicing equipment (fluids, batteries, pneumatic, etc.), checkout and maintenance equipment, and other auxiliary equipment items such as auxiliary power, ground heat exchanger. POCC (mission control) equipment is excluded.

It is assumed that a minimum of GSE will be required principally handling and transportation (dollies and shipping containers, etc.) equipment and a beam-builder and assembly jig checkout set. The SCAFE control microprocessors programming will also include built-in test capability, thus minimizing the external checkout GSE requirements. It is assumed that electronics checkout equipment (for CDHS and transponder system) and servicing and auxiliary equipment noted above will be available. Standard test equipment is also excluded.

1500 Support Operations

This cost element includes all labor, material, and services necessary for support operations activities. Support operations are defined to include transportation, logistics support, spares, storage, training, and all other peripheral activities. The transportation of the SCAFE payload between Convair and JSC and KSC was not analyzed in detail; however, for purposes of the study, a dedicated CSA aircraft was assumed both for: (1) the qualification article (San Diego to JSC, and return), and (2) the flight article (San Diego to JSC to KSC and return to JSC).

Minimum spare and repair parts are assumed. Components will be repaired and, during launch preparation, parts will be available from the backup unit.

1600 Ground Operations

This cost element includes all material, labor, and services necessary for the preflight ground operations phase of the program. It includes the equivalent of Level IV integration at JSC, off-line preparation, Orbiter installation, launch, and postmission operations at KSC.

1610 "Level IV" Integration

These activities will be accomplished at JSC with the primary flight article and include the flight article test and functional checkout, EVA/IVA operations verification, simulation and training integration of GFE experiments, and the potential functional operation of the flight article in the thermal-vacuum chamber (Space Environment Simulation Chamber A).

1620 Off-Line Preparation

These activities, equivalent to Level III/II integration, will be accomplished at KSC preparing the flight unit for Orbiter installation, primarily by KSC personnel. Costs are estimated only for SCAFE-related personnel who provide monitoring and standby support to KSC personnel.

Functions to be accomplished include payload receiving and inspection, installation in Cargo Integration and Test Equipment (CITE) simulator and simulated Aft Flight Deck (AFD), a complete interface verification and compatibility check, an Orbiter mission sequence test, and removal from CITE.

1630 Orbiter Installation/Launch

These activities, equivalent to Level I integration, are accomplished at KSC primarily by KSC personnel. Costs are only estimated for SCAFE payload personnel providing monitoring and standby support for KSC crews. The functions include moving the payload to the OPF, installing it in the Orbiter payload bay and aft flight deck, connecting and verifying the interfaces, the Orbiter integrated test, Shuttle buildup and move to launch pad, and the count-down and launch.

1640 Post-mission Operations

These activities will be accomplished at KSC and involve payload safing upon Orbiter landing, removal of the SCAFE payload from the Orbiter bay and aft flight deck at the OPF, moving of the payload to the O&C building for post-mission processing including equipment disassembly, storage, or shipping, as appropriate. Only SCAFE support personnel are included in the estimate.

1650 Maintenance and Refurbishment

This element includes all post-flight SCAFE payload maintenance and refurbishment undertaken prior to storage or reflight. The location of this activity depends on payload disposition. For purposes of the current cost estimate, maintenance and refurbishment are excluded.

1700 Mission Operations

This cost element includes all labor and services required for mission control, data handling/processing, and mission operations support. The identification and definition of any unique POCC hardware (consoles, etc.) is TBD and not included in the current estimate. POCC user charges are excluded from this element and are included in WBS 2000.

1710 Mission Control

The SCAFE orbital flight is designed for full autonomous on-board control. The POCC will only provide monitoring and quick-look data functions and standby fault diagnosis assist. The POCC operation includes a six-week preparation period (POCC reconfiguration, preparation, integration, test, crew familiarization, and training), a one-week flight support (launch and orbital operations), a one-week retrieval, disassembly, and clean up, and a three-month free-flyer data acquisition monitoring activity prior to revisit (Flight 2).

1720 Data Handling/Processing

This cost element covers data reduction and tape or hard copy data preparation as well as data handling processing associated with POCC quick-look data activities.

1730 POCC Software

In addition to available standard POCC and data processing software routines, it is estimated that an additional 2000 words of payload unique software will be required for data display, data formatting, etc.

1740 Mission Operations Support

This item covers all backup and support personnel necessary to support WBS cost elements 1710, 1720, and 1730.

1800 Facilities

This cost element includes all facilities or related services during development, test, or manufacturing, integration at JSC, integration at KSC, or mission support (POCC).

1810 Development, Test, and Manufacturing Facilities

It is currently estimated there are no new capital facilities required for the development, test, or manufacturing of the SCAFE. It is anticipated that thermal vacuum tests will be conducted in the JSC Space Environment Simulation Chamber A. (User charges for this facility are not included in the current estimate.) Other associated costs are included under System Test cost element 1300.

Other development or operations training facilities are also assumed available such as a simulator for development or training with the RMS, simulator for flight operations docking, and buoyant tank facility or other EVA training simulators.

1820 Integration Facilities (JSC)

None.

1830 Integration/Position Processing Facilities (KSC)

None.

1840 Mission Support Facilities (POCC)

None.

1900 Program Management/Administration

This cost element includes all labor, services, and materials necessary for program management/administration for all three phases of the program. It includes program administration, subcontract management, program planning and control, configuration management, data management and documentation, and other services necessary for the overall conduct of the program.

2000 Shuttle Transportation User Charges

This cost element includes all user charges associated with the STS for preparation, launch, on-orbit activities, and return to earth. It includes the basic transportation charge, plus all additional charges for optional supporting services, such as energy kits, EVA, second RMS, MMU, etc., and any user charges related to the POCC operations. It is assumed that the basic shuttle user charge includes all Shuttle-related activities such as on-line payload installation (OPF), MDC activities, flight crew costs, and other common ground operations/mission operations and activities.

3000 Tracking and Data Acquisition

This cost element includes all necessary related user charges associated with the NASA tracking and data acquisition facilities and services, including TDRSS, STDN, NASCOM, etc., not included in the basic STS user charge, both during the Shuttle on-orbit phase as well as the SCAFE platform free-flying phase.

5.3.3 SCAFE PROGRAM COST ESTIMATE

5.3.3.1 Total Program Cost. The preliminary cost estimate for the SCAFE is summarized below in Table 5-9 and detailed in Table 5-10. Costs are presented for the nonrecurring (development), the recurring production (flight hardware), and recurring operations phases of the program. The estimate includes all payload incurred costs through the first launch (1982) of the fabrication experiment, including three months of experiment orbital monitoring and data acquisition. The second flight

and GFE experiments are excluded. The costs are estimated in current constant FY 1977 dollars and prime contractor fee is not included.

It is assumed that three complete units are produced, an engineering test prototype, a qualification unit refurbishable to a backup flight unit, and a primary flight unit. Cost for refurbishing the qualification unit as a flight backup is included, but the refurbishment of the flight unit upon its return from the first flight is not. All flight platform avionics, electrical power, and their associated GSE were assumed essentially off-the-shelf and little or no component development was necessary.

Table 5-9. SCAFE program cost summary.

<u>Cost Element</u>	<u>Cost by Program Phase (1977 M\$)</u>		
	<u>Nonrecurring (Development)</u>	<u>Recurring- Production</u>	<u>Recurring- Operations</u>
Flight Hardware			
Platform Spacecraft	2.27	.92	-
Airborne Support Equipment	16.35	3.36	-
Flight #2	-	-	-
GFE Experiments	-	-	-
System Engineering & Integration	3.72	-	-
System Test	8.38	.21	.03
GSE (Peculiar)	.93	-	-
Support Operations	.10	-	.84
Ground Operations	-	-	.38
Mission Operations	.05	-	.18
Facilities	0	0	0
Program Mgmt/Admin	<u>1.59</u>	<u>.22</u>	<u>.07</u>
	<u>33.39</u>	<u>4.71</u>	<u>1.50</u>
Phase C/D Total		39.60	
Shuttle User Charge		21.42	
Prephase C/D		<u>2.30</u>	
Program Total		<u>63.32</u>	

ORIGINAL PAGE IS
OF POOR QUALITY

Table 5-10. Total SCAFE program cost estimate.

WBS	COST ELEMENT	COST - 1977 M \$		
		Nonrecurring (Development)	Recurring Production (Manufacturing)	Recurring Operations
PRE PHASE C/D				
	Phase B Definition Study	.30	-	-
	Selected Long Lead Technology	2.00	-	-
	Beam Builder	(1.50)	-	-
	Assembly Jig	(.50)	-	-
PHASE C/D				
1100	SCAFE Flight Hardware			
1110	Platform Spacecraft (Flight 1)	2.27	.92	
1111	Structure/Mechanical	(.49)	(.17)	-
1112	Communication/Data Mgmt	(.18)	(.19)	-
1113	Electrical Power	(.73)	(.35)	-
1114	Attitude Control & Stabilization	(.16)	(.02)	-
1115	Rendezvous and Docking	(.05)	(0)	-
1116	Experiments/Instrumentation	(.66)	(.19)	-
1120	Airborne Support Equipment (Flight 1)	16.35	3.36	
1121	Beam Builder	(7.78)	(1.86)	-
1122	Assembly Jig	(5.62)	(1.20)	-
1123	Controls and Displays	(.06)	(.03)	-
1124	Software	(1.35)	-	-
1125	FSE/IFHW	(1.53)	(.24)	-
1126	Experiments/Instrumentation	(.01)	(.03)	-
1130	Flight 2 Hardware	-	-	-
1140	GFE Experiments/Equipment	-	-	-
1200	System Engineering & Integration	3.72	-	-
1210	System Eng/Sustain Engineering	(2.02)	-	-
1220	System Integ/Analytical Integ	(.96)	-	-
1230	Product Assurance	(.74)	-	-
1300	System Test	8.38	.21	.03
1310	Engineering Test Prototype	(1.68)	-	-
1320	Qualification Test Article	(4.28)	-	-
1330	System Test Ops	(1.02)	-	(.03)
1340	Test Software	(.01)	-	-
1350	Test Article Refurb	(.88)	-	-
1360	Test Support	(.51)	-	-
1370	Acceptance Test	-	(.21)	-
1400	GSE (Peculiar)	.93	-	-
1500	Support Ops	.10	-	.84
1600	Ground Ops	-	-	.38
1610	"Level IV" Integration (JSC)	-	-	(.288)
1620	Off Line Preparation (KSC)	-	-	(.067)
1630	Orbiter Installation/Launch (KSC)	-	-	(.010)
1640	Post Msn Ops	-	-	(.019)
1650	Maintenance/Refurb (Post Flt)	-	-	(TBD)
1700	Mission Operations	.05	-	.18
1710	Mission Control	-	-	(.060)
1720	Data Handling/Processor	-	-	(.055)
1730	POCC Software	(.05)	-	-
1740	Support	-	-	(.060)
1800	Facilities	0	-	-
1810	Dev/Test/Mfg	0	-	-
1820	Integration (JSC)	0	-	-
1830	Integration/Post Msn Ops	0	-	-
1840	Mission Support	0	-	-
1900	Program Management/Admin	1.59	.23	.07
	Subtotal	33.39	4.71	1.50
	Phase C/D Project Total		39.60	
2000	Shuttle Transportation		21.42	
3000	Tracking & Data Acquisition		TBD	
	Pre-Phase C/D Total		2.30	
	Grand Total		63.32	

C-5

5.3.3.2 Annual Funding Requirements. The annual funding requirements for the SCAFE program are shown in Table 5-11. This funding distribution was established by spreading individual cost elements in accordance with the program schedule shown in Figure 5-2. Shuttle funding was spread in accordance with the Space Transportation System User Handbook, dated June 1977.

Table 5-11. Annual funding requirements.

	FY79	FY80	FY81	FY82	Total
Development					(35.7)
Phase B	0.3	-	-	-	0.3
Selected Long Lead					
Technology Development	1.0	1.0	-	-	2.0
Phase C/D	-	7.7	22.4	3.3	33.4
Production	-	-	3.9	0.8	(4.7)
Operations					(22.9)
Experiment Ops	-	-	0.5	1.0	1.5
Shuttle User Charge	-	4.3	7.4	9.7	21.4
Total	1.3	13.0	34.2	14.8	(63.3)

6

MANUFACTURING

One fabrication task was included in the SCAFED study. A high-fidelity prototype beam segment, representing the selected beam configuration (Section 2.1), was designed and manufactured for demonstration purposes and as a possible future test specimen.

6.1 DESIGN

The prototype beam segment design is shown in Figure 6-1. In both the Convair proposal and the Part II Study Plan, a two-bay beam specimen was identified. However, the possibility of future structural testing of the beam segment suggested at least three-bays to provide an interior bay, free of end effects. Accordingly the three-bay design of Figure 6-1 was prepared.

Beam cross section geometry, bay spacing, and end cutoff provisions are identical to the SCAFEDS baseline. Similarly the geometry and laminate materials in both the caps and cross-members are identical to the baseline. The diagonal cord also is of the correct fiber (20-end S-glass roving) and resin (P-1700 polysulfone). However, the current cord product is available only in flat (ribbon) form, rather than the preferred circular cross section, and falls somewhat short of the desired resin content (18-20% average vs 26%). Further cord development is, therefore, indicated, but strength, creep, and joining tests on the current product are encouraging and vendor costs to provide circular material with sufficient resin are estimated at less than \$5K.

The spotweld pattern is similar in arrangement and spacing to the baseline but employs weld sizes for which tips already exist and both machine schedules and strength data are available. The circular cord-capture spot provides less cord bond length than the special rounded triangular spot in the baseline design. Consequently cord tear-out strength may be limited and planning of future tests should acknowledge any such limitation. Cord joint strength well in excess of the baseline preload values is expected, however, and consequently the diagonals are installed with preload per the baseline.

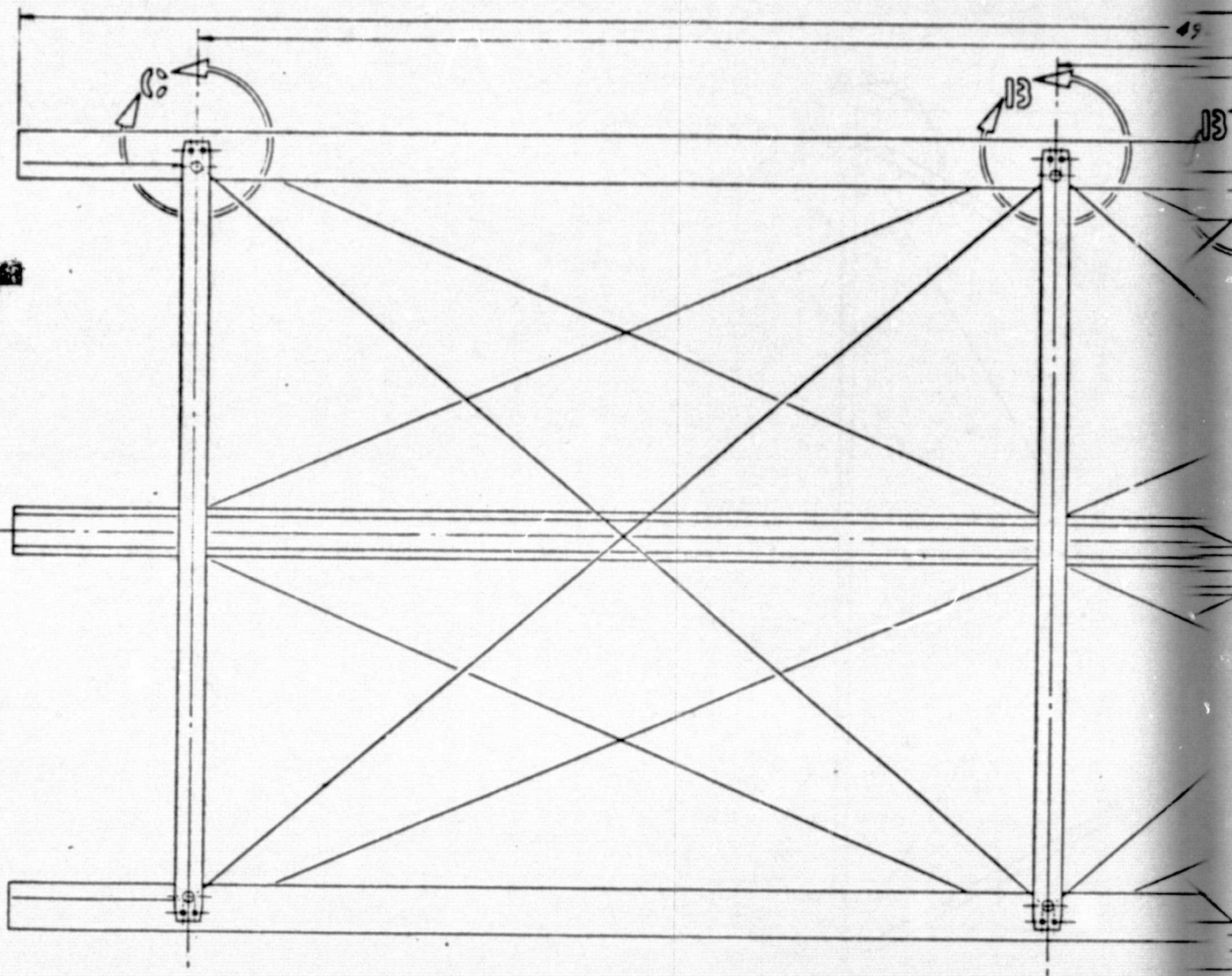
6.2 FABRICATION

Beam fabrication was governed by a manufacturing plan which defined material preparation and tooling requirements and provided detailed sequences of operations for both detail parts fabrication and beam assembly. Caps and cross-members were laid up in individual plies over full-length aluminum male tools and formed/consolidated under vacuum at 589°K (600°F). A residual pressure of .68-1.01 N/cm² was retained during cooldown to prevent springback. Detail part cross-section geometry and free-edge straightness conformed well to drawing requirements although some

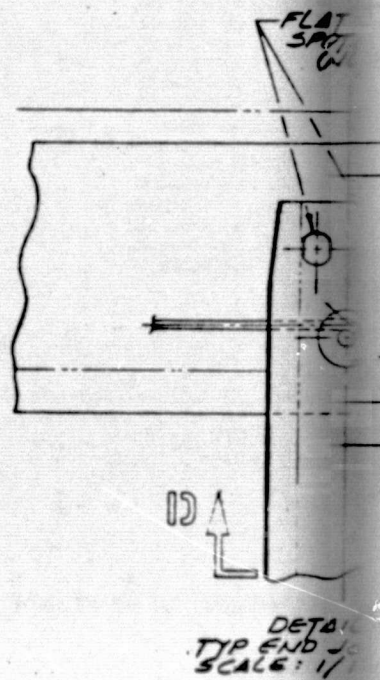
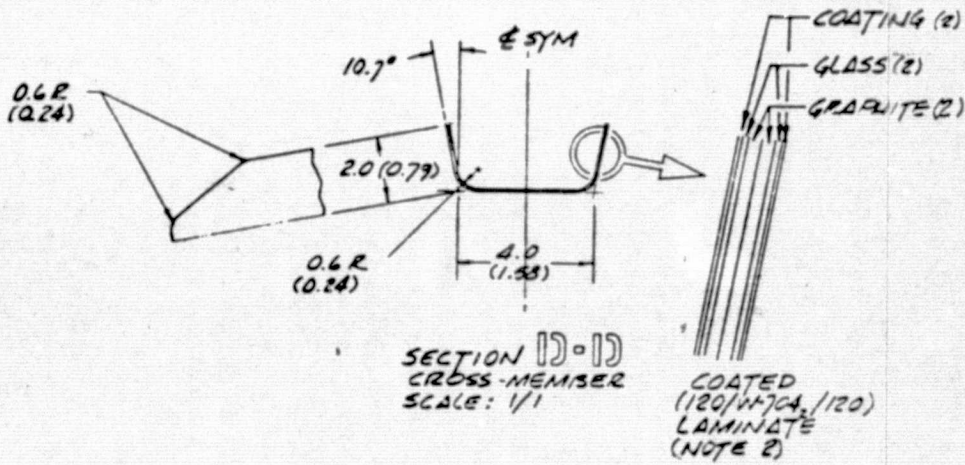
transverse wrinkling occurred during cooldown. This resulted from the interplay between shrinkage of the aluminum tool and friction at the part surface due to residual vacuum. Two of the three caps were noticeably wrinkled but were readily smoothed by a local "ironing-out" process using a flat ultrasonic tip in conjunction with an internal mandrel. The baseline titanium dioxide/resin coating was simulated by conventional white paint since thin, pigmented resin film, suitable for the individual ply layup approach, was unavailable. Parts were coated at the detail level and touched up after beam assembly.

To facilitate assembly operations sequencing, parts and cap/cross-member joints were numbered, as illustrated in Figure 6-2. Prior to permanent joining, caps and cross-members were accurately positioned, using temporary tooling, and pilot drilled at the pierce-weld hole for later use of an alignment pin and CLECO assembly clamps. All pairs of small spotwelds (Figure 6-1) were made prior to cord installation, in order to provide rigidity for handling and cord tensioning. Figures 6-3 and 6-4 illustrate the arrangement of beam elements, tooling, and welder in the first cap and cross-section closeout weld positions. Welds were made using a commercial, bench-supported Branson ultrasonic welder. Specific weld parameters (pressure, weld time, and hold time) were developed in a concurrent Convair-funded technology program. Figure 6-5 shows typical weld preparation at the stage of assembly shown schematically in Figure 6-3.

To maximize cord bond length within the pierced spot (to ensure preload retention) cords were installed individually in each bay rather than in the baseline continuous "zig-zag" manner. Figure 6-6 illustrates the typical setup for cord installation and subsequent pierce-weld accomplishment. The baseline 44.5 ± 8.9 N tension was maintained in each cord as it was welded in place, and preload retention to date is excellent. The completed beam segment is shown in Figure 6-7. Following customer acceptance, it will be shipped to NASA/JSC for display and structural testing.



ORIGINAL PAGE IS
OF POOR QUALITY



49
490.2 (192.99)

440.2 (181.18)

316.8 (124.72)

173.4 (68.27)

~~REINFORCING FRAME~~

2

FLAT ULTRASONIC
SPOTWELD (2)
(NOTE 4)

④
PIERCED/FLAT
ULTRASONIC SPOTWELD
(NOTE 4)

CAP REF

6.5MM

1.9
(0.75)

1.4
(0.55)

4.0 (1.57)

CORD REF

13

DETAIL ①
TYP END JOINT
SCALE: 1/1

13

DETAIL ②
TYP INTERIOR JOINT
SCALE: 1/1

COAT
(120/W-7)
LAMIN
(NOTE

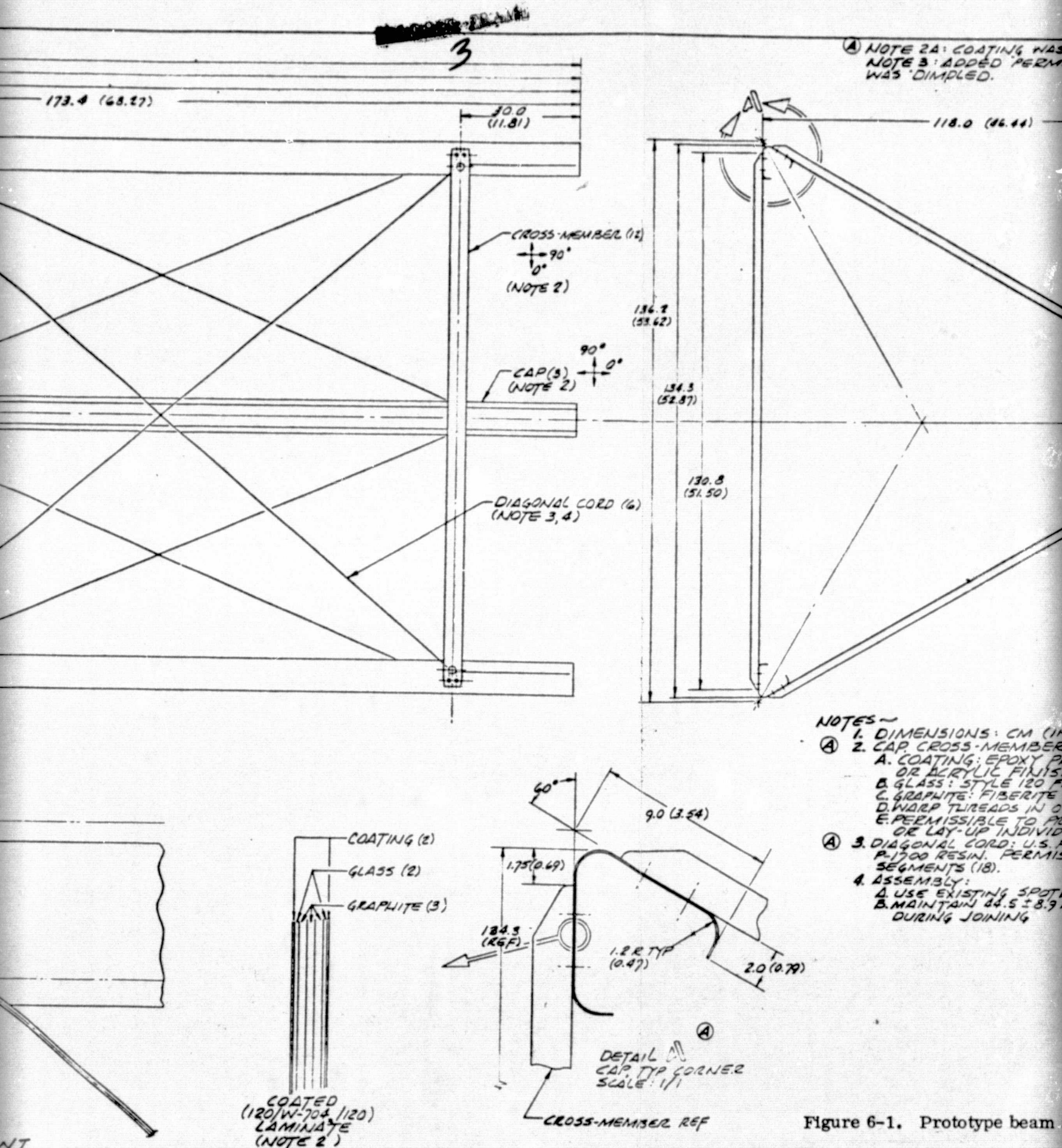
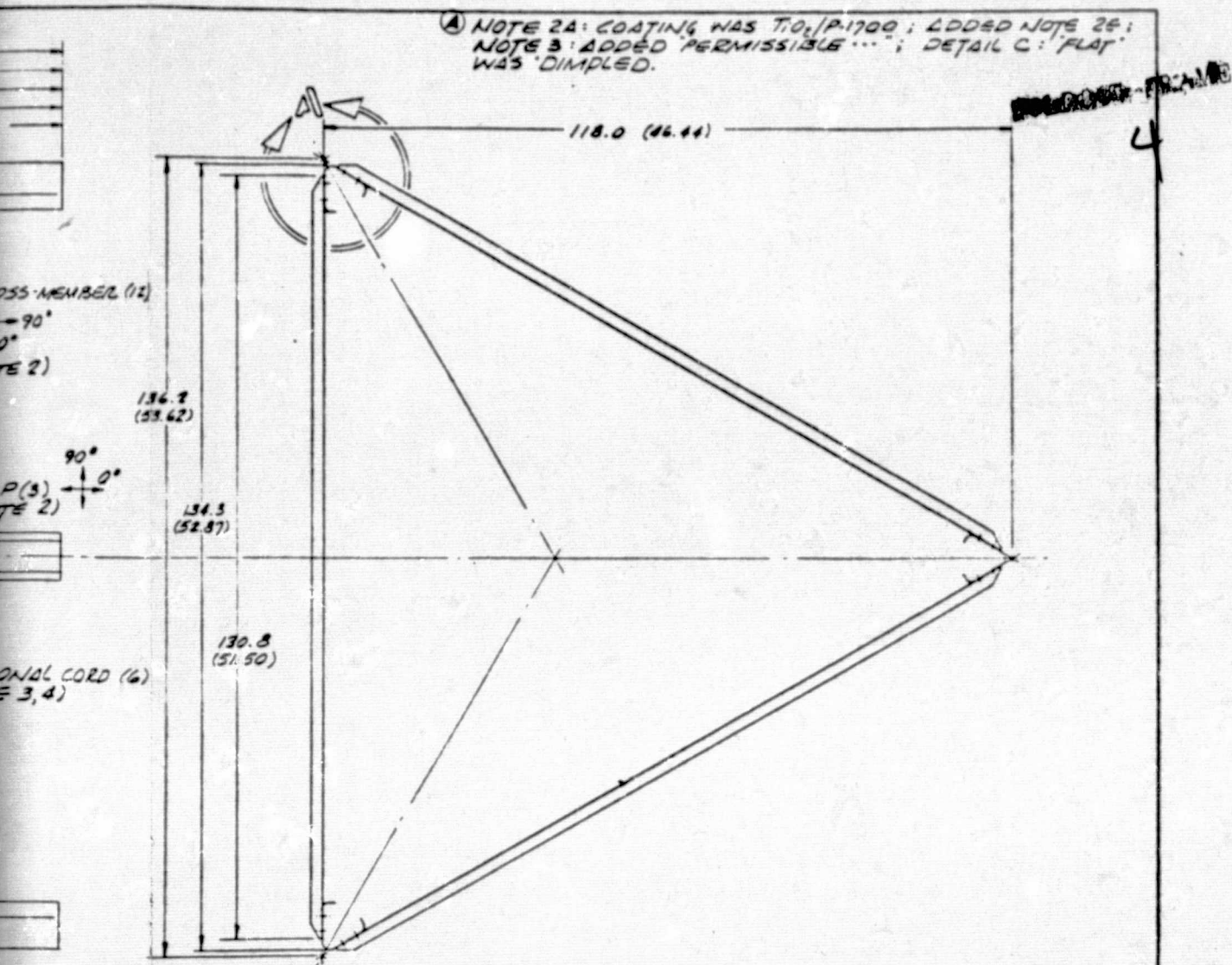


Figure 6-1. Prototype beam



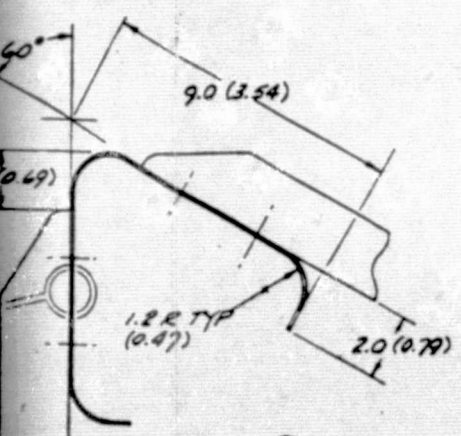
NOTE 2A: COATING WAS TIO₂/P-1700; ADDED NOTE 2E: NOTE 3: ADDED 'PERMISSIBLE...'; DETAIL C: 'FLAT' WAS 'DIMPLED'.

CROSS-MEMBER (12)
-90°
0°
TE 2)

90°
0°
P(3)
TE 2)

DIAGONAL CORD (6)
F 3, 4)

- NOTES~
1. DIMENSIONS: CM (IN)
 2. CAP CROSS-MEMBER MAT'L'S & MFG:
 - A. COATING: EPOXY PRIME; WHITE POLYURETHANE OR ACRYLIC FINISH COAT
 - B. GLASS: STYLE 120 FABRIC / P-1700 RESIN
 - C. GRAPHITE: FIBERITE STYLE W-702 FABRIC / P-1700 RESIN
 - D. WARP TILERS IN 0° DIRECTION (TYP BOTH FABRICS)
 - E. PERMISSIBLE TO PRE-CONSOLIDATE FLAT LAMINATE OR LAY-UP INDIVIDUAL PLYS & POST-CURE
 3. DIAGONAL CORD: U.S. POLYMERIC 20E 5-Glass ROVING / P-1700 RESIN. PERMISSIBLE TO INSTALL IN ONE-BAY SEGMENTS (18).
 4. ASSEMBLY:
 - A. USE EXISTING SPOTWELD TIPS
 - B. MAINTAIN 84.5 ± 8.9 N (19 ± 2 LB_f) CORD TENSION DURING JOINING



DETAIL A
CAP TYP CORNER
SCALE: 1/1

CROSS-MEMBER REF

Figure 6-1. Prototype beam segment.

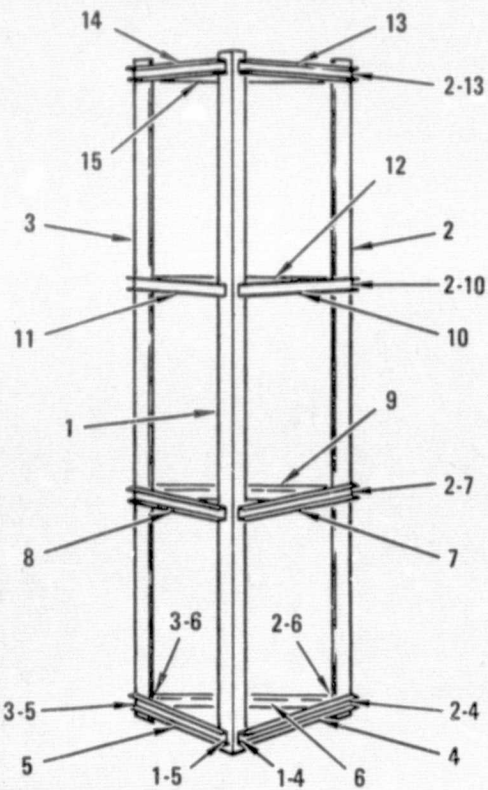


Figure 6-2. Part and joint numbers.



Figure 6-5. Typical flat-weld preparation.

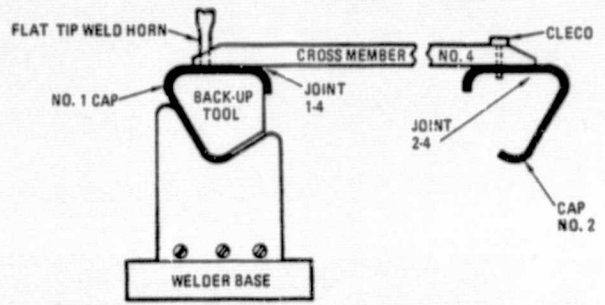


Figure 6-3. Flat-weld setup: first cap.

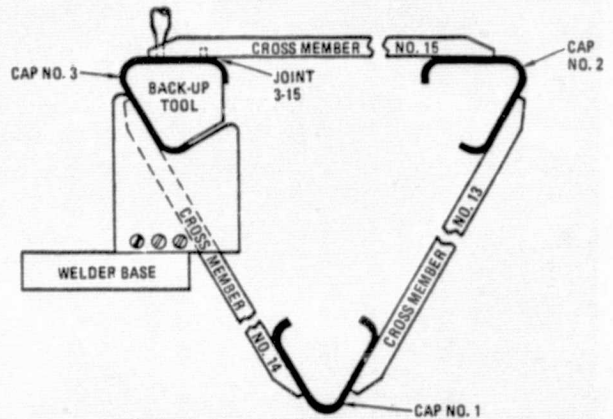


Figure 6-4. Flat-weld setup: cross-section completion.

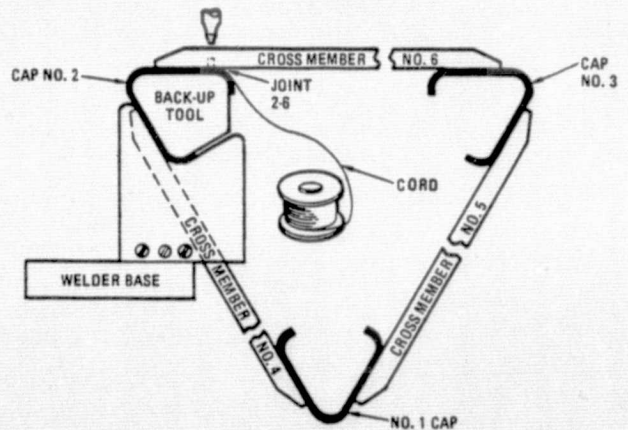


Figure 6-6. Cord installation/pierce-weld setup.

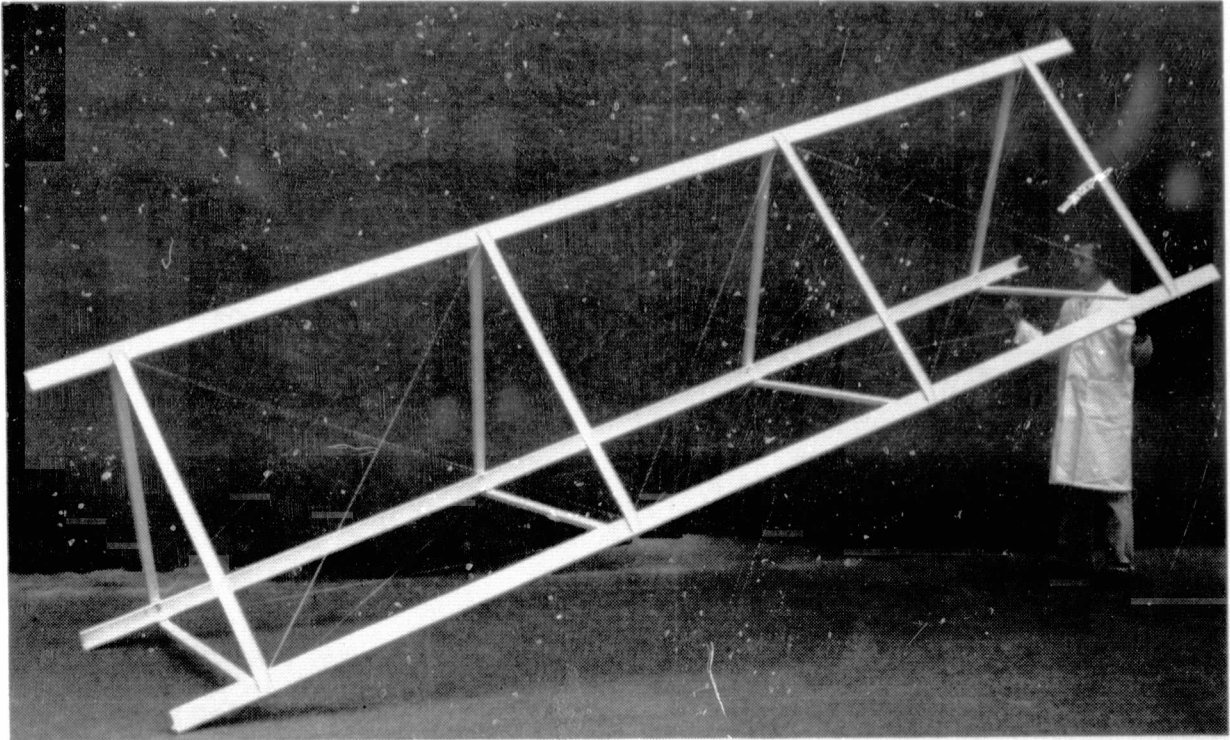


Figure 6-7. Completed beam segment.



CONCLUSIONS AND RECOMMENTATIONS

This section summarizes the noteworthy conclusions drawn from the SCAFE study effort and provides recommendations for subsequent program effort to implement the development plan.

7.1 CONCLUSIONS

Conclusions are presented in the same groupings/sequence as preceding text.

7.1.1 SYSTEM DESIGN

7.1.1.1 Structure/Materials

- a. The baseline platform is compatible with the storage/fabrication/assembly capabilities of the manufacturing systems. It accommodates the current mission requirements but is not optimized for the purpose. Final configuration/arrangement depend on better definition of the purpose/application of completed platform. In the event a configuration change is required, several alternative platform concepts have been identified which are feasible/compatible with the basic fabrication systems concept.
- b. The baseline equilateral triangular beam accommodates inter-beam joints without special end fittings or auxiliary piece parts.
- c. The open cross section beam cap is easy to form and exhibits a large margin of safety in the SCAFE application.
- d. The rigid post/diagonal cord sidewall concept results in lightest beam and permits preload to ensure constant shear/torsional stiffness. Beam distortion is insensitive to cord preload variation due to tolerance.
- e. The selected ultrasonic weld joints require no loose parts and produce no debris. The two-ply joint has been successfully demonstrated with several tip configurations. Development of the cord capture joint is in progress.
- f. The selected hybrid laminate material results in low energy requirement for forming, has high stiffness, low CTE, and uses low-cost pitch fiber.
- g. The selected resin impregnated S-glass cord requires low preload, which it sustains without creep, permits compact storage, and is compatible with both the joining process and the orbital environment.
- h. The selected TiO_2 thermal control coating maintains peak temperatures well within the maximum structural use temperature of the selected polysulfone resin system. Coating optical property degradation due to radiation exposure is minimal for the SCAFE mission duration.

7.1.1.2 Platform Fabrication System

- a. Automatic fabrication of the baseline platform is feasible using state-of-the-art electromechanical devices and materials technology.
- b. The areas of greatest development required to support the final design of the beam builder and assembly jig include:
 - 1. Full development of the rolltrusion process (currently in progress at Convair).
 - 2. Material heating elements and temperature controls.
 - 3. Differential cap drive control process.
 - 4. Refinement of the proposed ultrasonic welding processes.
 - 5. Platform drive and positioning control process.
- c. Scale-up limitations for the selected beam builder concept cannot be defined without further knowledge of potential applications. Potential scaled-up beam configurations must first be identified and defined in sufficient detail to allow system dynamics to be analyzed for possible growth constraints.
- d. Roll-in-a-can storage of cap material has a potential problem of introducing impulse loads on the beam builder if the material does not unwind uniformly. This may require the addition of a damper arm in the storage canister to absorb the energy of the rapidly unwinding roll. The unwinding characteristics of the material are subject to further studies and materials testing before a conclusion can be reached here.

7.1.1.3 Avionics and Controls

- a. Fabrication process control
 - 1. Control and monitor operations and concept implementation have been performed for the automated processes associated with both beam builder and assembly jig operation.
 - 2. Analyses performed during the study indicate all functions are within the current state-of-the-art with development required in several areas. Specifically, control functions (ACU and BCU) required are well within the memory and speed capability of current microcomputer-based systems.
 - 3. Beam builder and assembly power requirement have been defined and are well within Orbiter capabilities.
- b. Orbiter interfaces
 - 1. Control and monitor concepts are compatible with Orbiter crew and equipment utilization capability. Orbiter/crew only provide executive control over platform assembly functions (leaving detailed/real-time operations to beam builder and assembly jig automated operations).
 - 2. Few SCAPE-peculiar panels are required and can be accommodated with payload-dedicated space at the MMS and OOS.
 - 3. Orbiter software support functions were evaluated and found generally acceptable, although all needed functions are not currently available.
- c. Platform-attached systems
 - 1. Preliminary work in this area defined instrumentation required for SCAPE platform test purposes, and identified avionics to support this function.

7.1.1.4 Alternate Beam Concept. As a consequence of the post-ATP addition of this task, permissible emphasis was limited by compensating reductions in other task areas. However, preliminary exploratory effort indicated the following:

- a. The baseline geodetic beam is heavier than a corresponding triangular beam regardless of fiber material. Element size precludes the use of high modulus material due to storage diameter constraint.
- b. Automated fabrication of the baseline geodetic beam is feasible with a shuttle-compatible fabricator.
- c. Increased geodetic beam node count would alleviate weight and material problems at expense of machine complexity.
- d. Inter-beam joints are very complex unless centerline fittings are used. The geodetic concept appears best in single-span axial load applications rather than in multispan bending.

7.1.2 FLIGHT MISSION

- a. The SSAFE system and mission operation can more than adequately meet program objectives.
- b. The platform can be fabricated/assembled, test instrumentation installed and checked out, and all tests performed on one 7-day orbiter flight.
- c. To take advantage of the shuttle weight and volume capability, additional applications experiments can be carried into orbit and set up on the same shuttle flight. It is most cost-effective to carry equipment up to the capability of the shuttle on the mission. If all such equipment cannot be set up in a nominal 7-day mission, a short extension is more cost-effective than a revisit mission.
- d. Construction of the beams/platform can be fully automated, leaving the EVA capability of the astronauts for attachment and checkout of supporting subsystems and additional applications experiments.
- e. The free platform can be stabilized adequately for a revisit mission occurring with a nominal 2-month time period.
- f. No constraints, outside of nominal shuttle altitude capability, were found to restrict the SSAFE orbit. The selected fabrication orientation: eliminates need for attitude control maneuvers during fab/test; reduces loads and RCS propellant consumption by using rate mode duty cycles in two axes with $\pm 10^\circ$ attitude error; avoids viewing into either sun or earth-reflected light; provides communication coverage; and requires no maneuvering for thermal reasons.
- g. The system is Orbiter compatible: weight and c.g. are well within limits; support reactions are low; the software interface is compatible; although experiment mass properties extremes are beyond baseline values used in VRCS sizing, the system is adequate for control. Two MMUs have been baselined for mission, but assembly jig geometry/elevation in the cargo bay may impose special support provisions for one MMU.

7.1.3 ANALYSES

7.1.3.1 Mass Properties. System weight is low but inertias in two axes change significantly during the fab/assembly/equipment installation/test sequence. Consequently, the stable gravity gradient attitude of the total system changes during mission.

7.1.3.2 Stability/Control

- a. A constant, earth-fixed attitude is preferred throughout mission. The orbiter VRCS can operate in rate mode in two axes yet maintain maximum attitude error within $\pm 10^\circ$.
- b. Duty cycles for closed-loop attitude control show very low frequencies.
- c. The free platform can be stabilized for post-separation activities using existing qualified dampers.

7.1.3.3 Structural Dynamics

- a. Natural frequencies of system lower modes are widely separated from even the highest VRCS impulse frequencies.
- b. Resulting displacement/acceleration responses are low and support loads are much lower than preliminary values used for initial structural sizing.

7.1.3.4 Stress

- a. Beam internal loads are very low.
- b. Loads and distortion due to space heating effects are negligible.

7.1.3.5 Thermodynamics

- a. The heating/forming system power requirement is well within shuttle capability.
- b. Active (platen) cooling of the formed cap section is required to achieve temperatures below the structural usage limit within the nominal 40-second pause interval. Platen cooling also provides a final "sizing" of the formed cross section.
- c. Insulating the strip material storage canisters permits higher initial temperature for the forming process, which further reduces energy requirements.
- d. Element maximum temperature extremes are low and variation with orbit time is small due to platform material and coating characteristics.

7.1.4 PROGRAMMATICS

7.1.4.1 Development

- a. SCAFE equipment is state-of-the-art but a nominal development time is needed to make sure the equipment components will operate properly and can be combined into an effective total system.
- b. The mid-June 1982 launch date can be met with a minimum risk development program if: (1) the beam builder and assembly jig subsystems are developed in parallel with Phase B; and (2) the Phase B contractor also performs Phase C/D.

- c. For low-cost and nominal schedule, qualification requirements should be confined to safety and operational requirements only.

7.1.4.2 Cost

- a. For low total cost, existing equipment listed in the NASA Low Cost Program Office CASH catalog, should be used even though some items might provide greater capability than required.
- b. Total program costs, excluding shuttle user charges, are estimated at \$41.9M.
- c. The ability to accomplish all fabrication/assembly/equipment installation/test activities on a single shuttle flight saves \$19.9M in shuttle user charges for the now unneeded revisit mission.

7.1.5 FABRICATION. A high-fidelity beam segment has been built, permitting near-term evaluation and test of the fundamental structural concept.

7.2 RECOMMENDATIONS

Based on the SCAFE program work completed to date, near-term effort is indicated in several categories. Recommended studies of platform applications, definition of a beam builder development article, further definition of SCAFE programmatics/hardware, suggested manufacturing/test activity, and remaining evaluation of the alternative beam concept are summarized in the following subsections.

7.2.1 PLATFORM APPLICATIONS. Develop and define uses or capability of the beam builder and jig fixtures to construct potentially useful structural configurations.

- a. Perform a screening evaluation of potential platform uses or applications to select candidates which best benefit from a single flight of a large structure, either Orbiter-attached or as a free-flying satellite. Specific categories might include:
 - 1. Large structure characterization/test/demonstration (rigidity/shape/flatness; dynamics; gravity/drag/solar pressure interaction; operations; and multiple services)
 - 2. Materials test bed
 - 3. Systems demonstration (solar cell installation/function; SEPS; attitude control; microwave transmission/radiometry/multiple public services; illumination)
 - 4. Direct measurement of orbital environment
- b. Develop configuration/arrangement and mission operations requirements for candidate uses. Evaluate SCAFE platform applicability. Develop alternative structural concepts and configurations such as curved beams, stiffer platforms, gravity gradient balanced options, etc.
- c. Select preferred application concepts including experiment or operational equipment, structure, fabrication and assembly equipment, functional systems operations, and test and evaluation approaches. The requirements and design of the selected equipment, supporting subsystems, and applications experiments should be analyzed as a total system, instead of separately, to be most

cost-effective. Supporting subsystems should be sized, with adequate margin for contingencies, from the total systems approach.

- d. Prepare a detailed concept design of selected application equipment installation. Subsystem equipment should be nominally oversized both to accommodate a variety of candidate application experiments, and to assure low risk cost/schedule development.
- e. Conduct supporting analyses in the areas of flight mechanics, thermal, structural dynamics, stability and control, mass properties.
- f. Evaluate compatibility of selected application approach with the Orbiter.
- g. Evaluate and define the impact of any potential flight constraints in the areas of attitude control, vehicle orientation, and lighting requirements during Orbiter-attached and free-flight mission phases.
- h. Define the mission operations required to integrate the selected application approach and accomplish the flight experiment. Also consider:
 1. Development of additional applications experiments to go aboard the first SCAPE flight so that an alternate would be ready if a selected experiment's development fell behind schedule.
 2. Investigation of one or more revisit missions (including the capability to raise the platform orbit for longer life) carrying additional applications experiments to fully realize the effectiveness of the space-constructed platform.
 3. Investigate additional dynamic response tests with concentrated masses on the beam to determine if required for future platform applications.

7.2.2 SCAPE DEVELOPMENT. Further define the Part II platform and fabrication equipment concepts and provide the programmatic for a flight program including the selected application.

- a. Perform selected analyses and design trades on the Part II beam, beam builder, assembly jigs/fixtures, and Orbiter interfaces. Analytical effort should specifically include:
 1. Evaluation of beam builder and assembly jig temperature variation, and resulting structure distortion, to assess the need for auxiliary shielding or low coefficient of thermal expansion structure.
 2. More detailed characterization of material heating/forming/cooling and heating system operation.
 3. Dynamic modes/responses update to account for the effects of: operational forcing functions (beam builder cycles and assembly jig step-through); beam length variations during fabrication; mid-bay beam support on the assembly jig; and subsystems/equipment installation on the platform. Where possible, incorporate revised element stiffnesses and test data for damping and material properties.
 4. Additional system stability evaluation (and corresponding RCS duty cycles/propellant consumption) for all steps in the flight mission sequence.

- b. Design trade activity should include:
 1. Beam builder process/technique options from the NASA/MSFC LSSFE Program (NAS8-32471) vs. corresponding SCAFEDS options.
 2. Beam cross-member section options to improve differential drive capability and possibly improve clip feed system.
 3. Clip feed system concepts for alternate cross-member section option(s) vs. SCAFEDS baseline.
 4. Beam cap thickness reduction.
 5. Alternate strip material forms: woven single ply vs. laminated
 6. Beam builder and assembly jig shielding and/or low CTE (i.e., composite) structure vs. current metallic concepts, if indicated by thermal/distortion analyses.
 7. EVA bridge mechanism/control concepts.
 8. Beam builder/assembly jig latch concepts for: boost stowage; cross-beam fabrication.
 9. Additional techniques/sensors for beam & platform excitation and deflection measurement.
 10. Cross-beam welder concepts.
- c. Orbiter interface efforts should include:
 1. Definition of caution, warning, safety interfaces.
 2. Additional emphasis on software function requirements to guide definition of Orbiter payload support capability.
 3. Definition of the cradle structure and associated mechanisms (pivot, deployment/latching, emergency jettison).
 4. Mission-peculiar supports for one MMU, if required, due to assembly jig stowage envelope.
 5. Definition of location/configuration of SCAFE umbilical interface.
 6. Definition of the Orbiter-to-ACU/BCU control link.
- d. Prepare detailed concept design changes to the Part II final configuration of the beam builder and assembly jigs and fixtures. Effort should specifically include:
 1. Further quality assurance/reliability studies to: determine the extent of electro/mechanical redundancy required (to minimize the number of motor drives required); assist in defining in-process QA techniques/requirements.
 2. Evaluation of environmental impacts on fabrication system elements: resolve any vacuum operation issues; define insulation/shielding requirements/provisions.
 3. Detail design studies to define/select and establish preliminary specifications for all electro-mechanical drives and associated sensors. Identify special materials, lubrications, and environmental protection techniques applicable to each drive. Refine design concepts to maximize utilization of common elements for best cost-effectiveness.
 4. Define control software and overall intra-machine timing and synchronization, including: detailed machine timeline/diagrams, including in-process QA allowances and identify potential for machine cycle speed-up; process

control parameters and timing for welders; real-time software executive for beam builder and assembly jig controllers.

5. Beam builder update to incorporate latest features of rolltrusion process.
 6. Definition/selection of: data multiplexer elements on beam builder; data bus/command decoder link.
 7. Develop platform data analysis algorithms for deriving platform response characteristics from raw data. (May include identification of special equipment for Orbiter installation.)
 8. Analyze details of power switching/control and arm/safe function definition/implementation.
 9. Determine quantity/locations of TV monitors required in bay and on beam builder or assembly jig, and define individual requirements in terms of viewing angle, distance.
 10. Design illumination system for beam builder and assembly jig. Size and select components and mounting location.
- e. Revise the SSAFE requirements document to reflect changes and additions from the above effort. Organize/issue as system specification for Phase B.
 - f. Prepare changes to the Part II development plan considering the engineering for the selected experiment approach. Specifically identify the need/extent of any required facility modifications to accommodate beam lengths required for thermal vacuum qualification testing.
 - g. Develop a revised program cost estimate.

7.2.3 BEAM BUILDER DEVELOPMENT ARTICLE. Define and develop a ground-based beam builder to demonstrate the capability to automatically fabricate composite structure. Subsequently modify the ground-based beam builder to perform as a test/training simulator if the SSAFE is approved as a flight project.

- a. Prepare a detailed concept design of the ground test beam builder.
- b. Define a development test plan for utilization of the ground test beam builder.

7.2.4 MANUFACTURE AND TEST

- a. Conduct tests on the prototype beam segment, fabricated in Part II, to evaluate strength, stiffness, and structural damping.
- b. Conduct structural components tests to determine cap section crippling strength and column failure mode/load.
- c. Determine physical/mechanical properties of selected materials, including effects of exposure to orbital environment.
- d. Fabricate and test prototypes of key beam builder and assembly jig mechanisms. Upon successful individual demonstration, operate in proper functional sequence using a prototype control system.

7.2.5 ALTERNATIVE BEAM CONCEPT. Although task effort was limited, as noted above, several areas of concern were identified. These indicate the directions in which additional study should be conducted in order to more fully evaluate the cylindrical geodetic beam concept for applicability to large space structures.

- a. Develop better sizing criteria; optimize for typical applications.
- b. Improve methods of analysis, particularly nodal joints.
- c. Conduct detail design studies of the beam and any required end fittings; develop/test joints.
- d. Investigate element/grid optimization.
- e. Conduct subscale beam tests to correlate analytical methods.
- f. Conduct fabricator trades; consider provisions for beam-to-beam joints; define impact of node count variation.